MEASUREMENT OF EMISSIONS FROM BRAKE AND TYRE WEAR

Final Report – Phase 2

Report for: Department for Transport

Ref. T0414a TETI0037

Ricardo ref. ED14775   Issue: Issue 2   05/09/2025

Customer:
Department for Transport

Customer reference:
T0414a TETI0037

Confidentiality, copyright and reproduction:

This report is the Copyright of the Department for Transport (DfT) and has been prepared by Ricardo AEA Ltd under contract T0414a TETI0037 dated 2nd February 2023. The contents of this report may not be reproduced, in whole or in part, nor passed to any organisation or person without the specific prior written permission of the Department for Transport. Ricardo accepts no liability whatsoever to any third party for any loss or damage arising from any interpretation or use of the information contained in this report, or reliance on any views expressed therein, other than the liability that is agreed in the said contract.

Ricardo reference:
ED14775

Contact:
Louisa Kramer, Gemini Building, Fermi Avenue, Harwell, Didcot, OX11 0QR, UK

T: +44 (0) 1235 753 315
E: louisa.kramer@ricardo.com

Author:
Jon Andersson, Michael Campbell, Jason Southgate, Ian Marshall, Gary Waite, Simon de Vries, Louisa Kramer

Approved by:
Louisa Kramer
Signed

Date:
05/09/2025

EXECUTIVE SUMMARY

Policy Problem

Non-exhaust emissions (NEE) from brake wear, tyre wear, road wear, and resuspension of dust have become a significant source of particulate matter (PM_{10} and $PM_{2.5}$) emissions from road transport in the UK and other countries. However, there are still large gaps in our understanding of the factors affecting NEE.

With the increase in traffic volumes on the road and growth rate in the uptake of electric vehicles, NEE and their contribution to particulate matter in the atmosphere has received more attention in recent years. The new Euro 7 emissions standard includes, for the first time, limits for brake and tyre wear PM_{10} emissions.

Although the focus for NEE has primarily been on particulate mass, particle number is also important to consider. Euro 7 will include exhaust particle number (PN) emissions standards for solid particles greater than 10 nm diameter (PN10), and this is also to be controlled in the future for brake emissions.

Client and Motivation

The Department for Transport (DfT) commissioned this research to fill these gaps and potentially inform policy on reducing brake and tyre wear. Ricardo, in collaboration with ARUP AECOM, was tasked with investigating the variables affecting particle emissions from brake and tyre wear.

Research Questions

In the first phase of this project Ricardo successfully developed a system and methodology for measuring and characterising particles emitted from brake and tyre wear, under real driving conditions. For Phase 2, the systems were optimised, and the following research questions were addressed:

1. What variables affect particle emissions from brake and tyre wear?
2. How do different brake and tyre components influence emissions?
3. What is the impact of regenerative braking and particle reduction devices on NEE?

Importance of the Work

Non-exhaust emissions are now a dominant source of particulate matter emissions from road transport. Understanding and mitigating these emissions is crucial for improving air quality and public health. This study aims to provide insights that could lead to effective policy measures to reduce NEE.

Key Findings

- **Brake Wear Emissions**: Low dust and ceramic pads showed the lowest particle mass ($PM_{2.5}$) and particle number (PN10) emissions. No significant differences were found between budget and premium brake discs. PN10 and $PM_{2.5}$ emissions increased when the vehicle test mass was increased during the real drive emission (RDE) tests on the chassis dynamometer.

- **Brake Technology Effects**: Regenerative braking in PHEV and EV vehicles significantly reduced $PM_{2.5}$ emissions compared to ICE vehicles, but minimal impact was observed on PN10.

- **Tyre Wear Emissions**: Larger tyres (18") had higher wear rates, but no significant effect on $PM_{2.5}$ and PN emissions. Tyre emissions were dominated by volatile particles.

- **Particle Reduction Technologies**: The TAMIC system reduced $PM_{2.5}$ emissions from brake wear by over 40%. The Tyre Collective device captured large particles from the tyre but had no significant effect on smaller $PM_{2.5}$ emissions.

Approach

Tests on different brake pads and tyres were conducted on a chassis dynamometer, on-road, and on test tracks. Various instruments were used to measure particulate matter and particle number concentrations. The brake pads tested included budget, premium, organic, and low metallic pads, and a set of aged pads. The tested tyres varied by supplier/composition, design, size and age. To study the effect of regenerative braking on brake wear emissions, tests were also performed on three different vehicles, a VW Caddy (internal combustion engine), VW Golf GTE (Plug in hybrid) and VW eGolf (electric).

Summary of Findings

- Certain brake pad compositions can result in lower particle emissions, but higher cost does not necessarily mean lower emissions.
- Regenerative braking technology significantly reduces $PM_{2.5}$ emissions.
- Tyre mass emissions are dominated by particles larger than 2.5 µm, with little difference observed between different tyre sizes, costs, or ages.

Recommendations

- Implement policies promoting the use of low dust and ceramic brake pads.
- Encourage the use of vehicles with regenerative braking technologies in areas where $PM_{2.5}$ control is critical.
- Further research on particle reduction devices to enhance their effectiveness in capturing smaller $PM_{2.5}$ emissions

This study provides valuable insights into the variables affecting NEE and offers potential solutions to reduce these emissions, contributing to better air quality and public health.

CONTENTS

GLOSSARY

Term	Meaning/expansion
μm	micrometres (10^{-6}m)
4WD	Four wheel drive
ABS	Anti-lock braking system
AM	Ante meridiem
APC	AVL Particle Counter
CoV	Coefficient of variance
CPC	Condensation particle counter
CVS	Constant volume sampler
DfT	Department for Transport
DMS	Differential Mobility Spectrometer
Dp	Particle diameter
EEPS	Engine exhaust particle sizer
ELPI	Electrical low-pressure impactor
ESC	Electronic stability control
EV	Electric Vehicle
FMPS	Fast mobility particle sizer
GC/MS	Gas chromatography / mass spectrometry
GF/A	Whatman glass fibre filter, type A
GPS	Global positioning system
HEPA	High efficiency particulate air (filter)
ICE	Internal combustion engine
I/O	Input/output
ID	Internal diameter
ISO	International standards organisation
kph	Kilometres per hour
LACT	Los Angeles Congested Traffic (drive cycle)
LCV	Light Commercial Vehicle
LEZ	low emission zone
LS	Low steel (brake pads)
lpm	Litres per minute
MEXA	Motor exhaust (emissions) analyser
MPEC	Mobile Particle Emission Counter
mph	Miles per hour
MT	Manual transmission
NAO	Non-asbestos organic (brake pads)

Term	Meaning/expansion
NEE	Non exhaust emissions
nm	Nanometre (10^{-9}m)
OBD	On-board diagnostics
OPC	Optical particle counter
PG-42	~42 minutes duration particle generation cycle
PHEV	Plug-in hybrid
PM	Particulate mass or particulate matter
PM_{10}	PM sampled with an inlet of 50% efficiency at 10µm
$PM_{2.5}$	PM sampled with an inlet of 50% efficiency at 2.5µm
PN	Particle number
RDE	Real Driving Emissions
SPCS	Solid particle counting system
STC	Shoreham Technical Centre
TGA	Thermogravimetric analyser
VERC	Vehicle Emissions Research Centre
WLTC	World harmonised light-duty test cycle
WLTP	World harmonised light-duty test procedure

1. INTRODUCTION

Ricardo, in collaboration with the Arup AECOM consortium have been contracted by Department for Transport (DfT), to improve current understanding of vehicle brake and tyre wear particle emissions which can be used to inform future legislation and policies aimed at reducing non-exhaust emissions (NEE).

Phase 1 of the project was completed at the end of 2022 and involved the development of a "proof-of-concept" system for sampling tyre and brake wear particles from light duty-vehicles. A summary of the outcomes from Phase 1 is provided in Section 1.1 below. In Phase 2 the system developed in Phase 1 was optimised and used to investigate the influence of variables that can affect particle emissions from brake and tyre wear.

1.1 PHASE 1 SUMMARY

In Phase 1, Ricardo designed, built and tested a prototype system to measure brake and tyre wear under real-world conditions. The system was installed on the front driver wheel of a small light duty van and consisted of three sampling points, 1) a brake enclosure to sample particles from brake wear, 2) a tyre duct fixed to the wheel hub carrier to sample particles from behind the tyre and 3) sampling probes for ambient measurements of particles. Each sampling inlet was connected to a sampling tunnel, via conductive tubing, from which real-time measurements of particle number and particle mass were taken. Testing of the system was undertaken in a chassis dynamometer facility; on a nearby test-track; and on public roads in an urban area.

For the brake wear sampling, the system performed very well. Real-time non/low volatility particle number emissions corresponded to real-time braking events, with emissions around 2 - 5 x 10^9 #/km/brake. The lowest emissions were seen at lowest speeds. Real-time particle mass emissions also aligned with braking events, and mass emissions (~$PM_{2.5}$) were around 1 mg/brake/km. The brake enclosure was also installed on the rear wheel of a passenger car to assess the transferability of the enclosure. The non-volatile emissions were higher from the rear wheel when compared to the front wheel of the van, however, this may be related to the different pads and discs that were installed on the car.

Measurements of tyre wear emissions were more challenging than for brakes. For the urban road and track tests it was found that the tyre emissions could not be isolated from background contributions (ambient and road wear particles). The tests showed that measuring tyre emissions in the chassis dynamometer is possible, and spikes in particle number and particle mass were observed during braking events, but these were much lower than the emissions observed from the brakes. A recommendation was given to enclose more of the tyre to help to improve particle collection efficiency and reduce the interference from background emissions.

Full details of the system and results from the tests are presented in the Phase 1 report[1].

1.2 OBJECTIVES OF PHASE 2

For Phase 2 of the project the primary aim was to use the measurement systems developed in Phase 1 to fill in gaps in current knowledge on tyre and brake emissions. Specific objectives of Phase 2 were to:

1. Investigate the influence of variables affecting particle emissions from tyre wear. Including tests with different tyre composition, varying age (mileage) of the tyre and different tyre sizes.
2. Investigate the influence of variables affecting particle emissions from brake wear. Including variations in brake and disc materials, and age of the brake components.
3. Investigate the impact of the use of regenerative braking (the collection and storage of kinetic energy during braking in a form suitable for immediate or later use) on non-exhaust emissions of vehicles. Assessing the potential benefits of the use of regenerative braking on particle emissions and whether this offsets any increases in NEE due to the greater weight of electric vehicles.
4. Estimate the impact of technologies aimed at reducing particle emissions from brake and tyre wear. This work focussed on assessing the performance of particle collection devices for removing/filtering brake and tyre emissions.

This report presents the details and results from Phase 2 of the project. Section 2 provides details of the four test vehicles used in study. Section 3 describes the changes and updates that were made to the brake and tyre wear sampling system from Phase 1 to improve the collection efficiency of particles, and modifications

---

[1] [Measurement of Emissions from Brake and Tyre Wear. Final Report - Phase 1 (2022)](#)

undertaken to enable installation on multiple vehicles. Sections 4 and 5 present an overview of the test facilities and particle measurements systems used in Phase 2. Details of the different drive cycles, including those on the chassis dynamometer, on road, and on the test track, are presented in Section 6. Section 7 provides information on the different brake and tyre components that were tested, the rationale for choosing each of them, and preparation that was undertaken to precondition the components before testing. Sections 8 to 11 present the results from the tests on the brakes, tyres, braking technologies (i.e. regenerative braking) and particle reduction systems. Finally, Sections 12 and 13 present a discussion of the sampling system and the instrumentation used in the test, as well as the final conclusions and recommendations.

2. TEST VEHICLES

Four test vehicles were employed in the Phase 2 test work. The two vehicles (Volkswagen Caddy Van and Audi A4 car) previously used during Phase 1 were retained, and a further two vehicles (Golf GTE and eGolf) were added. The additional vehicles were specifically employed to study brake technology impacts on emissions. The study required three vehicles built upon nominally the same platform covering standard internal combustion engine (ICE), plug-in hybrid (PHEV) and full electric vehicle (EV) categories. Since the VW Caddy is built upon the Golf VII platform, a gasoline Golf GTE (PHEV) and eGolf (EV) of similar registration dates (late 2016 to early 2017) were sourced.

The VW Caddy ICE features no regenerative braking, the PHEV has variable regenerative braking levels dependent on operating mode but was used in electric mode (e-mode) where regenerative braking is maximized, and the EV features the highest levels of regenerative braking.

The Audi A4 was used purely for tyre emissions testing in this phase of the project.

On receipt all vehicles had a valid periodic technical inspection certificate (UK MOT) but were also subjected to an internal Ricardo safety check, which is a more thorough evaluation of key vehicle safety aspects. For example, the safety check must be performed every 3 months, to qualify a test vehicle for any on-road or chassis dynamometer testing.

For braking tests on the Caddy, Golf GTE and eGolf, the front right-hand brake pads, disc and calliper were enclosed, and for tyre wear testing, emissions were sampled from the right-hand front wheel of the Audi. Detailed descriptions and diagrams of sampling approaches can be found for brakes in Section 3.1 and for tyres in Section 3.2.

The Caddy was initially equipped with 16" wheels. These were swapped for 18" wheels in the Phase 1 project to create more space for the development of sampling systems for both brakes (including enclosures) and tyres. The larger 18" wheels allow for better energy dissipation, and this could potentially lead to small reductions in particle emissions compared to the original 16" wheels. Tyre testing on the Audi included both 16" and 18" sizes.

2.1 VW CADDY

The VW Caddy (Figure 2-1) is a compact light-duty diesel van built upon the VW Golf platform. Key properties of the vehicle are given in Table 2-1. The vehicle features hydraulic braking with standard anti-lock braking system (ABS), electronic brake-force distribution, brake assist and servo assistance, but no regenerative braking.

The Caddy has a published kerb weight (weight of the vehicle without passengers or cargo) of ~1445 kg but was weighed at 1895 kg when carrying a full fuel tank, driver and all the project measurement equipment on-board.

Table 2-1: Properties of the VW Caddy.

Registration	HJ64 SZG
Transmission	Manual transmission, 5 forward gears, front wheel drive
Engine capacity (cc)	1598
Fuel type	Diesel

Registration	HJ64 SZG
Peak power & torque	55kW; ~230 Nm
Gross Vehicle weight (kg)	2310
CO_2 emissions (g/km)	149
Peak power (kW)	55
Front Brakes	Vented disc
Date registered	28 Oct 2014

Figure 2-1: VW Caddy test vehicle.

2.1.1 Caddy Test Masses

For almost all chassis dynamometer testing the test mass was set to 1900 kg, to match the test mass experienced on the road.

Additionally:

- To study test mass effects on emissions, one chassis dynamometer test was performed with each brake pad and disc combination with the test mass increased to 2100 kg
- For a one-off test during brake technology evaluations on the chassis dynamometer, it was necessary for the Caddy to be tested at a representative mass of a standard gasoline Golf TSI of the same platform and vintage. The Golf VII TSI has kerb weight of 1375 kg, and so for testing purposes a driver and cargo contribution of 125kg was added, and a test mass of 1500 kg was used

2.2 GOLF GTE

The Golf GTE is a gasoline plug-in hybrid version of the VW Golf (Figure 2-2). It features a 1.4 litre turbocharged 4-cylinder engine in combination with an electric motor. The braking system features ABS, electronic stability control (ESC) and automatic post-collision braking. Further properties of the Golf GTE are provided in Table 2-2.

Figure 2-2: VW Golf GTE.

Table 2-2: Properties of the Golf GTE.

Registration	GF66 XTK
Transmission	6 speed DSG automatic transmission, front-wheel drive
Engine capacity (cc)	1395
Fuel type	Gasoline
Peak power & torque (e-machine + ICE combined)	150 kW; 350 Nm
Electric motor	75 kW
Gross vehicle weight (kg)	2020 kg
CO_2 emissions (g/km)	35
Front Brakes	Vented disc
Date registered	November 2016

The Golf GTE has several modes of operation:

- Electric mode (e-mode), where the vehicle operates only under electric power. Range is ~30 miles. This is the default/ start-up mode of the vehicle. Under e-mode, regenerative braking usage is higher than in hybrid (H-mode). In this project, testing was solely executed in e-mode.
- Hybrid mode, where the vehicle blends both the ICE and e-machine. The vehicle switches to H-mode when the HV battery is depleted, but H-mode can be selected at key-on.
    - GTE mode, when the vehicle uses ICE and e-machine to produce greatest performance. Regenerative braking use can be higher than in E-mode
- Charge mode, where the ICE is forced to generate electricity to charge the battery while driving. This enables pre-charging of the high voltage battery prior to entering an urban low emission zone (LEZ), for example.

In this project the vehicle was always operated in the default E-mode, as this mode best represents 'average' use by a driver. When a sequence of tests was conducted on a single day the vehicle was charged overnight before starting the sequence.

2.2.1 GTE Test Masses

The kerb weight of the Golf GTE is 1585 kg, and a test mass of 1700 kg was generally employed in this project. For one-off tests, where the test mass was matched to the weight of the Caddy (Section 2.1.1), 1900 kg was employed – this being just below the gross vehicle weight.

2.3 eGOLF

The eGolf is the original fully electric model of the VW Golf (Figure 2-3). Key properties of the vehicle are given in Table 2-3. The braking system features ABS, ESC, and automatic post collision braking.

Like the GTE, the eGolf features multiple operational modes:

- Normal mode – energy efficiency and performance are given equal weighting
- Eco mode – the vehicle's systems are optimized for maximum efficiency and improved range
- Eco+ mode – reduces power output and ancillary usage to maximise range

Regenerative braking options can be selected alongside the operational modes. As a default, a moderate level of regenerative braking (similar to D2 below) is automatically selected in Normal mode, and that is the setting used in this project.

Regenerative braking is a major element of the eGolf's strategy for energy efficiency, with several levels available to the driver:

- Drive modes 1, 2 and 3 (D1, D2, D3) provide increasing levels of regenerative braking to individual preference, engaging when the driver lifts off the accelerator.
- Braking mode (B-mode) provides a more aggressive braking option, aimed at maximising energy recovery in urban driving

Figure 2-3: VW eGolf test vehicle.

Table 2-3: Properties of the eGolf

Registration	LO17 PHV
Transmission	Single speed automatic, front wheel drive
Engine capacity (cc)	[-]
Fuel type	EV
Peak power & torque (combined)	85 kW; 270 Nm
Battery capacity & charge time (generic data, as information is not supplied in the vehicle manual)	24.2 kWh & ~8 hours (AC 3.6 kW)
Gross vehicle weight (kg)	~1960 kg
CO_2 emissions (g/km)	[-]
Front Brakes	Vented disc
Electric range (new)	Up to 118 miles
Electric range reported when tested	~110 miles
Date registered	June 2017

2.3.1 eGolf Test Masses

The kerb weight of the e-Golf is 1,585 kg, and a test mass of 1,700 kg was generally used in this project. For specific one-off tests, intended to isolate the positive effect of regenerative braking on brake emissions from the negative effect of vehicle mass, a test mass of 1,900 kg was employed to match the weight used for the Caddy. As with the GTE, the test mass was safely below the gross vehicle weight.

2.4 AUDI A4

Like the Caddy, the Audi A4 (Figure 2-4) was also used in the Phase 1 project, both for brake and tyre emissions experiments. In this later phase, it was used purely for tyre emissions testing, with the sampling and measurement equipment all situated off-vehicle (Section 3.2.4).

Figure 2-4: Audi A4 Test Vehicle.

Key properties of the Audi A4 are given in Table 2-4.

Table 2-4: Properties of the Audi A4.

Registration	MJ14OFO
Transmission	Manual transmission, 6 forward gears, front wheel drive
Engine capacity (cc)	1798
Fuel type	Petrol
Gross Vehicle weight (kg)	2060
CO_2 emissions (g/km)	141
Peak power (kW)	125
Tyre size	255/35/R19
Date registered	08 Oct 2015

A reference test mass of 1825kg was used for the Audi A4 testing.

2.5 CHASSIS DYNAMOMETER TERMS

A summary of chassis dynamometer terms employed in the project is given in Table 2-5. For any given vehicle, the highway terms differ between the two test facilities used (VERC: Vehicle Emissions Research Centre and VATF: Vehicle Anechoic Test Facility; Section 4), while the dynamometer terms are constant.

It should be noted that in the braking technology investigations (Section 9), the Golf GTE and eGolf were always tested with the same terms, so the same test weight and body shape was assumed. Alternatively, the Caddy was both used to represent an light commercial vehicle (LCV), where specific dyno and highway terms (as well as test mass) were used, and to represent a typical gasoline Golf TSI, where the same dyno terms as the GTE and eGolf were employed, but a more representative test mass was used.

Table 2-5: Chassis dynamometer and highway load terms

	Caddy	Caddy	Golf GTE	Golf GTE	eGolf	eGolf	Caddy	Audi A4
Facility	VERC	VERC	VERC	VERC	VERC	VERC	VATF	VATF
Test Inertia (kg)	1900	1500	1700	1900	1700	1900	1900/2100	1825/2025
Dyno Configuration	Four Wheel	Four Wheel	Four Wheel	Four Wheel	Four Wheel	Four Wheel	Two Wheel	Two Wheel
Dyno A (N)	35.9	10.09	10.09	35.9	10.09	35.9	35.9	127.75
Dyno B (N/km/h)	0.17	-0.1859	-0.1859	0.17	-0.1859	0.17	0.17	0
Dyno C (N/km/h2)	0.0381	0.0322	0.0322	0.0381	0.0322	0.0381	0.0381	0.04941

3. SAMPLING SYSTEM

3.1 BRAKES

Phase 1 of the concept development aimed to establish a methodology for sampling brake wear particle emissions in a controlled manner and to identify the necessary next steps to optimize the sampling system. The lessons learned from the design and testing process are as follows:

1. The total airflow required to efficiently transport the particles from the brake enclosure to the onboard particle counting devices (electrical low pressure impactor (ELPI+) and eFilter) within the sampling tunnel proved challenging. The flow rate reached around 180-190 litres per minute (l min⁻¹), but the axial fan design was not optimal due to flow restrictions at the brake enclosure. A flow rate of over 300 l min⁻¹ was desirable to ensure optimal transport efficiency of the particle distribution for Phase 2.

2. During Phase 1 testing, maintaining a constant flow was difficult, which was traced to leakage from the dilution boxes caused by pressure buildup ahead of the brake enclosure restriction, heat generated from the equipment also had an influence on maintaining constant flow.

3. The axial fans that provided airflow to the filters and sampling system had open inlets located relatively close to the rear doors of the vehicle when installed in the caddy. To prevent airflow restriction, the rear doors had to remain open, creating issues during testing in wet conditions.

4. Heat buildup in the dilution tunnel, caused by the significant heat generated by two high-powered vacuum pumps attached to the ELPI devices, along with the downstream vacuum pump and eFilter pump, resulted in substantial warming of the rear enclosure. This issue was partially resolved by keeping the rear doors open but underscored the concern mentioned in point 3.

5. The bulky nature and high-power demand of the installed equipment posed challenges for the duration of testing.

3.1.1 Improvements / evolution from Phase 1

Having identified the areas for improvement outlined above, the following actions were undertaken on the Phase 1 initial system in preparation for Phase 2 testing, with consideration given to the particle counting systems identified. Figure 3-1 illustrates the optimized sampling setup. Starting at the furthest point upstream, a blower directs air through a gate valve and into the high efficiency particulate air (HEPA) grade filter boxes, the air is then passed through micron grade filters to a blowby meter and then into the top of the brake enclosure. At the bottom of the brake enclosure is an outlet which is connected to a variable area (VA) flowmeter and then to the sample tunnel, from which each analyser sub-samples. A second blower, sucks against the sample tunnel (via a second gate valve) and exhausts the air outside the vehicle.

3.1.1.1 System Flow optimisation.

The most significant challenge in optimising the setup from Phase 1 was to improve the airflow without increasing power demand or requiring more space. Several alternative air delivery systems were considered to meet these requirements, and the final choice was to use high-powered leaf blowers. These blowers can generate high-velocity air flows with enough pressure to overcome the restrictions caused by the small ports in and out of the brake enclosure. Two units were selected: a Makita blower rated at 4.1 m³ min⁻¹ to blow into the filter boxes, and a KATSU blower rated at 3.2 m³ min⁻¹ downstream of the sampling tunnel to provide suction from the brake enclosure. Together, they had a combined power rating of 1150 W, split across two EcoFlow power packs. ~~with no peak load startup.~~

These blowers had a similar power demand to the original axial fans but offered an additional advantage. The downstream leaf blower replaced the larger Gast vacuum pump, which had a power rating of 800 W and a peak load exceeding 1000 W, often causing the EcoFlow power pack to shut down if not connected to mains power before testing began. The Gast pump was the largest power consumer, limiting the duration and number of tests that could be completed in a single day. Replacing it with a more efficient, lower-powered air delivery unit improved both the testing duration and the number of tests that could be completed.

3.1.1.2 Filter Air handling.

Optimizing the air delivery presented a new challenge. The HEPA filter box housings were not designed to operate under high inlet pressures. As a result, the increased flow from the blowers caused the filter boxes to expand slightly, which in turn led to the filter seals detaching and allowing unfiltered air to pass through.

To resolve this issue, a bead of silicone sealant was applied around the edge of the seal contact between the filter and the filter box to secure the filters in place. Additionally, a brace was installed around the filter box to minimize ballooning under high pressure.

A secondary set of 10-inch, 0.1 µm grade filters was added downstream of the filter boxes to mitigate the risk of particle entrainment in the event of filter failure or breaches. The addition of these filters did not result in any noticeable changes in airflow downstream of the filter boxes and could function as a standalone filter pack. This setup would allow for increased flow into the brake enclosure when the particle distribution of interest is above 0.1 µm.

3.1.1.3 Flow Path Optimization.

The flow path setup from Phase 1 was further refined to ensure uninterrupted airflow and minimize turbulence, which could lead to reduced flow rates and potential particle losses. To achieve this, every effort was made to keep hoses as short as possible with minimal bends. Since achieving higher flow was a priority, further modifications were made to both the inlet and outlet of the filter boxes. The outlet funnels were replaced with larger diameter "Y" pieces, and a similar configuration was applied to the inlet side where the blower connects. These changes helped create a smoother airflow path, reducing cumulative back pressure caused by turbulence. Additionally, all connections were carefully considered to eliminate restrictions and avoid abrupt changes in tube size.

3.1.1.4 Other Modifications.

One issue that needed resolution was the buildup of heat within and ventilation of the cabin. In Phase 1, one of the rear doors of the Caddy had to remain fixed in an open position. This presented a challenge during wet weather and also posed a risk of vehicle exhaust emissions being drawn back into the rear of the vehicle due to turbulent airflow. Emissions transported inside the vehicle could potentially contaminate the sampling system and affect the onboard instruments.

For Phase 2, the ventilation of the sampling tunnel was rerouted through a port cut into the rear door, allowing the doors to remain closed during testing. The inlet air was now drawn from inside the cabin, reducing the risk of external contamination. Additionally, the pumps used to provide system airflow were replaced with a more energy-efficient setup, eliminating the heat buildup caused by the older pumps. This change further reduced the cabin's internal temperature.
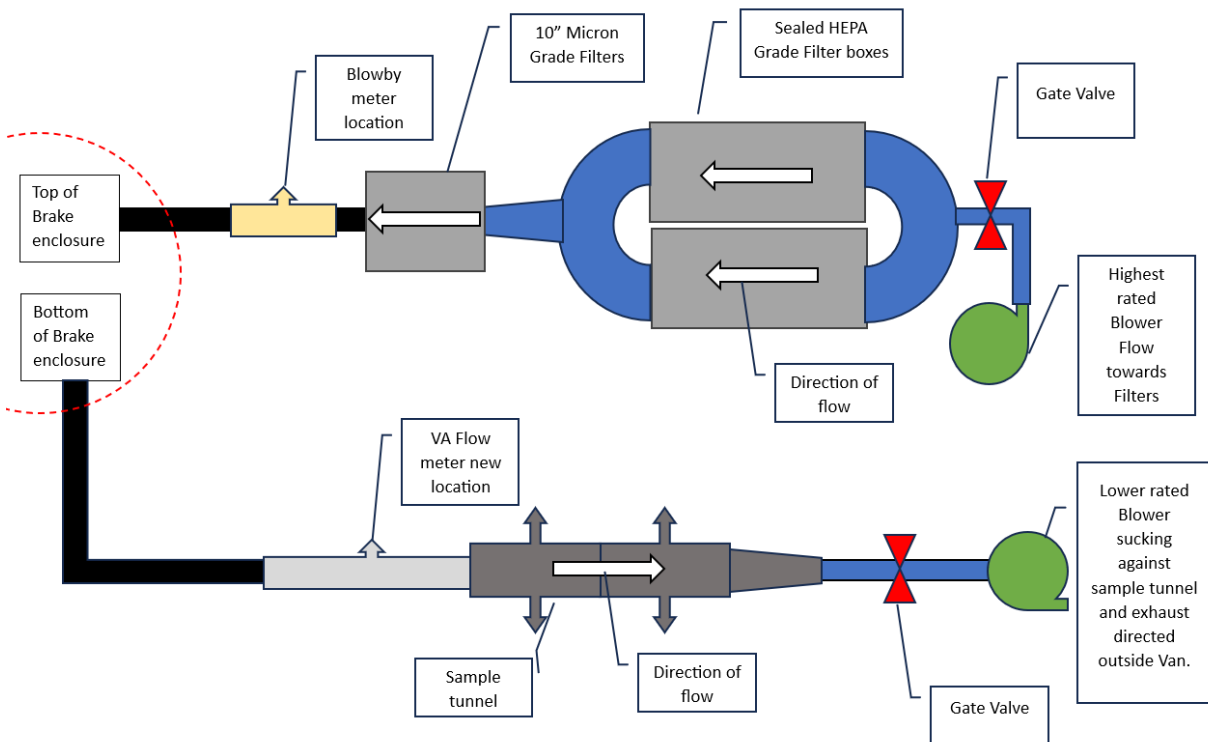
Figure 3-1: Flow schematic of optimised setup.

3.1.2 Evaluation of Sampling Setup

Tests were performed to ensure the sampling setup maintained optimal flow conditions. Positive flow into the brake enclosure was controlled to be equal to or slightly higher than the suction flow drawn from the enclosure into the onboard sampling tunnel. Additionally, the transport air was assessed for the presence of background particles that could be entrained in the flow stream, either due to inefficient filtration or unintended ingress into the sampling tunnel. These factors, influenced by the configuration and blowers used, were evaluated for their potential to interfere with particle number counts at low concentrations.

Another key consideration was the power demand of the system and its ability to maintain consistent flow over prolonged project testing. This assessment aimed to establish the stability of the blowers and ensure flow consistency during extended measurement periods.

3.1.2.1 Flow Evaluation

The blowers specified in Section 3.1.1.1 were installed and evaluated within the sampling system. Flow measurements were conducted simultaneously upstream of the brake enclosure and downstream of the sample tunnel.

The flow from the positive blower into the sampling enclosure was measured using an AVL 442 Blowby Airflow Meter, with a full-scale range of up to 600 l min^{-1}. This meter was positioned downstream of the filters and immediately before the brake enclosure, ensuring that any flow restrictions in the system were accounted for. The maximum flow into the enclosure was measured at 630 l min^{-1}. The flow exiting the sampling tunnel was measured using an inline mass flow meter (Model VA420). To ensure accuracy, the VA420 was calibrated against the AVL 442 Blowby Airflow Meter within the same setup. A calibration factor (slope) of 0.9045 was applied to align the readings. The maximum flow rate measured at the tunnel outlet was approximately 430 l min^{-1}.

To achieve an excess flow into the brake enclosure 10% greater than the flow drawn out, a gate valve installed at the blower inlet to the brake enclosure was adjusted to restrict the flow to approximately 475 l/min.

3.1.2.2 Battery Generator Capacity Evaluation

The EcoFlow battery generators used in the system have a maximum capacity of 2 kWh when fully charged. During Phase 1, the pumps supplying flow for the sampling system represented the highest power demand. As a result, the measurement campaigns were limited to less than one hour of testing before the generators required recharging.

To evaluate the power draw and determine the maximum measurement duration achievable with the new installation, the batteries were fully charged to 100%. Each blower was connected to its own individual EcoFlow battery generator. The sampling system was then activated and allowed to run continuously until the first battery reached 40% charge, at which point the test was stopped.

Based on the data collected, the maximum runtime was calculated for a full battery discharge from 100% to 5% capacity. For the blower installed in the sample tunnel, which had the highest power draw, the estimated maximum runtime was approximately 180 minutes. This represents a 120-minute increase compared to the original setup, significantly extending the testing time available per charge. However, this estimate excludes any additional power demands that may arise from other components in the installation.

3.1.2.3 Background Zero Evaluation

To validate the significant changes and optimizations made to the setup, the quality of the filtration and the integrity of the system were assessed through leak checks. This was achieved by comparing the ambient air to the air within the sample tunnel using a Scanning Mobility Particle Sizer (SMPS) system (TSI 3782 coupled with a TSI 3750 CPC) and a TSI Aerodynamic Particle Sizer (APS 3021). These instruments provided measurements across particle size ranges from 7 to 300 nm (SMPS) and from 0.5 to 20 μm (APS), respectively. The results of both scans were combined and are presented in Figure 3-3.
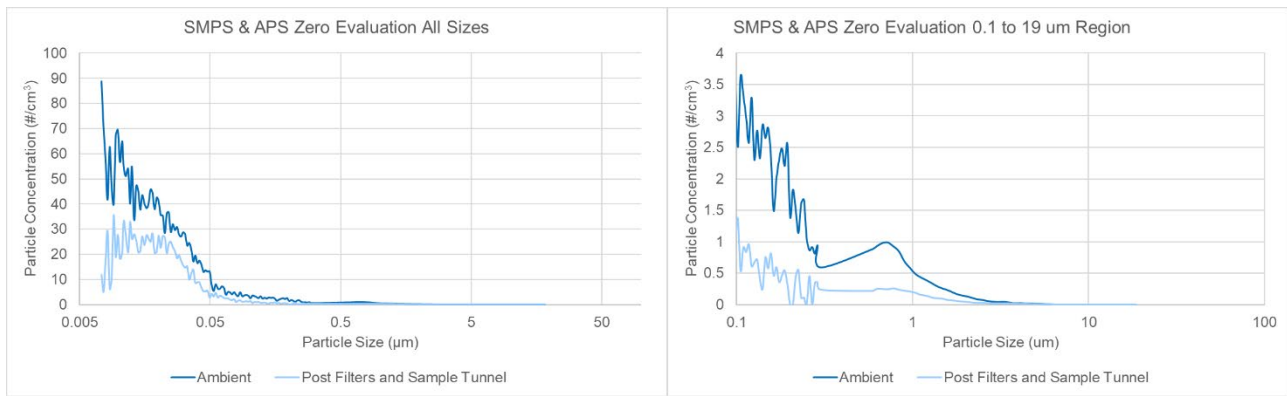
Figure 3-2: Particle concentrations measured by an SMPS and APS over a particle size range from 7 to 20 µm. The dark blue line represents ambient concentrations and the light blue line the concentrations once the air has passed through the filters and sample system. The left chart shows the concentrations for all size ranges, and the right chart shows a zoom-in of the concentrations for size ranges from 0.1 to 19 µm.

The system flows were configured as described in Section 3.1.2.1. A reduced particle concentration in the sample tunnel compared to ambient air indicated the absence of leaks in the system and confirmed that the filters were effectively reducing background particle concentrations. This result validated the filtration efficiency and ensured the integrity of the sampling setup.

3.1.3 Final system

3.1.3.1 Trolley installation – Brake measurements

To allow the easy in-lab use of all the equipment that had been mounted inside the Caddy for brake measurements, a 3-tiered trolley was procured. This allowed easy removal to and from the test facility as well as rapid connection to the test vehicle.

The sample tunnel was mounted on the shelf closest to the ground to allow the shortest possible 25 mm ID electrically conducting silicone pipes to be used to and from the vehicle brake enclosure. Both the hot and cold MPEC's were also located on the same shelf next to the sample tunnel, helping to keep sample lines short and the trolley's centre of gravity low. Other sampling instrumentation (Cambustion DMS500 and AVL APC+ PN10) were located on the floor near to the trolley, with suitably short connections to sample tunnel. On the next level a large HEPA filter and secondary filter were located. These were to remove any ambient particles from the air supplied to the brake enclosure.

The brake enclosure was not perfectly sealed. To increase the flow through the brake enclosure and to minimise the loss of material venting out, an additional vacuum pump was attached to the outlet of the sample tunnel. The flow through the sample tunnel from the brake enclosure and the flow of HEPA air to the brake enclosure was adjusted to give a venting flow loss of approximately 10% i.e. flow into the enclosure was 10% higher than the flow out of the enclosure.

Additionally, a 2kWh uninterruptible power supply (UPS) was located on the top shelf. When necessary, this allowed the instrumentation to be warmed up off-line and then moved into position, allowing more rapid set-up and efficient use of the test facility.

Further information on the brake measurement trolley can be found in Section 9.1.1.

3.1.3.2 Trolley installation – Tyre measurements

A wooden trolley was constructed to mount a large centrifugal "snail fan" fitted with an orifice and Mass Air Flow (MAF) sensor. This fan was the primary air mover to draw the sample, via a flexible pipe, from the tyre dust collector and past the emissions sample probe section. This trolley also housed any additional power supplies need by the instrumentation.

Both the hot and cold MPEC and the PN4 instrumentation was located on a floor-standing shelf unit next to the sample section. Other sampling instrumentation (Cambustion DMS500 and AVL APC+ PN10) were located on the ground with their connections attached to the sample section.

Further information on the tyre emissions measurement trolley can be found in Section 3.1.1.

3.1.4   Enclosures used with the three test vehicles

In Phase 1 three designs of brake enclosure were tested. The three enclosure designs used in phase 1 are described in more detail and illustrated in Section 5.1 of the phase 1 report[2]. In the first design, the outer face of the wheel was sealed, and a static rear (inner) plate fixed in place of the stone-guard enclosed the rear of the wheel and the brake. In the second, a bowl-shaped enclosure was fitted over the brake and attached to a similar rear plate as the first design, an opening around the wheel hub allowed the enclosure to remain static while the wheel rotated. In the third design, a similar bowl-shaped enclosure as in the second design was fitted to the hub (trapped between wheel and hub) so that it rotated, with the inner plate static as in the first design. None of the designs were completely sealed, although the location of the gap between the rotating and static components differs. The airflow into the enclosure is deliberately slightly higher than the sample flow out to ensure the sample is not contaminated with external particles. The tests suggested there was no significant difference between the three enclosures although the use of the wheel as the enclosure has slightly worse heat rejection, and there was some evidence that the static enclosure saw lower PN measurements thought to be due to less effective air mixing within the enclosure.

In this phase (2), the brake testing was carried out across three vehicles, although all three shared common brake components (which were moved from vehicle to vehicle) and instrumentation. The first enclosure design was chosen since the use of the wheel as the outer part of the enclosure facilitated the easy removal and refitting of the brakes from vehicle to vehicle. The wheel with the sealed face and the matching static inner plate were carried over from Phase 1 and were transferred between test vehicles along with the brake components and instrumentation, so all three vehicles used the same brake and enclosure components. The arrangement of the enclosure is shown in Figure 3-3 along with a picture of the sealed wheel fitted to one of the test vehicles.
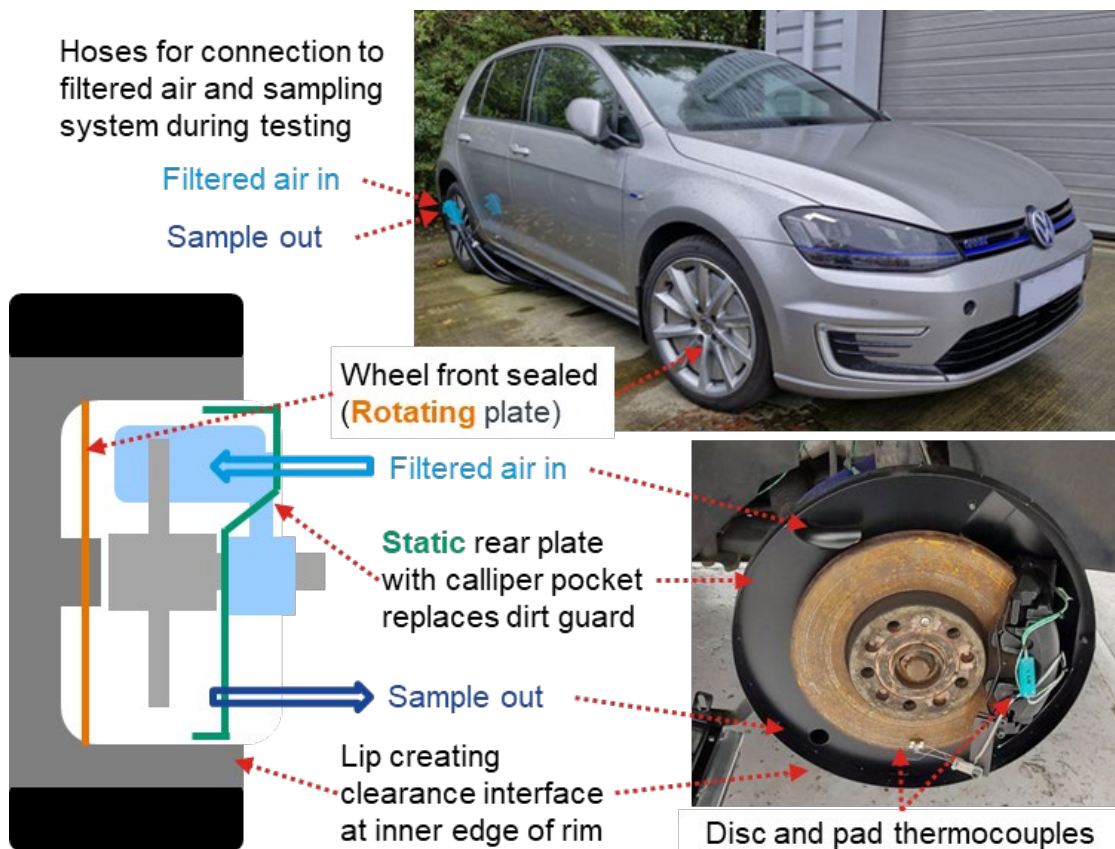

Figure 3-3: Brake enclosure for brake testing.

---

[2] Measurement of Emissions from Brake and Tyre Wear. Final Report - Phase 1 (2022)

3.2 TYRES

The development of an updated sampling system for measuring tyre particle emissions is described in this section.

3.2.1 Improvements / evolution from Phase 1

Review of phase 1 – smoke tests

In phase 1, a tyre particle sampling duct had been developed that enabled on-road testing. The requirement for the equipment to be on-board the vehicle and for the sample duct to be suitable for on-road use led to several constraints on the sampling system:

1. The space and power available on-board the vehicle limited the size of the sample tunnel and the pump used to draw air through the sample tunnel, limiting the flowrate of the sample tunnel.
2. To ensure a reasonable velocity of the sampled air past the tyre and into the sample inlet was achieved, the area of the sample duct opening was restricted by the available sample flowrate. Since the duct opening spanned the width of the tyre, this meant it had a narrow opening of limited height.
3. The sample duct was fitted to a front (driven and steering) wheel since they have the greatest wear rate. To enable the sample duct to be positioned close to the tyre and capture particles while turning, it was mounted via a bracket to the rear of the wheel hub/brake assembly. The duct could then move with the wheel in the horizontal plane when turning.
4. The steering geometry meant the lateral movement of the sample duct was accompanied by vertical movement, swinging up and out on left-hand steering and down and inwards on right-hand steering. This vertical movement, along with the need for the duct to clear uneven road surfaces (potholes and speed bumps included) and to not contact the underside of the vehicle body as that moved vertically (relative to the wheel) on the suspension, meant the vertical positioning of the duct was limited to a very narrow window.

In the conclusions of Phase 1 it was noted that this sampling arrangement could not collect the total particle emissions of the tyre, and its sampling efficiency was estimated as between 1:10 and 1:150 but could not be quantified. It was also noted that on-road emissions measured were relatively small compared to the background, but that vehicle dynamometer testing showed good repeatability. To develop an approach to tyre particle sampling for Phase 2 a qualitative assessment of the particle flows relative to the Phase 1 tyre sample duct was carried out using smoke. This used a smoke generator which produced particles from heated oil, the particles were ducted in front of the tyre (not blown) during both static and dynamic (on a vehicle dynamometer at 10kph and 50kph tests), and the result recorded as digital video. The test arrangement and a still from a video of a 10kph test are shown in Figure 3-4.
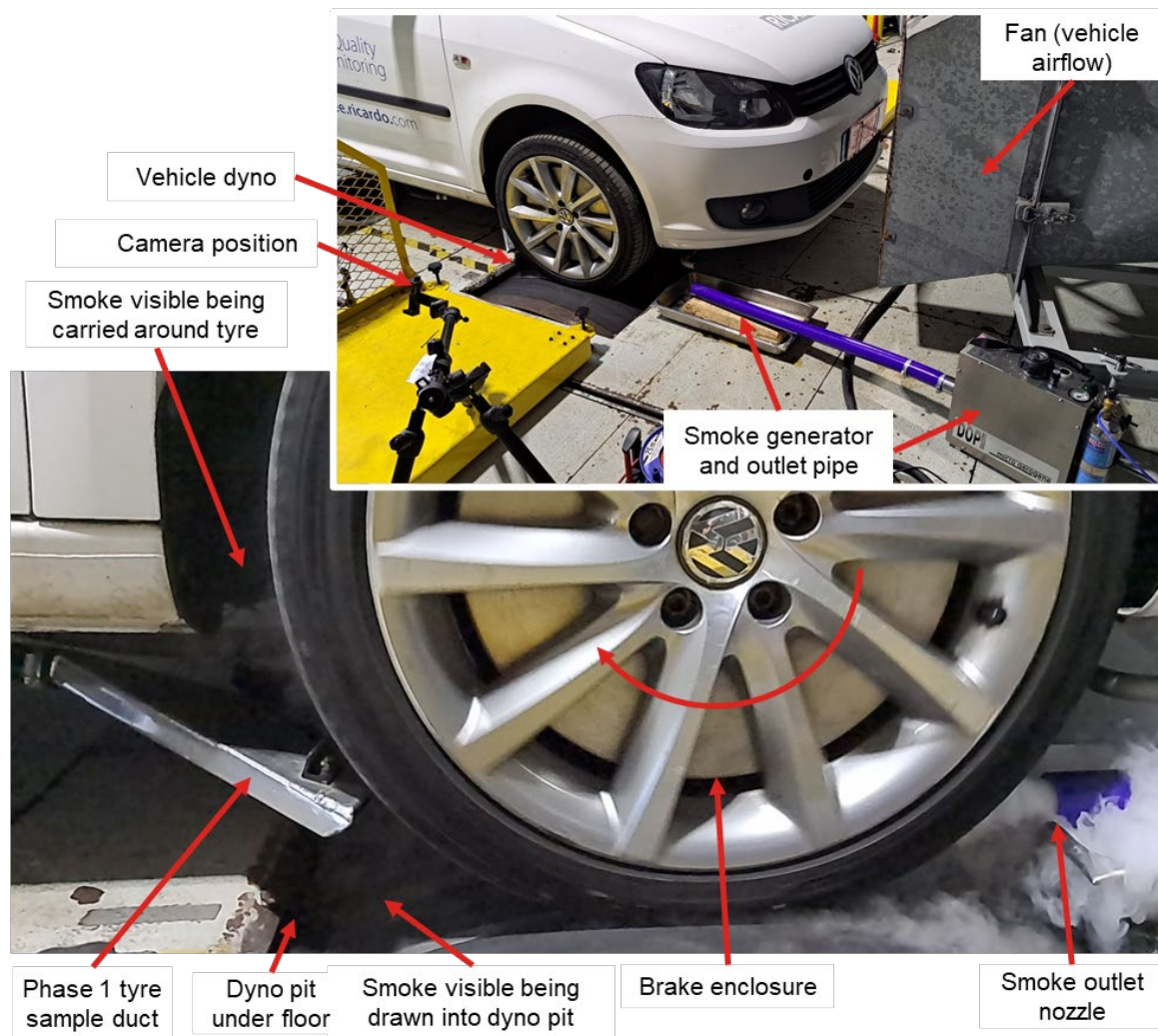
Figure 3-4: Set up for the tyre sampling duct smoke tests in the chassis dynamometer.

The smoke test provided some valuable insights:

- The sample draw of the duct was weak – smoke particles were drawn in only if their path entered the duct and were not diverted in.
- Air movement around the tyre was turbulent – particles may be carried out to the sides of the wheel.
- With the dyno pit extraction fan in use, a significant proportion of the smoke particles were drawn away through the gap between the dynamometer drum and floor. With the dynamometer pit extract switched off this was significantly reduced.
- At low speeds a thin layer of smoke particles was drawn around the wheel, close to the tyre, up into the wheelarch. This effect reduced as speeds increased and was limited by 50kph.

3.2.2 Tyre particle sampling design selection for Phase 2

A range of tyre particle sampling systems are observed in literature of other studies considering tyre abrasion and particle emissions. A selection of possible systems that may be applied to a tyre fitted to a vehicle is described below and summarised in the infographic in Figure 3-5. These range from a complex full enclosure which is more suited to laboratory tests, to sample probes which are more practical for testing on road.

- A full enclosure surrounds the tyre to capture all of the particles. This could be used as a reference design, however it is complex and requires modification to the vehicle, such as extending the axle. This type of enclosure is impractical for on road use. A wheel dynamometer is probably a better choice if the aim is for all particles to be captured, however this is not representative of real-world measurements.

- A particle enclosure surrounds the rear of the tyre. This is simpler to implement and can be fixed close to the contact point between the tyre and surface. It is expected that a large proportion of the particles can be collected with this type of enclosure. However, there may be unknown losses, and it is not suitable for on road use. This enclosure also requires a high flow rate for sampling.

- An underbody sample duct can be fixed to the underside of the vehicle and is simple to implement. This type of system can allow for testing on the road, however, for safety reasons it will need to be located further from the contact point between the tyre and road, which will likely result in unknown losses of particles and possible sampling of non-tyre material. A high flow rate is needed for sampling.

- A close mount sample duct sits behind the wheel and can move with the steering, therefore it can be used for on road tests. As for the underbody sample duct, this system will also result in losses of particles and contamination from non-tyre material. A medium to high flow is needed for the sampling.

- A sample probe is the simplest design and consist of one or more sampling inlets located behind the tyre. A low flow rate can be used, however only a small sub-sample of the particles emitted from the tyre will be sampled.
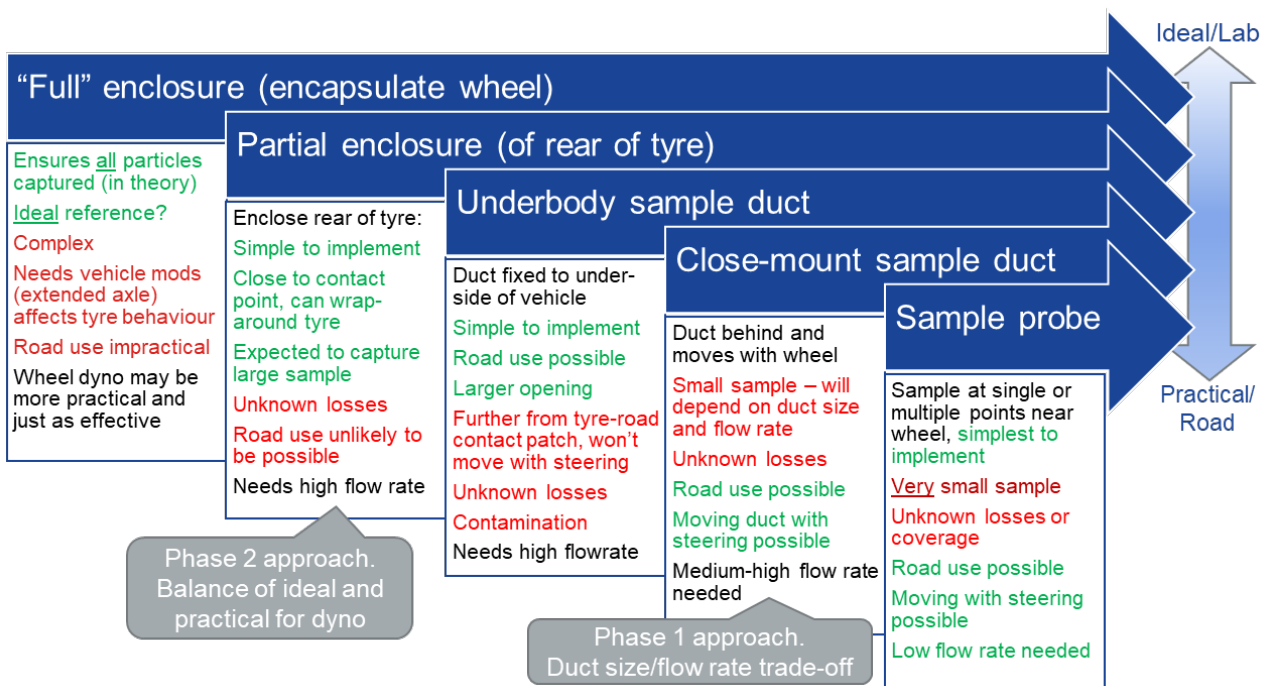
Figure 3-5: Range of potential tyre sampling approaches.

The system applied in Phase 1 could be classed as a close-mounted sample duct with greater coverage than individual probes but still able to be used on-road, but as noted its sample efficiency was low. Experience in Phase 1 showed that fitting a larger sample duct for road use is impractical unless it is fitted to the vehicle body. However, the inlet would then be located further from the tyre-road contact patch resulting in a lower particle capture efficiency. A full enclosure would in theory capture all emissions from the tyre and eliminate outside sources, making it an ideal reference for particle emissions measurement. However, the gap between tyre and wheel arch is insufficient to enclose a tyre on a vehicle so the axle may be extended to bring the wheel beyond the body and able to be enclosed, this changes the suspension geometry and weight distribution, which may affect the way the tyre behaves. For a study considering the real-world emissions of tyres, this approach was considered too far removed from road use. Also, no such system can be completely enclosed, and the smoke tests had shown the gap between the dynamometer drum and floor could allow particles to escape, so a full enclosure may be better represented by a tyre rig test.

After consideration of the potential approaches and discussion with Officials, the partial enclosure concept was selected for Phase 2. This is suited to vehicle dynamometer use as it is floor mounted and wraps around the rear of the tyre as illustrated in Figure 3-6. The duct height is constrained by the underbody of the vehicle, which can move on the vehicle suspension during dyno test accelerations and braking, although it is still able to be far larger than the close-coupled sample duct used in Phase 1.
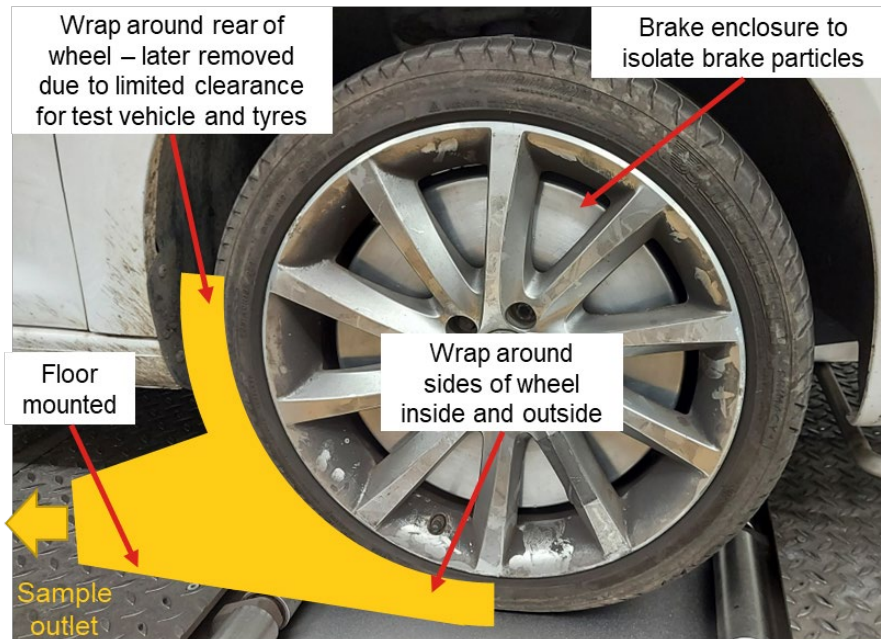
Figure 3-6: Partial tyre enclosure concept for vehicle dynamometer.

The duct design as implemented is shown in Figure 3-7, with key dimensions. The width is dictated by the widest tyre to be tested with 15 mm minimum clearance to each side, and as noted the height is restricted by the vehicle body. Indeed, the underside of the vehicle sill just made contact with the top of the duct under hard braking, demonstrating the duct was the maximum possible size. The lower edge of the duct extends over the dynamometer drum close to the tyre contact patch, and the sides extend forward so that they slightly overlap the sides of the tyre to channel any particles emitted into the duct. Initially, an upward extension around the rear of the tyre as high as the axle line was trialled, however there was found to be insufficient clearance between wheel and wheelarch with some of the larger tyres to be tested, since the vehicle body has some fore-and-aft movement relative to the wheel even when constrained on the dynamometer. The duct was fabricated from mild steel and painted to prevent rust particles. It was not fixed to the floor, it's weight and that of the duct behind it was sufficient to hold it in place, although if the vehicle contacted it the duct would move to avoid damage.
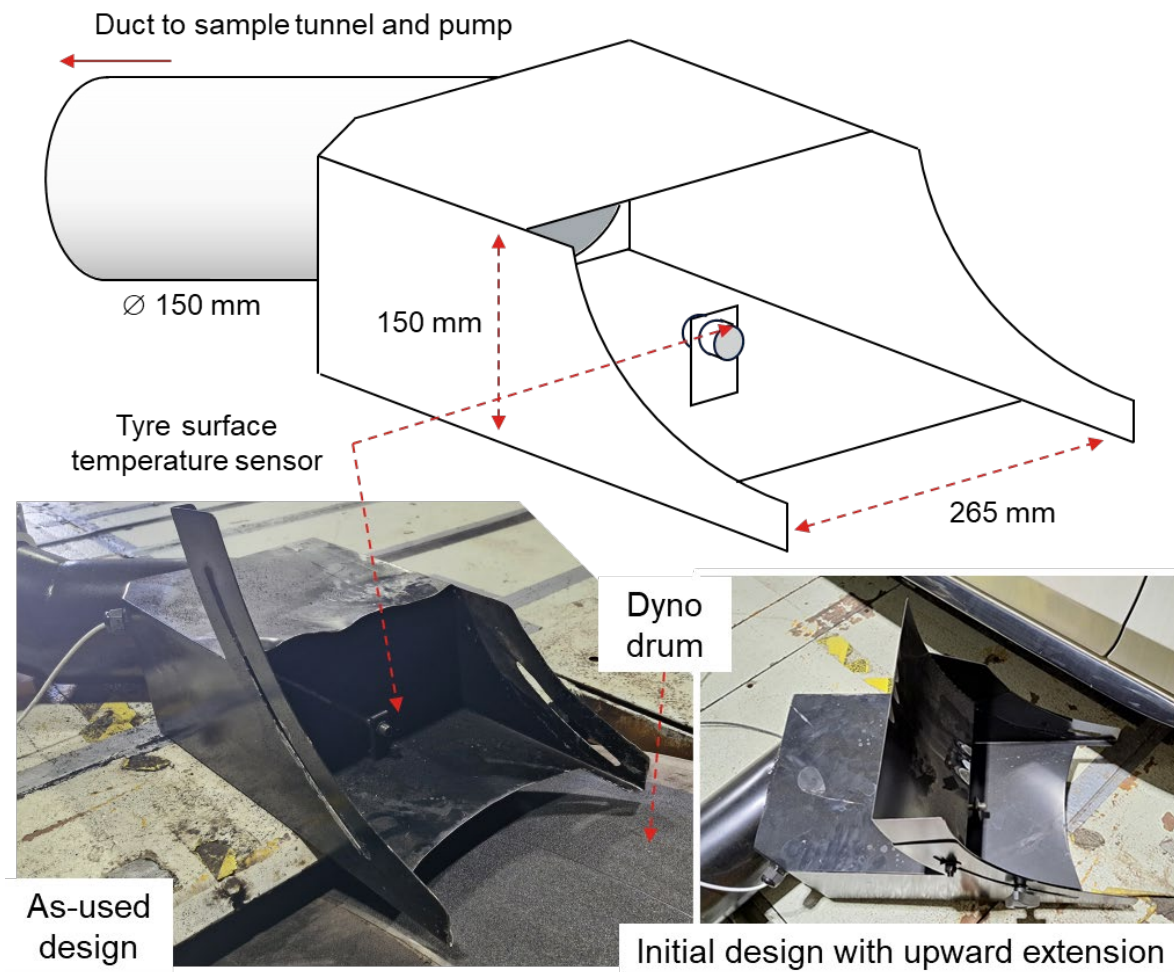
Figure 3-7: Sampling duct design and photographs.

Adopting dyno-only tyre emissions testing with the floor-mounted partial enclosure duct removes the constraint on sample tunnel and pump size and power demand. Instead, a large (150mm) bore pipe is connected to a large fan to draw sample flow through the sample duct, flow is measured after the sample positions using a hot-wire flow sensor and can be regulated through an orifice and a pair of by-pass valves. A hot wire sensor measures air flow by monitoring the current in a tungsten or platinum wire in the air flow, as the air flow increases more current is required to maintain the wire temperature. Such devices are commonly used to measure air flow into an engine and have the advantages of robustness, working over a range of air velocities including low speeds, being sensitive to changes in flow rate, and not requiring long flow straightening pipework

3.2.3 Preliminary experiments and development of facility and sample system

The floor-mounted tyre duct was initially tested in the vehicle emissions research facility (VERC). Further information on the VERC is provided in Section 4.1. The duct was connected to the sampling system, which was installed on a trolley as shown in Figure 3-8. The trolley housed the large sample fan to which the tyre sample duct was connected via a flexible hose, a mass air flow sensor, and a 50 mm diameter orifice. The sample flow was measured at 1110 litres/minute at the flow sensor. The particulate measurement instruments sampled immediately upstream of the orifice and flow measurement, and downstream of the flexible hose, which allowed the MEPCs to be mounted on the same trolley as the sample fan.

Figure 3-8: Photograph of initial tyre sampling set up on the chassis dynamometer.

The results of the initial tests were disappointing as unexpectedly low particle emissions were measured, and there was little obvious relationship between the drive cycle and the emissions profile of any of the instruments. These tests, comparisons to the results of tyre testing in Phase 1, root-cause analysis, a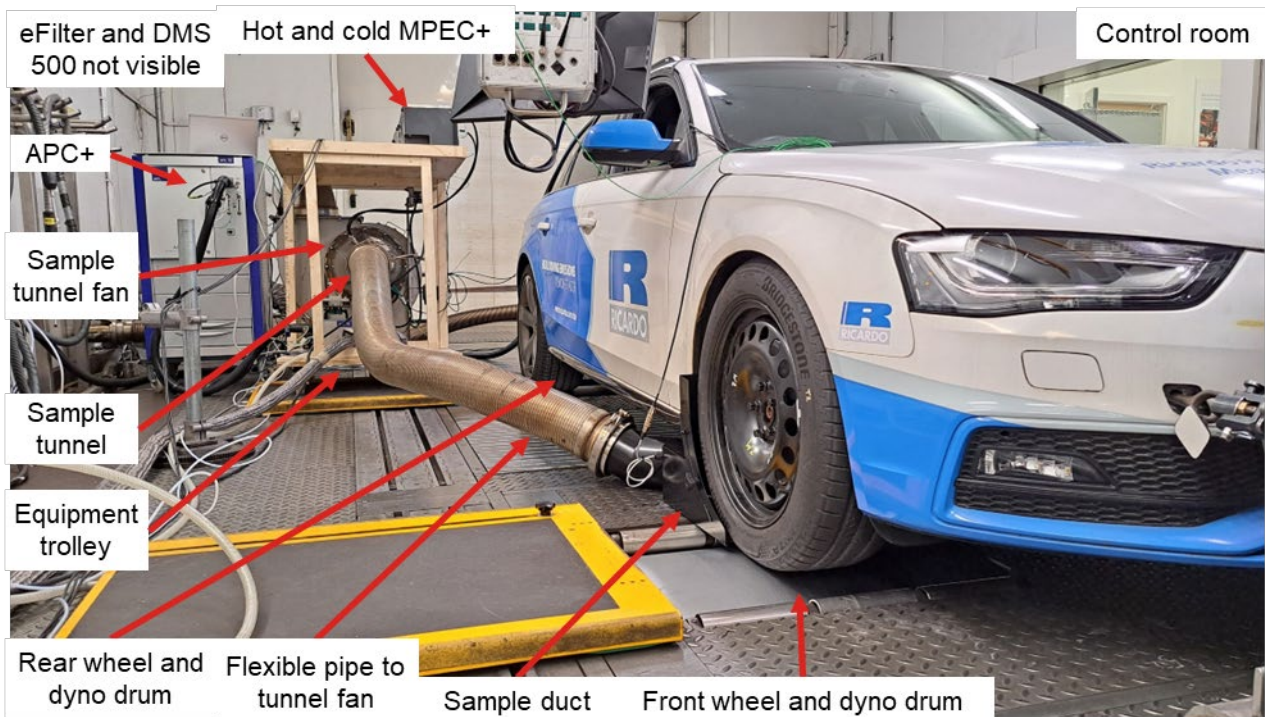nd investigations to understand the causes are described in Section 10.2.1. From these investigations following the initial tests and the consideration of factors leading to very low emissions detection, a number of changes were implemented:

- Testing would move to an alternative dyno facility which enabled the dyno pit extract to be disabled and had a rough textured dyno drum surface. Using the VATF described in Section 4.2 enabled both requirements to be met.

- The brake enclosure airflow would be configured to provide under-pressure within the enclosure, ensuring no particle leakage that could affect tyre particle measurements. The arrangement implemented is described in Section 3.2.4.3.

- The sample points would be moved upstream of the flexible pipe to ensure the sample would not be affected by any turbulence it caused, or any possible leakage. Flow rate measurement remained downstream of the flexible pipe. Since the sample system operates at near-ambient pressure and there are no gaps or obvious leaks, negligible leakage into the flexible pipe is assumed. The sampling system is detailed in Section 3.2.4.

- The sampling system would be modified to enable the flow rate to be varied.

- Measurements would include smaller particle sizes, down to 4nm, using the TSI 3775 CPC (PN4 system) as described in Section 5.2.3.

- Tyre temperature would be measured.

- Consider the need for, and validity of, background measurements.

3.2.4   Final system – trolley/off-vehicle installation

3.2.4.1   Sample system for tyre emissions testing

The final tyre particulate sampling system is illustrated schematically in Figure 3-9. Figure 3-10 shows the sampling system and instruments installed in the test facility (VATF) described in section 4.2. The sample duct fitted behind the tyre leads into the sample tunnel from which the six instruments detailed in Section 5 take their sample. A flexible pipe joins the sample tunnel to the fan via a mass air flow sensor, an orifice controls

the flow which can be varied via by-pass air valves between the orifice and the fan. Brake particles are prevented from entering the sampling system by an enclosure and vacuum as described in 3.2.4.3.
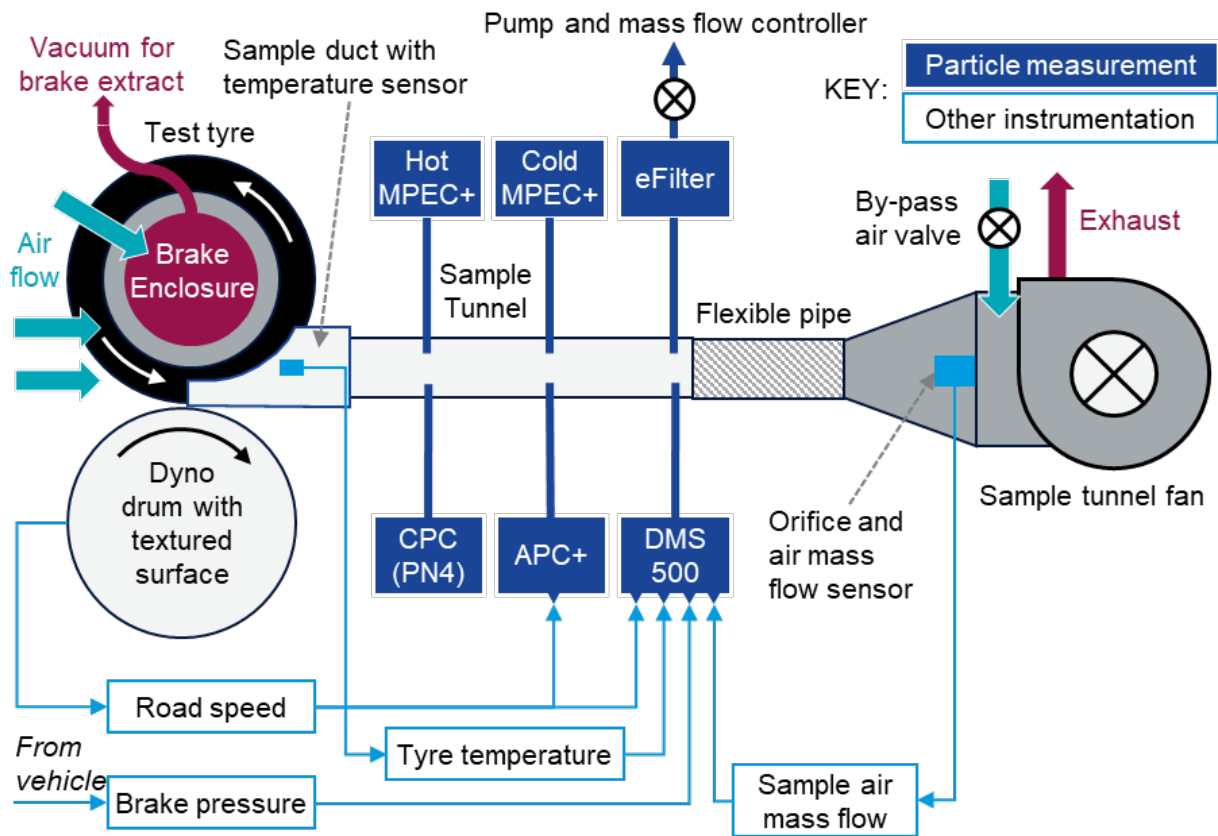

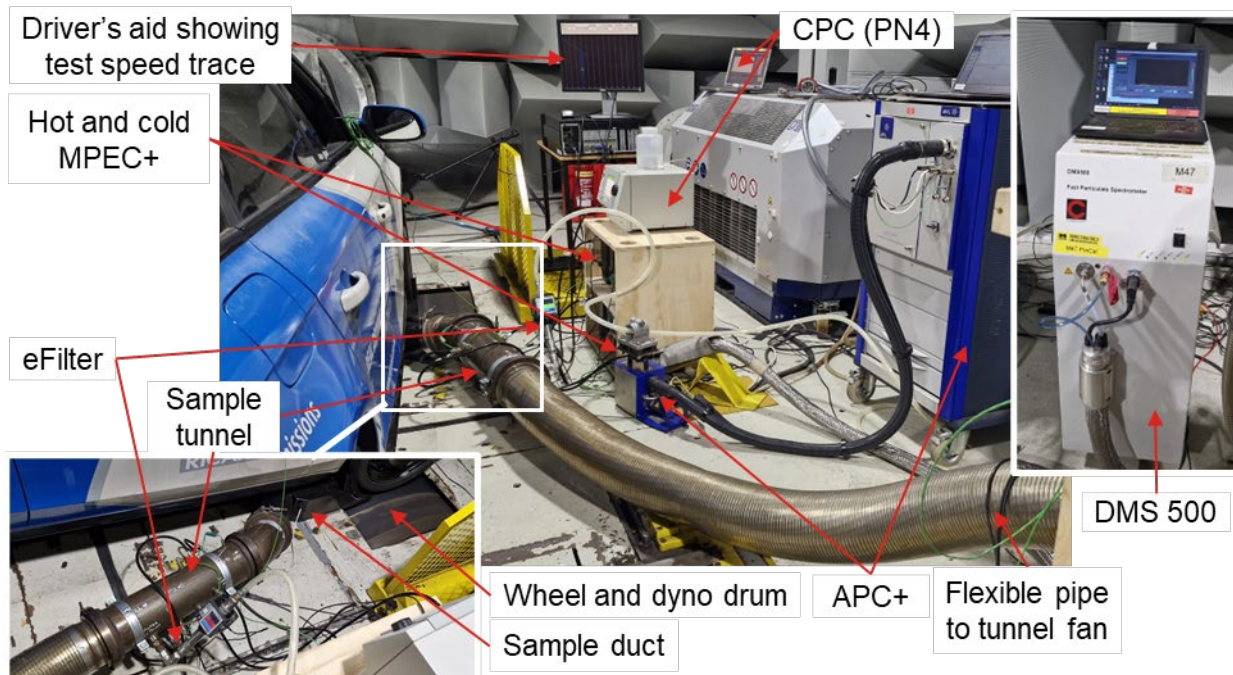Figure 3-9: Tyre particle sampling system schematic.

Figure 3-10: Tyre particle sampling system and instruments in the test facility.

The sample system was tested at a range of flow rates, some examples are provided in Table 3-1 along with the corresponding flow velocities at each point in the system. From the initial test there was a concern that a

high flow rate might lead to high dilution and low concentrations at the instruments (see Sections 3.2.3 and 10.2.1), however, there was no indication that decreasing flow rate improved measurement response. Since a velocity of ~1 metre/second is required to carry a particle of ~1mm, a flow rate of around 1700 litres/minute was used for testing as this ensures a flow velocity comfortably above 1 metre/second in the sample tunnel, although it may be a little lower in the sample duct itself. This was the highest flow rate possible with the mass air flow sensor fitted since that dictated the minimum size of the orifice. The face velocity at the tyre is estimated allowing for the area of duct open either side of the tyre and to the top, since the tyre itself blocks most of the duct opening, again a high flow rate provides the highest velocity between tyre and duct sides.

Table 3-1: Sample volume flow and velocities along system.

Volume flow (SLPM)	Volume flow (l/min @ 16 °C)	Velocity in tunnel (m/s)	Velocity in duct (m/s)	Estimated velocity at tyre (m/s)	Estimated velocity at tyre (kph)
250.2	262.4	0.247	0.110	0.302	1.1
334.4	350.8	0.331	0.147	0.403	1.5
548.0	574.8	0.542	0.241	0.661	2.4
765.4	802.8	0.757	0.337	0.923	3.3
1058.2	1109.9	1.047	0.465	1.276	4.6
1625.4	**1704.8**	**1.608**	**0.715**	**1.960**	**7.1**

3.2.4.2 Additional instrumentation

Additional instrumentation was installed to measure the following parameters:

- Road speed from the dynamometer.
- Brake fluid pressure from a sensor on the vehicle.
- Tyre tread surface temperature via an infra-red (non-contact) sensor installed within the duct as seen in Figure 3-7.
- An air mass flow sensor for the sample flow at the fan.

As shown in Figure 3-9, these instrumentation data were recorded on the DMS instrument which had available analogue inputs, although road speed was also recorded by the SPCS to facilitate data alignment.

In addition, a thermocouple was installed in the sample tunnel to record the sample air temperature, this was recorded on one of the MPEC+ instruments.

3.2.4.3 Brake enclosure for tyre emissions testing

The tyre emission testing has a different requirement of the brake enclosure compared to the brake tests. In this case, the purpose of the enclosure is to contain and extract brake particles, so they do not contaminate tyre particle measurements, therefore the temperature management and air mixing within the enclosure are not critical to measurement. The tyre testing used only one vehicle (the Audi A4), but a number of tyres of different types and sizes were tested (for 16" and 18" rims), each pre-fitted to a steel wheel to facilitate quick changes. Note that tyre testing on this vehicle in Phase 1 was on a rear wheel since the objective then had been to demonstrate the enclosure fitment to an alternative vehicle (most Phase 1 testing used the VW Caddy), however, Phase 2 testing was on the front wheel as it is subject to the greatest braking force and all the drive force for a front-wheel-drive vehicle. As the front brake was larger with different calliper and fixing locations compared to the rear, the previously fitted enclosure was not suitable.

A static enclosure design was selected since it could remain undisturbed though wheel swaps and did not require modifications to the wheels themselves. Also, the gap between static and rotating parts being at the hub rather than the outer edge of the enclosure was considered likely to minimise the potential for particles to escape. The enclosure was fabricated to fit around the brake assembly while fitting within the smallest of the steel wheels used (16"), and with a small clearance gap around the rotating wheel hub to minimise leakage. As with the brake sampling enclosure, inlet and outlet pipes were fitted to the rear plate, routed around brake and suspension components. However, in this case the outlet was connected to a vacuum and filter (Figure

3-11). An industrial vacuum cleaner (Karcher NT 40/1 Tact Te L) was used with nominal power of 1200W, maximum depression of 23kPa and flow of 39 litres/second. The brake enclosure inlet was left open to ensure the enclosure is at a vacuum, and so particles are extracted and not able to escape into the tyre sampling duct.
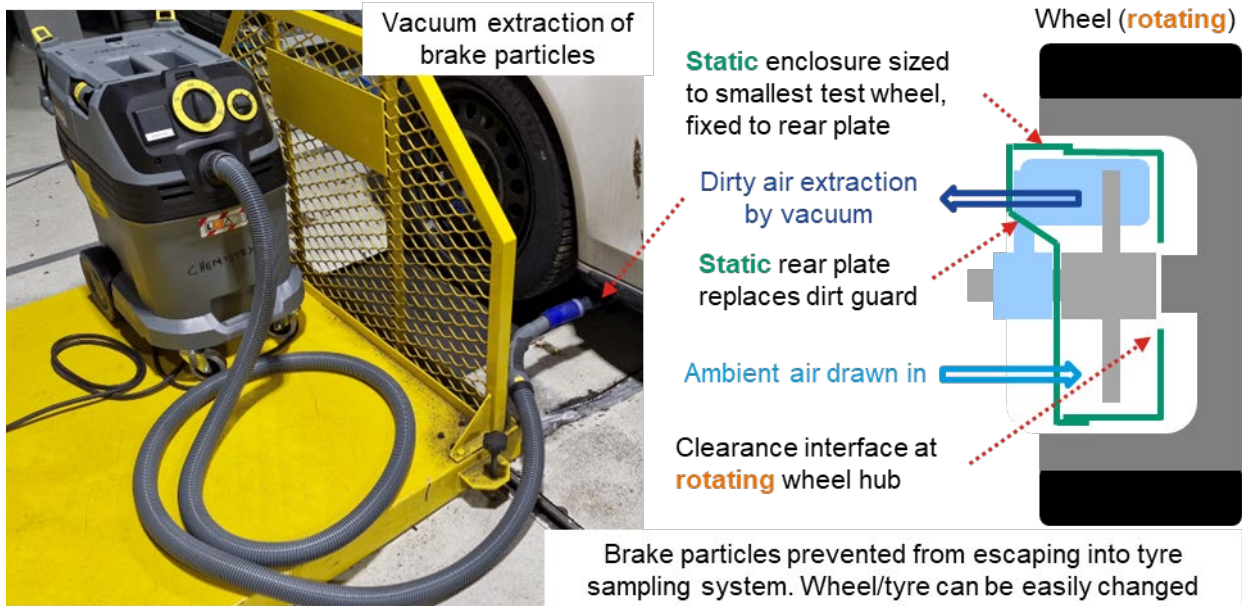

Figure 3-11: Enclosure and vacuum extraction of brake particles during tyre testing

4. TEST FACILITIES

4.1 VEHICLE EMISSIONS RESEARCH CENTRE (VERC)

The VERC at the Ricardo Shoreham Technical Centre provides a climatic 4-wheel drive (two axle) vehicle dynamometer with emissions measurement capability, along with a vehicle preparation and temperature stabilisation chamber known as a soak area. The emissions measurement provision meets all current tailpipe regulatory requirements for light duty vehicles, including gaseous pollutants, particle mass, and particle number, although in the brake tests only the particle number measurement was used (see Section 5). Brake tests were carried out at 23°C. The twin axle dynamometer enables braking forces to be contributed from both front and rear brakes.

The VERC also includes a filter paper weighing facility which was used for the filter papers used in the eFilter (see Section 5.4.1).

4.2 VEHICLE ANECHOIC TEST FACILITY (VATF)

The VATF at the Ricardo Shoreham Technical Centre comprises an anechoic chamber containing a single-axle drum dynamometer of 360kW capability designed for vehicle noise testing. While the anechoic (noise absorption) capability is not relevant, the facility offered some features that made it suitable for the tyre testing:

- The dynamometer drum is faced with a rough tarmac-like surface rather than the smooth steel of an emissions dynamometer (including the VERC). This was considered more representative of tyre-road behaviour in terms of heat and abrasion, as well as for noise (see below).
- The extract fan in the dynamometer pit can be turned off during testing, removing the vacuum in the gap between the dynamometer drum and the floor which could remove tyre particles ahead of the sampling system (see section 3.2.3).
- Unlike the emissions test facility (VERC) which must be used by multiple vehicles each day, the VATF could be exclusively used during the test period, allowing a more intense test schedule, and removing the need for test equipment and instruments to be installed for and removed after each test.

The VATF was also used for some brake testing due to its better availability and flexibility for scheduling longer tests, to minimise movement of the instruments between tyre and brake testing, and as the additional capabilities of the VERC (such as tailpipe emissions measurement and climatic control) were not required.

The VATF is fitted with a dynamometer control system with road-load simulation and a driver's aid (display) capable of running the transient tests required. There is no temperature control in the test cell, cell ventilation draws in ambient air from outside which is blown across the vehicle and extracted, so the cell temperature during testing is similar to the outside temperature. Across the test programme, facility temperatures at the start of the first PG42 cycle ranged from ~14°C to 23°C. A large fan at the front of the vehicle provides airflow to the radiator and under the vehicle in proportion to the road speed simulated by the dyno, and an extract is connected to the vehicle exhausts. Although there is no emissions measurement equipment installed in the facility, there is ample space for the particle measurement equipment required, much of which is common to both brake and tyre testing. One difference between the VATF and the VERC (which was used in Phase 1) is that the 2-wheel dyno provides for only front wheel braking, rather than the 4-wheel braking possible in the VERC.

Figure 4-1 shows the set up in the VATF for tyre testing, and Figure 4-2 the set up for brake testing.

Figure 4-1: Tyre testing in the VATF

Figure 4-2: Brake testing in the VATF

4.2.1　Dyno preparation for tyre testing

In reporting tyre emissions testing carried out at Karlsruhe Institute of Technology, (Schläfle, et al., 2023) stated that previous tyre testing had indicated a lack of "soiling" on the test drum "road" surface had altered the tyre such that it became "sticky", retaining smaller particles. Therefore, a small quantity of sand had been introduced to the test drum in which the tyre ran and allowed to stabilise ahead of testing. This was considered a potential factor in the lack of measurable particles in the initial test in the VERC (see Sections 3.2.3 and 10.2.1), although it was not clear from the paper whether this indicated a need for loose particles, or whether the surface used lacked sufficiently fine texture without the addition of sand. In the VATF as in most vehicle dynos the wheel on top of the drum (rather than inside as in some tyre test rigs) and so adding loose particles would not be practical, but ensuring the surface texture of the drum replicated that of small stones, sand, and other road dust was possible.

Although the dyno drum already had a section covered with an abrasive surface material, which was used in noise testing to provide a surface more representative of a road, it was decided to renew the material for the tyre emissions testing. The surface was renewed with an anti-slip Safety-Walk tape made by 3M, which has a mineral-coated, high friction slip-resistant and hard-wearing surface. The surface feel is like a coarse grade sandpaper, but it is sealed and dust free (see Figure 4-3). Over the duration of the tyre testing no significant wear of the surface took place, although the feel became slightly less sharp and changes in the way the surface reflected light corresponded to the wheel contact zone.

Other preparation included configuring an analogue output of road speed from the dyno controller (see 3.2.4.2), loading the test traces into the driver's aid, installing the sampling system described in section 3.2.4.1 and the measurement instruments described in section 5.

Figure 4-3: Coarse hard-wearing surface applied to dyno drum for tyre testing.

4.3　TEST TRACKS

The No.2 Inner Durability Circuit at MIRA Proving ground – in Nuneaton was used for the high speed braking tests on the test track (see section 6.6). The 3.8 km long circuit consists of 3 multi-lane straights connected by bends allowing acceleration and braking to be achieved within the test speed range required by the schedule.

5.　EMISSIONS MEASUREMENT SYSTEMS

5.1　CHANGES FROM PHASE 1

In Phase 1 of the project, two Dekati ELPI+ instruments were employed to provide number weighted particle size distribution data, including particle number (PN) through integration, both on the road and in the laboratory. One ELPI+ system was equipped with a heated inlet at 180°C, while the other operated at ambient temperature, the differential between the two enabling some understanding of the characteristics of the volatile particles emitted. However, the ELPI+ systems required sizeable vacuum pumps and were large instruments

intended for laboratory use that required significant power supplies. In addition, the volatile removal efficiency of the hot system was observed to lead to evaporation and recondensation of volatile particles. This evaporation-recondensation effect transformed a few large volatile particles into a large number of very small volatile particles, rendering both the integrated particle number emissions and the particle size distributions from the hot ELPI+ of limited value. Therefore, in Phase 2 of the project, to both save power and space and to improve discrimination of volatile and non-volatile particles, the ELPI+ instruments were replaced with dual Dekati MPEC+ (Mobile Particle Emission Counter) devices. These devices were specially modified to measure the particle count in the size range 10nm to >500nm, with one instrument configured to eliminate volatile particles and the other measuring total particles. The difference between the two, following correction for particle losses, indicates the level of volatile particle emissions.

The Dekati eFilter was retained from Phase 1, providing a filter-based measurement of $PM_{2.5}$ (particulate matter mass below 2.5 µm) emissions accompanied by a real-time signal, generated by a diffusion charger, enabling the second-by-second production of the particle-derived mass to be studied.

Other changes to the instrumentation used included the substitution of an AVL APC+ (AVL Particle Counter), measuring non-volatile particles >10 nm, according to future Euro 7 European exhaust emissions legislation, for the Horiba SPCS (Solid Particle Counting System, which measures non-volatile particles >23nm according to current European exhaust emissions legislation), and a particle size distribution device, the DMS500 (Differential Mobility Spectrometer) from Cambustion. The DMS500 was used in a modified form, covering the range from 5nm to 2.5µm. The DMS500 does not discriminate between volatile and non-volatile particles. These systems were used in the laboratory only.

Equipment used in Phase 1 and 2 is summarised in Table 5-1, with further details of specific devices used in Phase 2 given in the following sections.

Table 5-1: Equipment used in Phase 1 and Phase 2 programmes.

Metric	Phase 1	Brake (B) / Tyre (T) use Phase 1	Phase 2	Brake (B) / Tyre (T) use Phase 2
PM in the lab (real-time & gravimetric)	eFilter	B&T	eFilter	B&T
PM on the road (real-time & gravimetric)	eFilter	B&T	eFilter	[-]
Non-volatile PN in the lab	SPCS (PN23); hot ELPI+	B&T	APC+ (PN10); hot MPEC+	B&T
Non-volatile PN on the road	Hot ELPI+	B&T	Hot MPEC+	[-]
Volatile PN in the lab	Cold ELPI+	B&T	Cold MPEC+	B&T
Volatile PN on the road	Cold ELPI+	B&T	Cold MPEC+	[-]
Total PN > 4nm	[-]	[-]	3775 CPC	T
Particle size distribution	Hot ELPI+, Cold ELPI+	B&T	DMS500	B&T (lab only)

5.2 PARTICLE NUMBER (PN)

5.2.1 PN measurements using hot and cold MPEC

Particle number measurements were made using a pair of Dekati MPEC+ instruments[3]. The Dekati MPEC+ is an electrostatic charge-based device designed for the real-time measurement of particulate matter

---

[3] Brochure on the Dekati MPEC instruments.

emissions in various applications, including as a PN-PEMS device for on-road automotive legislative use. For automotive use, the MPEC+ employs a specialised diffusion charger (the e-particle number counter, ePNC) downstream of a heated inlet and volatile particle remover device (evaporation tube, ET). The ET is heated to 350°C, providing a more robust approach to eliminating the volatile particles than the 180°C inlet tube of the hot ELPI used in Phase 1. Together the inlet and ET aspects of the MPEC+ permit compliance with the volatile particle removal and counting efficiency requirements for PN-PEMS devices at Euro 6. These require specific counting efficiency ranges for particles up to 200nm, and permit a certain degree of over-counting of larger particles in the region of 200nm, which are the consequence of the tendency of large particles to accumulate multiple charges.
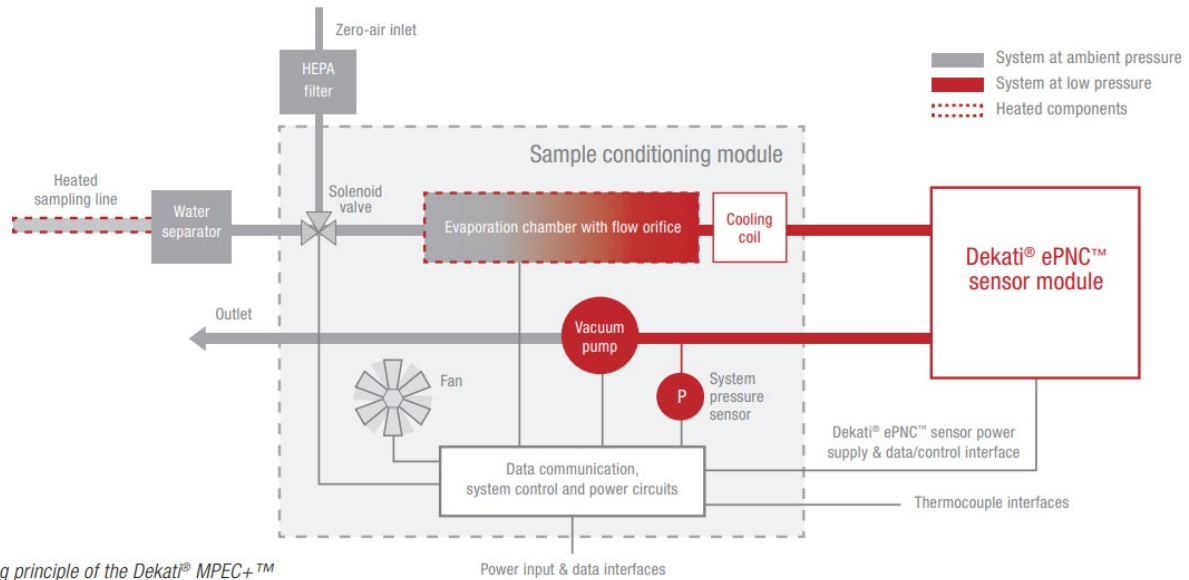

Operating principle of the Dekati® MPEC+™

Figure 5-1: Operating principles of the MPEC+ (courtesy of Dekati Ltd, Finland).

Two MPEC+ systems were employed, one "hot MPEC" was operated with the inlet and evaporation tube active and the other "cold MPEC" was operated with the inlet and evaporation tube at ambient temperature. The cold MPEC then measured "total" particles, with the hot MPEC measuring just non-volatile particles. The MPEC devices were also configured to measure particles >10nm rather than the >23nm lower limit requited for Euro 6 PN-PEMS measurements.

Temperature gradients in the hot MPEC lead to different thermophoretic losses in that instrument, than in the cold MPEC, and there will be other subtle differences in losses. Consequently, the Ricardo Particle Measurement Centre (PMC) performed a calibration on the two MPEC units in order to assess losses and potentially enable corrections. Once corrected, simultaneously collected hot MPEC results can be subtracted from cold MPEC results to provide information on the presence and magnitude of volatile particles.

5.2.1.1   ISO 17025 Calibration of the MPEC+ devices

Calibration of the Hot and Cold MPEC+ devices was conducted at Ricardo's Particle Measurement Centre in Oxfordshire UK, which holds ISO 17025 accreditation for the calibration of particle number counting and dilution devices. The linearity response of the MPEC+ units was evaluated by comparing their performance against a traceable transfer standard Scanning Mobility Particle Sizer (SMPS) at various reference particle number (PN) concentrations. Both the test instrument and the transfer standard were challenged with a charge-equilibrated, thermally treated, polydisperse soot aerosol, having a geometric median diameter (GMD) of 70 nm ± 20 nm and a geometric standard deviation (GSD) ≤ 2.1.

The counting efficiency of the particle number device, including the sample line, was assessed by comparing its performance against a transfer standard condensation particle counter (CPC). Both the test instrument and the transfer standard were challenged with charge-equilibrated, thermally treated, monodisperse soot aerosols with diameters of 200, 100, 70, 50, 30, 23, 15, and 10 nm. The presence of multiply charged particles was minimized, quantified, and corrected for as per ISO 27891.

5.2.1.2 Calibration results of the MPEC+ devices

The overall linearity response of the MPEC+ units for the polydisperse aerosol (Figure 5-2) showed a strong correlation with the cold MPEC+, with an approximately 20% higher efficiency in the hot MPEC. This increased efficiency is likely due to thermophoretic deposition in the hot MPEC.
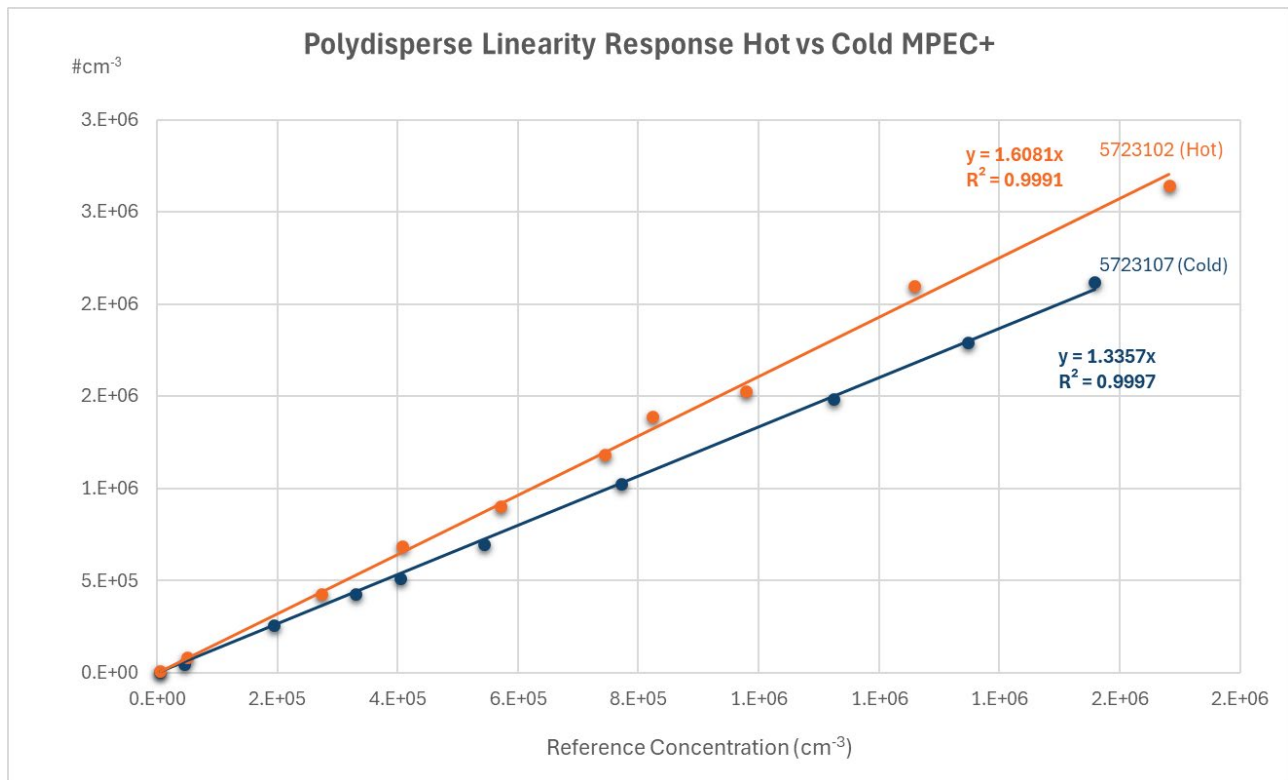
Figure 5-2: Polydisperse linearity response of the hot (red line) and cold (blue line) MPEC.

The monodisperse calibration showed that both the cold and hot MPEC units had similar detection efficiencies between 10 and 100 nm. However, at 200 nm, a significant difference was observed, with the hot MPEC showing a 50% increase in counting efficiency compared to the cold MPEC (Figure 5-3). Both units were directly compared to the same monodisperse aerosol sample simultaneously, suggesting that the difference was due to how the detectors operated at that specific time. Repeated measurements produced consistent results.

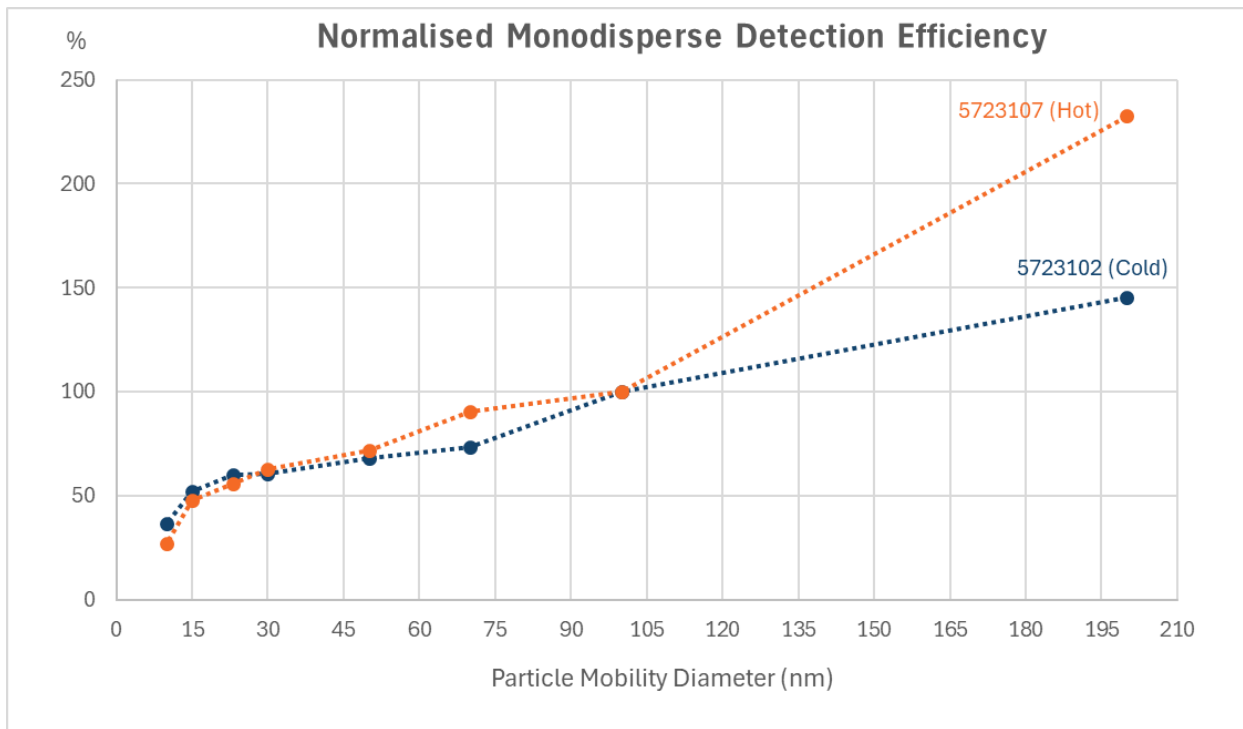Figure 5-3: Monodisperse efficiency response of the hot (red line) and cold (blue line) MPEC.

5.2.2 PN measurements using APC10

Non-volatile particle number emissions were measured during chassis dynamometer testing using an AVL APC+. The APC+ had been upgraded by the manufacturer to measure >10nm rather than the original 23nm lower limit, and the modifications also included the substitution of the original evaporation tube with a catalytic stripper. This provides the most robust approach for elimination of volatile particles. The APC+ system employs the principles of the measurement systems designed for regulatory tailpipe PN10 and PN23 emissions when sampling from a dilution tunnel but is primarily designed for raw exhaust sampling.

In overview: initial heated dilution at 150°C and a catalyst are employed to eliminate volatile particles. These then condition the sample aerosol into a stream of non-volatile particles that are counted by an integrated condensation particle counter.

Figure 5-4: AVL APC+ (courtesy of AVL List GmbH, Austria)

5.2.3 Measurements using TSI 3775 CPC (tyres only)

Total volatile plus non-volatile particles with a lower d50 of 4nm, and with an upper limit of < 1µm were measured with a TSI 3775 CPC. The TSI 3775 CPC is a condensation particle counter that measures up to 50,000 #/cm^3 in single particle count mode and 10^7 #/cm^3 in photometric mode. The 3775 CPC was introduced for the tyre particle counting, as it was considered possible that the dominant particle emissions from tyres, by number, could be sub-10nm volatile emissions and these would be difficult to detect and accurately count with other instruments employed.

Figure 5-5: TSI 3775 Condensation Particle Counter (courtesy of TSI Incorporated, Shoreview, MN, USA)

5.3 PARTICLE SIZE DISTRIBUTION

5.3.1 Particle size distribution using DMS500 2.5 µm

Particle size distributions in the range ~5nm to ~2.5 µm were determined using a differential mobility particle sizer (Cambustion DMS500,Figure 5-6). This instrument usually measures ~5nm to ~500nm but can be specially calibrated to measure up to 2.5 µm, and this extra calibration was undertaken specifically for the test programme. The DMS measures directly from the sample tunnel.

The DMS500 uses a unipolar corona discharge to apply a known charge to each sampled particle, which is proportional to its surface area. Charged particles flow into a classification section with a strong radial electrical

field. This field causes particles to drift through a sheath flow toward the electrometer detectors, carrying their known charge. The DMS features 22 parallel electrometer detectors in series that process real-time data at 10 Hz. These detectors measure particles at different distances down the column, depending on their aerodynamic drag-to-charge ratio. The measured charges on the electrometers are converted to particle concentrations on specific electrodes, with each electrometer corresponding to a specific size range. Together these enable number-weighted particle size distributions to be determined. The DMS500 software also includes corrections for particle losses: for example, in the sample line.

It should be noted that the DMS uses different inversion matrices, for spark ignition particles and diesel exhaust particles, which transform the charge distribution into the particle size distribution. The accuracy of the output size distributions is related to the size distribution, the morphology of the particles emitted and the chemical composition. In this work, since no matrix exists for brake and tyre emissions, the diesel matrix was employed, but the accuracy of the size distributions is therefore uncertain. Similar concerns would be present with other charge-based particle sizing instruments without dedicated inversion matrices. In the future a specific brake particle matrix may be produced by Cambustion.

Figure 5-6: Cambustion DMS500 (courtesy of Cambustion Ltd, Cambridge, UK).

5.4   PARTICULATE MASS (PM / PM$_{2.5}$)

5.4.1   Real-time and gravimetric PM$_{2.5}$ mass using eFilter

Particulate mass was measured by Dekati eFilter both on a glass-fibre filter (47 mm Whatman GF/A) and in real-time using the integral diffusion charger. The eFilter requires an additional external pump to draw the sample. A small sub-flow passes through the diffusion charger but is added back into the main flow so that element is also collected on the filtration substrate.

To visualise real-time particulate mass emissions appropriately, the cumulative mass determined by the diffusion charger is normalised so that it equals the gravimetric mass determined on the filter. As such, no specific mass-based calibration is required. Data are logged to an internal memory card during testing and exported using a card reader after the test is completed.

Figure 5-7: Dekati eFilter (courtesy of Dekati Ltd, Finland).

5.5 OTHER MEASUREMENTS

5.5.1 Brake emissions testing

As well as the emissions measurement instruments, other measurements were taken during testing to enable accurate interpretation of the emissions and to provide context. The additional measurements taken during brake emissions tests are detailed in Table 5-2. These measurement devices are illustrated schematically in Figure 3-1. The measurements were recorded at 1Hz throughout the tests using a Dewesoft DEWE43 data acquisition system which provided 8 analogue inputs and two Controller Area Network (CAN) bus inputs.

Table 5-2: Other measurements used in brake testing

Measurement	Source or sensor	Recording	Notes
Air flow into sample tunnel	Flow meter in brake enclosure outlet before sample tunnel	Not recorded	Used to set a fixed tunnel flowrate before test
Air flow into brake enclosure	Orifice meter in inlet pipe to brake enclosure, AVL blow-by meter type, calibrated to 550 litres/min	Dewesoft logger, analogue input	Used in all brake tests
Brake fluid pressure (bar)	Gauge pressure sensor installed in the vehicle brake pipe	Dewesoft logger, analogue input	Used in all brake tests
Brake disc temperature – right front (enclosed) (°C)	Brake disc sliding surface contact thermocouple	Dewesoft logger, analogue input	Used in all brake tests
Brake disc temperature – left front (normal) wheel (°C)	Brake disc sliding surface contact thermocouple	Dewesoft logger, analogue input	Used in all brake tests
Vehicle ECU data: Vehicle speed (kph), engine speed (rpm)	Vehicle On-Board Diagnostics (OBD) port	Dewesoft logger, Controller Area Network (CAN)	Used in all brake tests
GPS data: Vehicle speed (kph)	Dewesoft Global Positioning Satellite (GPS) sensor	Dewesoft logger, GPS	Used for track/road testing only

Note that the Global Positioning Satellite (GPS) data which included vehicle speed was not used in dynamometer tests, since the vehicle is not moving. Instead, the dynamometer road speed could be used to validate the speed from the vehicle ECU. Additional measurements were also available from the dynamometer

controller, although most had little relevance to the brake tests, being intended for vehicle exhaust emissions tests.

5.5.2 High-speed braking tests at proving ground

During the high-speed braking tests carried out at MIRA proving ground (test track), the emissions measurement comprised only the portable instruments: hot and cold Dekati MPEC+ and the eFilter. The AVL APC+ and Cambustion DMS were only used in laboratory (dyno) testing. As well as the additional measurements detailed above for brake testing, further instrumentation was used to enable consistent deceleration rates to be achieved.

A Racelogic Driftbox deceleration gauge with a head-up display was used to provide data to the driver. The device uses GPS position measurement and sophisticated motion sensors at $10\,\mathrm{Hz}$ resolution to calculate instantaneous road speed and deceleration.

A brake pedal effort gauge was also trialled initially, intended to enable repeatable pedal effort. This device connected to the brake pedal pad with a head-up display visible to the driver, enabling consistent force to be applied to the brake pedal. However, it was found that consistent pedal force did not lead to consistent decelerations, since the speed and temperature sensitivity of the brake pad resulted in changes to the pad-disc friction coefficient, so the device was not used.

5.5.3 Tyre emissions testing

The additional measurements taken during tyre emissions tests are detailed in Table 5-3. These are shown schematically in Figure 3-9. Tyre emissions testing was carried out only using a vehicle dynamometer, and with no need for GPS or vehicle ECU data, a dedicated data acquisition system was not required, instead spare analogue input channels on the measurement instruments were utilised.

Table 5-3: Other measurements used in tyre testing

Measurement	Source or sensor	Recording
Road speed of the vehicle (kph)	Analogue output from the dynamometer controller	Analogue input channel on the DMS instrument Also recorded by the AVL APC+ for data alignment
Brake fluid pressure (bar)	Gauge pressure sensor installed in the vehicle brake pipe	Analogue input channel on the DMS instrument
Tyre surface temperature (°C)	Infra-red (non-contact) temperature sensor installed within the sample duct, directed at the tyre tread surface, as seen in Figure 3-7	Analogue input channel on the DMS instrument
Sample tunnel air flow	Air mass flow (hot wire) sensor at the tunnel orifice	Analogue input channel on the DMS instrument
Sample tunnel temperature	Thermocouple (K-type) in the sample tunnel near the instrument sample points	Analogue input channel on an MPEC instrument

6. TEST CYCLES, VEHICLE OPERATION AND DRIVING STYLES

Several vehicle operation approaches were used during the project. These included regulatory drive cycles usually used for emissions testing (Worldwide Harmonized Light Vehicles Test Cycle, WLTC) and sections of recognised cycles used for brake measurements (in the Particle Generation 42 minutes cycle, PG42). In addition, two short Real Driving Emissions (RDE) cycles were tested, one on the chassis dynamometer and the other on the road. These are derived from a fully compliant RDE test, so comply with most of the parameters required for regulatory RDE testing, excepting the duration, which is reduced to ~1 hour in both cases.

Furthermore, on both test tracks and chassis dynamometer, individual controlled braking events were studied. These included low speed braking on the Ricardo drive-by site (≤ 50 mph), high speed braking at the MIRA proving ground[4] (≤ 80 mph) and a chassis dynamometer based bespoke drive cycle developed to comparatively evaluate braking severity effects on tyre emissions from consistent and different speeds.

Details of the drive cycles and approaches used are given in the following sections.

6.1 PG42 TEST CYCLE

The PG42 cycle, as shown in Figure 6-1, is a bespoke drive cycle developed by Ricardo from the high particle emitting sections of the LACT (initial ~1400s of PG42) and WLTP brake dynamometer cycles (last ~1150s). The test lasts ~42 minutes and covers a distance of approximately 50 km.
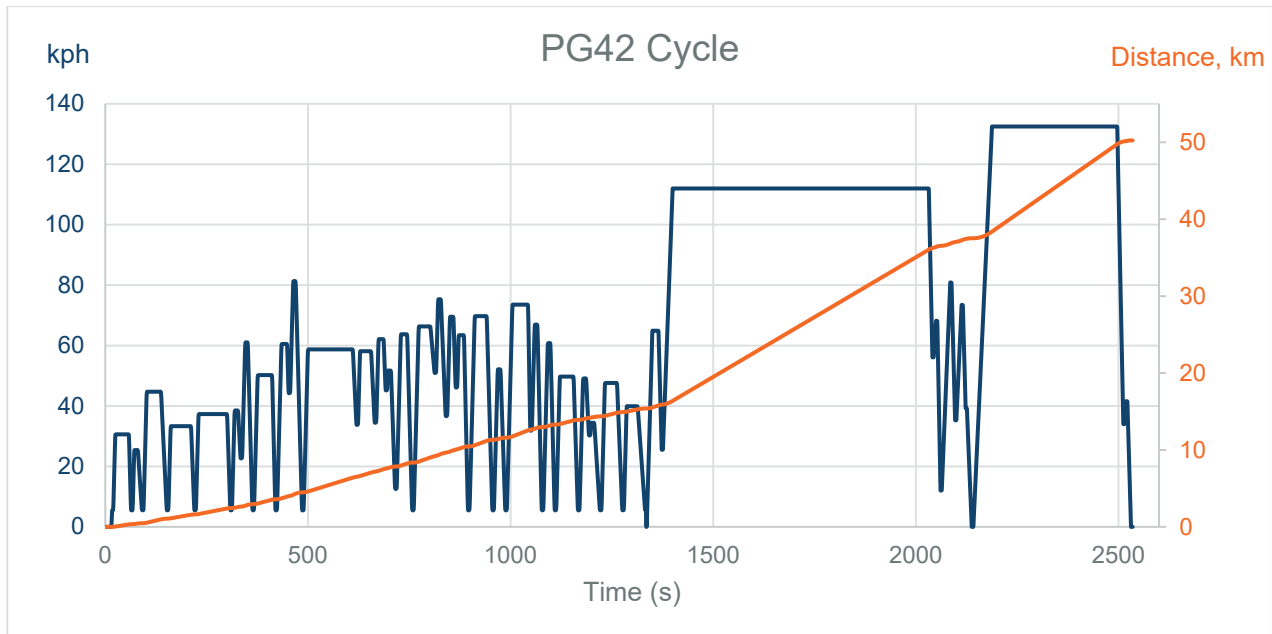

Figure 6-1: PG42 Cycle. The blue line represents the speed at different times and the orange line represents the cumulative distance during the cycle.

6.2 WLTC TEST CYCLE

The WLTC is the certification cycle first used at Euro 6c (Figure 6-2). It is of 30 minutes duration, ~23 km distance and comprises urban, rural and motorway driving elements.

---

[4] Proving Ground Surfaces - HORIBA MIRA Test Capabilities (vehicletesting.solutions)
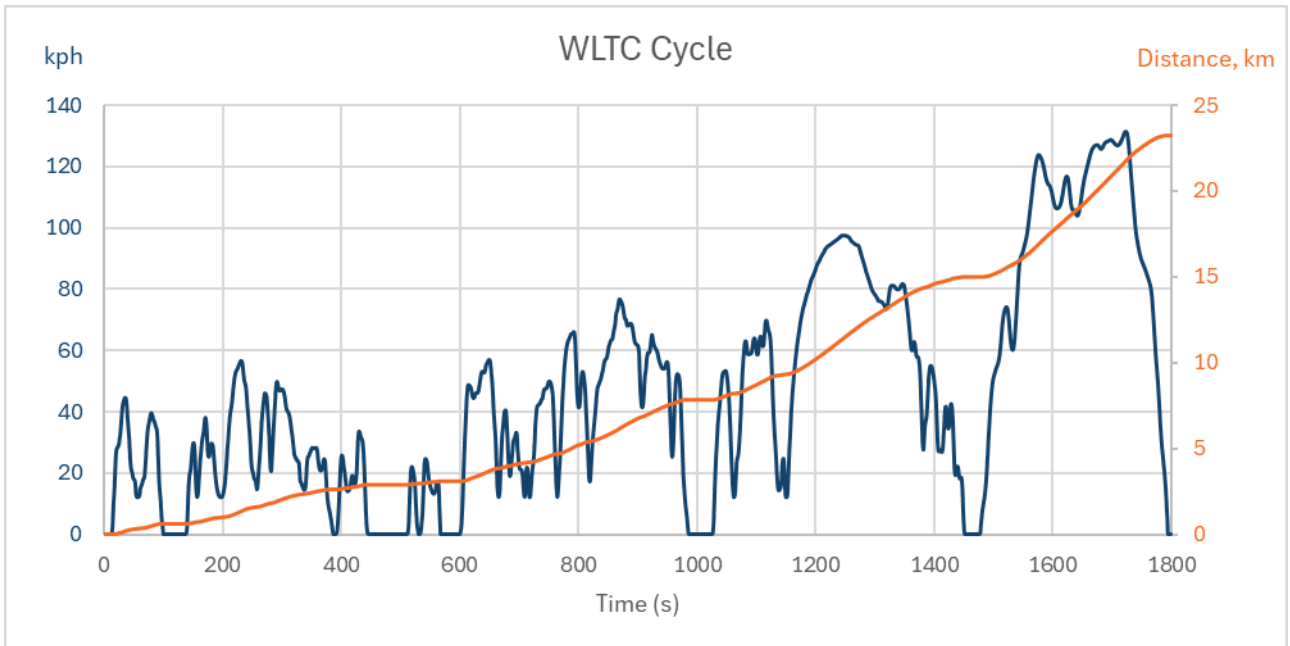
Figure 6-2: WLTC cycle. The blue line represents the speed at different times and the orange line represents the cumulative distance during the cycle.

6.3   DYNO RDE TEST CYCLE

The dyno RDE cycle is a cut-down version of a drive trace drawn from a ~105 minutes real-world "eastbound" RDE cycle, a test route that is regularly executed on the roads around Ricardo. It comprises urban, rural and motorway driving, lasts just over 1 hour and covers a distance of ~46 km (Figure 6-3).
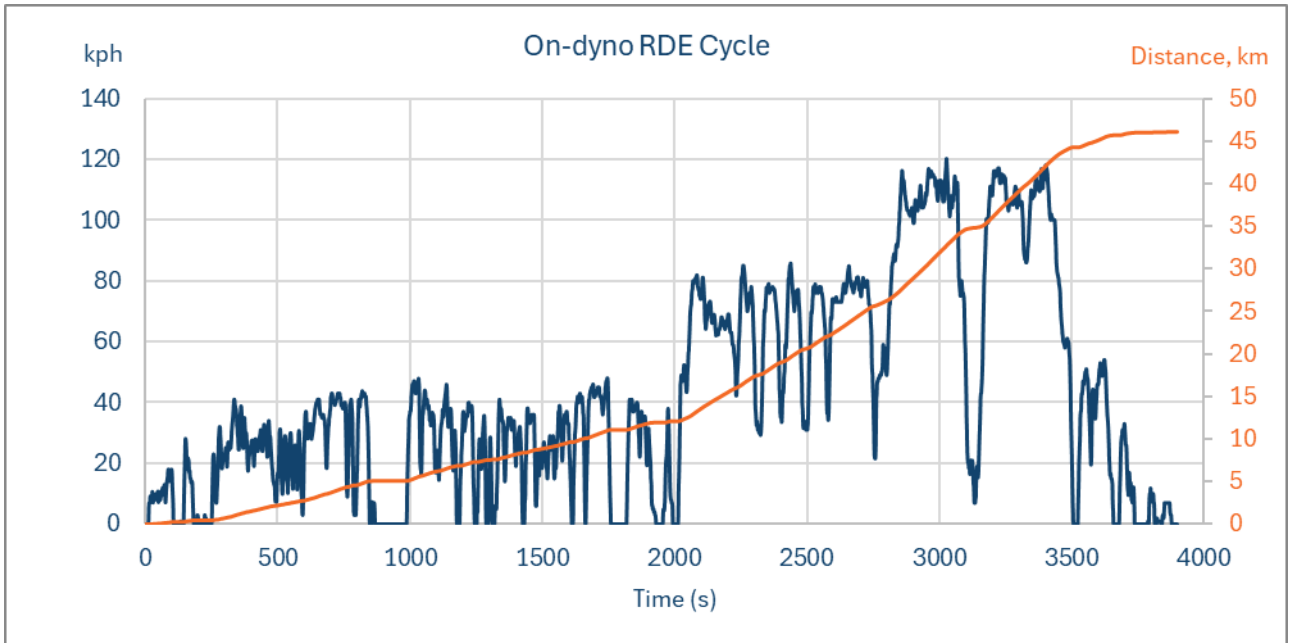

Figure 6-3: On-dyno RDE. The blue line represents the speed at different times and the orange line represents the cumulative distance during the cycle.

6.4   ON-ROAD RDE TEST CYCLE

The on-road RDE is similarly a cut-down version of the eastbound RDE route, with some minor route tweaks to ensure ~1/3 each of urban, rural and motorway operation (Figure 6-4). Trip distance is ~46 km and typically takes around 1 hour to complete.
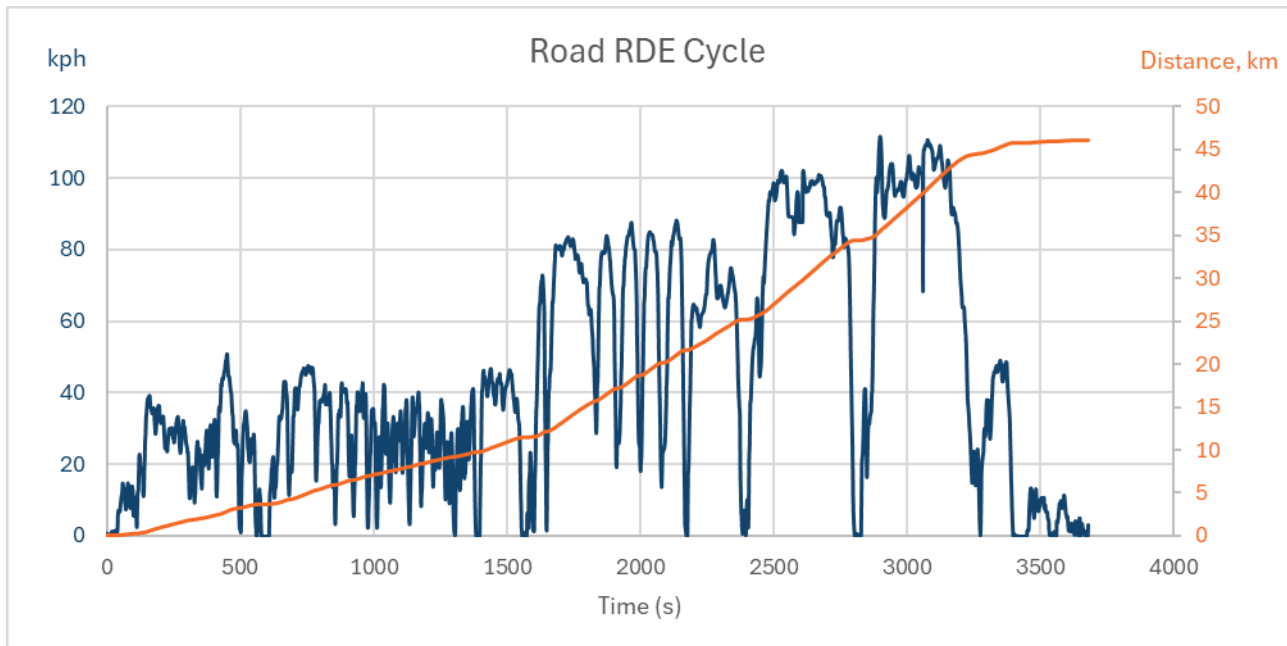
Figure 6-4: On-road RDE. The blue line represents the speed at different times and the orange line represents the cumulative distance during the cycle.

6.5 DRIVE-BY GENTLE, MODERATE, DYNAMIC BRAKING

The Ricardo drive-by site was first employed for brake emissions measurements in Phase 1 of this project. This is a short private test track located directly north of the Ricardo site at Shoreham-by-Sea and aligned roughly north-south. During the testing, the test vehicle was repeatedly driven the length of the ~450 m track in both directions. The driver accelerated to the target speed and then performed braking manoeuvres—ranging from gentle, through moderate to dynamic, with the latter similar to an emergency stop. The study focused on repeat braking events at discrete speeds up to and including 50 mph (80 kph). Speeds greater than 50 mph were not achievable within the available 450 m distance for the VW Caddy

Drive-by testing was primarily employed for the investigation and comparison of the impact of increasing brake pad temperatures, emissions vs. temperature curves for different pad and disc types.

Exercises conducted on the drive-by site featured braking from five different speeds: 10 mph, 20 mph, 30 mph, 40 mph and 50 mph (corresponding to 16, 32, 48, 64 and 80 kph respectively), and in 3 different modes: gentle, moderate and dynamic. Each braking mode is subjective according to the driver employed, but in almost all cases the same driver was employed.

Each braking exercise in gentle, moderate or dynamic mode began at the lowest speed and ascended stepwise to the highest speed. Five repeats of each speed were conducted, resulting in 25 braking events in each mode. In all cases gentle braking was performed first, followed by moderate and then by dynamic braking.

Examples of gentle, moderate and dynamic braking are shown in Figure 6-5a,b,c respectively for a test using the combination of Pad 1 and Disc 1. The higher braking rates of moderate and dynamic braking compared to gentle braking leads to quicker throughput of the tests and shorter overall test duration.
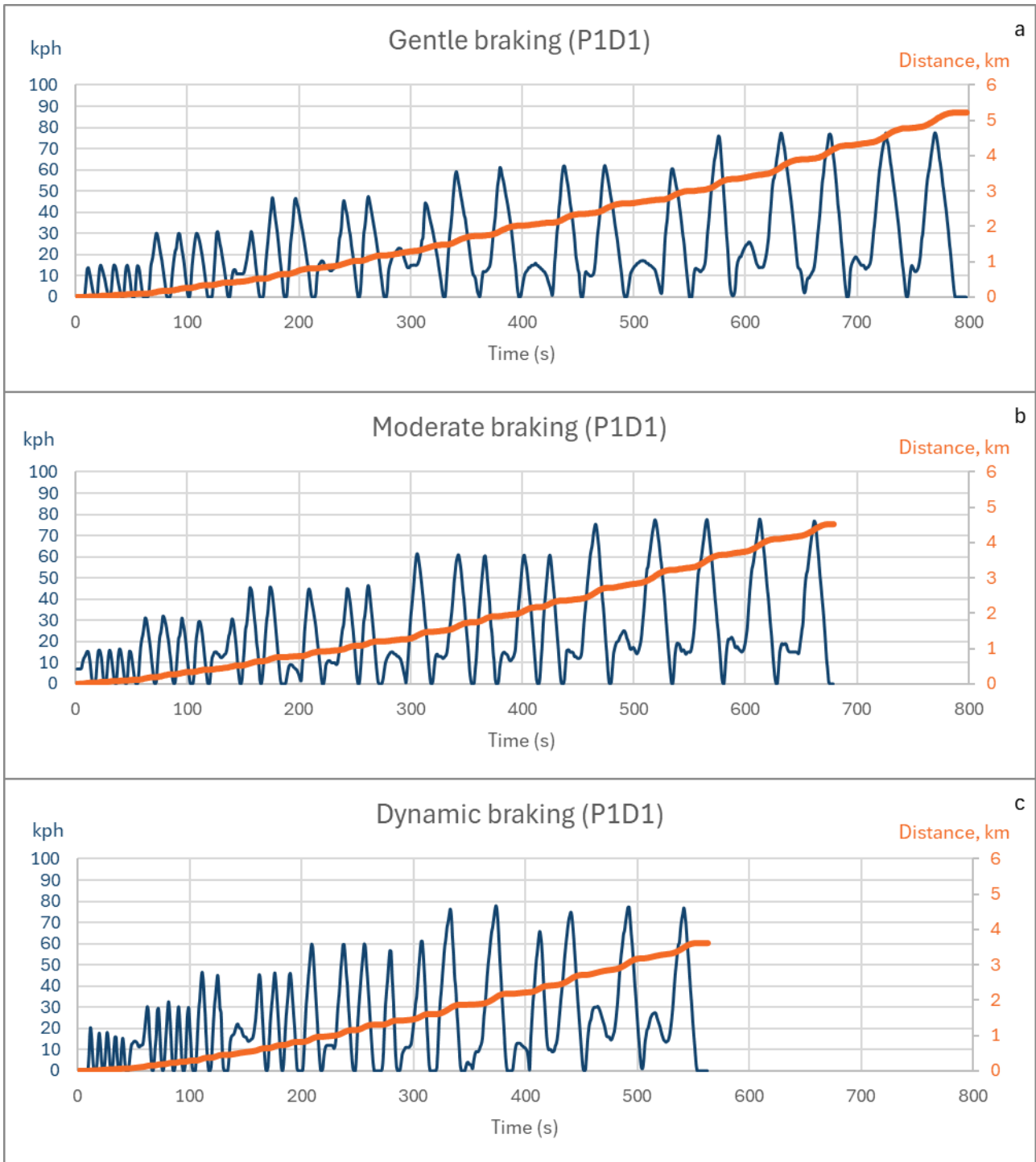
Figure 6-5: Drive-by a) gentle, b) moderate and c) dynamic braking cycles. The blues line represents the speed at different times and the orange lines represents the cumulative distance during the cycle.

In all cases braking rates were highest from the dynamic mode, lower from the moderate mode and lowest from the gentle mode of braking. An example of braking rates is shown in Figure 6-6, for the combination of Pad 1 and Disc 1.
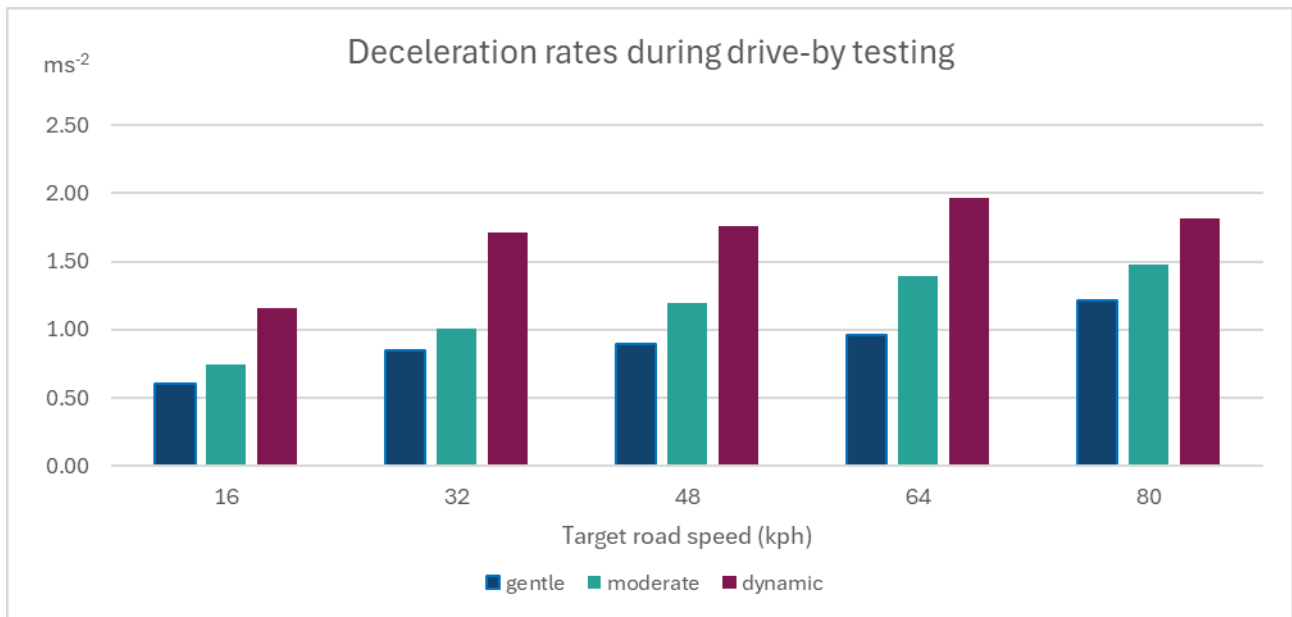
Figure 6-6: Drive-by braking rates for tests using Pad 1 and Disc 1

Braking rates from individual braking events in gentle, moderate and dynamic modes were determined as follows:

- The braking period was determined as the time when the braking pressure was >0.2 bar, and the vehicle speed was between the peak value (i.e., 30kph vs. 32kph nominal) and the first stop (0 kph).
- The maximum speed during the braking period was divided by the duration of the braking period (dv/dt) to determine the deceleration rate.

6.6 HIGH SPEED BRAKING ON THE TEST TRACK

A similar exercise to that conducted on the drive-by site was conducted on the inner durability circuit test track at MIRA. In this experiment, one pad and disc combination were tested at both similar and at higher speeds than those achievable on the drive-by site. The objective in this case was slightly different to that of the drive-by testing: the aim was to specifically evaluate the emissions of the pad and disc pair during braking from various speeds, when starting from a broadly consistent baseline pad temperature. This contrasts with the drive-by braking, where brake pad temperatures at the braking event increased with speed.

Testing comprised of two sets of braking events, moderate and dynamic braking, at different initial speeds.

Set#1 – moderate braking; deceleration targeted at 0.25G with initial braking temperature at ≤ 100°C (or a 5 minutes' pause, whichever was reached first). This was undertaken at the following speeds:

- 30 mph x 3 repeats
- 40 mph x 3 repeats
- 50 mph x 3 repeats
- 60 mph x 3 repeats
- 70 mph x 3 repeats
- 80 mph x 3 repeats

Repeats were then undertaken again at 50 mph and 80 mph.

The speed-time profiles of the moderate braking exercise are shown in Figure 6-7a with repeats at 50 mph and 80mph in Figure 6-7b.
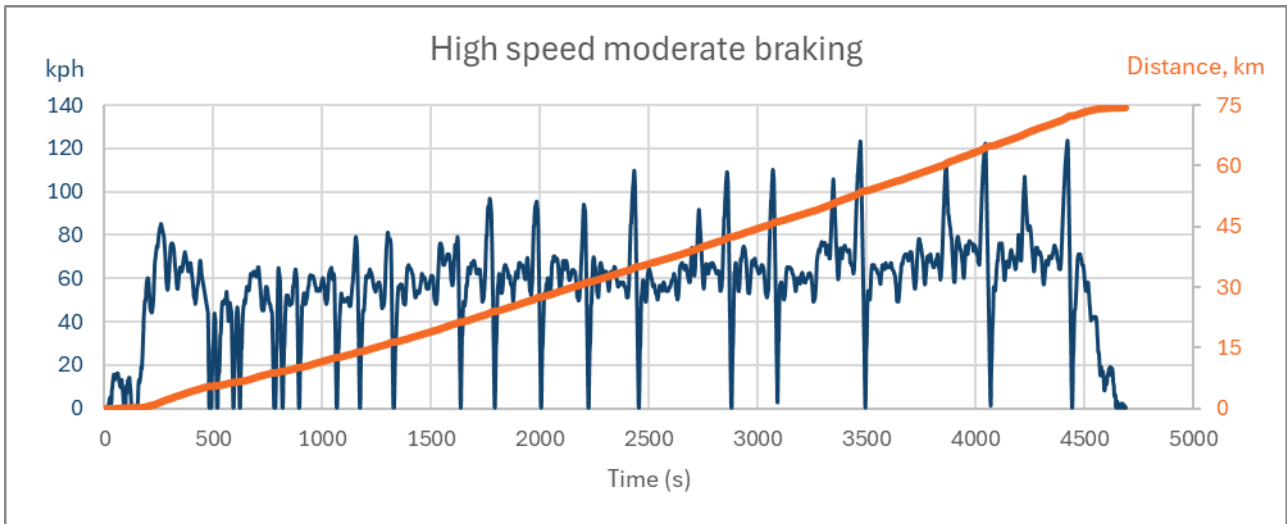
Figure 6-7 Moderate braking events at MIRA.

Following Set#1 the on-board batteries were recharged and then Set#2 – dynamic braking was executed.

Set#2 – dynamic braking; deceleration targeted at 0.5G with initial braking temperature at ≤ 100°C (or a 5 minutes' pause, whichever was reached first)

- 30 mph x 3 repeats
- 40 mph x 3 repeats
- 50 mph x 3 repeats
- 60 mph x 3 repeats
- 70 mph x 3 repeats
- 80 mph x 3 repeats

As for Set 1, repeats were undertaken again at 50 mph and 80 mph. The speed-time profile of the dynamic braking is shown in Figure 6-8.
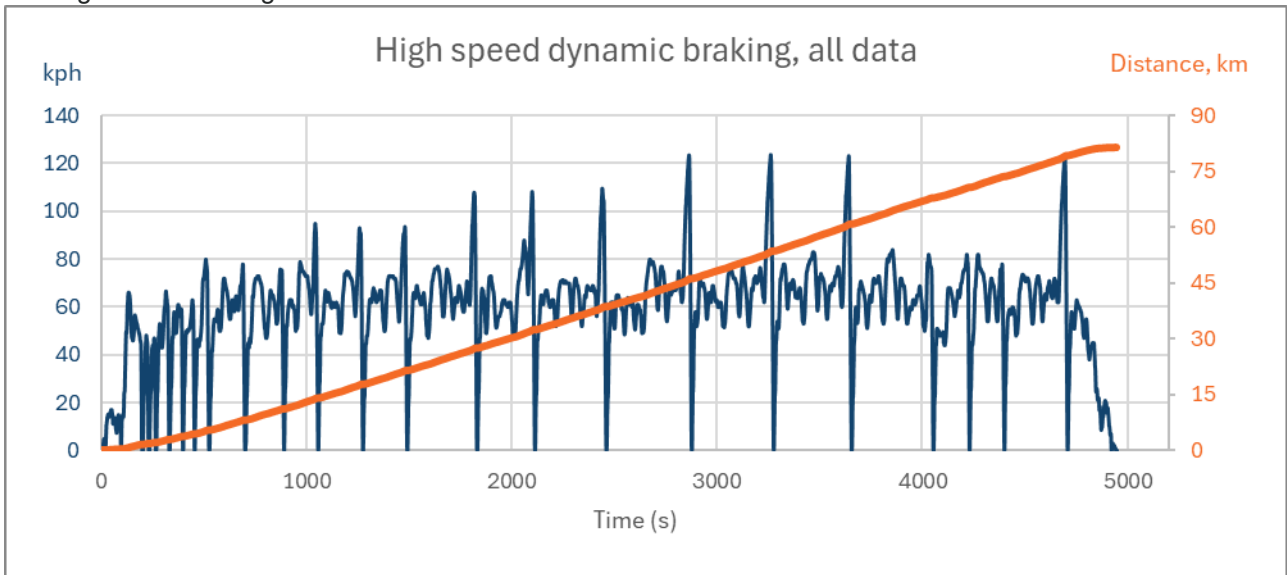

Figure 6-8: Dynamic braking events at MIRA

Deceleration events, calculated in the same manner as for the drive-by testing are shown in Figure 6-9.
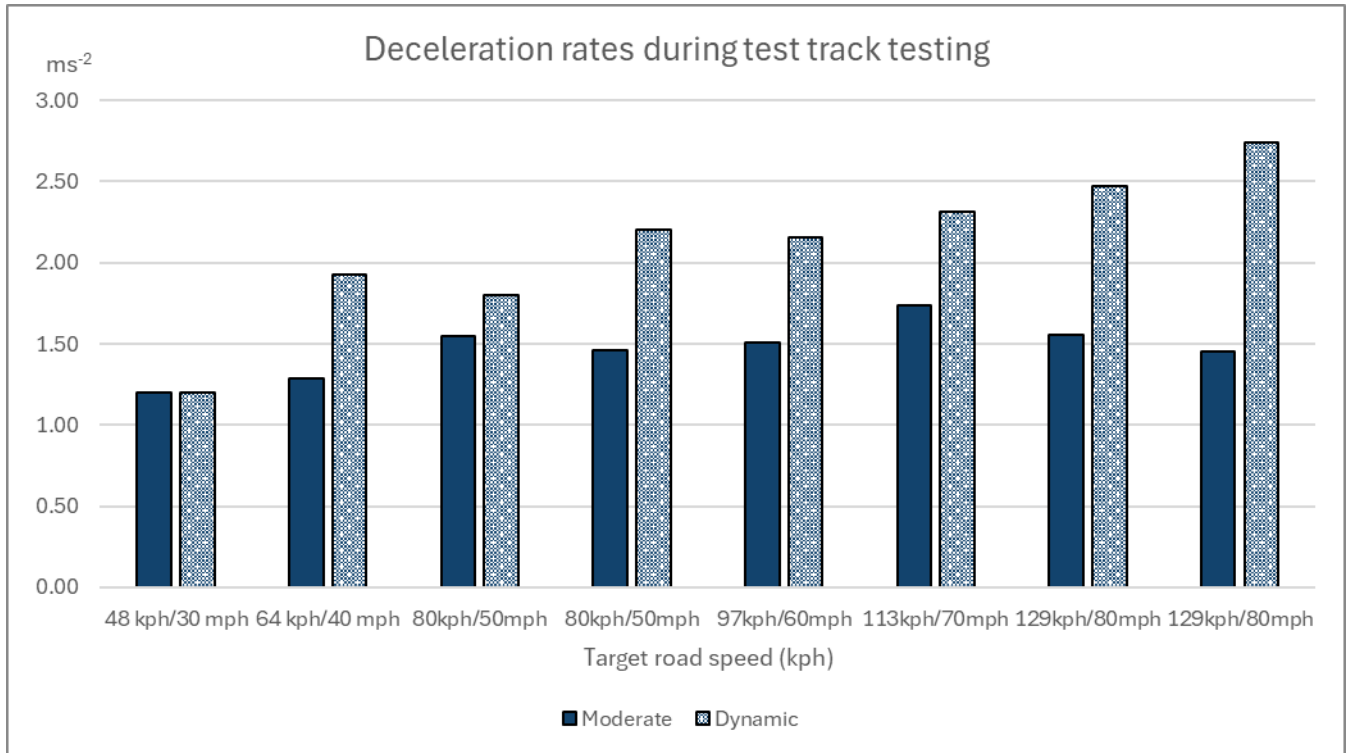
Figure 6-9: Deceleration rates during moderate and dynamic testing at MIRA

6.7 BESPOKE BRAKE AND TYRE EMISSIONS CYCLE

Ricardo was requested to investigate certain braking aspects on the chassis dynamometer. A bespoke cycle was developed using the following rules to achieve the required objectives:

- The cycle should last 90 -120 minutes
- Braking events should be discrete parts of the drive trace and acceleration profiles should be included
- Intervals should be introduced between braking events to include both cruises and idles – so both braking to rest and braking from higher to lower speeds
- Longer cruises to be employed when braking from higher speeds
- Different cruise speeds should use different tyre cooling periods
- There should be a fixed delay once a speed is achieved following both acceleration and deceleration
- There should be:
    - 3 x deceleration rates
    - 3 x cruising speeds
    - 30, 50, 80, 110kph speeds to brake from
- Some 30kph tests should be repeated after 110kph (to study residual heat effect in the tyre)
- Decelerations to be conducted in neutral / clutch down
- Some tyre-warming aspects to be studied e.g., accel, back-off, accel, back-off
- Tyre temps to be measured using an infra-red thermometer

The resultant cycle is shown in Figure 6-10, and contains braking events conducted in groups of three, starting from 30, 50, 80 and 110 kph.

- 30kph: braking is always to rest, under gentle, moderate or dynamic braking. The initial 9 braking events conducted at 30kph are repeated at the end of the cycle, in order to evaluate the effect of hot braking Vs. cold braking on emissions.
- 50kph: braking is to rest, 15kph or 30kph, and under gentle, moderate or dynamic braking
- 80kph: braking is to rest, 30kph or 50kph, and under gentle, moderate or dynamic braking
- 110kph: braking is to rest, 30kph or 80kph, and under gentle, moderate or dynamic braking
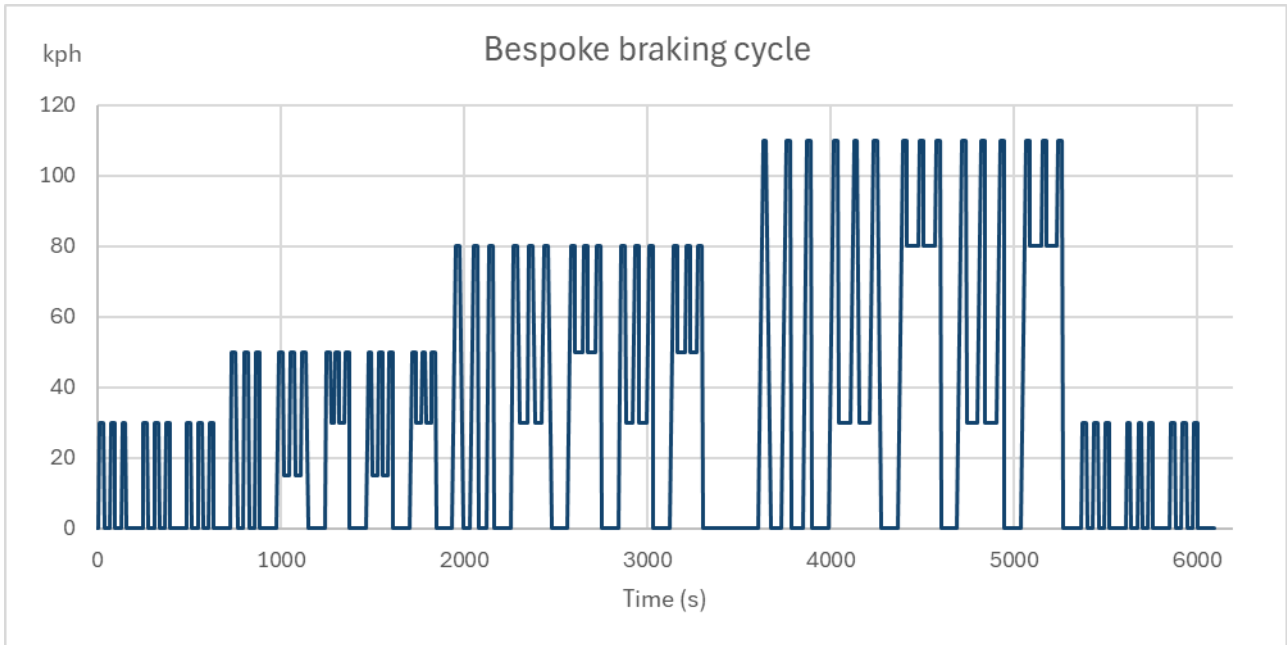
Figure 6-10: Bespoke braking cycle.

Target deceleration rates from peak speed to rest are given in Table 6-1, with a detailed breakdown of individual braking events given in Table 6-2.

Table 6-1: Deceleration rates from peak speed to rest, ms^{-2}

	dynamic	moderate	gentle
30	6.4	4.2	1.2
50	6.9	4.6	1.3
80	6.7	4.4	1.3
110	6.8	4.4	1.3

Table 6-2: Individual braking events within bespoke cycle

Braking event #	Nominal speed (initial)	Nominal speed (end)	Deceleration gentle/moderate/ dynamic	Short name
1	30	0	G	G-30-0
2	30	0	M	M-30-0
3	30	0	D	D-30-0
4	30	0	G	G-30-0
5	30	0	M	M-30-0
6	30	0	D	D-30-0
7	30	0	G	G-30-0
8	30	0	M	M-30-0
9	30	0	D	D-30-0
10	50	0	G	G-50-0
11	50	0	M	M-50-0

Braking event #	Nominal speed (initial)	Nominal speed (end)	Deceleration gentle/moderate/ dynamic	Short name
12	50	0	D	D-50-0
13	50	15	G	G-50-15
14	50	15	G	G-50-15
15	50	0	G	G-50-0
16	50	30	M	M-50-30
17	50	30	M	M-50-30
18	50	0	M	M-50-0
19	50	15	D	D-50-15
20	50	15	D	D-50-15
21	50	0	D	D-50-0
22	50	30	D	D-50-30
23	50	30	D	D-50-30
24	50	0	D	D-50-0
25	80	0	G	G-80-0
26	80	0	M	M-80-0
27	80	0	D	D-80-0
28	80	30	G	G-80-30
29	80	30	G	G-80-30
30	80	0	G	G-80-0
31	80	50	M	M-80-50
32	80	50	M	M-80-50
33	80	0	M	M-80-0
34	80	30	D	D-80-30
35	80	30	D	D-80-30
36	80	0	D	D-80-0
37	80	50	D	D-80-50
38	80	50	D	D-80-50
39	80	0	D	D-80-0
40	110	0	G	G-110-0
41	110	0	M	M-110-0
42	110	0	D	D-110-0
43	110	30	G	G-110-30
44	110	30	G	G-110-30
45	110	0	G	G-110-0
46	110	80	M	M-110-80
47	110	80	M	M-110-80
48	110	0	M	M-110-0
49	110	30	D	D-110-30
50	110	30	D	D-110-30
51	110	0	D	D-110-0

Braking event #	Nominal speed (initial)	Nominal speed (end)	Deceleration gentle/moderate/ dynamic	Short name
52	110	80	D	D-110-80
53	110	80	D	D-110-80
54	30	0	D	D-30-0
55	30	0	G	G-30-0
56	30	0	M	M-30-0
57	30	0	D	D-30-0
58	30	0	G	G-30-0
59	30	0	M	M-30-0
60	30	0	D	D-30-0
61	30	0	G	G-30-0
62	30	0	M	M-30-0
63	30	0	D	D-30-0

Individual braking events were isolated through the use of a braking pressure signal, such that the emissions from both brakes and tyres were quantified from the deceleration events in a bespoke cycle only.

7. COMPONENTS TESTED AND TEST PREPARATION

7.1 BRAKE SYSTEM COMPONENTS

7.1.1 Brake pad and disc variants

In order to cover the brake disc and pad variants available in the marketplace, options were identified from typical commercial retail websites and categorised based on cost, description and any specification claims relative to visible dust production.

From public domain information it was not possible to determine any significant material composition or specification of the brake disc material. Consequently, the discs were selected on the basis of piece cost. This discrimination allowed investigation into any relationship between piece cost and particulate emission.

A similarly limited amount of information was available in the public domain regarding friction material. Any reference to dust generation was focussed upon the visible dust in relation to roadwheel appearance and corrosion prevention.

Two groups of pad specifications were evident, the "Low metallic content" material, which is typically specified in European vehicles as a good compromise between performance, wear and thermal stability and "Organic" materials, which typically generate less visible brake dust, but can have a compromise in their thermal resistance.

The piece cost variation between the brake pads was significant, with "premium" pads being > 3x greater than some of the "budget" variants.

Table 7-1: Details of the brake pads and discs tested in the project.

Disc ref	Disc	Disc cost	Pad ref	*Pad	Pad cost	Pad description / material / rationale
D1	Eicher Brake disc – "Low cost"	£	P1	Pagid	£££	PA4309GF – Premium brake pad
D1	Eicher Brake disc – "Low cost"	£	P2	Eicher	£	"Budget" brake pad
D1	Eicher Brake disc – "Low cost"	£	P3	JPN	£	"Budget" brake pad
D1	Eicher Brake disc – "Low cost"	£	P4	Bosch	££	Low-metallic material – Typical of older friction material tuned for European driving style (thermal performance) rather than limiting visible brake dust.
D1	Eicher Brake disc – "Low cost"	£	P5	Vika	££	Organic friction material – typically lower visible dust
D1	Eicher Brake disc – "Low cost"	£	P6	SKAD	£	"Budget" brake pad
D1	Eicher Brake disc – "Low cost"	£	P7	Mintex	£££	Mintex are part of TMD Friction group – members of PMP working group – "Recognised" UK brand
D1	Eicher Brake disc – "Low cost"	£	P8	Jurid	£££	Low dust brake pads - Ceramic – "Recognised" European brand
D1	Eicher Brake disc – "Low cost"	£	P9	Zimmermann	£££	Low dust brake pads
Dx	Eicher Brake disc – "Low cost"	£	P10A	Pagid	£££	PA4309GF – Aged pads ~ 50,000 km
D2	Pagid Brake disc – "premium brand"	£££	P1	Pagid	£££	PA4309GF – Same pad set (P1) but tested

Disc ref	Disc	Disc cost	Pad ref	*Pad	Pad cost	Pad description / material / rationale
						on "premium" disc
Dx	Eicher Brake disc – "Low cost", same part as D1	£	Px	Pagid	£££	PA4309GF – Premium brake pad, same part as P1

7.2 TYRE VARIANTS

7.2.1 Wheel and tyre variants

In order to facilitate efficient testing, an original equipment steel wheel from Volkswagen was selected to be used for all the tests. The wheel was available in both 16" and 18" variants with a width appropriate for the tyres selected, for testing on both the VW Caddy and Audi A4.

Unlike brake pads, where the consumer has only manufacturer information upon which to assess suitability and performance of the product, passenger car tyres sold within the EU have to display a label (similar format to that applied to domestic white goods), that quantifies some key performance parameters. The C1 (Passenger car) tyre rating label is controlled under Regulation (EU) 2020/740 and previously under Regulation (EC) No 1222/2009. The label information classifies fuel efficiency, by way of a rolling resistance coefficient, wet grip performance and noise generation.

The original tyre label divided the fuel efficiency parameter into seven discreet "tiers" with A rating being the "best", but as tyre technology developed, the current regulation has reduced this to five tiers and added a wet grip performance parameter. Market analysis of tyres available in the test size, shows that despite the A to E scoring range, there were very few tyres available classified with less than a "C" rating. This is presumably due to customer expectation and technology improvements.

The tyres selected for testing in this project (as shown in Table 7-2) allowed a number of parameters to be included:

- Premium cost versus "budget" brands in both tyre sizes (T1-T8 vs. T9-T10)
- Summer construction and formulation vs. "All season" designated tyres within same brand (T3-T4 vs T7-T8)
- Tyre size - hence contact patch (T1-T10 vs. T15-T20)
- Tyre age / wear for same size and brand (T1-T2 vs. T1 –T14)

Specific tyre label properties are summarised in Figure 7-1.

Table 7-2: Details of the tyres tested in the project.

Tyre No.	Description	Tyre type	Fuel cons.	Wet grip	Tyre cost	Wheel no.	Wheel diameter	Notes
T1,T2	Bridgestone Turanza Eco 215/55R18 95T	Summer	A	B	£££	W1,W2	18"	Supplier variant
T3,T4	Michelin Primacy 4; 215/55R18 99VXL TL S1	Summer	A	B	£££	W3,W4	18"	Supplier variant
T5, T6	Goodyear EfficientGrip Performance 2; 215/55R18 99V XL	Summer	A	A	£££	W5, W6	18"	Supplier variant

T7, T8	Michelin CrossClimate 2 215/55R18 99V XL TL	All Season	B	B	£££	W7, W8	18"	Design variant
T9, T10	Landsail LS588 SUV; 215/55R18 99V	Summer	B	B	££	W9, W10	18"	Supplier variant
T11, 12	Bridgestone Turanza Eco 215/55R18 95T	Summer	A	B	£££	W11, W12	18"	11k km aged variant
T13, T14	Bridgestone Turanza Eco 215/55R18 95T	Summer	A	B	£££	W13, W14	18"	23k km aged variant
T15, T16	Bridgestone Turanza ECO 205/55R16 91H	Summer	A	B	££	W15, W16	16"	Size variant
T17, T18	Michelin CrossClimate 2 205/55R16 94V XL TL	All Season	B	B	££	W17, W18	16"	Size variant
T19, T20	Michelin primacy 4+ 205/55R16 91V TL	Summer	C	A	££	W19, W20	16"	Size variant
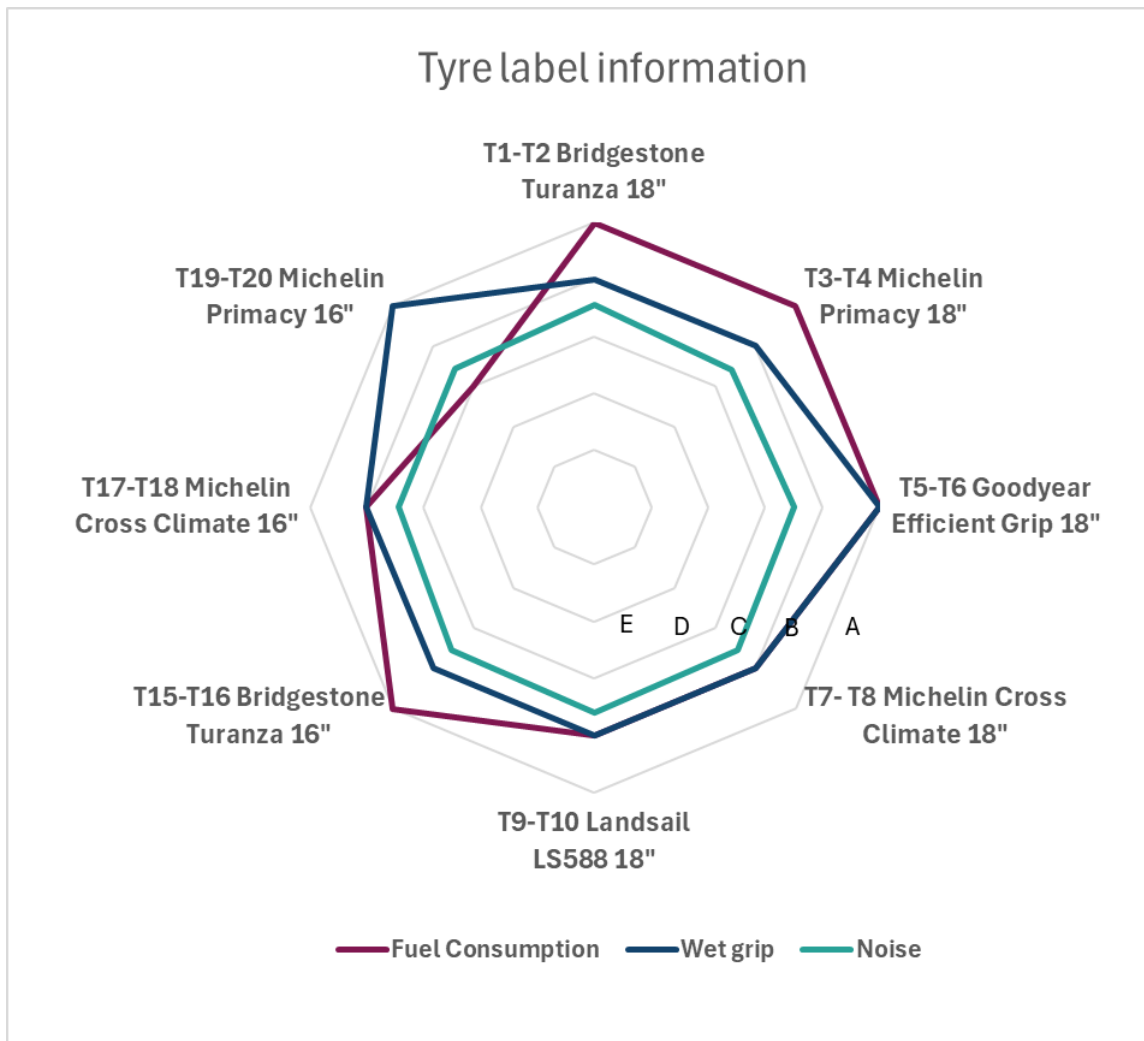
Figure 7-1: Tyre label information for the tyres tested in the project.

7.3 COMPONENT MANAGEMENT

Brake and tyre components procured for testing were also subjected to some basic metrology. For brake pads this entailed the measurement of weight and thickness, and for tyres this included both the measurement of weight (the tyre and wheel were measured together) and tread depth. Before any component weighing, the components were washed and dried.

Sufficient wheels were procured so that each tyre was paired with a dedicated wheel and no tyre changes were required in the project, just wheel changes. This prevented possible damage to the tyres when changes between tyre variants occurred, which may otherwise have resulted in some loss of tyre material.

To reduce any potential contamination, all components were located in a cool dry storage area until required for fitment on the vehicle. In addition, all changes of wheels/tyres, brake pads and brake discs were performed by in-house staff on-site at the Ricardo Shoreham Technical Centre.

7.3.1 Pad weighing and thickness measurements

Each set of pads was etched on the rear with an appropriate, unique designation. They were then weighed, and their thickness measured with a micrometer gauge (Mitutoyo, Japan, calibrated January 2024). Each measurement was made in triplicate and an average taken. Pad thickness was measured at six positions, as indicated by Figure 7-2, which shows a pad viewed from the friction material side. The thickness measurements included the backplate and any shims (thin pads between the pad and calliper), chamfers and other discontinuities were avoided. These measurement processes were conducted at the beginning, after ageing, and at the end of the test programme. Each set of 4 pads were then stored in individual, labelled, boxes in a cool dry place when not in use.
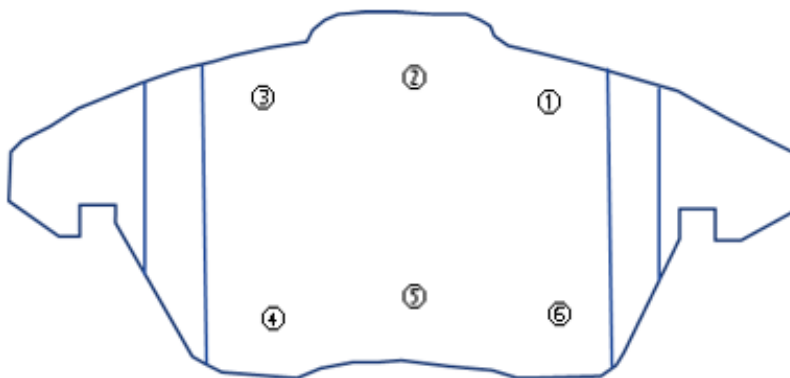

Figure 7-2: Locations on a brake pad for thickness measurements.

Brake discs were treated in a similar manner to brake pads. Disc thickness measurements were made according to the locations shown in Figure 7-3, at points every 60° and ~5 mm inside the disc perimeter, using a micrometer gauge. The disc was also weighed. Discs were stored alongside the pads until required for use.
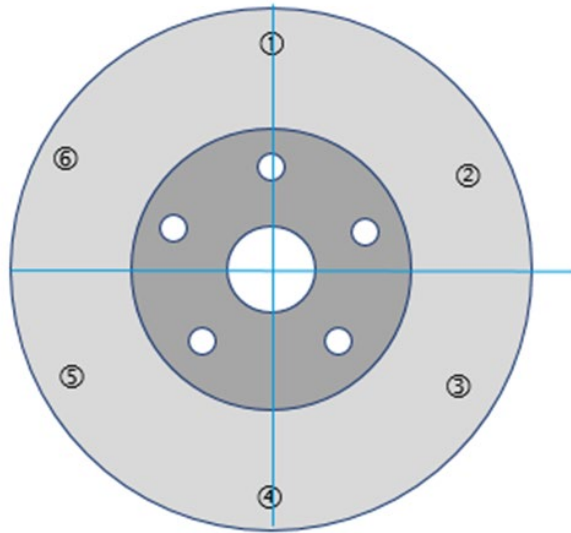
Figure 7-3: Locations on a brake disc for thickness measurements.

7.3.2 Tyre weighing and tread depth measurements

All the tyres/wheels were uniquely labelled by etching (wheel) and with a paint pen (tyres). Prior to weighing, the tyres/wheels were cleaned with water and a cloth then dried. Any obvious contaminants, such as stones and mud, were removed from the tread during this process. Tyres were then weighed on calibrated scales with 0.1g resolution.

Tread depth measurements were made on the centre tread, with three measurement locations on each tyre: (1) clockwise measurement position at 0° (tyre valve position). (2) second position at ~120° and (3) third position at ~240°. The tyre/wheels were then stacked and stored in a cool dry place ready for use. These measurements were made at the beginning, after ageing and at the end of the test programme.

7.4 TEST PREPARATION

7.4.1 Vehicle safety checks

Prior to any road or chassis dynamometer testing, vehicles are safety checked by internal Ricardo specialists. Ricardo vehicle safety checks are done nominally at 3 monthly intervals and are to ensure the on-going safety of the vehicle whilst it is on site being tested, and potentially driving on public highways or on a test track. The safety check does not eliminate the need for the annual government roadworthiness test (MOT) when the vehicle is to be used on a public highway.

Safety checks include several individual sub-tasks performed under each of the headings below:

- Tyre Condition – including pressure and tread depth
- Body Condition – including dents and stone chips
- Security and Safety Equipment – including wheel nut torques and glass
- Lights and Warning Lights – including head lights and dash warning lights
- Vehicle Controls and Equipment – including seat belts and steering
- Engine Compartment – including leaks and fluid levels
- Vehicle on Hoist – including suspension and brakes
- Road Test - check control and operation of steering, brakes, clutch, gearshift, speedometer, tachometer, temp gauge etc.

7.4.2 Preliminary preconditioning of brake and tyre components

The preliminary on-road brake and tyre preconditioning was conducted around the urban and rural sections of a fully compliant passenger real driving emissions (RDE) route near to the Ricardo site at Shoreham-by-Sea

(Figure 7-4). Together the urban and rural sections comprised ~50 km distance, so each set of tyres and brake pads, with an appropriate brake disc, was driven around those sections four times, resulting in an approximate preconditioning distance of ~200 km.
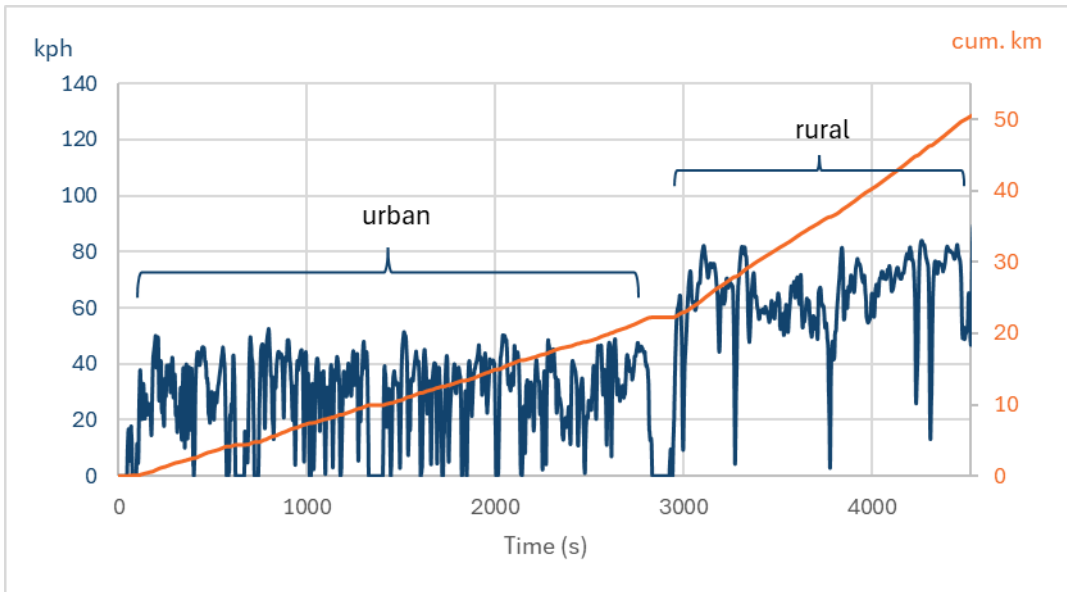

Figure 7-4: Urban and rural sections of the Ricardo eastbound RDE route. The cumulative distance travelled for one cycle is approximately 50 km.

8. BRAKE WEAR EMISSIONS RESULTS

8.1 TESTING PERFORMED

8.1.1 Tests per pad & disc combination

All tests were performed on the VW Caddy at 1900 kg test mass (the vehicle was weighed to establish the test mass), excepting selected tests that were conducted at 2100 kg to study the effect of additional test mass on emissions.

8.1.1.1 Tests per pad and disc combination

Pads P2 to P9 were tested with Disc 1 (D1), each over an identical protocol (Table 8-1).

Table 8-1: Test protocol for P2 to P10A, with either D1 or Dx, and for P1 with D2

Day	Test
Day 1	Chassis dynamometer PG-42 x 3
Day 2	On-road RDE x 3
Day 3 AM	Drive-by site gentle and moderate braking (80kph max)
Day 3 PM	Drive-by site dynamic braking (80kph max)
Day 4 AM	(1) RDE transposed to dyno (2) Same dynamometer RDE with increased weight (2100 kg)
Day 4 PM	Repeats, pad and/or disc change
Day 5	Reserved for repeats (if necessary)

Pad P10A (pad aged by 50,000 km) was tested over the same protocol as P2 to P9 (Table 8-1), but with Disc X (Dx), the service disc, which was nominally identical to D1 but was used for non-test activities such as moving the Caddy around geographically. Dx was used because P10A had an unevenly worn surface and it was considered possible that this could affect the surface of D1, which might then impact later testing of other pads. In fact, Dx was unaffected by the experiments with P10A, and was later used along with a set of service pads (Px, which were a nominally identical set to P1) for the brake technology testing.

P1 was tested twice, once with D1 and once with D2. With D1 a slightly extended protocol was followed. This included an extra drive-by site dynamic braking set, but with 200 kg higher test mass. With D2 the protocol shown in Table 8-1 was followed.

8.1.2   Test order and test dates during comparative brake pad and brake disc testing

Testing took place in the VATF, on the road and on the drive-by site. The test order was primarily dictated by the weather, with road and particularly drive-by testing not conducted when rain was present, forecast or had just passed. As a consequence, the on-road RDE and drive-by emissions testing of a particular combination of pads and discs did not often immediately follow their chassis dynamometer testing, as when rain was forecast, pads were changed to allow further testing to progress in the VATF. This approach facilitated the most efficient progression through the test programme, although it was predicted to increase risk of damage to the pad and discs through a greater number of pad and disc changes. In fact, no issues, nor damage to pads or discs, were encountered when changing brake components during the project.

Table 8-2 provides a summary of the test dates for the brake pad and disc combinations tested.

Table 8-2: Test dates for comparative brake pad and brake disc testing in 2024.

Pad & Disc	PG42	Dyno RDE	Road RDE	Drive-by
P1, D1	18/03; 16/05	16/05	20/05	20/05; 23/05
P1, D2	17/05	17/05	20/05; 22/05	23/05
P2, D1	15/05	15/05	28/05	29/05
P3, D1	14/05	14/05	24/05	24/05
P4, D1	03/05	03/05	30/05	31/05
P5, D1	08/04	08/04	17/04	18/04
P6, D1	09/04; 26/04	29/04	19/04	29/04
P7, D1	30/04	30/04	07/05	07/05
P8, D1	01/05	01/05	08/05	08/05
P9, D1	02/05	02/05	09/05	10/05; 13/05
P10A, Dx	20/03; 21/03	21/03	15/04	16/04

Test order for the PG42, chassis dyno RDE, road RDE and drive-by testing was as follows (pads with D1 unless otherwise stated):

- PG42: (P1)*, P10A + Dx, P5, P6, P7, P8, P9, P4, P3, P2, P1, P1 + D2
- Dyno RDE: (P1)*, P10A + Dx, P5, P6, P7, P8, P9, P4, P3, P2, P1, P1 + D2
- Road RDE: P10A + Dx, P5, P6, P7, P8, P9, P1, P1 + D2, P3, P2, P4
- Drive-by: P10A + Dx, P5, P6, P7, P8, P9, P1, P1 + D2, P3, P2, P4

(P1)* indicates measurements with P1D1 conducted prior to any secondary preconditioning (see Section 8.2)

8.2 SECONDARY PRECONDITIONING

Chassis dynamometer testing initially commenced in mid-March 2024 on the combination of P1, D1 following the planned ~200 km on-road preconditioning. However, despite the preliminary preconditioning, measurements of non-volatile PN10 (with APC) revealed a progressive reduction of emissions through a sequence of three PG42 tests (Figure 8-1a). This suggested that, with regard to particle number emissions, the pad/disc combination was not fully stabilised prior to the testing, and additional preconditioning was required. To validate this assumption, P10A – a pre-aged pad – was fitted and testing recommenced.

P10A is a nominally identical pad to P1, except it was pre-aged to 50,000 km on a Ricardo employee's own vehicle, and Dx is a nominally identical disc to D1 that was procured new at the outset of the project. Dx is the "service disc" used when the vehicle needs to be driven on the road without ageing either of the project discs (D1 and D2). It was anticipated that P10A would be a good example of stable PN emissions from P1, since it was a highly aged nominally identical pad.
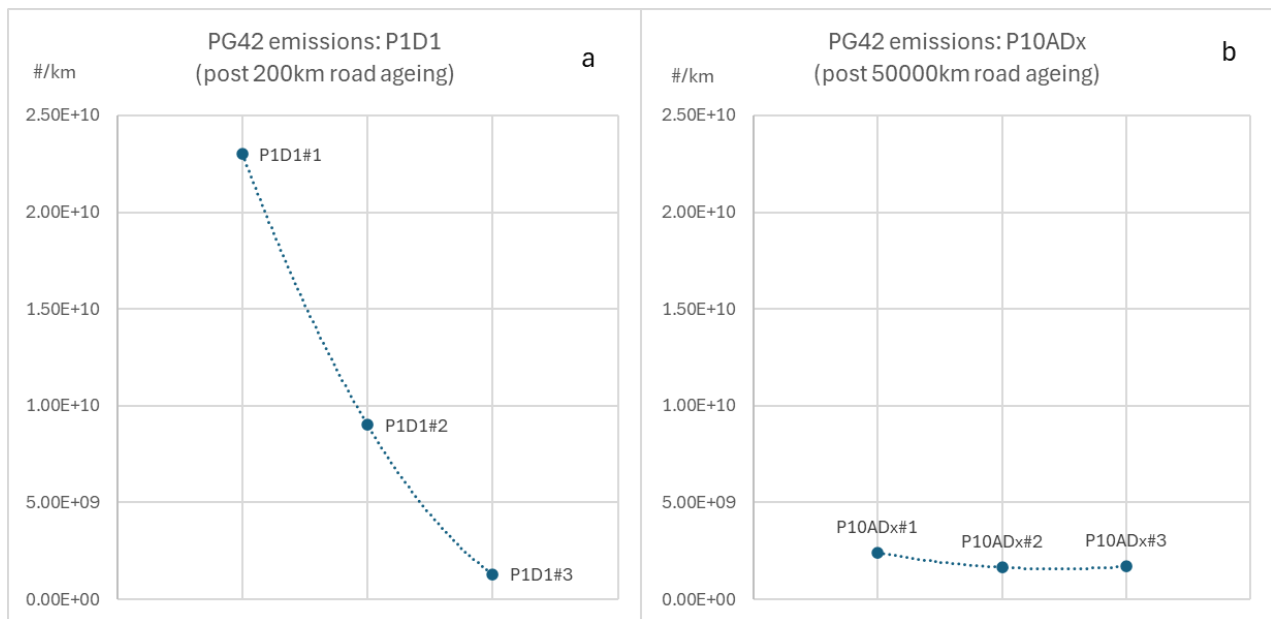
Figure 8-1: #/km emissions from (a) P1,D1 following the 200km road ageing & (b) P10A,Dx, aged ~50,000km on the road.

Three PG42 tests were conducted on P10A with Dx (as a reminder, Dx was selected for these tests only, as the P10A pads showed some signs of uneven wear and this could have conceivably led to minor damage to D1, that might have influenced later test on other pads). The results (Figure 8-2b) showed levels similar to the third test on P1, indicating that P1 had reached stabilisation after 200 km road ageing plus 3 x PG42 tests (an additional 150 km, albeit with some aggressive braking events included).

It was then agreed with DfT to conduct further secondary ageing, which comprised 3 x PG42 cycles on each of the other low mileage pads (P2, P3, P4, P5, P6, P7, P8 and P9). This ageing was executed on the chassis dynamometer. These pads were aged with Dx fitted.

Later testing of P1 in May during the main project, and following the secondary ageing, revealed emissions levels that were similar to those of P10A, and with similar variability (Figure 8-2). This confirmed that emissions were stable after the initial and secondary ageing was complete.
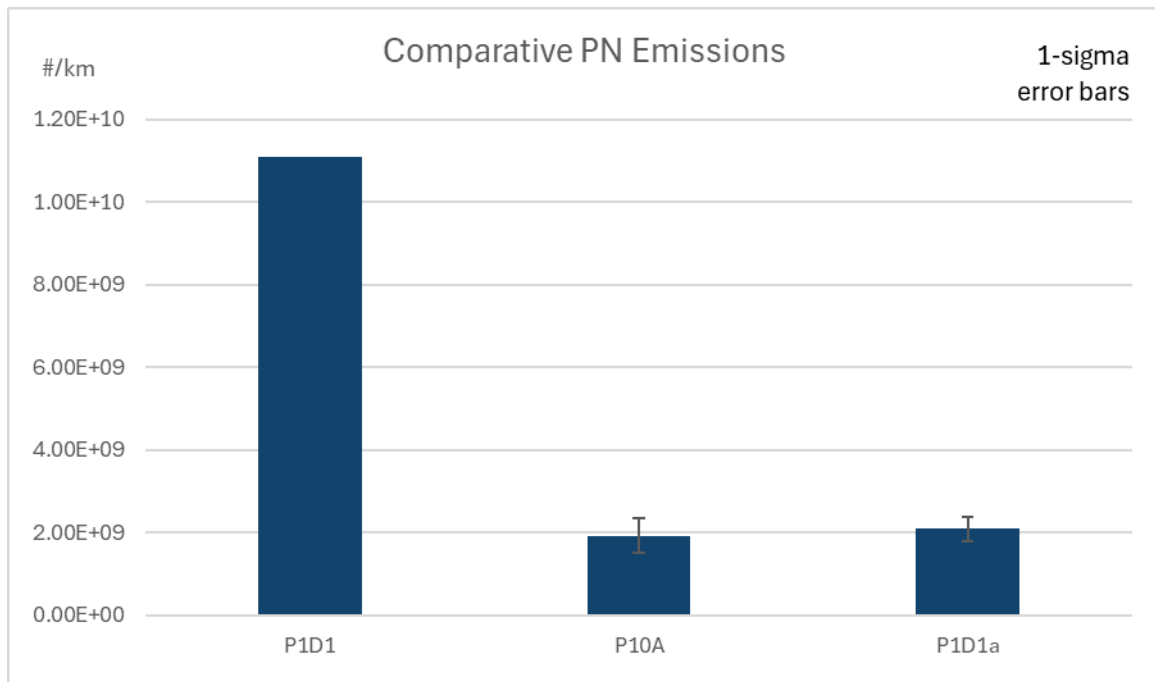
Figure 8-2: Average emissions from P1D1 (after preliminary aging only), P10A (50000 km road ageing) and P1D1a (after preliminary and secondary ageing).

The 3 x PG42 tests performed on P10A and Dx were accepted as the valid measurements for the test programme and were followed by chassis dyno RDE tests prior to the secondary ageing being conducted on the other pads.

8.3 BRAKE WEAR EMISSIONS RESULTS

8.3.1 Real-time brake emissions profiles

As observed in the Phase 1 study[5], brake wear particle number emissions have been seen to correspond to braking events, as indicated by brake pressure measurements. Using the first PG42 test on pad 7 and disc 1 as an example, in this section real-time traces are shown in Figure 8-3a-e for brake particle number emissions with APC10, cold MPEC, hot MPEC, DMS500 and eFilter respectively.

As expected, these data show strong emissions spikes, from all instruments employed, that correspond to braking pressure events. The least clean signal is from the DMS500, which is measuring total particles >5nm (Figure 8-3d). Since the cold MPEC, which measures total particles >10nm, (Figure 8-3b) does not indicate an appreciably different transient profile to the hot MPEC (non-volatile particles >10nm, Figure 8-3c), it is unlikely that extra spikes in the DMS500 data are volatile particles and more likely these are just noise from the electrometers of the DMS.

In general, the brake particle emissions do not appear to indicate outgassing of volatile materials (even during the high temperature part of the cycle, 800s to 1400s), so both volatile and non-volatile particles released are primarily related to the instantaneous application of the brakes. There does appear to be continuous low-level presence of particles throughout the drive cycle, best observed during the long cruises, but this is most likely indicative of the background, or residual, level of particles within the enclosure.

However, all the instruments employed do show occasional spikes of particle emissions that are not obviously associated with the brake pressure signal. These can be seen in Figure 8-3a-e at ~1350s and ~1400s, but are better observed, for the APC10 and cold MPEC, in Figure 8-3a,b which focus on the time range between 1000 and 1500s of the PG42 cycle.

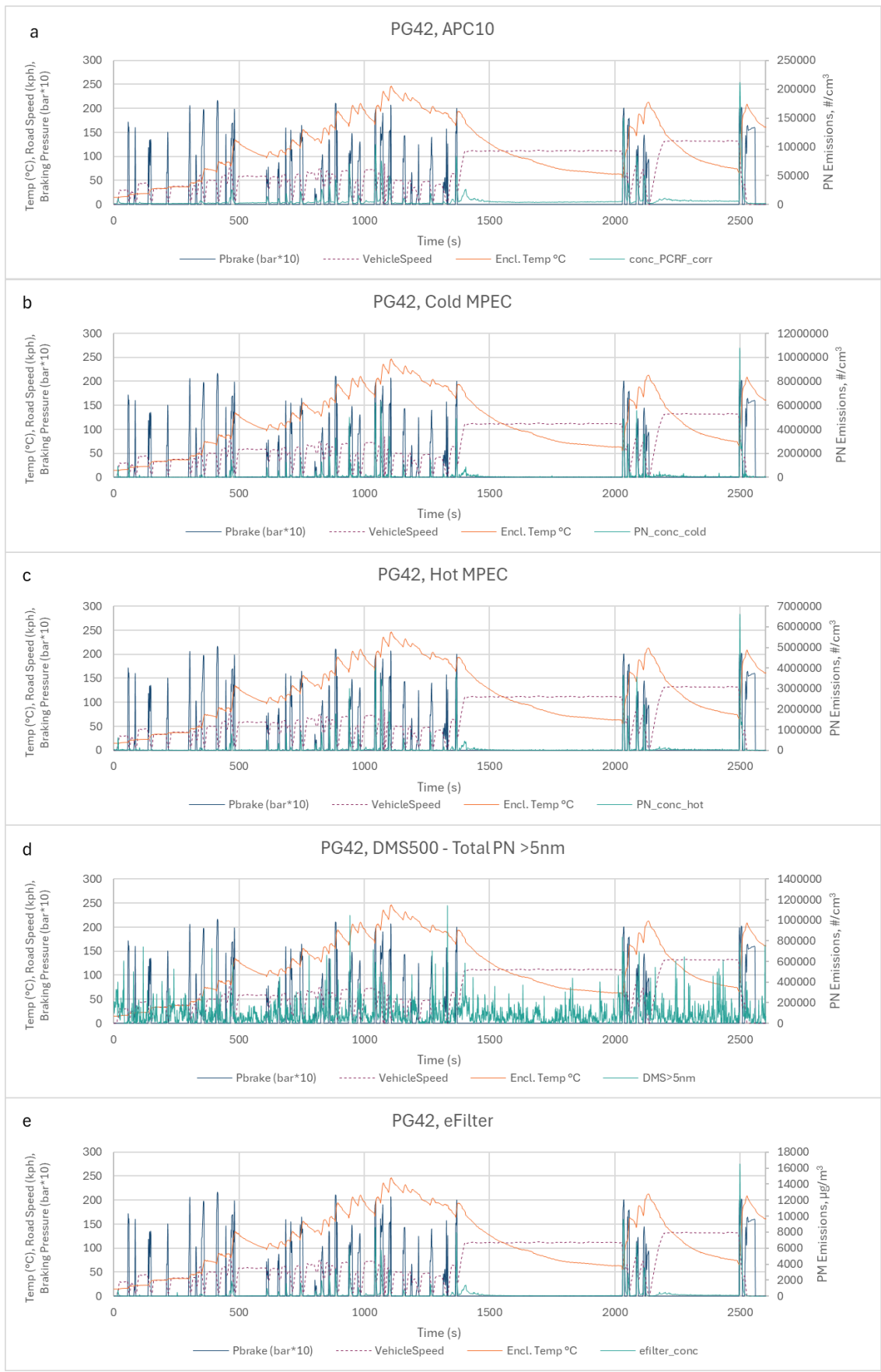[5] Measurement of emissions from brake and tyre wear - GOV.UK (www.gov.uk)

Figure 8-3: Example real-time particle emissions from the a) APC10, b) cold MPEC, c) hot MPEC, d) DMS500 and, e) eFilter, used in this study.

Considering the emission of non-volatile particles from the APC10 in Figure 8-4a, the shape of the spike at 1350s is different in the way it is formed when compared with the spikes seen after brake pressure is applied. The emissions also seem to hang up after the spike, which suggests that the pad may have stuck following the last application and may continue to stick for a short duration. The preceding brake application (~1317s to 1332s) is not a particularly "clean" apply - the pressure is inconsistent, peak pressure is reached more slowly and (possibly related to the application), there is no obvious temperature increase. This may have contributed to the sticking of the pad, and the effect seems to last beyond the next braking event (~1365s) but clears during the subsequent long cruise. Figure 8-4b confirms that, in-line with emissions during braking, there is no obvious release of additional volatile particles.
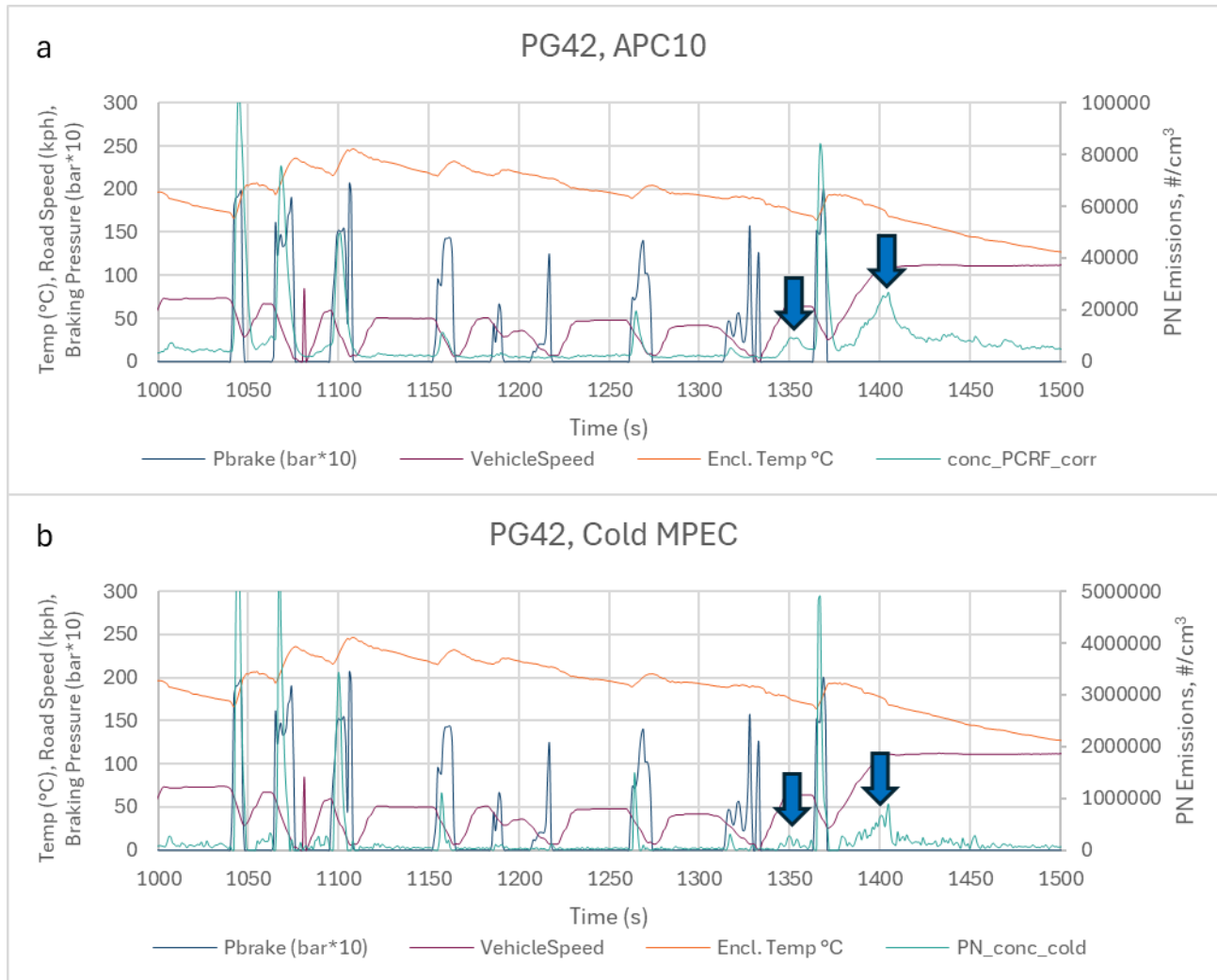
Figure 8-4: Particle emissions incorrespondent with braking pressure events as shown in the a) APC10 and, b) cold MPEC data.

It appears that there are emissions of particles that do not directly correspond to the application of brakes but are the consequence of prior braking events that may originate through the approach an individual driver takes to braking for a specific event. These events may contribute particle emissions in a real-world test (on chassis dynamometer or on-road) that might not be observed in a brake dynamometer test and so consideration may need to be given to factoring these emissions into 'real-world' expectations for emissions when compared to certification levels.

8.3.2 P1, high mileage pad (P1Dx) and premium Disc (P1D2)

Pad P1 (Pagid, PA4309GF, premium brake pad) was tested with Discs D1 (low-cost Eicher brake disc) and D2 (Pagid, premium brake disc), and was nominally identical (with the same manufacturer, same part number, but not the same batch nor identical mileage) to the high mileage pad (P10A). Dx was similarly of the same

specification as D1. This section compares results of tests between P1D1 and P1D2, and between P1D1 and P10ADx, investigating effects of high v low mileage on emissions and any differences between emissions between the disc variants, respectively.

8.3.2.1 *PG42 Cycle emissions at 1900 kg test mass*

Emissions results from PG42 cycles are presented for APC10 (non-volatile particles >10nm), cold MPEC (total particles >10nm), hot MPEC (non-volatile particles >10nm), gravimetric $PM_{2.5}$ by eFilter, real-time PM by eFilter, and integrated total PN 5nm to 2.5 µm from the DMS in Figure 8-5a – f respectively. Results show the mean of three sequential repeat tests, with error bars showing one standard deviation about the mean value.

Results of the cold MPEC, hot MPEC instruments and both gravimetric and real-time PM show similar trends, indicating that the aged pads (P10A) have lower emissions than those of P1, irrespective of disc type.

There is no obvious difference in emissions between D1 and D2, with any instruments.

Non-volatile PN10 emissions from the APC10 (which uses a catalytic stripper to eliminate volatiles) were similar between P1D1, P1D2 and P10ADx. This conflicts with the results of the H_MPEC (which uses an evaporation tube), potentially indicating that there are low/semi-volatile components in the sample aerosol, that the H_MPEC is unable to fully evaporate, but the APC10 can eliminate catalytically.

PG42 emissions from the APC10 (Figure 8-5a) were in range 2×10^9 #/km, with gravimetric $PM_{2.5}$ results (Figure 8-5d) ~1.8 mg/km from P10A and 3 – 3.5 mg/km from P1, the range covering both discs.

PN (5 nm to 2.5 µm; Figure 8-5f) from the DMS showed highly variable results from both Dx and D2. Both these discs had experienced substantially less mileage than D1, and this may indicate the need for extended ageing for discs when determining emissions below 10nm.
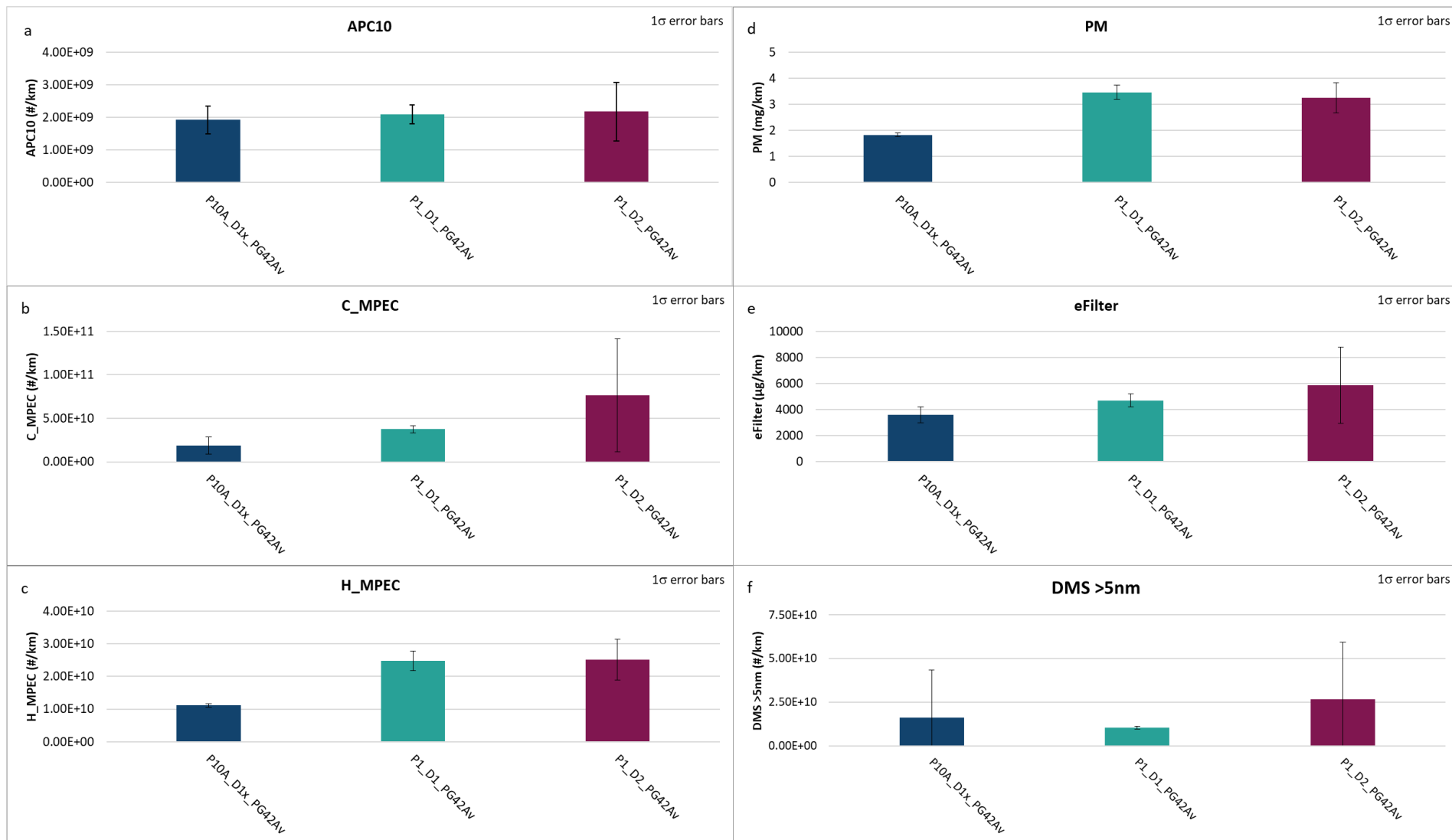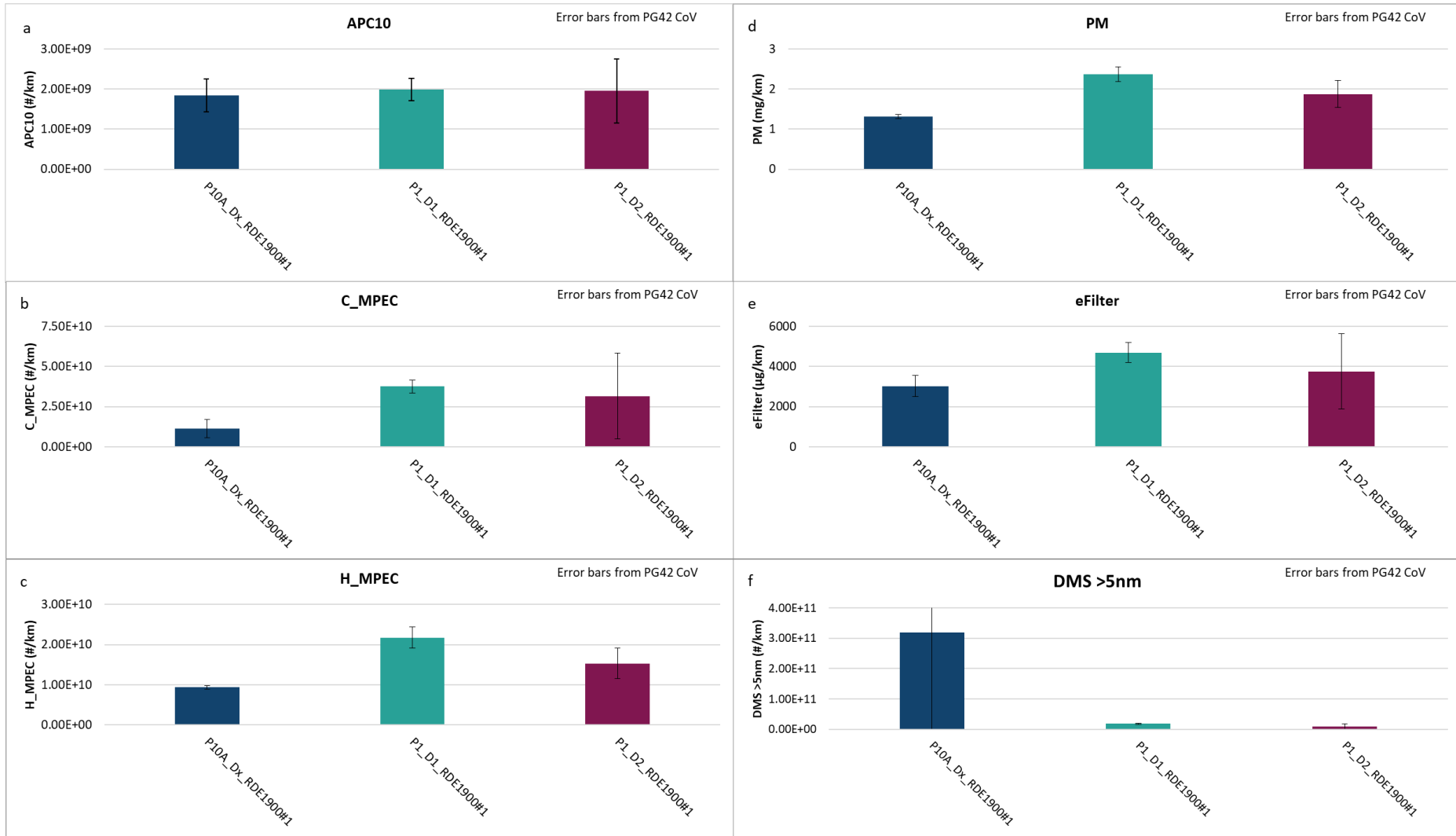
Figure 8-5: Comparative results from PG42 tests with P1D1, P1D2 and P10ADx as shown for the a) APC, b) cold MPEC, c) hot MPEC, d) gravimetric PM$_{2.5}$, e) eFilter PM and f) DMS500.
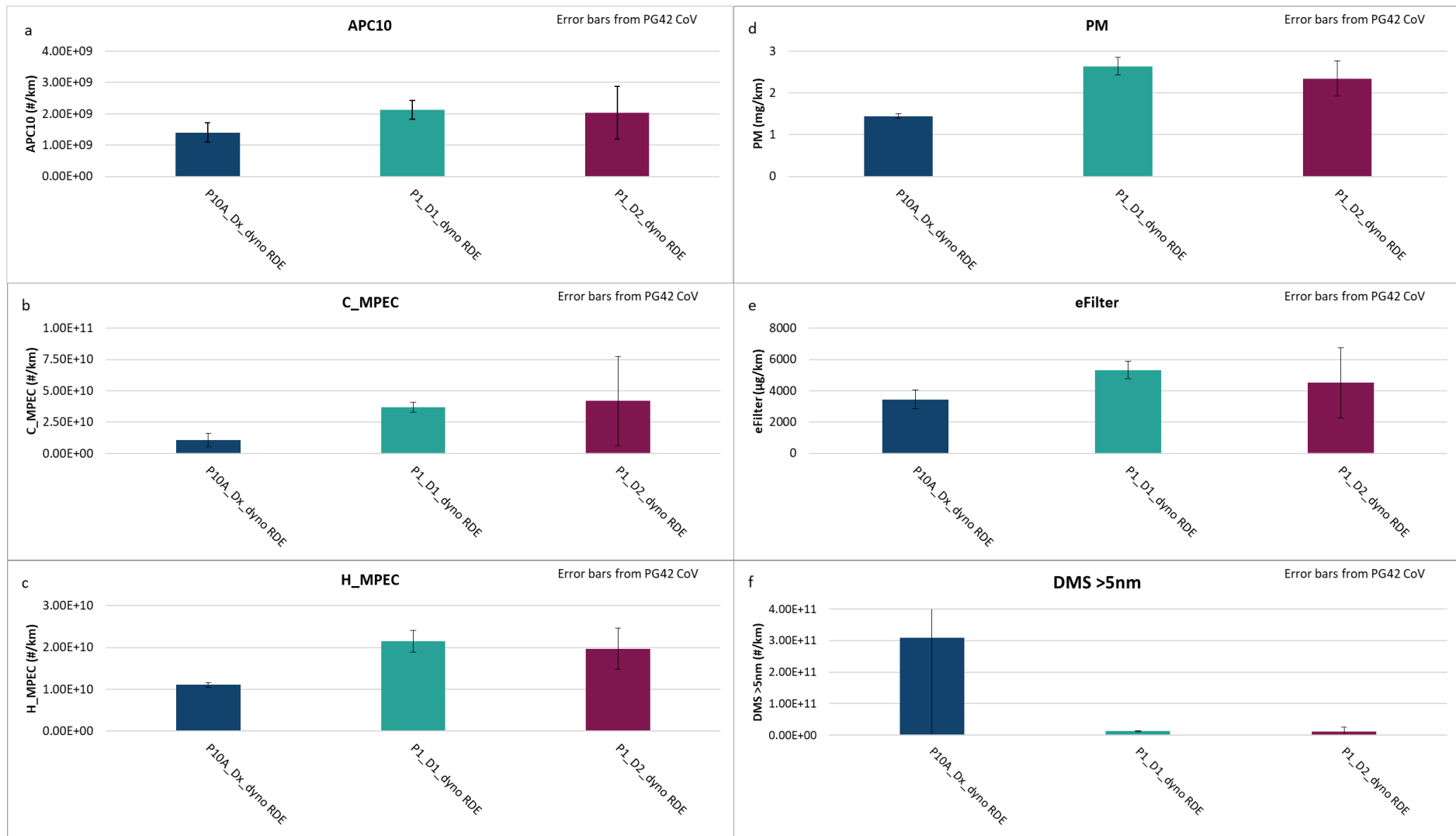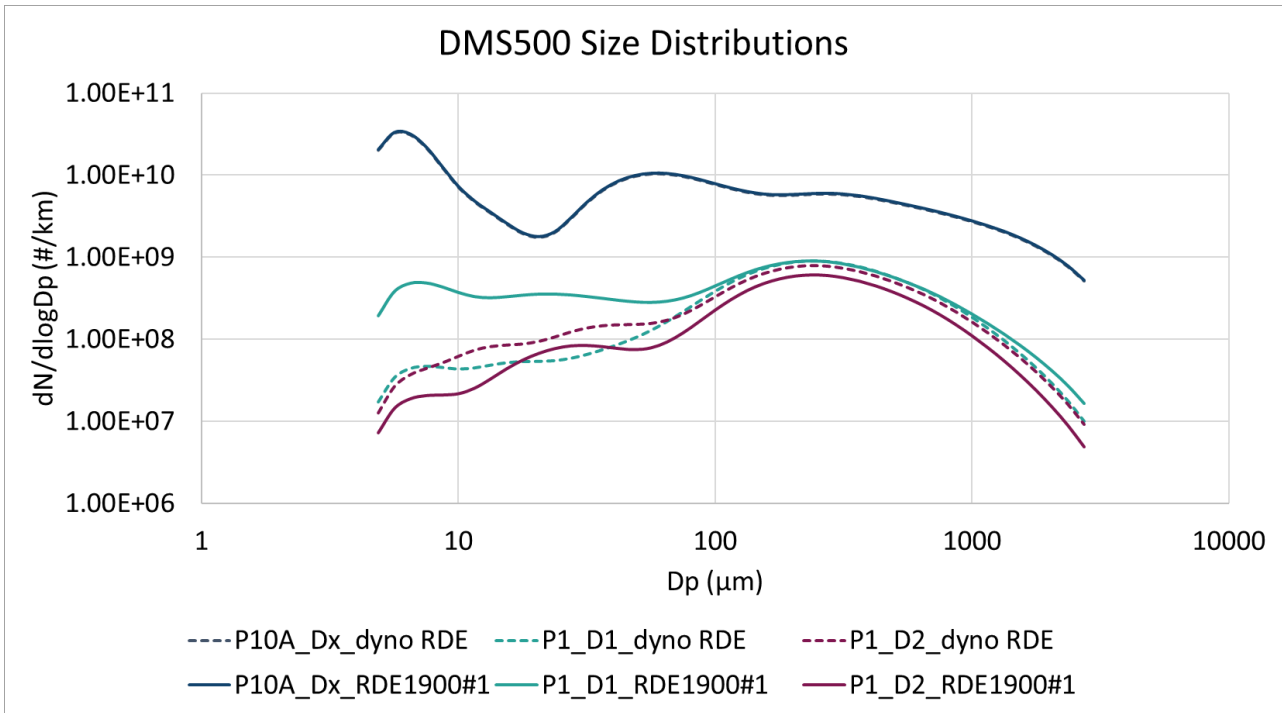
The particle size distributions from the DMS (Figure 8-6), show that the main differences in the particle number emissions between the three discs lie in the <100nm region, and may derive from volatile particles, since the APC10 does not appear to detect these emissions differences. There is also an apparent difference in the accumulation mode emissions (<100nm), which aligns with the observations of lowest particle emissions from P10A seen in both the MPECs and mass emissions data. This suggests that some of the particles in this size range above 100nm may also be semi-volatile. This is consistent with observations in Phase 1 of the project, where some brake wear particles >1 μm were evaporated and recondensed into a nanoparticle mode by the heated inlet of the hot ELPI.
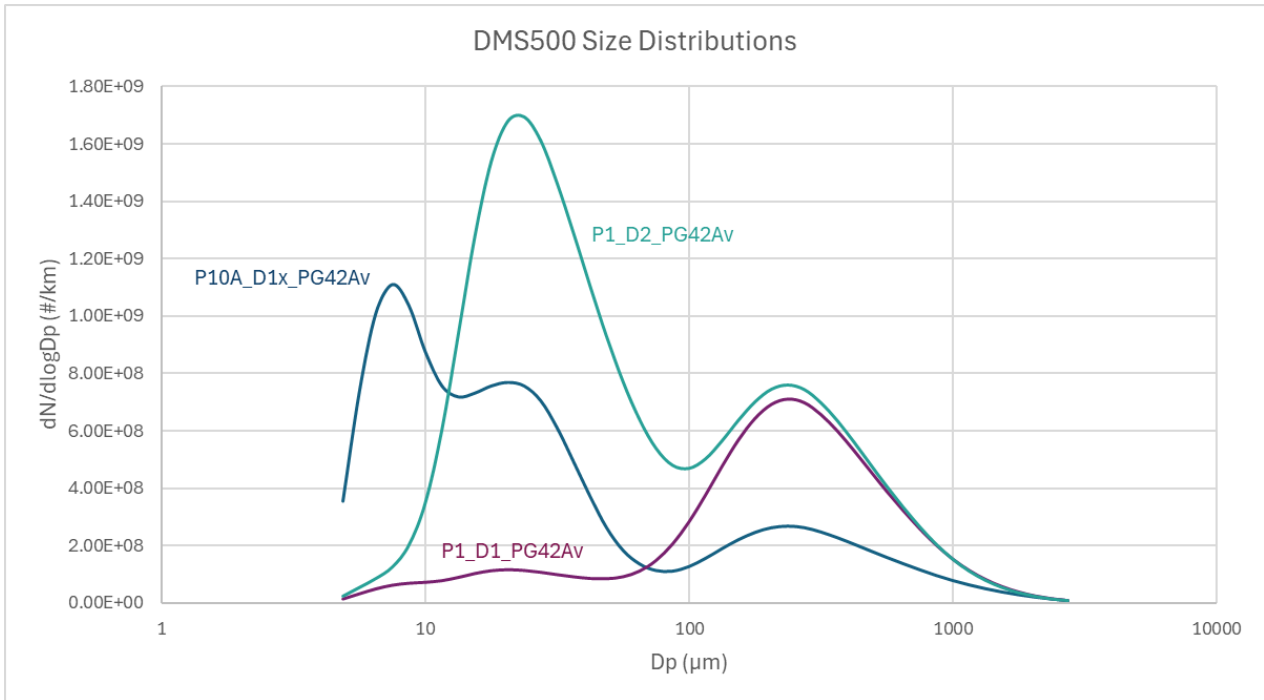
Figure 8-6: Particle size distributions measured by the DMS500 from PG42 cycle, P1D1, P1D2 and P10A, Dx.

It should be noted that, as Figure 8-5a-c shows, PN emissions determined by the MPECs are much larger (typically 10-20x, but up to 100x) than indicated by the APC10. This is likely to be due to a multiple charging effect in the MPECs, where larger particles (>200nm) accumulate multiple charges, and the greatest numbers of charges are associated with the largest particles. Since the MPECs' diffusion charger approach totals the individual charges, the actual number of particles present is overstated. This effect is discussed further in Sections 5.2.1 and 12, but its presence does not prevent the use of the hot and cold MPEC to discriminate differences between pads and discs.

8.3.2.2   Chassis dynamometer RDE emissions, at 1900 kg and 2100 kg test mass

Figure 8-7 and Figure 8-8 present the results from Chassis dynamometer RDE emissions tests, at 1900 kg and 2100 kg test mass, respectively, for the following measurements:

a.   APC10 (non-volatile particles >10nm).
b.   Cold MPEC (total particles >10nm).
c.   Hot MPEC (non-volatile particles >10nm).
d.   Gravimetric $PM_{2.5}$ by eFilter.
e.   Real-time PM by eFilter.
f.   Integrated total PN (5nm to 2.5 μm) from the DMS.

One-off tests were tested at each dynamometer load / test mass so, to enhance discrimination, data are shown with error bars that represent the percentage variation observed during the triplicate PG42 cycle tests.

Results at both 1900 kg and 2100 kg are broadly consistent with those from the PG42 cycle, wherein there is little or no discrimination between results from Disc 1 and Disc 2 with any of the measurement approaches. Alternatively, but again consistent with PG42 results, for MPECs and mass measurements with the eFilter, emissions from P10A + Dx are lower than from the other pad and disc combinations.

Mean APC10 results for both 1900 kg and 2100 kg tests for P10A are directionally below the means of the other pad + disc combinations, but on the basis of the standard deviation from the PG42 tests not significantly so for the 1900 kg results.

Integrated DMS data from both 1900 kg and 2100 kg data (Figure 8-7f and Figure 8-8f) showed similar results between Disc 1 and Disc 2, but substantially higher emissions from P10A with Disc x. Particle size distributions from P10A+Dx showed that emissions were elevated across the size range, but particularly high below 10nm (Figure 8-9). As with the PG42 testing, the use of low mileage discs may lead to both high variability and high particle number emissions, and so a rigorous disc break-in period, of at least 500 km, would be advised for future work should <10nm particle measurements be important.

The effect, on emissions, of increasing test mass from 1900 kg to 2100 kg is discussed in Section 8.3.2.2, where data from all pad and disc combinations is included.

Figure 8-7: Comparative results from chassis dyno RDE tests at 1900 kg with P1D1, P1D2 and P10ADx as shown for the a) APC, b) cold MPEC, c) hot MPEC, d) gravimetric PM$_{2.5}$, e) eFilter PM and f) DMS500,

Figure 8-8: Comparative results from chassis dyno RDE tests at 2100 kg with P1D1, P1D2 and P10ADx as shown for the a) APC, b) cold MPEC, c) hot MPEC, d) gravimetric $PM_{2.5}$, e) eFilter PM and f) DMS500.

Figure 8-9: Comparative particle size distribution results measured by the DMS5000 from chassis dyno RDE tests at 1900 kg and 2100 kg.

8.3.2.3 Road RDE tests, at 1900 kg

The results from the cold MPEC and hot MPEC instruments and real-time and gravimetric eFilter measurements collected during on-road RDE tests (at ~1900 kg test mass) are shown in Figure 8-10a to Figure 8-10d respectively. Triplicate tests were conducted.
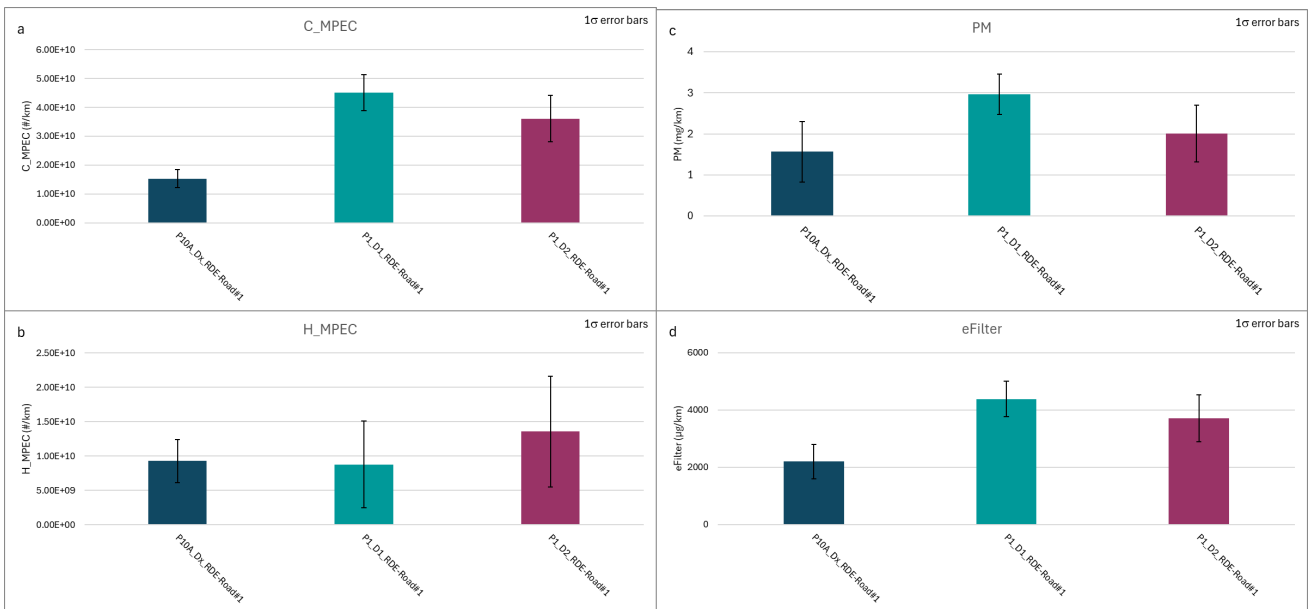
Figure 8-10: Comparative results from road RDE tests with P1D1, P1D2 and P10ADx as shown for the a) cold MPEC, b) hot MPEC, c) gravimetric PM$_{2.5}$ and d) eFilter PM.

P10A + Dx emissions from all four measurement approaches shown here were either similar to or lower than observed from P1D1 and P1D2, these results reflecting the general observations of PG42 and RDE tests on the chassis dynamometer. P1D1 and P1D2 always showed similar results to each other.

8.3.3 Emissions of pad variants with a single disc (D1)

The emissions of nine different pads (P1 to P9 inclusive) with a single disc are compared for PG42, dyno RDE and road RDE driving in this section. Although pad details can be found in Table 7-1, detailed chemical composition of the pads was not available, but manufacturers provide descriptors (or marketing claims) for the various pads, which can be summarised as shown in Table 8-3.

Table 8-3: Matrix plot for the various pad descriptors.

Brake Pads	Premium	Budget	Low Metallic	Organic	Recognised brand	Low dust
P1	1					
P2		1				
P3		1				
P4			1			
P5				1		1
P6		1				
P7					1	
P8					1	1
P9						1

Descriptors

From the descriptors, P5, P8 and P9 are advertised as low dust pads, while P4 is low metallic. Without any supporting information, these pads might be considered candidates for low PM and PN emissions. Similarly, the premium brand, P1, and recognised industry brands P7 and P8, might be expected to perform well emissions-wise. Alternatively, the budget pads P2, P3 and P6 might be expected to have shorter lifetimes, wear more quickly and consequently have higher PM and PN emissions.

8.3.3.1 Pad variants – PG42 tests

Triplicate PG42 cycles' particle number emissions results from the APC10, cold MPEC and hot MPEC are shown in Figure 8-11. It is clear that the measurement approach is able to discriminate between pads for PN, with average APC10 coefficient of variance (CoV) at 11%, cold MPEC CoV at 17% and hot MPEC CoV at 13%. Across the 3 instruments, highest PN emissions results are consistently seen from P7, P1, P6 and P5, while lowest emissions results are seen from P8, P4, P9 and P2. Anomalously cold MPEC values for P5 were observed, which are lower than hot MPEC values. This may suggest an issue with either the hot or cold instrument, or an artefact of particle formation in the hot MPEC caused by more abundant low volatility species in the P5 sample aerosol than the samples of other pads. Potentially, these low volatility species could fully, or partially, evaporate in the evaporation tube of the hot MPEC and recondense downstream into numerous small particles. This would result in the hot MPEC reporting higher emissions than the cold MPEC. The APC10 (equipped with a catalytic stripper which is highly effective at eliminating volatiles) results support the hot MPEC data rather than the cold MPEC data, which suggests there may have been an issue with the cold MPEC during that sequence of tests. Table 8-4 shows APC10 emissions from the pads, arranged from low to high (left to right) and indicates that the highest PN emissions pad, 5, emits ~2.5x higher than the lowest pad, P8.

Table 8-4: APC10 emissions (#/km) from PG42 cycles, in ascending order by pad number

Pad number	8	4	9	2	3	7	1	6	5
#/km	1.06E+09	1.2E+09	1.35E+09	1.44E+09	1.62E+09	1.81E+09	2.08E+09	2.13E+09	2.67E+09
Normalised	1.00	1.13	1.27	1.35	1.53	1.70	1.96	2.00	2.51
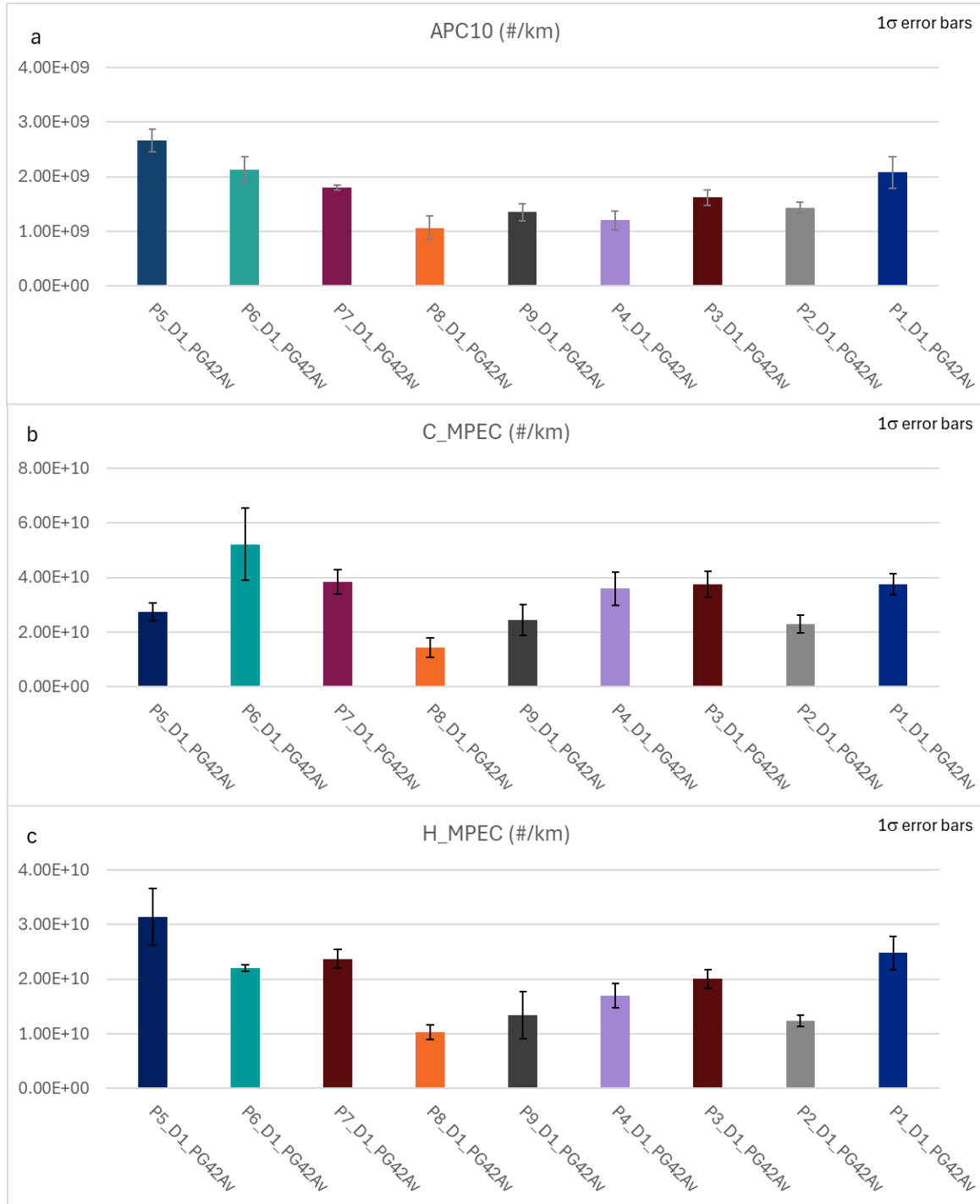
Figure 8-11: Comparative PN results from triplicate PG42 tests at 1900 kg as shown for the a) APC, b) cold MPEC and c) hot MPEC.

Results from the cold MPEC (Table 8-5) indicate a higher differential between lowest and highest emitting pads than the APC10 and hot MPEC (Table 8-6), which likely indicates that the levels of volatile materials emitted by the pads vary. These volatiles influence the APC10 results least, as it has the greatest ability to eliminate volatiles, the hot MPEC next and the cold MPEC most.

Table 8-5: Cold MPEC emissions (#/km) from PG42 cycles, in ascending order by pad number

Pad number	8	2	9	5	4	3	1	7	6
#/km	1.43E+10	2.28E+10	2.45E+10	2.74E+10	3.6E+10	3.74E+10	3.75E+10	3.84E+10	5.22E+10
Normalised	1.00	1.59	1.71	1.91	2.51	2.61	2.61	2.68	3.64

Table 8-6: Hot MPEC emissions (#/km) from PG42 cycles, in ascending order by pad number

Pad number	8	2	9	4	3	6	7	1	5
#/km	1.02E+10	1.24E+10	1.34E+10	1.7E+10	2E+10	2.2E+10	2.37E+10	2.48E+10	3.14E+10
Normalised	1.00	1.21	1.31	1.67	1.96	2.16	2.32	2.43	3.08

The comparative gravimetric PM and eFilter real-time results show similar effects to PN (Figure 8-12a, b respectively), with highest emissions from P5, P6, P7 and P1 and lowest emissions from P8, P2 and P9. Emissions range from 0.91 mg/km (P8) to 3.46 mg/km (P1) using the gravimetric method. eFilter data, shown in Figure 8-12b is intended to be scaled to equate to the gravimetric data shown in Figure 8-12a, so that real-time PM production can be studied, but comparative results strongly resemble those of the gravimetric mass approach.
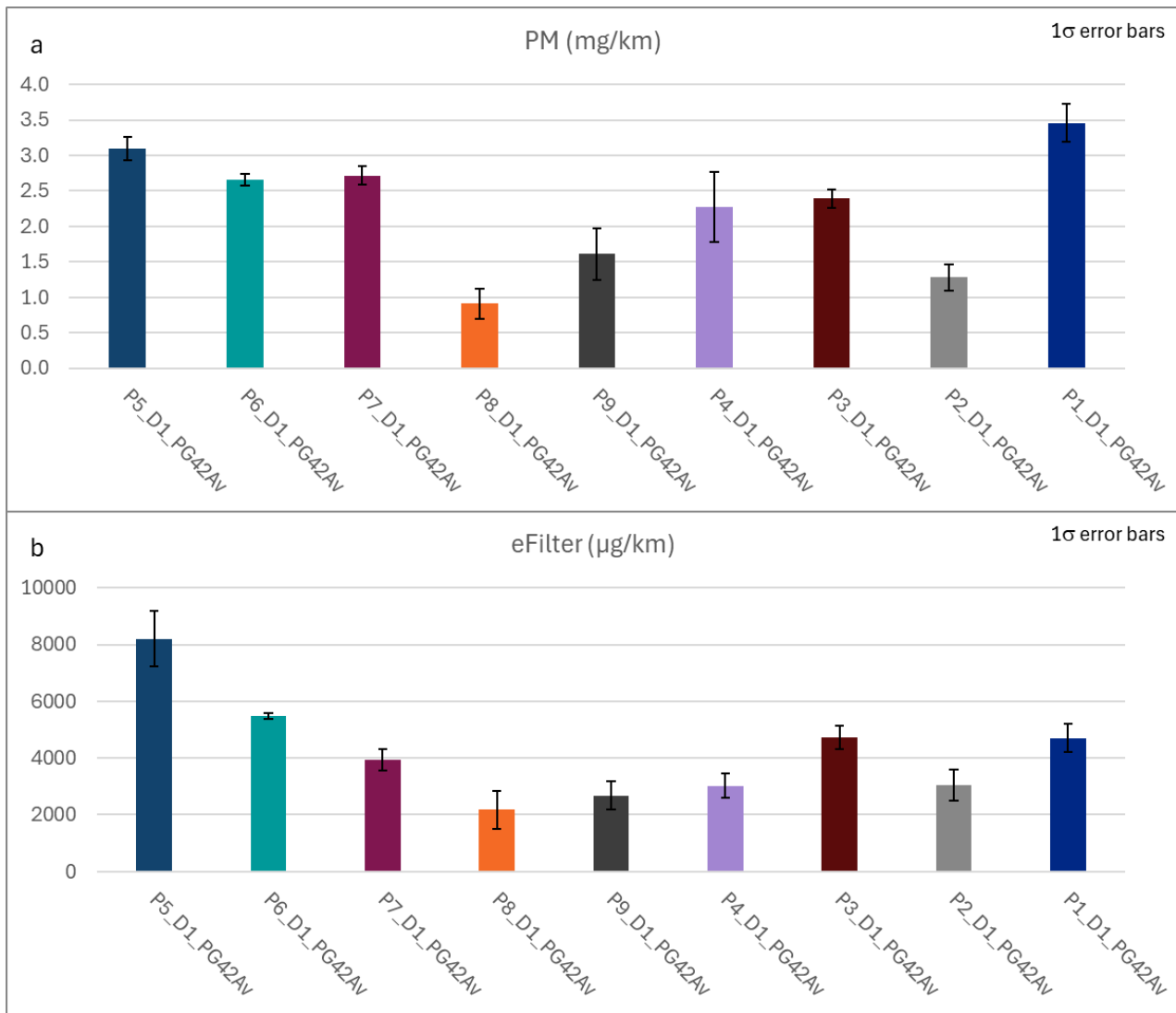
Figure 8-12: Comparative PM results from PG42 tests at 1900 kg as shown for a) gravimetric PM and b) eFilter PM.

PM emissions quantification includes both solid and volatile components, and the ratios of lowest to highest PM emissions from the gravimetric (Table 8-7) and real-time method (Table 8-8) are similar to that seen for the cold MPEC, with those three results in the range 3.55 to 3.81x.

Table 8-7: Gravimetric PM emissions (#/km) from PG42 cycles, in ascending order by pad number

Pad number	8	2	9	4	3	6	7	5	1
mg/km	0.91	1.28	1.61	2.27	2.39	2.66	2.72	3.09	3.46
Normalised	1.00	1.41	1.77	2.51	2.64	2.93	3.00	3.41	3.81

Table 8-8: eFilter PM emissions (#/km) from PG42 cycles, in ascending order by pad number

Pad number	8	2	9	4	6	3	7	5	1
µg/km	166.4	250.3	306.3	421.2	456.4	468.5	514.7	516.0	591.7
Normalised	1.00	1.50	1.84	2.53	2.74	2.81	3.09	3.10	3.55

In terms of both PN and PM, three of the four lowest emitting brake pads (over the PG42 cycle) are sold as low dust, or low metallic pads though, interestingly, budget pad P2 also shows consistently low emissions.

The highest $PM_{2.5}$ and PN10 emitting pads were not as consistently identifiable, but P7, P5 and P1 were always amongst the highest emitters. P7 was identified as low dust, P5 as high organic content (which may displace some metals) and P1 as a premium product. It seems that based upon current descriptors of pads, it is not possible to identify a low $PM_{2.5}$ or PN10 emitting product, albeit that the descriptors may still be valid for total wear and other characteristics such as extended life.

Figure 8-13 shows real-time particle number and mass emissions signals from the APC10, cold MPEC, hot MPEC and eFilter respectively, comparing a high emitting pad, P5, with a low emitting pad, P8. From these figures, it is clear that with both pads particulate emissions are produced in response to the same transient events irrespective of whether mass or number are considered, and if the measurand includes volatiles, or not. Emissions from P8 may be slightly higher than those of P5 in the first ~800s, but after that emissions from P5 dominate. These differences do not appear to be related to enclosed pad temperature, as consistently these temperatures are higher from P8 than from P5, but overall P8 emissions are substantially lower (Figure 8-14).
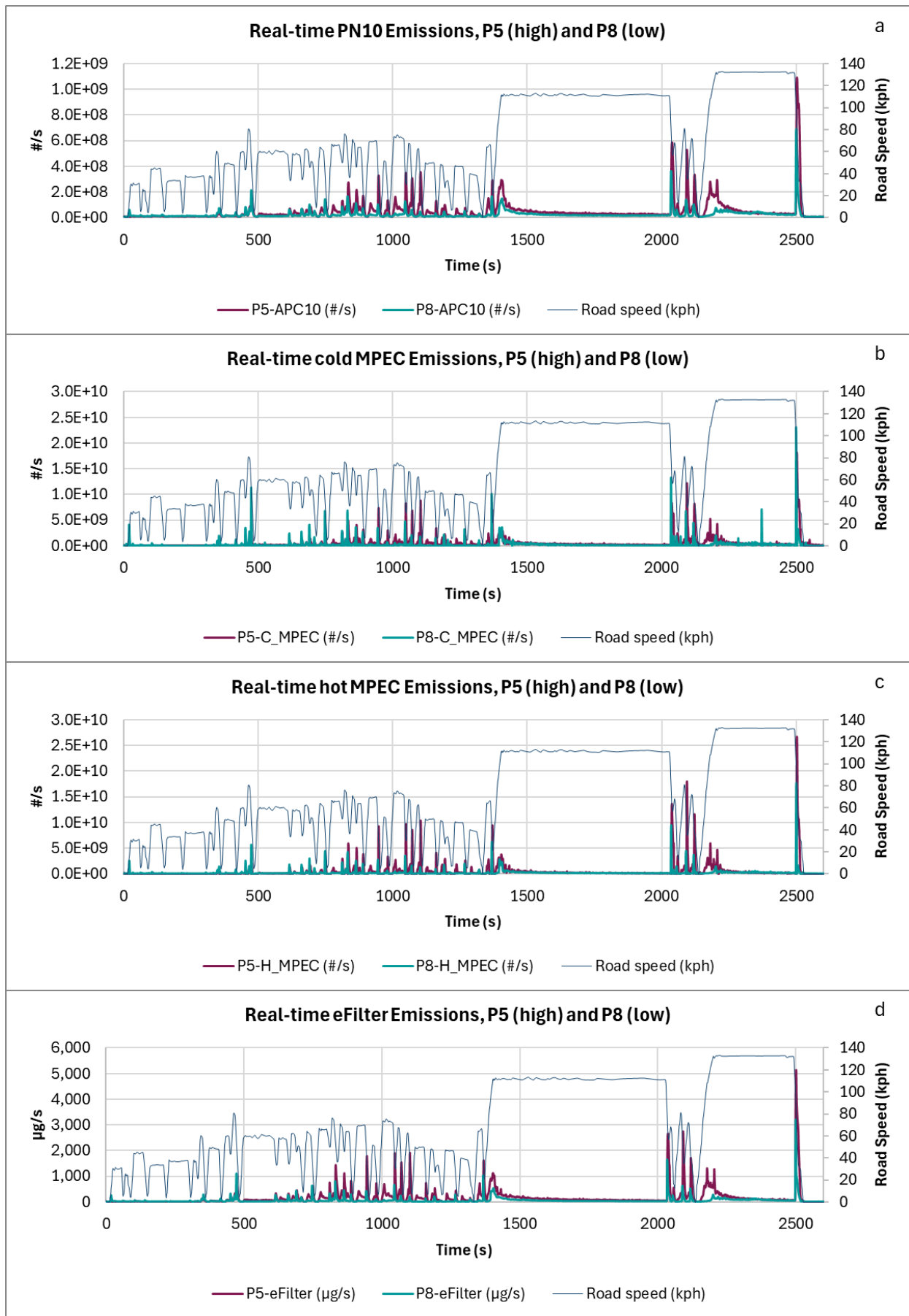
Figure 8-13: Real-time particulate emissions, P5 and P8 during PG42 cycles from the a) APC10, b) cold MPEC, c) hot MPEC and d) eFilter.

The chemical composition of the pads must play a major role in the emissions observed, but also it appears that P8 cools more rapidly than P5, as can be seen in the long cruise between ~1400s and 2050s in Figure 8-14, and heats up more rapidly (~2050s to 2150s). This is indicative of the different thermo-physical properties of P8. It is likely that P8 either contains less volatile material or much lower volatility materials than P5.
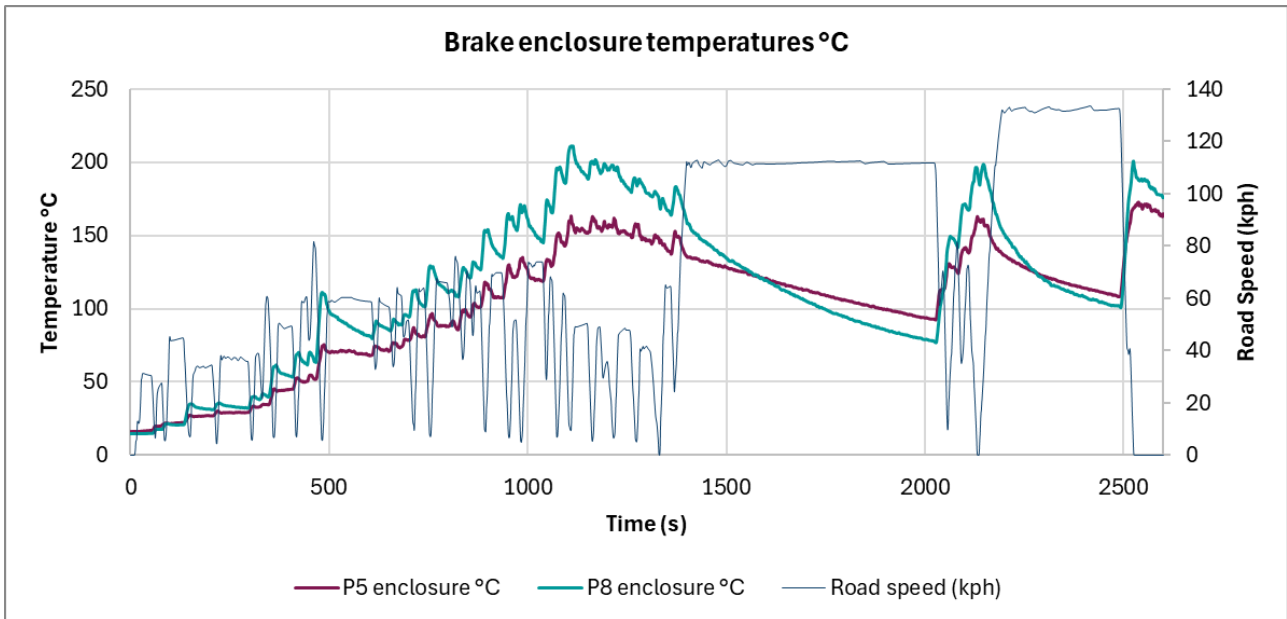
Figure 8-14: Enclosed pad temperatures during PG42 cycles, P5 and P8.

8.3.3.2   Pad variants – Dyno RDE tests at 1900 kg and 2100 kg

One-off chassis dynamometer RDE tests were conducted at both 1900 kg and 2100 kg test masses: these enable both pad-to-pad comparisons to be made, and the effect of increased test mass on to be assessed. The test mass effect is described independently in Section 0. Since the 1900 kg test and 2100 kg test are both singular tests, the percentage standard deviations (CoV) determined from the PG42 tests, also conducted on the chassis dynamometer, are applied to these data in Figure 8-15 (PN instrument results) and Figure 8-16 (PM instrument results) to indicate the potential scatter of the data. In these figures the 1900 kg and 2100 kg results are shown as pairs of bars for each pad variant. The initial plain bar shows the 1900 kg result and the subsequent dotted bar shows the 2100 kg result.
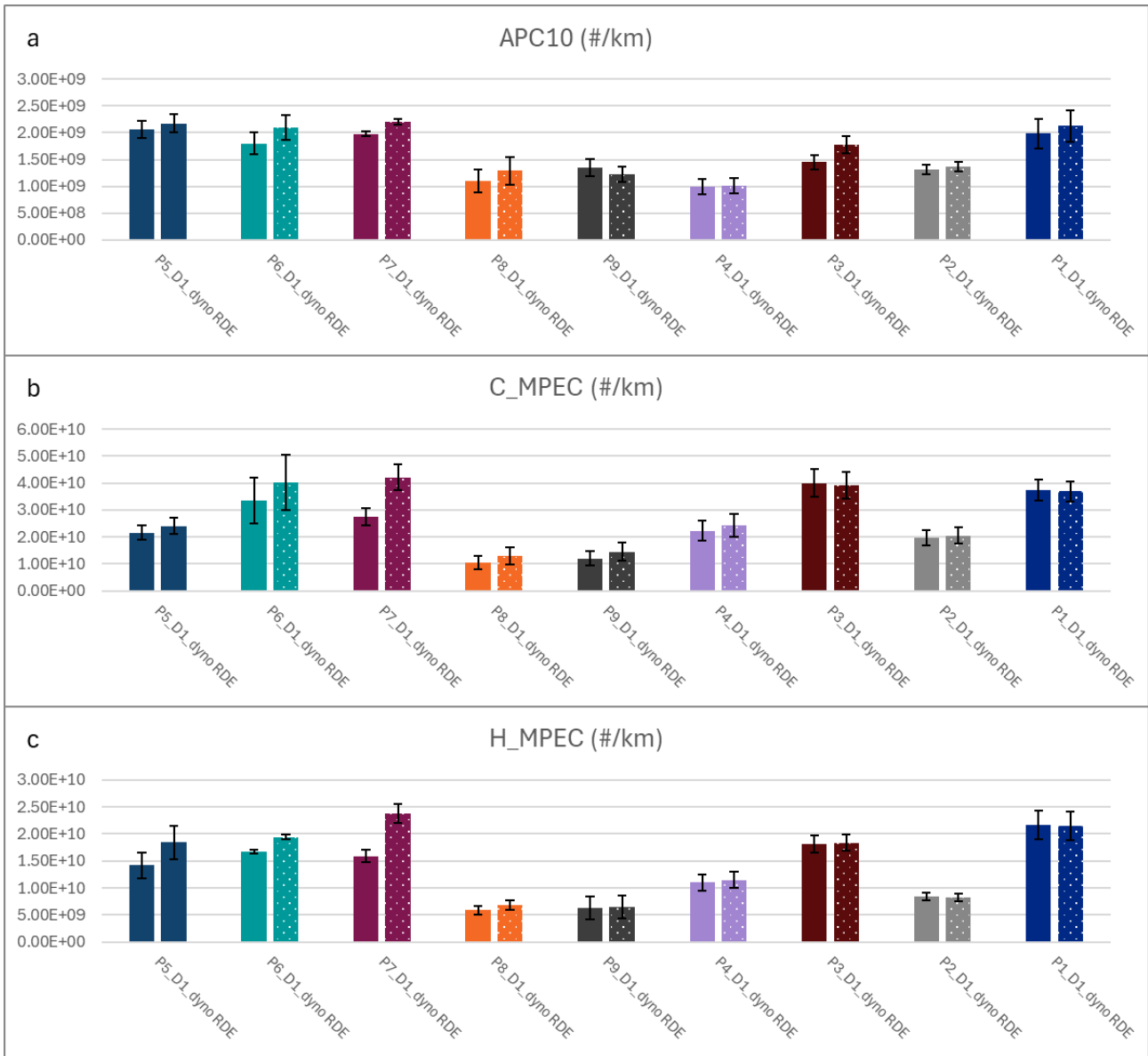
Figure 8-15: PN emissions from chassis dyno RDE tests at 1900 kg and 2100 kg measured by the a) APC, b) cold MPEC and c) hot MPEC.

The pads with lowest PN emissions (Figure 8-15a-c) measured with the APC10 and both MPECs are, as observed with the PG42 tests, P8, P9, P4 and P2, while P7, P5 and P1 remain amongst the highest emitters. Similarly, P8, P9 and P2 clearly have the lowest $PM_{2.5}$ emissions, while P4 is also lower than the other 5 pad variants (Figure 8-16a,b).

These observations are consistent with findings from the PG42 tests. There are limited emissions differences in either PN or PM between the 1900 kg and 2100 kg tests, although where differences are observed and potentially significant, emissions appear higher from the 2100 kg tests.
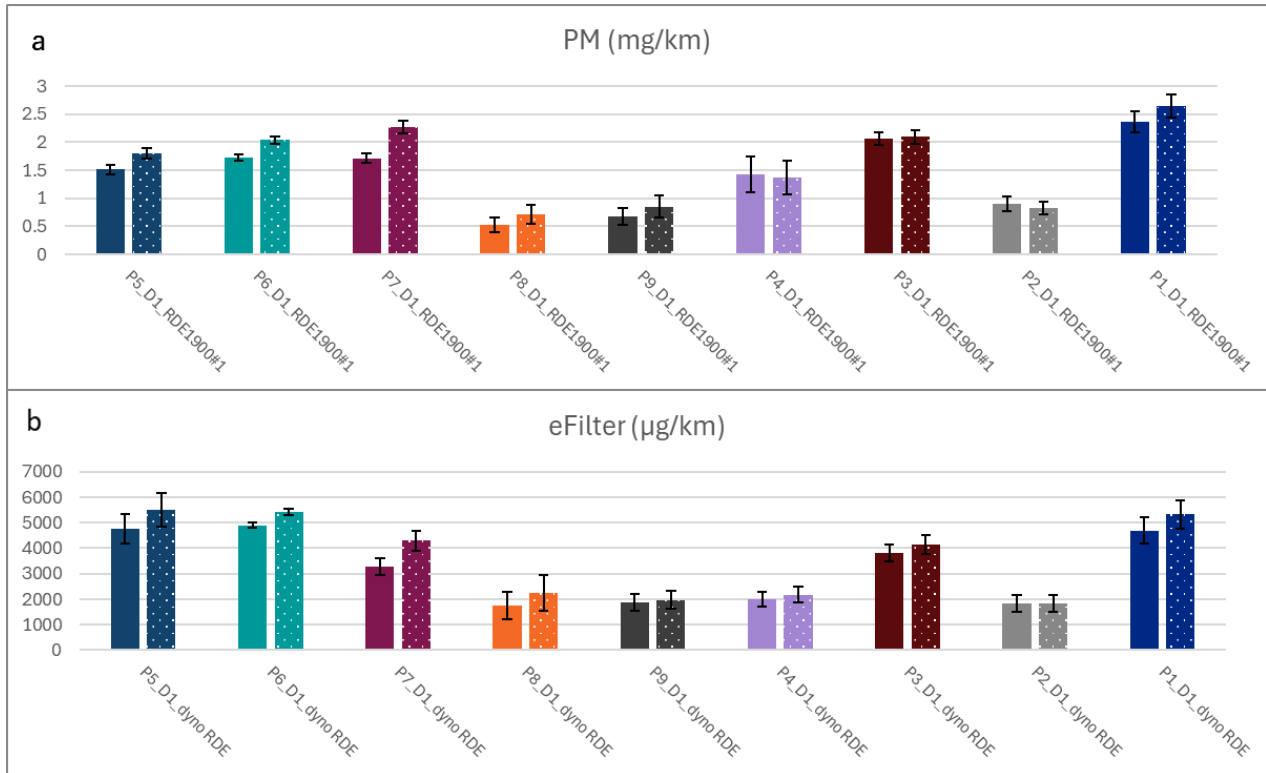
Figure 8-16: PM emissions from chassis dyno RDE tests at 1900 kg and 2100 kg

The ratios of lowest to highest emissions on the dyno RDE cycles also broadly agree with the results of the PG42 tests. These clearly indicate the lowest ratios for the APC10 and higher ratios for the instruments that detect volatile particles (Table 8-9) and generally similar ratios to the PG42 tests (<~2.5 for the APC10 and > 3 for the other approaches). Ratios from the higher test mass 2100 kg tests also tended to show higher values than the 1900 kg tests, potentially through greater heat input to the pad & disc pairing liberating more volatile materials from the pads with formulations most susceptible to volatile loss.

Table 8-9: Emissions and emissions ratios from the highest and lowest emitting pads on the dyno RDE cycles

	Min 1900 kg tests	Min 2100 kg tests	Max 1900 kg tests	Max 2100 kg tests	Max/Min 1900 kg tests	Max/Min 2100 kg tests
APC10 (#/km)	1.00E+09	1.01E+09	2.06E+09	2.21E+09	2.06	2.19
CMPEC (#/km)	1.04E+10	1.06E+10	3.99E+10	4.20E+10	3.85	3.96
HMPEC (#/km)	5.86E+09	6.50E+09	2.17E+10	2.38E+10	3.71	3.67
eFilter (µg/km)	2.52E+02	2.28E+02	7.66E+02	1.01E+03	3.04	4.42
Filter PM (mg/km)	0.53 (P8)	0.71 (P8)	2.36 (P1)	2.64 (P1)	4.50	3.72

8.3.3.3 Pad variants – On road RDE

From on-road RDE tests, emissions measurements are confined to the mobile systems, namely the MPECs and the eFilter. Triplicate tests were performed and the standard deviation of those three tests is shown as error bars in Figure 8-17a-d, which compares emissions from the pad variants. It should be noted that the on-road RDE tests would be expected to show higher variability than the chassis dyno RDE tests, since although the route is fixed, the ability of the driver to exactly replicate how the route is driven is confounded by factors such as the weather and the influence of other road users.

Nevertheless, it is apparent that across the instruments and metrics used, the lowest emitting pads are definitely P8 and P9, with P4 emissions also relatively low, while highest emissions are from P1.
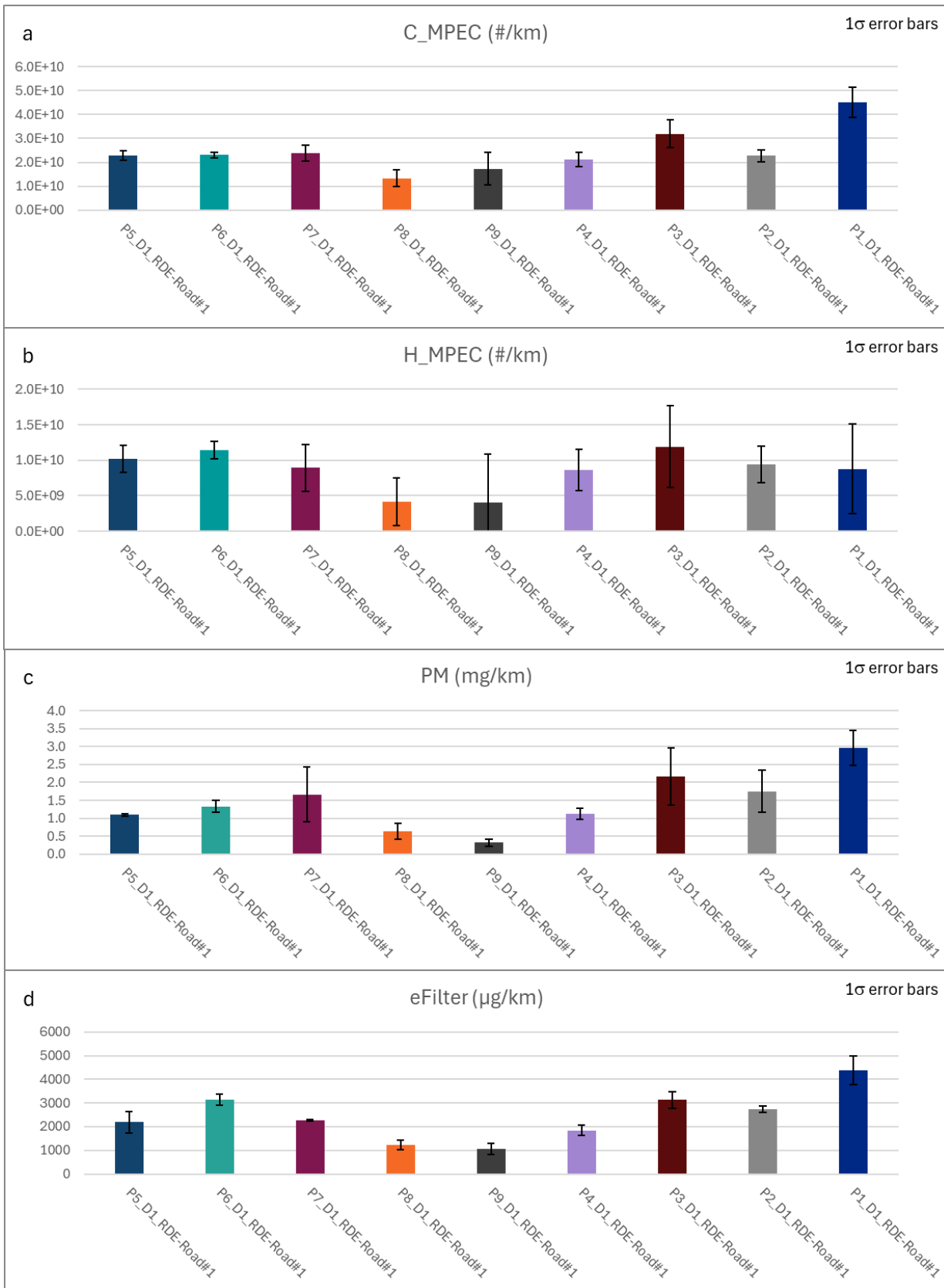
Figure 8-17: PN and PM emissions from on-road RDE tests at ~1900 kg measured by a) cold MPEC b) hot MPEC, c) gravimetric PM and d) eFilter.

This data highlights that chassis dyno cycles and on-road RDE tests show the same trends, but that, due to improved repeatability, greater discrimination is possible, and a wider variety of measurement systems can be used, in the laboratory.

Max/Min ratios from the road RDE, where the Caddy's natural weight when loaded with the measurement systems is approximately 1900 kg, were generally similar to those from the chassis dyno RDE tests conducted at 1900 kg (Table 8-10).

Table 8-10: Emissions ratios from the highest and lowest emitting pads on the dyno and road RDE cycles

	Road RDE Min	Road RDE Max	Road RDE Max/Min	Dyn 1900 kg Max/Min
CMPEC (#/km)	1.33E+10	4.51E+10	3.38	3.96
HMPEC (#/km)	3.99E+09	1.19E+10	2.98	3.67
eFilter (µg/km)	1062.26	4386.11	4.13	4.42
Filter PM (mg/km)	0.32	2.97	9.23	3.72
*Filter PM (mg/km)	0.64	2.97	4.63	3.72

*One potential anomaly is the high Max/Min ratio for gravimetric PM, where Pad 9 gave a very low mean emissions result (0.32 mg/km). The next lowest emitting pad, P8 (consistently the lowest emitting pad in other cycles' data), gave a result of 0.64 mg/km and if this is used to calculate the Max/Min a value more consistent with other cycles is obtained.

8.3.3.4 Emissions magnitudes and emissions factors

In this section, the objective of generating emissions factors for PN10 and PM$_{2.5}$ emissions is given initial consideration. This is achieved using the various chassis dyno cycles' and the on-road RDE emissions test results.

The average emissions results from the APC10, MPECs and eFilter, for the 9 different pad variants and PG42, dyno RDE (1900 kg and 2100 kg tests) and on-road RDE were compiled. On instrument and cycle-specific bases, the average emissions across all pads, and relevant standard deviations were calculated. Across all cycles and instruments, the standard deviations were in the range 30-40%. The resultant mean values represent a cross-section of emissions from each instrument and driving cycle. These data are compared graphically between the various drive cycles for APC10, cold MPEC, hot MPEC, eFilter real-time and eFilter gravimetry respectively, in Figure 8-18a-e.

From the APC10 (Figure 8-18a), used only during chassis dynamometer tests, particle number (PN10) emissions were similar across the PG42 and both RDE cycles with an average emissions rate of ~1.6x10^9 #/km. From the chassis dyno cycles, emissions from the hot MPEC (Figure 8-18c) ranged from ~1.3 to 1.9x10^{10} #/km, with road RDE emissions lower at ~ 8.6x10^9 #/km. However, total particle number emissions from cold MPEC, Figure 8-18b, were similar across road and chassis dyno RDE cycles: in the range 2.46 to 2.83x10^{10} #/km, with PG42 emissions higher at ~3.2x10^{10} #/km. Considering that the MPEC systems report higher than the APC10 (discussed elsewhere, e.g. Sections 5.2.1 and 12), if an analyser similar to the APC10 was employed for on-road PN measurements during the RDE testing, it can be roughly estimated - using the relationship between APC10 and hot MPEC in the dyno cycles - that emissions of non-volatile PN10 would be observed in the range 0.72x10^9 #/km to 1.05x10^9 #/km.

Mean gravimetric PM$_{2.5}$ emissions, as shown in Figure 8-18e, were consistent across RDE cycles, including both road and chassis dyno, in the range 1.43 to 1.52 mg/km, while PG42 cycle emissions were substantially higher, at an average of 2.27 mg/km.

PM calculated using the real-time eFilter signal, shows a slightly lower response for the road RDE tests than for the chassis dyno tests, though not significantly so. The eFilter real-time signal is intended to be normalised to the simultaneously collected filter PM.
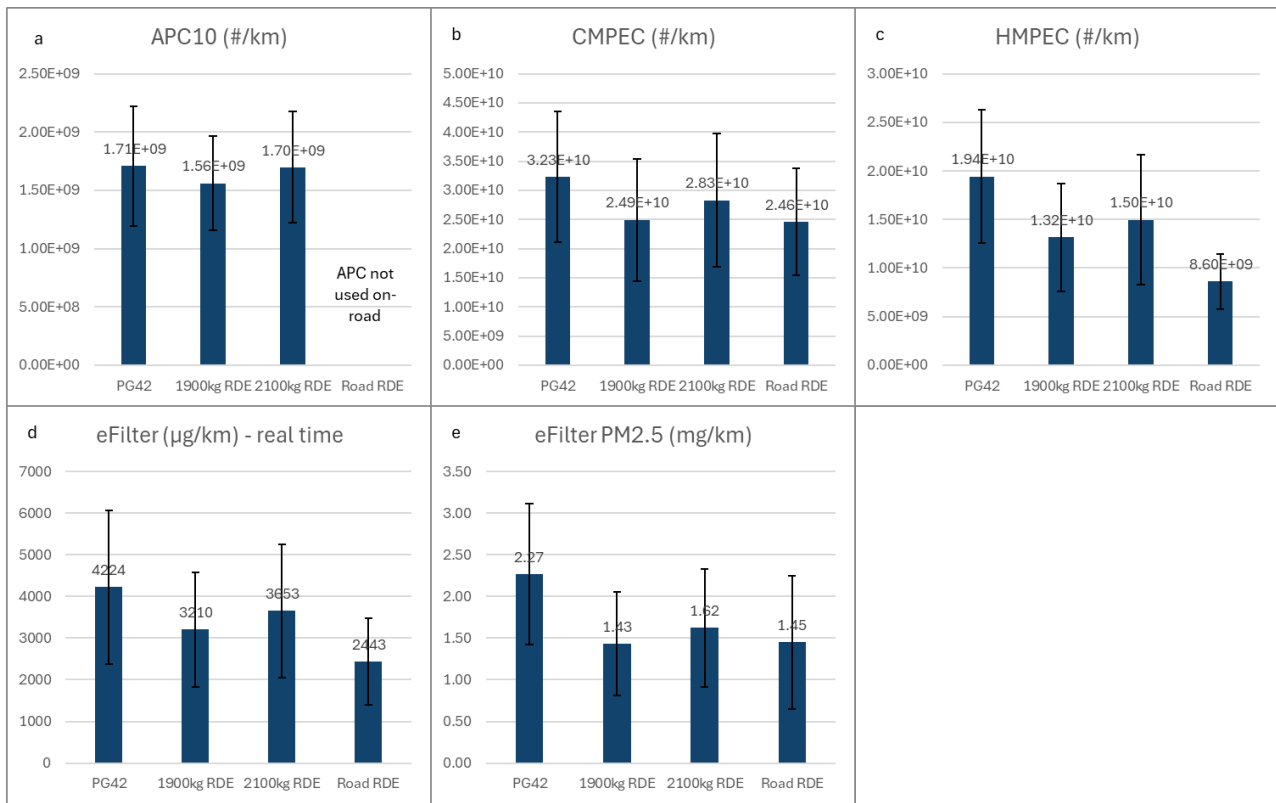
Figure 8-18: Brake emissions results averaged across all pad variants for the different test cycles as measured by a) APC, b) cold MPEC, c) hot MPEC, d) gravimetric PM and e) eFilter.

8.3.3.5 Relationship between emissions levels and brake pad cost

Comparisons between normalised brake pad cost and normalised $PM_{2.5}$ (mg/km) and $PN10$ (#/km) emissions are shown in Figure 8-19. There is no obvious correlation between lower emissions and higher cost, for either $PN10$ or $PM_{2.5}$ emissions.
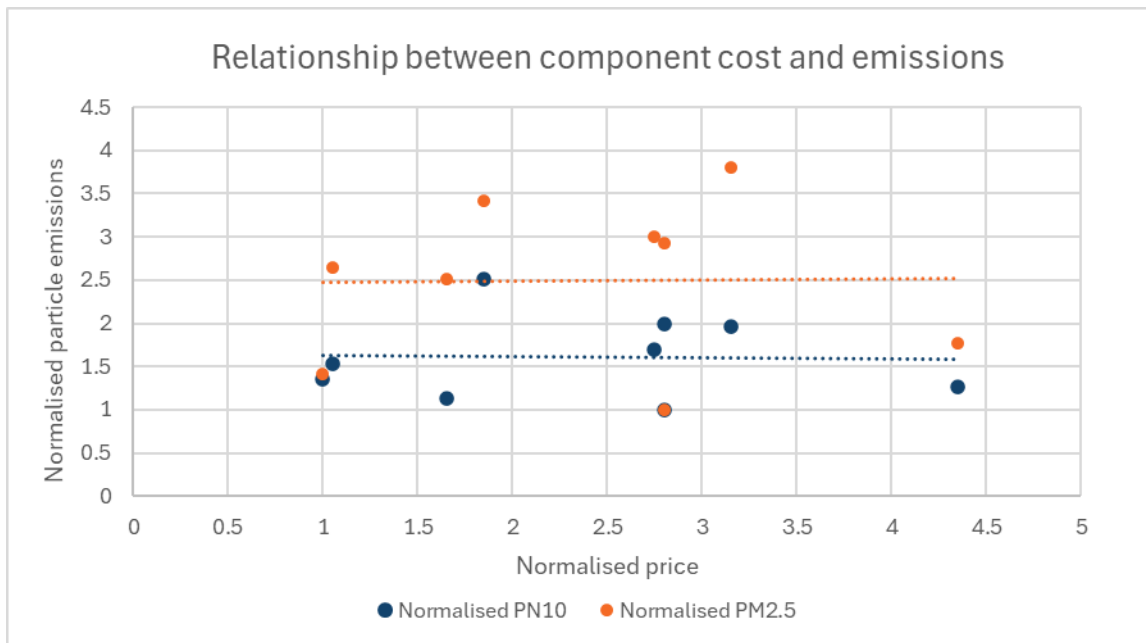

Figure 8-19: Relationship of $PM_{2.5}$ and $PN10$ emissions with brake pad cost.

8.3.4 Effects of increasing Chassis dynamometer RDE test mass from 1900 kg to 2100 kg

The impact of adding 200 kg to the weight of a test vehicle (noting that this does not exceed the GVW) was studied through comparison of the dynamometer RDE tests conducted at 1900 kg and 2100 kg. This increase would be the equivalent of carrying 2 additional 80 kg passengers each with a 20 kg suitcase. Although a visual comparison of 1900 kg and 2100 kg data can be made using Figure 8-15 and Figure 8-16 in Section 8.3.3.2, a regression analysis provides an improved way of visualising any effects of the higher test mass. Data from the comparison, shown in Figure 8-20 are drawn from P1 to P9 inclusive.

Figure 8-20a-c show that PN emissions as measured by APC10, hot MPEC and cold MPEC are ~9%, 13% and 11.5% respectively, higher at 2100 kg test mass than at 1900 kg test mass. An origin is forced on these charts since there is no reason to anticipate any offset when the same instruments, test facility and vehicle are used in th experiment. The differential in PN emissions between 2100 kg and 1900 kg tests is consistent with the ~10.5% increase in test mass applied.
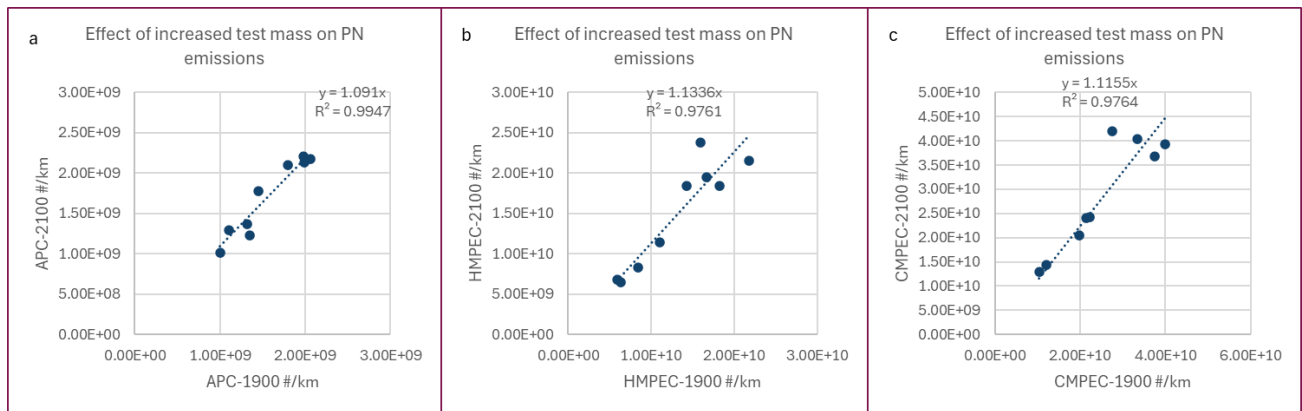
Figure 8-20: Correlations between 1900 kg and 2100 kg test mass PN results on chassis dyno RDE cycles as measured by a) APC, b) hot MPEC and c) cold MPEC.

Correlations between gravimetric and eFilter real-time PM emissions also show emissions increases with high test mass (Figure 8-21), gravimetric $PM_{2.5}$ emissions being increased by ~12.5% and eFilter real-time results by ~14%.
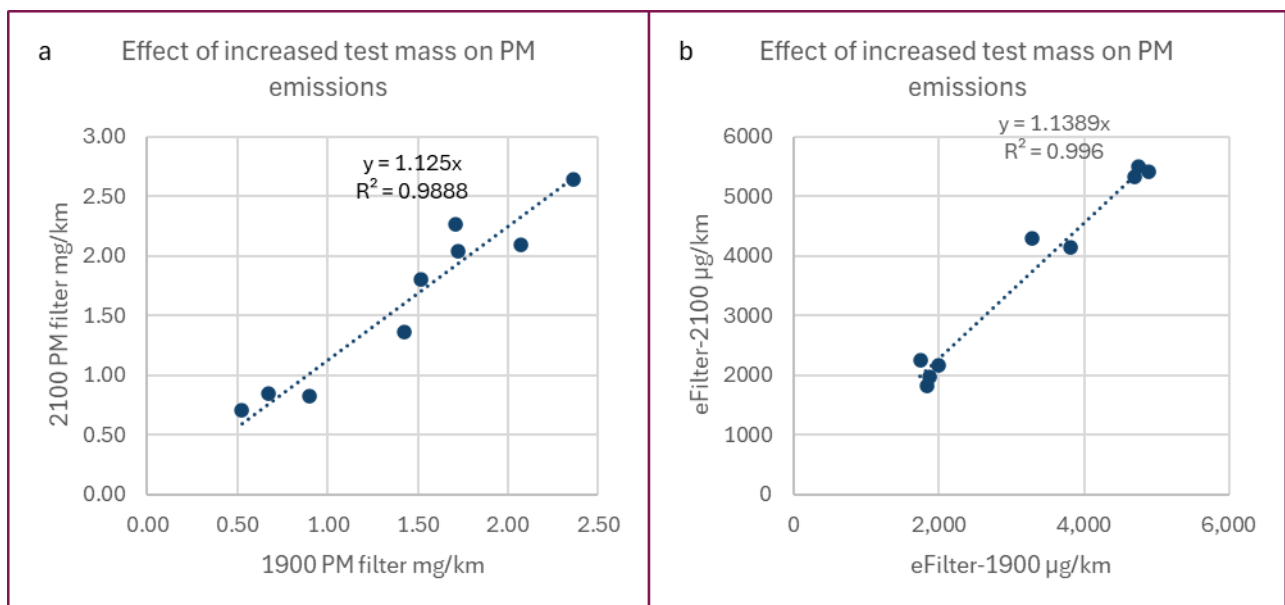
Figure 8-21: Correlations between 1900 kg and 2100 kg test mass PM results on chassis dyno RDE cycles

8.3.5 Drive-by testing

Drive-by testing included gentle (gen), moderate (mod) and dynamic (dyn) driving tested sequentially in that order, with 5 repeated braking events conducted at 5 different speeds, resulting in 25 braking events per mode.

Tests were conducted on all pads with the Caddy at its normal weight of 1900 kg. One additional test was performed using P1 and D1 under dynamic braking only, with the vehicle loaded to 2100 kg. This test can be identified as P1D1*.

As the tests progressed, the braking system became progressively hotter and so in effect emissions and temperature data was acquired. Both the enclosed braking system and unenclosed braking system were monitored, through the use of disc-based rubbing thermocouples.

PN measurements were made using hot and cold MPEC instruments, with real-time mass measured using the eFilter. One cumulative $PM_{2.5}$ filter was collected across all gen, mod and dyn testing combined on each pad + disc combination.

It should be noted that during the moderate braking tests of one pad and disc combination (P2D1) the cold MPEC recorded no data. However, there was a strong correlation between the hot MPEC response and the cold MPEC response from the gentle and the dynamic braking (Figure 8-22) that bracketed the moderate tests both in terms of disc temperatures and chronologically. The moderate braking cold MPEC data was therefore simulated using the relationship in Figure 8-22 and the hot MPEC results.

The relationship between the cold MPEC and hot MPEC in Figure 8-22 indicates around 20% lower PN levels from the hot MPEC than from the cold MPEC. This is consistent with the approximate level of thermophoretic losses present in the hot MPEC and may indicate that the level of volatile materials present is relatively low.
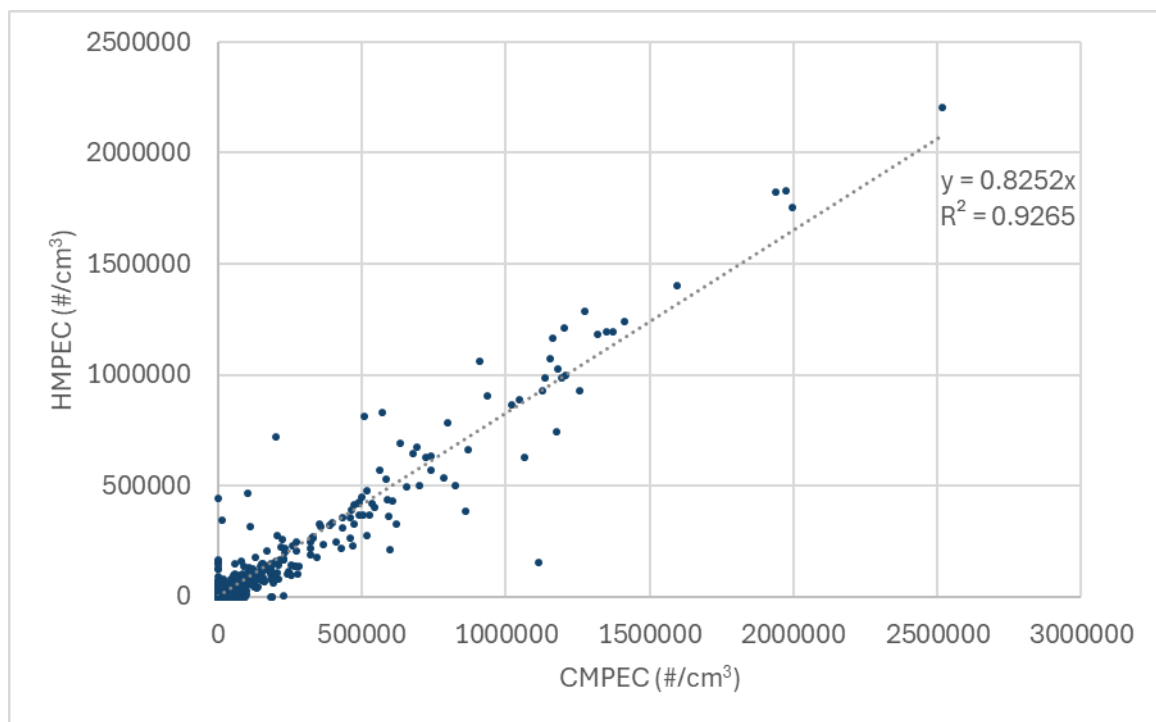
Figure 8-22: Relationship between hot and cold MPEC results, P2D1 - gentle and dynamic braking.

8.3.5.1 Emissions, braking styles and disc temperatures

As reported in previous sections (e.g., 8.3.3) different brake pads have been observed to generate different emissions levels under nominally identical drive cycle conditions. The same is true of discrete braking events executed during the gentle, normal and dynamic testing.

As Figure 8-23 shows, at all speeds, brake temperatures increase from gentle to moderate to dynamic braking, with temperatures broadly similar between different pads. The same driver was used for the braking experiments, but there will have been some natural variability in their behaviour.
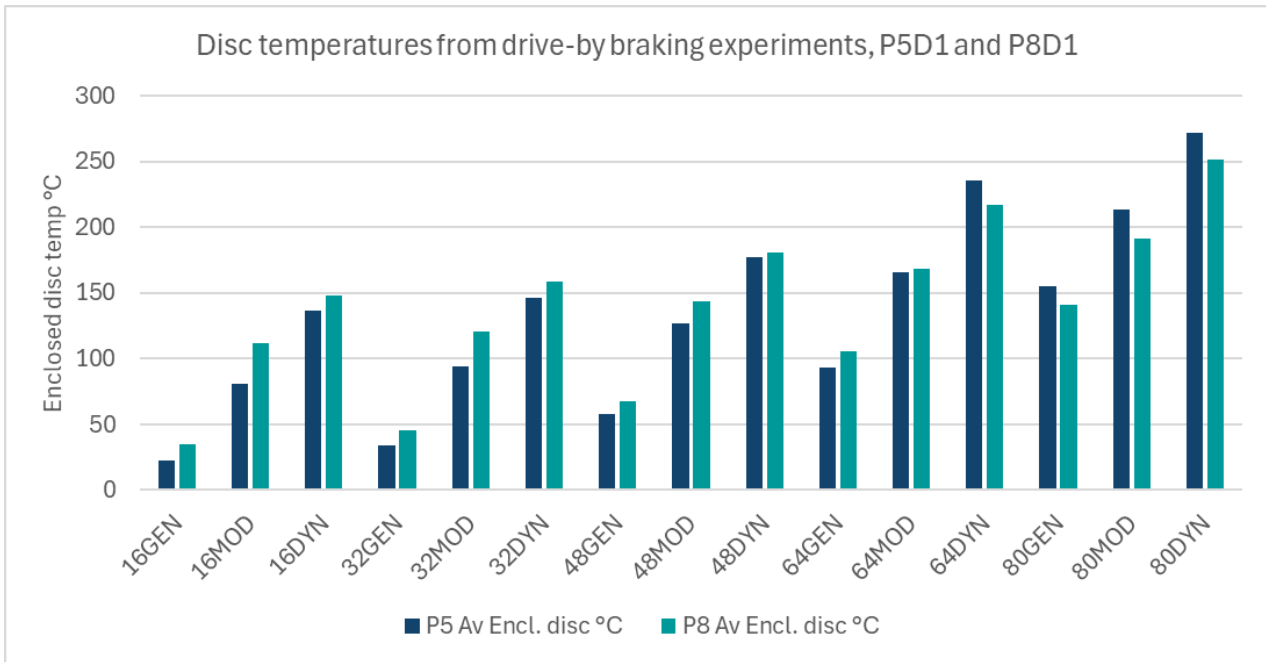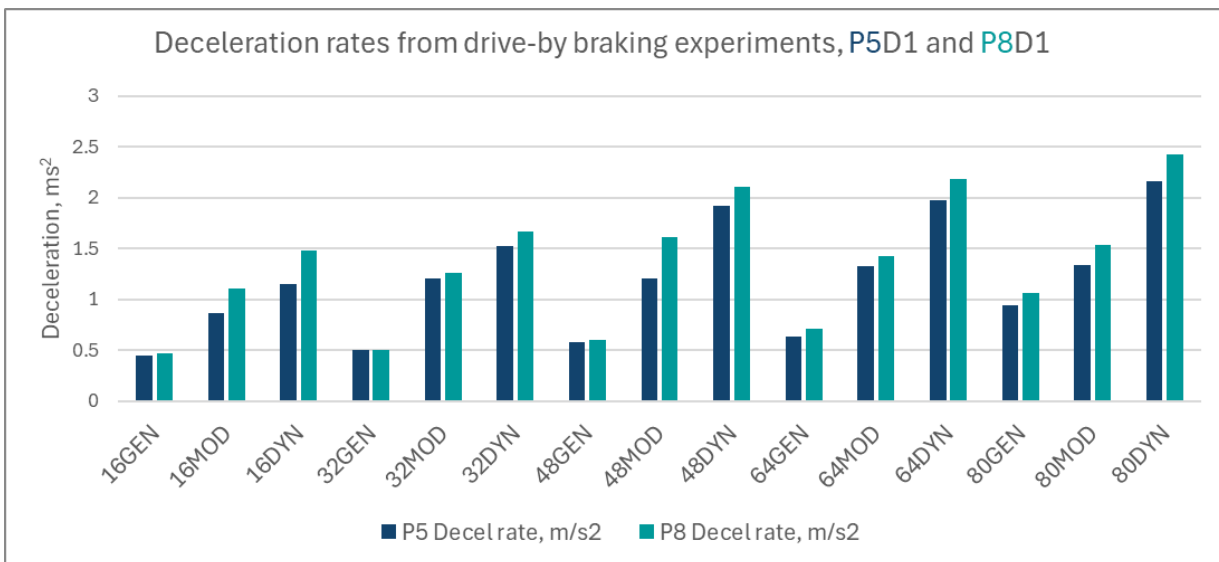
Figure 8-23: Comparative disc temperatures during gentle, moderate & dynamic braking, for high (P5) & low (P8) emitting pads.

As a consequence, we do see some differences in the deceleration rates under gentle, normal and dynamic braking which could potentially lead to different temperatures and emissions levels. Figure 8-24, for example, consistently shows higher deceleration rates from P8 than from P5. It should be noted however, that the composition of pads is also likely to be a factor in the temperature observed since, for example, braking events from 80kph show lower disc temperatures from P8 (Figure 8-23) despite higher deceleration rates, and overall P5 requires lower deceleration rates to reach a given temperature than P8 (Figure 8-25).

Figure 8-24: Comparative deceleration rates during gentle, moderate & dynamic braking, for high (P5) & low (P8) emitting pads.
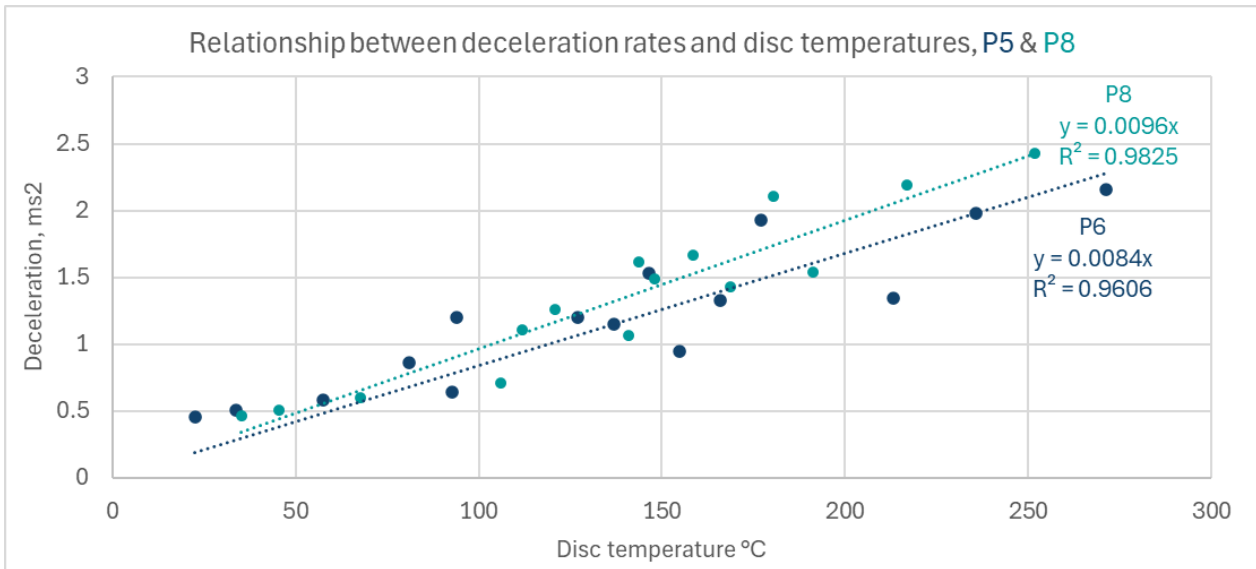
Figure 8-25: Relationship between disc temperature and deceleration rate for P5 and P8.

As reported in the Phase 1 study, the sampling approach used required the brake pad, calliper and disc to be enclosed and which relies on the filtered air passing through the enclosure to cool it, does not fully enable the enclosed disc to match the unenclosed disc temperature. The unenclosed and enclosed disc temperatures are well correlated though, as shown in Figure 8-26. However, there are variances between pads e.g., for P7 and P8 (Figure 8-27), which may be due to exotherms produced by volatile components combusting during braking; differences in heat rejection from different pad types; differences in pad and disc contact areas and contact durations related to formulations, or to other - or combinations of - factors.

PN and PM emissions measured from an enclosure are likely to be over-estimates of the actual emissions compared to an identical but unenclosed pad and disc pair.
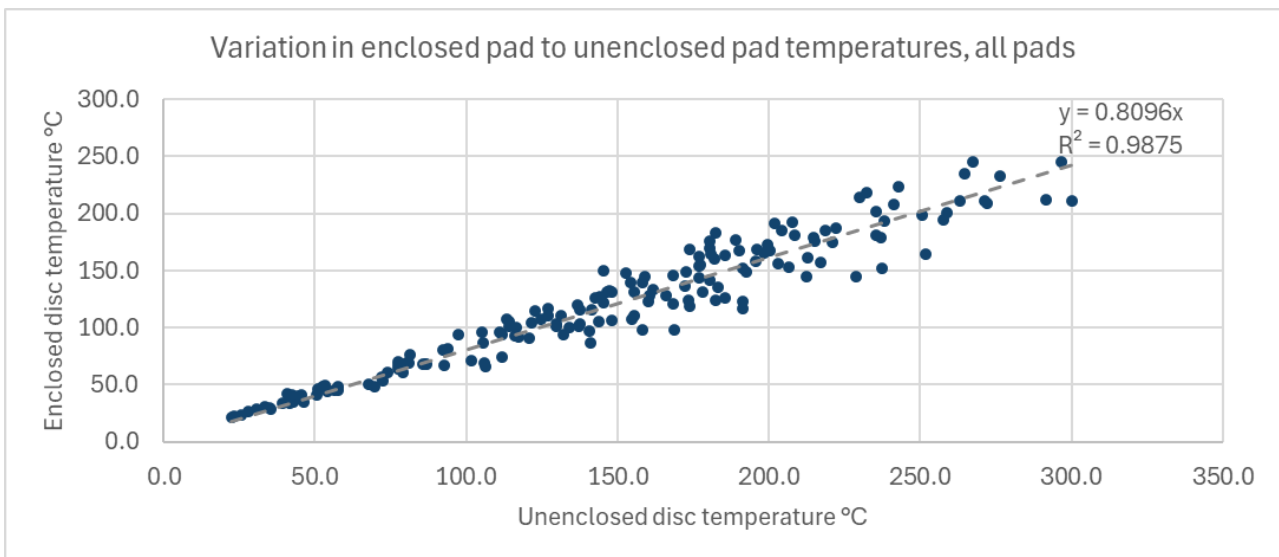
Figure 8-26: Variation in enclosed pad to unenclosed pad temperatures, all pads.
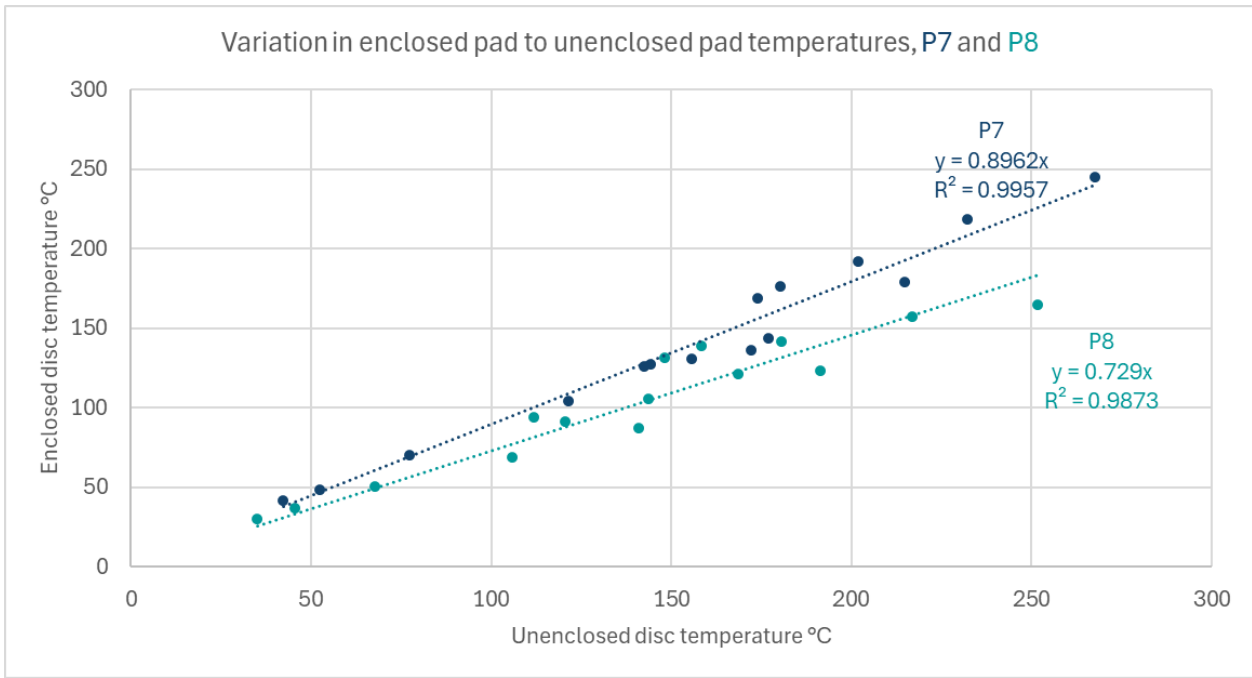
Figure 8-27: Variation in enclosed pad to unenclosed pad temperatures, P7 and P8.

8.3.5.2 Aged vs. newer pads (P1D1 & P10AD1), and budget vs. premium discs (P1D1 & P1D2)

Emissions versus temperature curves from P1D1, P1D2 and P10AD1 drive-by tests are shown in Figure 8-28a, b and c for cold MPEC, hot MPEC and eFilter data respectively. Each chart shows the R^2 value for an exponential fit to the instantaneous particles/s data and corresponding temperature. The following observations can be made:

- Emissions of both eFilter and MPECs are lowest from P10A, higher from P1D1 and highest from P1D2. This is broadly in-line with observations from chassis dyno cycles

- Exponential curve fits provide a reasonable fit for P1D2, better for P1D1 data, and an excellent fit for P10A data. P10A is the highly aged pad and D1 is more aged than D2. Potentially the "curing" of the disc and pad with age modifies the emissions characteristics of the disc and pad combination. This may be related to changes in volatile loss from the pads and discs over time.

- The poorest exponential fit with P1D2 would be related to disc evolutionary effects rather than the pad, and this suggests that both pads and discs are important influences on both volatile and solid particle emissions
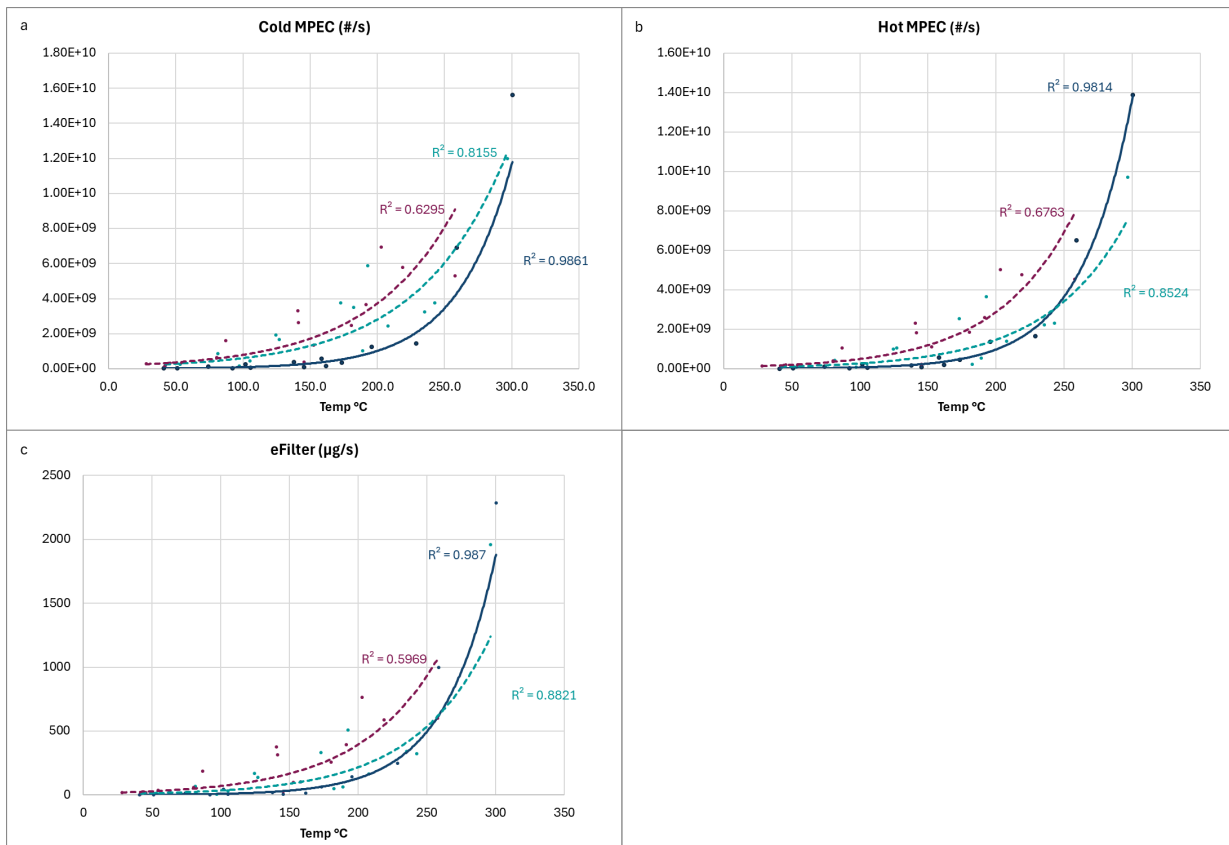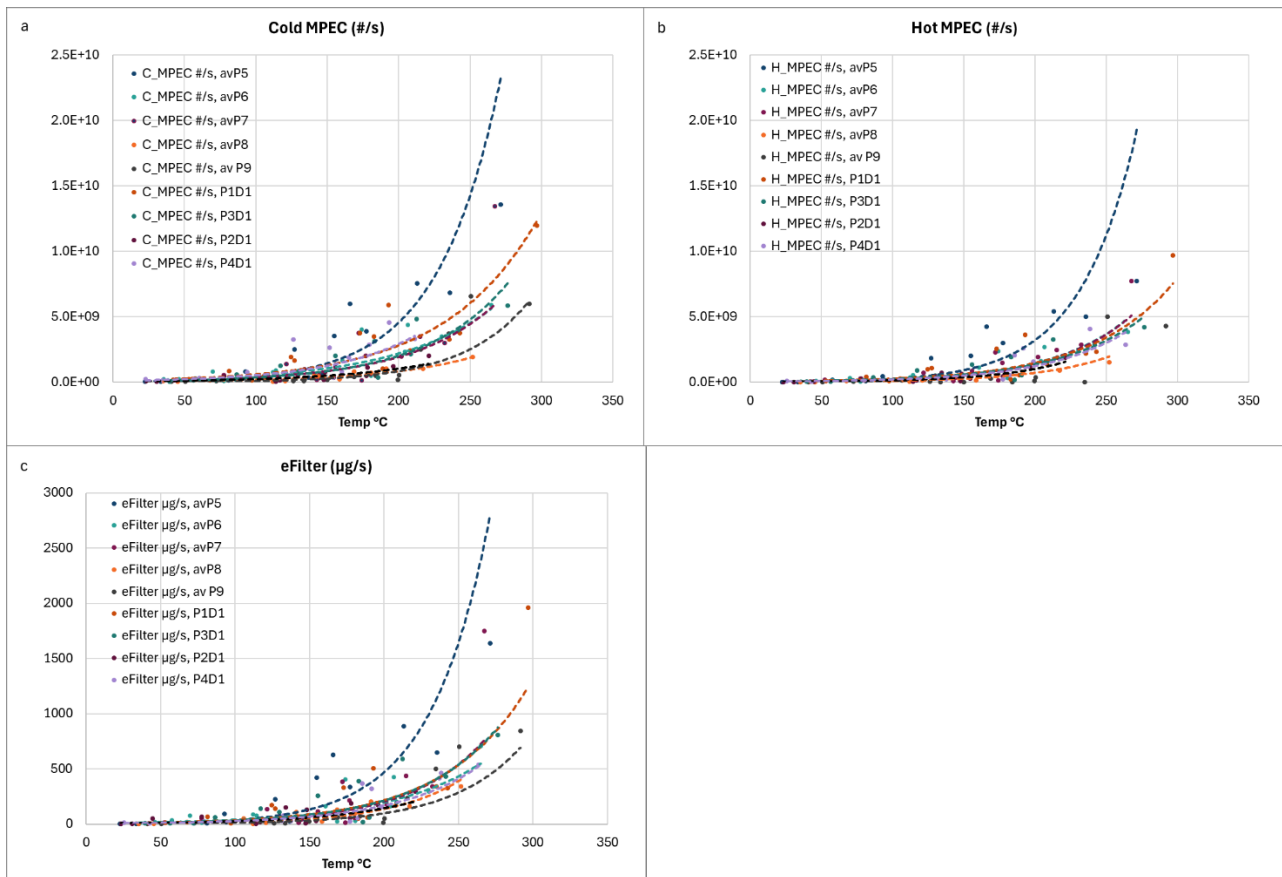
Figure 8-28: Emissions versus temperature curves from P1D1, P1D2 and P10AD1 gentle, moderate and dynamic drive-by tests, as measured by a) cold MPEC, b) hot MPEC and c) eFilter.

Since there are consistent increases in PN and PM emissions with temperature, and it is clear from Figure 8-23 that at equal speeds brake disc temperatures are higher from dynamic braking than moderate braking and lowest from gentle braking, particulate emissions increase with braking dynamicity. This is demonstrated, by comparing (for example) Figure 8-30, Figure 8-31 and Figure 8-32.

8.3.5.3 Pad variants with a single disc

Figure 8-29a, b, c shows emissions versus temperature curves for cold MPEC, hot MPEC and eFilter data respectively, featuring 9 pad variants with D1. Exponential curve fits are shown for all pads.

These charts indicate that P5 (organic composition) clearly has the highest particle number emissions while low dust pads P8 and P9 have the lowest particle number emissions. These observations are entirely consistent with the comparative emissions seen from chassis dynamometer and road RDE testing. Other pads seem to be grouped together, although P1 (premium pad) is at the top of this group.

Interestingly, P9 emissions are similar to or lower than P8 in cold MPEC and eFilter data (where volatile materials are measured) but emissions are higher than P8 in the hot MPEC data. This may indicate a higher volatile fraction in the emissions of P8 than from P9.

Notably, the high temperatures reached in the dynamic braking exercises reveal that lower emissions are achieved under all types of braking with the low dust formulations used in P8 and P9.

Figure 8-29: Emissions versus temperature curves from nine pads and one disc during gentle, moderate and dynamic drive-by tests, as measured by a) cold MPEC, b) hot MPEC and c) eFilter.

8.3.5.4 High and low emitting pads under gentle, moderate and dynamic operation

Figure 8-30, Figure 8-31 and Figure 8-32 respectively, present comparisons between all pads and discs emissions during gentle, moderate and dynamic drive-by tests. Each figure contains 15 individual graphs and presents cold MPEC data in the first column, hot MPEC data in the second column and eFilter data in the final column. 16kph, 32kph, 48kph, 64kph and 80kph data are shown in rows 1 to 5 respectively.

From gentle braking (Figure 8-30), highest emissions are generally seen from P1D2, which may be an indication of elevated emissions related to the low mileage disc. Low emissions are consistently seen from P10A (high mileage, aged pad), P2 (budget pad), P8 and P9 (both low dust pads).

From moderate braking (Figure 8-31), there are no consistent high emitters across all speeds, although at 48kph and above, P5 is clearly highest from all measurement approaches. Lowest emitters were P2, P8 and P10A. P9 appears to have higher emissions than these three pads at 80kph.

Pads 2 and 8 show consistently low emissions from dynamic braking (Figure 8-32). P9, which is a low emitter under moderate and gentle driving conditions shows relatively high emissions compared to P2 and P8, as does P10A. These effects are likely related to the pad composition and the highest temperatures experienced by the pads. There are no pads that show consistently high emissions at 16kph and 32kph, but at 48kph and above P5 and P10A feature prominently in the highest emitting pads.
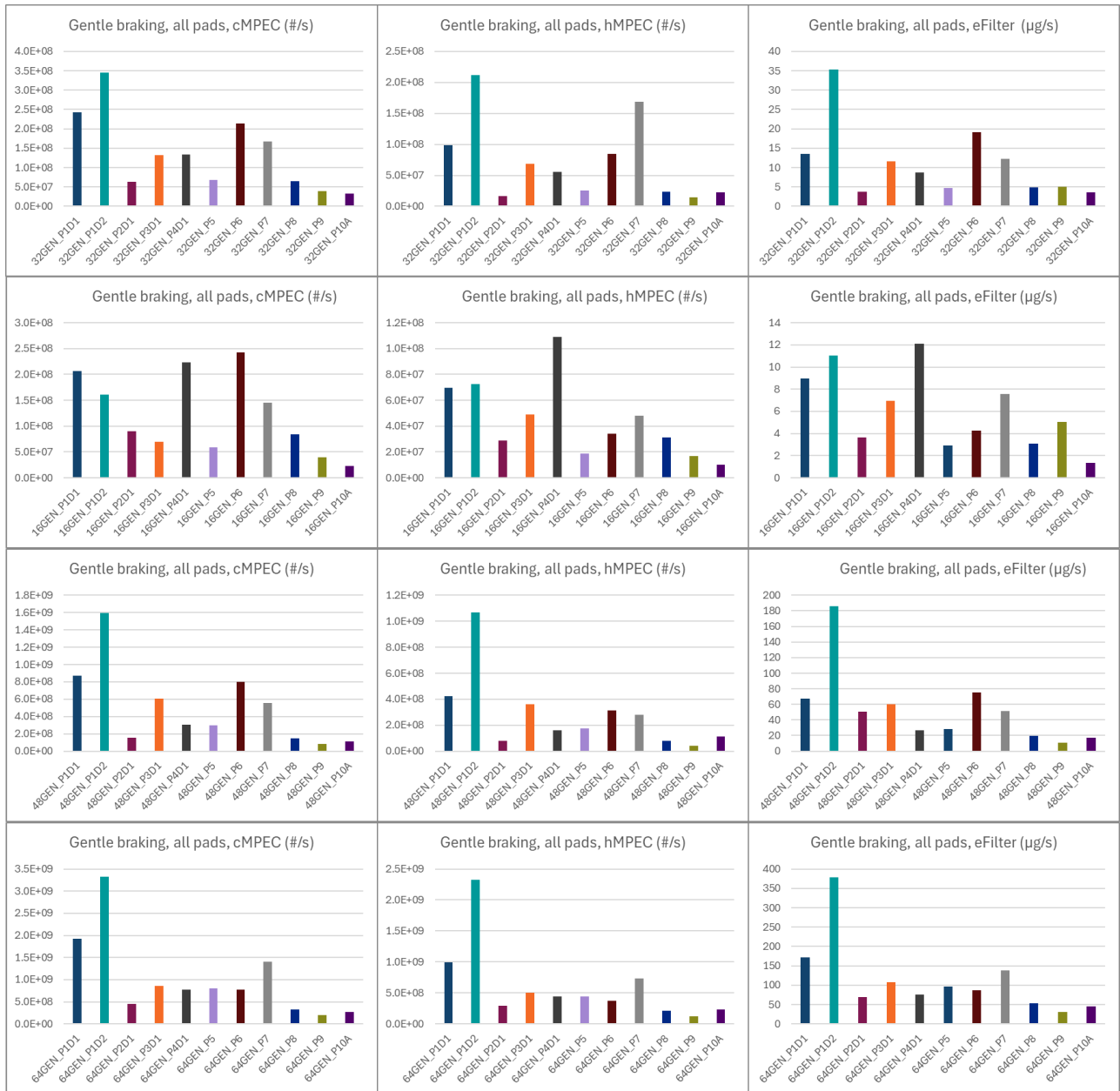
Figure 8-30: Gentle drive-by emissions, 16, 32, 48, 64 and 80kph nominal speeds, all pads with D1.

Figure 8-31: Moderate-style drive-by emissions, 16, 32, 48, 64 and 80kph nominal speeds, all pads with D1.

Figure 8-32: Dynamic-style drive-by emissions, 16, 32, 48, 64 and 80kph nominal speeds, all pads with D1.

8.3.6 Test track braking from elevated speeds

As described in Section 6.6, higher speed braking events, that were impossible on the drive-by site, were studied on the test track at MIRA. In this study an additional control was added, in contrast to the drive-by braking exercise, such that between each braking event the brake temperature was allowed to stabilise. Measurements were made using the non-metallic Pad 4 and Disc 1, a combination that showed low to moderate emissions during the chassis dyno PG42 testing (Section 8.3.3.1).

Moderate and dynamic braking events were studied, with measurements made using cold and hot MPEC instruments plus the eFilter. Deceleration rates for the moderate and dynamic braking events are compared in Figure 6-9, indicating significantly higher rates with the dynamic braking.

8.3.6.1 Moderate Braking

Figure 8-33a-f show unit/s emissions (lefthand column) and unit/km emissions (righthand column) for the eFilter, cold MPEC and hot MPEC instruments. Error bars show 1-sigma. All instruments showed a roughly linear increase in emissions, for unit/km (Figure 8-34) and also unit/s emissions, with road speed between 48kph and 128kph, and that emissions were repeatable (when 80 kph and 128 kph were revisited).
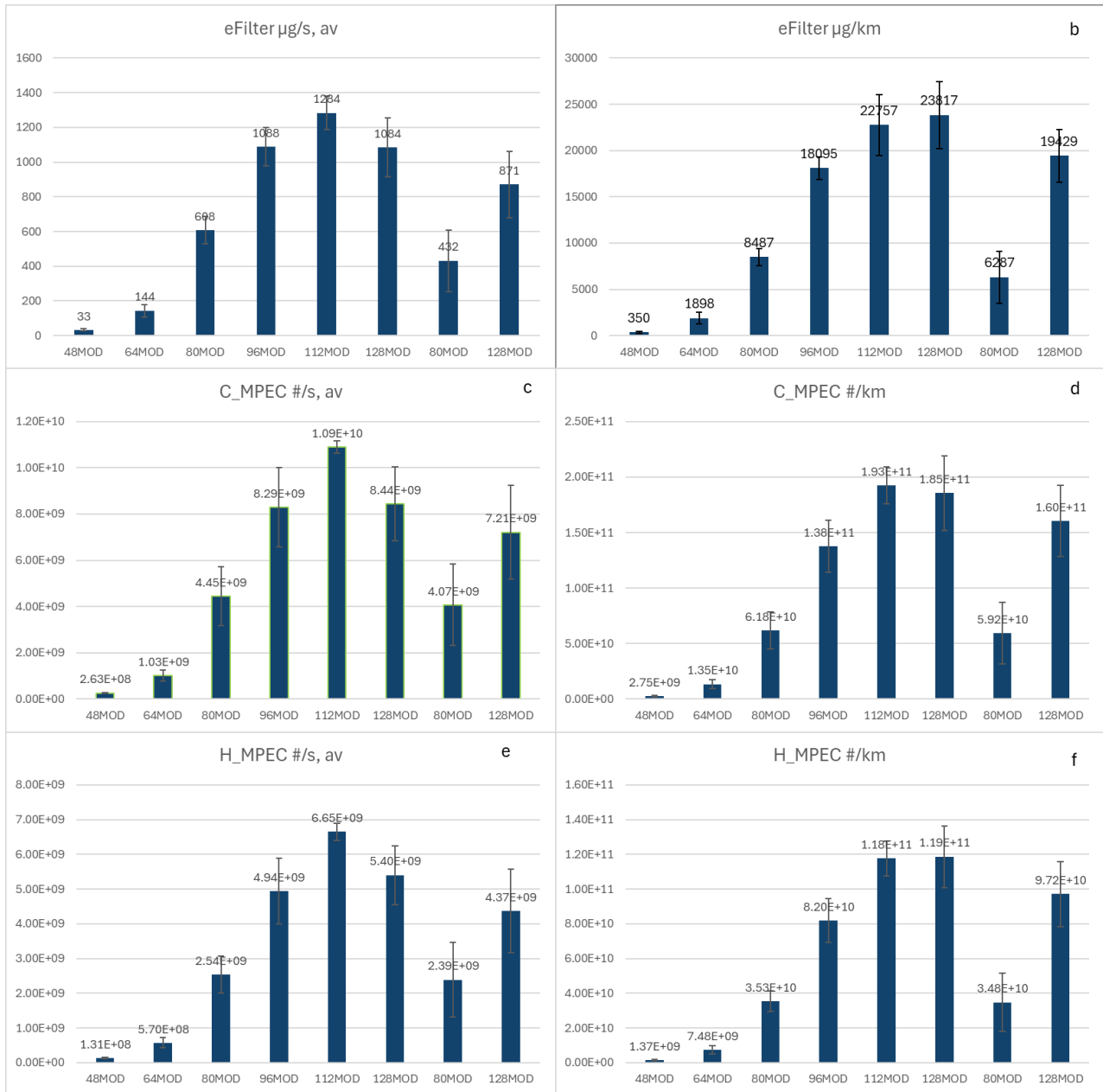
Figure 8-33: Emissions from moderate braking events from 48 kph to 128 kph, on a test track using P4D1, as measured by eFilter (top) cold MPEC (middle) and hot MPEC (bottom).

On an emissions per km basis, between 48kph and 128kph, eFilter mass emissions increased by a factor of ~70, from ~0.35 mg/km to 23.8 mg/km. With the cold MPEC the increase factor was similar, from ~2.75×10^9 #/km to ~1.9×10^{11} #/km and slightly higher for the hot MPEC (factor ~85) from ~1.37×10^9 #/km to ~1.2×10^{11} #/km.

These increases in emissions were associated with increases in the enclosed disc temperature from ~ 60°C to ~150°C (Figure 8-35).
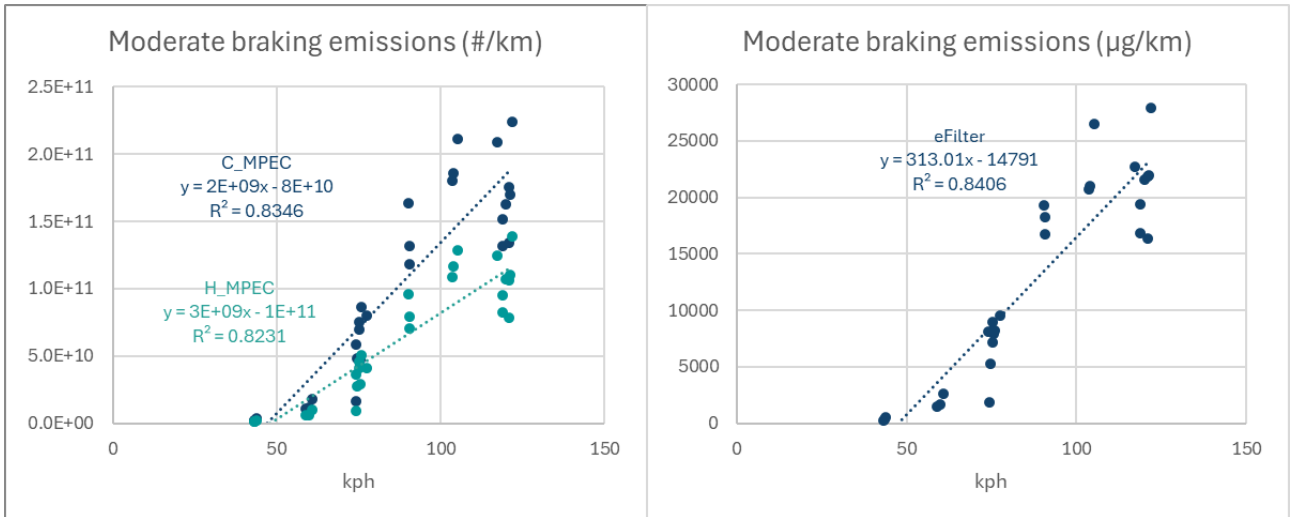
Figure 8-34: Moderate braking emissions measured by the cold and hot MPECs (left) and the eFilter (right) with initial speeds from 48 kph to 128 kph, increase in a linear relationship with temperature.
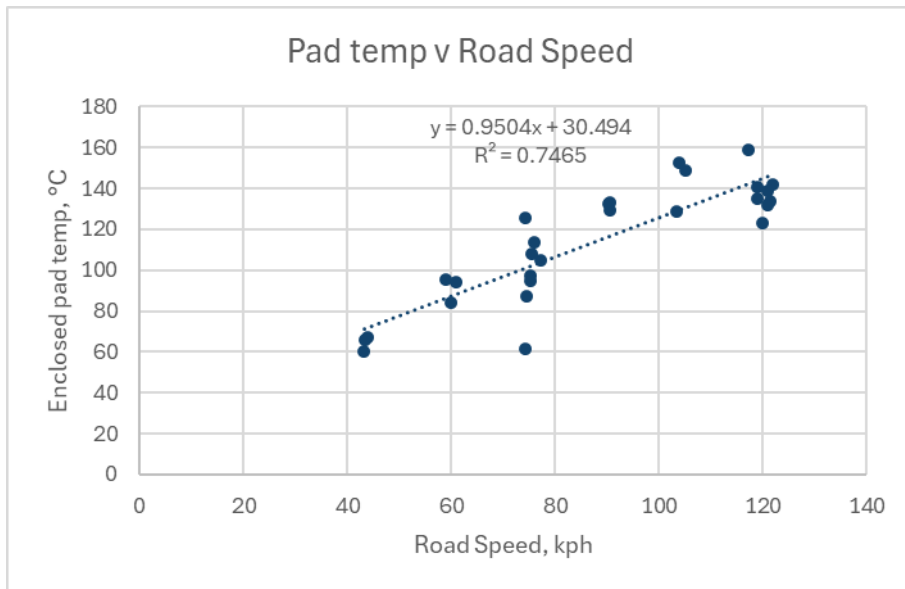

Figure 8-35: Moderate braking emissions, enclosed pad temperature vs initial braking velocity.

8.3.6.2 Dynamic braking

Figure 8-36a-f displays emissions in unit/s (left column) and unit/km (right column) for the eFilter, cold MPEC, and hot MPEC instruments, with error bars representing 1-sigma uncertainty. Emissions increased with a generally quadratic relationship with in both #/km (Figure 8-37) and #/s emissions. This characteristic was present in both moderate and dynamic data, with the gradient increased at the higher deceleration levels. Additionally, dynamic braking emissions were less consistent than moderate results when speeds of 80 kph and 128 kph were revisited.

Between 48 kph and 128 kph, mass emissions per kilometre increased significantly across all instruments. For the eFilter, emissions rose by a factor of approximately 100, from around 0.27 mg/km to 27.9 mg/km. The cold MPEC showed a slightly smaller increase, with emissions growing by a factor of about 87, from approximately 3.52×10^9 #/km to 3.06×10^{11} #/km. The hot MPEC displayed the lowest increase, with emissions rising by a factor of roughly 45, from around 3.61×10^9 #/km to 1.64×10^{11} #/km.

These increases in emissions were associated with increases in the enclosed disc temperature from ~ 60°C to ~150°C (Figure 8-38).
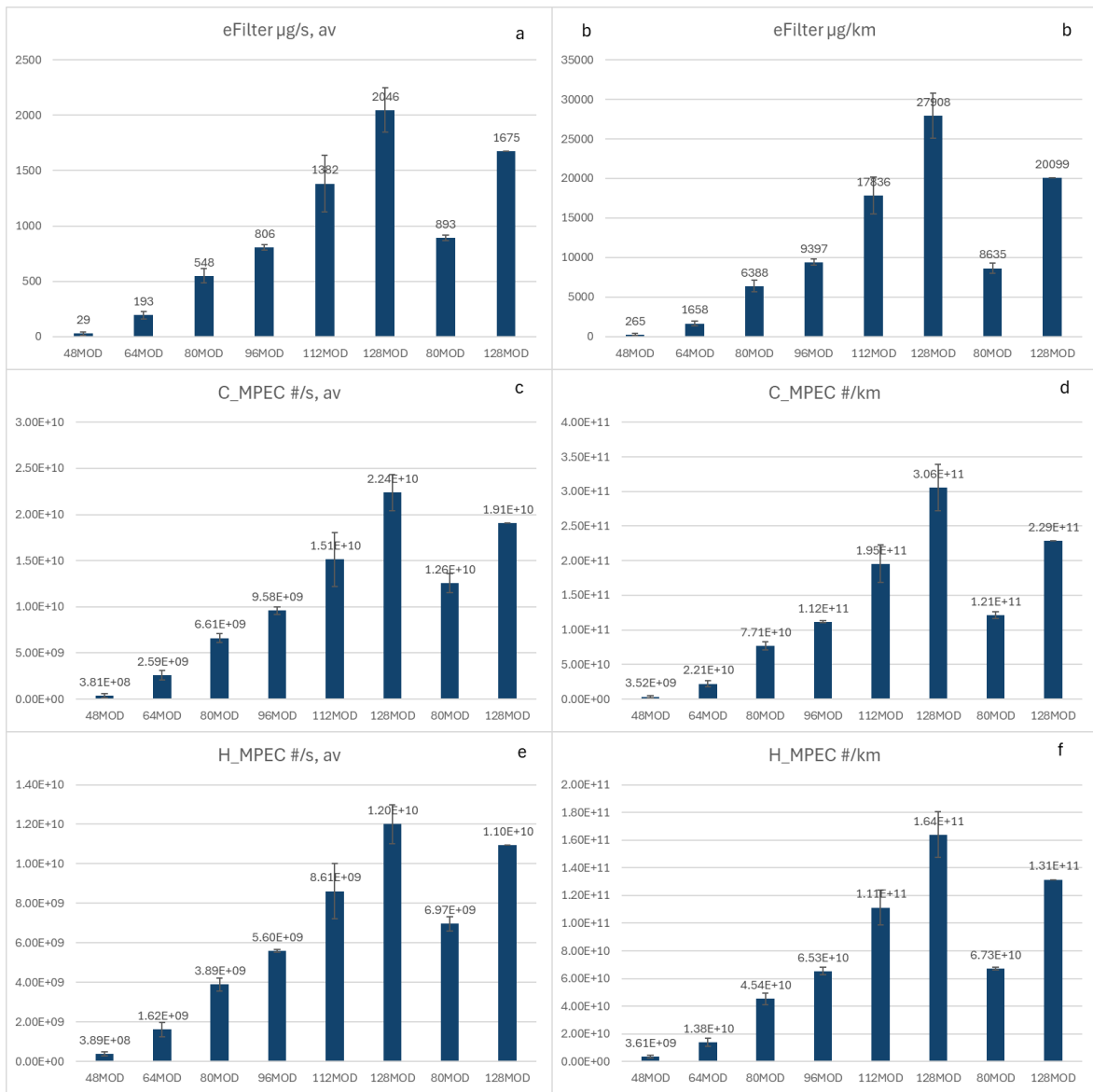
Figure 8-36: Dynamic braking emissions, initial speeds 48 kph to 128 kph, increase with temperature, as measured by eFilter (top) cold MPEC (middle) and hot MPEC (bottom).
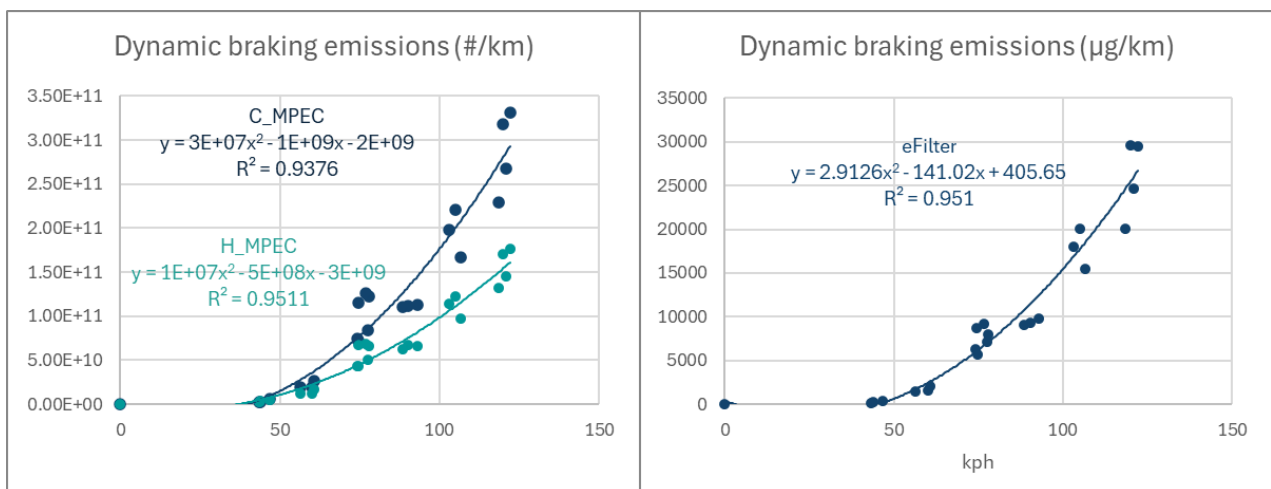

Figure 8-37: Dynamic braking emissions, measured by the cold and hot MPECs (left) and the eFilter (right) with initial speeds from 48 kph to 128 kph, increase in a quadratic relationship with temperature.
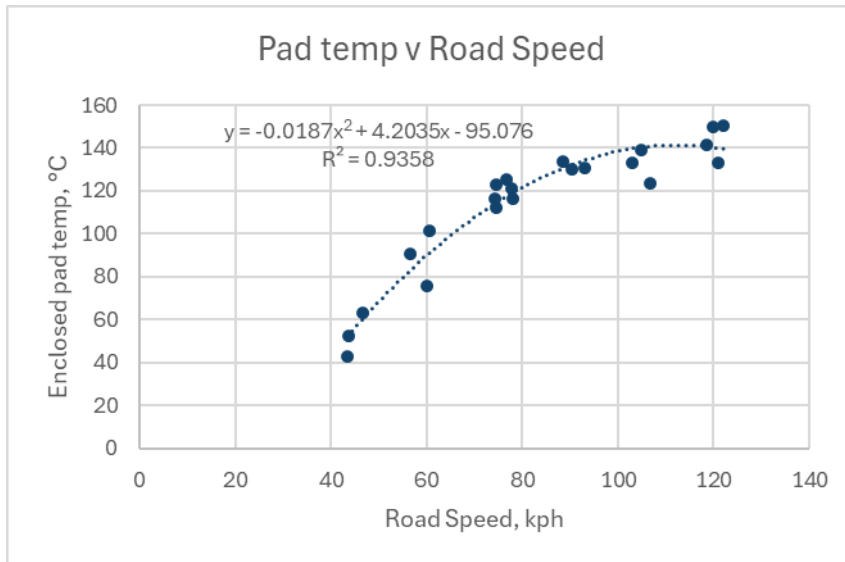
Figure 8-38: Dynamic braking emissions- enclosed pad temperature vs initial braking velocity shows quadratic relationship.

8.3.6.3 Moderate vs. dynamic braking

As shown in Figure 8-39, including 1-sigma error bars, PN emissions from both the cold MPEC and the hot MPEC were higher from dynamic braking than from moderate braking, with cold MPEC emissions ~28% higher and hot MPEC ~17% higher.
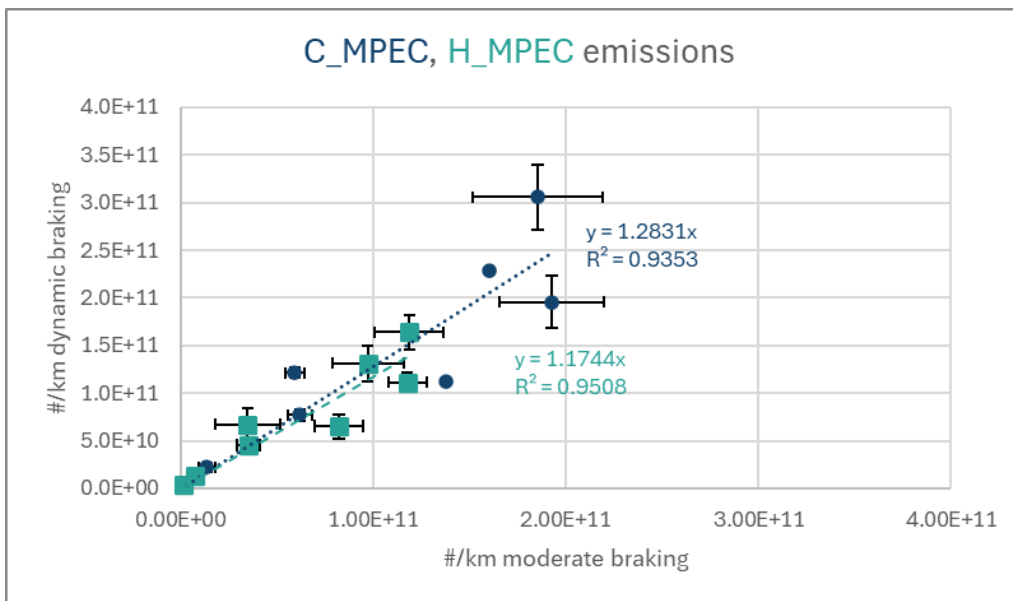
Figure 8-39: PN emissions from the MPEC systems comparing moderate versus dynamic braking.

Conversely, the eFilter emissions shown in Figure 8-40a were ~9% higher from the moderate braking than from the dynamic braking. It is not clear what led to this unexpected observation, but since PN emissions were higher from dynamic braking, this must have resulted from a reduction in emissions of a relatively few larger particles that did not affect the PN substantively. As Figure 8-40b shows, the braking was certainly more aggressive in the dynamic phase than in the moderate phase.
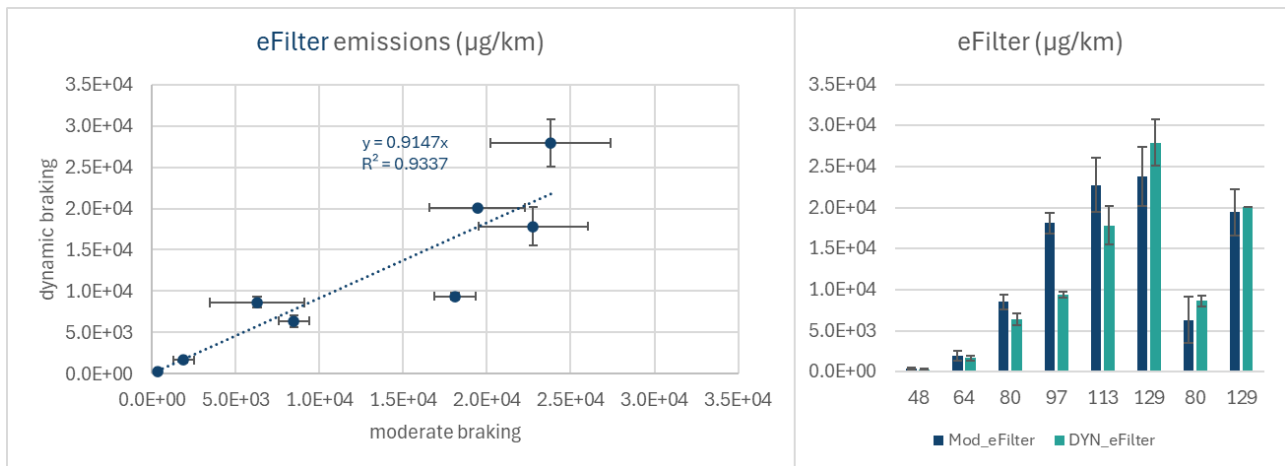
Figure 8-40: a) Relationship between real-time PM emissions from the eFilter for moderate and dynamic braking, b) column chart showing the moderate and dynamic eFilter emissions when braking under different speeds.

8.4 BRAKE PAD METROLOGY

8.4.1 Pad Weights

Each set of brake pads comprised 4 individual elements: 2 pads for the left-hand side front wheel and two for the right-hand side. Each pad set is numbered, for example: the four P1 pads would be identified as P1-1 (left-hand outboard), P1-2 (left-hand inboard), P1-3 (right-hand inboard) and P1-4 (right-hand outboard) with pad numbers 3 and 4 situated inside the enclosure for emissions measurements.

Brake pads were weighed when new, following preliminary ageing, after secondary ageing and once the brake pad emissions evaluations were completed. Prior to weighing, brake pads were cleaned using a commercial brake cleaning product (Napa Brake and Clutch Cleaner[6]). Average mass losses across the four pads were calculated and these data used to determine pad wear evolution by distance, and wear rates.

Results of average pad weight losses for P1 to P10A are given in Table 8-11, with final weight loss rates shown graphically in Figure 8-41. Note that the 5,0000 km pre-aged brake pad, P10A, has only initial (as received) and final weights, as it was not subject to either the preliminary road mileage or secondary PG42 preconditioning experienced by the other pads.

It should be noted that due to the challenges of weighing small mass changes on relatively heavy pads and potential inconsistencies when cleaning them, on some occasions pad masses increased slightly following preconditioning steps, meaning that negative wear rates are reported (e.g., P6 following preliminary ageing; Table 8-11). However, at the end of testing all pads showed positive mass losses.

Table 8-11: Mass loss from brake pads in mg/km.

	Total PM	Total PM	Total PM
	After preliminary ageing, ~200 km (mg/km)	After Preliminary & secondary ageing, ~350 km (mg/km)	After preliminary & secondary ageing and testing, >740 km (mg/km)
P1	0.78	-1.00	2.27
P2	2.95	4.20	3.23
P3	0.75	1.86	3.42
P4	1.02	2.17	2.62
P5	1.26	1.94	4.24
P6	-2.07	2.72	3.20

---

[6] Napa Brake and Clutch Cleaner

	Total PM	Total PM	Total PM
P7	1.16	1.09	2.13
P8	0.93	2.20	2.50
P9	2.01	2.70	2.64
P10A	N/A	N/A	5.38
Average P1 - P9	0.98	1.99	2.92
STDEV P1 - P9	1.35	1.41	0.66
Average all			3.16
STDEV all			1.00

At ~5.4 mg/km, the brake wear emissions rate from the highest mileage pad, P10A, was substantially higher than from any of the other pads, indicating that wear rates may increase as pads age. P1 is a nominally identical pad to P10A but with ~1165 km of accumulated mileage rather than the ~50,500 km of P10A. The wear rate of P1, at ~2.27 mg/km is ~42% of that recorded for P10A.

Evolution of mass emissions rates for individual pads varies (Figure 8-41a), but there may be an underlying trend of increasing emissions rates with mileage (Figure 8-41b) supporting the observation of highest rates with the highest mileage pad, P10A.

Given that the apparent average increase in wear rates for pads P1 to P9 appears to increase by ~2 mg/km between 200 km and 750 km, and the wear rate of P1 at ~1200km is ~2.3 mg/km and that observed by a similar pad (P10A) at ~50,500 km is ~5.4 mg/km, it seems likely that the increase in wear rate with distance is much slower at higher mileages than at low mileages.
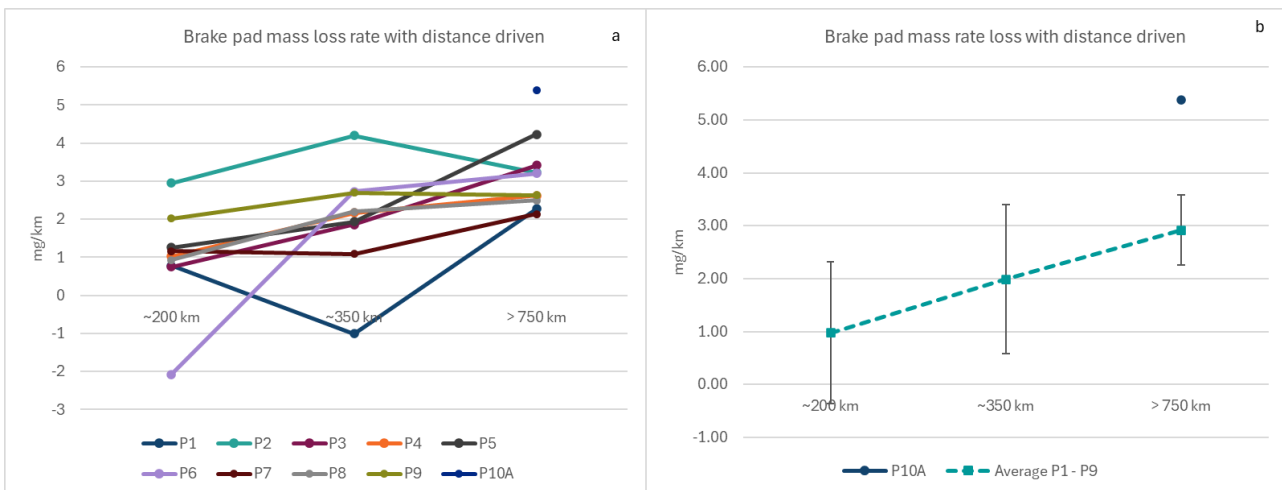
Figure 8-41: Brake pad mass loss rates with distance driven for a) all pads, b) P10A and the average of P1 to P9.

Aggregated brake pad wear rates are shown in Figure 8-42, indicating that typical brake pad mass emissions over the first ~1,000 km of use are of the order 3 mg/km.
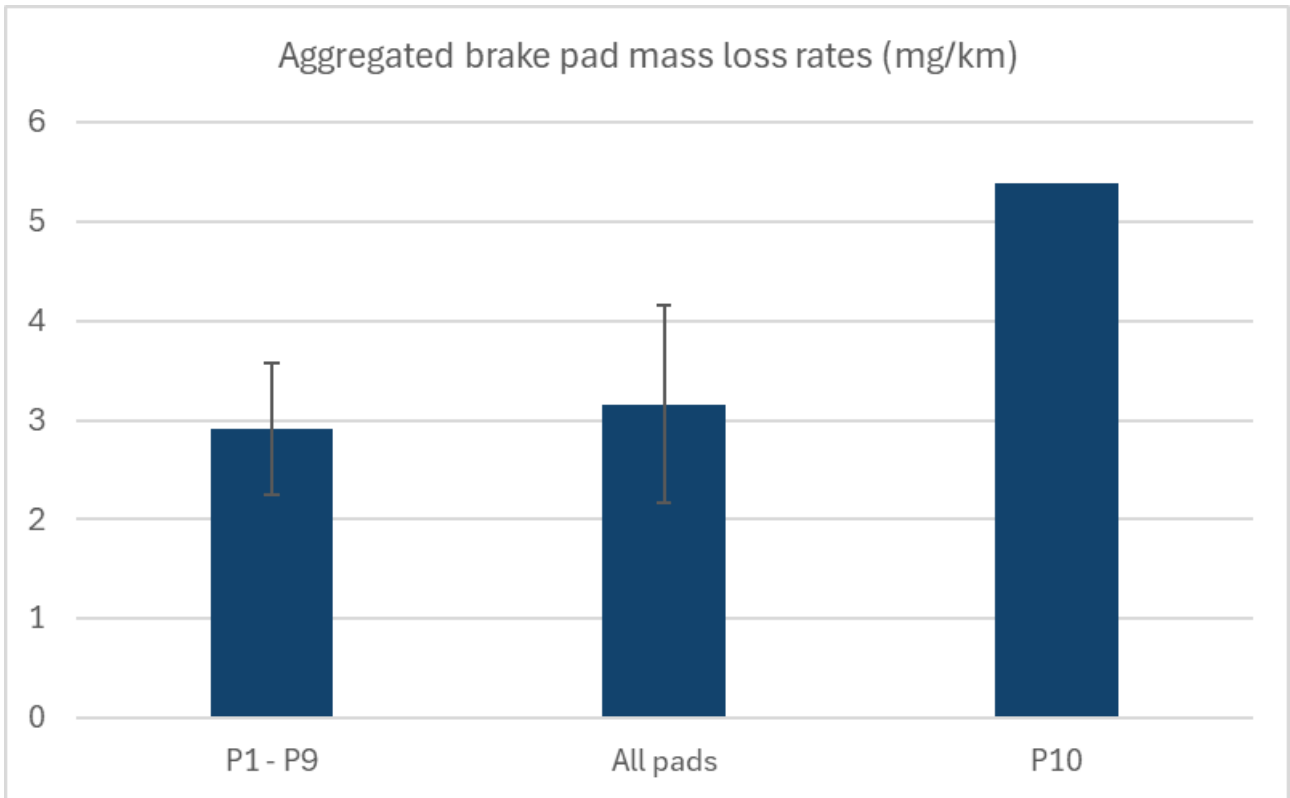
Figure 8-42: Aggregated brake pad mass loss rates.

Pads showing the lowest wear appear to emit ~2.5 mg/km. Considering Pads P1 to P9, the lowest emissions were observed from P1, P4, P7 and P8, and the highest from P5 and P3 (Figure 8-43). Of the low emitters, P1 is a premium pad, P4 is a low metallic material pad, P7 is a "recognised UK brand" and P8 is a ceramic pad – all these might be expected to be longer-life and thus potentially have lower emissions. With higher

emitters, P5 is a low dust organic friction material pad, which might lead to higher losses of resins/binders, while P3 is a budget pad: both these could conceivably be expected to show higher mass loss rates.
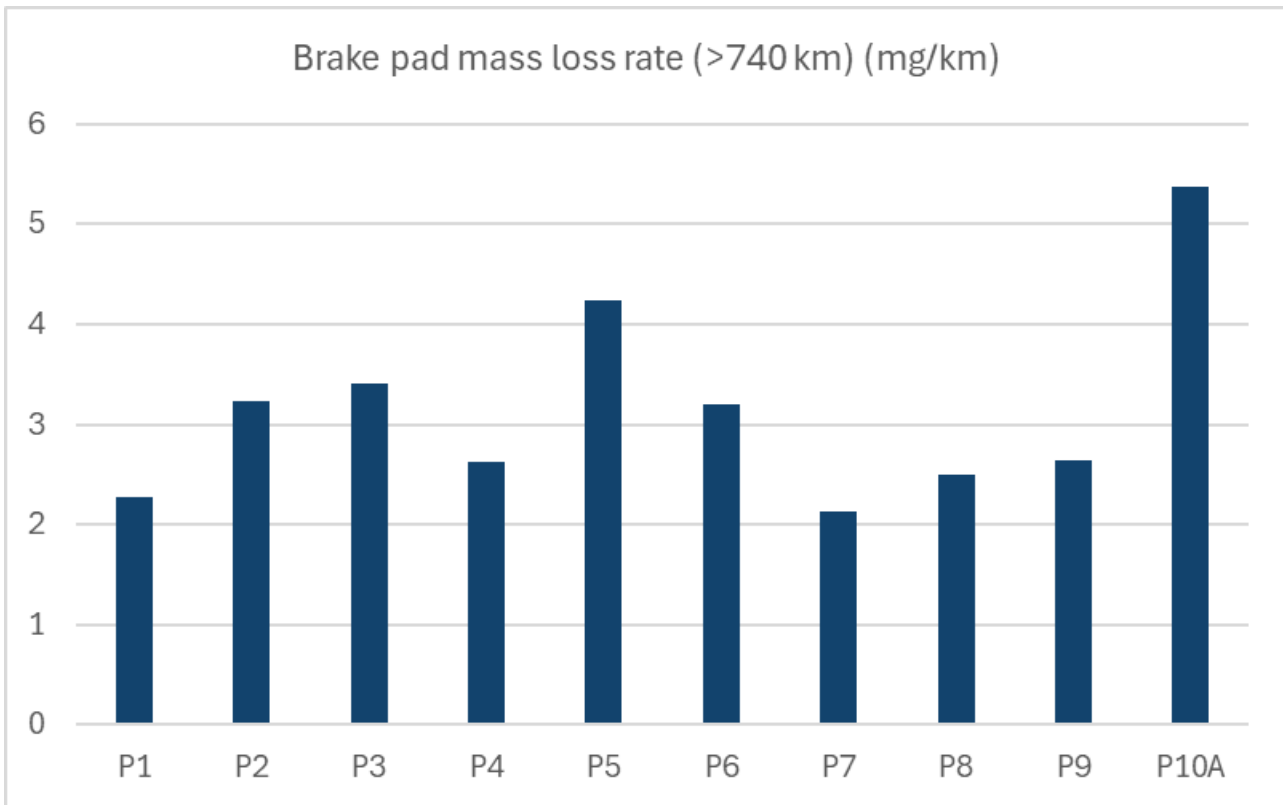
Figure 8-43: Brake pad mass loss rates, P1 to P10A in mg/km for distances above 740 km.

8.4.2 Pad Thicknesses

Each brake pad was measured for thickness using a micrometer gauge (Mitutoyo, Japan, calibrated January 2024), with measurements made at six points on the pad surface (Section 7.3.1).

Brake pads were measured alongside the weighing exercises: when new, following preliminary ageing, after secondary ageing and once the brake pad emissions evaluations were completed. From the six measurements average thicknesses for each of the four pads were calculated, and these data used to determine pad wear. The average pad thickness data is shown in Table 8-12.

Table 8-12: Thickness loss from brake pads, µm/km.

	After preliminary ageing, ~200 km (µm/km)	After Preliminary & secondary ageing, ~350 km (µm/km)	After preliminary & secondary ageing and testing, >740 km (µm/km)
P1	0.43	0.43	0.29
P2	0.56	0.40	0.29
P3	0.45	0.44	0.41
P4	0.35	0.37	0.30
P5	0.26	0.13	0.20
P6	0.31	0.37	0.27
P7	0.24	0.26	0.22
P8	0.39	0.33	0.27
P9	0.49	0.50	0.37
P10A	N/A	N/A	0.20

	After preliminary ageing, ~200 km (µm/km)	After Preliminary & secondary ageing, ~350 km (µm/km)	After preliminary & secondary ageing and testing, >740 km (µm/km)
Average P1 - P9	0.39	0.36	0.29
STDEV P1 - P9	0.11	0.11	0.07

Despite the high mileage (P10A) pad showing the highest mass loss rate after >740 km, it showed the lowest wear thickness reduction rate. In general, this observation of lower thickness reduction rate with higher mileage seems to be supported by data of many individual pads (Figure 8-44a) and the average trend (Figure 8-44b).

After the completion of testing (744 km to 1165 km) the typical thickness loss from Pads P1-P9 appears to be ~0.3 µm/km (Figure 8-45).

A comparison of P1 (0.29 µm/km) and P10A (0.20 µm/km) (Figure 8-46) indicates a reduction in the wear rate of ~0.09 µm/km between 1165 km and 50500 km, compared to a greater reduction (~0.14 µm/km) over the first 1165 km. This suggests a significant slow-down in wear rate evolution at higher mileages, although the dyno ageing clearly contains some aggressive braking that would likely occur less often in normal road use.

Across P1 to P9, pad thickness reduction rates, from mileages >740 km, range from just above 0.2 µm/km to above 0.4 µm/km. P3 and P9 appear to wear substantially more than the other pads (>0.35 µm/km), while P5 and P7 are lower. Unlike the weight-based effects (Section 8.4.1) there are no obvious links between pad types/descriptions and the trends seen with pad thickness changes.
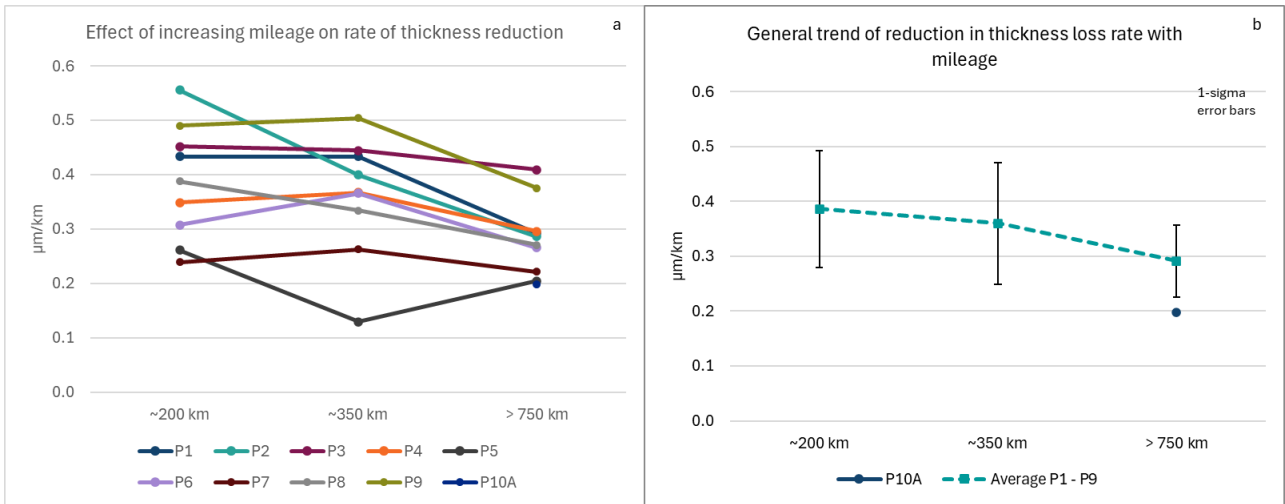
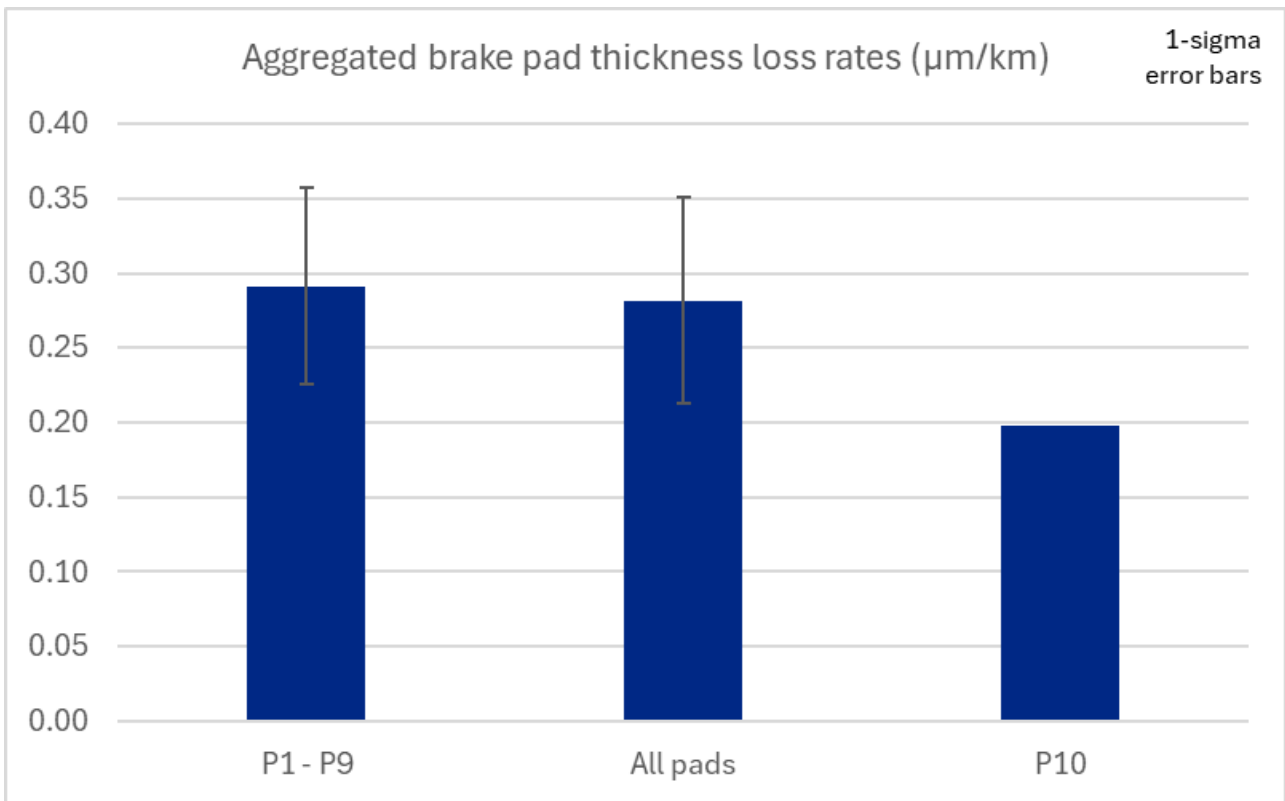Figure 8-44: Brake pad thickness loss rates (µm/km) with distance driven.

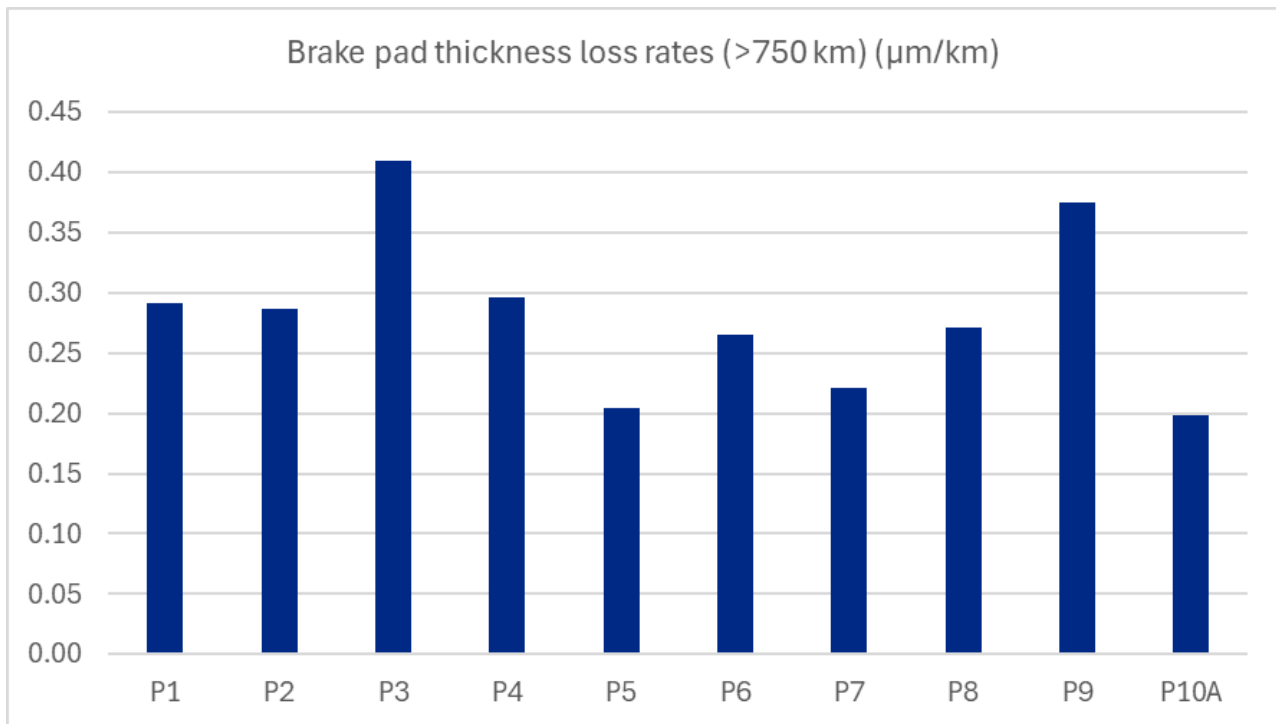Figure 8-45: Aggregated brake pad thickness loss rates in µm/km.

Figure 8-46: Brake pad thickness loss rates, P1 – P10A in μm/km, for mileages > 750km.

8.5 BRAKE WEAR EMISSIONS DISCUSSIONS/SUMMARY

It should be noted that testing was performed on a two-wheel drive dynamometer, so braking forces on the measured pad and disc combination would be 50% on each front wheel, rather than approximately 35% on each front wheel, since braking forces are split ~70% front and 30% rear during 4-wheel braking. As a consequence, emissions factors for a single front wheel could be potentially 30% lower than quoted here.

8.5.1 Disc variants and high mileage pad, P10A

a) Real-time particle emissions corresponded to, and aligned with, instantaneous braking events

b) There were no substantial indications of outgassing of volatiles during braking events

c) Occasional spikes of emissions were observed that were not aligned with brake pressure events. These could be due to brake stiction and release. Potentially these could lead to over-estimates of PN emissions in a ISC or certification test, and so should be prevented from occurring, as far as possible.

d) It appears that aged brake pads have lower PM and PN emissions than lower mileage pads, suggesting an evolutionary mechanism during their lifetime

e) There does not seem to be any substantial difference in PM and PN emissions between a low-cost brake disc (D1) and a premium brake disc (D2). However, it should be noted that a brake system aimed at low emissions would likely comprise a sympathetic pad and disc pair, and this might deliver more benefits than a random pairing of pad and disc.

f) Brake discs may need an elevated mileage break-in process in order to produce stable PN emissions, especially volatile PN10 emissions.

- From the experiments comparing the disc types and aged and unaged pads, PN10 (APC10) emissions from the PG42 cycle were ~2×10^9#/km, with gravimetric $PM_{2.5}$ emissions in the range 1.5 to 2.5 mg/km. Hot MPEC and cold MPEC emissions reported as ~10x and ~20x those of the APC10, due to multiple charging effects on particles larger than ~1μm. Real-time eFilter results were consistent with those of the gravimetric PM. The DMS500 reported similar size distributions from all pad and disc combinations, but occasionally significant differences in magnitude between tests that were not supported by the results of other instruments.

- On dyno RDE tests at 1900 kg and 2100 kg test masses indicated similar magnitudes of emissions and results trends to those observed from the PG42. Emissions from the 2100 kg tests appeared to be higher than from the 1900 kg test (see Section 8.5.3d) below)

g) On-road short RDE tests using MPECs and eFilter (real-time and gravimetric) supported the comparative results seen on the chassis dynamometer: there was little discrimination in emissions due to higher temperatures observed in the enclosure between D1 and D2 and from the pad-to-pad comparisons, and lowest emissions were seen from P10A.

8.5.2 Comparison of pad variants, all tested with D1

a) Consideration of triplicate PG42 cycles' particle number emissions results from the APC10, cold MPEC and hot MPEC indicates that the enclosure-based sampling and measurement approach is able to discriminate between pads variants for PN, with average APC10 coefficient of variance (CoV) at 11%, cold MPEC CoV at 17% and hot MPEC CoV at 13%.

b) From APC10 and the MPECs, highest PN emissions results were consistently seen from P7, P1, P6 and P5, while lowest emissions results were seen from P8, P4, P9 and P2. Pads 8 and 9 are nominally "low dust", Pad 4 was "low metallic" which would seem to align with lower PN emissions. P2 is a budget pad, but this does indicate that inexpensive low emissions pads do exist on the market

c) APC10 results indicated that across the range of results the highest PN emissions pad, P5, had 2.5x higher emissions (~$2.5x10^9$ #/km) than the lowest pad, P8 (~$1x10^9$ #/km).

d) The range of results from the cold MPEC indicated a higher differential between lowest and highest emitting pads than the APC10 and hot MPEC. This likely indicates that the levels of volatile materials emitted by the pads vary. The volatile constituents influence the APC10 results least, as it has the greatest ability to eliminate volatiles, the hot MPEC next and the cold MPEC most.

e) The comparative gravimetric $PM_{2.5}$ and eFilter real-time results showed similar effects to PN, with highest emissions from P5, P6, P7 and P1 and lowest emissions from P8, P2 and P9. The high to low range of $PM_{2.5}$ emissions was from ~1 mg/km (P8) to ~3.5 mg/km (P1).

f) A comparison of the lowest emitting pad P8 and a high emitting pad P5, showed that even if the enclosure temperature of P8 tests was higher, PN and PM emissions were lower. P8 also heated and cooled more quickly than P5 during testing. This is indicative of the different thermo-physical properties of P8, which was a ceramic pad. It is likely that P8 also either contains less volatile material or much lower volatility materials than P5.

8.5.3 Pad variants – dyno RDE tests at 1900 kg and 2100 kg; on road RDE at 1900 kg

a) From both 1900 kg and 2100 kg chassis dynamometer RDE tests, the pads with lowest PN emissions measured with the APC10 and both MPECs were, as observed with the PG42 tests, P8, P9, P4 and P2, while P7, P5 and P1 remained amongst the highest emitters. PN emissions ranged from ~$1x10^9$ to $2x10^9$ #/km.

b) P8, P9 and P2 showed the lowest $PM_{2.5}$ emissions, while P4 was also lower than the other 5 pad variants. PM ranged from ~0.5 mg/km to ~2.5 mg/km.

c) From on-road RDE tests it is apparent that across the instruments and metrics used, the lowest emitting pads were P8 and P9, with P4 emissions also relatively low, while highest emissions were seen from P1.

d) There was a consistent increase in both PN10 and $PM_{2.5}$ emissions when test mass was increased from 1900 kg to 2100 kg during on-dyno RDE tests. PN emissions as measured by APC10, hot MPEC and cold MPEC were ~9%, 13% and 11.5% respectively, higher at 2100 kg test mass than at 1900 kg test mass.

e) Gravimetric and eFilter real-time PM emissions also showed emissions to be higher with the extra 200 kg test mass: gravimetric $PM_{2.5}$ emissions increased by ~12.5% and eFilter real-time results by ~14%.

8.5.4 Average emissions across all pads, discs and cycles

a) PN emissions from the APC10 used only during chassis dynamometer tests, produced emissions levels that were similar across the PG42 and both RDE cycles with an average emissions rate of ~$1.6x10^9$ #/km

b) Mean gravimetric $PM_{2.5}$ emissions were consistent across RDE cycles, including both road and chassis dyno, in the range 1.43 to 1.52 mg/km, while PG42 cycle emissions were substantially higher, giving an average of 2.27 mg/km

8.5.5 Findings of drive-by site investigations of gentle, moderate and dynamic braking

a) PN and PM emissions were highest from dynamic braking and lowest from gentle braking.

b) Considering emissions from different disc types and from the aged pads (P10A), through using MPEC' and eFilter measurements, PN and PM emissions were lowest from P10A, higher from P1D1 and highest from P1D2. This is broadly in-line with observations from chassis dyno cycles. Exponential fits were the best options for temperature v emissions curves, providing a reasonable fit for P1D2, better for P1D1 data, and an excellent fit for P10A data. Potentially the "curing" of the disc and pad with age stabilises the volatile emissions characteristics of the disc and pad combination, which would suggest that both pads and discs are important influences on both volatile and solid particle emissions.

c) The exponential fits to eFilter and MPEC emissions versus temperature curves for the 9 pad variants and disc 1, indicate that P5 (organic composition) clearly has the highest particle number emissions while low dust pads P8 and P9 have the lowest particle number emissions. These observations agree with PG42, dyno RDE and on-road RDE findings. Other pads seem to be grouped together, although P1 (premium pad) is at the top of this group. Notably P9 emissions are similar to or lower than P8 in cold MPEC and eFilter data (where volatile materials are measured) but emissions are higher than P8 in the hot MPEC data. This may indicate a higher volatile fraction in the emissions of P8 than from P9, or the emissions of some larger particles carrying a high charge level. The emissions seen at the high temperatures reached in the dynamic braking exercises reveal that lower emissions are achieved under all types of braking (likely to be encountered in normal use) with the low dust formulations present in P8 and P9.

d) Due to higher disc temperatures observed in the enclosure than for the unenclosed disc, reported PM and PN emissions may be higher from this study than in the real-world. However, the differential is not anticipated to be large, since the effect of temperature on emissions in the typical drive cycle temperature regime would be less than a factor of two at the highest temperatures, and this would only be for a fraction of the cycle duration.

8.5.6 Test track braking from ~48kph to ~128kph

a) During test track braking exercises, where temperatures were permitted to stabilise between individual braking events, measurements were made with eFilter and MPECs. For moderate braking, results showed a roughly linear increase in emissions, for unit/km and also unit/s emissions, with road speed between 48kph and 128kph, and that emissions were repeatable when 80 kph and 128 kph were revisited at the end of the measurement set. For dynamic braking the emissions increase was better represented by a quadratic fit.

b) On an emissions per km basis, for moderate braking between 48kph and 128kph, eFilter mass emissions increased by a factor of ~70, from ~0.35 mg/km to 23.8 mg/km. With the cold MPEC the increase factor was similar, from ~2.75×10^9 #/km to ~1.9×10^{11} #/km and slightly higher for the hot MPEC (factor ~85) from ~1.37×10^9 #/km to ~1.2×10^{11} #/km. These increases in emissions were associated with increases in the enclosed disc temperature from ~ 60°C to ~150°C.

c) Between 48 kph and 128 kph, for dynamic braking, mass emissions per kilometre increased significantly across all instruments. For the eFilter, emissions rose by a factor of approximately 100, from around 0.27 mg/km to 27.9 mg/km. The cold MPEC showed a slightly smaller increase, with emissions growing by a factor of about 87, from approximately 3.52×10^9 #/km to 3.06×10^{11} #/km. The hot MPEC displayed the lowest increase, with emissions rising by a factor of roughly 45, from around 3.61×10^9 #/km to 1.64×10^{11} #/km. This suggests a higher level of volatile material being released under dynamic braking than under moderate braking, despite the enclosed disc temperature increase from ~ 60°C to ~150°C being essentially the same as that observed from the moderate braking. Potentially this suggests higher short-term local temperatures with dynamic braking than moderate braking that don't translate to higher bulk disc temperatures.

8.5.7 Brake pad metrology – weights and thicknesses

a) Brake pads were weighed when new, following preliminary ageing, after secondary ageing and once the brake pad emissions evaluations were completed. Some pad masses increased slightly following an ageing step, meaning that negative wear rates were reported for that step, but this only occurred twice and at the end of testing all pads showed positive mass losses.

b) The highest mileage pad (~50,000 km), P10A, exhibited a brake wear mass reduction rate of ~5.4 mg/km, significantly higher than other pads, suggesting pads may show increased wear rates with age. P1, a similar pad with lower mileage (~1165 km), had a wear rate of ~2.27 mg/km, about 42% of P10A's rate.

c) Aggregated mass loss data showed typical brake pad emissions over the first ~1000 km were around 3 mg/km. Pads P1, P4, P7, and P8 had the lowest emissions (~2.5 mg/km), while P5 and P3 had the highest. Lower emissions were linked to premium, low metallic, recognized brands, and ceramic pads, whereas higher emissions were generally associated with low dust organic and budget pads.

d) Despite the high mileage pad (P10A) showing the highest mass loss rate after >740 km, it exhibited the lowest wear thickness reduction rate. This trend of lower thickness reduction with higher mileage is supported by data from various pads. Typical thickness loss from Pads P1-P9 after testing (744 km to 1165 km) was ~0.3 µm/km. Comparison of P1 (0.29 µm/km) and P10A (0.20 µm/km) indicates a reduction in wear rate of ~0.09 µm/km between 1165 km and 50500 km, suggesting a significant slow-down in wear rate at higher mileage.

e) Across Pads P1 to P9, thickness reduction rates for mileages >740 km range from just above 0.2 µm/km to above 0.4 µm/km. Pads P3 and P9 show substantially higher wear (>0.35 µm/km), while Pads P5 and P7 show lower wear. There were no obvious links between pad types/descriptions and thickness reduction trends, unlike weight-based effects.

9. BRAKING TECHNOLOGY RESULTS

9.1 TESTING PERFORMED

Braking technology emissions tests were performed on the 4WD chassis dynamometer in the 4WD-capable VERC, rather than the 2WD VATF, since EV and PHEV may utilise all four wheels for regenerative braking, and functions such as traction control may not work in a fully representative manner on a two-wheel drive chassis dynamometer. This also means that fully representative braking forces are experienced by the instrumented front brake.

9.1.1 Technical Approach

Tests were performed on the VW Caddy (ICE), VW Golf GTE (PHEV) and VW eGolf (EV), with two distinct approaches taken:

- Fixed test mass: all vehicles were evaluated at a fixed test mass of 1900 kg – equal to the typical mass of the VW Caddy with all the measurement equipment on-board, as used in the brake wear emissions testing (Section 8). From these data, a comparison of results represents a direct comparison of the impact of the regenerative + friction braking capabilities of the EV and PHEV with the friction-only braking capacity of the ICE. This comparison enables the benefits of regenerative braking on brake particle emissions to be determined independently of vehicle mass. This aspect was included since one important question asked of this study was whether reductions in particle emissions from regenerative braking are offset by the typically higher test mass of EV and PHEV.

- Variable test mass: the ICE LCV, PHEV and EV were tested at representative masses (1900 kg, 1700 kg, 1700 kg respectively), while in addition the ICE was also subjected to limited testing at a mass and dynamometer terms representative of a typical lighter ICE passenger Golf (1500 kg). From these data insights into real comparative emissions of the vehicles, including both contributions of the braking system technology and the test mass, are achieved.

Due to the selection of ICE, PHEV and EV with a shared vehicle platform it was possible to equip the three test vehicles with the same calliper, brake pad and disc sets, so these are eliminated as variables when comparing emissions between vehicles. Testing was performed using the service pads (Px, Pagid PA4309GF)

and service disc (Dx, Eicher low-cost disc), see Table 7-1 for further details. Similarly, wheels, tyres and brake enclosures were common between the three vehicles, also eliminating these as potential confounding variables when comparing emissions.

The front brake specification for the VW Golf GTE (PHEV) consists of a Ø312 mm front brake disc, with the same brake calliper piston diameter as the VW Caddy and VW eGolf but mounted at a larger effective radius by way of revised calliper anchor bracket. The rear brake specification is common across all three vehicles. The larger diameter brake disc increases the front bias of the braking system by approximately 2% and the available brake torque available by approx. 11% for a given pressure. The brake specification change is probably to reflect the vehicle performance, mass and customer expectation for the PHEV vehicle.

Fitment of the smaller front brake disc and calliper to the PHEV would make a small difference to the regenerative braking system performance. Detailed investigation of the regen strategy applied to the PHEV and EV was outside the scope of this project, however, for the dynamometer based drive cycles applied and aim of the project, this approach was considered acceptable. The change in brake bias and brake torque was likely to result in compromised driveability caused by a mismatch between the driver braking demand and the regenerative brake torque applied. The difference was expected to be within the typical system tolerance applied when considering friction variability, vehicle loading and "real world" driving conditions.

For the braking technology investigations, emissions measurements were performed with the measurement equipment, pumps, filters and other sampling and measurement system elements externally installed on a trolley (Figure 9-1). Only the enclosure and transport tubing for the air input and sample outlet were installed to the vehicle. This approach permitted rapid changes between vehicles and accelerated test throughput, while avoiding the complexities of accommodating large amounts of equipment in the two relatively small passenger cars (PHEV and EV).
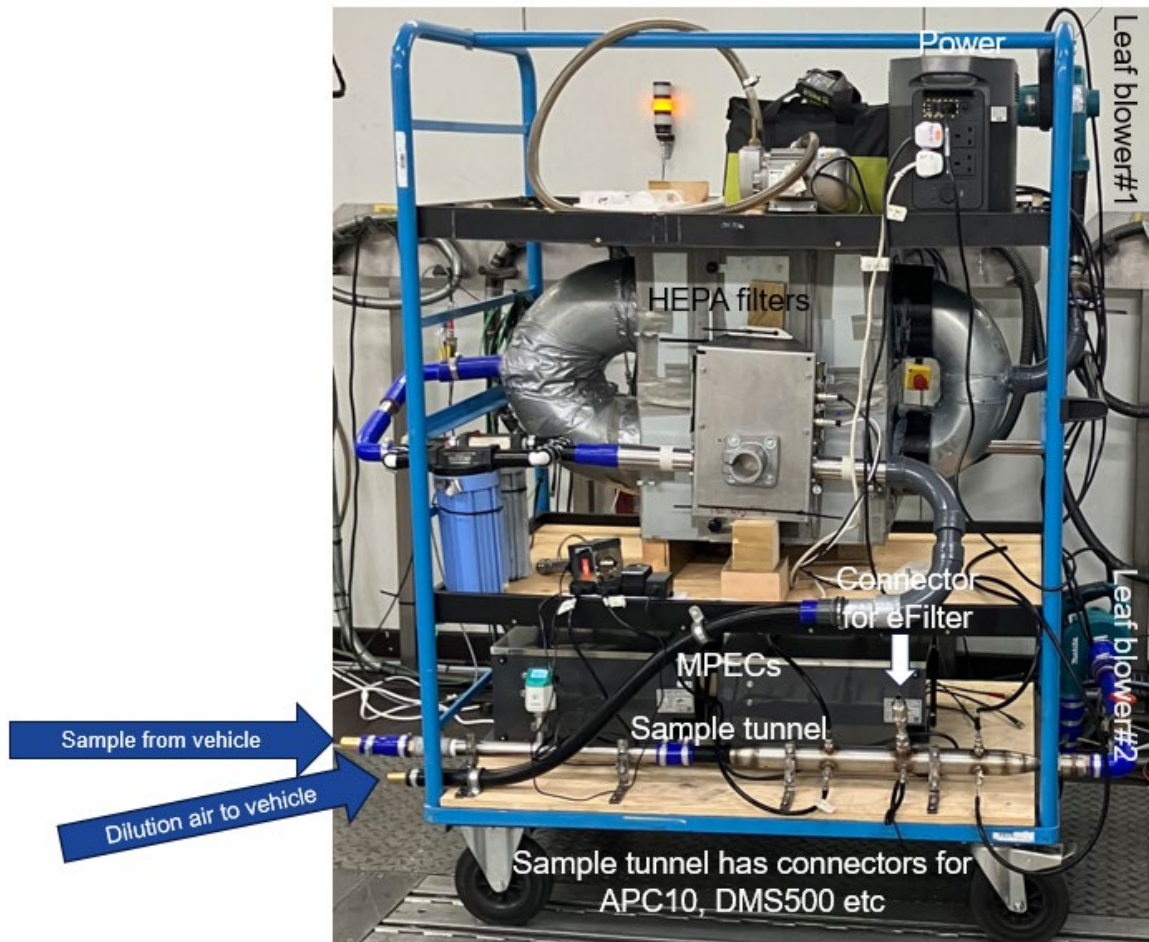
Figure 9-1: Sampling trolley used for brake technology sampling on ICE, PHEV and EV.

During tests on the PHEV and EV, measurements of currents were made using a Hioki PW 3390 power meter (Figure 9-2a) and current clamps were attached to the high voltage lines under-bonnet (Figure 9-2b). These data were employed to investigate the activation, or not, of regenerative braking.

Figure 9-2: (a) Hioki Power Meter; (b) current clamp.

9.1.2 Tests per vehicle

The ICE, PHEV and EV were tested over identical protocols, excepting a subset of additional tests performed when the ICE LCV was tested with changed test mass and dynamometer terms in order to simulate a lighter passenger car on the same platform, such as a Golf TSI. Emissions tests were restricted to the PG42 cycle, on-dyno RDE and bespoke cycle.

The PHEV was tested in e-mode (Section 2.2) and the EV was tested in normal mode (Section 2.3). Both vehicles were fully charged prior to the first PG42, dyno RDE and the bespoke cycle. However, despite the EV range showing as 102 – 110 miles following an overnight charge, the vehicle was unable to complete any more than one PG42 on a full charge, despite the length of the PG42 cycle being ~50km (31 miles). The impact of this was that the EV testing took longer than expected while measures were taken to recharge the vehicle between tests. These issues are discussed in Section 9.2.2.

Table 9-1 summarises the tests planned, identifying the test masses used. Tests highlighted in grey were compared to investigate the effects of regenerative and friction braking, tests highlighted in blue were compared to determine emissions of actual vehicle types, including their realistic test masses.

Table 9-1: Testing planned for braking technology investigations.

Test Cycle	ICE (Caddy)	PHEV (Golf GTE)	EV (eGolf)	ICE (Caddy test as Golf TSI)
PG42#1	1900 kg	1900 kg	1900 kg	1500 kg*
PG42#2	1900 kg	1700 kg	1700 kg	[-]
PG42#3	1900 kg	1700 kg	1700 kg	[-]
Dyno RDE#1	1900 kg	1900 kg	1900 kg	1500 kg*
Dyno RDE#2	1900 kg	1700 kg	1700 kg	[-]
Dyno RDE#3	1900 kg	1700 kg	1700 kg	[-]
Bespoke	1900 kg	1700 kg	1700 kg	[-]

*Dynamometer terms matched to those of the PHEV and EV at 1700 kg.

The various tests were performed over a period of ~2 months due to restrictions in VERC access. The intervening periods saw tyre testing performed in the VATF. A list of braking technology tests by date, including some repeats and failures, is shown in Table 9-2. Note that the same colour scheme is employed as for Table 9-1, with tests highlighted in red to investigate the effects of regenerative and friction braking and tests highlighted in blue to determine emissions of actual vehicle types.

Table 9-2: Testing performed for braking technology investigations

Date	Test performed
02/07/2024	Caddy - PG42 #1, 1900 kg
02/07/2024	Caddy - PG42 #2, 1900 kg
02/07/2024	Caddy - PG42 #3, 1900 kg
03/07/2024	Caddy - dyno RDE #1, 1900 kg
03/07/2024	Caddy - dyno RDE #2, 1900 kg
03/07/2024	Caddy - dyno RDE #3, 1900 kg
10/07/2024	Golf GTE - PG42 #1, 1900 kg
10/07/2024	Golf GTE - PG42 #2, 1700 kg
10/07/2024	Golf GTE - PG42 #3, 1700 kg
11/07/2024	Golf GTE – Bespoke, 1700 kg
12/07/2024	Golf GTE - dyno RDE#1, 1700 kg
12/07/2024	Golf GTE - dyno RDE#2, 1700 kg
12/07/2024	Golf GTE - dyno RDE#3, 1700 kg
16/07/2024	eGolf - PG42 #1, 1900 kg
16/07/2024	eGolf - PG42 #2 - Battery ran out near EOT

17/07/2024	eGolf - dyno RDE#1, 1700 kg
17/07/2024	eGolf - dyno RDE#2 - eFilter data lost
18/07/2024	eGolf – Bespoke, 1700 kg
30/07/2024	eGolf - PG42 #2, 1700 kg
30/07/2024	eGolf - PG42 #3, 1700 kg
31/07/2024	eGolf - dyno RDE#3, 1700 kg
31/07/2024	eGolf - dyno RDE#4, 1900 kg
19/08/2024	Golf GTE - PG42, 1900 kg
22/08/2024	Caddy - PG42, 1500 kg
22/08/2024	Caddy - dyno RDE, 1500 kg
23/08/2024	Caddy – Bespoke, 1900 kg
23/08/2024	Caddy - PG42 #1, 1900 kg
28/08/2024	eGolf - PG42 #1 1700 kg
30/08/2024	GTE - dyno RDE, 1900 kg

9.1.3 Effect of regenerative braking energy recovery on brake disc temperature

Testing on the 4WD chassis dynamometer allowed limited analysis of the effect of regenerative braking on particulate generation to be investigated. The Hioki Power Analyzer in conjunction with current clamps at the traction battery allowed the regenerative contribution to be calculated.

The expected total energy over the PG42 cycle could be calculated and compared to the actual energy measured by summation of the vehicle speed and acceleration over each 1 second increment using the following equation:

$$E = \sum \frac{1}{2} m (v_2 - v_1)^2$$

Where E is the energy measured, m is the mass of the vehicle and v_2-v_1 is the increment in vehicle speed over 1 second.

From the dynamometer, the total power, front axle power and rear axle power were measured. Table 9-3 shows values for two PG42 tests on the E-Golf vehicle. The front and rear values approximately sum to the total power value, with the front axle seeing both "Max" positive and "Min" negative values, representing traction and braking, whilst the rear axle shows only negative (braking) values. The brake proportion of front axle ~ 80%, rear axle ~ 20%, reflects the hydraulic + regenerative proportioning of the vehicle. The values measured were consistent from test to test, demonstrating good repeatability of the driver and the test equipment.

Table 9-3: Test to test repeatability of power flow and energy flow.

Test name	Expected total energy (kJ)	Calculated total energy (kJ)	Max total dyno power (kW)	Min total dyno power (kW)	Max front power (kW)	Min front power (kW)	Sum of all front axle dyno power - positive (kW)	Sum of all front axle dyno power - negative (kW)	Max rear dyno power (kW)	Min rear dyno power (kW)
VERC_1034	1188745	1189883	63.96	-97.48	68.37	-77.77	28079	-6896	0	-19.72
VERC_1259	1188745	1188278	69.79	-95.62	69.79	-76.93	27961	-6923	0	-18.69
Difference (%)			-8.35	1.95	-2.03	1.09	0.4	-0.4	0	5.51

The Hioki Power Analyzer measured current via clamps, but no traction battery voltage data was recorded. Consequently to calculate power at the traction battery, a fixed traction battery voltage of 400v was assumed.

In reality the battery voltage would change as battery state of charge (SoC) varies. This gives a consistent approach for test to test comparison, but not absolute values.

Regenerative energy could be calculated by taking the dynamometer front axle power over the cycle (positive is traction, negative is regenerative or deceleration) and comparing it to the Hioki calculated power which represents the power seen at the battery (ignoring losses). For the E-Golf, the positive (traction power) should be the same from both instruments, but the negative (deceleration power) should only represent the regenerative energy recovered to the traction battery, the balance being friction braking.

Applying a fixed assumption of 400 volts for the traction battery gives a poor correlation between the actual measured power and that calculated from the current clamp. Since the only source of traction power to the vehicle is the battery, the measured and calculated traction powers were normalized and that constant then applied to the regenerative power calculation. The "constant" represents a combination of the actual voltage, inertia values applied to the dynamometer, losses and calculation accuracy over 1 second sampling period.

Table 9-4: Power and regenerative braking proportion for two PG42 tests.

Test name	Sum of all front axle dyno power - positive (kW)	Sum of all front axle dyno power - negative (kW)	Constant applied	Calculated power - positive (traction)	Calculated power - negative (regenerative)	Friction braking contribution (kW)	Regenerative braking proportion (%)
VERC_1034	28079	-6896	226	28066	-3526	(-6896) - (-3526) = -3370	48.90%
VERC_1259	27961	-6923	219	27958	-3515	(-6923) - (-3515) = -3408	50.80%

Over the PG42 cycle, where a maximum deceleration of 2.2 m/s^2 is required, approximately 50% of the braking energy was recovered to the battery via regenerative braking (Table 9-4). This represents a higher proportion than that seen in a typical "real world" situation.

Figure 9-3 and Table 9-5 show that the regenerative braking contribution results in significantly lower brake disc temperatures over the cycle when compared to the temperatures developed by the friction brakes on the ICE vehicle. The lower temperatures reflect the significant regenerative braking contribution on the front axle.

Table 9-5: Disc temperatures during two PG42 cycles using the E-Golf.

Test name	Front disc average (°C)	Front disc peak (°C)	Rear disc average (°C)	Rear disc peak (°C)
E-Golf (P1 3-4 D1-2 PG42_2_eGF)	41. 4	86.2	34.8	60
E-Golf (P1 3-4 D1-2 PG42_3_eGF)	35.5	72.2	29.8	51.2
VW Caddy	101	217.1	N/A	N/A
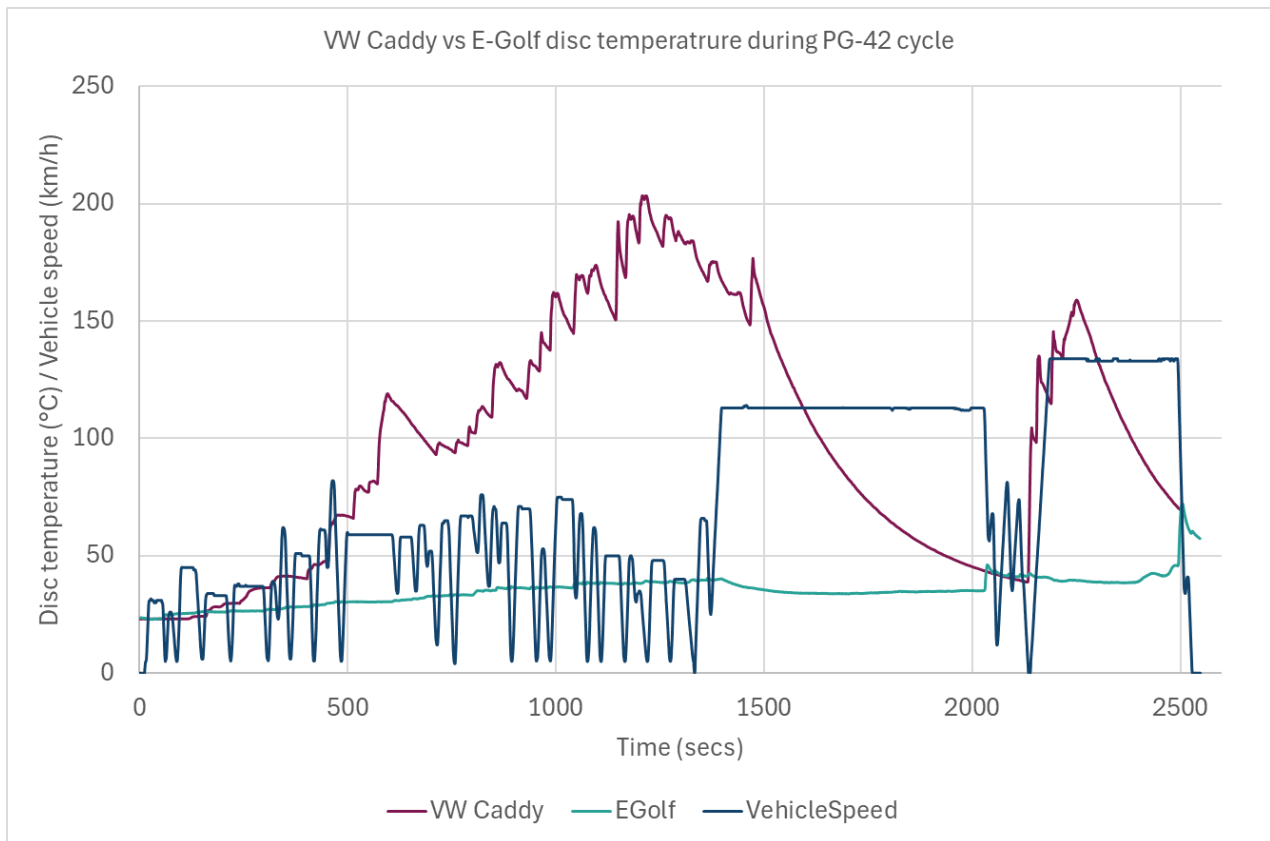
Figure 9-3: Front brake disc temperature comparison between the VW Caddy and the E-Golf over a PG42 cycle.

9.2 BRAKE TECHNOLOGY EMISSIONS RESULTS

This section presents results of comparative brake particle emissions measurements from ICE, PHEV and EV vehicles constructed on the same platform, employing the same braking hardware (callipers, discs and pads) and driven over the same tests: PG42, dynamometer RDE and bespoke cycles. The main differences between the vehicles are the presence of regenerative braking with the EV and PHEV, with a greater proportion of regenerative braking being available to the EV, and a range of test masses.

Between them, the three drive cycles used cover a wide range of vehicle operation, from low to high speed and from gentle to dynamic braking, and so common trends between the three cycles will be indicative of representative differences in emissions between the vehicles.

Results are split into two parts, the first addressing emissions differences between the vehicles, and so incorporating both the influences of test mass and braking technology, while the second reports on tests with aligned vehicle test mass and measures braking technology (frictional plus regenerative) in isolation.

It should be reiterated that the trends identified for both mass and number metrics apply to the $PM_{2.5}$ range only.

9.2.1 Emissions of ICE, PHEV and EV using appropriate test masses and vehicle-specific dyno terms

PN emissions from ICE, PHEV and EV are presented for PG42, on-dyno RDE, and bespoke cycles in Figure 9-4, Figure 9-5 and Figure 9-6, respectively. It should be noted that in these figures, the bespoke cycle is treated as an emissions cycle and the results shown represent the cumulative contribution of all the 63 individual braking events, on a particles/km basis.

Results show a reasonably consistent trend in that ICE PN emissions results from cold and hot MPEC at 1900 kg are higher than PHEV results at 1700 kg, which are higher than EV results at 1700 kg. The lower emissions observed from EV than PHEV, at the same test mass, is indicative of a higher level of regenerative braking leading to lower brake particle emissions. Higher emissions from the ICE at 1900 kg, is due to the higher test mass, the use of only frictional braking, or a combination of the two. Differences between cold MPEC and hot

MPEC are consistently > 20 % (Figure 5-2), indicating the likely presence of volatile particle emissions. Particle emissions from the ICE at 1500 kg test mass are similar to, or higher than, the emissions of the EV, and lower than the hot MPEC results from the PHEV, which indicates that for low volatility particles test mass is an important factor in reducing emissions. Cold MPEC results are higher than hot MPEC results, which indicates the presence of at least some volatile particles that can be eliminated by the volatile particle remover of the hot MPEC.

Conversely, there is relatively little difference between the emissions of the wholly non-volatile PN10 particles measured by the APC10 during PG42, dyno RDE and bespoke cycles (isolated and magnified in Figure 9-7a, b, and c respectively) between any of the vehicles / test masses evaluated, excepting perhaps slightly elevated PN from the ICE at 1900 kg during the bespoke cycle. This may indicate that the primary impacts of regenerative braking and test mass in the $PM_{2.5}$ regime are on volatile and semi-volatile particle emissions and not on wholly non-volatile materials. Emissions are consistent between vehicles at ~1.5×10^9 #/km from the PG42 cycle, and ~2×10^9 #/km from the on-dyno RDE, with bespoke emissions at ~5×10^9 #/km from the ICE at 1900 kg and ~3×10^9 #/km from the PHEV and EV.

Higher non-volatile particle emissions from the ICE than the PHEV and EV in the bespoke cycle could derive from the extra 200 kg test mass during several braking events that are harsher than seen in the PG42 and on-dyno RDE cycles.
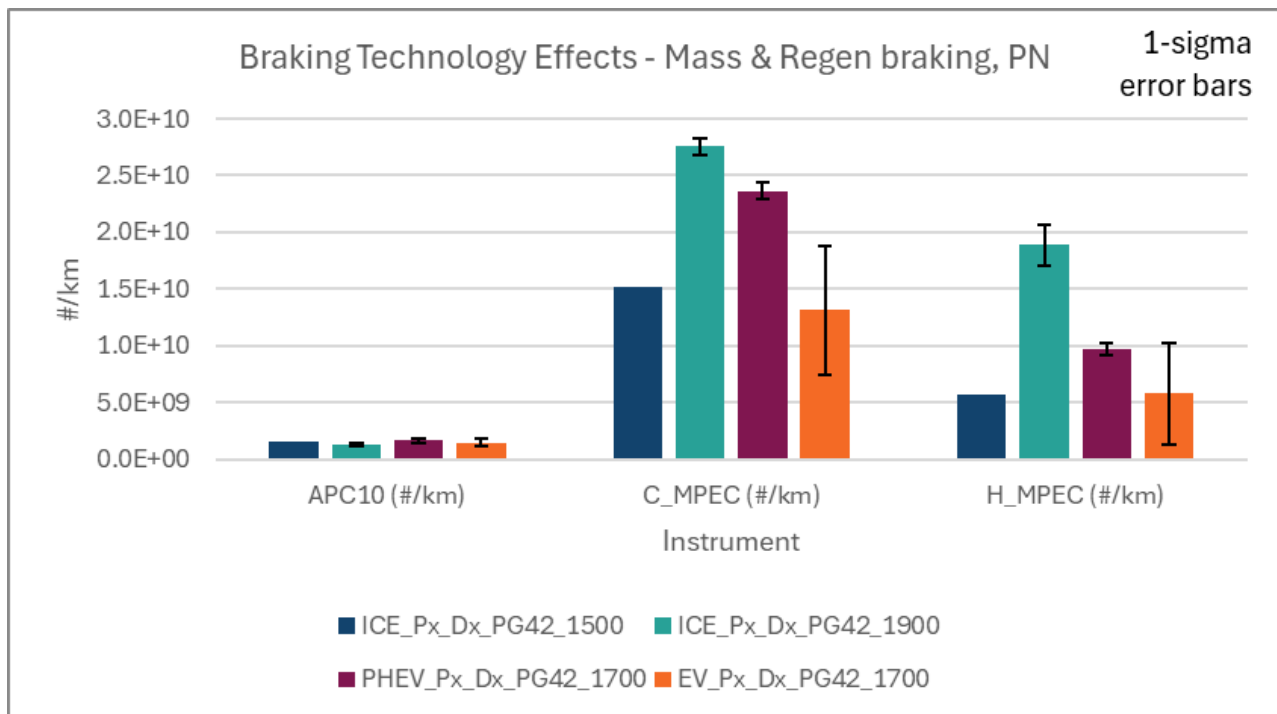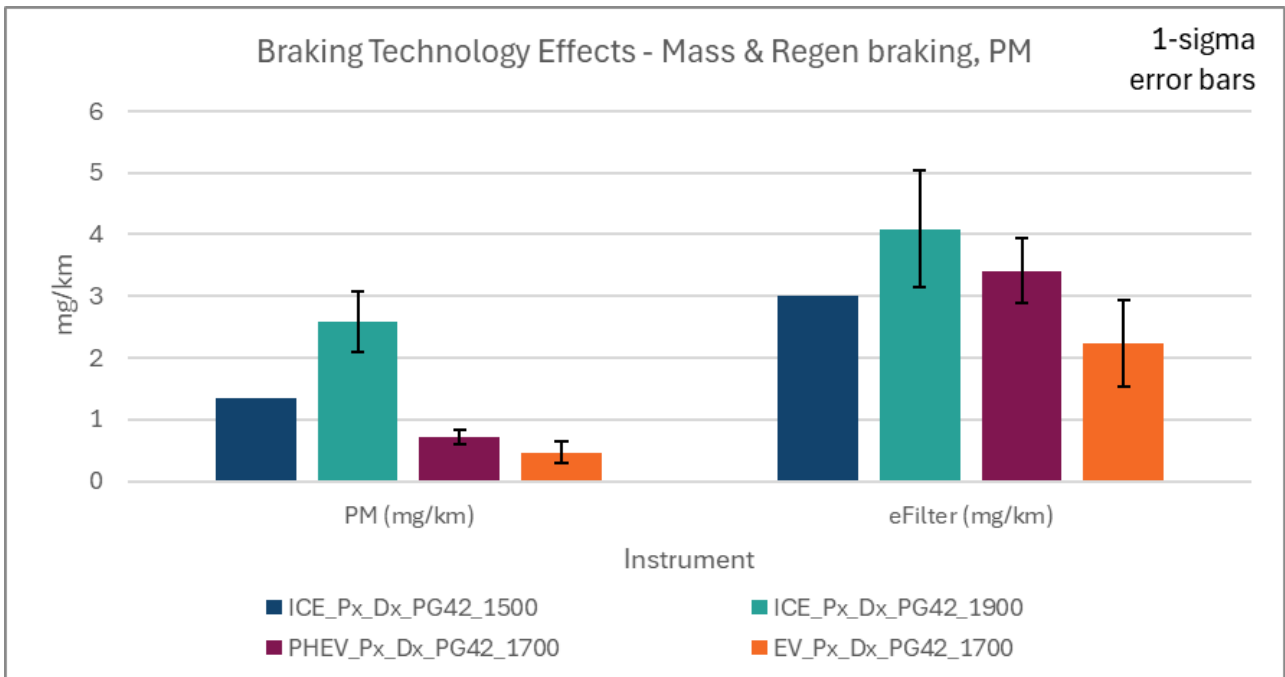

Figure 9-4: PG42 PN emissions under different test masses and braking technology effects.
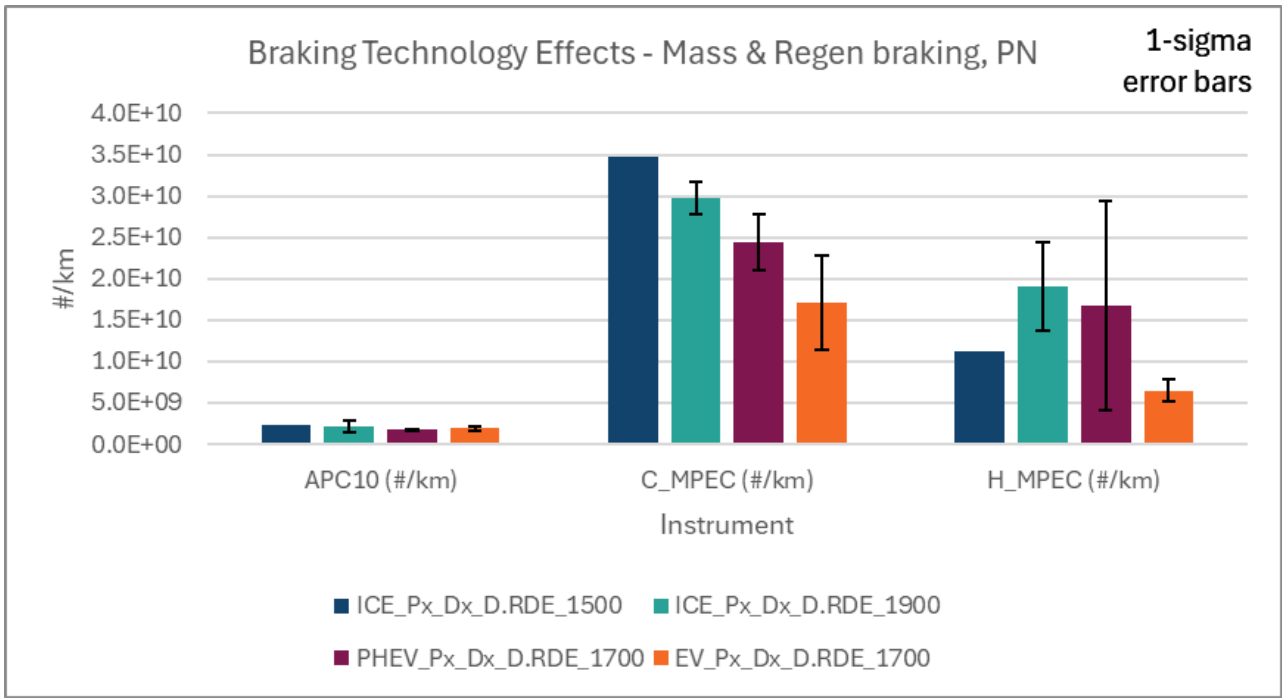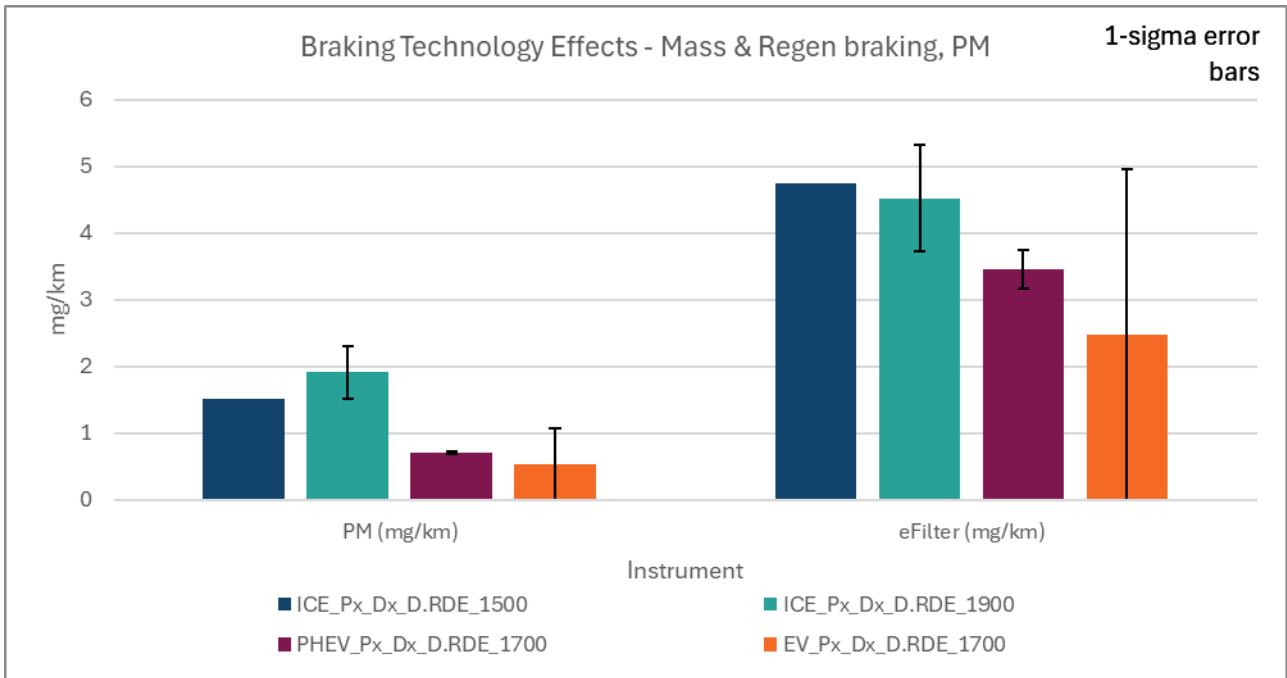
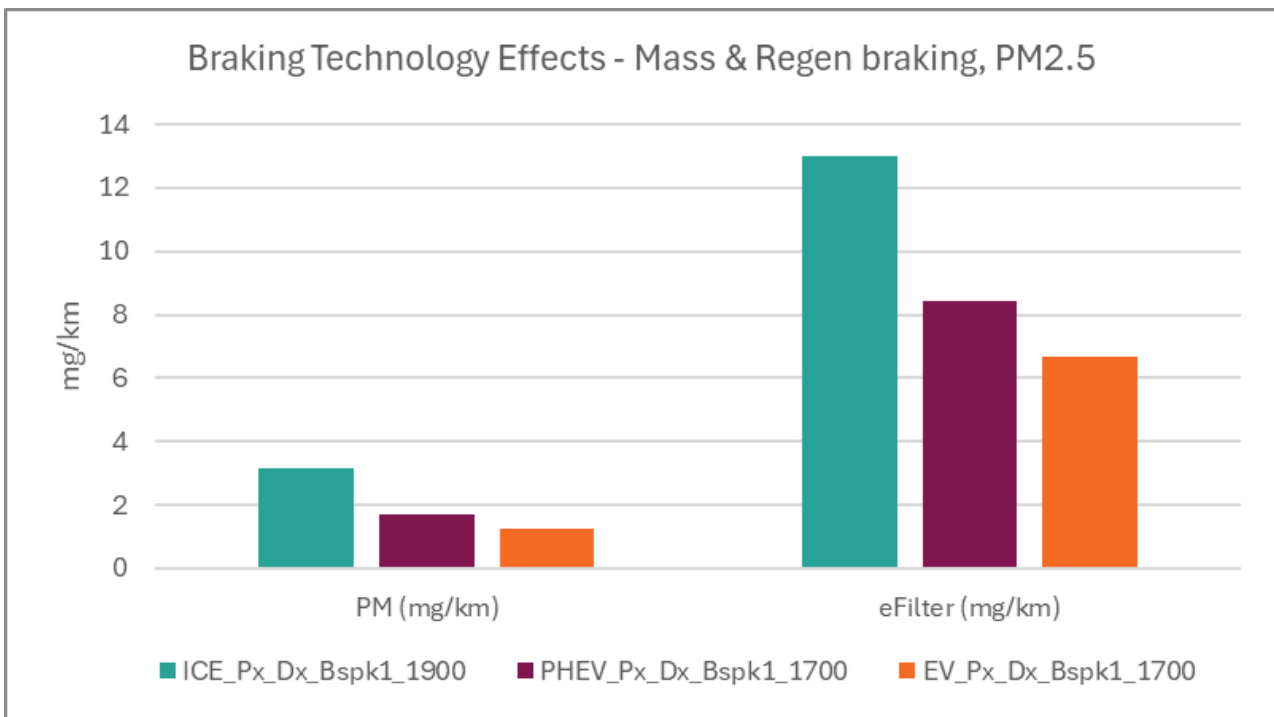Figure 9-5: On-dyno RDE PN emissions – test mass and braking technology effects
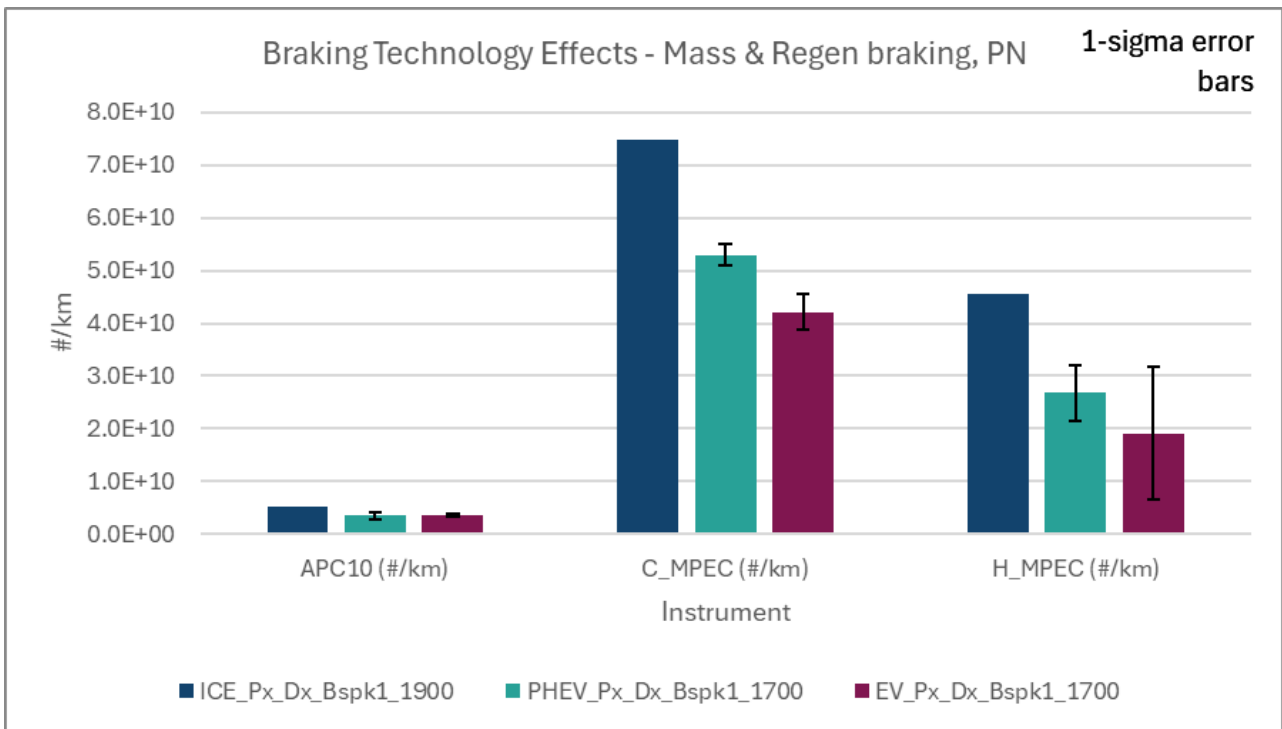
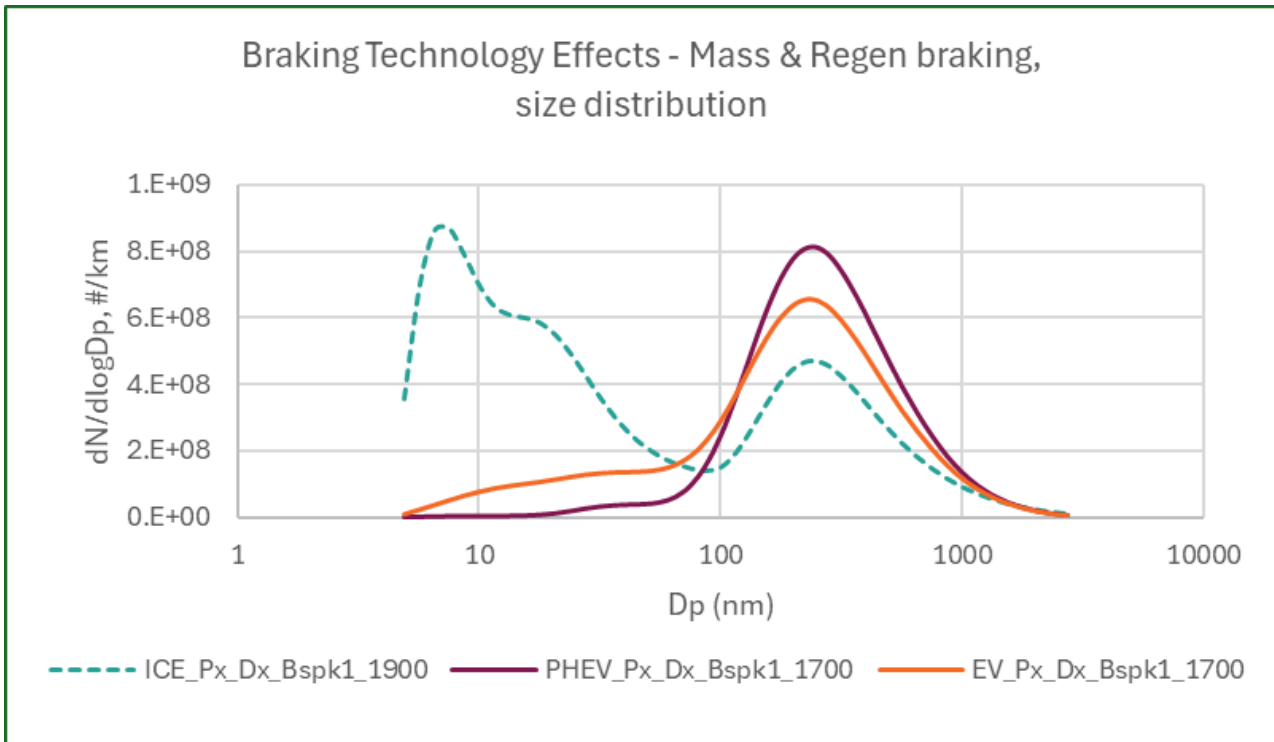Figure 9-6: Bespoke cycle PN emissions – test mass and braking technology effects
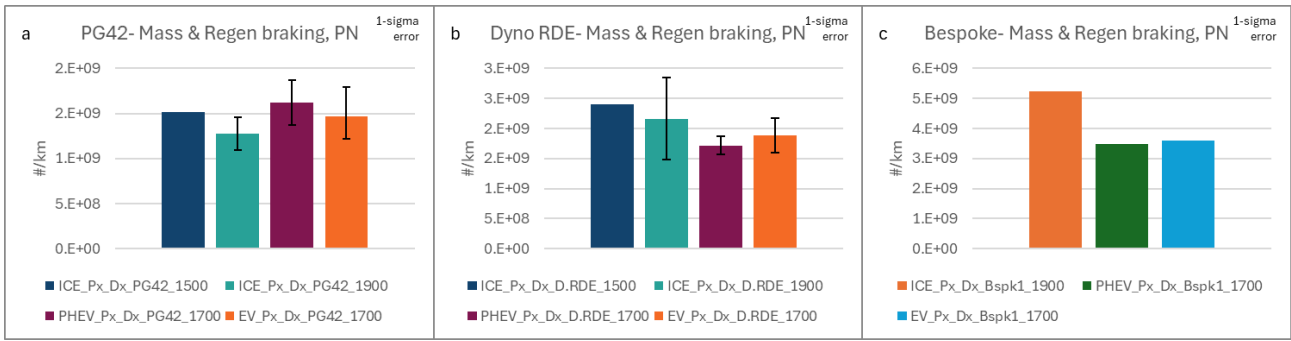
Figure 9-7: PN10 emissions measured by the APC10 for a) PG42 cycle, b) on dyno RDE cycle and c) bespoke cycle, under different test masses and braking technology effects.

PM (PM$_{2.5}$) emissions for the PG42, on-dyno RDE, and bespoke cycles are shown in Figure 9-8, Figure 9-9, and Figure 9-10, respectively. All three charts show a similar trend, that gravimetric PM is highest from the ICE, the PHEV is next highest, and the EV is lowest. Gravimetric PM$_{2.5}$ emissions from the ICE are typically in the range 2 to 3 mg/km from the three cycles, 0.6 to 1.6 mg/km from the PHEV and 0.3 to 1.2 mg/km from the EV. Emissions rankings are consistent with eFilter data from the three drive cycles. The eFilter PM data reports considerably higher than the gravimetric PM, which is likely to be due to the multiple charging effect of large particles that also leads to the apparent high PN observed from the MPECs. Average gravimetric PM$_{2.5}$ emissions from the ICE did not exceed 2.5 mg/km from either PG42 or dyno RDE cycle, and emissions from the PHEV and EV were less than 30% of this level.

The 1500 kg ICE data (light-blue bars) from the PG42 and chassis dyno RDE cycles in Figure 9-8 and Figure 9-9, respectively, indicate that while emissions are lower than from the 1900 kg ICE, the drop in test mass of 400 kg does not reduce the gravimetric PM$_{2.5}$ emissions to the levels observed from either PHEV or EV. The comparative data from the eFilter are less definitive, but the 1700 kg EV emissions are consistently lower than the 1500 kg ICE.

Figure 9-8: PG42 PM emissions – test mass and braking technology effects.

Figure 9-9: On-dyno RDE PM emissions – test mass and braking technology effects.

Figure 9-10: Bespoke cycle PM emissions – test mass and braking technology effects.

Number-weighted particle size distributions from the PG42 (Figure 9-11), chassis dyno RDE (Figure 9-12) and bespoke cycle (Figure 9-13) are shown below. All cycles show bimodal character, with a sub-100nm mode showing a peak below 20nm and a >100nm mode showing a peak in the range 200nm to 300nm. In the >100nm mode, which is likely to be the main $PM_{2.5}$ mass-containing mode, emissions are always highest from the 1900 kg ICE, next from the PHEV and lowest from EV. The 1500 kg ICE mode is always higher than that from the EV. Emissions from the <100nm mode appear more variable than from the mode of larger particles and are likely dominated by emissions of volatile or semi-volatile particles.
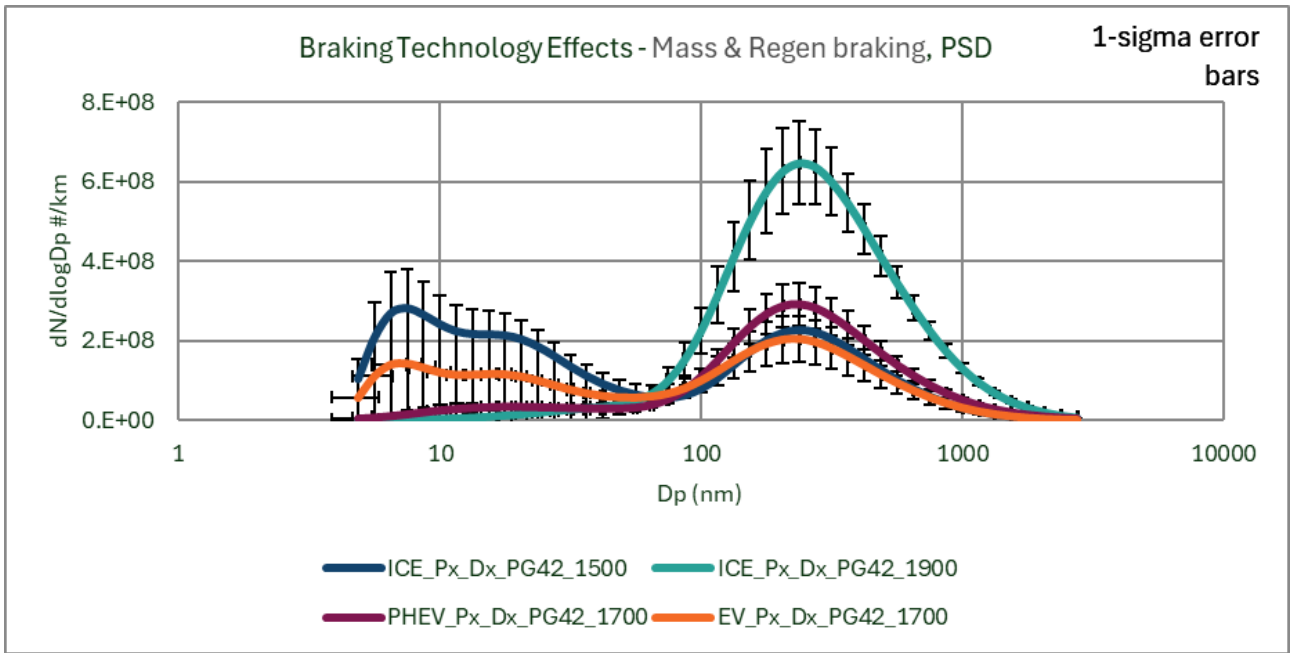
Figure 9-11: PG42 particle size distributions – test mass and braking technology effects.
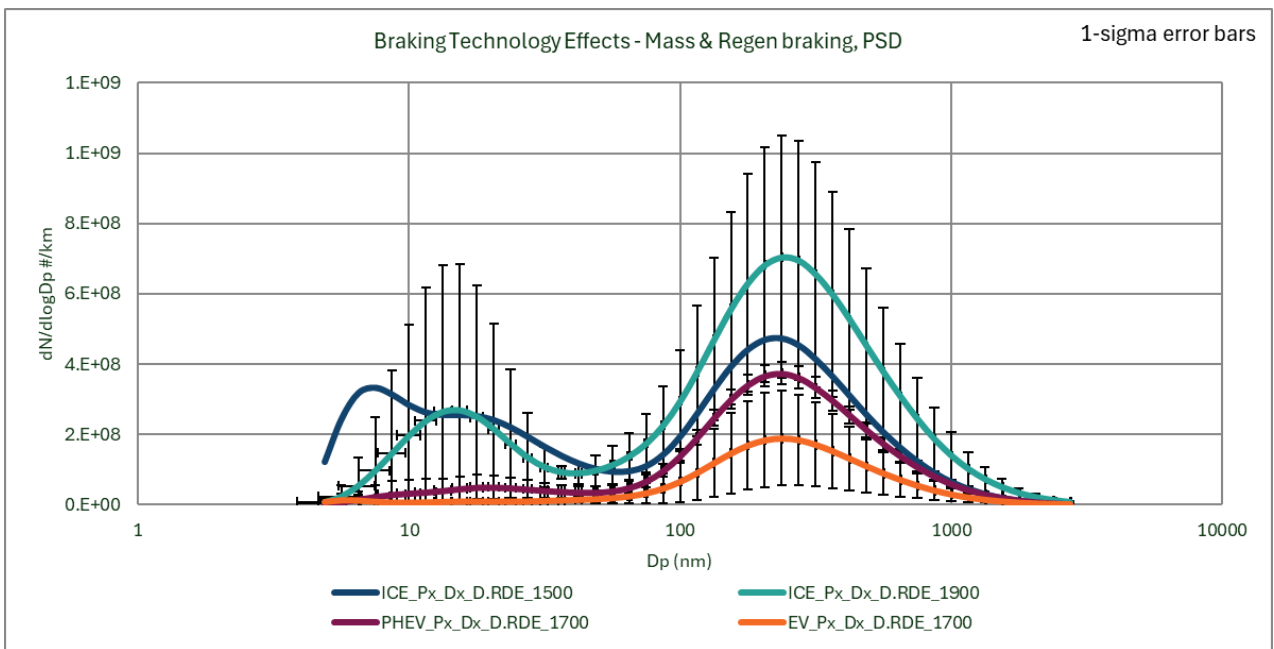
Figure 9-12: On-dyno RDE particle size distributions – test mass and braking technology effects.

Figure 9-13: Bespoke cycle particle size distributions – test mass and braking technology effects.

9.2.1.1 Bespoke cycle analysis – individual braking events

The bespoke cycle (Figure 6-10) was designed to permit the comparison of discrete braking events from different speeds (30kph, 50kph, 80kph and 110kph) and severities (gentle, moderate, dynamic), including braking to rest, braking from a fixed speed to a fixed lower speed and the impact on emissions of braking from a given speed when the braking system is cool (at the start of the bespoke cycle) and when the braking system is hot (at the end of the bespoke cycle after high-speed braking has been conducted). In this section results from the ICE, PHEV and EV are presented, with ICE tested at 1900 kg and the PHEV and EV tested at 1700 kg. Emissions effects are shown for PN10 (APC10) and for PM (eFilter). The cold and hot MPEC instruments were also employed, but since the majority of PN emissions from braking events are solid particles, emissions trends for these closely resemble emissions measured by the APC10, and their results are not shown.

Each bespoke cycle includes 63 discrete braking events (Table 6-2) but many of these events are executed in close proximity to nominal repeats. To simplify the presentation of results, these repeats are averaged. Results are presented as particles/km or mass/km, which given the short distances over which braking is executed, results in some high specific emissions levels.

In charts throughout this section ICE results are shown as dark blue bars, PHEV results as orange bars and EV results as grey bars.

9.2.1.1.1 Braking events at 30 kph – ICE, PHEV and EV

Figure 9-14 shows PN10 and PM emissions, respectively, from gentle, moderate and dynamic braking events of the ICE vehicle when started from a 30 kph cruise. Six bars are shown. From the left the initial two bars show first cool and then hot gentle braking emissions, the next two bars cool and then hot moderate braking and the final two bars cool and then hot dynamic braking.

It is clear that for gentle and moderate braking from 30 kph there are slightly higher emissions from the hot than the cool braking system, but for dynamic braking there is a greater increase when the braking system is hot. Braking emissions from 30kph in gentle, moderate and dynamic manner appear to have similar emissions levels when the braking system is cool. Effects on braking observed are consistent between PN and PM.
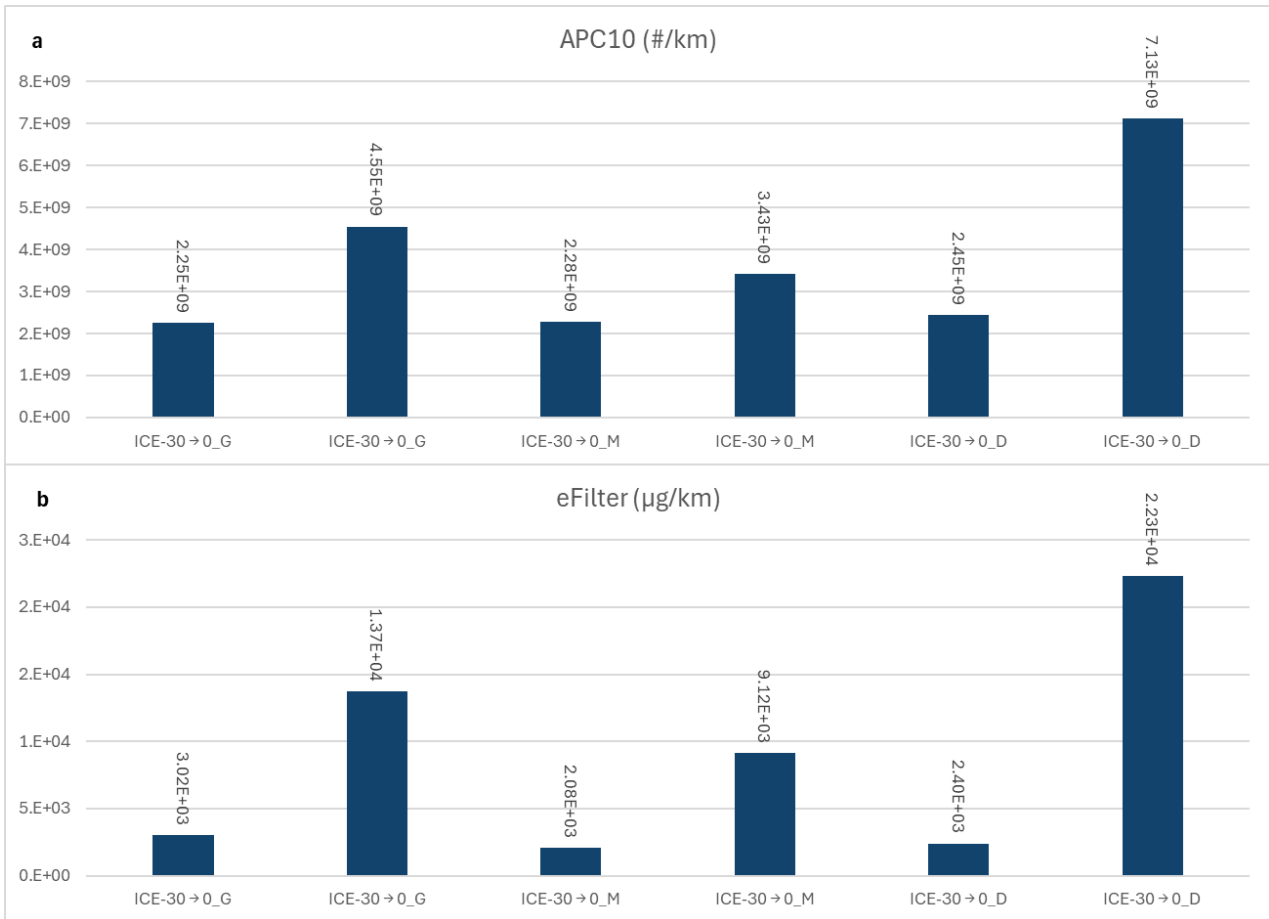
Figure 9-14: a) PN10 and b) PM emissions for ICE braking events at 30 kph.

Figure 9-15 shows PN10 and PM emissions from gentle, moderate and dynamic braking events at 30 kph, and featuring data from the ICE, PHEV and EV vehicles. Several effects are apparent:

- ICE PN10 emissions are higher than, or similar to, PHEV and EV emissions

- EV PN10 emissions are consistent across all tests, while PHEV and ICE emissions vary

- From the hot 30kph tests at the end of the bespoke cycle, PN10 emissions from ICE and PHEV are 3x the levels from the EV

- For PM emissions from comparable tests, ICE > PHEV > EV
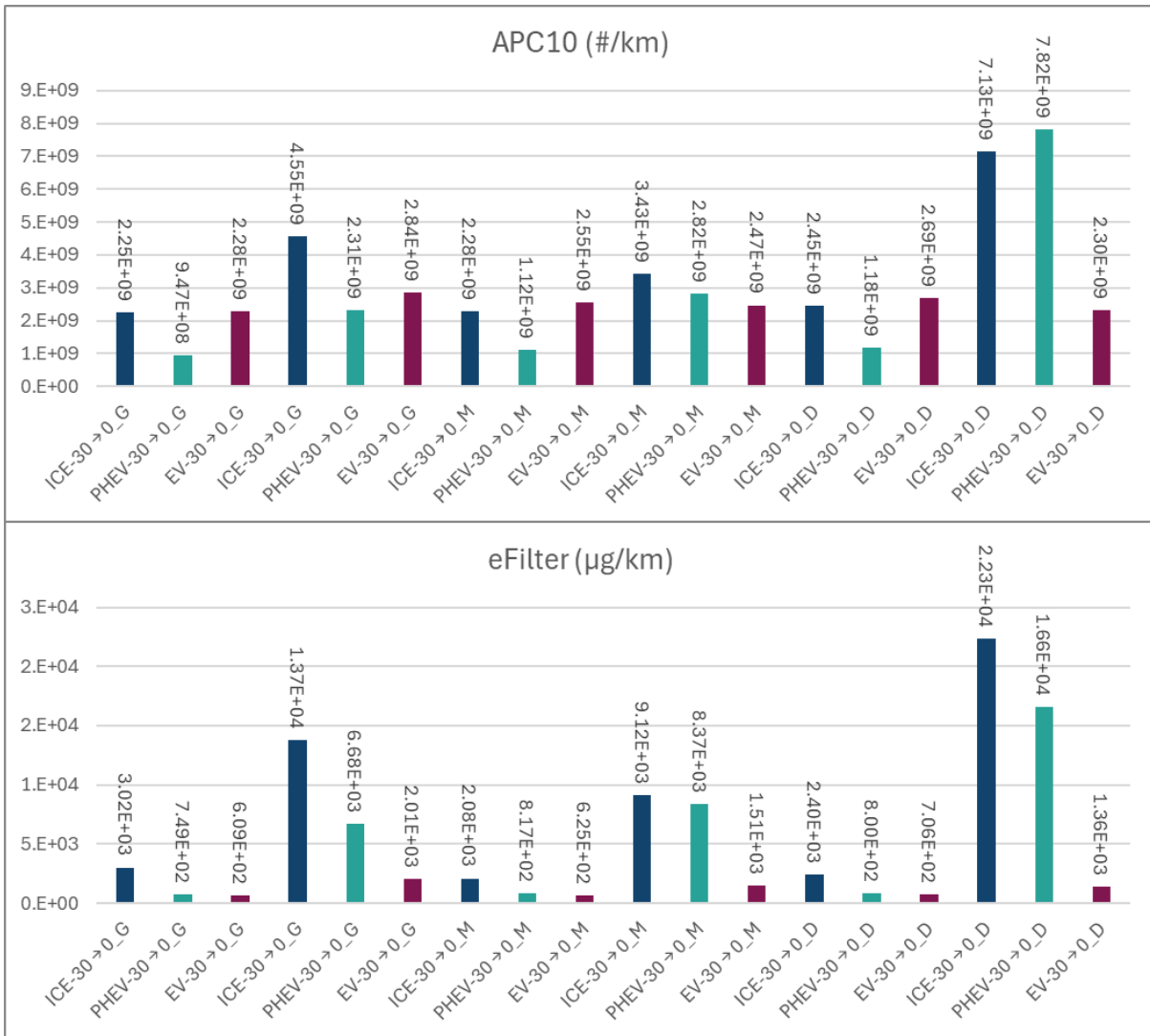
Figure 9-15: a) PN10 and b) PM emissions, from braking events from 30 kph for ICE, PHEV and EV vehicles.

9.2.1.1.2 Braking events at 50kph – ICE, PHEV and EV

Braking events from the ICE vehicle, starting at 50 kph, are shown in Figure 9-16. Note that not all conditions were tested with all vehicles. This figure provides the following indications:

- Gentle or moderate braking from 50 kph to a lower speed (50 to 15 kph, gentle; 50 to 30 kph, moderate) results in lower emissions than braking from 50 kph to rest
- When braking from 50 kph to rest PN and PM emissions are higher from moderate and dynamic braking than from gentle braking
- Dynamic braking from 50 kph to 30 kph, 15 kph and to rest shows highest emissions when braking to rest and lowest emissions when braking to 30 kph
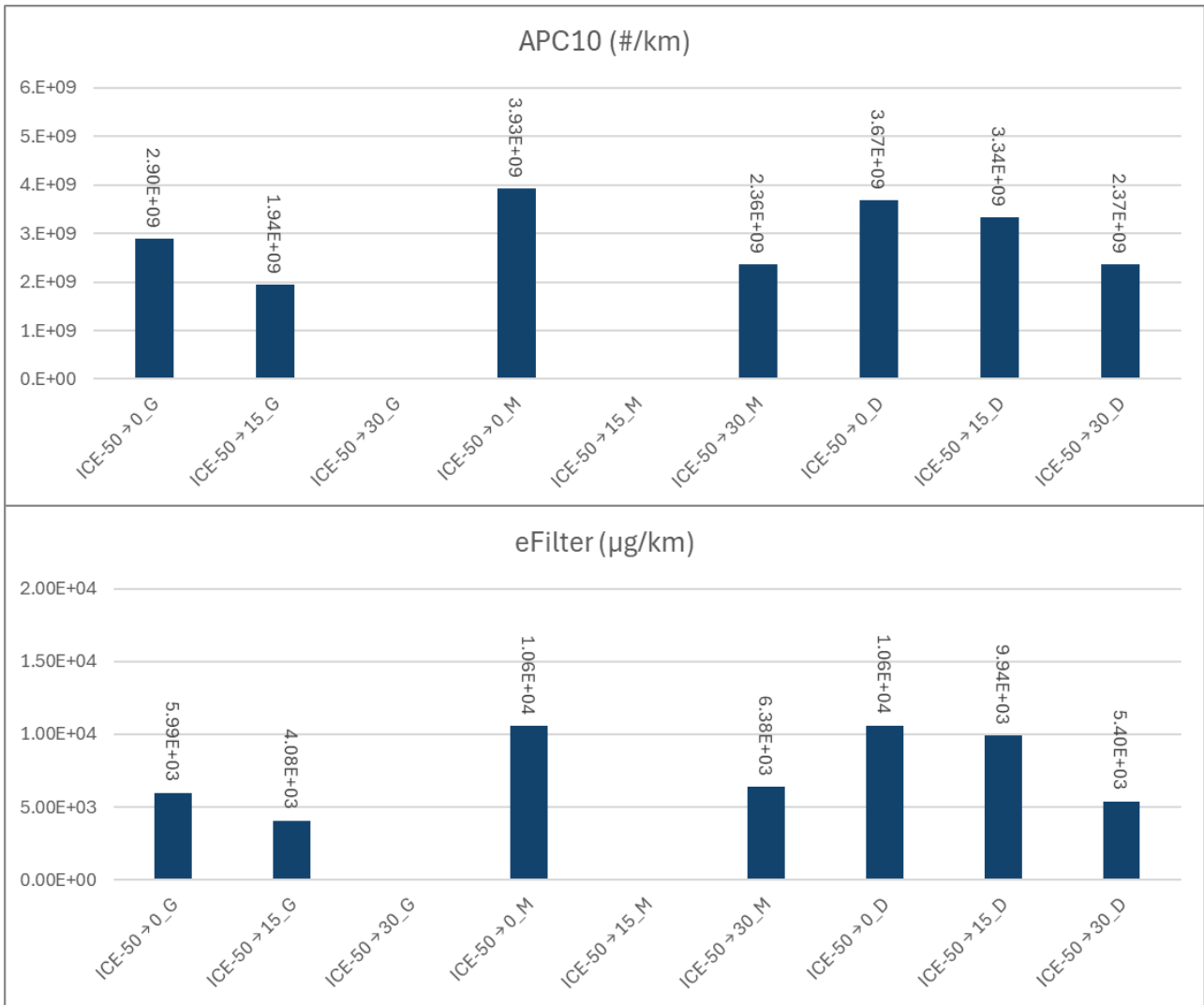
Figure 9-16: a) PN10 and b) PM emissions for ICE braking events at 50 kph.

Emissions from braking events of ICE, PHEV and EV vehicles, commencing at 50 kph, are shown in Figure 9-17. Results indicate the following:

- PN emissions are broadly similar between all vehicles
- PM emissions tend to be slightly higher from the ICE, and slightly lower from the EV
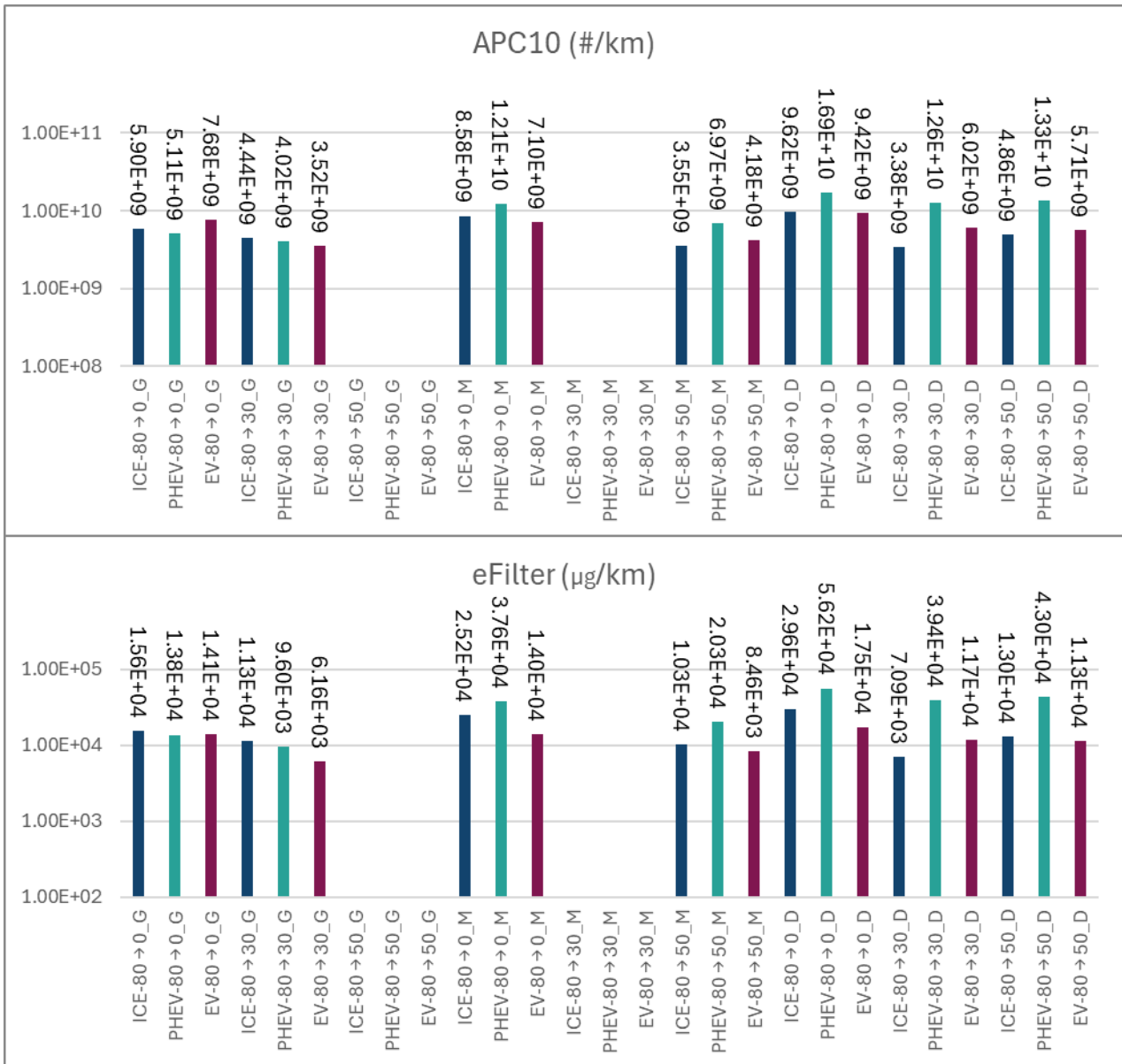- Moderate and dynamic braking emissions are higher than emissions with gentle braking
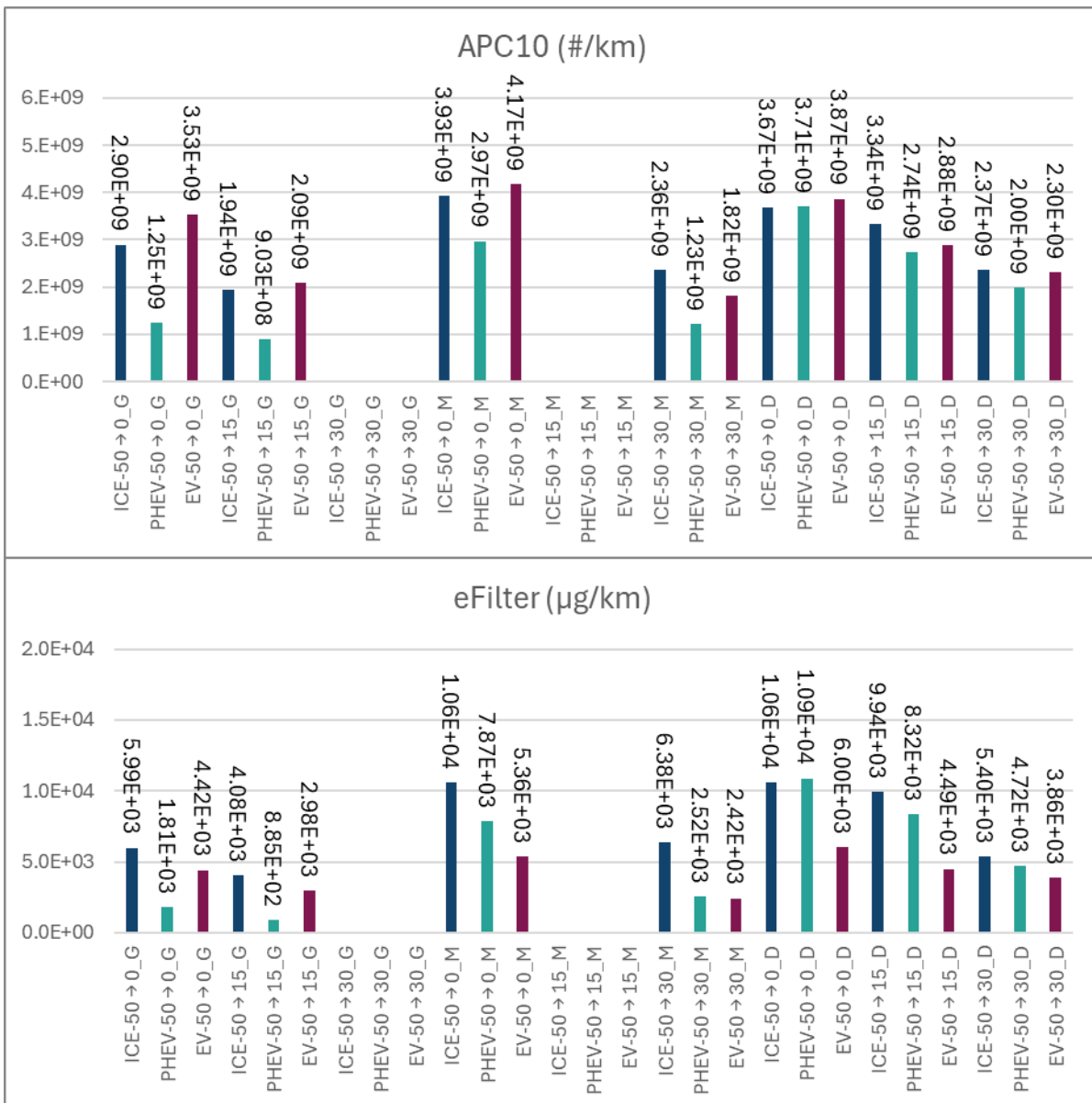
Figure 9-17: a) PN10 and b) PM emissions, from braking events from 50 kph for ICE, PHEV and EV vehicles.

9.2.1.1.3   Braking events at 80kph – ICE, PHEV and EV

Emissions of braking events from the ICE vehicle, starting at 80 kph, are shown in Figure 9-18. This figure provides the following indications:

- When braking from 80 kph to rest using gentle, moderate and dynamic styles, PN and PM emissions increase with dynamicity

- Dynamic braking from 80 kph to 50 kph or 30 kph shows lower emissions than when braking to rest
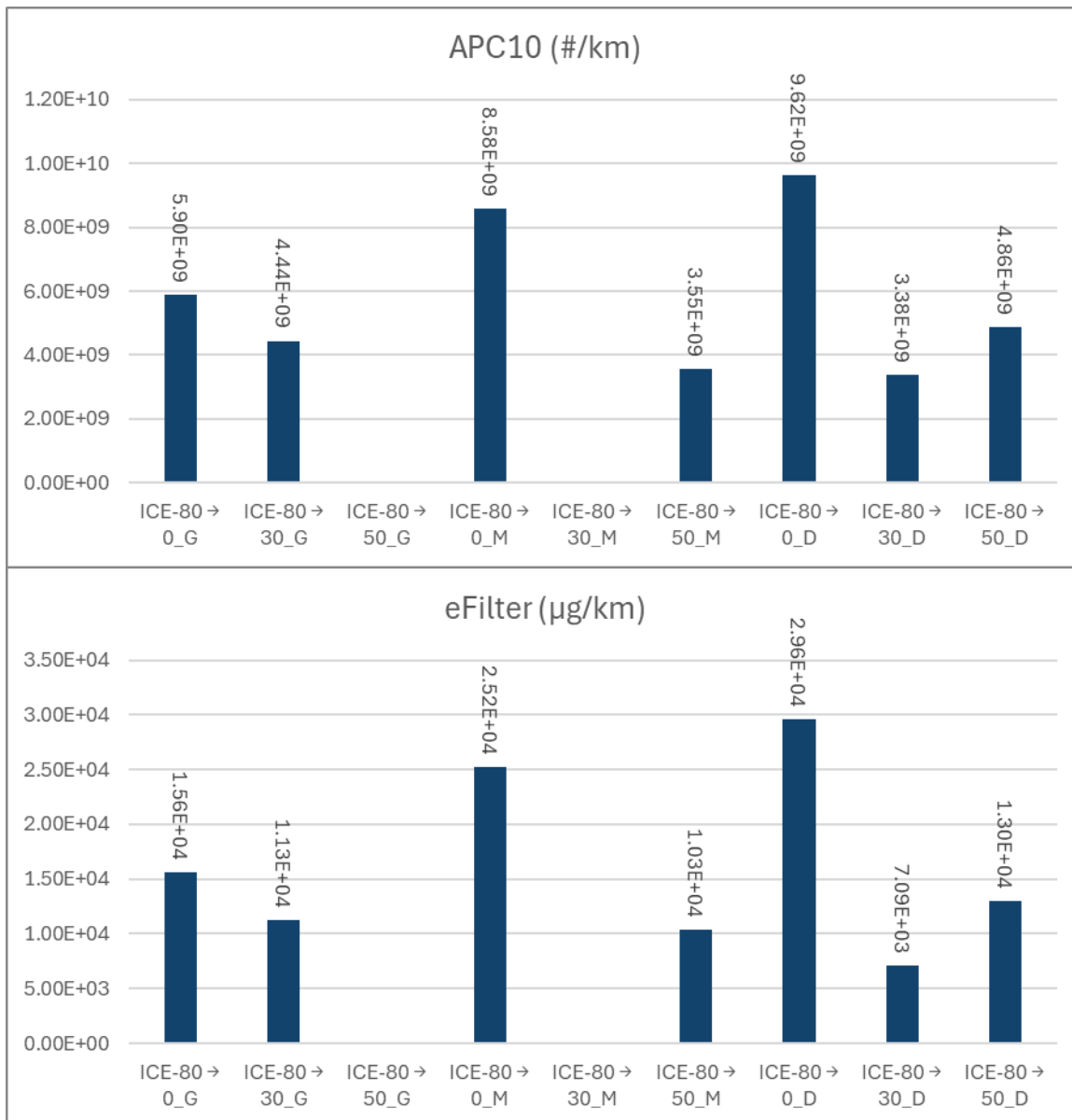
Figure 9-18: a) PN10 and b) PM emissions for ICE braking events at 80 kph.

Emissions from braking events commencing at 80 kph, on ICE, PHEV and EV are shown in Figure 9-19. The following observations can be made:

- Interestingly, unlike the 50 kph and 30 kph data, PHEV emissions tend to be highest of the 3 vehicles. The lower power E-machine applied in the PHEV may contribute less regenerative braking at high speed where it is potentially in its torque limited region, however this does not explain why the emissions would be greater than the ICE vehicle, which is wholly reliant upon friction braking.

- EV emissions are similar to ICE

- Dynamic braking from 80 kph to 50 kph or 30 kph shows lower emissions than when braking to rest, but emissions are relatively similar. In this case, heat build-up in the braking system may become a greater factor in determining the emissions than the length and time of the braking event.

Figure 9-19a,b: a) PN10 and b) PM emissions, from braking events from 80 kph for ICE, PHEV and EV vehicles.

9.2.1.1.4 Braking events from 110kph – ICE

Emissions from braking events commenced at 110kph are shown in Figure 9-20. Unlike lower speeds, all braking events were conducted towards the end of the bespoke cycle (Figure 6-10). During braking from 110kph to rest, PM and PN emissions are highest from dynamic braking and lowest from the gentle braking, When braking from 110kph to rest and braking from 110kph to lower speeds, PN emissions seem to reduce excepting 110kph to 30kph, where both PN and PM emissions were higher than from any other braking event from 110kph. The reason for this anomalous result is not clear.
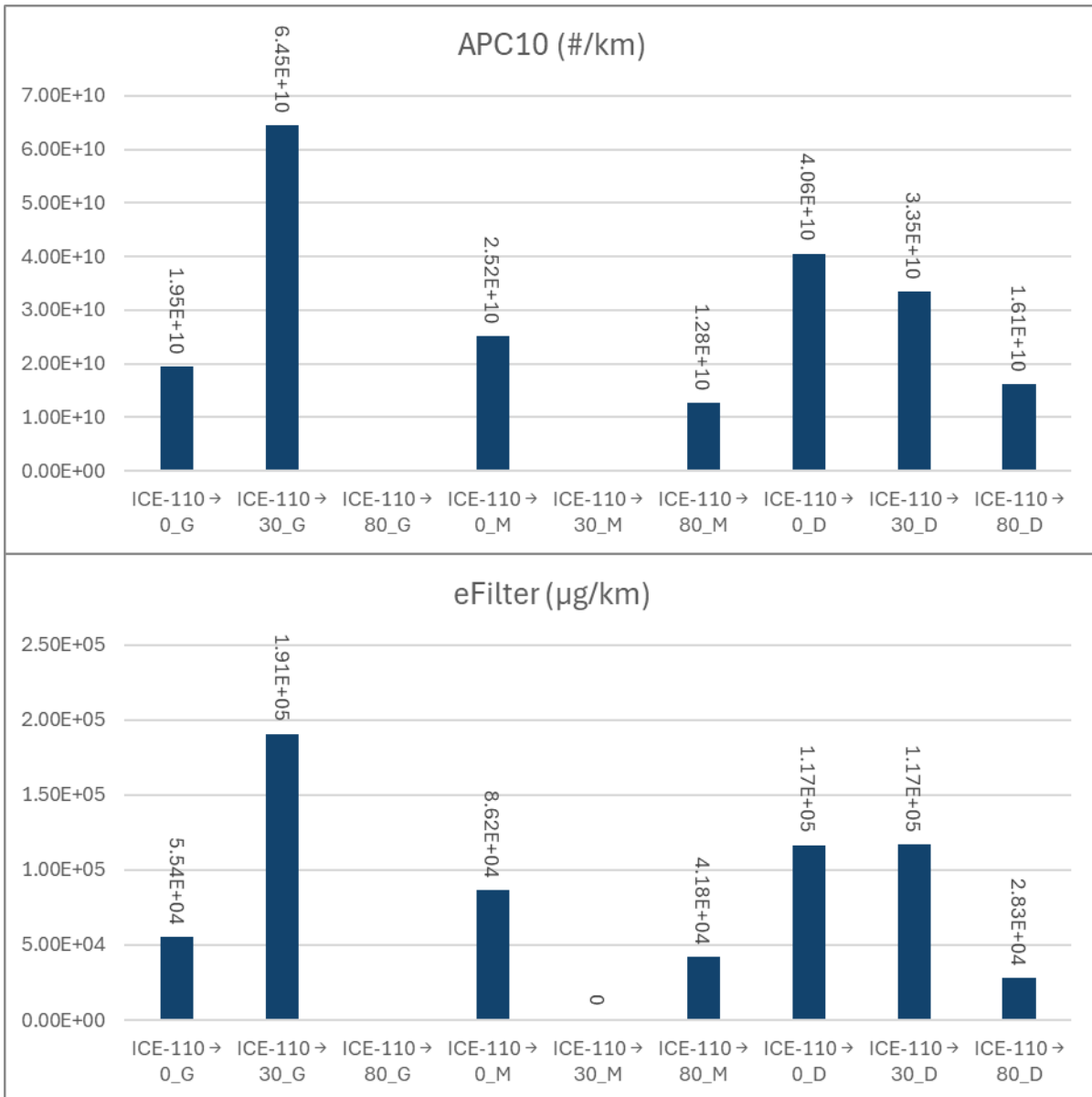
Figure 9-20: a) PN10 and b) PM emissions for ICE braking events at 110 kph.

PN10 and PM emissions from the ICE, PHEV and EV from braking events commencing at 110kph are shown in Figure 9-21 a and b. These data show the following:

- Broadly similar emissions are observed from the ICE and PHEV, which may indicate they are both solely, or predominantly in the PHEV case, employing friction braking at this speed.

- PN and PM emissions from the EV are at least 80% lower than those of the ICE and PHEV from all moderate and dynamic braking events. This suggests that the regenerative braking of the EV provides a significant benefit at higher speeds.

- With all three vehicles, there is a general trend of slightly lower PN and PM emissions when braking from 110 kph to 80 kph or 50 kph compared to braking to rest.
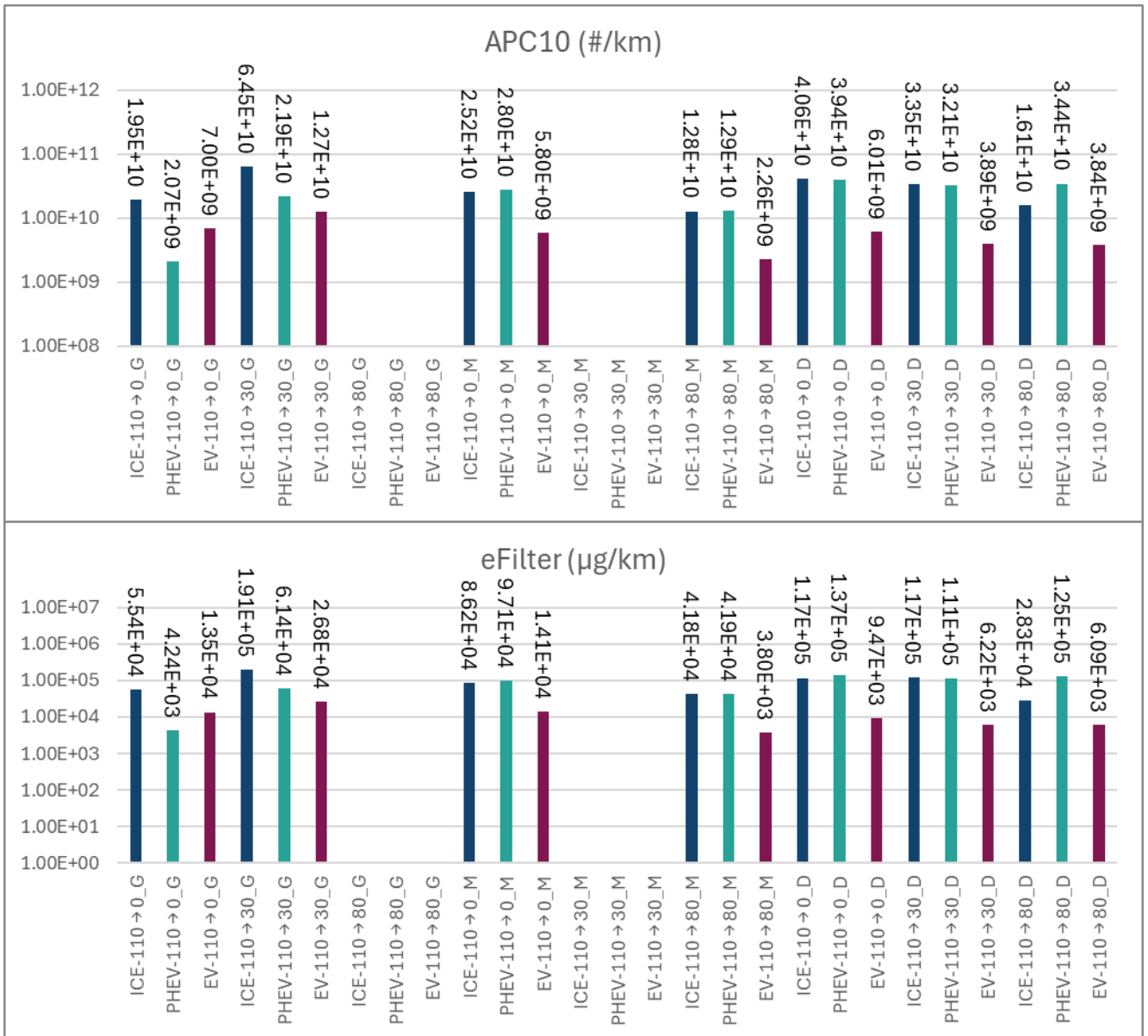
Figure 9-21: a) PN10 and b) PM emissions, from braking events from 110 kph for ICE, PHEV and EV vehicles.

9.2.1.1.5 Emissions with increasing vehicle speed

Using dynamic braking as an example, Figure 9-22, Figure 9-23 and Figure 9-24 for ICE, PHEV and EV respectively, show that both PN10 and PM emissions tend to increase as the speed at which braking is initiated increases. Each of these figures shows braking from 30 kph through to 110 kph, including all tests where there is braking to rest plus any braking to other, lower speeds. The data at 50, 80 and 110 kph is bracketed by the cool and hot 30 kph test data.

From the ICE, PN and PM emissions are relatively consistent (within a factor of ~3) from braking events starting at 30kph to 80kph. Conversely, when braking from 110kph to rest, ICE emissions increase by approximately one order of magnitude when compared to braking to rest from 80kph. PHEV emissions increase when braking from 80kph, and then increase again when braking from 110kph. EV emissions are higher at 80kph and 110kph than at 30kph and 50kph, but at the higher speeds are consistently lower than the ICE and PHEV.
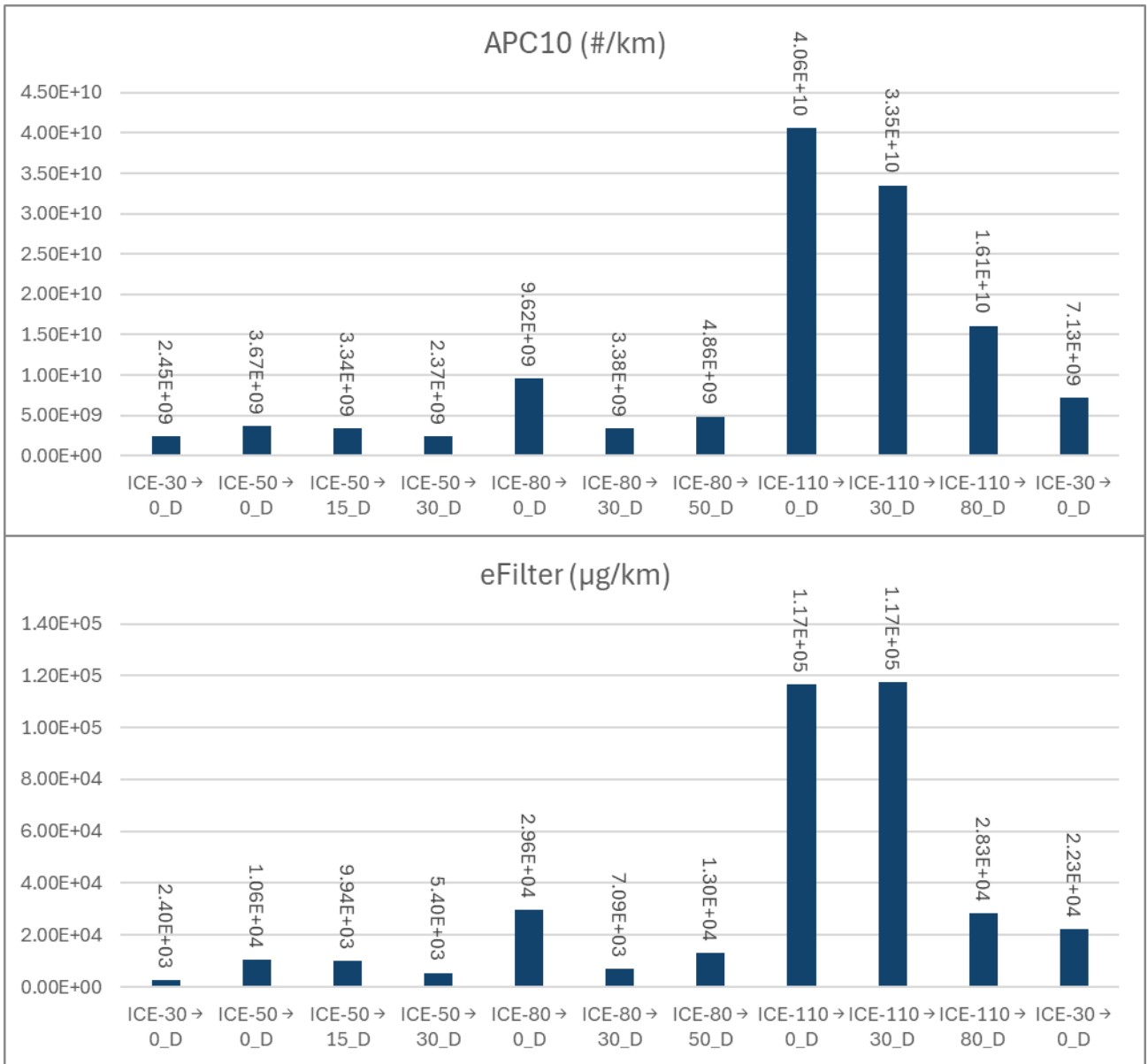
Figure 9-22: a) PN10 & b) PM emissions for dynamic ICE braking events from different initial speeds
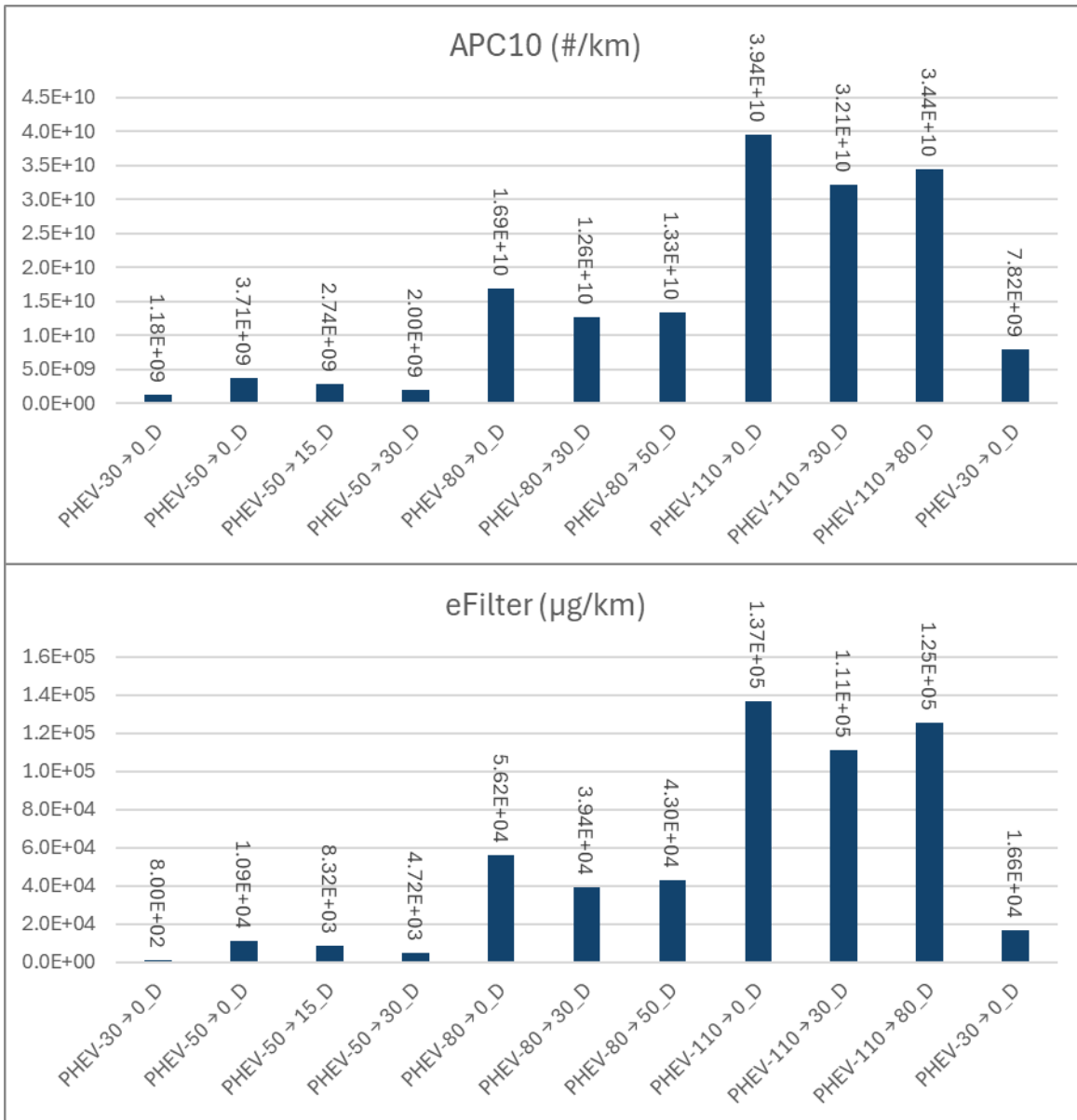
Figure 9-23: a) PN10 & b) PM emissions for dynamic PHEV braking events from different initial speeds
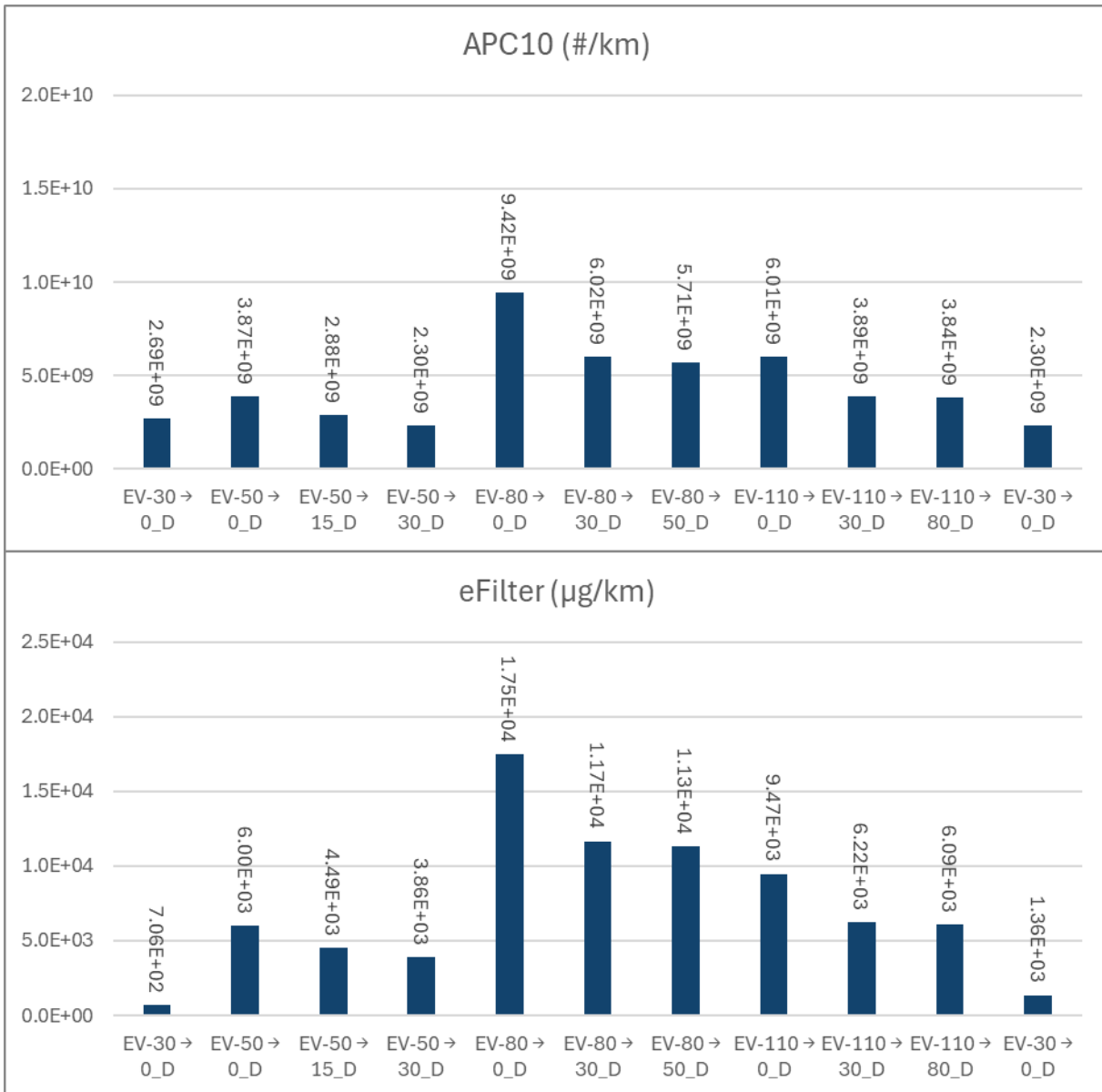
Figure 9-24: a) PN10 & b) PM emissions for dynamic EV braking events from different initial speeds.

9.2.1.1.6 Real-time emissions profiles from the bespoke cycle

Real-time emissions profiles from bespoke cycles driven on the ICE, PHEV and EV are shown in Figure 9-25, Figure 9-26 and Figure 9-27 respectively. Each figure is split into cool 30 kph, and 50 kph to 80 kph sections on the left, and the 110 kph sections, and hot 30 kph sections on the right. A sharp spike of emissions closely corresponds to each braking event, with large differences between emissions at 110 kph and lower speeds. There is also some evidence of limited particle release from all three vehicles during the acceleration part of the discrete events of the bespoke drive cycle. These figures also clearly illustrate that lowest emissions are seen from the EV in the highest speed section.
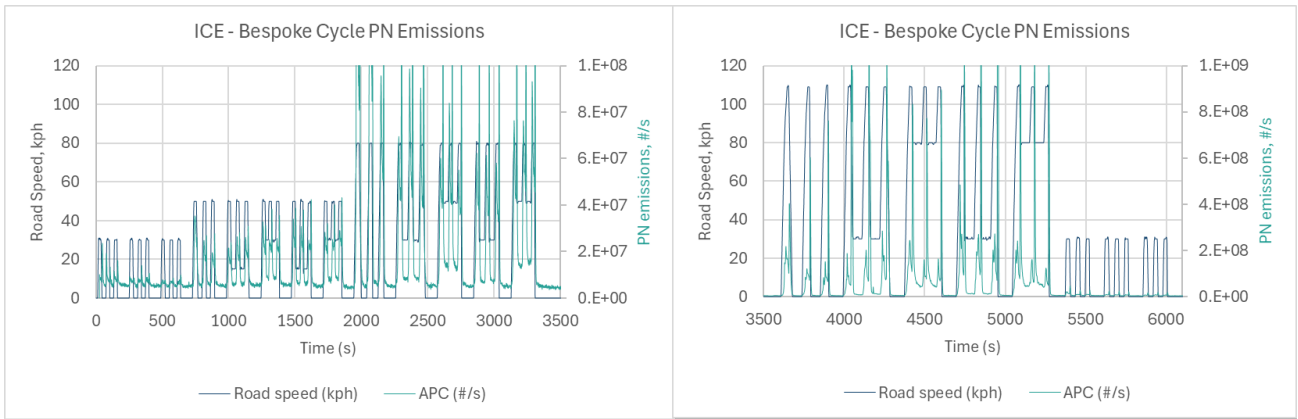
Figure 9-25: Real-time bespoke cycle PN emissions from the ICE (linear scale).
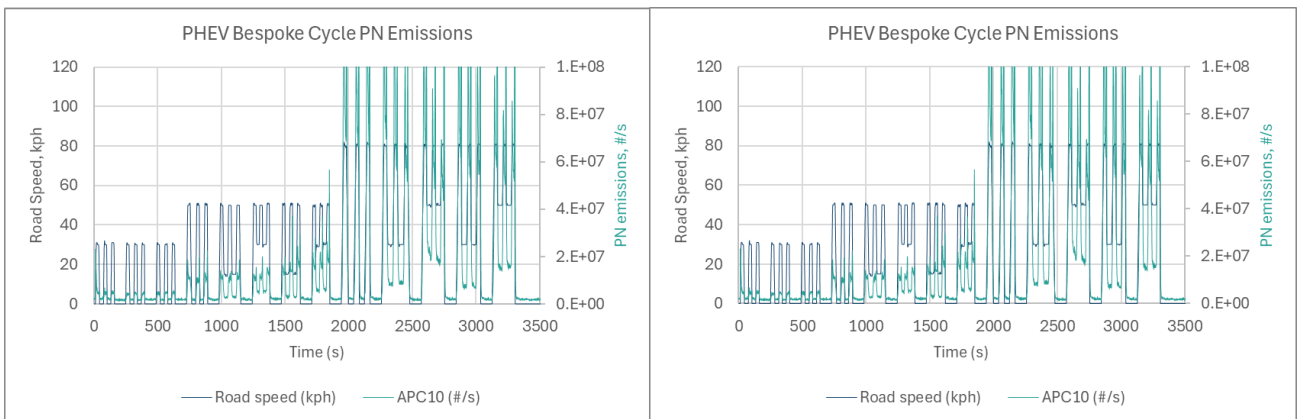
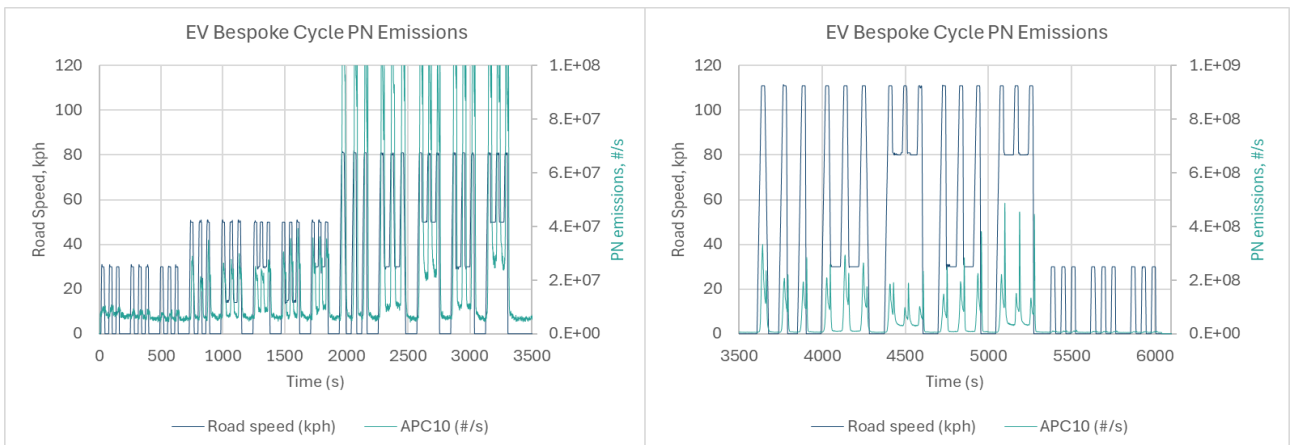Figure 9-26: Real-time bespoke cycle PN emissions from the PHEV (linear scale).

Figure 9-27: Real-time bespoke cycle PN emissions from the EV (linear scale).

9.2.2   Emissions from ICE, PHEV and EV using 1900 kg test mass and matched dyno terms

The comparative effects of the ICE vehicle's friction braking and the PHEV and EV vehicles' combined regenerative braking plus frictional braking are described in this section. All tests were conducted at a constant test mass of 1900 kg.

Figure 9-28 and Figure 9-29 respectively, show PN10 emissions from PG42 and RDE cycles. Each figure includes emissions from the APC10, plus cold and hot MPECs. Comparisons are between triplicate PG42 and RDE tests on the ICE and single tests on the PHEV and EV, so results should be considered indicative only.

APC10 data shows much lower emissions and minimal difference between the ICE, PHEV and EV from either PG42 or RDE cycle. A magnified view of these two cycles' data, shown in Figure 9-30, confirms similar emissions levels from all technologies from the PG42 cycle at ~10^9 #/km and from the on-dyno RDE cycle at ~ 2 x 10^9 #/km. The higher emissions from the RDE cycle may be due to a higher number of braking events in roughly the same distance driven.
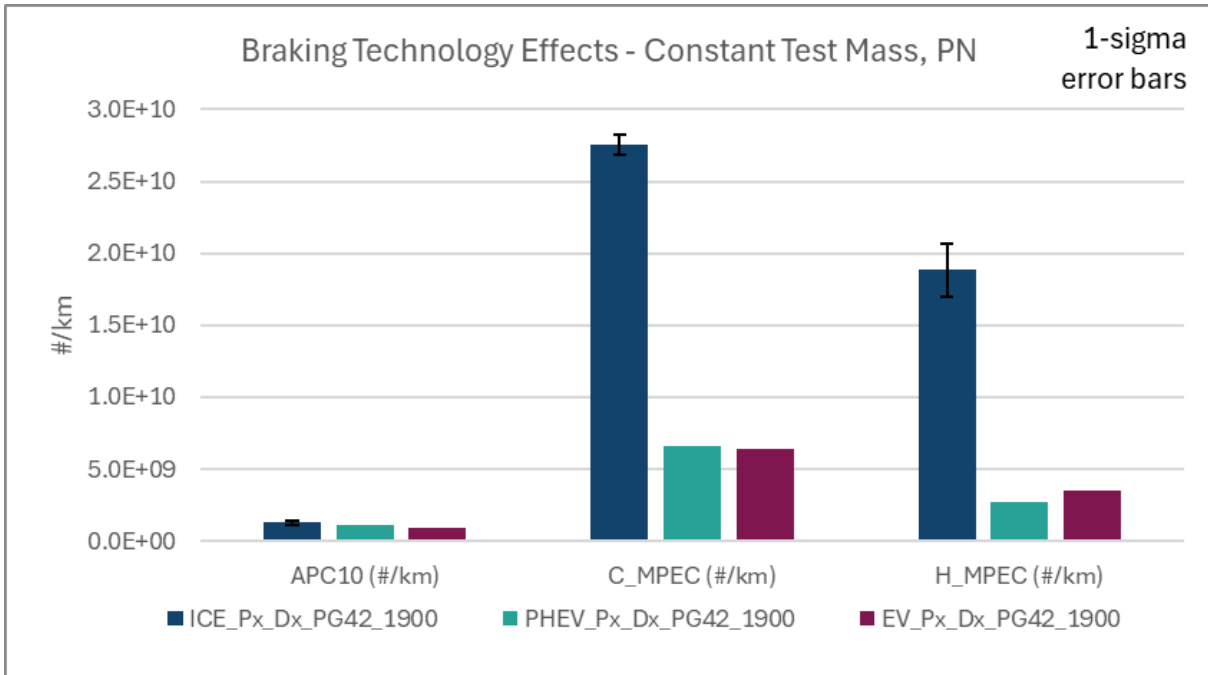

Figure 9-28: PG42 PN emissions - braking technology effects.
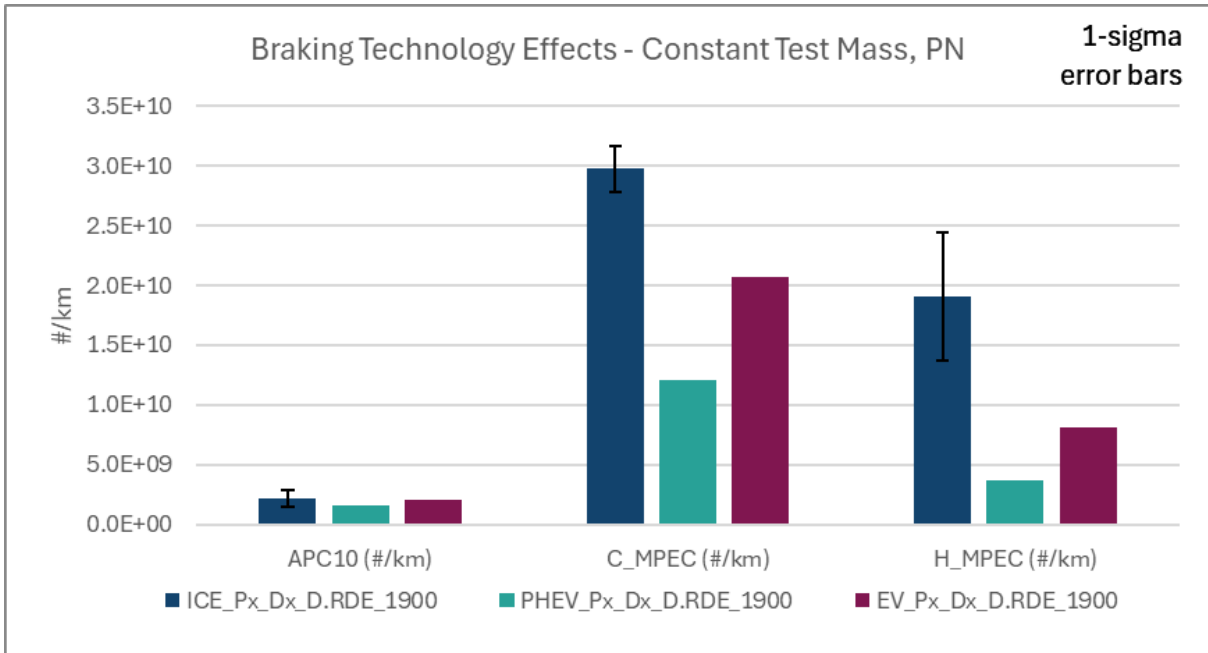
Figure 9-29: On-dyno RDE PN emissions – braking technology effects.
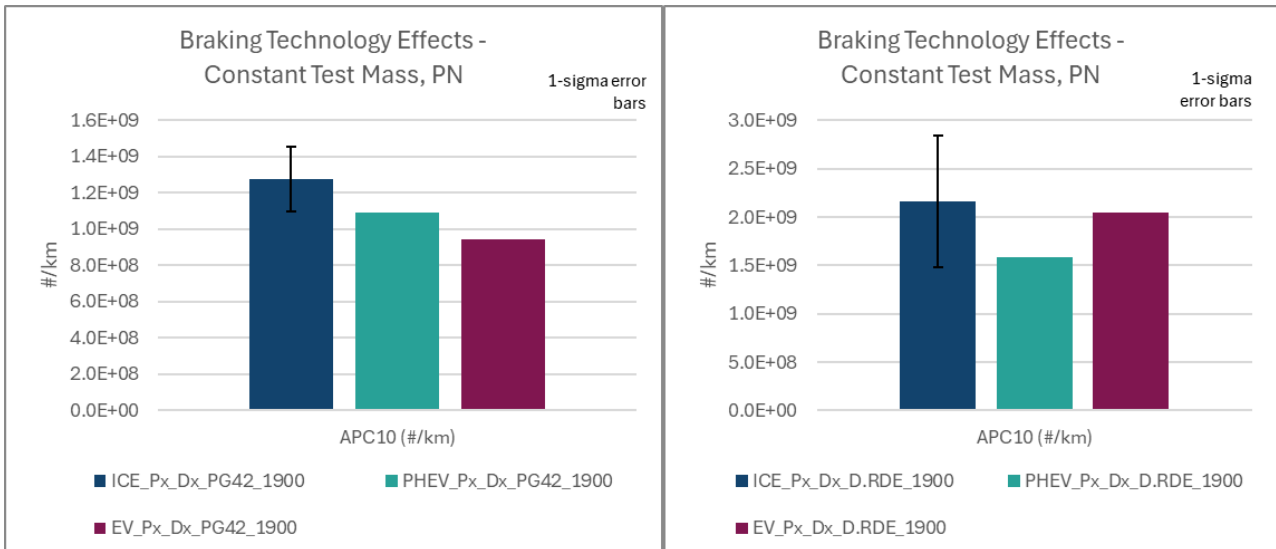
Figure 9-30: Braking technology PN emissions – APC10 only.

Conversely, both cold and hot MPEC emissions are clearly highest with the ICE vehicle from the PG42 and RDE cycles, most likely indicating that there are volatile and semi-volatile particle emissions present in the MPEC data that the APC10 eliminates. It is also conceivable that the ICE vehicle emits a greater proportion of larger particles that collect and carry higher charge levels, and this too would contribute to the discrimination observed between the different vehicles' results. However, the PM mass, for both PG42 (Figure 9-31) and on-dyno RDE (Figure 9-32), shows a similar effect - of highest emissions from the ICE - to the MPECs and this metric would be comprised of both solid and volatile constituents.

The PM mass data shows little obvious discrimination between the emissions of the PHEV and the emissions of the EV from either PG42 (Figure 9-31) or on-dyno RDE (Figure 9-32), though emissions are typically 20-30% of the ICE levels and well below 1 mg/km.
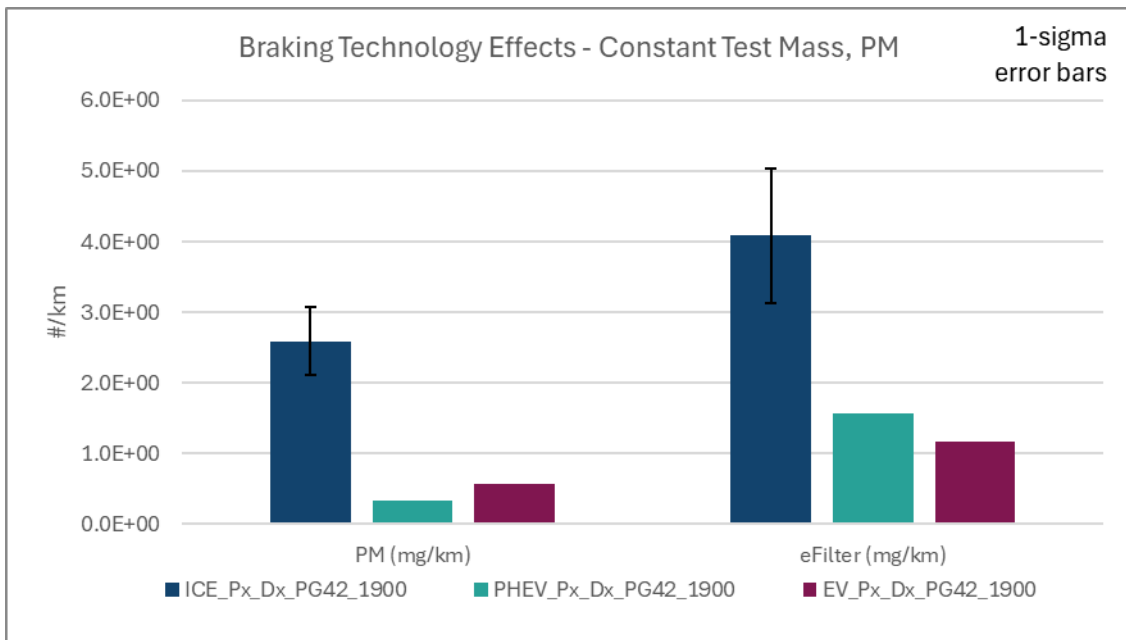

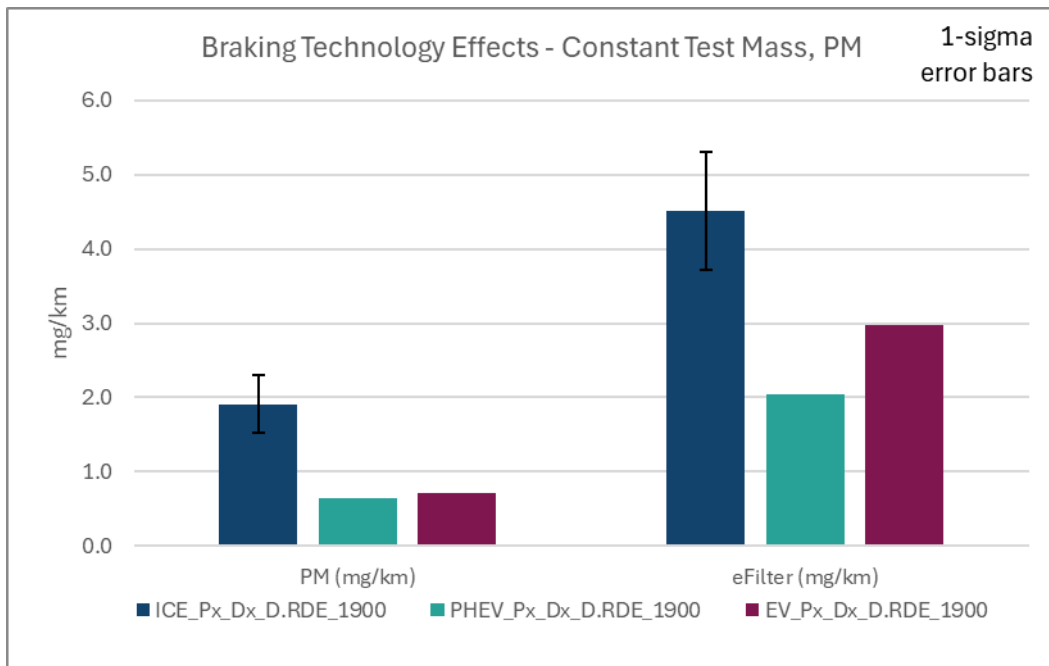Figure 9-31: PG42 PM emissions – braking technology effects.

Figure 9-32: On-dyno RDE PM emissions – braking technology effects.

Thermogravimetric analysis (TGA) of three filters from the bespoke cycle tests showed higher volatile proportion in the PM from the ICE, as well as substantially higher mass overall, indicating a higher emission of volatile materials from that vehicle (Figure 9-33).
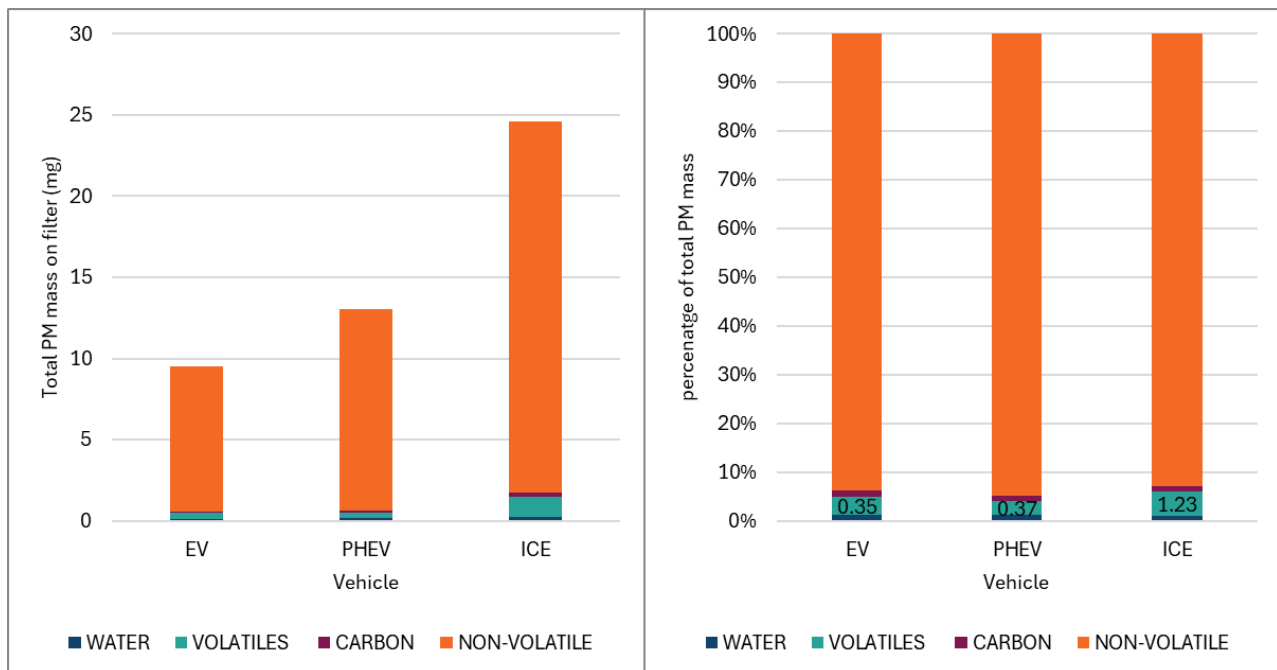

Figure 9-33: PM filter masses and TGA proportional chemical composition from bespoke cycles on 3 vehicles.

Particle size distribution data (Figure 9-34) does not indicate an obvious shift in the particle size distributions >100nm, but does indicate some variability in the <100nm region between vehicles – this likely to be related to the presence of volatile particles.

The particle size distribution data indicates bimodal character, with lowest emissions in the >100nm mode from the EV, higher from the PHEV and highest from the ICE when considering both PG42 and RDE cycles. A second mode, at below 50nm, appears substantially highest from the PHEV on both PG42 and RDE cycles and lowest from the EV.
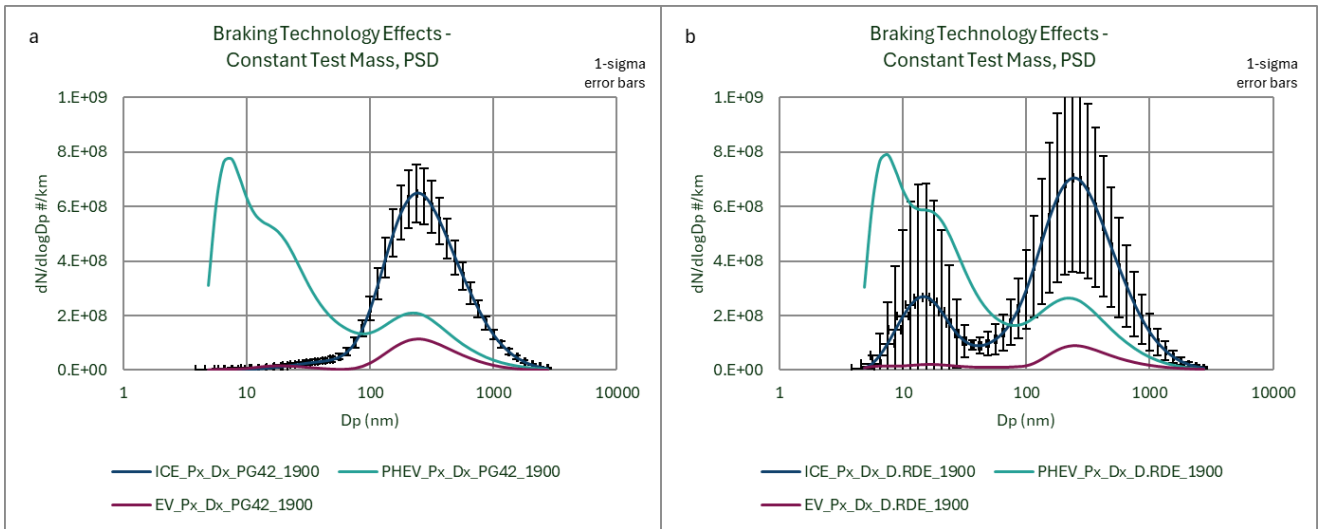
Figure 9-34: Braking technology particle size distributions, PG42 (a) and on-dyno RDE (b).

Given that all three vehicles are equipped with the same braking systems, it is possible that these large differences in <50nm particle emissions are due to the release of volatile particles. However, as Figure 9-35 shows, the temperatures experienced by the disc and pad are much greater when the ICE is tested than when the PHEV and EV are tested, and it would be logical to anticipate greater volatile release at higher temperatures. In addition, braking pressures are generally greater from the ICE than from the PHEV and EV (Figure 9-36), and there is no evidence of high PN10 observed with the cold MPEC from the PHEV test (Figure 9-37). On this basis, it is possible that the variable <50 nm mode results may be related to the instrument rather than the emissions.
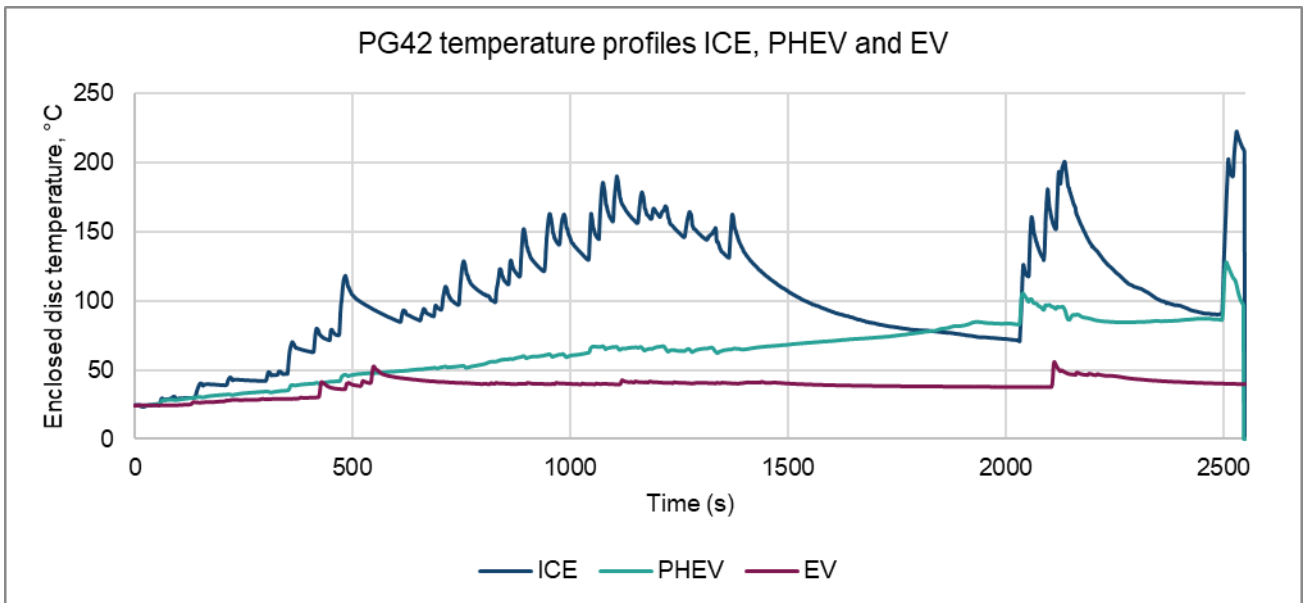

Figure 9-35: PG42 (1900 kg) all vehicles, enclosed disc temperature.

Note that the greater temperature increase/heat accumulation in the enclosure with ICE will increase volatile release. This effect will be present in the real world – ICE brakes will generally be hotter than PHEV and EV brakes – and so volatile particle emissions will be higher from ICE. That effect will be slightly magnified with the enclosure approach to sampling, where heat loss is reduced compared to the unenclosed brake.
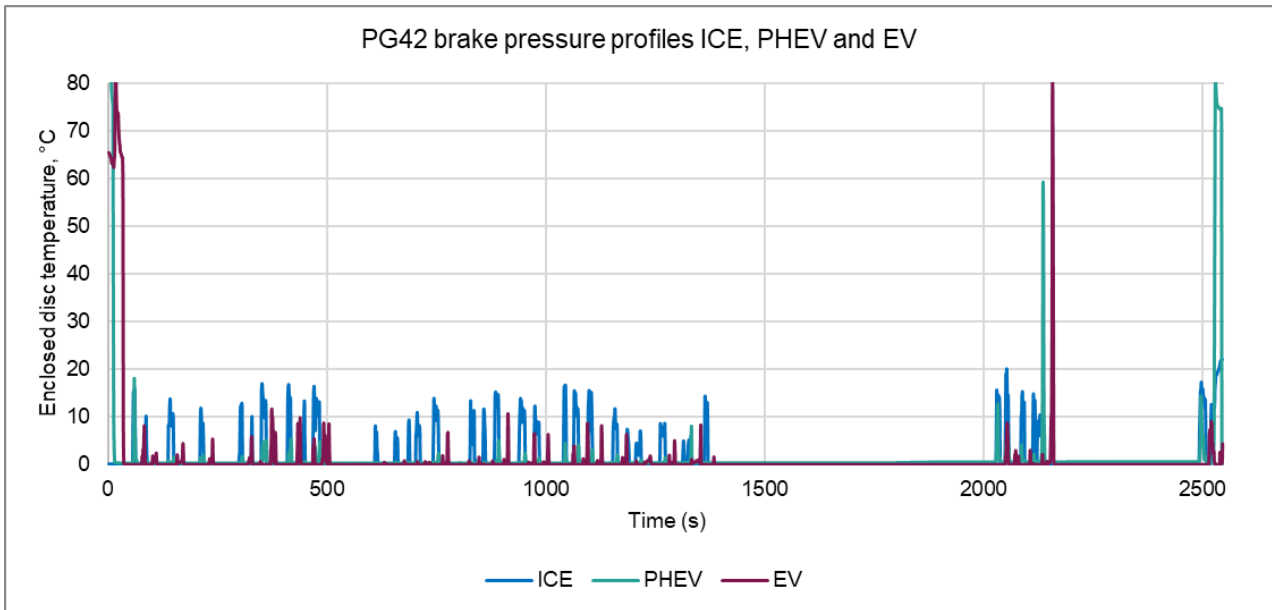
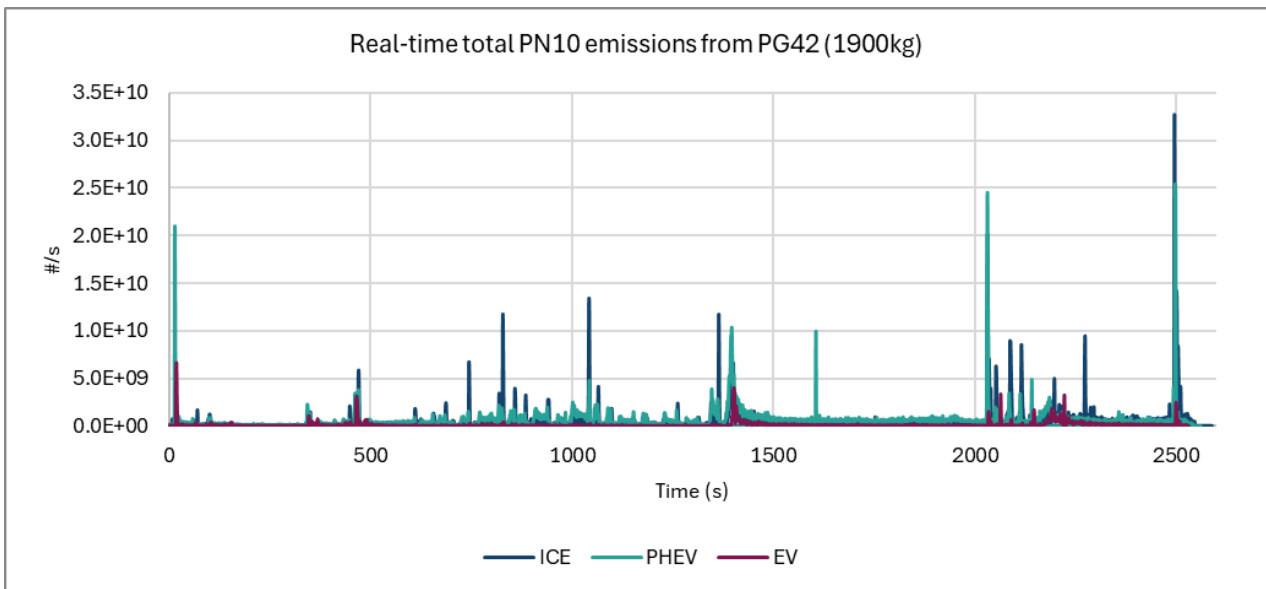Figure 9-36: PG42 (1900 kg) all vehicles, brake pressure profiles.

Figure 9-37: PG42 (1900 kg) all vehicles, real-time cold MPEC PN10 data.

9.3 BRAKE TECHNOLOGY DISCUSSIONS/SUMMARY

9.3.1 Mass and regenerative braking combined

a) There are minimal differences in non-volatile PN10 emissions between vehicle types except for slightly elevated emissions from the ICE at 1900 kg during bespoke cycles. Emissions from the PG42 cycle were ~1.5x10^9 #/km from ICE, PHEV and EV, emissions from the dyno RDE were ~2.0x10^9 #/km and emissions from the bespoke cycle at 3-5x10^9 #/km. This suggests that increased regenerative braking and lower test mass have minimal effect on non-volatile particles and they primarily reduce the release of volatile and semi-volatile materials.

b) From the MPEC instruments that measure volatiles as well as non-volatiles, the ICE at 1900 kg vehicle showed the highest PN emissions, followed by PHEV, with EVs showing the lowest emissions. This trend is consistent across PG42, On-dyno RDE, and bespoke cycles.

c) Higher test mass (1900 kg) in ICE vehicles leads to significantly higher emissions compared to PHEV and EV at 1700 kg. The increased emissions are attributed to the use of frictional braking and higher vehicle mass.

d) EVs benefit from higher regenerative braking capacity, resulting in lower brake particle emissions compared to PHEVs and ICE vehicles.

e) Cold MPEC emissions were consistently higher than hot MPEC emissions, and by more than 20%. This indicated the likely presence of some volatile particles that are reduced in the hot MPEC.

f) Gravimetric $PM_{2.5}$ emissions were highest from ICE vehicles (2-3 mg/km), followed by PHEV (0.6-1.6 mg/km), and lowest from EVs (0.3-1.2 mg/km). Real-time eFilter data supports these trends.

g) Particle size distribution measurements showed a bimodal distribution with peaks below 20nm and between 200 and 300nm. The >100nm mode, which contains the main $PM_{2.5}$ mass, has the highest emissions from 1900 kg ICE, followed by PHEV, and lowest from EV. The <100nm mode is more variable and was dominated by volatile / semi-volatile particles.

h) A comparison of PN10 and $PM_{2.5}$ emissions of the ICE at both 1900 kg and 1500 kg and the PHEV and EV, both at 1700 kg, indicated that for PM, the reduction in test mass to 1500 kg with the ICE did not provide the same benefit in emissions as the increase in mass with the PHEV and EV accompanied by the addition of regenerative braking. Therefore, although PHEV and EV come with increased vehicle weight, their use of regenerative braking still delivers a mass emissions benefit. Non-volatile PN10 emissions, alternatively, saw limited benefits of either regenerative braking or reduced test mass on emissions.

i) PN10 and PM emissions from the bespoke cycle on all vehicles showed slightly higher emissions from a hot braking system than from a cool braking system. The differential was greatest with dynamic braking. When braking at 30 kph, the differences in emissions between gentle, moderate and dynamic braking were limited, at 50 kph dynamic emissions were noticeably highest, while at 80kph and 110 kph, emissions clearly increased with braking dynamicity. Emissions were always highest when braking from 110 kph. Higher emissions were also observed, at all speeds, when braking to rest, than when braking to a lower speed.

j) Comparisons between vehicle specific emissions from the bespoke cycle showed similar PN10 emissions levels from ICE, PHEV and EV at 30 kph and 50 kph, but highest emissions from the PHEV at 80 kph. This may be due to a switch from regenerative braking to friction braking at this speed. At 110 kph emissions from the ICE and PHEV were similar, while EV emissions were ~80% lower. This likely reflects the continuing use of regenerative braking in the EV and its absence with the other vehicles. Effects on PM were broadly similar to PN10.

9.3.2 Emissions from ICE, PHEV and EV using 1900 kg test mass and matched dyno terms

a) PN10 data from the APC10 showed minimal differences in emissions between ICE, PHEV, and EV across both PG42 and RDE cycles, with similar levels around 1×10^9 #/km for PG42 and 2×10^9 #/km for dyno RDE. The higher emissions in the RDE cycle may be due to a greater number of braking events over the same distance.

b) Both cold and hot MPEC emissions were highest from ICE vehicles, likely due to volatile and semi-volatile particles excluded from measurement by the APC10. Though particle size distributions in the >100nm regime were similar in profile, ICE vehicles also emitted more of the larger particles that carry higher charge levels, probably contributing to the observed differences.

c) PM mass emissions were highest in ICE vehicles, around 2 mg/km from both PG42 and dyno RDE cycles, with PHEV and EV emissions being 20-30% of ICE levels and well below 1 mg/km. Brake system temperatures were much higher with the ICE vehicle, and thermogravimetric analysis (TGA) indicated a higher volatile proportion and overall mass in PM from ICE vehicles, suggesting higher emissions of volatile materials despite the use of the same pad and disc.

10. TYRE WEAR EMISSIONS RESULTS

10.1 TESTING PERFORMED

Tyre emissions testing was performed on the two-wheel drive chassis dynamometer in the VATF, using the Audi A4 vehicle. Consequently, Emissions measurements were made using the same instrumentation

employed in the brake wear emissions experiments, but with the addition of the condensation particle counter measuring PN4 (Section 5.2.3). The same test cycles as employed in the brake wear experiments were used, excepting that the bespoke cycle was tested as standard across all tyres.

Tyres tested are summarised in Section 7.2 and shown in Table 7-2. Each tyre is associated with its own unique wheel, such that Tyre 1 is associated with Wheel 1. Together the combination is identified as W1.

Testing included tyres that can be grouped in several categories, that enable different comparisons to be made:

10.1.1 Size variants

In this category, nominally identical, or highly similar, tyres in 16" and 18" versions were tested, including:

- **Tyre 17** (Michelin CrossClimate 2 205/55R16 94V XL TL) 16" and **Tyre 7** (Michelin CrossClimate 2 215/55R18 99V XL TL) 18"
- **Tyre 20** (Michelin Primacy 4+ 205/55R16 91V TL) 16" and **Tyre 4** (Michelin Primacy 4; 215/55R18 99VXL TL S1) 18"
- **Tyre 16** (Bridgestone Turanza ECO 205/55R16 91H) 16" and **Tyre 2** (Bridgestone Turanza Eco 215/55R18 95T) 18"

10.1.2 Mileage variants

In this category, tyres of the same baseline type, but with different degrees of ageing, were tested:

- **Tyre 2** (Bridgestone Turanza Eco 215/55R18 95T), 18" – procured new
- **Tyre 12** (Bridgestone Turanza Eco 215/55R18 95T), 18" – aged ~11,000 km
- **Tyre 14** (Bridgestone Turanza Eco 215/55R18 95T), 18" – aged ~23,000 km

10.1.3 Supplier variants

In this category, similar tyres from different manufacturers were compared. All are 18" tyres intended for UK summer use:

- **Tyre 4** (Michelin Primacy 4; 215/55R18 99VXL TL S1)
- **Tyre 6** (Goodyear EfficientGrip Performance 2 215/55R18 99V XL)
- **Tyre 7** (Michelin CrossClimate 2 215/55R18 99V XL TL)
- **Tyre 10** (Landsail LS588 SUV; 215/55R18 99V)

In addition, **Tyre 7** is a tyre of different structure/composition. It is not a winter tyre as might be seen in northern Europe but is designed for colder operation.

10.1.4 Tyre test order and internal check

The test order of tyres commenced with the 16" tyres and completed with the 18" tyres.

It was considered likely that the 16" tyres would wear more than the 18" tyres for two reasons:

- Firstly, at any given speed the smaller wheels and tyres are rotating more quicky, and so must slow more when braking;
- Secondly, the contact patch that brakes the vehicle is smaller and thus experiences greater forces and potentially greater wear and particle release

Since the roller of the VATF had been coated with 3M walkway tape to create an abrasive surface more like asphalt (Section 4.2.1), it was considered possible that this surface might wear and evolve during the test programme. To study this, an internal standard was introduced to assess any changes throughout the test campaign and to enable consideration of a drift correction of the results if necessary. The internal standard saw repeats of the first tested tyre and wheel combination (W17) three further times. These were nominated as W17, W17b, W17c and W17d. It should be noted that a full suite of drive cycles was not tested for W17b to W17d, instead triplicate PG42 tests were undertaken each time.

The order of testing was therefore as follows, with further detail in Table 10-1.

- W17 ► W20 ►W16 ►**W17b** ►W2 ►W12 ►W7 ►**W17c** ►W10 ►W4 ►W6 ►W14 ►**W17d**

[Key: 16" tyres, 18" tyres; *internal standard*]

When the full test plan was completed, a few tests were repeated. Following these a further three PG42 tests (W17e) were undertaken.

Table 10-1: Summary of planned tyre and wheel tests, along with test dates.

Test order	Tyre number	Description	Wheel number	Wheel diameter	Notes	Test date
1	T17,T18	Michelin CrossClimate 2 205/55R16 94V XL TL	W17,W18	16"	Size and design variant	5/6 Aug
2	T19,T20	Michelin primacy 4+ 205/55R16 91V TL	W19,W20	16"	Size variant	12/13 Aug
3	T15,T16	Bridgestone Turanza ECO 205/55R16 91H	W15,W16	16"	Size variant	2/3 Sep
1b	T17,T18	Michelin CrossClimate 2 205/55R16 94V XL TL	W17,W18	16"	Size and design variant PG42 only	5/6 Sep
4	T1,T2	Bridgestone Turanza Eco 215/55R18 95T	W1,W2	18"	Supplier variant	9/10 Sep
5	T11,T12	Bridgestone Turanza Eco 215/55R18 95T	W11,W12	18"	11k km aged variant	12/13 Sep
6	T13,T14	Bridgestone Turanza Eco 215/55R18 95T	W13,W14	18"	23k km aged variant	16/17 Sep
7	T7,T8	Michelin CrossClimate 2 215/55R18 99V XL TL	W7,W8	18"	Design variant	19/20 Sep
1c	T17,T18	Michelin CrossClimate 2 205/55R16 94V XL TL	W17,W18	16"	Size and design variant PG42 only	23/24 Sep
8	T9,T10	Landsail LS588 SUV; 215/55R18 99V	W9,W10	18"	Supplier variant	26/27 Sep
9	T3,T4	Michelin Primacy 4; 215/55R18 99VXL TL S1	W3,W4	18"	Supplier variant	30 Sep/1 Oct
10	T5,T6	Goodyear EfficientGrip Performance 2; 215/55R18 99V XL	W5,W6	18"	Supplier variant	3/4/ Oct
1d	T17,T18	Michelin CrossClimate 2 205/55R16 94V XL TL	W17,W18	16"	Size and design variant PG42 only	7/8 Oct

10.1.5 Daily order of test cycles

Testing on each individual tyre variant took two days, with the same sequence of tests conducted:

- Day#1: PG42#1 ►PG42#2 ►PG42#3 [60 mins cooling] ►On-dyno RDE, 1850 kg ►WLTC
- Day#2: Bespoke cycle ► [60 mins cooling] ► On-dyno RDE, 2050 kg

Due to the potential influence of heat accumulation in the tyre and roller surface on PM and PN emissions, where repeat tests were deemed necessary the preceding test in the daily sequence (unmeasured) was driven as a preconditioning. Similarly, the tests on any given day were split into two batches, separated by a 60 minutes' cool down period, to allow the tyres and roller to return to ambient conditions.

10.2 ADDITIONAL EXPERIMENTS

10.2.1 Initial tyre testing in the VERC

Initially it was intended to execute the tyre wear emissions test programme in the VERC facility, however two initial tests using the floor-mounted enclosure and higher sample flow (Section 3.2) revealed unexpectedly low particle emissions. This finding was in contrast to the results of the Phase 1 project. In addition, a recent

publication (Schläfle, et al., 2023) suggested that tyres rotating on a stainless steel relatively unfeatured roller led to stickiness of the tyres and inhibition of particle emissions. The low particle emissions were explored in a number of experiments, in order to guide further tyre testing.

10.2.1.1 Comparison of Initial Phase 2 PG42 particle emissions results with Phase 1 emissions

Phase 2 non-volatile PN10 and real-time mass emissions are shown in Figure 10-1a,b. There is little obvious relationship between the emissions profile and drive cycle from either of the instruments. There is a tendency towards increased PN10 as the test progresses – this could be due to the impact of tyre heating.

The eFilter shows high emissions at the start of test, but these commence before the vehicle moves – possibly the instrument is settling down after the flow was started. Much of the data from both instruments looks like noise, or to a continuous emission of materials (e.g., volatiles).

This contrasts with the Phase 1 emissions where clear spikes of emissions were observed to be coincident with braking events (Figure 10-2a,b).
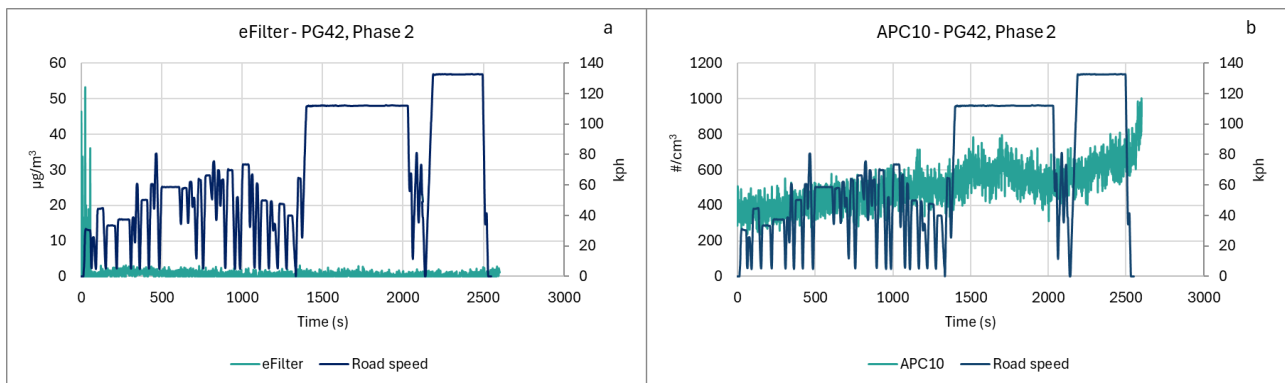

Figure 10-1: (a) Real-time mass and (b) Non-volatile PN from PG42, Phase 2.
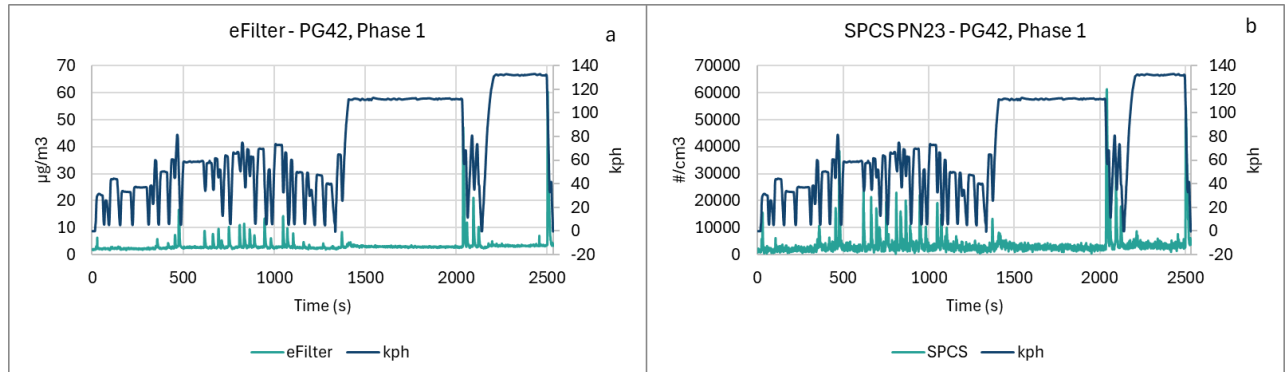

Figure 10-2: (a) Real-time mass and (b) Non-volatile PN from PG42, Phase 1.

These results suggested that either much lower particulate emissions were observed from the tyre on the Audi compared to the tyre tested on the Caddy in Phase 1 which could derive from a number of sources, or the Caddy emissions in Phase 1 were higher, again for a number of possible reasons.

A comparison of emissions levels from PG42 cycles in Phase 1 and 2 indicated substantially higher average particle concentrations in Phase 1. Values shown in red are below sensitivity limits, and levels measured in Phase 2 were ~ 5-8 times lower than in the Ph 1 work.

A root cause analysis was performed to explore possible factors leading to the results observed in the Phase 1 and preliminary Phase 2 measurements.

	APC10/SPCS (#/cm³)	cold MPEC/ ELPI (#/cm³)	hot MPEC/ ELPI (#/cm³)	eFilter (µg/m³)
Phase 1 PG42 (approx. mean of all tests)	4,100	6,000	2,000	3.4
Phase 2 PG42 - 15 Jan	524	3163	232.7	0.69
Ratio	7.8	1.9	8.6	4.9

10.2.1.2 Possible root-causes for low tyre particulate emissions in preliminary Phase 2 measurements

The root-cause analysis, shown in Figure 10-3 and described below, focuses on the lower levels of particles seen in the preliminary Phase 2 study, compared to the Phase 1 results. There are two possible reasons for the low levels of particles, either the solid particles are not seen, or solid particles are not generated.

Solid particles not seen:

- Particles not penetrating the sampling system due to issue with the sampling system design.
- Particles below detection limits, due to sample over-diluted (from an air leak or too high flow), or the instrument is not sensitive enough, or there is high noise measurement system.
- Particles are lost through the chassis dynamometer evacuation or other means, for example: turbulent flow, sample transfer losses, or the sample flow/face velocity is inadequate.

Solid particles not detected:

- Different tyre used in Phase 1 and Phase 2.
- Difference in tyre pressures.
- Other differences in the testing between phase 1 and 2, such as inertia.
- Solid particles detected in Phase 1 were not from tyre wear, e.g. possible leakage from brake enclosure.
- Solid particles are produced, but above 2.5 µm and low in number.
- Smooth chassis dynamometer surface does not create tyre wear particles.
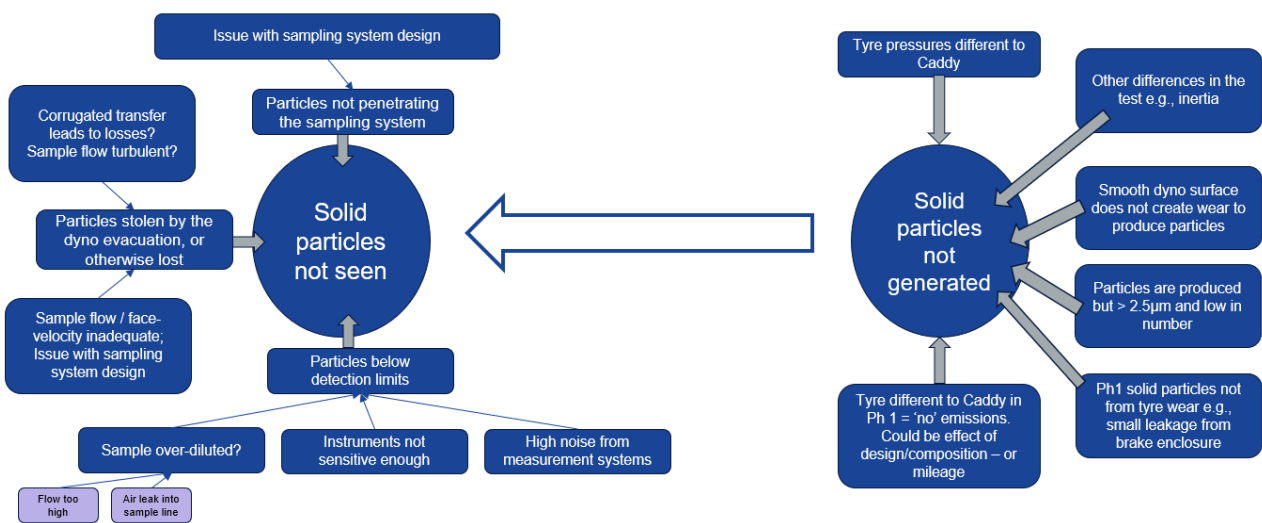

Figure 10-3: Possible root-causes for low tyre particulate emissions levels.

The most likely potential factors were considered to be:

- The dyno is diverting the particles away from the floor-mounted enclosure due to lower face velocity.

- The new sampling system is running at too high a flow rate and the concentrations are diluted to, or below, the detection limits of the measurement instruments.

- Particle emissions are very low from the tyre being tested, lower than the tyre tested previously.

- The solid particles we detected previously were leakage from the brake enclosure, which is left in place and operational to avoid contaminating the near-by tyre emissions sample. In Phase 1 this was operated exactly as for brake wear measurements, in that air is both pushed into the enclosure and pumped out. This may lead to leakage of brake particles due to overpressure in the enclosure. However, the phase 2 sampling system, which is configured to evacuate the brake enclosure to a vacuum cleaner, does not have this leakage as the enclosure is in an underpressure environment.

From the root-cause analysis, selected experiments and reviews of Phase 1 data were conducted in order to inform how to progress tyre testing in Phase 2.

In parallel the possibility of testing tyre wear in the VATF rather than the VERC was explored. The VATF has a dyno roller with a more road surface-like coating, which might lead to the production of higher particle emissions.

10.2.1.3 Do particles transit through the tyre sampling system to the analysers?

The sampling system was configured to draw from the exhaust of a non-DPF diesel. The vehicle was idled for ~5 mins, then started and the engine allowed to stabilise (cat heating was permitted to complete), the throttle was then blipped a few times and then the engine allowed to settle at idle. Measurements were made with eFilter, hot and cold MPECs, with a PM sample also taken via the eFilter.

Particles were clearly observed to rise at ~300s with the eFilter and also with the hot MPEC (there were some issues with logging data from the cold MPEC) (Figure 10-4). This provided evidence that particles can be detected from the sampling system if they are present at high concentrations.
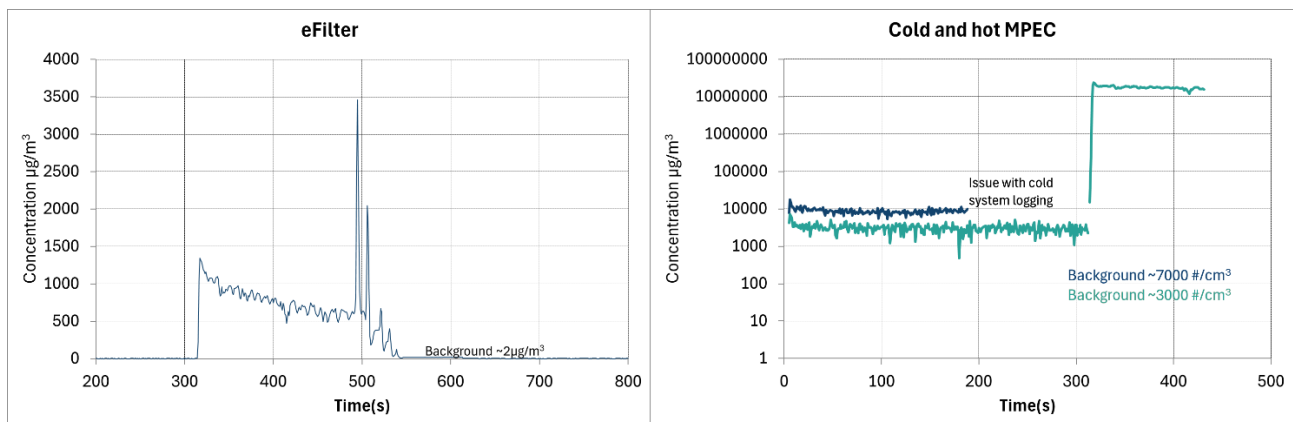
Figure 10-4: Particles observed to transit the tyre sampling system, measured by the a) eFilter and b) the hot and cold MPECs.

10.2.1.4 Measurements with sampling system situated directly behind tyre of DPF diesel vehicle

Emissions measurements were made using the tyre sampling system with a DPF-equipped diesel operating on the chassis dynamometer. The vehicle was selected to avoid, as far as possible, contamination of the sample with tailpipe particle emissions, but it was not equipped with extensive regenerative braking capabilities. The inlet of the system was mounted as close as possible to the rear wheel.

Emissions measurements made with the eFilter and the PN4 condensation particle counter (CPC) are shown in Figure 10-5. The PN4 system was employed since it was considered possible that tyre emissions could be dominated by semi-volatile species, and given the high dilution in the sampling system these would likely appear as very small particles.

The eFilter data (Figure 10-5a) showed spikes of emissions situated on top of a continuous emission of particles. Substantial mass was detected continuously. Between drive cycle events there was no return to

baseline observed, but there was an increase in underlying emissions across the cycle duration. This may have been volatile release with increasing tyre temperature. Potentially the spikes seen above the baseline of "volatile emissions" may be solid particles originating from the engine, brakes or tyre.

Emissions from the PN4 CPC (Figure 10-5b) also showed spikes of emissions situated on top of a continuous elevated particle level. No return to baseline was observed during the cycle, but an increase in underlying emissions during cycle duration was seen. As with the eFilter data spikes above the continuous emissions level may have been solid particles.

This experiment indicated that the sampling system could detect particles at low levels, and that tyre emissions may be dominated by volatile particles with periodic solid particle emissions also present.
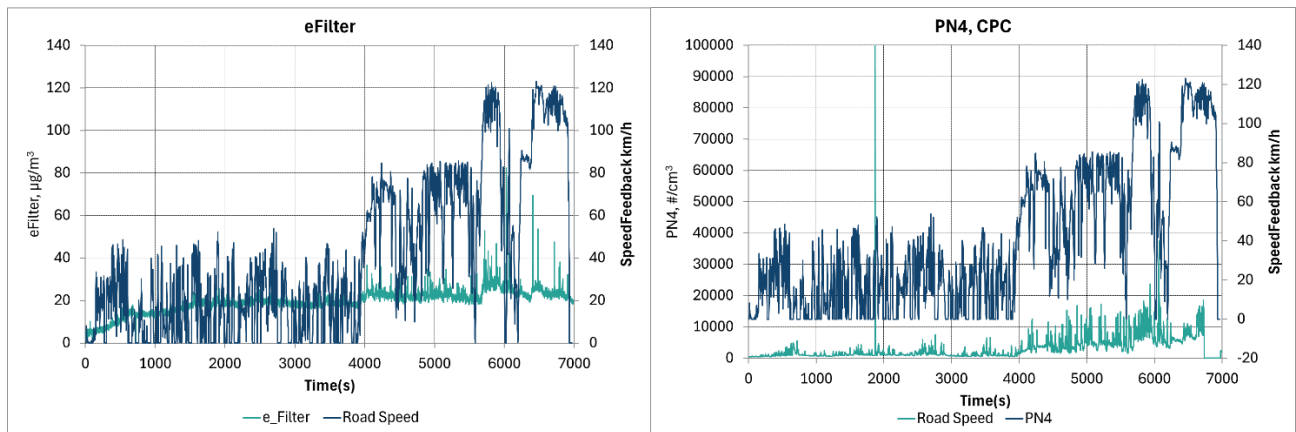

Figure 10-5: Real-time a) PM and b) PN emissions from the rear tyre of a DPF-equipped diesel in the VERC.

10.2.1.5 Measurements with sampling system situated directly behind tyre of an EV

Emissions measurements were made using the tyre sampling system with an EV operating on the chassis dynamometer. The vehicle was selected as it produces no tailpipe emissions and uses regenerative braking for almost all braking events. The inlet of the system was mounted as close as possible to the rear wheel.

Real-time mass measurements with the eFilter are shown in Figure 10-6a, while PN measurements with the cold and hot MPEC are shown in Figure 10-6b.
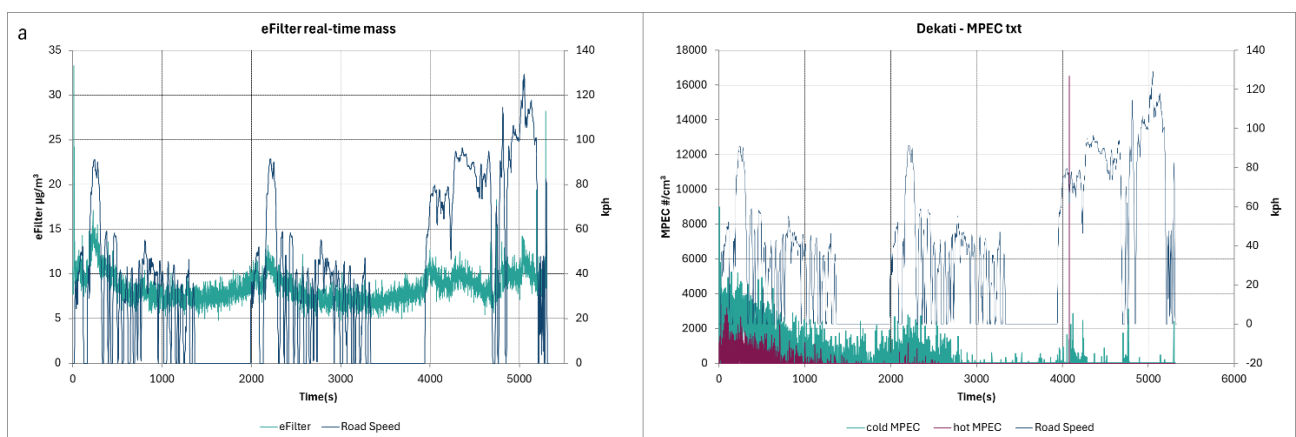

Figure 10-6: Real-time a) PM and b) PN emissions from the rear tyre of an EV in the VERC.

From these measurements there was good evidence of eFilter mass emissions deriving from cycle – mostly on accelerations. These emissions seem to generate and comprise the raised "background levels" seen in the earlier DPF diesel test. These particles may be volatiles are dominate the emissions of tyres when tested on a typical steel roller, like that present in the VERC.

There was some evidence for PN emissions in response to the hardest accelerations in the early part of the drive cycle (first 300s). The two MPECs showed < 50% of the particles are solid and the rest to be volatile. PN levels were low – and may be artificially raised due to multiple charging on 100nm+ particles.

The lack of discrete spikes of emissions above the continuous emissions level during the EV tests, suggests that these were generated from mechanical braking or tailpipe particle emissions in the earlier DPF diesel testing. Tyre particle emissions may therefore comprise relatively few large particles (detected by eFilter) and mostly volatile / semi-volatile emissions otherwise.

10.2.1.6 Comparison of Ph1 brake and tyre emissions

Brake and tyre wear emissions profiles from PG42 cycle testing in Phase 1 were reevaluated (Figure 10-7). A comparison of brake wear PN emissions (non-volatile PN23, measured by SPCS) with tyre wear emissions (SPCS), shows similar profiles, but with the tyre emissions at levels two orders of magnitude below those of the brake emissions. This could indicate ~1% leakage of brake wear particles from the brake enclosure during tyre sampling, due to overpressure in the enclosure, as described in Section 10.2.1.2, with these particles drawn into the tyre emissions' sampling inlet.

Comparison of PM filters from the brake and tyre tests showed deep black particulate material from the brake sampling and light grey uniform deposit from the tyre sampling. The tyre sampling material appeared to be more like volatiles than solid particles. eFilter data from Phase 1 also suggested different densities for the particulate material of brakes and tyres, implying different chemistries.
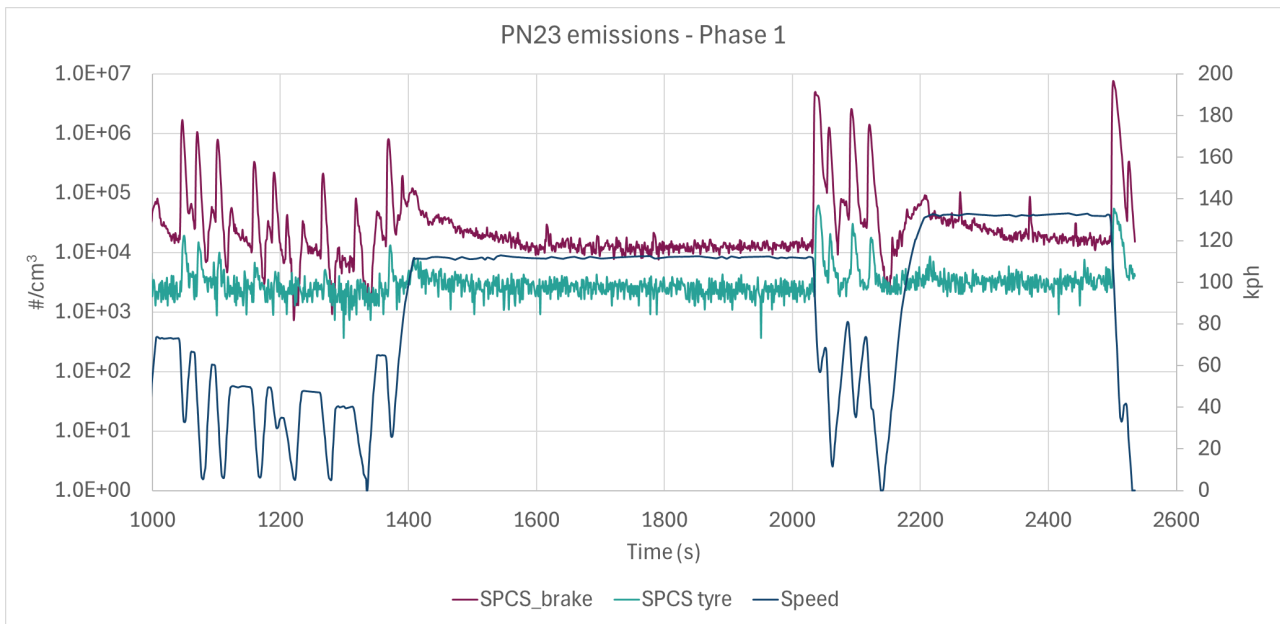
Figure 10-7: Comparative SPCS brake and tyre emissions profiles from a PG42 cycle, Phase 1 of the project.
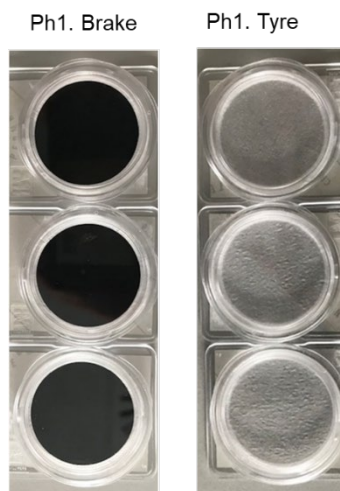

Figure 10-8: PM filters sampled during brake and tyre testing in the Phase 1 project.

From this analysis, it was considered possible that brake particles were being sampled alongside tyre emissions in Phase 1, and this possibility would be eliminated by creating underpressure in the brake enclosure during testing.

10.2.1.7 Overview and outcomes

Several experiments, described in Section 10.2, indicated that when tested on a steel roller, particle emissions from tyres may be dominated by volatiles, with many of these potentially <10nm. Solid particles can also be detected, but measures should be taken to ensure that brake wear particles do not contaminate the samples.

A surface more representative of asphalt was required in order to study and potentially enable the production of solid particles, and so a decision was made to move tyre testing to the VATF, where the roller would be freshly covered with a hard-wearing abrasive surface (3M walkway tape, Section 4.2.1). Measurements in the VATF included the PN4 system, to detect very small particles.

10.2.2 VATF testing

The VATF as used for the tyre testing is described in Section 4.2, and was prepared for the testing as recorded in Section 4.2.1, using the sampling system and instruments as detailed in Section 3.2.4 and Section 5. The significant factors changed between the initial VERC tyre test and the tyre tests in the VATF were:

- The use of a rough surface of the dynamometer drum for the test tyre to run on.
- The extract fan in the dynamometer pit being disabled during testing to minimise tyre particles being removed ahead of the sampling system.
- The addition of PN4 particle measurement with a TSI 3775 CPC.
- Sample points for all instruments being moved immediately downstream of the sample duct, rather than being downstream of the flexible sample pipe.

10.2.3 Background measurements

Prior to commencing comparative tyre emissions measurements, several VATF facility background measurements were made, and the results compared with initial PG42 cycles' emissions. All the instruments employed during actual tyre evaluations were used to collect background data, with the facility set-up exactly as for tyre emissions sampling excepting that the test vehicle and chassis dynamometer were switched off. These comparisons were made with the intention of determining whether backgrounds should be collected and subtracted from results obtained from the various instruments. Some further background investigations with similar outcomes were undertaken during the tyre particle reduction device evaluation described in Section 11.2.4.2.

One set of emissions and background results is discussed in the following sections.

10.2.3.1 PN4 background and emissions

Data on both a real time basis and averaged across the sampling period/cycle are presented for PN4 in Figure 10-9a and Figure 10-9b respectively, comparing three PG42 cycles' data (dark blue, light blue and grey) with a facility background collected beforehand (red). Figure 10-9a also shows the drive trace of a PG42 cycle (dashed line).
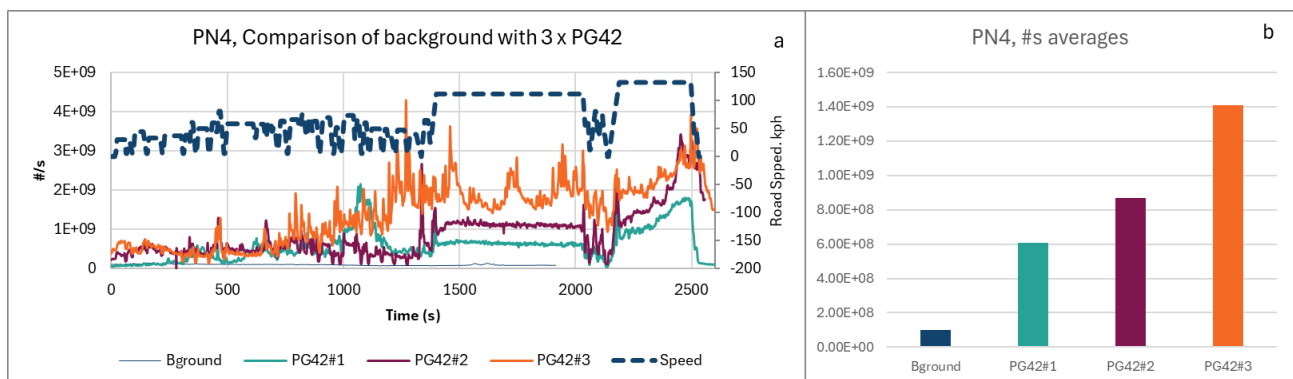

Figure 10-9: a) real time PN4 emissions and b) average PN4 emissions from background and PG42 cycles.

These data clearly indicate that PN4 emissions from PG42 cycles are well above the level of the background, measured prior to the PG42 tests, for the whole duration of the cycle. It should be noted that PG42#3 indicates different particle emissions behaviour than the two prior tests. Emissions spiking is observed during the long cruise from ~1400s to 2000s that is not observed in the other two tests. Despite investigations, it has not been possible to identify a source of these particles linked to the tyre. Therefore, it is possible that an outside source of particles has influenced this particular PG42 test. Clearly this could suggest a background contribution, but the background would be very different to that measured before the test started (shown in red).

In addition, PG42#1 shows an emissions peak between ~900s and 1250s that is not present in the other two PG42 tests. Since these are visible to the PN4 they could be volatile or non-volatile, and any size from 4nm upwards. They could be contributions from the background or a spontaneous release of emissions from the tyre.

10.2.3.2 APC10 background and emissions

In addition to PN4 measurements, which include both solid and volatile particles >4nm, the APC10 was employed to measure non-volatile PN >10nm. Using the same chart formats shown for the PN4 continuous data, Figure 10-10a shows #/s data, while Figure 10-10b shows the same data magnified on the y-axis. These charts do not indicate the spiking in PG42#3 between 1400s and 2000s seen with PN4, so this suggests the

presence of either non-volatile particles <10nm, volatile particles in the <2.5 μm region or both during PN42#3. These particles would not necessarily be emissions from the tyre.

In addition, the average #/s levels of the background collected before the test (Figure 10-10c) were higher than the average emissions from PG42#2 and #3. This is despite the observation of particle emissions peaks at ~2500s corresponding to the hard deceleration at the end of the PG42 cycle. Since these peaks are visible, emissions at this point in the cycle must be higher than the background (and instrument noise) present simultaneously. Again, this highlights the unrepresentative nature of a background sampled before the tests.
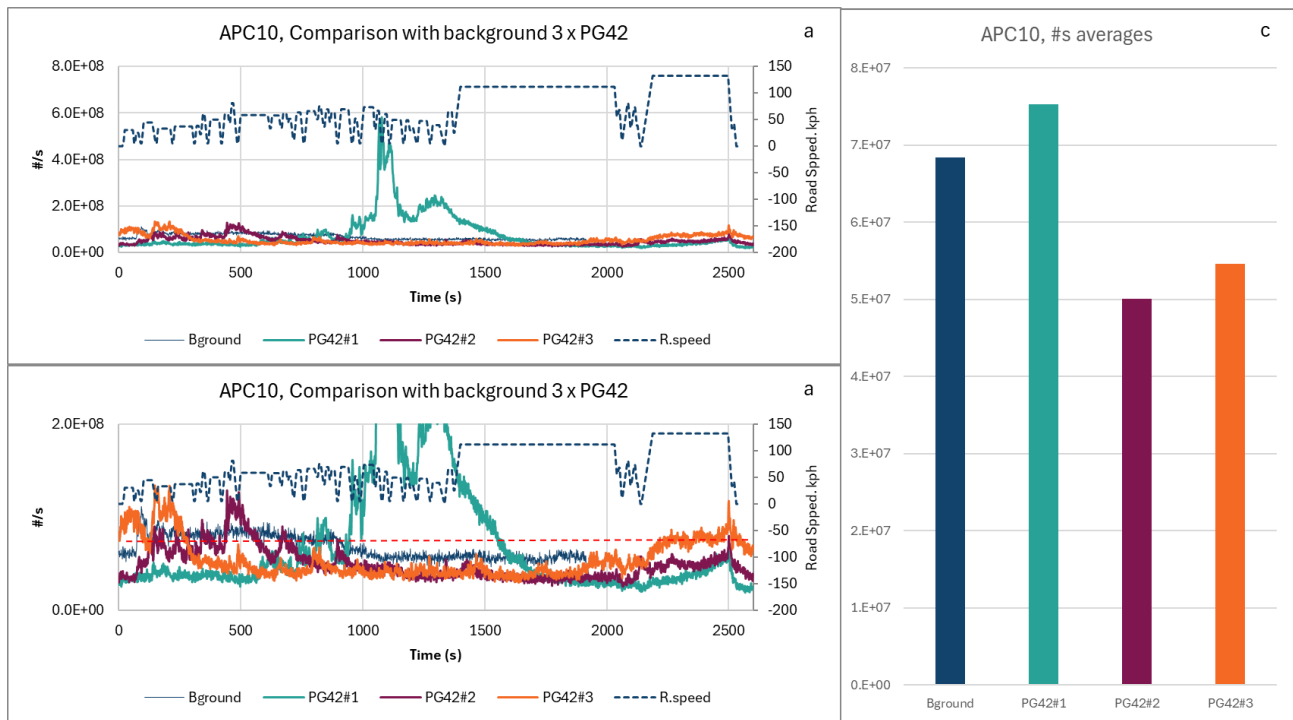
Figure 10-10: a) Real-time emissions from background and PG42 cycles measured by the APC10, b) the same chart magnified at low emission levels, c) average emissions from background and PG42 cycles.

The large peak of emissions seen with the PN4 instrument between ~900s and 1250s is more significant in the context of non-volatile PN10 emissions measured by APC10. The emissions event dominates the overall emissions and lasts from ~900s to ~1600s. It is not clear what the source of this event is.

10.2.3.3 Cold MPEC background and emissions

In this section, real-time (Figure 10-11a,b) and average (Figure 10-11c) #/s emissions of total (volatile and non-volatile) particle number emissions from background and PG42 cycles measured by the cold MPEC, are compared.

The cold MPEC data from PG42#3 (but not the other two PG42 tests) also shows the emissions spiking in the cruise between 1400s and 2000s exhibited by the PN4 system and, as shown in Figure 10-12, the real-time traces are highly similar to the PN4 throughout the drive cycle, with the cold MPEC (PN10) reading ~40-50% of the PN4 levels. Both instruments measure total particles (solids plus volatiles), and this suggests that ~50% of the PN emitted during the drive cycle lie between 4nm and 10nm, and this size range contributes a significant proportion of the emissions spikes.

In the other two PG42 cycles, PG42#1 and #2, the average emissions (Figure 10-11c) are very close to the background levels, despite the emissions peaks at ~2500s being well above the mean background level (Figure 10-11b).
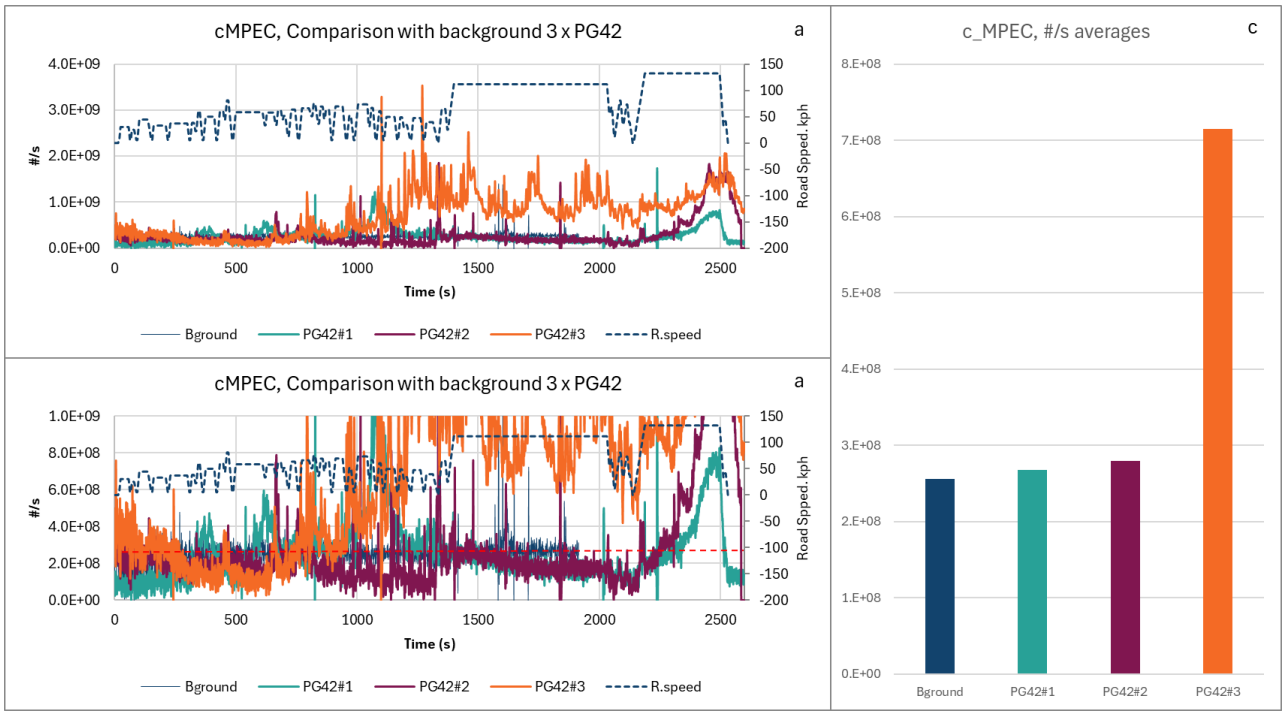
Figure 10-11: a) Real-time emissions from background and PG42 cycles measured by the cold MPEC b) the same chart magnified at low emission levels, c) average emissions from background and PG42 cycles.
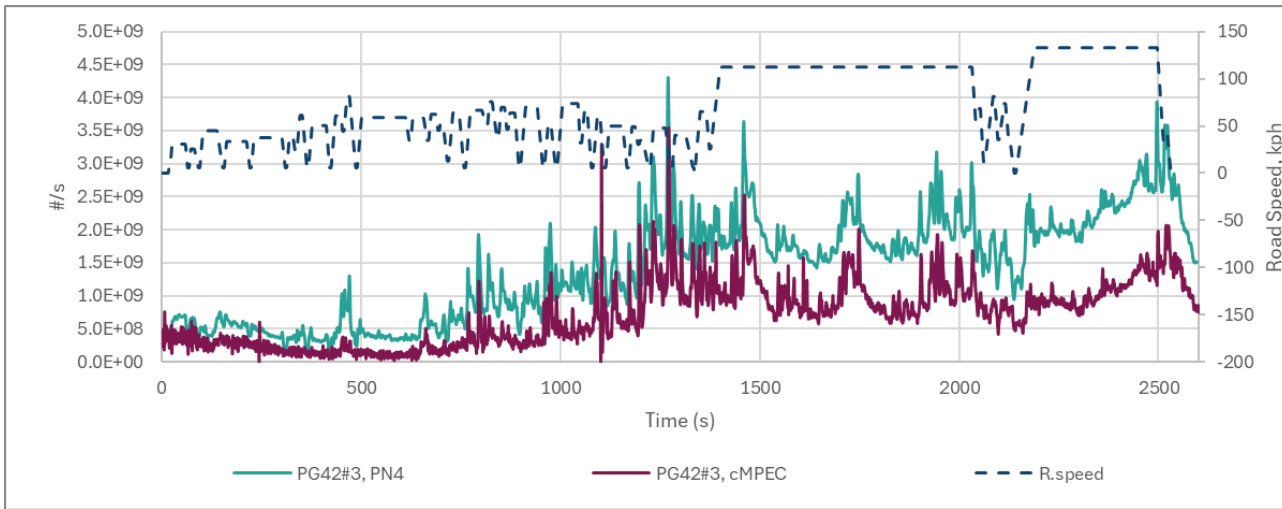

Figure 10-12: Real-time emissions from PG42#3 measured by the CPC (PN4) and cold MPEC, along with the vehicle speed trace.

10.2.3.4 Hot MPEC background and emissions

Comparisons of the real-time and cumulative PG42 cycle and background emissions measured with the hot MPEC, Figure 10-13a,b, show that the PG42 cycles' hot MPEC emissions levels are generally dominated by noise, that the strong peak usually observed at ~2500s is not apparent in any of the results, and that background levels sample prior to the tests are similar to, and at times higher than, sample levels. Highest emissions were observed from PG42#1 (Figure 10-13c), where the peak of non-volatile particles observed in the APC10 results between ~900s and 1600s is also apparent. Figure 10-14 shows that after the first ~400s of PG42#3, hot MPEC emissions are in the noise below the detection limit and the similarity with the APC10 signal is poor. Alternatively, during PG42#1 where emissions levels were higher (Figure 10-15), the agreement between APC10 and hot MPEC is improved, indicating less of a sensitivity challenge for the hot MPEC.

These data indicate that during tyre emissions tests on PG42 cycles the hot MPEC is often functioning at or below its detection limit, that hot MPEC background can be higher than the samples, and that prior background samples are not necessarily representative of the background present during measured emissions cycles.
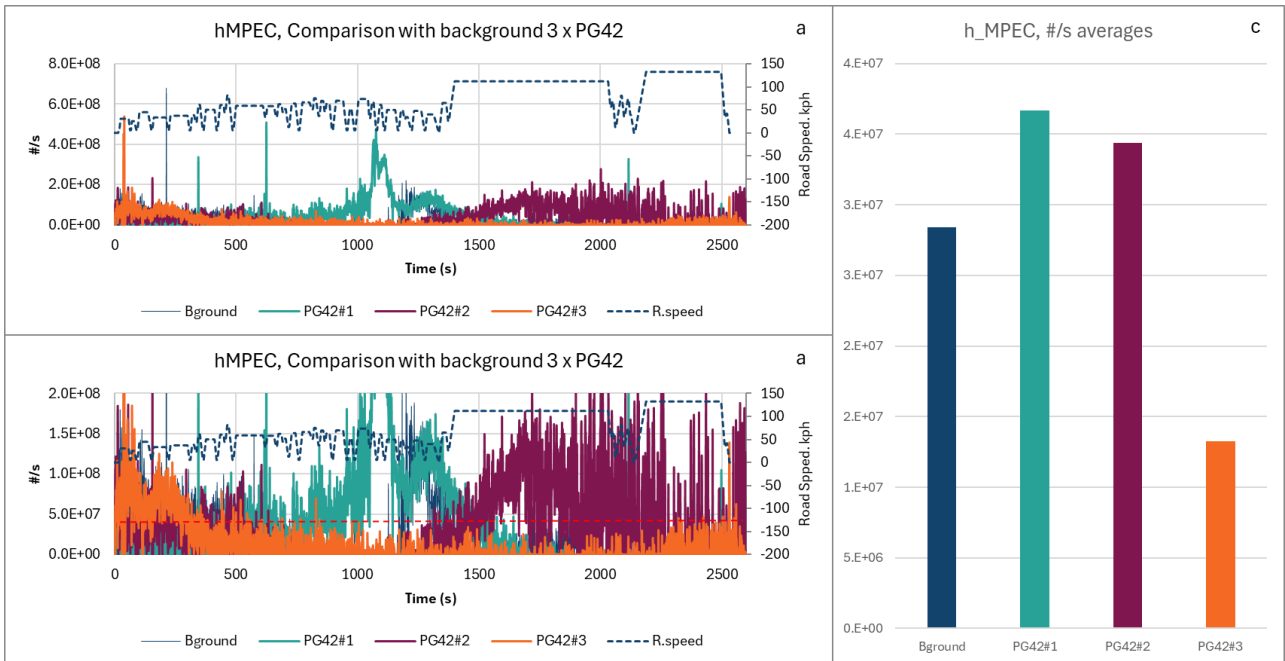

Figure 10-13: a) Real-time emissions from background and PG42 cycles measured by the hot MPEC b) the same chart magnified at low emission levels, c) average emissions from background and PG42 cycles.
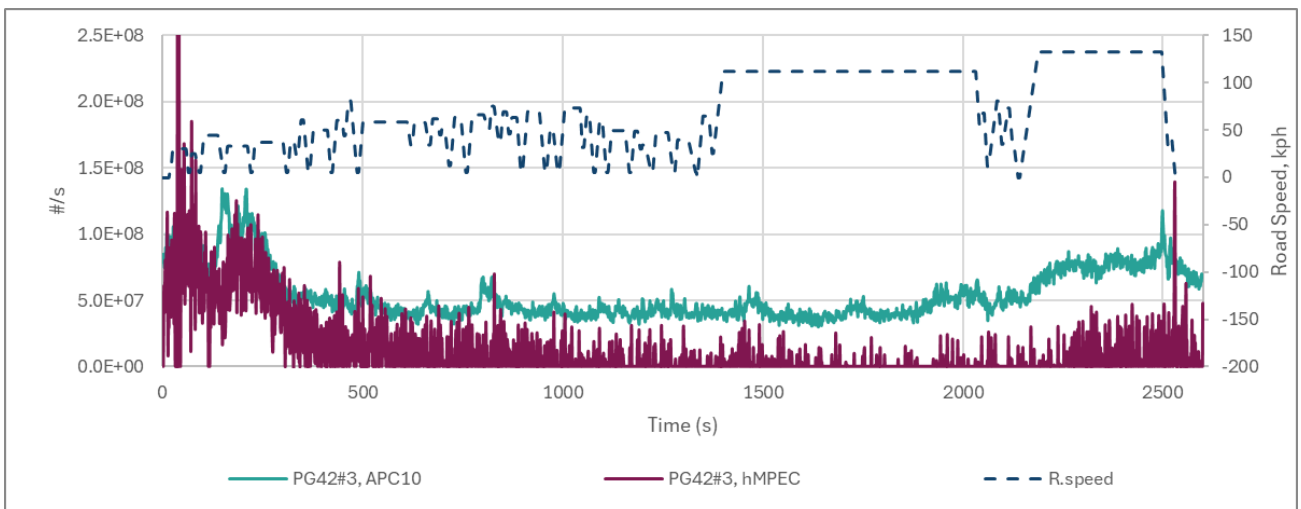

Figure 10-14: Real-time emissions from PG42#3 measured by the CPC (PN4) and hot MPEC, along with the vehicle speed trace.
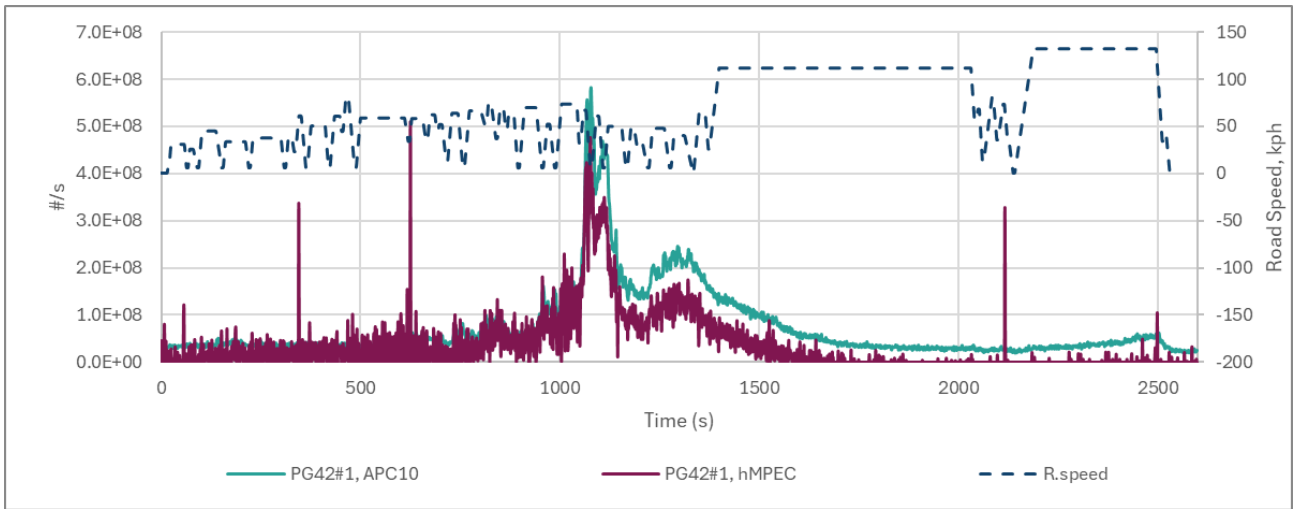
Figure 10-15: Real-time emissions from PG42#1, APC10 and hot MPEC.

10.2.3.5 eFilter background and emissions

eFilter background levels were typically similar on average to PG42 test results, although PG42#3 showed a higher emissions level overall, and PG42#1 and PG42#2 were lower for the first #10 minutes than the background taken before testing started (Figure 10-16a,b).
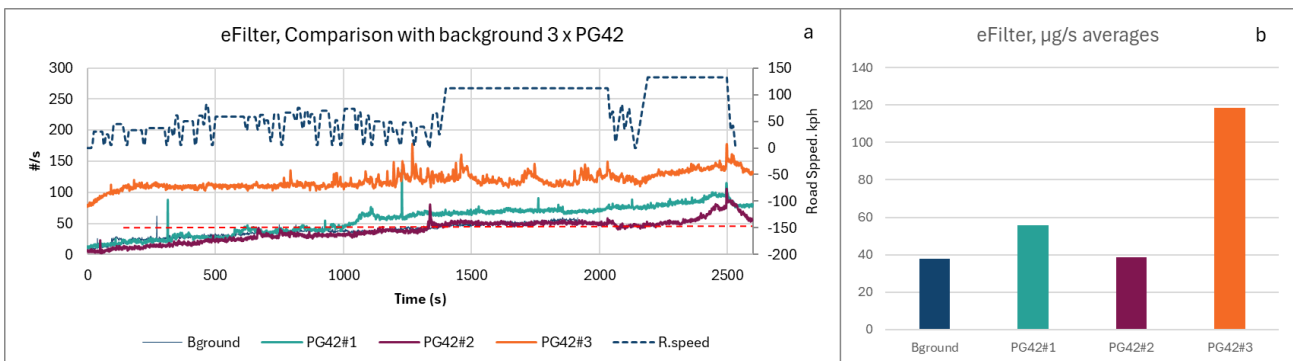

Figure 10-16: a) Real-time emissions from background and PG42 cycles measured by the eFilter, b) average emissions from background and PG42 cycles.

10.2.3.6 eFilter Gravimetric PM_{2.5} background and emissions

The gravimetric PM_{2.5} background collected with the eFilter prior to the three PG42 tests was higher than any of the test results (Figure 10-17). This observation is different to that of the real-time eFilter, and the most likely explanation is that the glass fibre PM filters employed collect gas-phase volatiles as well as particles, while the eFilter measures only particle phase materials. On this basis we would expect the filter-based measurements to be considerably higher, but in fact the eFilter emission is many times higher than the filter approach. The simplest explanation for the higher eFilter masses is the presence of a relatively few massive particles that contribute a disproportionate charge contribution when the mass is calculated. These particles do not have the same impact on filter mass.
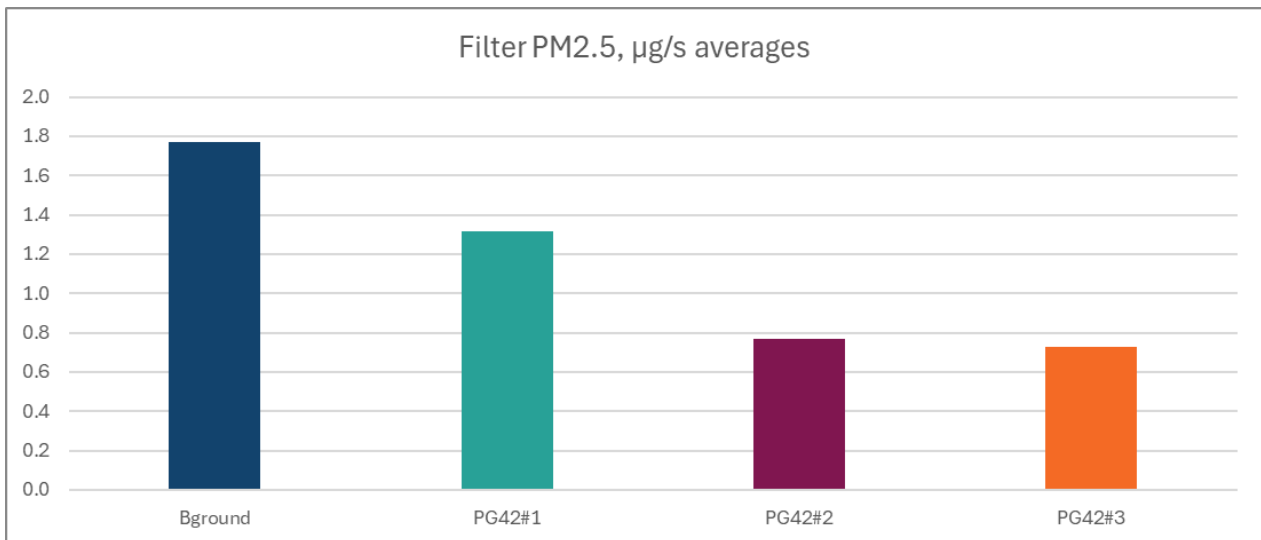
Figure 10-17: Average gravimetric emissions from background and PG42 cycles from the eFilter.

10.2.3.7 Summary

Comparisons of background measurements with PG42 tyre emissions sample measurements showed that the responses of some instruments were above measured background levels (PN4, APC), some were borderline but could show obvious transient events in drive cycles (e.g. cold MPEC) despite being below the typical continuous background concentrations, and others were close to or below the background concentrations (hot MPEC, eFilter). In addition, it was not possible to gain confidence that a background sampled before a sequence of emissions tests was representative of the background present during those emissions tests.

The subtraction of an unrepresentative background risks eliminating tests completely from the database, even though it is visually clear that individual events of particle production are apparent within those tests. It is possible that the inlet-duct sampling approach used in this project benefits from the outgassing of materials from the tyre. This outgassing into the duct may restrict the ingress of ambient particles and gases while the emissions event occurs. This possibility would need further investigation to verify. If this is the case, the subtraction of any background would likely be inappropriate.

For these reasons it was decided not to collect or subtract backgrounds during the tyre test programme. The resulting mass and number emissions levels from tyre measurements are therefore "maximum" ones, as there is likely to be some background contribution of volatile and solid particles during each test.

For future work tyre emissions measurements could be made in a facility fed with filtered air to minimize background, or a duplicate set of instruments run in parallel to determine simultaneous background levels. For the latter, however, it is challenging to determine exactly where the inlet for these samples would be positioned.

10.3 RESULTS OF TYRE TESTING

This section describes tyre metrology, plus particle number and mass emissions from various tyres. Testing results primarily focus on emissions from the PN4, non-volatile PN10 (APC10), total PN10 (cold MPEC) and gravimetric $PM_{2.5}$ (filter PM) approaches. Gravimetric $PM_{2.5}$ is included, despite the background experiments suggesting that emissions levels were below the background (Figure 10-17), both because $PM_{2.5}$ is a key metric and because evidence from Section 10.3.3 demonstrates that $PM_{2.5}$ results can discriminate emissions between sequential tests and must therefore be above the background for at least some of those tests.

10.3.1 Tyre Metrology

Tyre weight measurements were made of the unused tyres, after the initial ~200 km on-road ageing and end-of testing (following completion of all the chassis dynamometer testing). Exceptions were the two aged tyres: W12, with ~11,000 km initial mileage and W14, with ~23,000 km initial mileage. Tread depth measurements were first made following the initial ageing. In addition, the test mileages, due to additional experiments and repeats, were higher from some tyres than others. To allow like-for-like comparisons between all tyres, wear

rates presented are based upon tyre + wheel mass losses and tread depth reductions, both calculated for the delta and distance covered between post ageing and end-of test measurements.

It should be noted that the distances between post-ageing and end of test ranged from ~360 km to ~1030 km, and mass losses were < 80g, excepting the high mileage tyres. Although the tyres were cleaned and inspected prior to weighing, it is possible that some small stones/chips remained embedded in the tyres. If present these would increase the wheel + tyre weights and potentially influence the apparent wear rates for mass loss.

10.3.1.1 Mass-based tyre emissions wear rates

Mass based tyre wear data from the 10 tyres tested are summarised in Table 10-3. Within this table, subsets of data addressing [a] wheel size variants, [b] mileage effects and [c] manufacturer and design variants with 18" tyres are isolated.

In part [a] of the table, the first column indicates the number of the wheel + tyre combination plus the tyre diameter in inches, in part [b] the first column identifies the number of the wheel + tyre combination plus the approximate post-ageing mileage in 1,000's of km, and finally in part [c] the first column identifies the wheel + tyre combination plus the tyre diameter. In addition, within part [c], [18*] identifies that W7 is an 18" tyre design variant. Details of tyre specifications can be found in Table 7-2.

Table 10-3: Summarised weighing and distance-related weight loss data from the tyres tested

[a] 16" wheels vs. 18" wheels

Wheel	Initial (g)	Post-ageing (g)	Post-test (g)	Ageing distance (km)	Test distance (km)	Wear rate (post-ageing, mg/km)
W17 [16]	16703.9	16696.3	16690.0	210.8	1032.5	6.1
W7 [18]	22060.9	22052.7	22045.1	199.6	365.1	20.7
W20 [16]	17203.6	17190.1	17177.9	215.7	317.0	38.4
W4 [18]	22497.8	22486.6	22462.2	194.7	363.3	67.2
W16 [16]	15607.5	15600.2	15521.3	214.0	636.1	124.0
W2 [18]	20616.9	20624.7	20558.4	223.7	587.0	113.0

[b] Mileage effects

Wheel	Initial (g)	Post-ageing (g)	Post-test (g)	Ageing distance (km)	Test distance (km)	Wear rate (post-ageing, mg/km)
W2 [0]	20616.9	20624.7	20558.4	223.7	587.0	113.0
W12 [11k]	N/A	20761.7	19747.6	~11,000	956.1	1060.7
W14 [23k]	N/A	20643.4	19597.7	~23,000	317.0	3298.2

[c] Manufacturer and design variables with 18" tyres

Wheel	Initial (g)	Post-ageing (g)	Post-test (g)	Ageing distance (km)	Test distance (km)	Wear rate (post-ageing, mg/km)
W2 [18]	20616.9	20624.7	20558.4	223.7	587.0	113.0
W7 [18]	22060.9	22052.7	22045.1	199.6	365.1	20.7
W10 [18]	22666.6	22648.1	22603.1	196.3	411.7	109.3
W4 [18]	22497.8	22486.6	22462.2	194.7	363.3	67.2
W6 [18]	21680.0	21667.2	21652.1	197.9	314.8	48.0

A comparison of tyre wear rate emissions between 16" and 18" tyres is shown in Figure 10-18Figure . These data suggest that total tyre wear emissions are higher from 18" tyres than from 16" tyres (W17, W7 and W20, W4) or broadly similar (W16, W2). In addition, it's clear that the Michelin CrossClimate 2 215/55R18 99V XL TL tyres (W17,W7) have lower wear than the Michelin Primacy 4; 215/55R18 99VXL TL S1 tyres (W20, W4), with emissions from the Bridgestone Turanza Eco 215/55R18 95T tyres (W16, W2) highest of the three pairs.

At an average of ~120 mg/km wear from a single front wheel, W16 and W2 show emissions rates higher than recent literature values for tyre wear (Giechaskiel, et al., 2024), which report ~110 mg/km per vehicle, but W17 and W7 showed much lower levels, averaging ~13.5 mg/km. Front wheel tyre wear would be expected to be higher than rear wheel wear, testing in this project on PG42 cycles was designed to promote wear, and the front two wheels provide all the braking on the two-wheel drive chassis dyno used, so higher than average emissions are perhaps not unlikely. It is also possible that the surface used on the roller of the chassis dynamometer promotes greater wear than would asphalt, but this is considered unlikely.
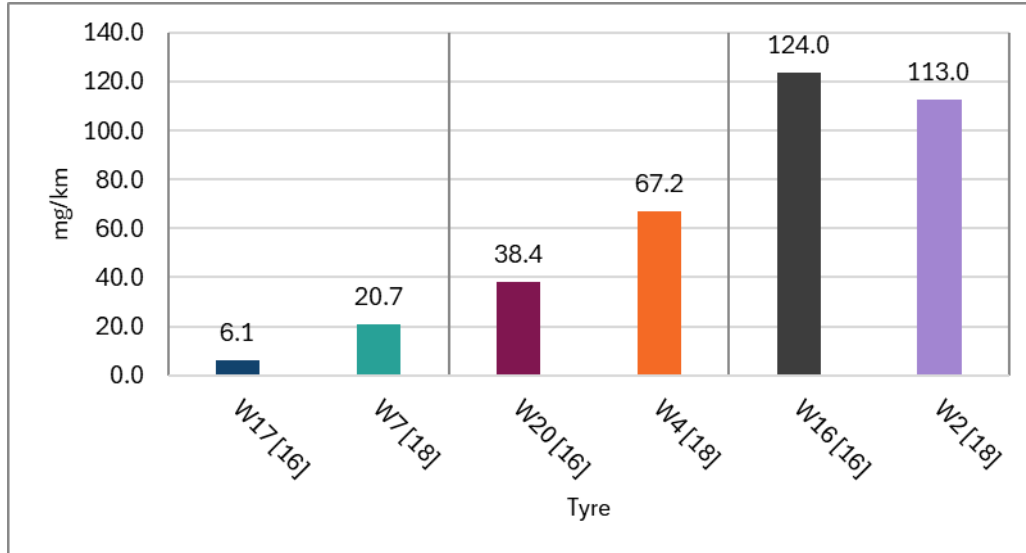
Figure 10-18: Effect of 16" and 18" size on mass-based tyre wear rates.

The effect of accumulated tyre mileage on mass-based tyre wear emissions rates is shown in Figure 10-19. Prior to the test programme ageing, W2 was a new tyre, W12 had driven ~11,000 km and W14 ~23,000 km. A further 587 km, 956 km and 317 km respectively were added to W2, W12 and W14 before the end of test measurements. All tyres were 18" Bridgestone Turanza Eco 215/55R18 95T types.

Results indicate that tyres of this type with elapsed mileages of >10,000 km have substantially higher mass emissions rates, and that the mass emissions rates continue to rise as the mileage increases. W12 (~12,000 km total elapsed mileage) emits approximately 1 g/km of tyre wear, while W14 (~23500 elapsed mileage) emits ~ 3.3 g/km of tyre wear. This is ~300 times higher than the emission rate of the same tyre type (W2) at ~800 km.
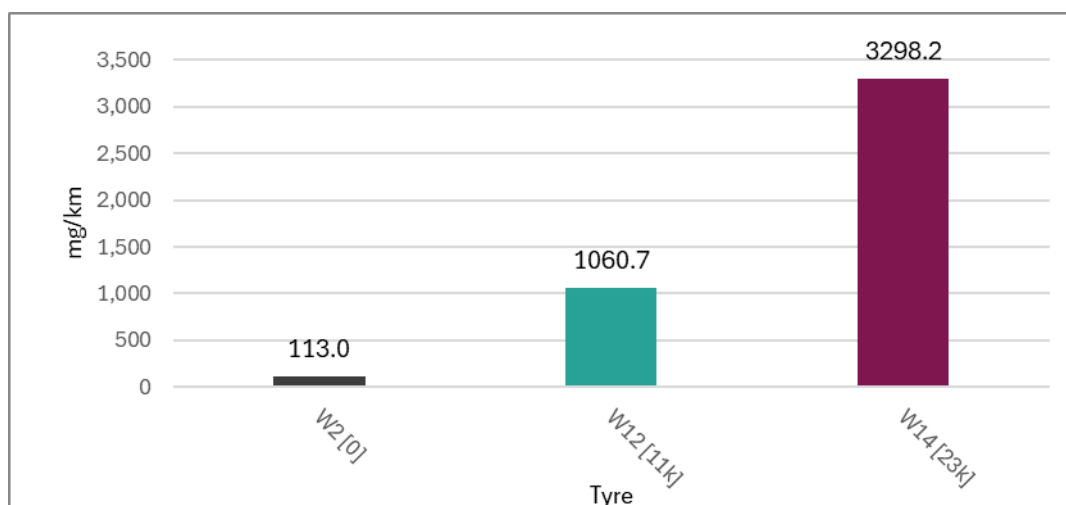

Figure 10-19: Effect of elapsed mileage on mass-based tyre wear rates.

Comparisons between 18" tyre wear mass emissions rates plus manufacturer and design variables are shown in Figure 10-20. W2 and W10, which are 18" summer tyres, both show similar mass emissions rates of ~110

mg/km. From the tyre labelling data (Figure 7-1) both have similar ratings for noise and wet grip, while W2 claims better fuel economy. W10 is lower price.

W4 (summer), W6 (summer) and W7 (all-season) have lower mass emissions rates than W2 and W10, at ~67 mg/km, ~48 mg/km and ~21 mg/km respectively. Noise ratings are matched between these tyres (also with W2 and W10), but their manufacturers claim better fuel consumption for W4 and W6 than for W7, and W6 has a higher wet grip rating than W7 and W4. W2, W4 and W6 all claim the highest fuel economy ratings. W7, which shares its status with W10, has the lowest fuel economy rating of all the 18" tyres.

There is clearly no correlation between fuel economy ratings and the wear rates observed in this study. This is perhaps counter-intuitive as lower tyre-to-road friction might be expected to accompany lower wear. Notably, W7, the sole all-season tyre - which has a relatively poor fuel economy rating and would be comprised of a softer compound for winter use - appears to show the lowest wear rate. It should be noted, though, that project mileage was relatively low, and it may take longer for tyre property effects to manifest.
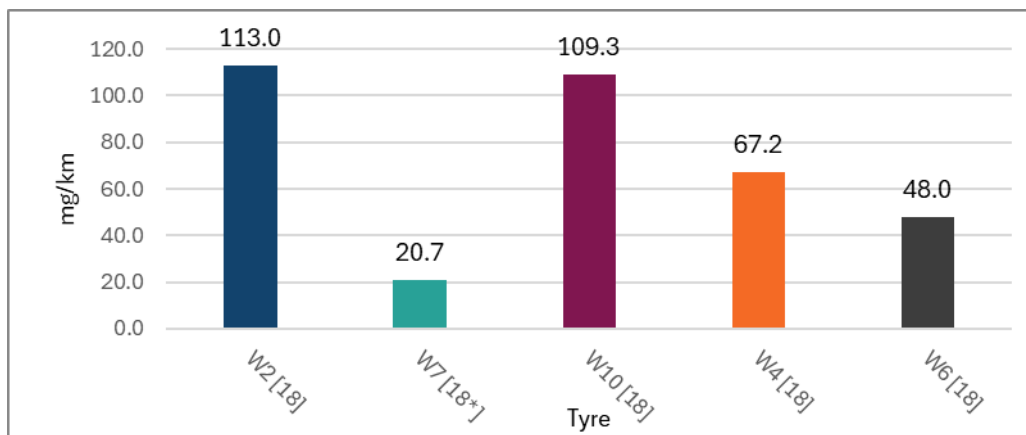

Figure 10-20: Comparison of 18" tyre wear mass emissions rates, manufacturer and design variables.

Overall (excluding the two high mileage tyres) the average mass emissions rate for the 18" tyres was 71.6 ± 39.7 mg/km, and the average mass emissions rate for the 16" tyres was 56.2 ± 60.2 mg/km. Including all "low mileage" tyres gives an average mass emissions rate of 65.8 ± 45.0 mg/km.

10.3.1.2 Tyre tread depth measurements

Tyre tread wear was determined using a digital tyre tread depth gauge with range 0 to 25 mm and precision of 0.01 mm (PCL, UK[7]). First measurements were made following initial road mileage (~200 km per tyre), with final measurements after the completion of all testing. Tread measurements were made in three locations of the central groove, spaced at ~120° intervals around the circumference of the tyre, with the three measurements averaged to determine a single tread depth value. Wear rates have been calculated in µm/km, which equates to mm/1,000km.

Tyre tread wear data from the 10 tyres tested are summarised in Table 10-4, Table 10-5 and Table 10-6. Table 10-4 addresses wheel size variants, Table 10-5 shows mileage effects, and Table 10-6 compares data from manufacturer and design variants for 18" tyres.

Table 10-4: Tyre tread depth differences - tyre size effects.

Wheel	Post ageing depth, mm	post test depth, mm	ageing distance, km	test distance, km	wear rate post-ageing, µm/km
W17 [16]	6.61	6.58	211	1032	0.03

---

[7] Digital Tyre Tread Depth Gauge

Wheel	Post ageing depth, mm	post test depth, mm	ageing distance, km	test distance, km	wear rate post-ageing, µm/km
W7 [18]	7.23	7.09	200	365	0.37
W20 [16]	7.50	7.36	216	317	0.44
W4 [18]	6.77	6.65	195	363	0.31
W16 [16]	5.82	5.48	214	636	0.53
W2 [18]	5.33	5.22	224	587	0.19

Table 10-5: Tyre tread depth differences - tyre mileage effects.

Wheel	Post ageing depth, mm	post test depth, mm	ageing distance, km	test distance, km	wear rate post-ageing, µm/km
W2 [0]	5.33	5.22	224	587.0	0.19
W12 [11k]	5.58	3.40	11000	956.1	2.28
W14 [23k]	4.95	3.09	23000	317.0	5.85

Table 10-6: Tyre tread depth differences - tyre manufacturer and design effects.

Wheel	Post ageing depth, mm	post test depth, mm	ageing distance, km	test distance, km	wear rate post-ageing, µm/km
W2 [18]	5.33	5.22	224	587	0.19
W7 [18]	7.23	7.09	200	365	0.37
W10 [18]	7.50	7.25	196	412	0.62
W4 [18]	6.77	6.65	195	363	0.31
W6 [18]	6.96	6.86	198	315	0.31

Figure 10-21 compares tread wear results of nominally identical 16" and 18" tyres. Notably, as seen for tyre mass loss in Figure 10-18, W17 (Michelin CrossClimate 2 205/55R16 94V XL TL) has the lowest wear rate, but W7, the 18" version of this tyre, does not show the same low mass and depth wear rates. Potentially this indicates a formulation difference between the two tyres. Excepting this pair, both W20 + W4 (Michelin Primacy 4 tyres, by ~30%) and W16 + W2 (Bridgestone Turanza ECO tyres, by ~65%) showed higher tread depth loss from the 16" tyres than the 18" tyres. This would be consistent with the 16" tyres having higher sidewalls, experiencing more flexion during the road ageing and hence greater heat build-up and wear, plus the smaller contact patch would lead to greater pressure per unit area and higher wear.
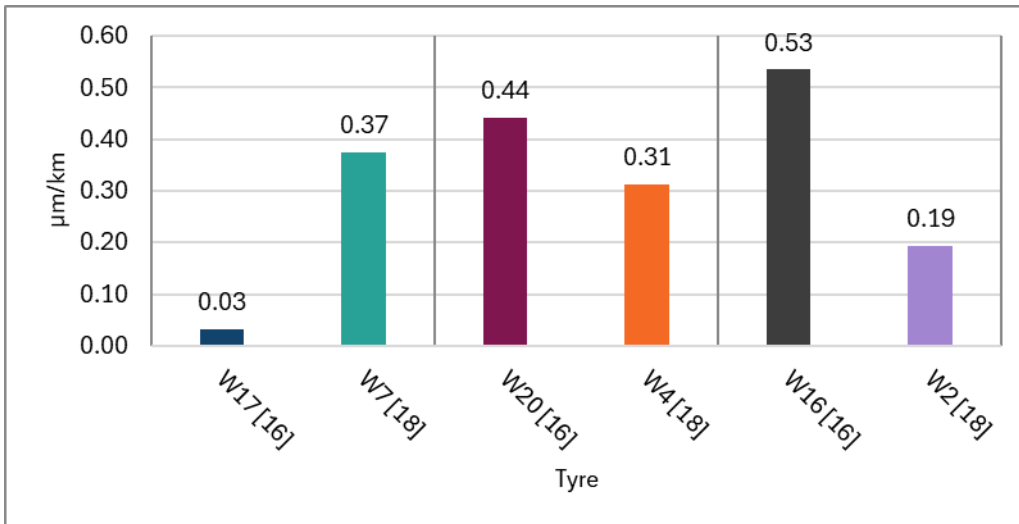
Figure 10-21: Tyre size influences on tyre tread wear rates.

The effects of increased mileage on three nominally identical 18" Bridgestone Turanza tyres are shown in Figure 10-22. The low mileage tyre (W2) had covered ~800 km, W12 had covered ~12,000 km (11,000 of this pre-ageing) and W14 had covered ~23,500 km (23,000 km pre-ageing). There is a clear acceleration in tyre tread depth wear rate as mileage increases. This correlates closely with the observed effects on tyre mass lost rate (Figure 10-23). It is possible that the tyre material fatigues with distance driven and the reduce tread depth increases local stresses, further increasing wear.
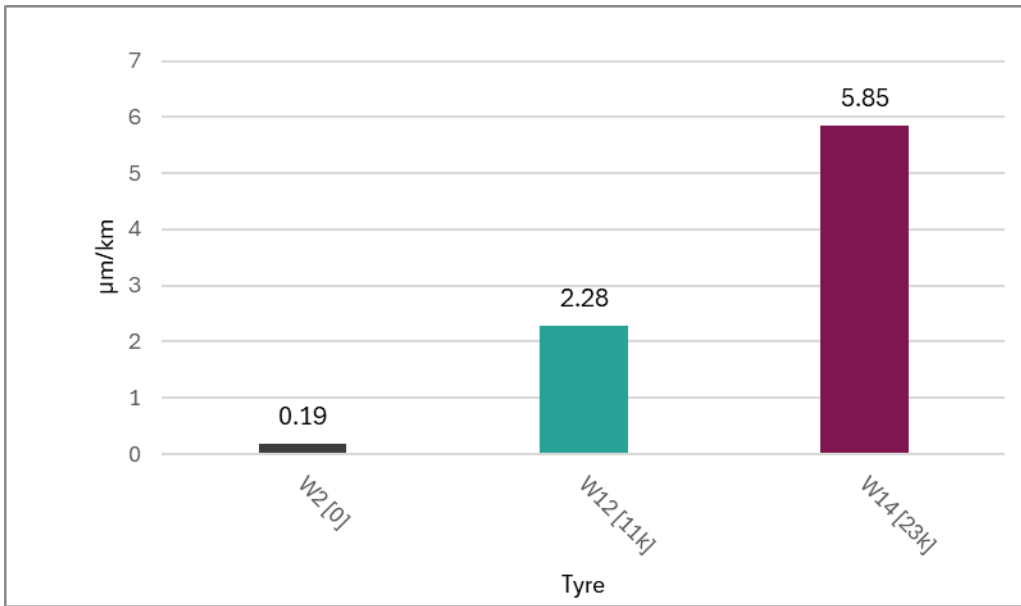
Figure 10-22: Tyre mileage impacts on tread depth wear rates.
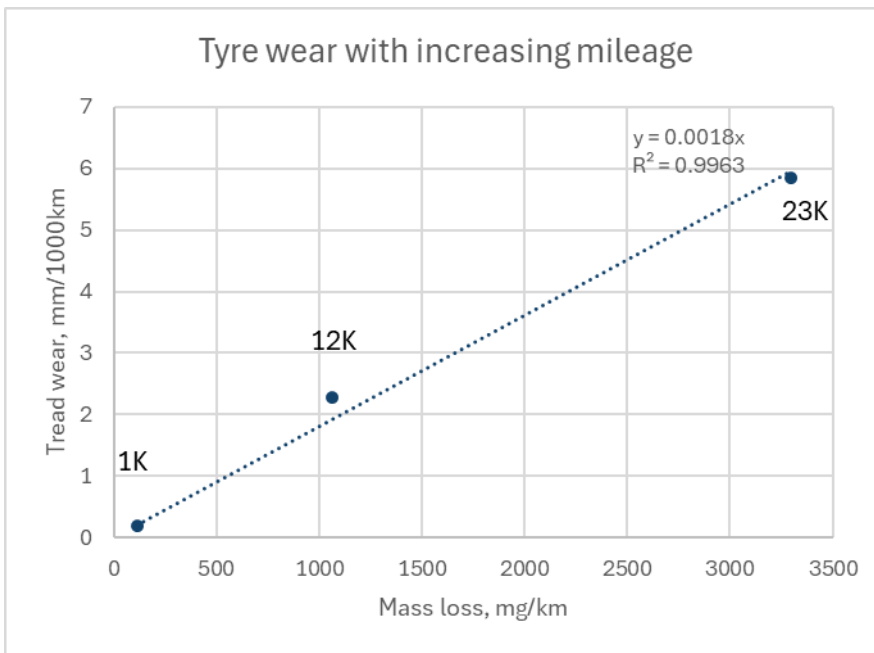
Figure 10-23:Correlation between tyre mass loss and tyre tread wear, W2, W12 and W14.

Tyre wear rates were similar between 4 out of 5 of the 18" tyres compared in Figure 10-24 at 0.2 to 0.4 µm/km, with only W10 appreciably higher, at 0.6 µm/km. W10 is a low budget tyre, that might be expected to show more rapid tread wear. It was also (Figure 10-20) one of the two tyres with the highest mass loss rate. Interestingly, W2, which shows the lowest tread depth loss in Figure 10-24, showed the highest mass loss rate. This, and differences between other 18" tyres, may indicate different tyre rubber densities. Because of these possible density differences, there is no strong relationship between tread depth and mass loss wear rates for the 18" tyres (excluding the type shown in Figure 10-25).
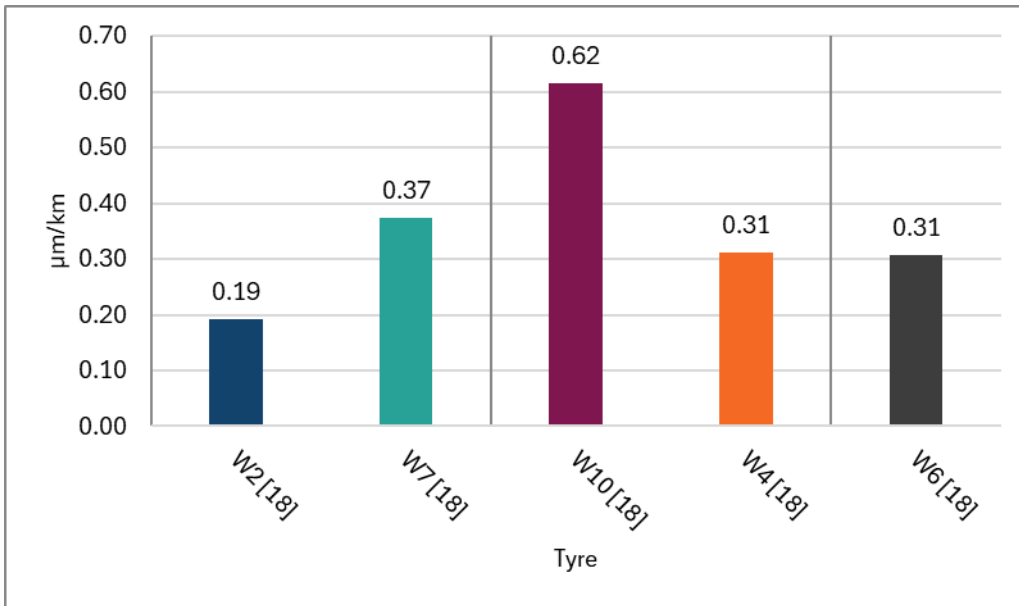
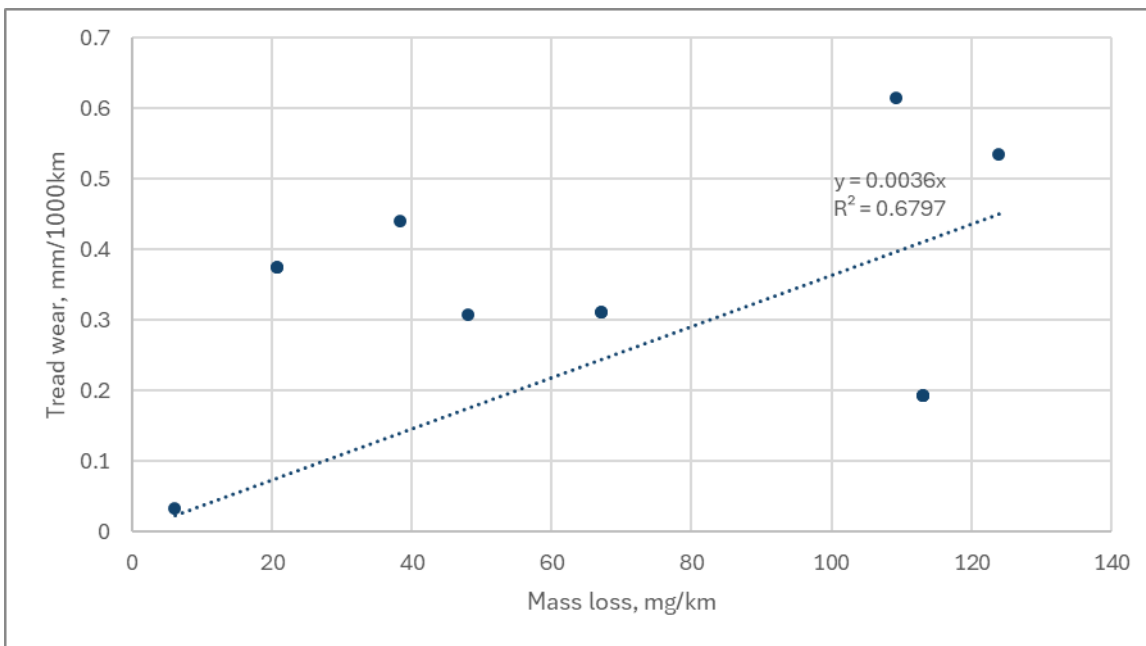Figure 10-24: Comparison of tread wear rates from different 18" tyres.

Figure 10-25: Correlation between tyre mass loss and tyre tread wear for 18" tyres.

10.3.2 Real-time tyre emissions profiles

Real-time traces from the emissions cycles tested tend to show emissions peaks related to aggressive braking events and to the highest speed parts of the cycle. As an example, emissions of all PG42 tests, and a high emitting PN4 test on wheel/tyre W20 respectively, are shown from PN4 (Figure 10-26), cold MPEC (Figure 10-29) and APC10 (Figure 10-31) instruments in this section.

Of the instruments used in the test programme, total PN4 emissions are always the highest irrespective of drive cycle. For PG42 PN4 emissions, as shown in Figure 10-26, the dominant particle production event is observed after ~2200s of the cycle. This results from a high-speed cruise and abrupt braking event, following an aggressive acceleration. At this point of the cycle the tyre surface temperature is at its highest point of ~40°C, as illustrated for the test on W20 in Figure 10-27. Emissions from W20 (Figure 10-28), show the post 2200s peak to continue beyond the point that the vehicle has come to rest, which suggests release / outgassing of materials in response to prior activity rather than instantaneous effects. The same figure also indicates

spikes of PN emissions related to both acceleration and braking events earlier in the cycle, but these are very small compared to the event at the end of the cycle.
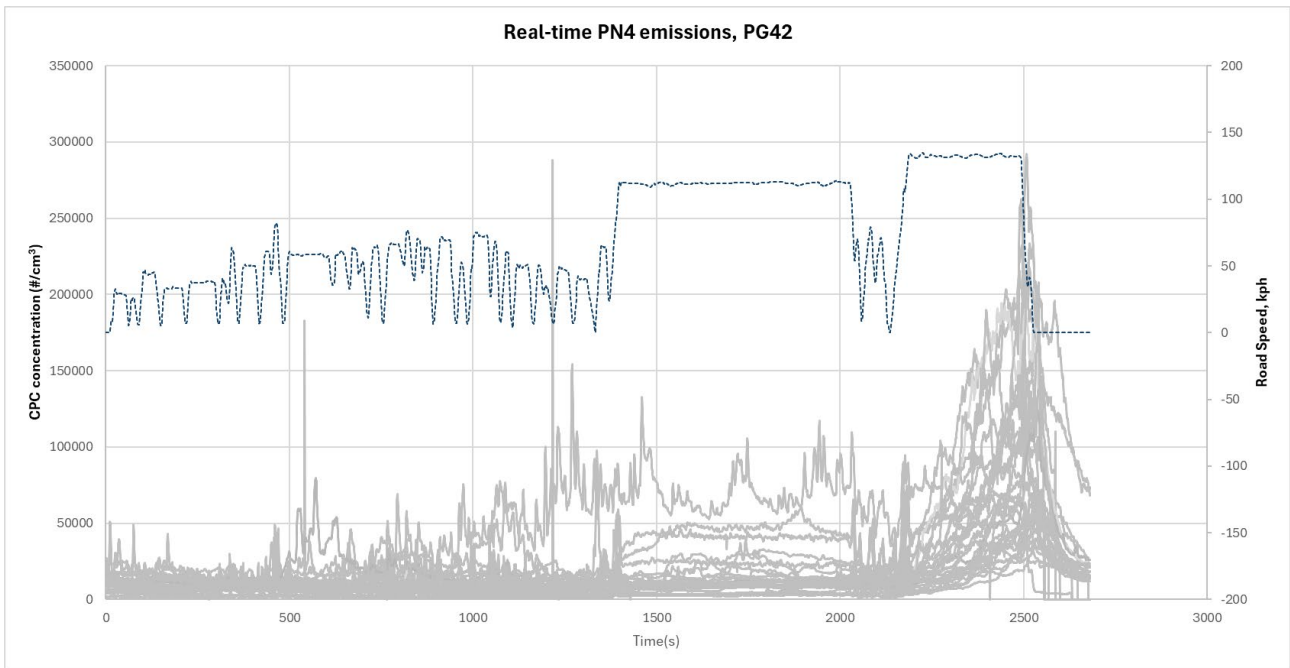

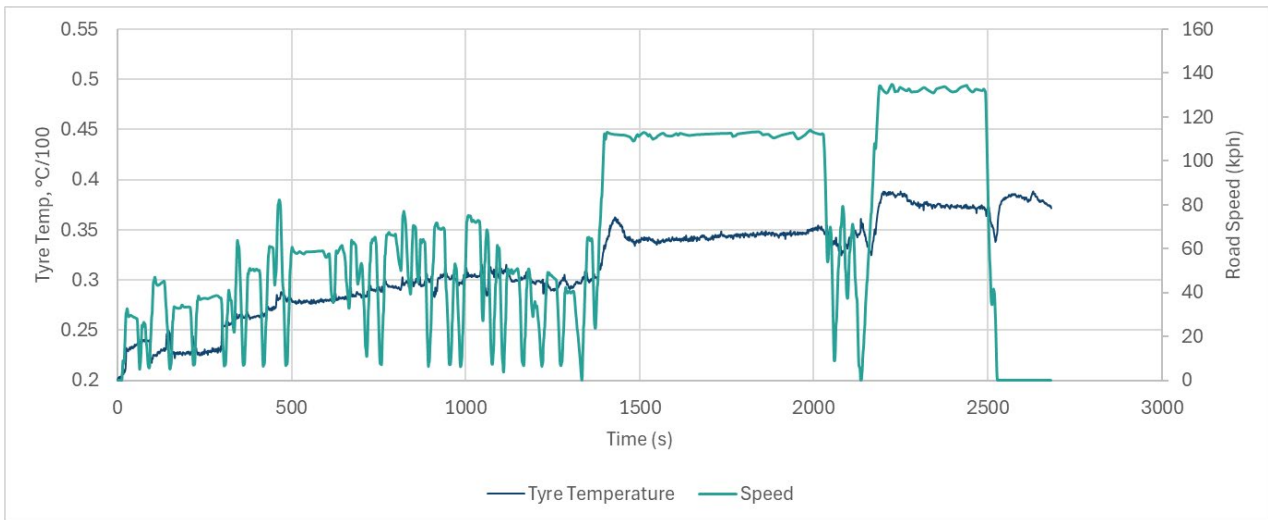Figure 10-26: PN4 emissions from a PG42 test showing data from all wheels and tyres.
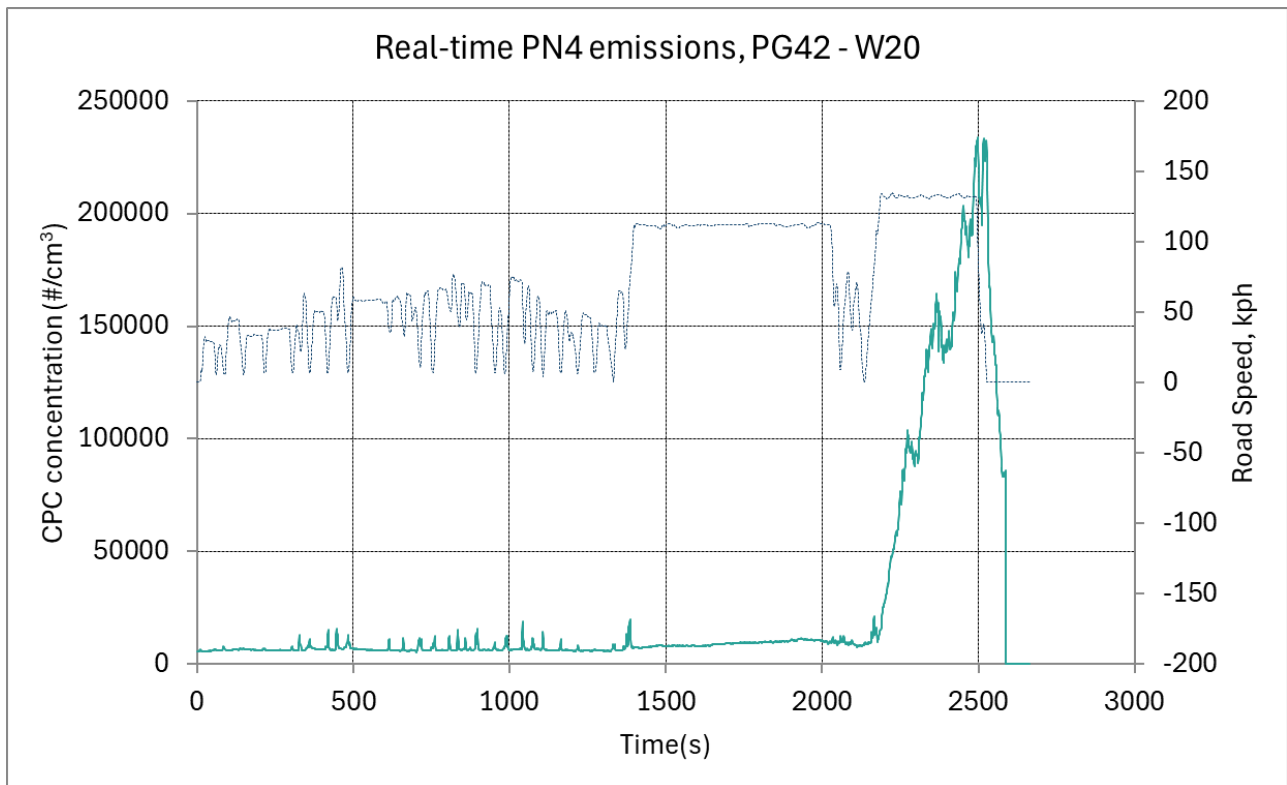

Figure 10-27: Tyre temperature during the PG42 cycle.

Figure 10-28: PN4 emissions from a PG42 test with W20.

Total PN10 emissions are shown from the cold MPEC in Figure 10-29. While this does indicate the presence of the same major particle production event beyond 2200s, the magnitude relative to the rest of the cycle is much diminished, and the data are generally less clean, showing many spikes of electrical interference. The sensitivity of the PN4 device which runs without dilution and uses a CPC to count each particle individually at low levels (up to ~10000#/cm^3) and in photometric mode at higher concentrations, is much greater than the cold MPEC which relies on charging the particles and counting the total charges using an electrometer.

Nevertheless Figure 10-30 clearly shows the presence of the peak at the end of the cycle from the test on W20.

Like the PN4 system, the APC10 also relies on a CPC to count the particles. However, it also features a volatile particle remover, including a catalyst, to eliminate volatiles and includes a dilution step of ~100x. Together these hugely reduce the concentration of particles that reach the CPC. As shown in Figure 10-31, this impacts sensitivity and the ability to discriminate between tyre emission and background levels, but the dominant emissions peak at the end of the cycle can still be observed (Figure 10-32).
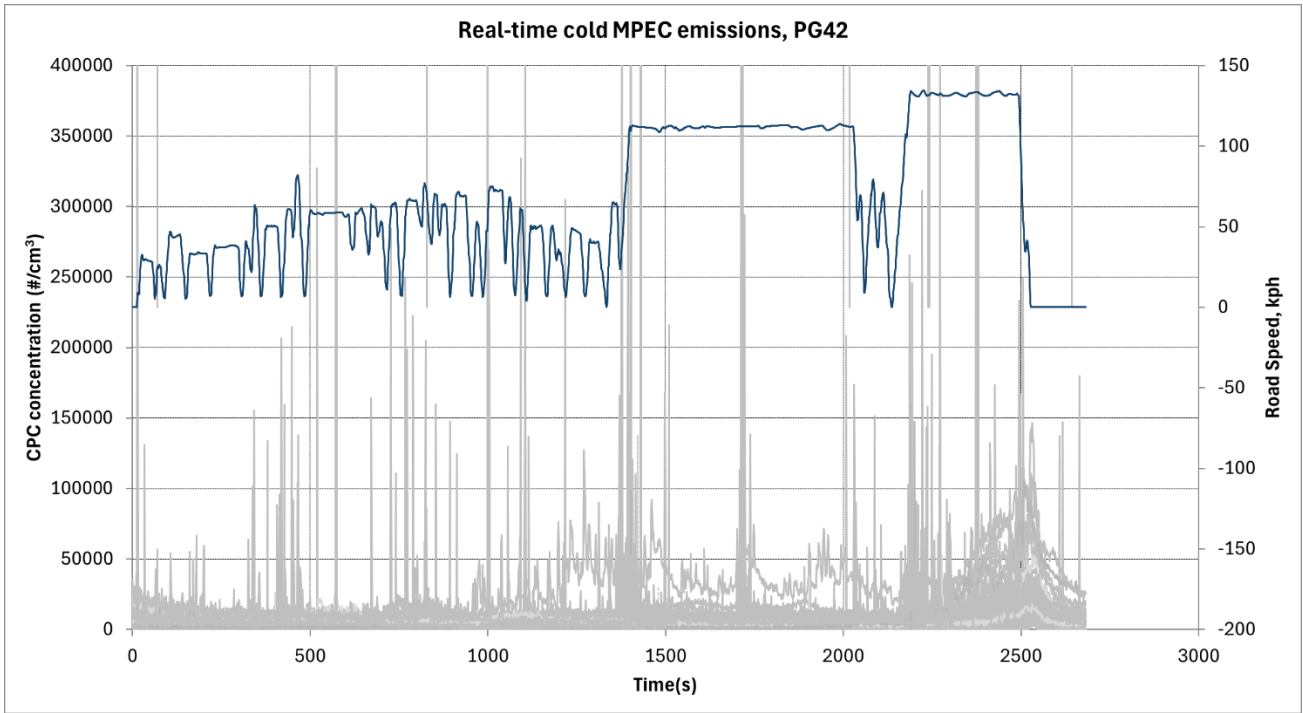
Figure 10-29: Cold MPEC emissions from a PG42 test showing data from all wheels and tyres.
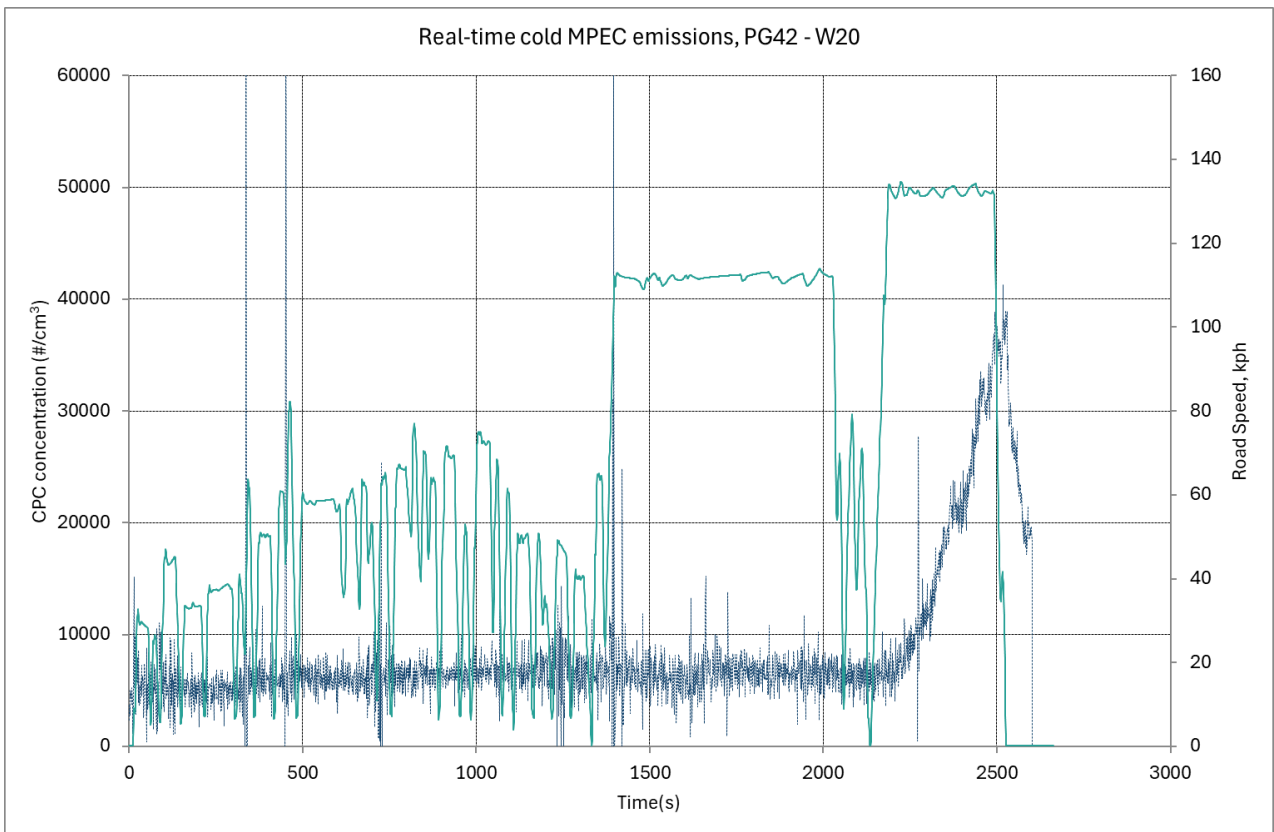

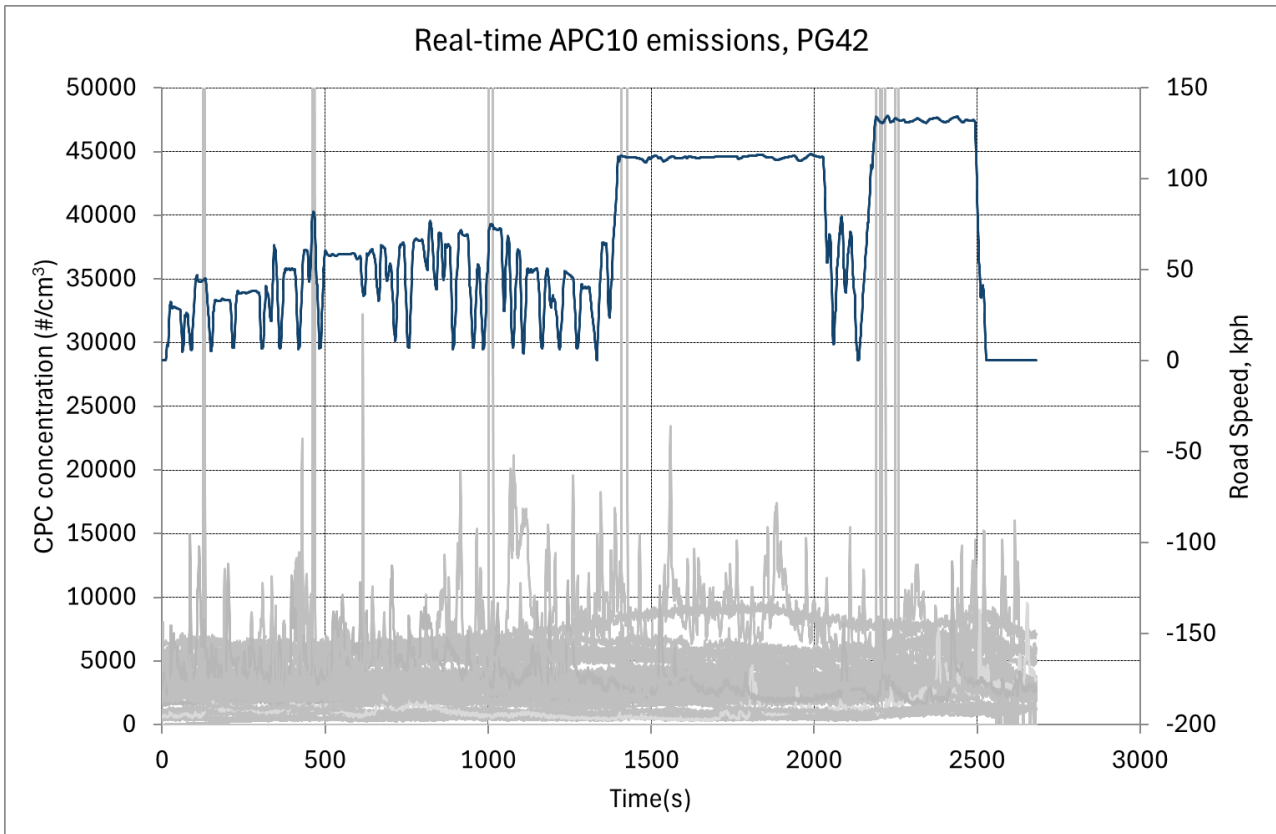Figure 10-30: Cold MPEC emissions from a PG42 test with W20.

Figure 10-31: APC10 emissions from a PG42 test showing data from all wheels and tyres.
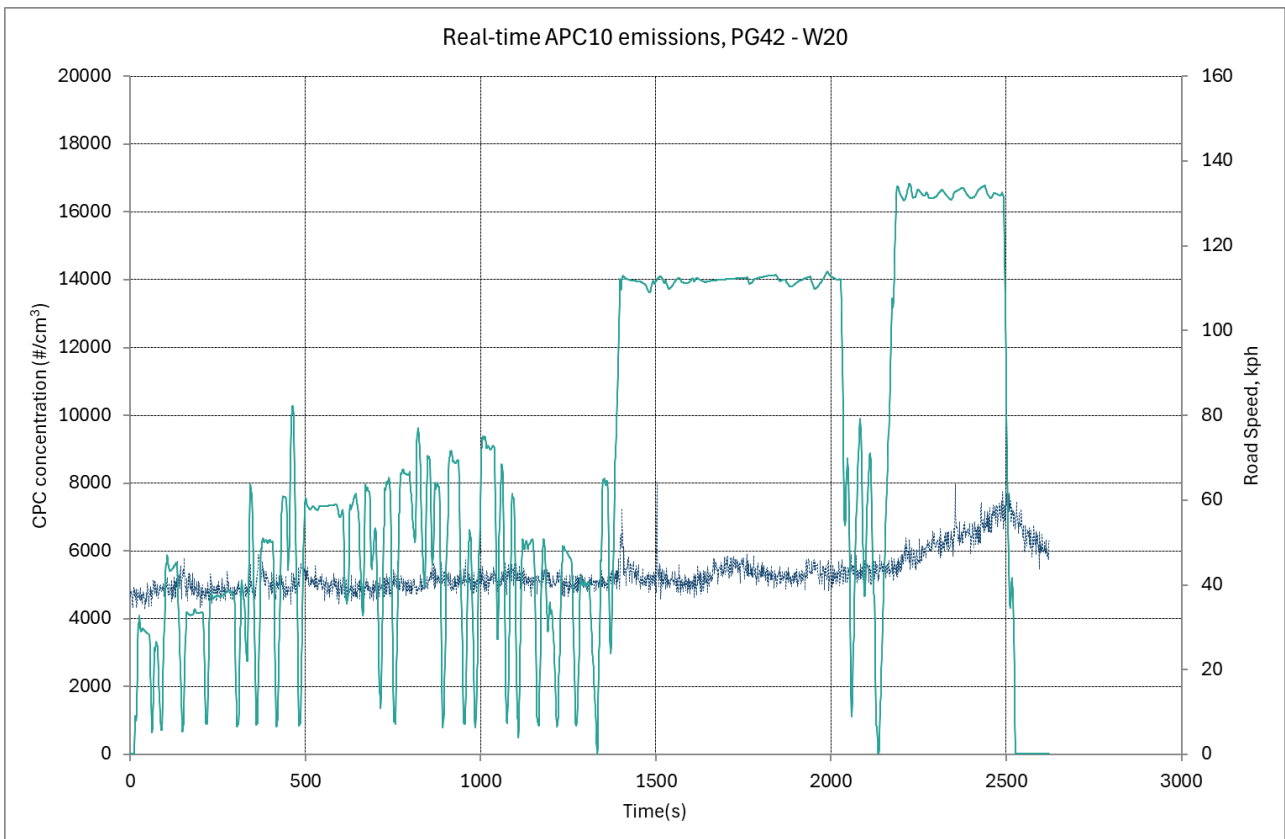

Figure 10-32: APC10 emissions from a PG42 test with W20.

Emissions of total PN4, total PN10 (cold MPEC) and non-volatile PN10 (NVPN10, APC10) from W20 are shown in Figure 10-33. Figure 10-33a shows the entire PG42 cycle, and Figure 10-33b the period following 2200 s, with the emissions shown on a log scale.
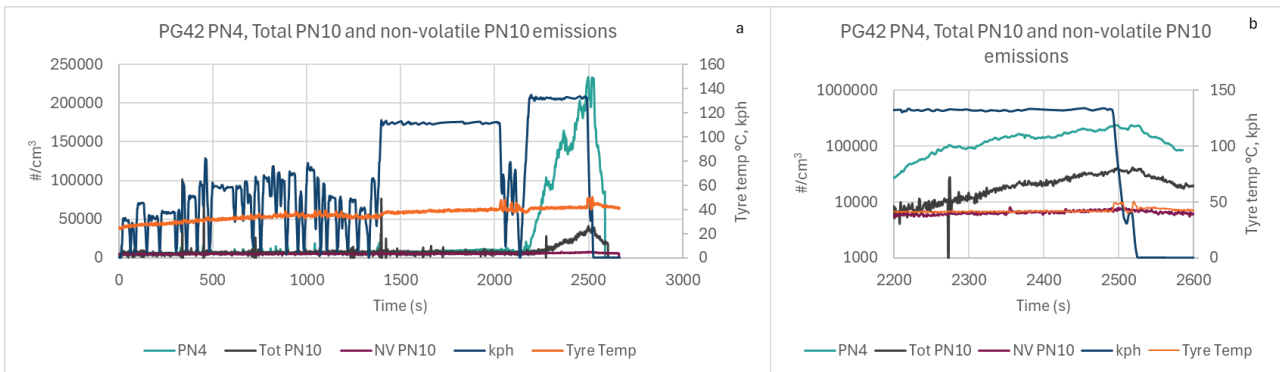

Figure 10-33: a) Total PN4, total PN10 and non-volatile PN10 emissions, b) section of the data from 2200 seconds onwards. Data are from a PG42 cycle test of W20.

These data indicate that total PN10 emissions are typically ~an order of magnitude less of those observed for PN4, which indicates that ~90% of the PN4 emissions are in the 4-10nm range. Similarly, non-volatile PN10 emissions are approximately an order of magnitude lower than total PN10, so ~90% of the PN10 emissions are volatile and only ~1% of PN4 particles are solids. This highlights the challenge of measuring non-volatile PN emissions from drive cycles in which there are not extreme particle production events.

For example, peak concentrations of PN4 on W20 from the dyno RDE cycle at 2025kg are ~30,000 #/cm^3 compared with ~220,000 from the PG42 (Figure 10-34a), indicating a large reduction in volatile particles emitted, and the emissions from the three instruments are much closer together (Figure 10-34b). In the WLTC cycle (Figure 10-35a), peak concentrations of PN4 are ~50,000 #/cm^3 but data from both cold MPEC and hot MPEC appear to be below the instrumental noise threshold / background level.
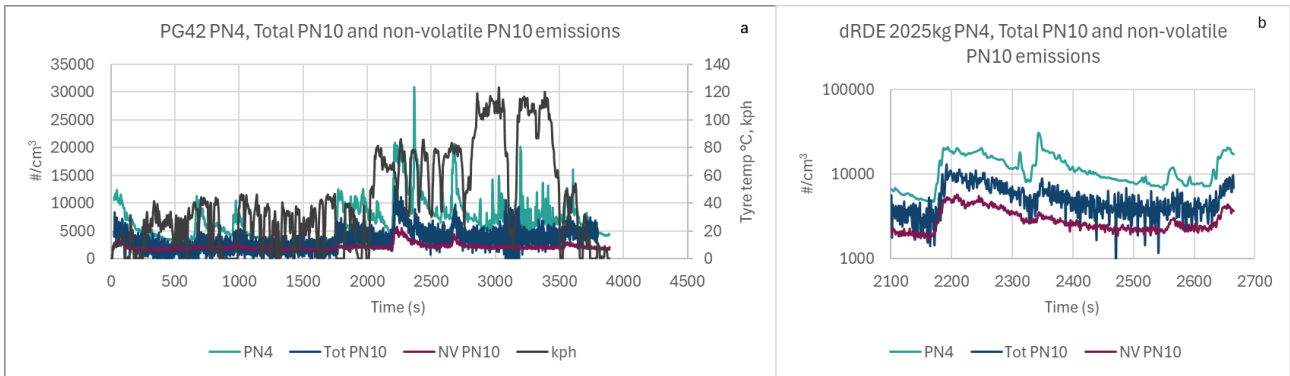
Figure 10-34: a) Total PN4, total PN10 and non-volatile PN10 emissions, b) section of the data from 2200 seconds onwards. Data are from a dyno RDE cycle test of W20 at 2025 kg.
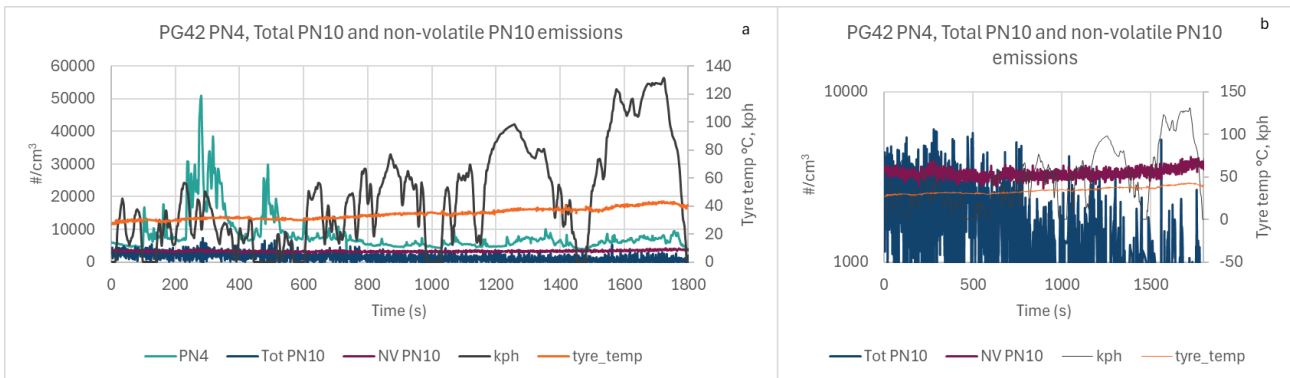

Figure 10-35: a) Total PN4, total PN10 and non-volatile PN10 emissions, b) section of the data from 2200 seconds onwards. Data are from a WLTC test of W20.

These assessments indicate that the focus for comparing real-time emissions between tyres should be on PN4, APC10 and cold MPEC instruments.

10.3.3 Effect of cycle order on tyre emissions

The tyre wear emissions tests conducted in this programme were performed over two days for each set. 3 x PG42 tests, a dyno RDE (dRDE) at 1835 kg and a WLTC tested on the first day and there was a 1h pause between the last PG42 and the dRDE to allow tyre temperatures to stabilise. On the second day, the bespoke test was performed first, followed by a 1h pause and then the dRDE at 2025 kg.

As Figure 10-36 shows for W17, W14 and W6 tests respectively (representing tyres evaluated at the start, middle and end of the test campaign), there is no evidence of a consistent trend in either increasing emissions or reducing emissions across a day of testing. This suggests that emissions from the different cycles can be viewed in isolation without accounting for an influence of the previous cycle(s).
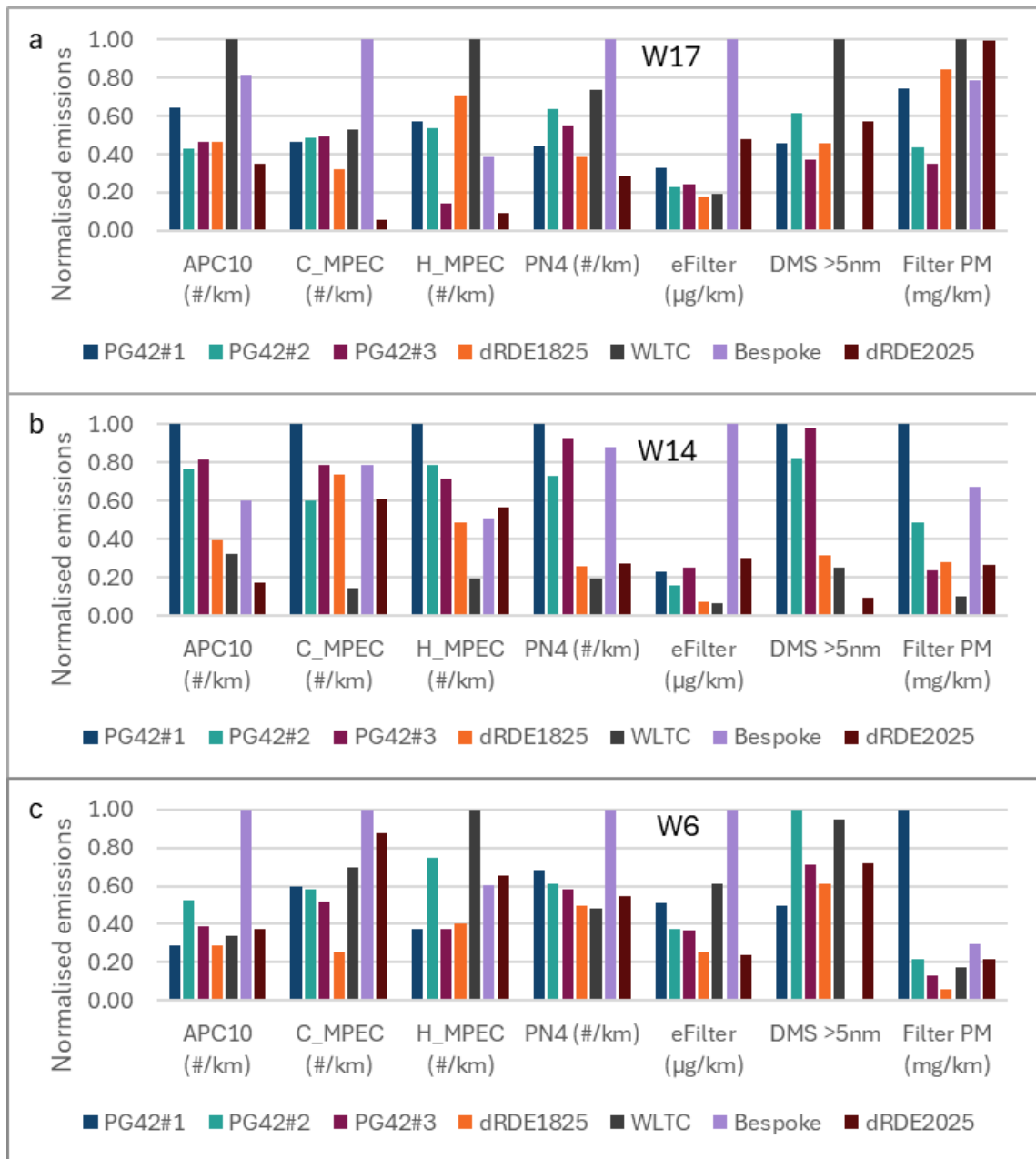
Figure 10-36: Normalised emissions from a) W17 (early), b) W14 (mid) and c) W6 (end) tyre tests.

The possibility of evolutionary trends between repeat cycles has also been investigated. This can be studied by looking at the 3 consecutive PG42 cycles from all tyres tested, as shown in Figure 10-37. This indicates that there are no obvious test order trends in the PN data (with APC10, cold MPEC and PN4 shown) but there is an apparent trend in $PM_{2.5}$ data. PM emissions decrease consistently between the first test and the subsequent two tests. Potentially, this is related to the warm-up of the tyre inhibiting the release of larger more massive particles, while not impacting the smaller volatile and non-volatile particles that dominate the particle number emissions.

There is only one non-compliance with the $PM_{2.5}$ evolutionary effect: the very last PG42 test on W17e. Inspection of this filter showed an abnormally high level of "oversized" single particulate materials (only individual particles > 50 – 70 μm are visible to the naked eye), which is likely to be the source of the high mass (Figure 10-38). Tyre wear PM filters generally have a few of these larger particles but is not clear why this one sample is different. This trend of reduced $PM_{2.5}$ emissions after a "cold start" may also exist on the road, and so quantifying these emissions in a regulatory procedure could require a cold and hot weighting approach.

For comparisons of emissions between tyres the triplicate PN and PM results obtained from PG42 cycles have been averaged, although the evolutionary effect on the PM results creates large standard deviations.
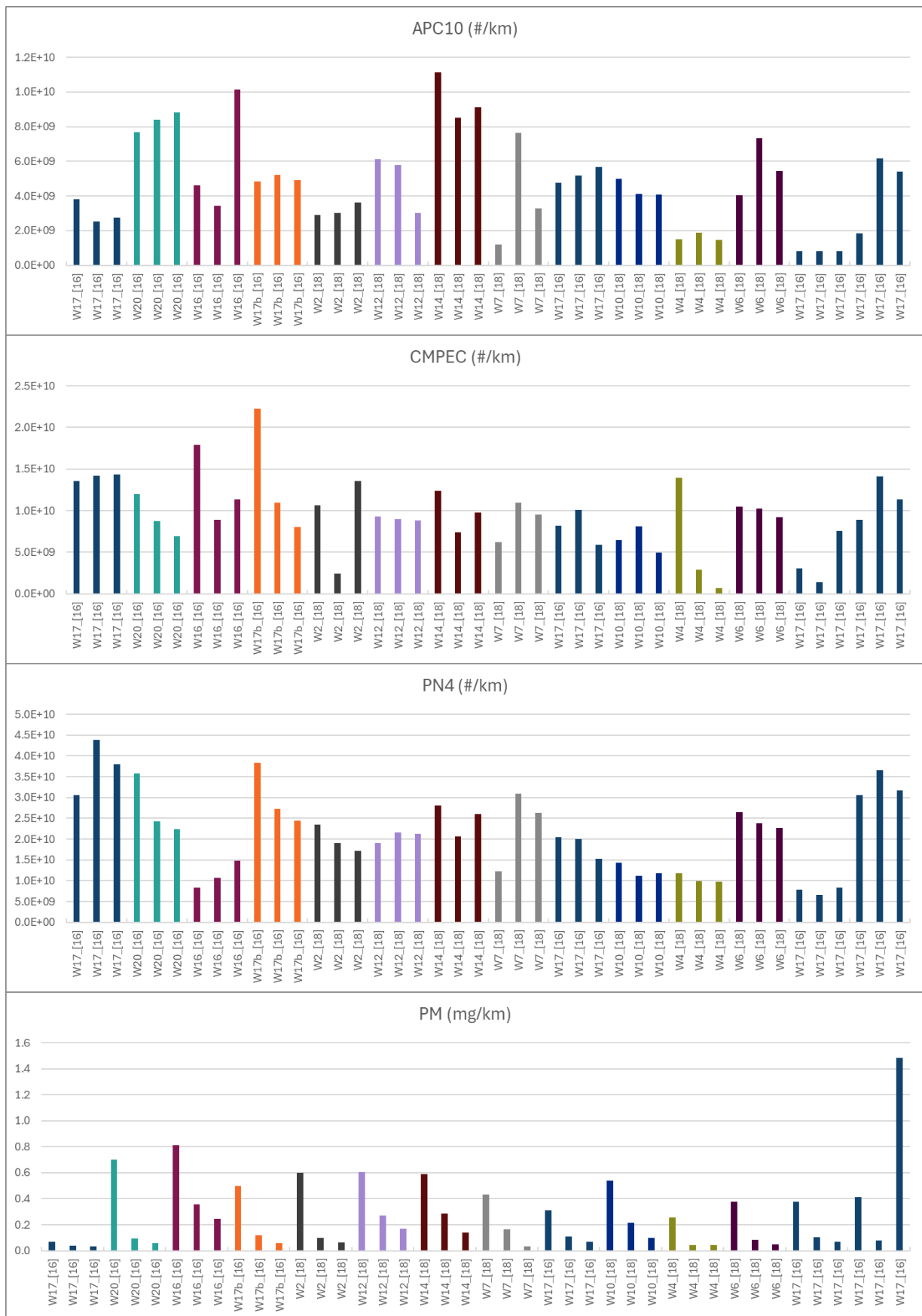

Figure 10-37: PG42 test to test repeatability for (a) APC10, (b) cold MPEC, (c) PN4, and (d) PM.

Figure 10-38: PM filters from W17e PG42 tests, showing high >2.5 µm particles from the third test.

10.3.4 Check for time trends in particle emission data across the project duration

W17 was tested 5 times during the test programme, including bracketing tests at the outset and end of all other testing. These reference tests were included to evaluate whether the 3M walkway tape surface applied to the chassis dyno roller evolved during the project, resulting in a trend on results that might need correcting in the final dataset. Figure 10-39a-d shows test ordered results of 15 PG42 tests for APC10, Cold MPEC and PN4, and 14 tests for PM$_{2.5}$ respectively. The final, unexpectedly high, PM$_{2.5}$ result discussed in the previous section is omitted from Figure 10-39d.
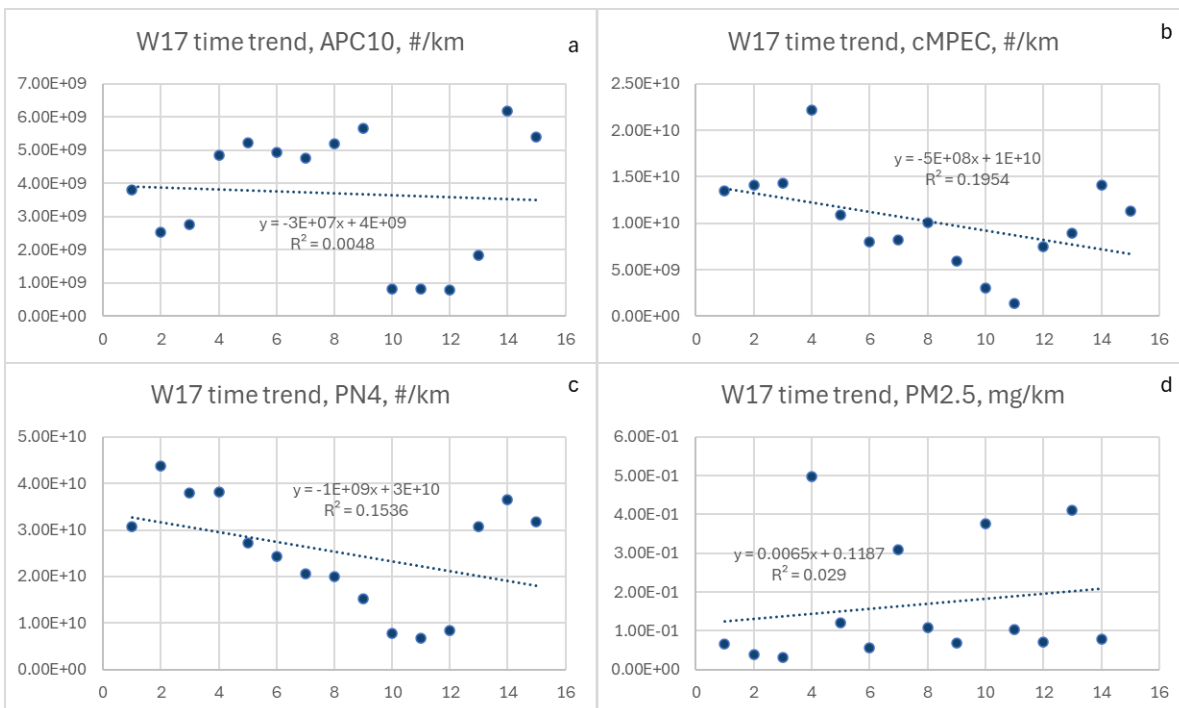
Figure 10-39: Time trends in W17 tests for (a) APC10, (b) cold MPEC, (c) PN4, (d) gravimetric PM$_{2.5}$.

The time-series data from W17 tests indicates no obvious trend in either non-volatile PN10 emissions from the APC10 or in the PM$_{2.5}$ data, and very weak downward trends with time for total particles >4nm (PN4) and total particles >10nm (cold MPEC). Therefore, no adjustments of results of tyre emissions through the test programme are considered necessary.

10.3.5 Effects of tyre size on emissions

This section presents an evaluation of the influence of tyre size on emissions through the comparison of nominally identical (or highly similar) tyres with 18" and 16" diameters. Three pairs of tyres, each pair from a different manufacturer, were compared, using data from APC10, cold MPEC, PN4 and filter-based PM.

Results are shown for PG42, dyno RDE at 1825kg, dyno RDE at 2025 kg, WLTC and from the bespoke cycle treated as a simple emissions test. All cycles data excepting the PG42, which is drawn from at least triplicate tests and is shown with one standard deviation error bars, was from single tests only. Therefore, the analysis seeks consistent trends between the two tyres across the five cycles.

The three pairs of tyres tested were W17 and W7; W20 and W4; W16 and W2. Basic information on these tyres is given in Table 10-7 and tyre rating details can be found in Table 7-2. The commercial descriptions of the three tyres are as follows:

The Michelin CrossClimate 2 is an all-season tyre known for its exceptional traction in various conditions, durable tread design, enhanced ride comfort, low noise levels, and optimized fuel efficiency.

The Michelin Primacy 4+ is a premium touring summer tyre known for its excellent dry and wet handling, low rolling resistance, quiet ride, and good wear resistance, though it has slightly longer wet braking distances compared to some competitors.

The Bridgestone Turanza Eco is a premium summer tyre designed for eco-friendly vehicles, featuring Enliten technology for reduced weight and lower rolling resistance, excellent wet and dry grip, enhanced fuel efficiency, and a quiet, comfortable ride.

Table 10-7: Pairs of tyres compared to explore the influence of tyre size on wear particle emissions.

Tyre	Description	Size
W17	Michelin CrossClimate 2 205/55R16 94V XL TL	16"
W7	Michelin CrossClimate 2 215/55R18 99V XL TL	18"
W20	Michelin Primacy 4+ 205/55R16 91V TL	16"
W4	Michelin Primacy 4; 215/55R18 99VXL TL S1	18"
W16	Bridgestone Turanza ECO 205/55R16 91H	16"
W2	Bridgestone Turanza Eco 215/55R18 95T	18"

10.3.5.1 Non-volatile PN10 emissions, APC10

Comparative non-volatile PN10 particle emissions measured from the five cycles on all three pairs of tyres are shown in Figure 10-40.

The PG42 data for the first pair (W17 and W7) shows similar levels of emissions from the two tyres and no obvious directional trend across the other cycles. There does not appear to be any tyre size-related impact on non-volatile PN10 from this tyre type.

The tyre pair W20 and W4, shows a significant difference in PN10 emissions on the PG42 cycle, with higher emissions from the 16" variant. This effect of higher emissions with smaller tyres is consistently observed across the other test cycles and ranges from ~80% on the PG42 to ~20% on the bespoke cycle. There is no consistent effect observed for the pair of tyres W16 and W2.

Figure 10-40: Non-volatile PN10 emissions compared between pairs of matched specification tyres of 16" and 18" sizes.

10.3.5.2 Total PN10 emissions, cold MPEC

Total PN10 emissions from the cold MPEC on the PG42 cycle were similar between all three pairs from the PG42 cycle, and there were no consistent trends in emissions across the other test cycles (Figure 10-41). It is therefore not possible to identify any difference between the emissions of the 16" and 18" tyres.
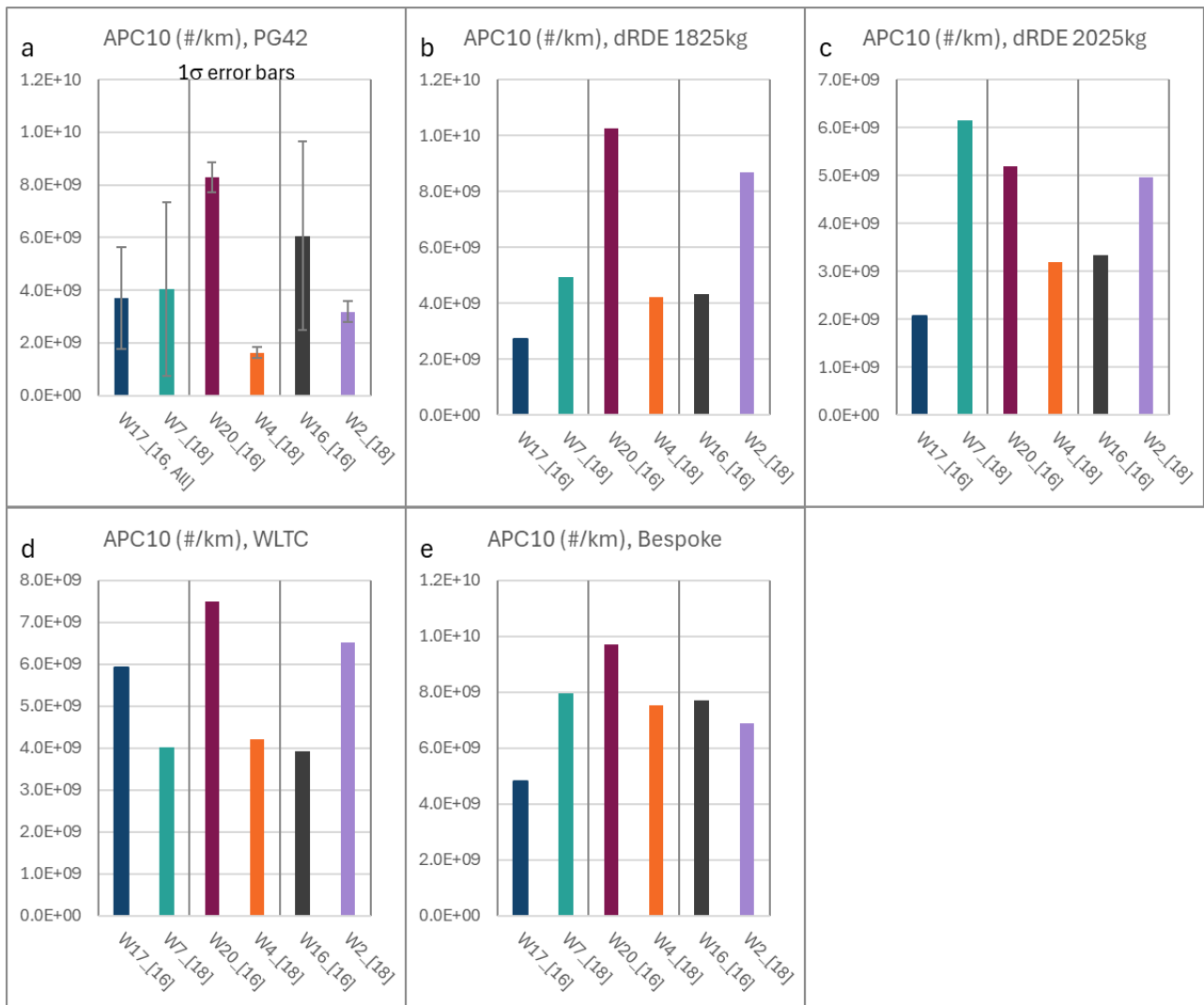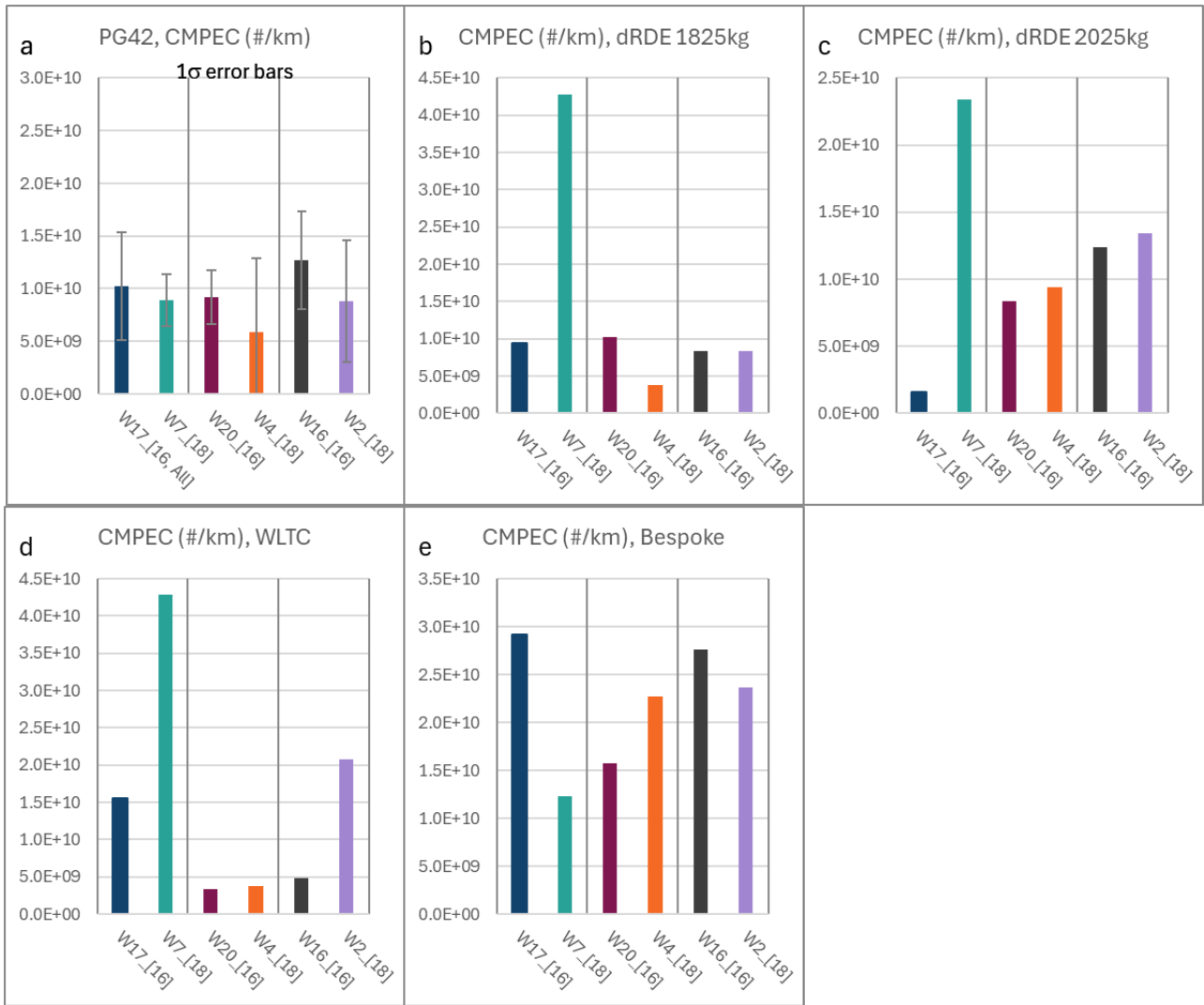
Figure 10-41: Total PN10 emissions compared between pairs of matched specification tyres of 16" and 18" sizes.

10.3.5.3 Total PN4 emissions

Total PN4 emissions results from the five test cycles are shown in Figure 10-42. There is no consistent trend in emissions between the pair of tyres W17 and W4 while, excepting the bespoke cycle, there is a consistent reduction in PN4 emissions between the 16" tyre W20 and the 18" tyre W4, in agreement with the APC10 result. The third pair (W16, and W2) indicates higher PN4 emissions with the 18" tyre than from 16" tyre across all cycles.
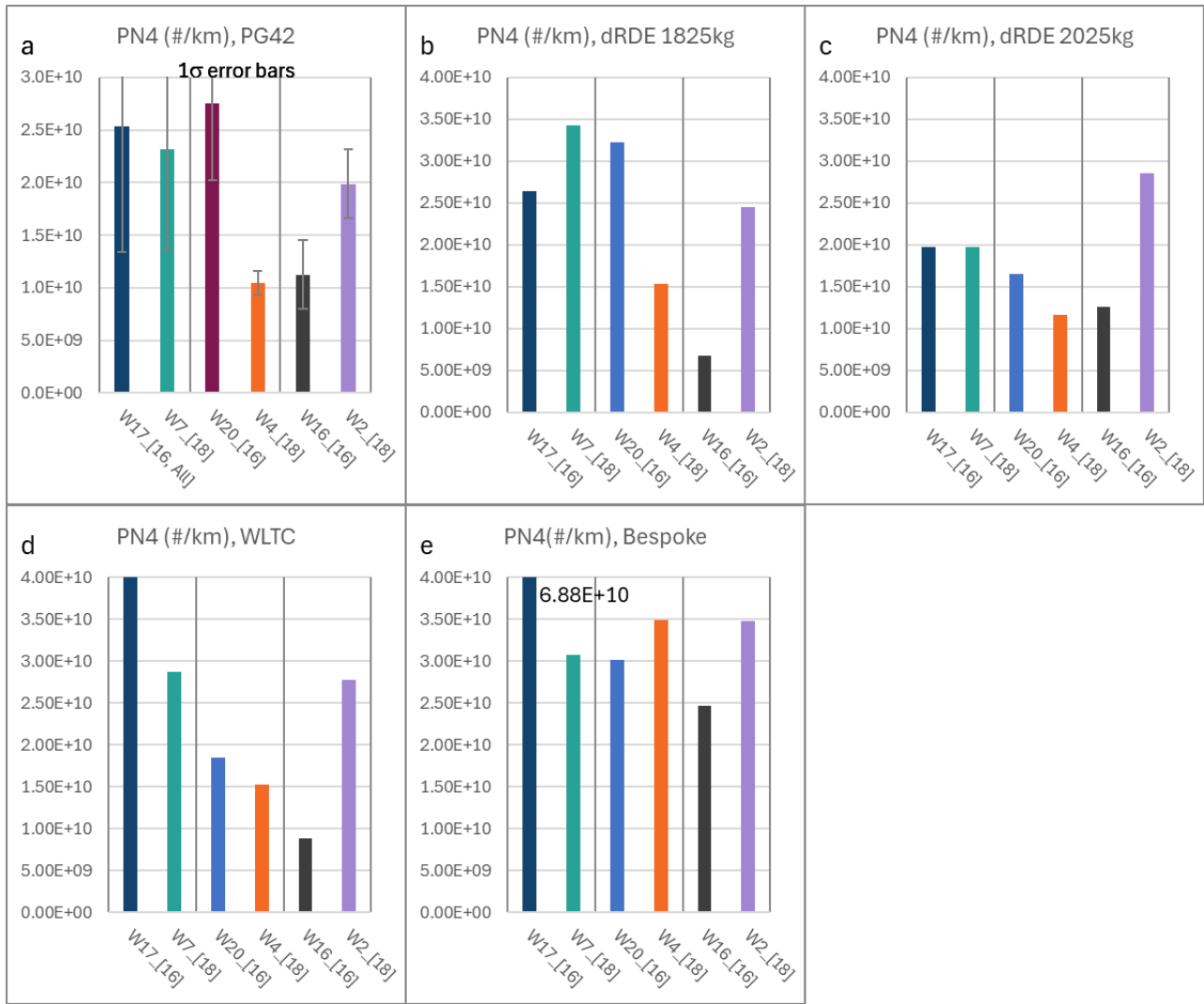
Figure 10-42: Total PN4 emissions compared between pairs of matched specification tyres of 16" and 18" sizes.

10.3.5.4 PM₂.₅ *(filter) emissions*

$PM_{2.5}$ results from gravimetry are compared between the three tyre pairs, and across the five test cycles, in Figure 10-43. The first pair of tyres, W17 and W7, show a general trend of higher emissions from the 18" tyre than the 16" tyre, although the PG42 results were similar. Both the other pairs of tyres, W20, W4 and W16, W2 show generally higher emissions from the 16" tyre than from the 18" tyre.
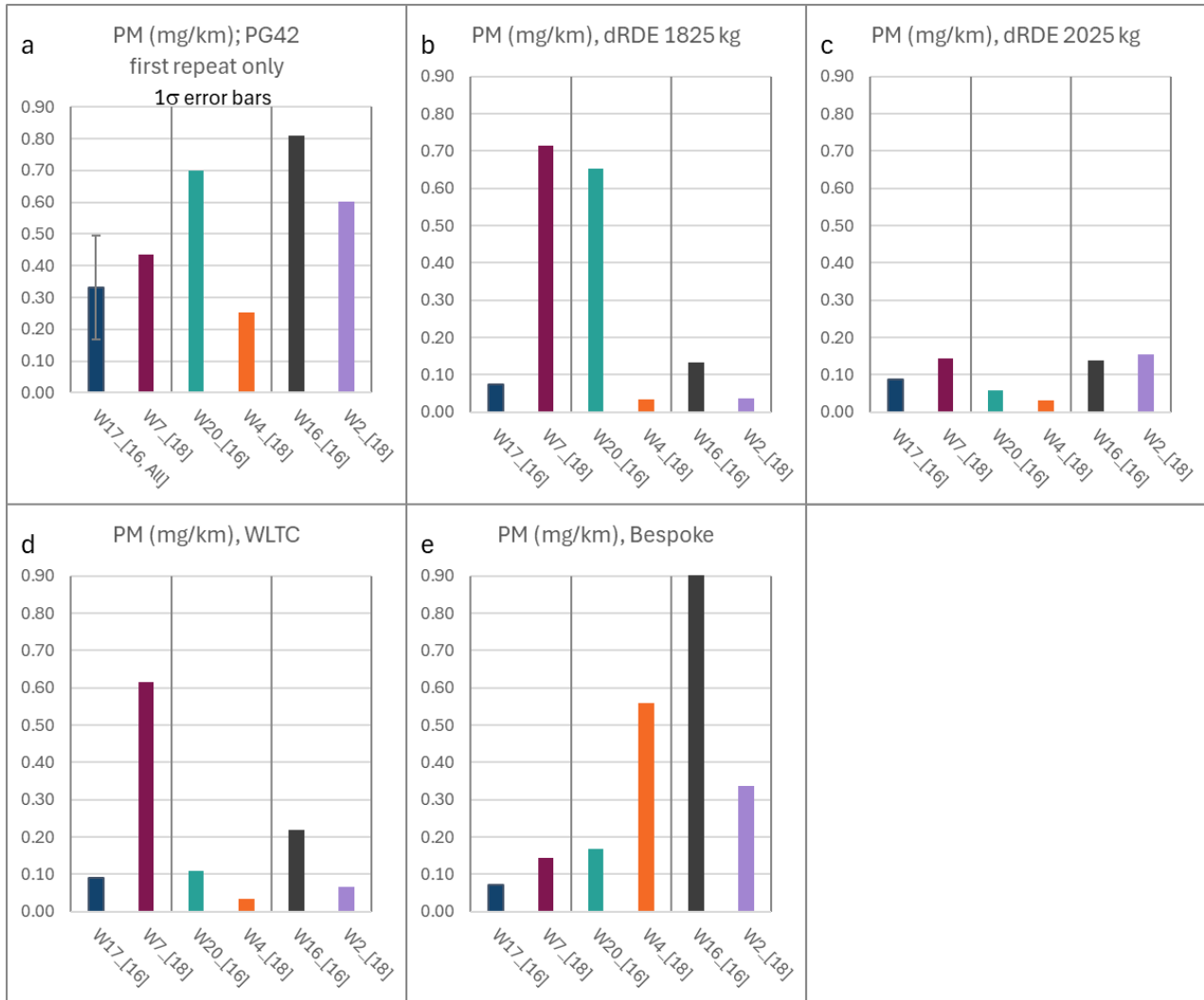
Figure 10-43: PM$_{2.5}$ emissions compared between pairs of matched specification tyres of 16" and 18" sizes.

10.3.5.5 Summary of tyre size effects on emissions

Generally, across the three pairs of tyres, there is no obvious increase in particle number or mass emissions between 18" tyres and 16" tyres, since results across the various cycles and instruments are inconsistent. In addition, the impact of the background is not well understood. However, the pair W20 and W4 did indicate higher emissions from 16" tyres than 18" tyres for the majority of cycles and for APC10, PN4 and PM$_{2.5}$. The effects observed with W20 and W4 may be related to the specific formulation of the tyre, but that detailed information is not available in the public domain.

10.3.6 Effects of tyre age/mileage on emissions

This section compares three tyres of nominally identical composition but having experienced three different degrees of usage. The tyres, described in Table 10-8, are 18" Bridgestone Turanza Eco tyres with <1000 km (W2), >11,000 km (W12) and >23,000 km (W14) accumulated mileage. The commercial description describes the Bridgestone Turanza Eco as a premium summer tyre designed for eco-friendly vehicles, featuring Enliten technology for reduced weight and lower rolling resistance, excellent wet and dry grip, enhanced fuel efficiency, and a quiet, comfortable ride.

Emissions data are shown from PG42, dyno RDE (1825 & 2025 kg), WLTC and bespoke cycles.

Table 10-8: Tyres used to explore the influence of elapsed mileage on wear particle emissions

Tyre	Description	Size	Mileage
W2	Bridgestone Turanza Eco 215/55R18 95T	18"	< 1000 km
W12	Bridgestone Turanza Eco 215/55R18 95T	18"	> 11,000 km
W14	Bridgestone Turanza Eco 215/55R18 95T	18"	>23,000 km

10.3.6.1 Non-volatile PN10 emissions, APC10

Comparative non-volatile PN10 emissions for the three differently aged tyres, and across the 5 different drive cycles, are shown in Figure 10-44. While results from the PG42 cycle (Figure 10-44a) suggest an increase in non-volatile PN10 with increasing mileage, other cycles' data do not support this observation. In fact, dRDE and WLTC cycles suggest lowest non-volatile PN10 from the highest mileage tyre. Consequently, no obvious conclusions can be drawn from this comparison.
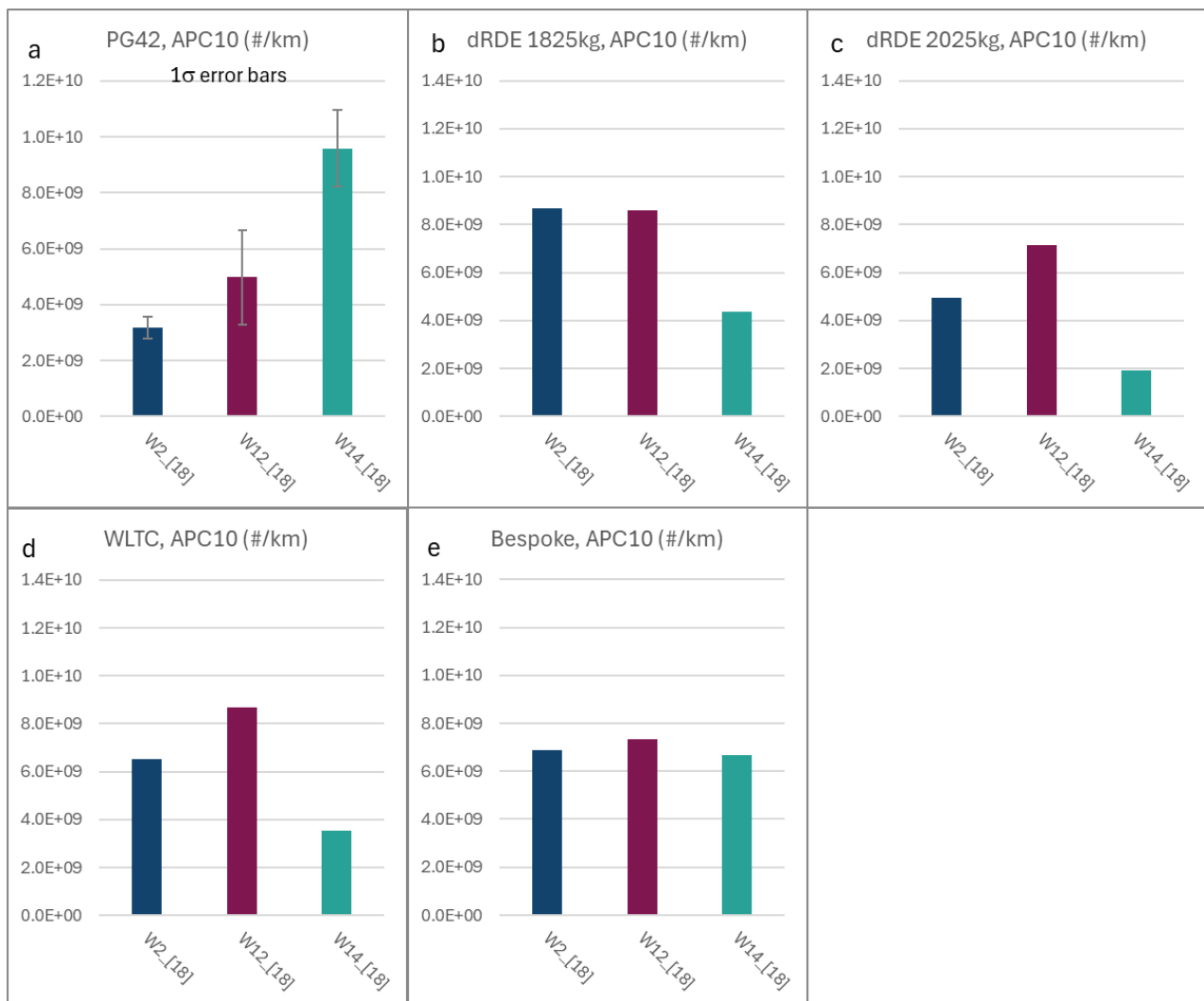

Figure 10-44: Non-volatile PN10 emissions compared between tyres with <1000 km, >11,000km and >23,000 km accumulated mileage.

10.3.6.2 Total PN10 emissions, cold MPEC

Figure 10-45 shows comparisons of emissions results from the cold MPEC. Results suggest that either there is no difference in emissions with mileage, or perhaps the very highest mileage tyre shows lower emissions. If this is the case, the contrast with APC10 data (e.g., a Figure 10-44a; Figure 10-44e) and cold MPEC data would imply that the reduction in PN would be through a reduction in volatile particles. This could relate to curing of the tyre over prolonged operation.
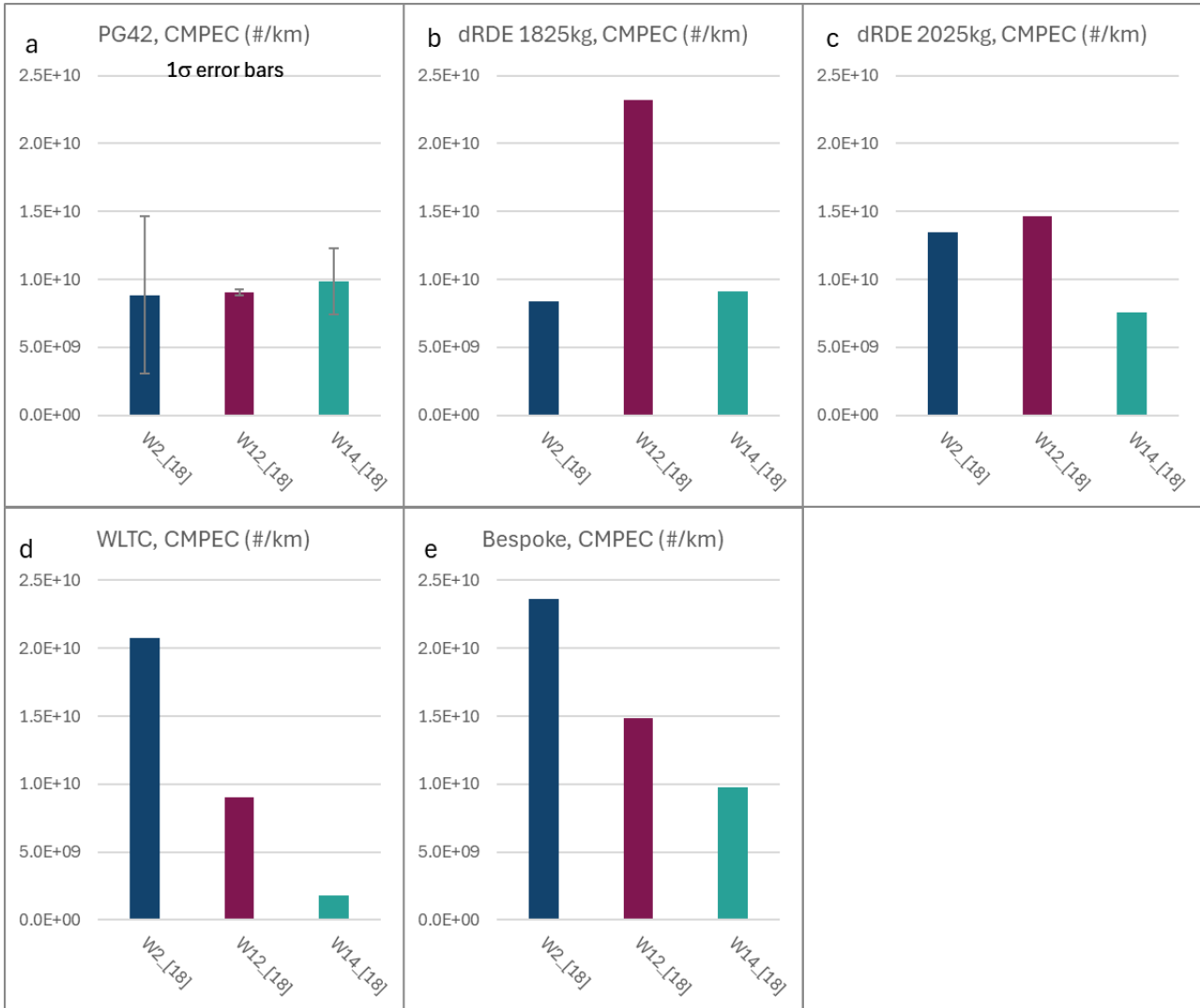
Figure 10-45: Total PN10 emissions compared between tyres with <1000 km, >11,000 km and >23,000 km accumulated mileage.

10.3.6.3 Total PN4 emissions

Total PN4 emissions comparisons between the three tyres and across the 5 cycles are shown in Figure 10-46. Trends between the tyres are similar to those seen from the cold MPEC, and results support the suggestion that volatile PN emissions could reduce at high mileages.

Figure 10-46: PN4 emissions compared between tyres with <1000 km, >1,1000 km and >2,3000 km accumulated mileage.

10.3.6.4 PM$_{2.5}$ (filter) emissions

There were no obvious trends in PM$_{2.5}$ observed in the comparisons between tyres of different mileages, across the five drive cycles tested (Figure 10-47).
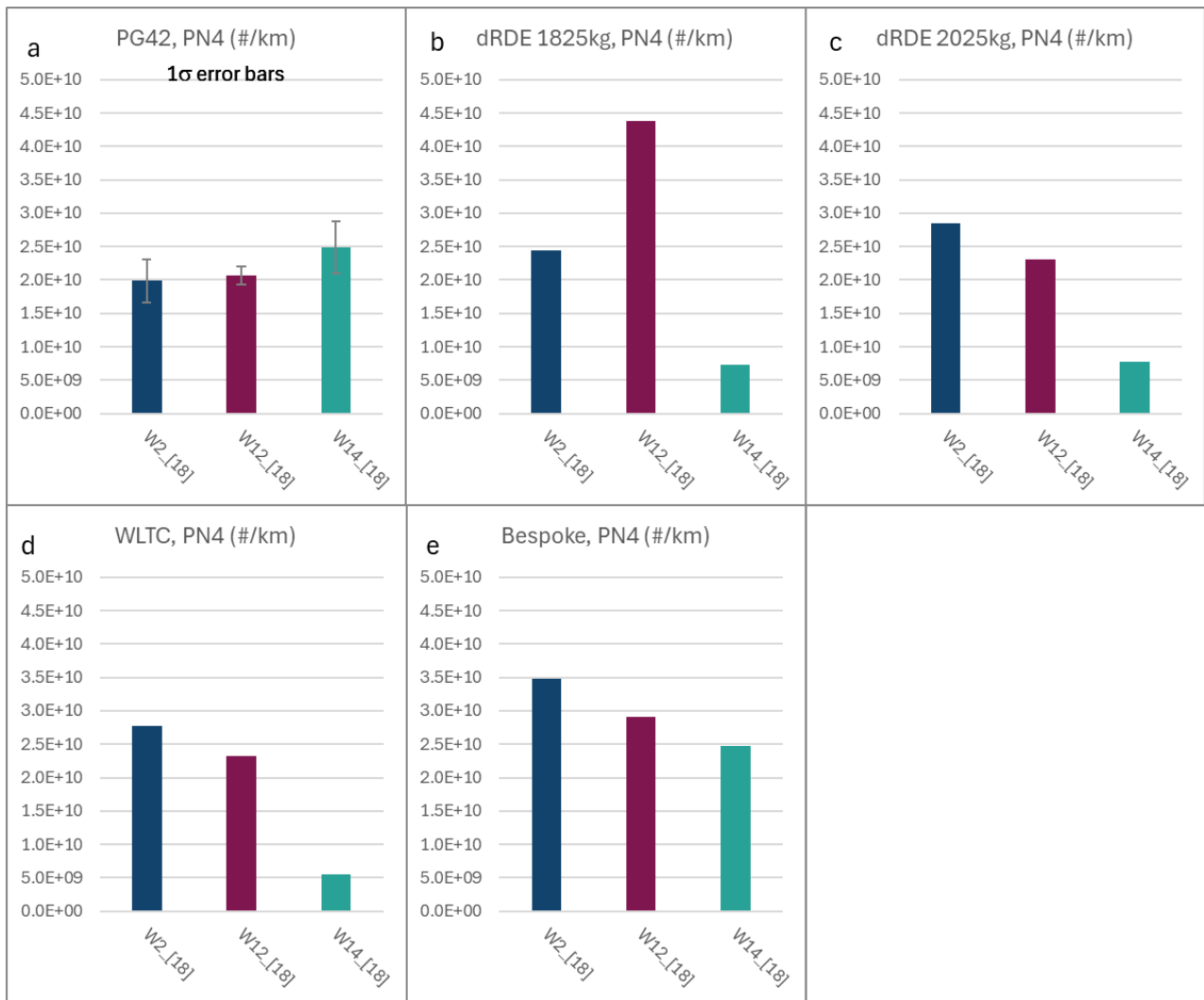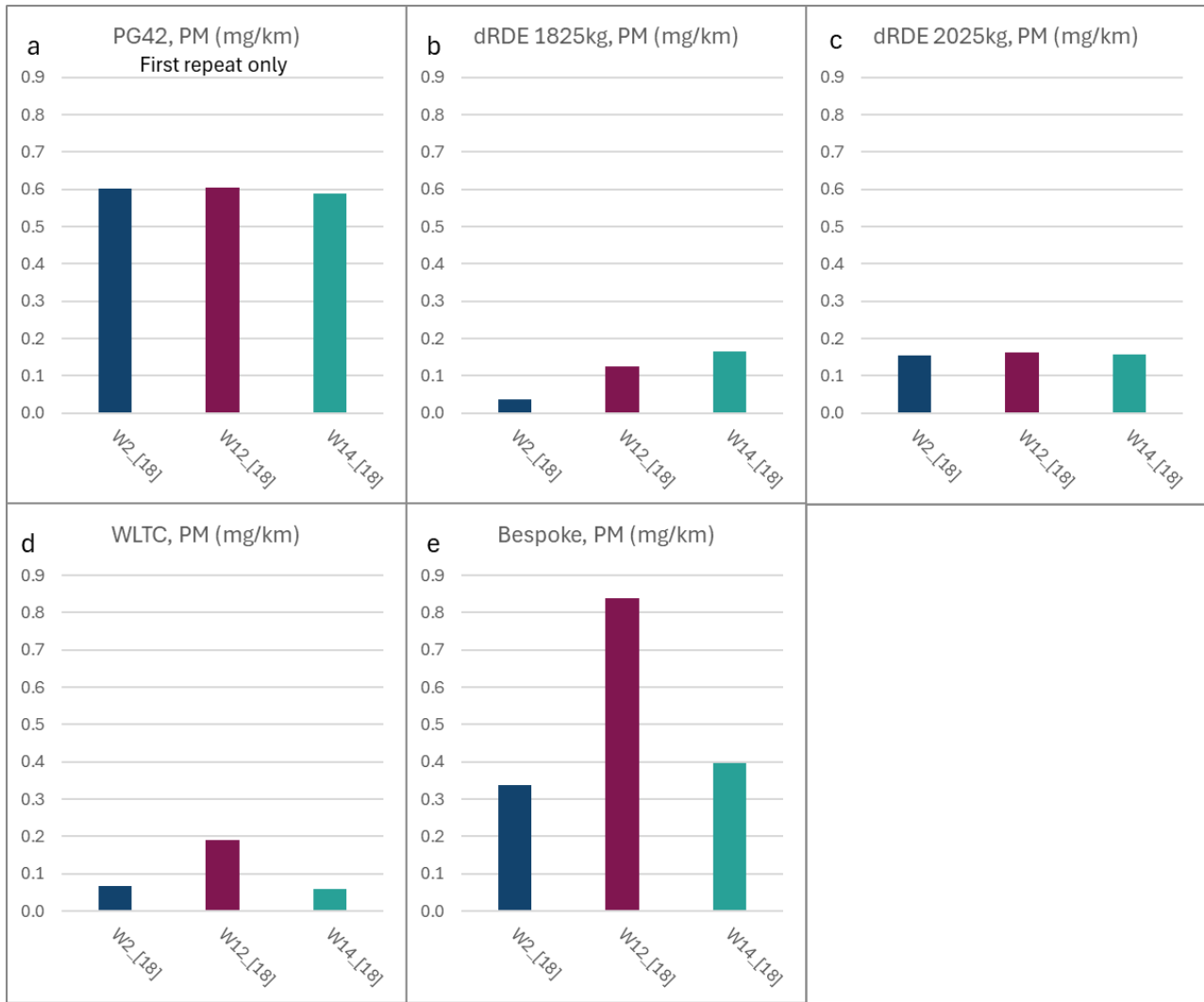
Figure 10-47: PM$_{2.5}$ emissions compared between tyres with < 1000 km, > 11,000 km and > 23,000 km accumulated mileage.

10.3.6.5 Summary of tyre mileage effects on emissions

There were no stand-out effects of different tyre mileage on PM$_{2.5}$ or PN emissions, excepting the possibility that higher tyre mileages may lead to a reduction in volatile particle number emissions.

10.3.7 Variations in emissions between manufacturer tyres and tyre design

Five tyres from four different manufacturers, as shown in Table 10-9, were compared using emissions from the PG42, dRDE cycles (1825 kg and 2025 kg), WLTC and bespoke cycles. Emissions are presented from triplicate PG42 cycles (excepting PM, where just the first result is used) and single tests on the other cycles, from APC10, cold MPEC, PN4 and filter PM$_{2.5}$ measurements.

Tyre/wheel combination W7 is an all-weather UK tyre suitable for use all year round, including in severe snow, as well as in summer and features a "Vee" tread pattern. The other 4 tyres were UK summer or standard all-season tyres.

Table 10-9: Tyres used to explore differences between manufacturers and tyre design on particle emissions.

Tyre	Description	Size	Commercial description
W2	Bridgestone Turanza Eco 215/55R18 95T	18"	The Bridgestone Turanza Eco is a premium summer tyre designed for eco-friendly vehicles, featuring Enliten technology for reduced weight and lower rolling

Tyre	Description	Size	Commercial description
			resistance, excellent wet and dry grip, enhanced fuel efficiency, and a quiet, comfortable ride
W7	Michelin CrossClimate 2 215/55R18 99V XL TL	18"	The Michelin CrossClimate 2 215/55R18 99V XL TL is an all-season tyre designed for excellent performance in dry, wet, and light snow conditions, featuring a V-formation tread pattern, Thermal Adaptive compound, and 3PMSF certification for severe snow service
W10	Landsail LS588 SUV; 215/55R18 99V	18"	The Landsail LS588 SUV 215/55R18 99V is an all-season performance tyre designed for SUVs and CUVs, featuring a silica compound for enhanced wet traction and fuel efficiency, optimized tread design for reduced road noise, and large shoulder blocks for improved dry traction and handling
W4	Michelin Primacy 4; 215/55R18 99VXL TL S1	18"	The Michelin Primacy 4 215/55R18 99VXL TL S1 is a premium summer tyre designed for high safety and longevity, featuring EverGrip technology for superior wet braking, a tread pattern optimized for water evacuation, and MaxTouch Construction for even wear and improved fuel efficiency
W6	Goodyear EfficientGrip Performance 2 215/55R18 99V XL	18"	The Goodyear EfficientGrip Performance 2 215/55R18 99V XL is a premium summer touring tyre designed for enhanced mileage and fuel efficiency, featuring Mileage Plus Technology for increased tread elasticity, excellent wet and dry handling, and a quiet, comfortable ride

10.3.7.1 Non-volatile PN10 emissions, APC10

Results of non-volatile PN10 emissions, comparing five tyres and five instruments, are shown in Figure 10-48.
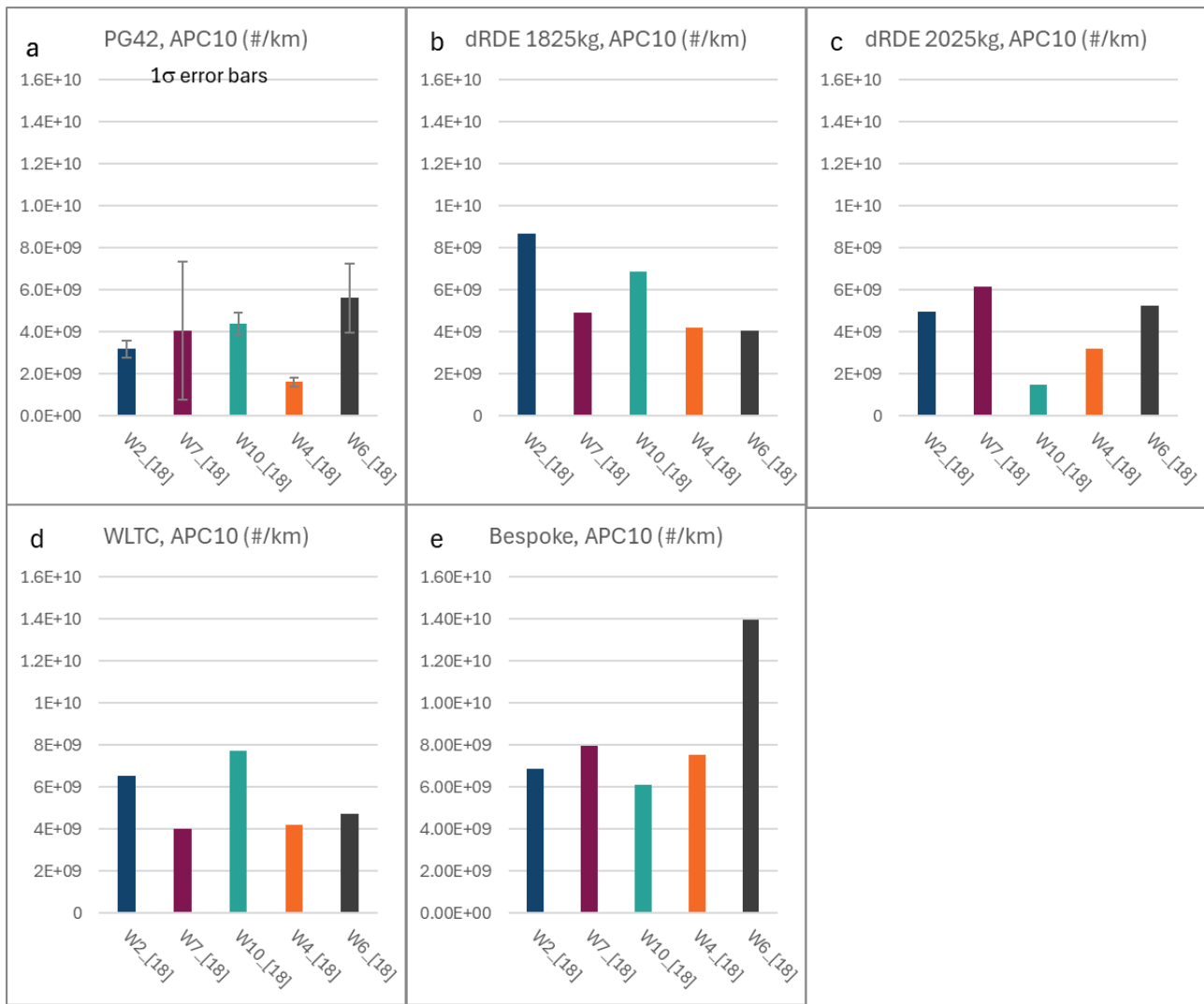
Figure 10-48: Non-volatile PN10 emissions compared between 18" tyres of different manufacturers and designs.

Emissions from W4 generally appear towards the low end of the non-volatile PN10 emissions range when compared with the other tyres. This is a summer tyre that may be harder than other tyres and wear less in the tests performed, releasing fewer solid particles. There are no other obvious trends in emissions across the drive cycles.

10.3.7.2 Total PN10 emissions, cold MPEC

Figure 10-49 illustrates the comparative analysis of total PN10 emissions across five different tyres and instruments, measured using the cold MPEC.

W7 generally shows similar, or higher, emissions of total PN10 than other tyres. This is a softer tyre designed for winter use and may wear more, and release more volatile materials and particles than other tyres. Emissions of other tyres are broadly similar to each other across the five cycles.

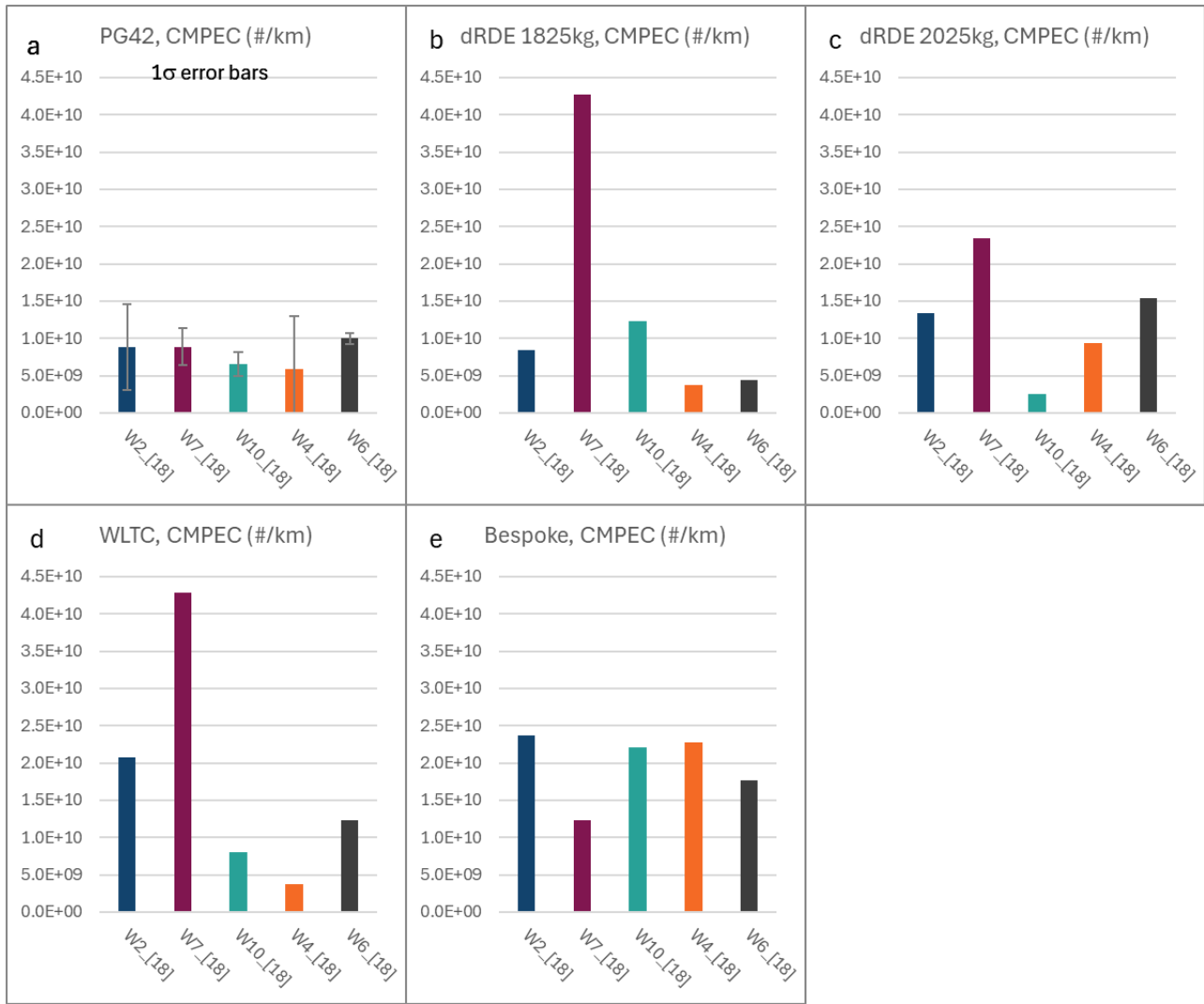Figure 10-49: Total PN10 emissions compared between 18" tyres of different manufacturers and designs.

10.3.7.3 PN4 emissions

Total PN4 emissions of five tyres collected from the PG42, dRDE, WLTC and bespoke cycles are shown in Figure 10-50.
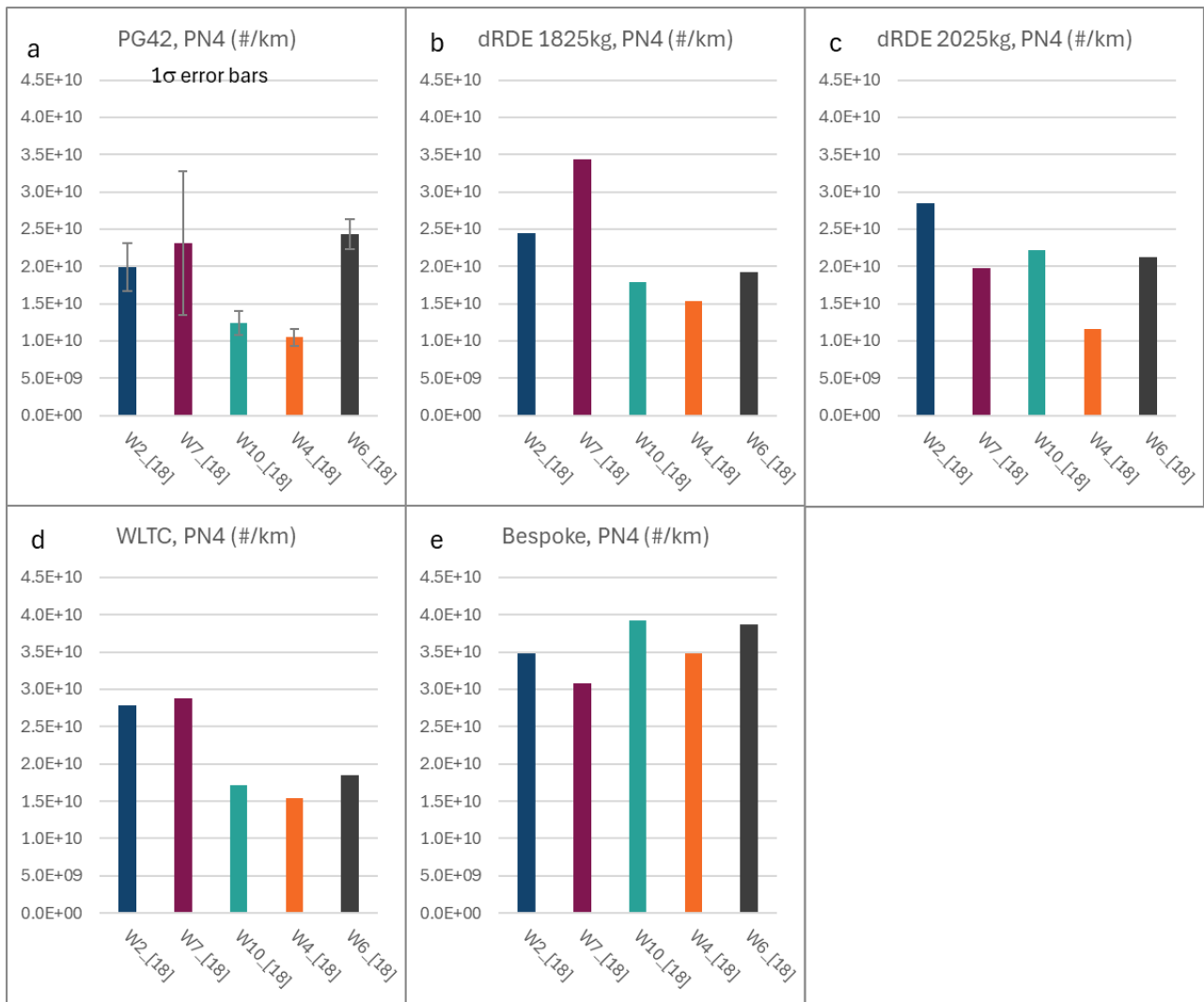
Figure 10-50: PN4 emissions compared between 18" tyres of different manufacturers and designs.

Emission results suggest generally lowest emissions from W4 and possibly a tendency towards higher emissions from W7. These trends would be consistent with a harder summer tyre showing lower solid and volatile emissions (W4), and a more versatile softer all-weather tyre giving higher emissions.

10.3.7.4 PM$_{2.5}$ (filter) emissions

Filter-based PM$_{2.5}$ emissions collected using the eFilter, comparing five tyres and five instruments, are shown in Figure 10-51. Excepting the bespoke cycle, W4 shows lowest PM$_{2.5}$ emissions from all cycles, while W7 is among the highest emitters. W4 may be a generally low emitting tyre for both volatile and non-volatile contributors to PM$_{2.5}$, as seen from the APC10, PN4 and cold MPEC results. Alternatively, while W7 shows high PM$_{2.5}$ and relatively high total PN10 emissions, it is unlikely that volatile materials would comprise all of the large differences in mass observed from the dRDE 1825 kg and WLTC measurements. Potentially these high emissions could derive from a few (not sufficient to impact APC10 measurements) relatively large solid particles that are more easily released by the softer W7 tyre than the other tyres studied.
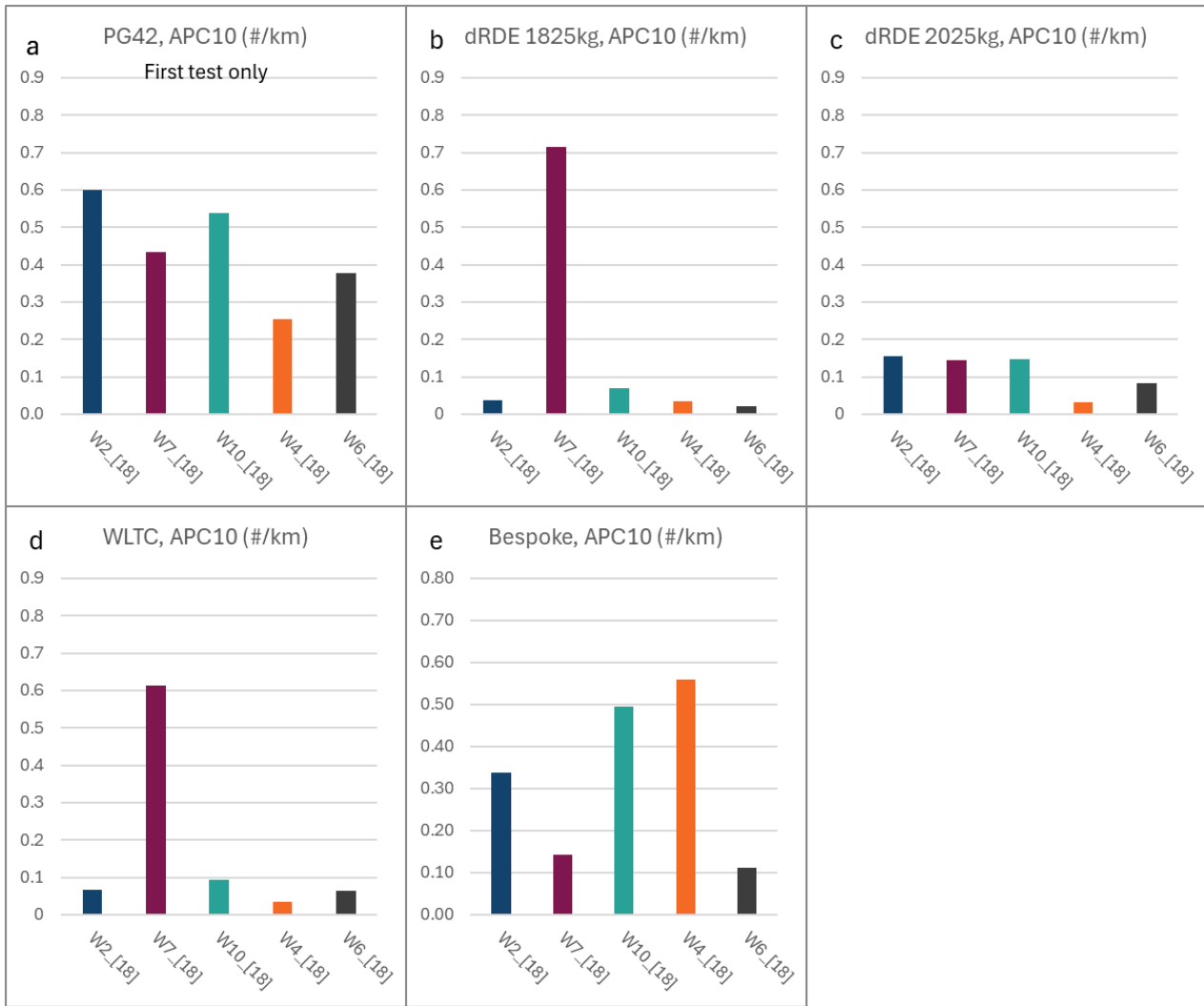
Figure 10-51: Filter-based PM$_{2.5}$ emissions compared between 18" tyres of different manufacturers and designs.

10.3.7.5 Summary of tyre manufacturer and design effects on emissions

The summer tyre, W4, appears to show generally lower emissions of both PN10 (solid and total) and PM than other tyres. This is a harder compound summer tyre, and its specific formulation may tend towards lower emissions. Conversely, W7, which is an all-season tyre able to provide good grip even under conditions of substantial snow, is likely to be softer and this may generate higher PN and PM$_{2.5}$ emissions. However, these comparisons are made from limited data and differences observed may not be significant.

10.3.8 Observations from bespoke cycle real-time data

Unlike a conventional real-world drive cycle such as the RDE or WLTC, by design the speed vs. time events of the bespoke cycle are intentionally separated (Figure 6-10). Emissions peaks are therefore more clearly resolvable and can be related to individual events, including to individual brake pressure applications (Figure 10-52).
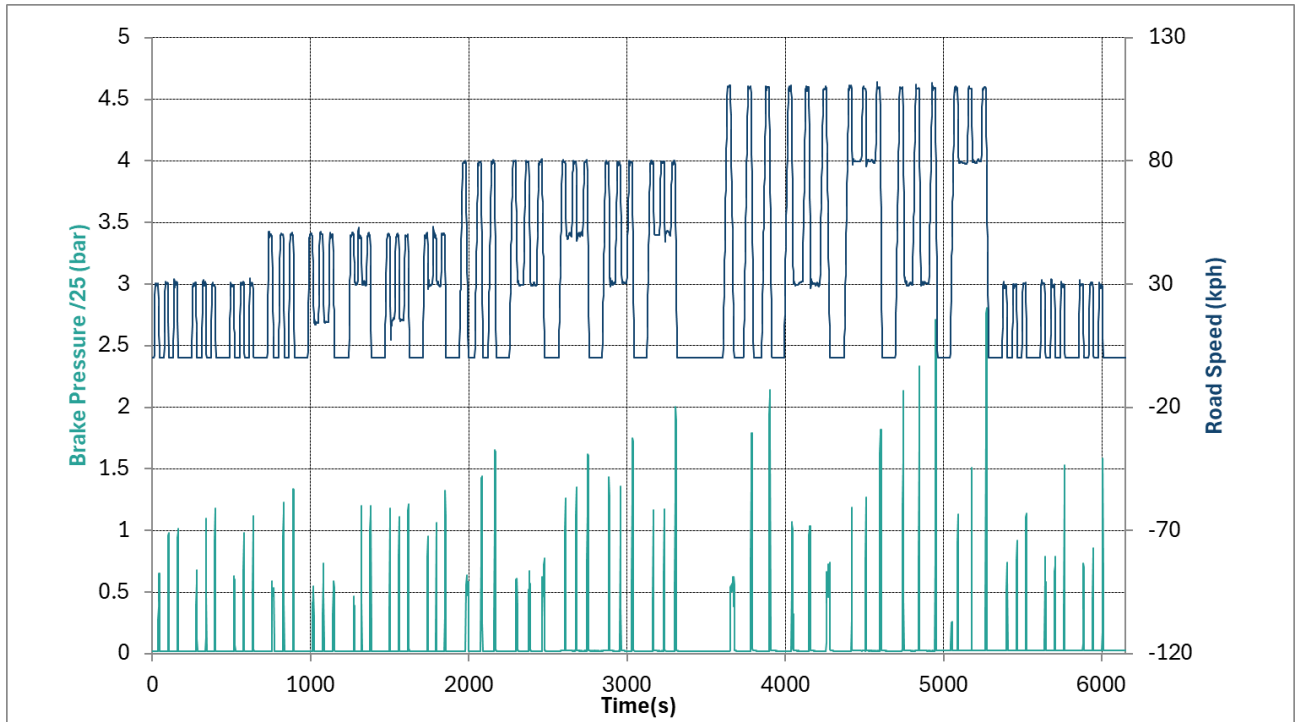
Figure 10-52: Typical road speed and discrete brake pressure events from the bespoke cycle.

It should be noted that some tyres showed unusual emissions profiles from the bespoke cycle (see Section 10.3.9.5) and so discussions of the relationship between drive-cycle events and instantaneous particle emissions focus on W17, which showed a clear and straightforward relationship.

10.3.8.1 Tyre temperatures

As Figure 10-53 shows for W17 and W7, tyre temperatures rise and fall throughout the bespoke cycle. At ~5000s, during the braking events from the highest speeds, tyre temperature reaches a peak ~14 to 15°C higher than the start temperature. Temperatures drop away relatively quickly after 5000s, but the braking events at 30kph at the end of the cycle take place at higher tyre temperatures than those at the start of the cycle.
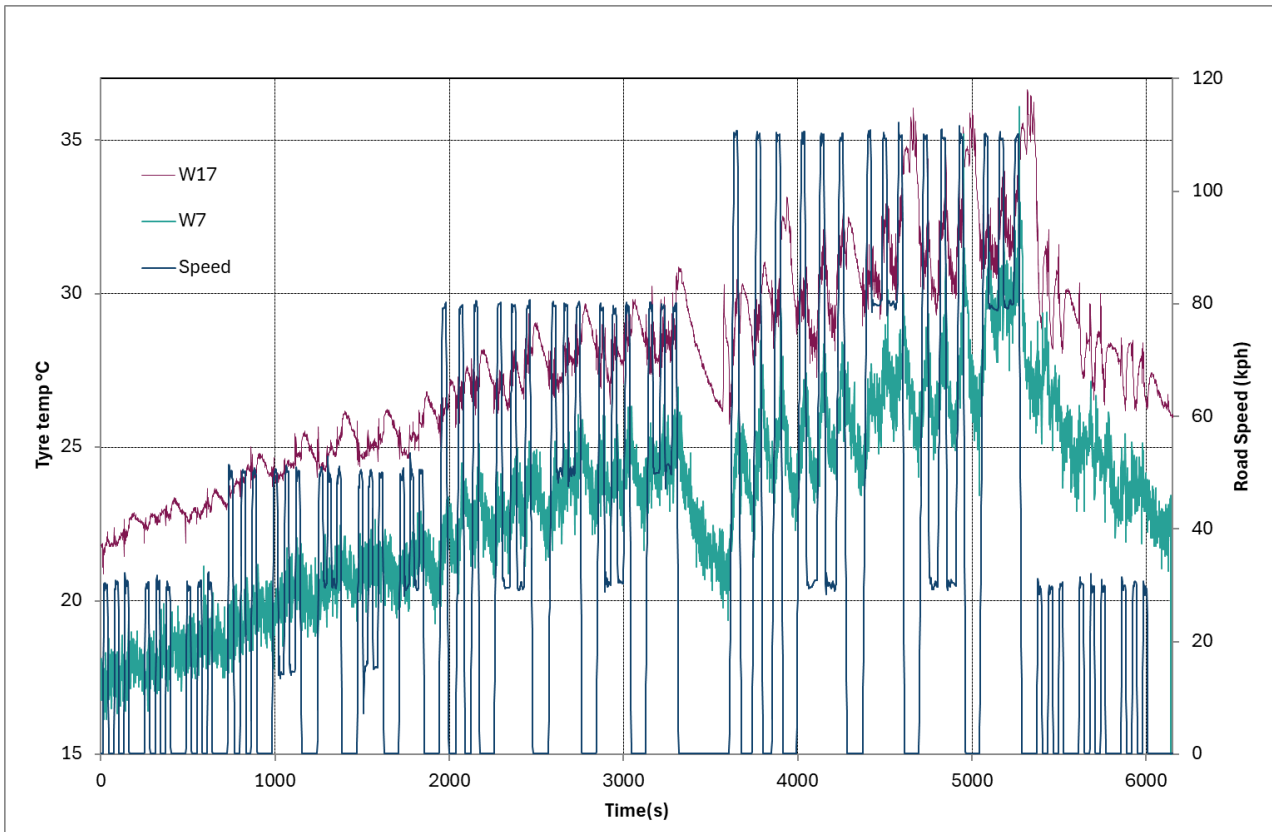
Figure 10-53: Tyre temperatures rise and fall throughout the bespoke cycle.

W17 and W7 are matched tyres excepting their diameter. At 16" diameter, W7 has a smaller contact patch than W17 and, as Figure 10-54 shows, the tyre would require the absorption of more energy per unit area and therefore heats up more when braking from higher speeds than the larger W7 tyre. Note that the two y-axes begin at different temperatures but are similarly scaled to enable the comparison.
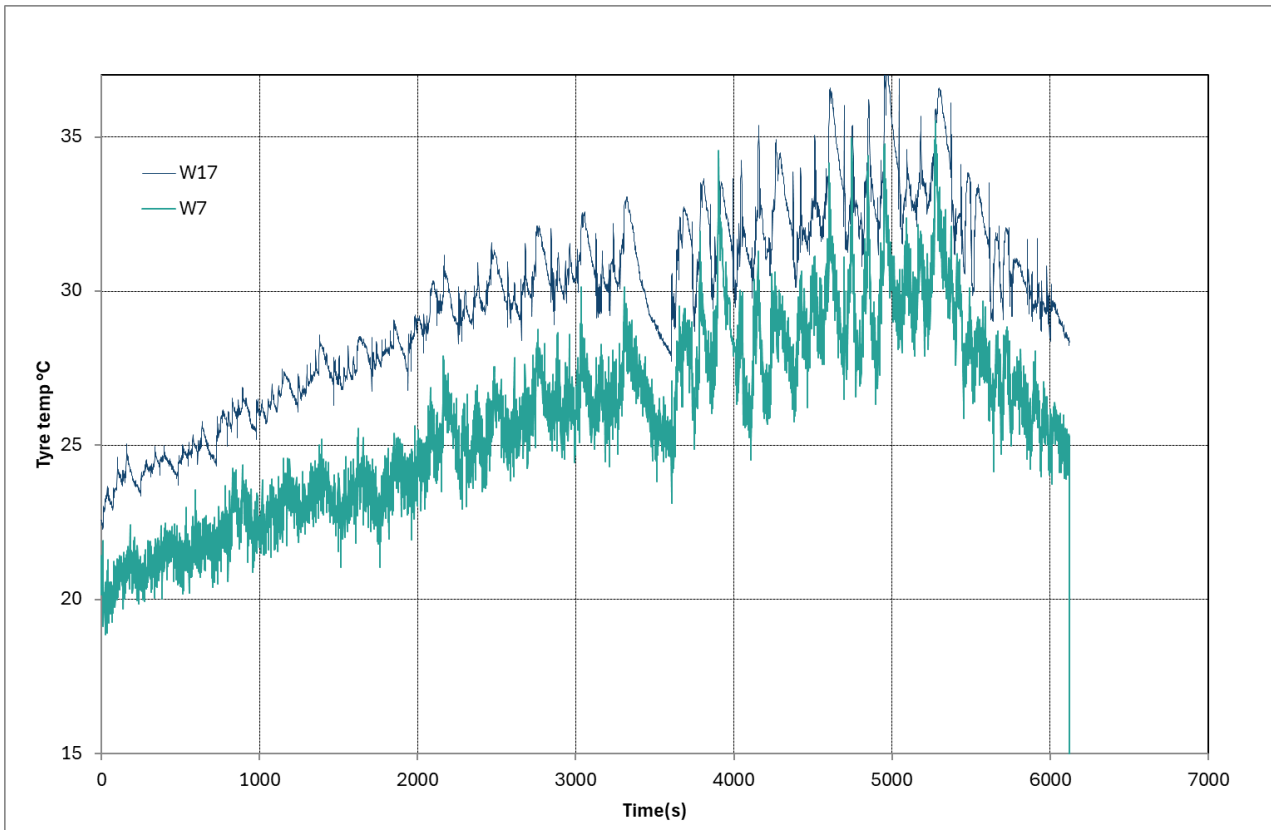
Figure 10-54: W17 (16" tyre) shows higher tyre temperature increases in the bespoke cycle than W7 (18").

10.3.8.2 PN emissions from tyre braking events

Total PN4, total PN10 and non-volatile PN10 emissions can all be seen to increase with braking from higher speeds (Figure 10-55), which leads to the higher tyre temperatures observed. The sources of the particles observed are explored in the following sections.
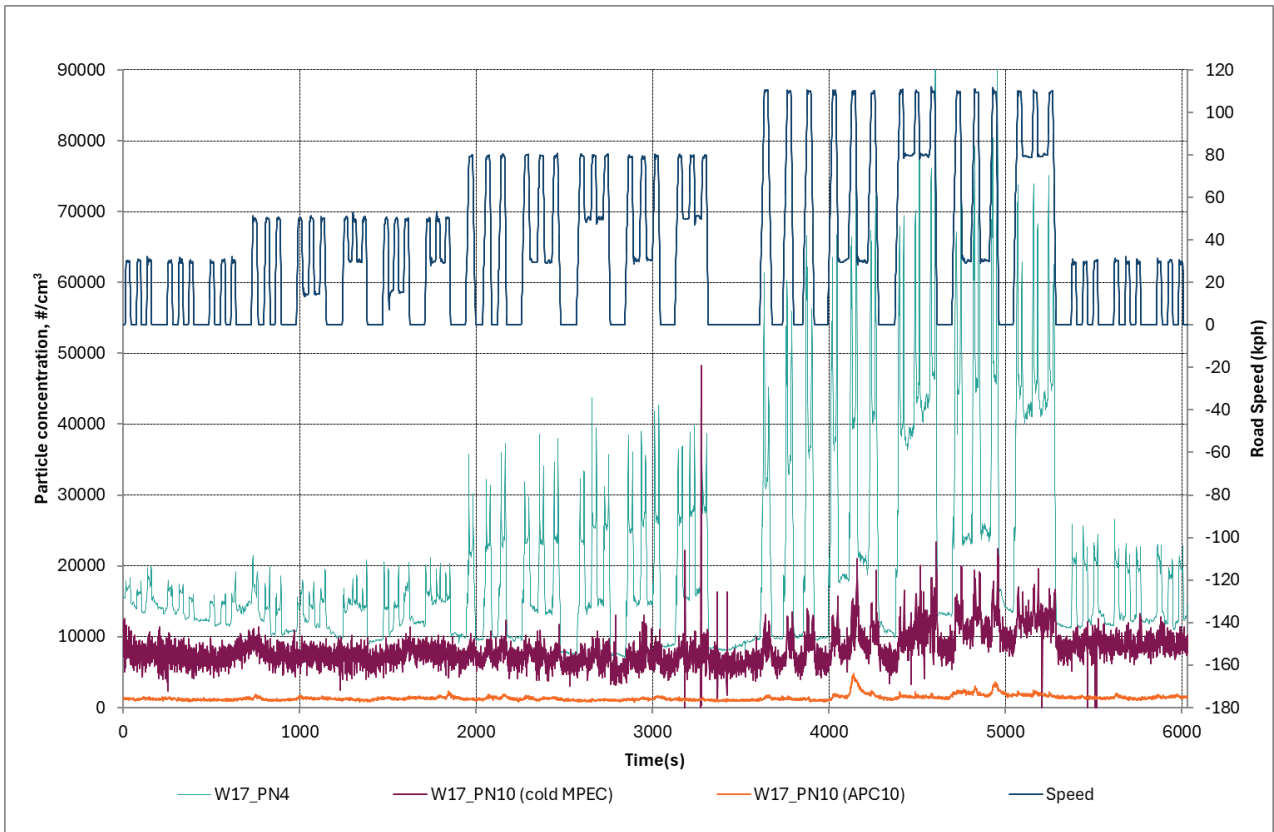
Figure 10-55: PN emissions increase with initial speed of the braking event.

Six drive cycle accelerations to 100kph with intermediate cruises or idles are shown from W17 in Figure 10-56. Real-time particle emissions traces are shown for total PN4, total PN10 and non-volatile PN10 (APC10) instruments.
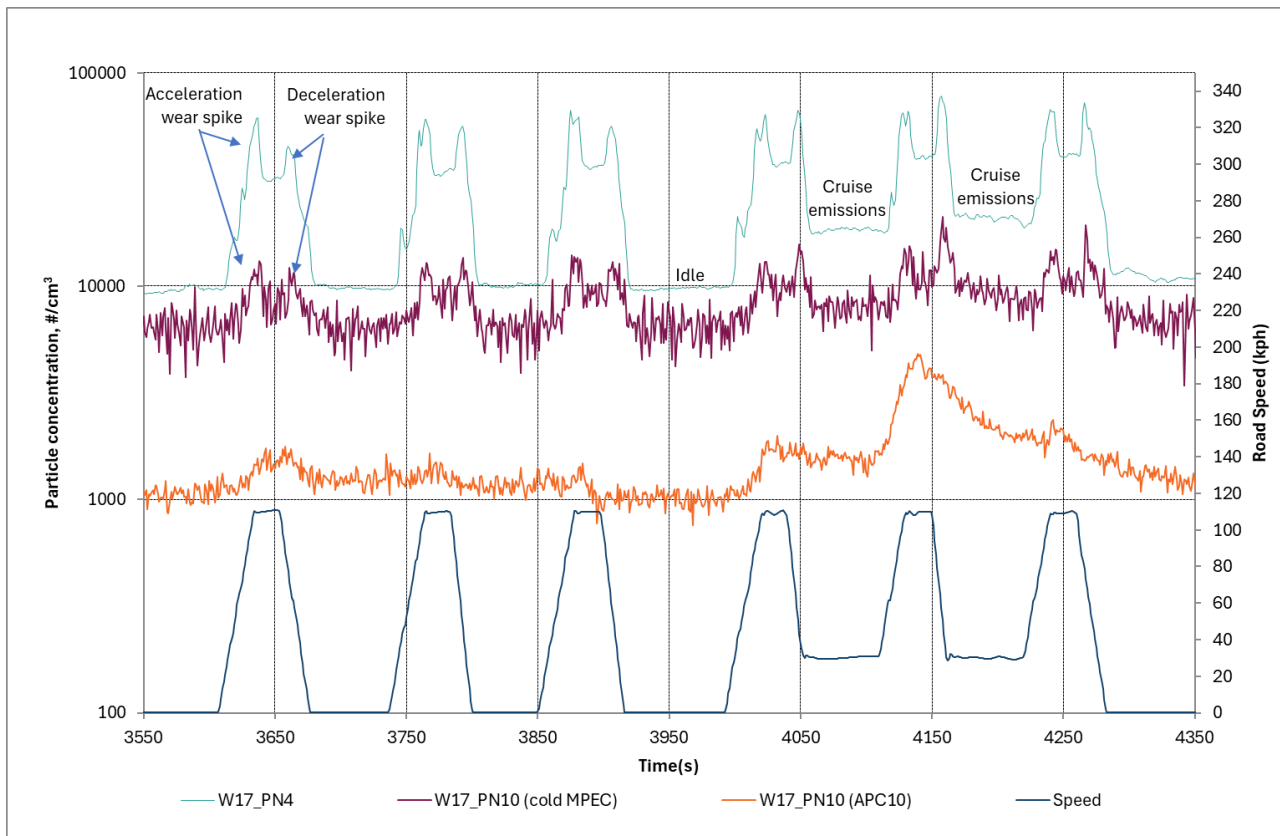
Figure 10-56: Real-time tyre emissions of PN4 and PN10 from 100kph braking events, W17.

The PN4 data clearly shows highest levels of emissions (concentrations > 10000 #/cm^3, averaging 23674 #/cm^3 across the period 3550s to 4350s), PN10 levels were ~65% lower (averaging 8351 #/cm^3) and non-volatile PN10 levels were ~94% lower than PN4 (averaging 1513 #/cm^3). These data also suggest that volatile particles comprise ~82% of total PN10 emissions.

Each single braking event from 110kph demonstrates clearly through the PN4 data, and the same effect is apparent in the total PN10 data, that particle emissions spikes are generated from both accelerations and decelerations (see 100kph event between ~3600s and 3680s in Figure 10-56). In addition, particle emissions are both elevated above idle levels and stable during cruise conditions (apparent between 4050 and 4250s). These data indicate that braking from a higher speed down to a lower speed creates fewer particle emissions than braking to rest. A higher speed cruise shows higher PN emissions (e.g., between levels at 4150s and 4200s) than a lower speed cruise (e.g., 4100s).

It is more difficult to discern emissions effects in the APC10 data, due to the lower concentrations measured (the APC10 data employs dilution at ~150:1, so an average concentration of ~10 #/cm^3 is reaching the particle counter). There do appear to be non-volatile particle production events that correspond to the main braking events of the cycle, but these are at much lower levels than seen for volatile particles.

10.3.8.3 Effect of cool or hot braking on tyre emissions

The bespoke cycle features a repeated set of measurements at the start and end of the cycle, these are braking events of different severities from 30 kph. At the start of the cycle, the tyres are relatively cool, while at the end of the cycle these 30 kph events follow braking from 110kph and the tyres will be substantially hotter (see Figure 10-53). As Figure 10-54 shows for (a) the initial braking events and (b) the last braking events of the cycle on W17, PN4, total PN10 and non-volatile PN10 emissions all appear to be higher at the end of the cycle than at the start of the cycle. The average concentrations from the two sets of three braking events between 487s and 646s and between 5855s and 6015s are compared in Table 10-10.

The increment between hot and cold tyre PN emissions at 30 kph is higher from non-volatile PN10 particles (~44%) than for total PN10 particles (~31%) and total PN4 particles (~19%). This may be since the increase in non-volatile particles is a greater proportion of the 'background continuum' of emissions than for the total particles. However, the fraction of non-volatile particles in total PN10 remains relatively constant at 15 to 17%

suggesting that the total PN10 composition remains broadly constant during both hot and cold tyre braking events.
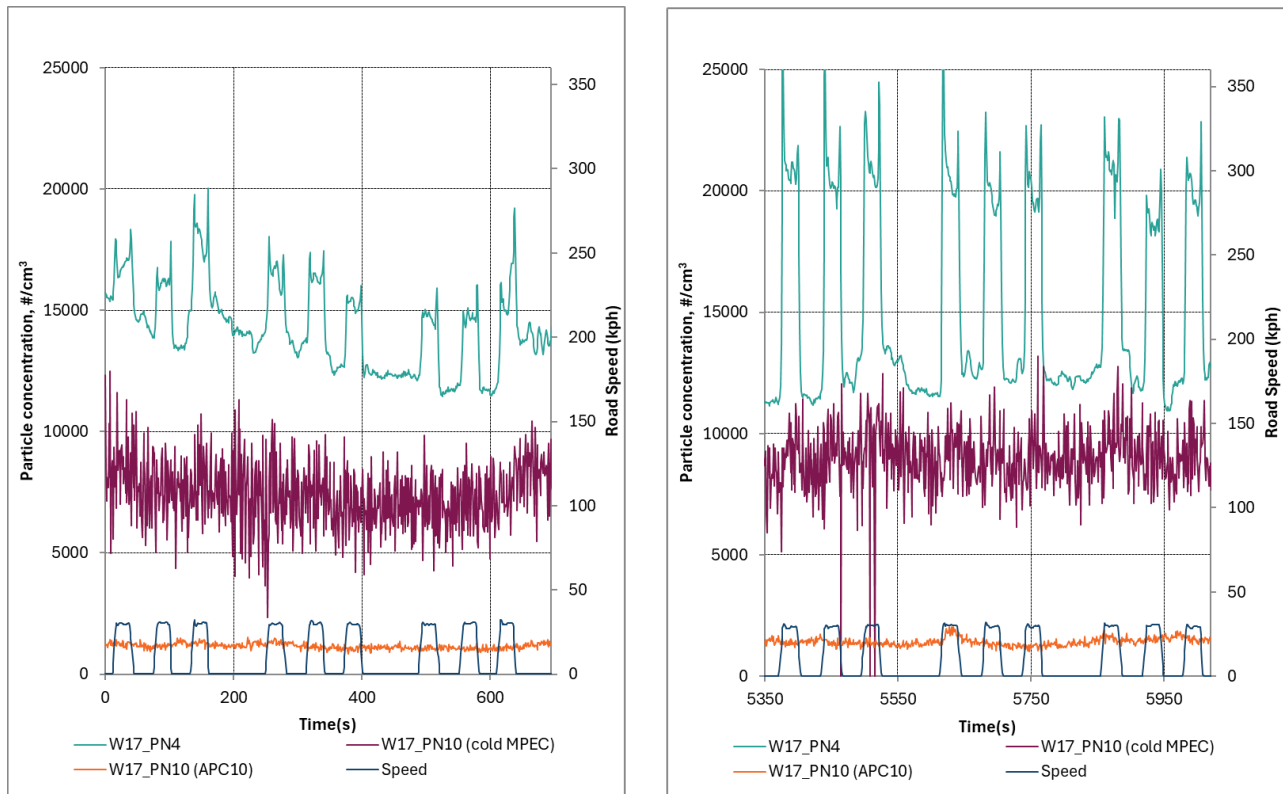

Figure 10-57: PN emissions from a) cool 30 kph braking and b) hot 30 kph braking.

Table 10-10: Differences in PN concentrations with hot and cold braking systems.

	Cool brake system (250s – 410s), #/cm³	Hot brake system (5610s – 5770s), #/cm³	% increase with hot braking
Total PN4	13506	16078	~19%
Total PN10	6955	9120	~31%
Non-volatile PN10	1062	1527	~44%
Non-volatile PN10 fraction	15%	17%	~2%

From an air quality standpoint, it appears that lower temperature tyres emit lower particle emissions, of both solid and volatile particles in the $PM_{2.5}$ range. This implies that generally lower speeds will not only reduce particles emitted in response to each individual braking event, but the lower speeds will moderate tyre temperatures and have a further benefit on reducing tyre particle emissions in the $PM_{2.5}$ range.

10.3.8.4 Tyre to tyre comparisons and general trends in braking emissions from, and to, different speeds

Bespoke cycle emissions data was collected from all the tyres tested. In the following sections, these data are considered in two ways. Firstly, to look at trends and effects on emissions generated by braking to and from different speeds within the bespoke cycle. These are considered by reviewing PN4 and non-volatile PN10 data from W17; and secondly, to briefly consider any comparative differences in trends between tyres in terms of tyre size, tyre mileage and manufacturer (this complementary to data from Sections 10.3.5, 10.3.6 and 10.3.7) using non-volatile PN10 data. The APC10 data are selected to eliminate, as far as possible, variations in bespoke emissions that derive from volatile materials.

10.3.8.4.1 Trends when braking to and from different speeds

Figure 10-58 and Figure 10-59 show average braking emissions (any emissions generated from tyres during accelerations are not included) of PN4 and non-volatile PN10 respectively generated when testing W17 over the bespoke cycle using. From these data the following observations can be made:

- In general, particle emissions, on a per km basis, are not greatly different between gentle, moderate and dynamic braking. This is likely because the longer distances taken to stop when braking from higher speeds offset the higher particle concentrations emitted by more dynamic braking

- There is no consistent relationship of higher #/km emissions when braking from higher speeds to rest (e.g., from 80kph to rest) than from lower speeds to rest (e.g., 50kph to rest)

- When braking from a higher speed to a lower speed (e.g., 110kph to 80kph) emissions are lower than when braking to an even lower speed (e.g., 100kph to 50kph), at least with dynamic braking. With dynamic braking the trend can be seen for both PN4 and PN10 data and with each of three initial speeds (50kph, 80kph and 110kph) dropping to two or three lower speeds
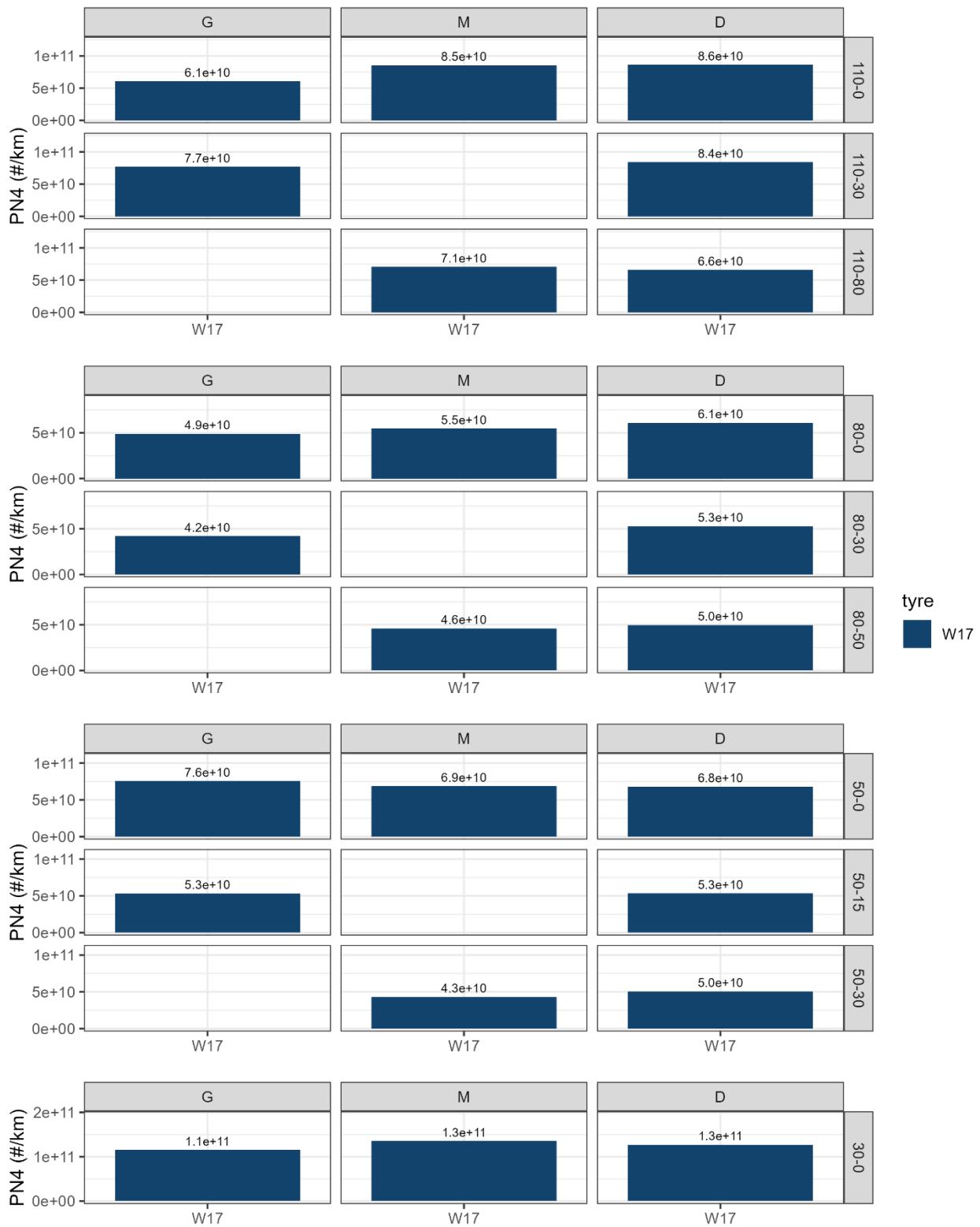
Figure 10-58: Summary of PN4 emissions from W17, during the bespoke cycle tests.
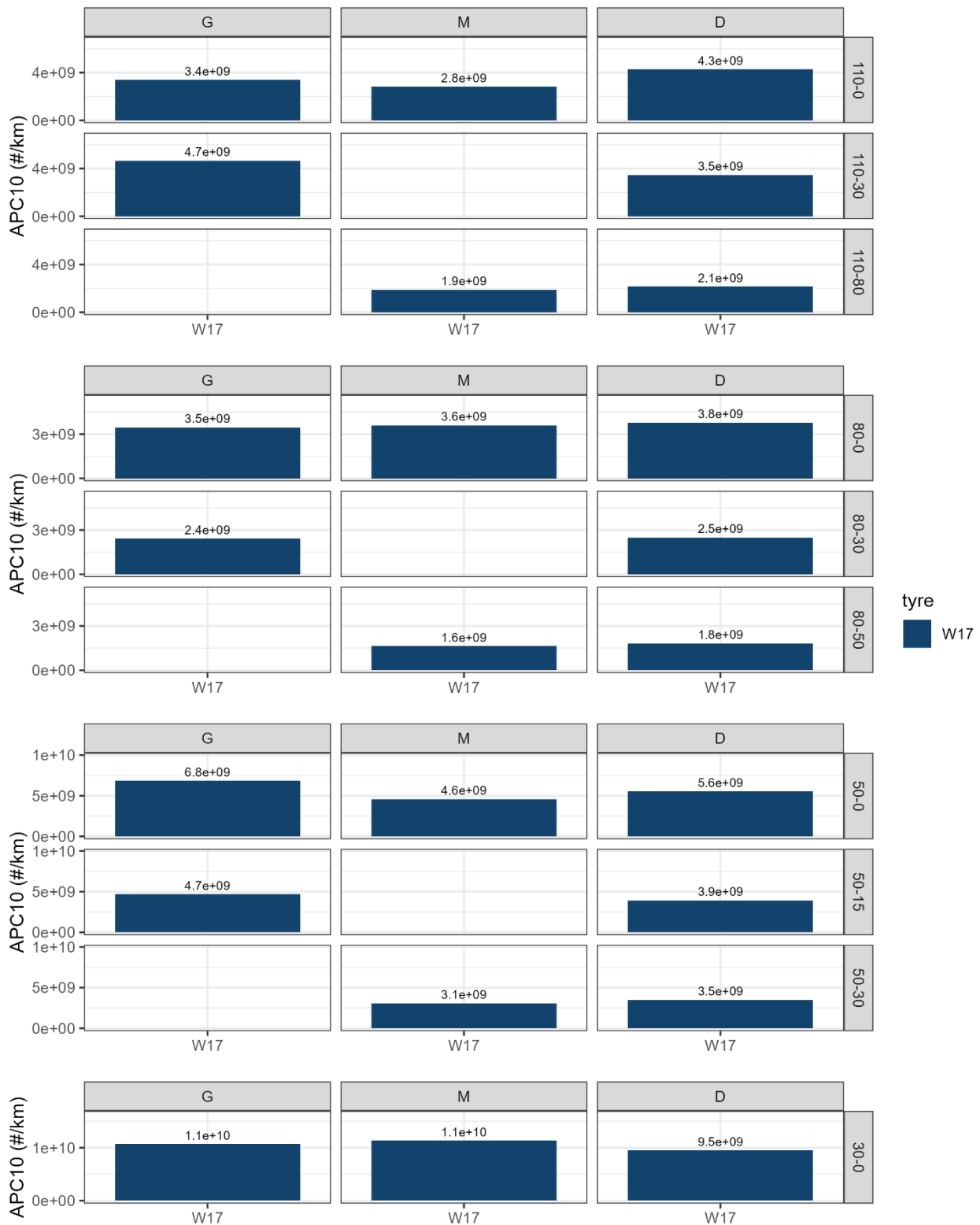
Figure 10-59: Summary of non-volatile PN10 emissions from W17, during the bespoke cycle tests.

10.3.8.4.2 Comparative bespoke cycle non-volatile PN10 emissions from different tyre sizes

Figure 10-60 shows bespoke cycle non-volatile PN10 emissions from three pairs of tyres. Each pair of tyres comprises a nominally identical, or very similar, formulation but the tyre diameter is smaller with the first (16") tyre, e.g., W17 than with the second (18") tyre of the pair, e.g. W7.

Results suggest that for two of the three pairs of tyres (W20, W4 and W16, W2) emissions are consistently higher across all speed and braking dynamics with the 16" tyres than with the 18" tyres. However, for the first pair (W17, W7) the opposite is true.

Potentially the smaller contact area of the lower diameter tyres leads to higher non-volatile PN10 emissions but given that the comparative data lacks a statistical basis, it is probably not valid to conclude any definitive trend from these observations and further work would be advised.
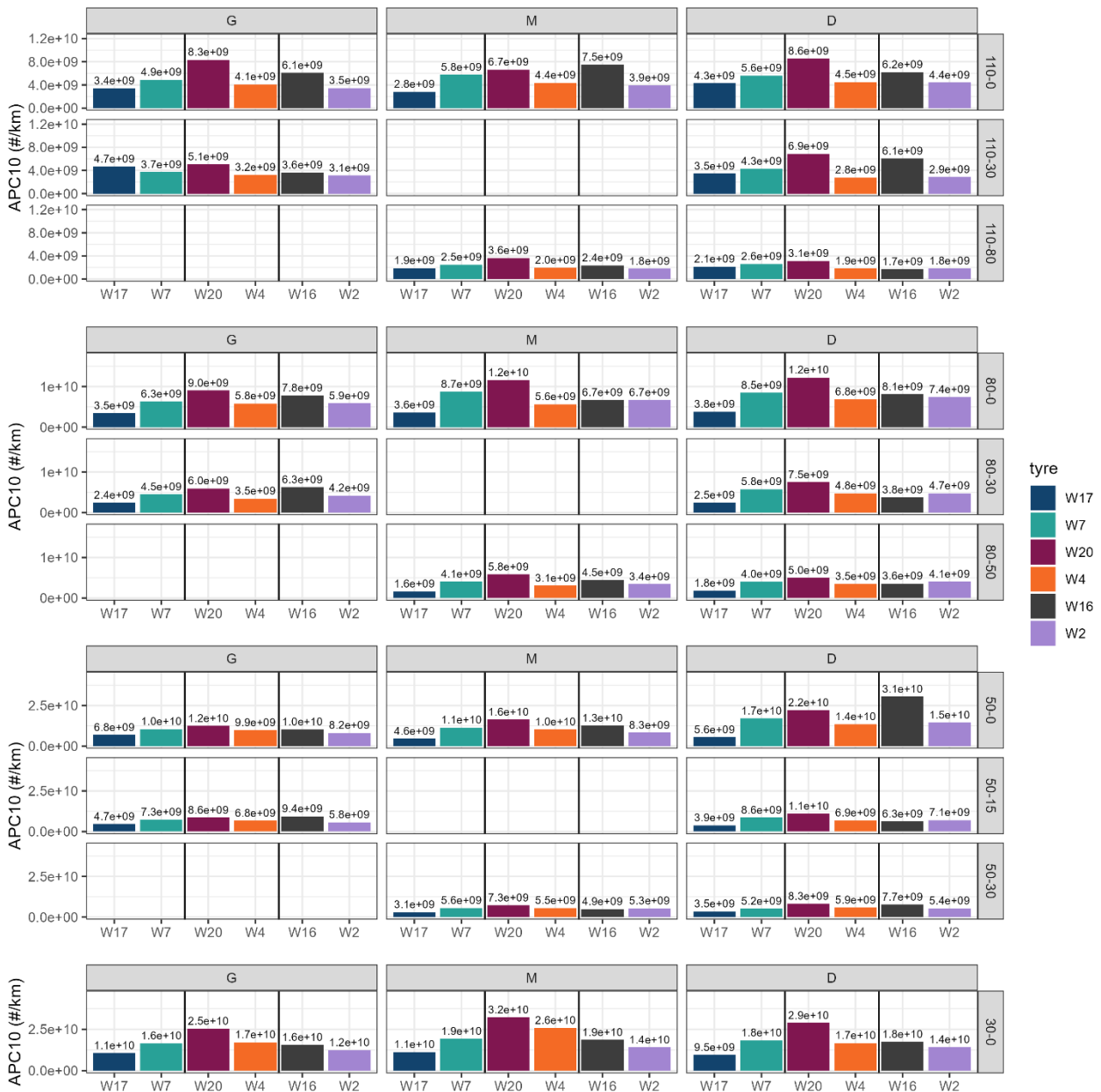
Figure 10-60: Bespoke cycle non-volatile PN10 emissions summary, 16" vs 18" tyres.

10.3.8.4.3 Comparative bespoke cycle non-volatile PN10 emissions with different mileage tyres

There are no consistent trends, on non-volatile PN10 emissions from bespoke cycles, between road speeds and braking dynamics from tyres with different elapsed mileages (Figure 10-61).
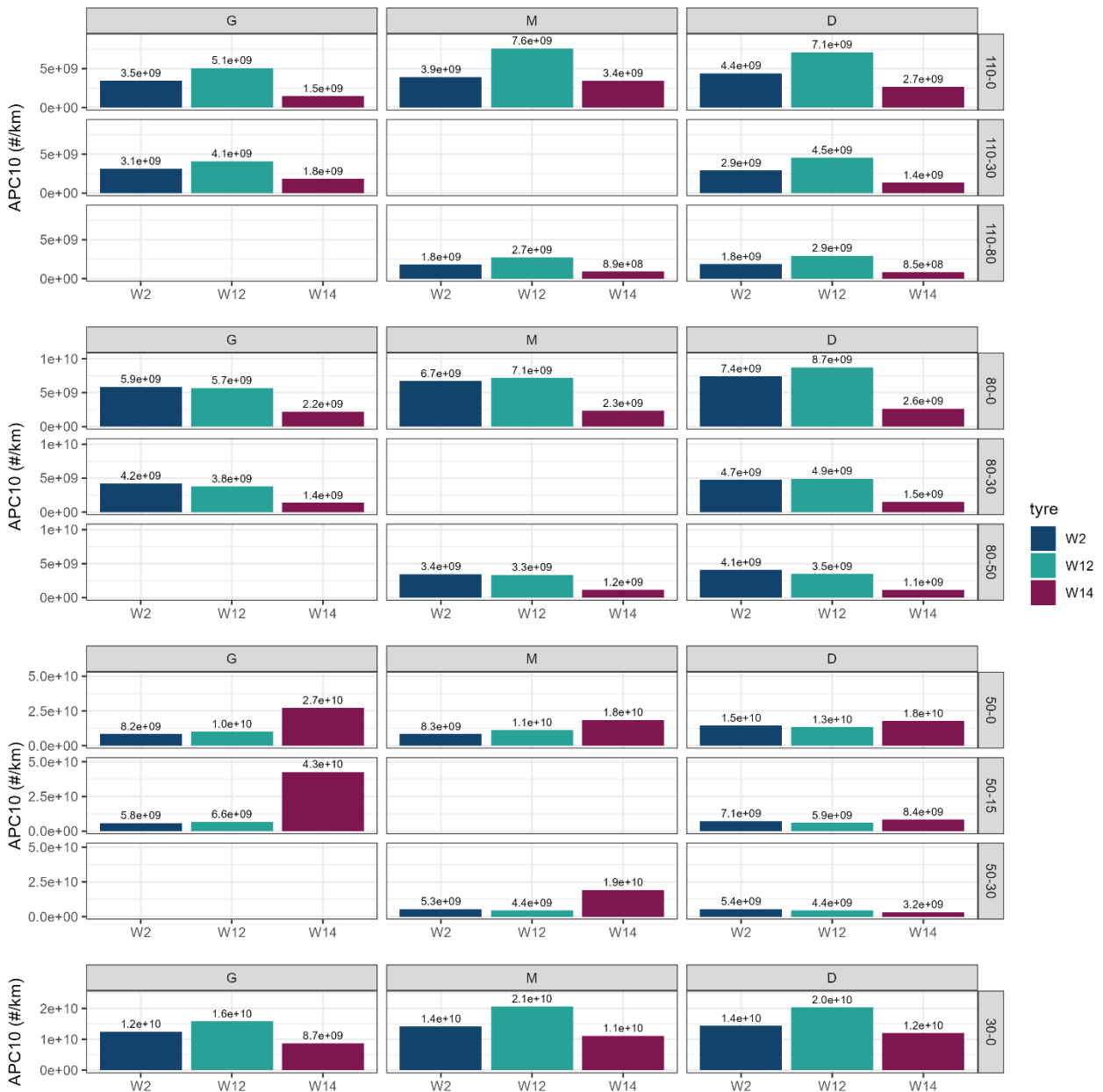
Figure 10-61: Bespoke cycle non-volatile PN10 emissions summary, tyre mileage effects.

10.3.8.4.4 Comparative bespoke cycle non-volatile PN10 emissions between 18" tyres of different designs and from different manufacturers

There are no consistent trends, on non-volatile PN10 emissions from bespoke cycles, between different 18" tyres (Figure 10-62). Emissions from W6 do appear higher in many cases, but W6 in particular, showed unusual emissions behaviour during two bespoke cycle repeats. Examples of unusual bespoke cycle emissions behaviour, including W6, is explored in Section 10.3.9.5.
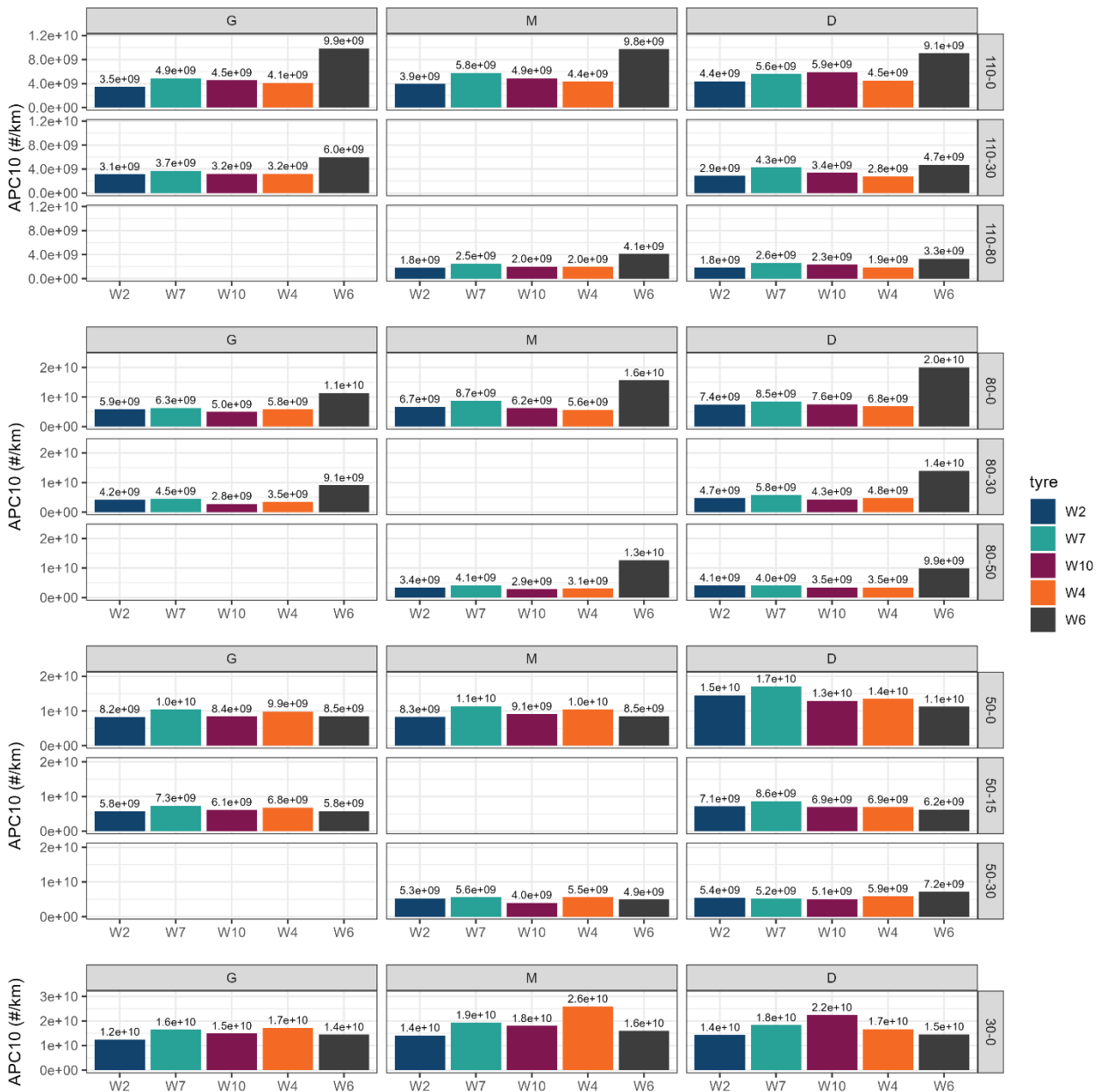
Figure 10-62: Bespoke cycle non-volatile PN10 emissions summary, manufacturer and design comparisons.

10.3.9 Miscellaneous

10.3.9.1 Averaged PN and PM emissions per km across all tyres and cycles

Average non-volatile PN10, total PN10, total PN4 and $PM_{2.5}$ (gravimetric) emissions from the test programme are shown in Figure 10-63a-d. In each chart, the first five columns show the results from each drive cycle averaged across all tyres. The penultimate column shows the average of the results from all the cycles (All; averaged averages), and the final column shows the averages of the first four drive cycles only, omitting the bespoke cycle (All (no BSPK)). The bespoke cycle is omitted because it is an artificial drive cycle, and it may be less representative than the other cycles.
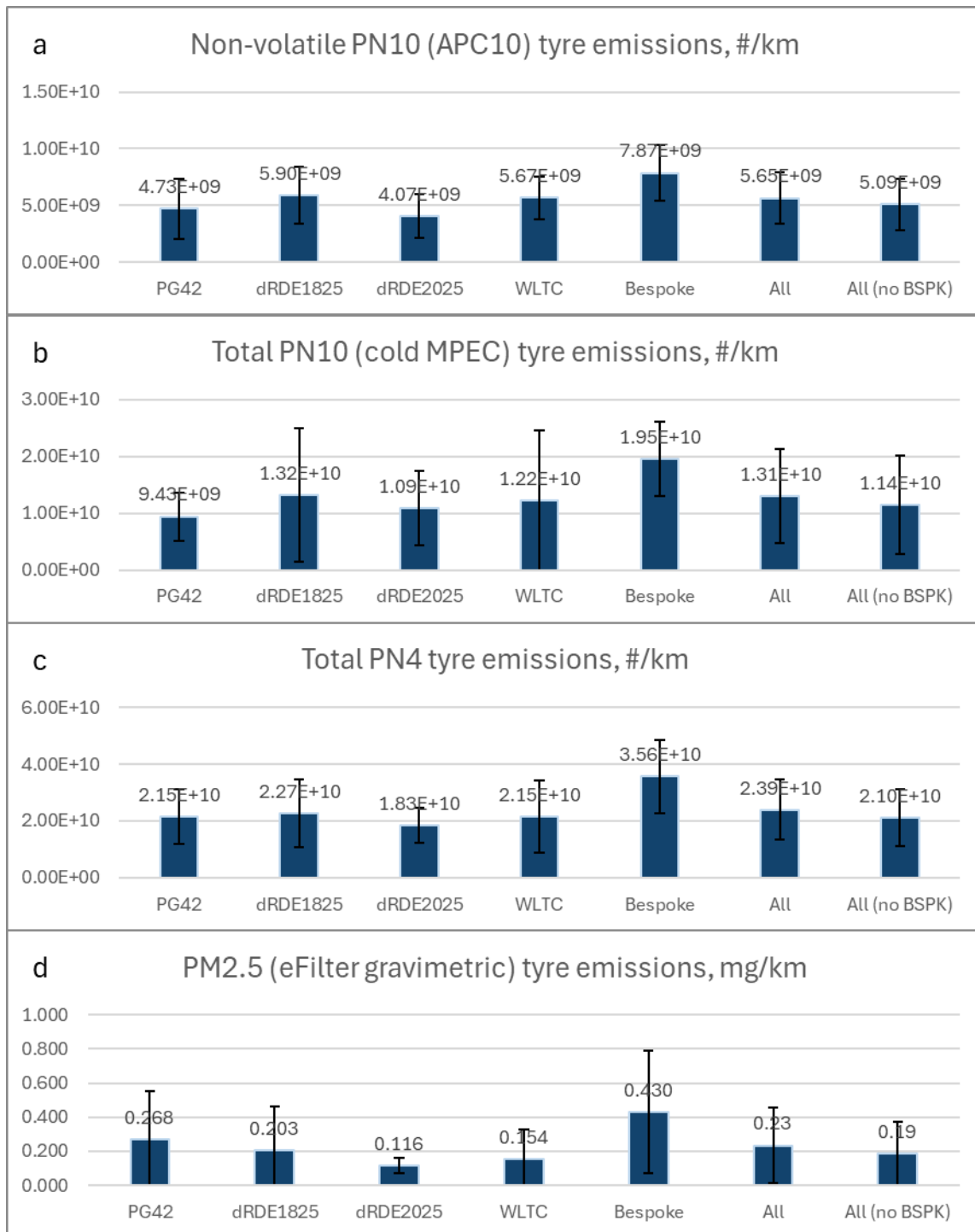
Figure 10-63: Cycle specific and averaged emissions factors for a) non-volatile PN10, b) total PN10, c) PN4, d) gravimetric PM$_{2.5}$.

The data in the final two columns represent potential typical emissions factors for the most reliable metrics used in this project. Excluding bespoke cycle results, Table 10-11 indicates that non-volatile PN10 emissions from tyres are of the order 5 x 10^9 #/km ± 44%, total PN10 emissions are ~1.1 x 10^{10} #/km ± 76%, Total PN4 emissions are approximately twice those of PN10, at 2.1 x 10^{10} #/km ± 48%. PM$_{2.5}$ emissions are well below 1 mg/km, but highly variable, at ~0.19 mg/km ± 103%.

Table 10-11: PM$_{2.5}$ and PN emissions averaged across all cycles.

	APC10 (#/km)	cMPEC (#/km)	PN4 (#/km)	PM$_{2.5}$ (mg/km)
Mean	5.09E+09	1.14E+10	2.10E+10	0.19
STDEV	2.24E+09	8.67E+09	1.01E+10	0.19
CoV (%)	44%	76%	48%	103%

From Section 10.3.1.1, average mass-based tyre emissions wear rates were ~66 mg/km ± 45.0 mg/km. The average PM$_{2.5}$ emission was ~0.19 mg/km, so ~0.3% of the wear emissions rate. However, a substantial proportion of the PM$_{2.5}$ is likely to be volatile material and so the contribution of the solid particle proportion, present in PM$_{2.5}$, to the overall mass-based wear emissions rate will be even lower.

10.3.9.2   PM filter masses and images

Figure 10-64 shows a collection of filters taken during the tyre sampling. The masses collected on PM filters used for gravimetry ranged widely. Highest masses on each tyre were collected from the first PG42 cycle in the sequence of 3, or from bespoke cycles. The 10 highest filter masses ranged from 0.871 mg to 2.107 mg. The lowest 10 filters ranged in mass from ~25 µg to ~54 µg and were collected from a variety of different cycles. From a total of ~ 110 filters only 6 showed collected masses above 1 mg, while 25 masses were below 100 µg.

Almost all filters appeared completely white, indicating either collection of levels of single particles smaller than the visible threshold (~50 µm to 70 µm) at concentrations below the level at which agglomeration would occur on the filter, or merely collection of gas phase and semi-volatile materials. Figure 10-64 shows a selection of filters, equally spaced across the range, from the lowest collected mass to the highest.

Figure 10-64: Images of tyre wear PM filters of different sampled weights.

Of the filters shown in Figure 10-64, only those with the highest masses: 487 µg from a bespoke cycle on W2, 774 µg from a bespoke cycle on W4 and 2107 µg from Tyre W17 on its final PG42 cycle (see also Section

10.3.3), show any sign of discoloration. For these filters with the highest loadings the material collected appears to be a very light grey fine dust. Some filters (e.g., with 487 µg, 774 µg and 2107 µg loadings) also indicate the presence of individual black particulates much larger than the PM$_{2.5}$ range sampled.

Together, these observations suggest that almost all tyres and drive cycles emit very limited levels of solid materials in the PM$_{2.5}$ range, occasionally very fine dust is emitted and much larger (100's of µm in diameter) particles are present, some of which may reach the PM filter.

10.3.9.3 Particles recovered from the transfer system from tyre sampling inlet to analysers

Following completion of testing, the sampling and transfer system was disassembled to investigate the potential deposition of tyre wear particles in elements of the transfer line. In the phase 1 study, there had been uncertainty regarding the effectiveness and efficiency of the sampling duct employed, and so an alternative approach was used in this study. In this phase of the study a much larger inlet, but still with relatively high inlet flow velocity of ~100 cm/s, was used. This inlet flow is similar to that used in PM$_{2.5}$ samplers.

Within the sampling system between the inlet and pump, large quantities of black particulate materials were found in several locations (Figure 10-65), comprising individual particles visible to the naked eye, so of at least 50 µm in diameter. These particles will comprise emissions from all the different tyres tested in this project. Along with the clear profile of PN4 emissions, the presence of these particles in the transfer system is clear indication that the plume of particles released from the contact patch between tyre and roller is entering the sample inlet.

Figure 10-65: Particulate material recovered from the transfer system.

When this investigation is considered along with the filter images and the emissions measurements, it appears that PM$_{2.5}$ emissions contain a minimal level of solid particles, and they are likely dominated by volatile materials. The major contribution of tyre wear to mass emissions appears to be the production of much larger solid particles, and so the primary influence of wear is likely the emissions of volatile species and releases of microplastics, rather than PM$_{2.5}$.

10.3.9.3.1 Tyre wear macro-scale particle size distributions

The size distributions of the supermicron tyre wear particles were determined through sieving granulometry, where sieves of different mesh diameters are used to discriminate particles by their physical diameters. Tyre wear from each sampling location was separated into 10 size fractions, with the smallest fraction containing all material below 53 µm and the largest fraction all material above 2.8mm. For the smallest size fraction, a lower limit of 2.5 µm was assumed, since minimal PM$_{2.5}$ mass was detected in this study. These size fraction data were then used to plot particle size distributions (Figure 10-66).

Results showed that, within the resolution of the size bins used, particle size distributions at all sampling locations were similar, indicating modes in the size distributions at ~53 µm, 250 µm and 600 µm.

The size-fractionated tyre wear samples have been collected into separate jars for future study, if required.
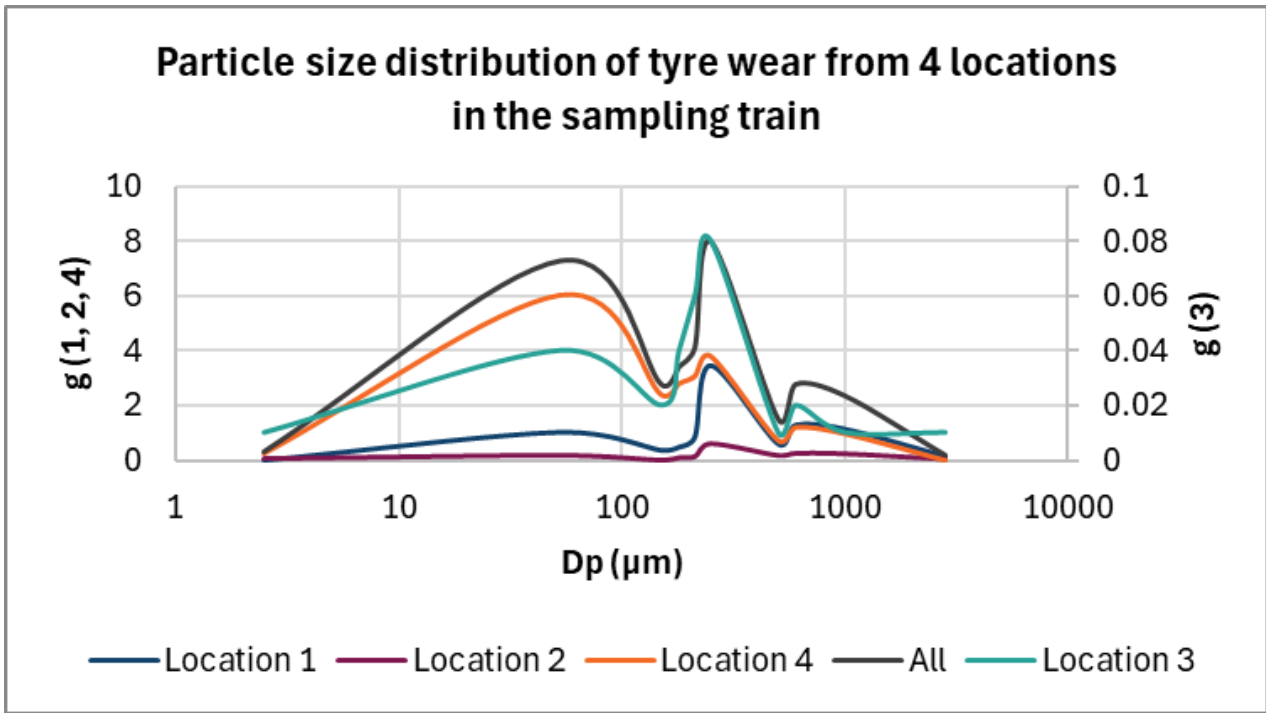
Figure 10-66: Tyre wear size distributions from four locations in the sampling train.

10.3.9.4 Are cycle-averaged PN4 emissions concentrations related to average tyre temperature?

Since the test facility temperature was uncontrolled, the start temperatures of tyres could vary by a few degrees from day to day. It was considered possible that emissions of volatile-dominated PN4 could be related to tyre temperature, and this could be a source of variability in results. W17 was tested over five separate sets of 3 x PG42 cycles and so offers an opportunity to explore this. However, as Figure 10-68 shows, for data from both the 2nd and 3rd PG42 cycles in each set of repeats, there is no obvious relationship between higher average drive cycle tyre temperatures and higher PN4 emissions concentrations.
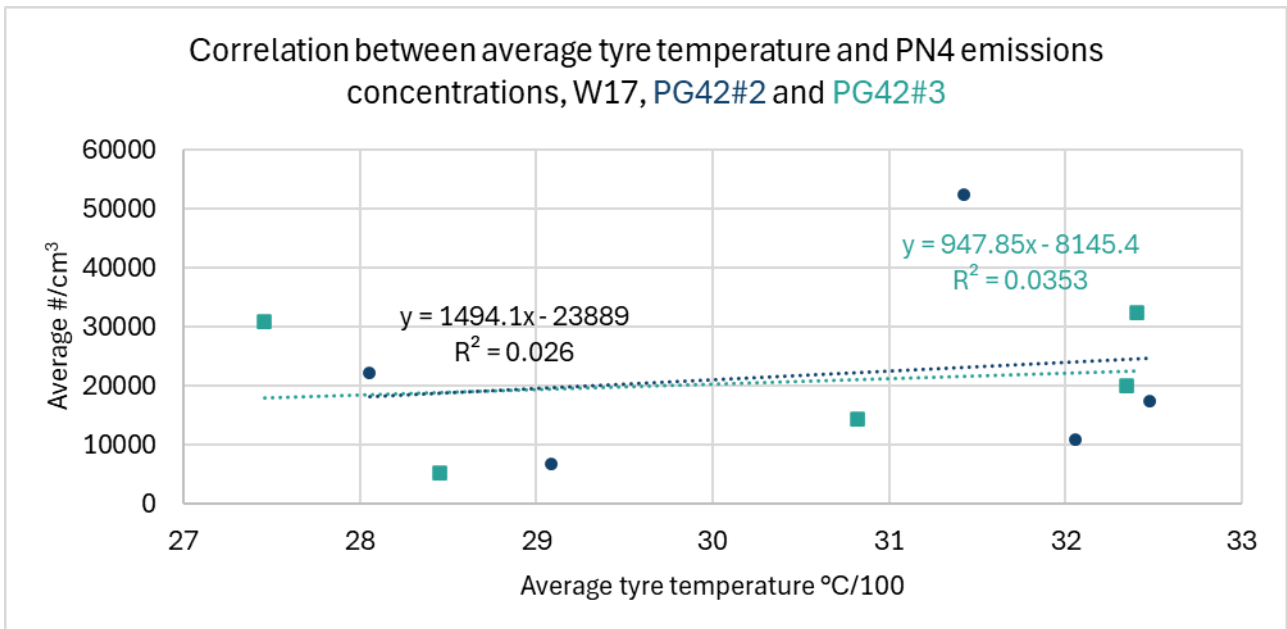
Figure 10-67: Relationship between average tyre temperature and PN4 emissions concentrations for PG42 tests on W17.

10.3.9.5 Anomalous emissions events during bespoke cycles

Several tyres showed unusual emissions profiles during bespoke cycle testing. These resulted in large, long duration, emissions periods. Emissions peaks were often observed in data from both total particle (e.g. PN4) and non-volatile (e.g., APC10) instruments. Two notable examples are W14 and W6 emissions.

The W14 bespoke cycle featured a large emissions event from just after the start of the cycle to ~1750s (Figure 10-68). This occurred in the lowest temperature part of the bespoke cycle. It may simply be an event that has occurred in the background during the drive cycle but if so, it is not clear what the origin would be since the facility was closed to entry during the test. It may also be an emissions event from the tyre, perhaps related to release of particles from a localised hotspot when coarse particle wear occurs. This event dominates the overall emissions of the bespoke cycle, and leads to high apparent emissions from the early parts of the cycle.
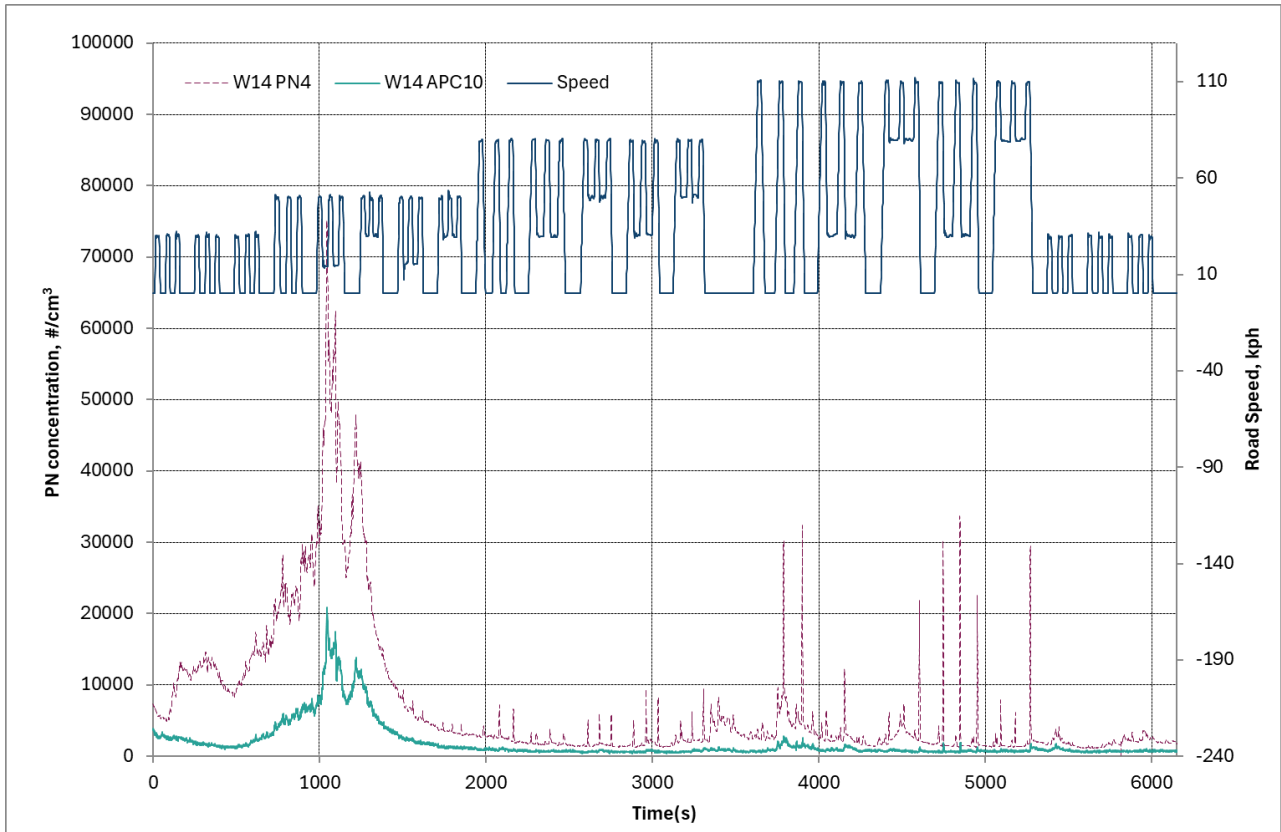
Figure 10-68: PN4 and non-volatile PN10 emissions from the bespoke cycle on W14.

Testing of W6 also showed an unusual emissions profile, and to investigate further a repeat cycle was performed. Figure 10-69 shows the results of the two tests using the PN4 instrument. The two W6 cycles showed inconsistent particle emissions traces across the bespoke cycle and were also dissimilar. This is not likely to be an instrument effect, since tests performed immediately before and after these bespoke cycle tests showed expected results.
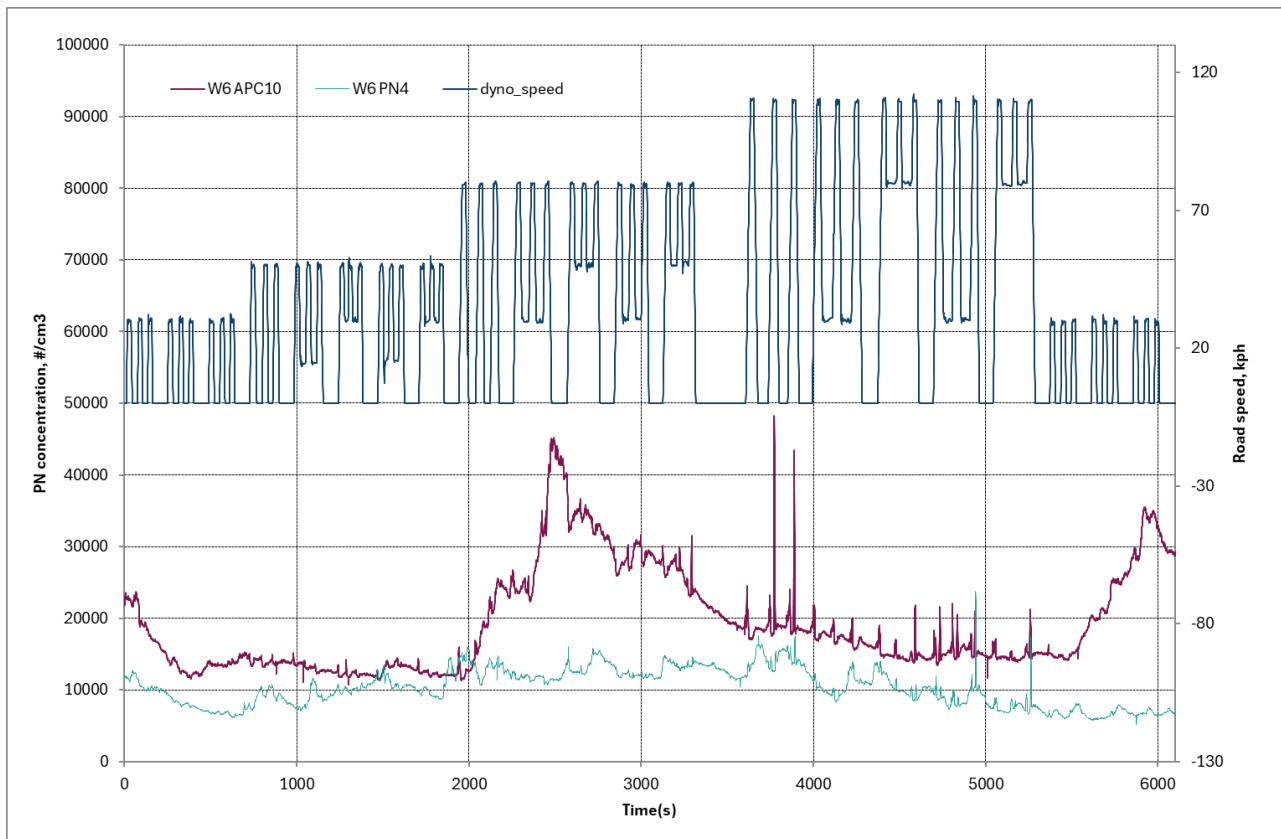
Figure 10-69: PN4 (grey) and PN10 results from two bespoke tests on W6.

It may be that the (PM$_{2.5}$ regime) emissions characteristics of certain tyres are unrepeatable and unpredictable. For example, the bespoke test shown by the blue line does indicate emissions from two events near 5000s of the cycle, but few other discrete events. It is impossible to rule out a confounding effect of background particle contributions, but while emissions from the test represented by the blue line are consistently lower than those shown by the grey line, the grey line test shows emissions spikes well above baseline levels, but the blue line does not.

10.4 TYRE WEAR EMISSIONS DISCUSSIONS/SUMMARY

10.4.1 Comparison of Phase 1 and Phase 2 tyre emissions measurements in the VERC

Lower tyre particle emissions were seen from the Audi in Phase 2, than seen from the Caddy in Phase 1 of this study, although both were tested in the VERC. After eliminating potential influences such as emissions below analyser detection limits and particle transport challenges that may have limited particles being detected by the analysers, this effect was considered to be related to the challenge of the tyre surface becoming sticky when running on the clean steel surface of the VERC roller, and this restricting the release of particles in the PM$_{2.5}$ range. A comparative analysis of phase 1 and 2 data also indicated a reasonable probability that tyre particle measurements in phase 1 were contaminated by brake particle emissions escaping from the brake enclosure during tyre tests.

It should be noted that testing was performed on a two-wheel drive dynamometer, so braking forces on the measured tyre would be 50% on each front wheel rather than approximately 35% on each front wheel, when braking forces are split ~70% front and 30% rear during 4-wheel braking. As a consequence, emissions factors could be potentially 30% lower than quoted here. In addition, the influences of cornering, lower or higher tyre pressures and wheel alignment on wear and emissions were not studied in this work, and all could lead to higher emissions factors.

10.4.2 Tyre wear emissions measurements in the VATF

Testing was moved from the work to the VATF where the roller could be coated with a hard-wearing textured surface to promote emissions, and the brake enclosure was continuously evacuated during testing to eliminate the possibility of particle leakage. A total PN4 measurement without dilution was added to evaluate emissions of sub 10nm particles.

Tyre background measurement concentrations showed that some instruments' responses were consistently well above background levels (APC10, PN4), some were just above (e.g., cold MPEC) and others close to or below background levels (hot MPEC and eFilter). Backgrounds were inconsistent and could be seen to vary substantially between pre and post-test measurements. It was not possible to confidently understand if any background collected was representative of that experienced during a test, and so generally no backgrounds were subtracted or sampled.

10.4.3 Mass-based tyre wear rates

Mass based tyre wear rates indicated that losses may be greater from 18" tyres than from 16" tyres from the same manufacturer and matched specification. Tyre wear was measured only from the front wheel on the driver's side. Highest emitting tyres showed approximately 120 mg/km emissions, while lowest emitting tyres were closer to 20 mg/km. High-end emissions were above recent literature values, but it should be noted that tests were performed on a 2-wheel drive chassis dynamometer so higher braking forces would be experienced at the front wheels than from the same vehicle when tested on the road. There did appear to be variations in mass emissions rates between products from different tyre manufacturers.

Accumulated mileage showed a large effect on mass-based tyre emissions rates. On the same tyre type with approximately 1000, 12,000 and 23,500 km ageing, the two higher mileage tyres emitted approximately 1.1 and 3.3 g/km of material, the highest emission rate being ~300 times higher than seen from the lowest mileage tyre. The mass emission rate appears to accelerate with at higher mileages.

When different 18" tyres (with elapsed mileages of ~ 1000 km or below) were compared, there was a wide spread of emissions rates, approximately 20 mg/km to ~115 mg/km. There was no correlation of mass emissions rates with tyre fuel economy ratings, and in fact the lowest wear rate was seen from the tyre with the lowest fuel economy rating.

Average tyre wear mass rate, including all 16" and 18" tyres with ~1000 km or lower elapsed mileage, was 65.8 ± 45 mg/km.

10.4.4 Tyre tread wear rates

Tyre tread wear determination, based upon tread depth measurements, was performed on the same tyres. Comparative treadwear depth measurements indicated that two of three pairs of tyres showed more tread wear from the 16" variant than from the 18" variant. Differences of 30% and 65% were seen. The other pair of tyres showed much lower wear from the 16" tyre, and it is suggested that this might indicate a formulation difference between the two tyre sizes from this particular manufacturer.

Increased mileage had a similar effect on tread depth loss rate as it had on tyre mass loss. From 1000 to 12,000 to 23,500 kilometres, wear rates increased from 0.2 µm/km to 2.3 µm/km and reached 5.9 µm/km at the highest mileage. Wear rate at the highest mileage was approximately 30 times that at the lowest mileage.

Tread wear rates of 18" tyres at mileages of ~1000 kilometres or less were in the range 0.2 to 0.6 µm/km. The tyre showing the highest tread depth wear rate showed the lowest mass wear rate. This may indicate that the tyre is composed of a lower density rubber compared to the other tyres.

10.4.5 Real-time tyre emissions profiles

Real-time tyre emissions results from one test showed highest emissions from the PN4 measurements, with peaks of emissions corresponding to aggressive braking events and high-speed cruise operation. Both the cold MPEC and the APC10 showed corresponding emissions events but at substantially lower levels. Results indicated that from a PG42 test, the emissions reported from the APC10 (non-volatile PN10) were about 1% of PN4 levels, while emissions from the cold MPEC (total PN10) were about 10% of PN4 emissions.

10.4.6 Test sequence and test order effects

The position of the test cycle within a day's sequence—whether first, last, or any other—had no noticeable impact on per km emissions of volatile or non-volatile particle numbers, or on mass.

There was no evidence of a consistent trend in either increasing or reducing (mass or number) emissions across a days' testing. This suggests that emissions from the different cycles can be viewed in isolation without needing to account for any influence of the previous cycle(s).

10.4.7 Potential evolution of the chassis dyno roller surface with time

The possibility of evolutionary trends between repeat cycles was also investigated. This was studied by reviewing the results of the 3 consecutive PG42 cycles from all tyres tested. There were no obvious test order trends in the PN data, but there was an apparent trend in $PM_{2.5}$ data. PM emissions decreased consistently between the first test and the subsequent two tests. Potentially, this is related to the warm-up of the tyre inhibiting the release of larger more massive particles, while not impacting the smaller volatile and non-volatile particles that dominate the particle number emissions. This would suggest that multiple short cold trips could have a higher overall $PM_{2.5}$ emission that the same overall distance driven in a single trip.

Repeat measurements of triplicate PG42 cycles on a designated wheel and tyre were performed at intervals throughout the tyre emissions test programme. These extra measurements were included to monitor whether ageing or wear of the textured surface was impacting results. No discernible time-related drift in PN or $PM_{2.5}$ emissions was observed.

10.4.8 Effects of tyre properties on PN and $PM_{2.5}$ emissions

When comparing emissions of PN and $PM_{2.5}$, produced over various drive cycles and between matched 16" and 18" tyres, there was no clear effect of tyre size observed.

Similarly, there were no clear-cut effects of different tyre mileage on $PM_{2.5}$ or PN emissions, excepting the possibility that higher tyre mileages may lead to a reduction in PN4 and PN10 volatile particle number emissions.

When comparing tyre manufacturer and design effects on emissions of 18" tyres, the summer tyre W4, with its harder compound and specific formulation, was seen to have lower emissions of both PN10 (solid and total) and PM compared to other tyres. In contrast, the all-season tyre W7, designed to provide good grip even in substantial snow, is likely softer and may produce higher PN and $PM_{2.5}$ emissions. However, these comparisons are based on limited data, and the observed differences may not be significant.

10.4.9 Bespoke cycle testing

Bespoke cycle testing enabled clear visualisation of individual braking events, particularly with PN4, where acceleration, braking and cruise emissions were observed. Braking from a high speed to a lower speed showed lower particle emissions than when braking all the way to rest. There also appeared to be higher tyre particle emissions when braking from a given speed (e.g., 30kph) to rest when the tyres were hot, than when tyres were cooler. However, there were no clear differences between tyre sizes, mileage or manufacturer/design in emissions of PN or $PM_{2.5}$.

Some anomalous emissions profiles were observed during tyre testing over bespoke cycles. These contributed to the difficulties of comparing bespoke cycle emissions between tyres. The anomalies manifested as large emissions events that weren't obviously correlated with drive cycle events. When one tyre showing a bespoke cycle featuring an anomaly was repeated, another anomaly was observed. It is considered possible that effects were not related to background variation and instead indicate that total PN4 and PN10 emissions characteristics of certain tyres may be unrepeatable and unpredictable.

10.4.10 Tyre wear emissions factors

Typical tyre emissions factors for the most reliable metrics used in this project, excluding bespoke cycle results, indicated that non-volatile PN10 emissions from tyres were of the order 5×10^9 #/km $\pm$ 44%, total PN10 emissions were ~1.1×10^{10} #/km $\pm$ 76% and Total PN4 emissions were approximately twice those of PN10, at 2.1×10^{10} #/km $\pm$ 48%. $PM_{2.5}$ emissions were well below 1 mg/km, and highly variable, at ~0.19 mg/km $\pm$ 103%.

10.4.11 Collected PM filter masses

The masses collected on PM filters used for gravimetry varied significantly. The highest masses, ranging from 0.871 mg to 2.107 mg, were typically collected from the first PG42 cycle or bespoke cycles. In contrast, the lowest masses, between ~25 µg and ~54 µg, came from various cycles. Out of approximately 110 filters, only six had masses above 1 mg, while 25 had masses below 100 µg. Most filters appeared completely white, suggesting the collection of single particles smaller than the visible threshold (~50 µm to 70 µm) or retention of gas phase and semi-volatile materials at low concentrations.

10.4.12 Size distributions of supermicron tyre wear granules

The size distributions of supermicron tyre wear particles were determined using sieving granulometry, which separates particles by physical diameter using sieves of various mesh sizes. Tyre wear samples from each location were divided into 10 size fractions, ranging from particles smaller than 53 µm to those larger than 2.8 mm. A lower limit of 2.5 µm was assumed for the smallest fraction due to the minimal $PM_{2.5}$ mass detected gravimetrically (~0.2 mg/km). These size fractions were used to plot particle size distributions, revealing similar patterns across all sampling locations, with modes at approximately 53 µm, 250 µm, and 600 µm.

10.4.13 Relationship between PN4 emissions and tyre temperatures

PN4 emissions were observed to contain a large proportion of volatile particles, and as such were used as a benchmark for studying whether average tyre temperatures influenced emissions levels. No obvious relationship between higher average drive cycle tyre temperatures and higher PN4 emissions concentrations was observed.

11. PARTICLE REDUCTION DEVICE EVALUATIONS

11.1 BRAKE PARTICLES

The Tallano "TAMIC" system was installed and tested during the last two weeks of October 2024. Testing was undertaken in the VATF.

11.1.1 Tallano TAMIC System

The Tallano "TAMIC" system is a brake particle reduction technology intended for applications including light-duty vehicles. The device aims to reduce particle emissions released from the braking system during brake applications. The TAMIC system components must be integrated directly into a vehicle's braking mechanism. It comprises a collection module, suction system, and filtration unit. During braking, friction between the brake pads and rotors releases particles, which the TAMIC system captures in real-time. In the primary intermittent operational mode, capture of particles is actuated by a signal from the vehicle. In the tests at Ricardo this signal was provided by the identification of current flow to the brake lights. In a second mode, the vacuum operates continuously. The system employs a vacuum to redirect particles from the brake pad contact area, which is specially machined and profiled to direct particles, to the vacuum system where they are sent to a filter contained in an aluminium vessel. The filter has high efficiency for collecting particulate material over a wide particle size range.

During intermittent mode, the TAMIC system has a spin-up delay time for the sampling vacuum that follows the initial braking signal, a period of collection of particles, and then a spin-down period.

11.1.1.1 Brake pads employed

The brake pads used in the evaluation of the TAMIC system at Ricardo were P3, previously tested on the VW Caddy in the main brake wear test programme. These were sent to Tallano for modification and compatibility with the TAMIC system. The modifications made can be seen in Figure 11-1.

The slot in the front face of the pad is positioned near the trailing edge to capture particles as they leave the contact area, carried by the rotation of the disc.

The previously tested P3 pads were employed so that the data from their original testing could be used as a baseline to assess the impact of the TAMIC device. P3 pads were selected because they showed roughly median emissions levels of all pads tested on the test cycles to be evaluated, and the original test data was very repeatable. In both the original test work and the TAMIC evaluation, P3 was tested with disc 1 (D1) to ensure best comparability of data.
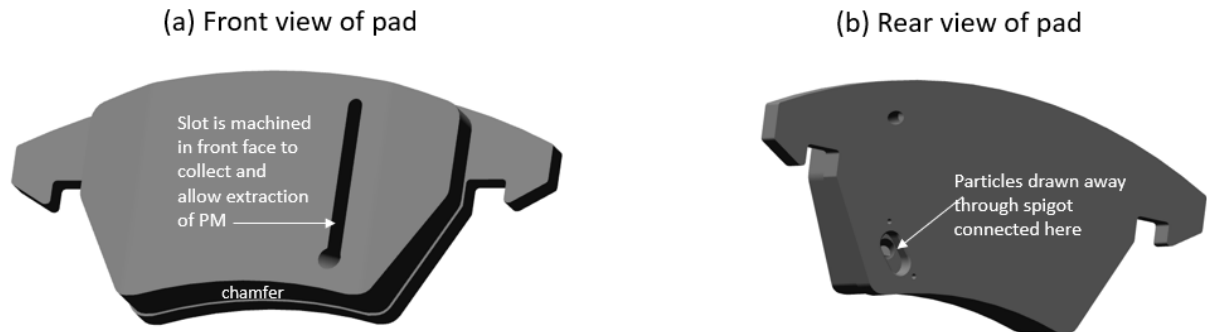

Figure 11-1: 3d CAD drawings of the a) front and b) back views of the P3 pads employed in this project (Courtesy of Tallano)

11.1.2 Installation

The TAMIC system was installed on the VW Caddy during the penultimate week of October, during a short visit by Tallano engineers. The initial tasks were to fit a pair of machined pads to the driver's side wheel - that was also fitted with disc 1 – and to assemble the modified, new calliper fist with the existing calliper elements, including the rubbing thermocouple (Figure 11-2). A few modifications were necessary to these components to ensure proper fitment. These were carried out in the workshops at Ricardo.
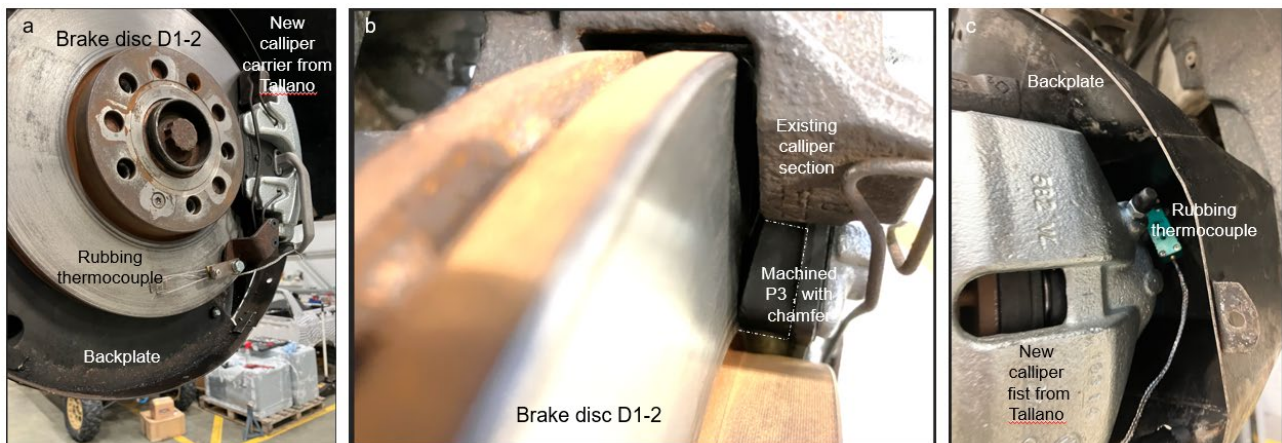
Figure 11-2: a) backplate, b) brake disc, c) calliper, machined pad and rubbing thermocouple.

The two pads were each modified by Tallano with "evacuation spigots" (Figure 11-3a) from which brake wear particulate materials were removed and transported to the filter element. The existing sampling system backplate was drilled by Ricardo away from the existing plumbing of the Ricardo sampling system (Figure 11-3b), to enable the evacuation spigots of the two P3 pads to connect to a pair of evacuation lines transporting the collected particulate materials to the filter (Figure 11-3c).

Figure 11-3: a) rear of pad P3 with evaluation spigot, b) backplate with inlet and outlet lines c) spigot evacuation lines.

The evacuation lines and the sample-out line of the Ricardo sampling system are routed under the vehicle and up into the body (Figure 11-4a), where they join the stripy black and yellow hoses of the TAMIC system, delivering the PM to the filter unit through the action of the TAMIC vacuum system (Figure 11-4b,c). The TAMIC system is set into two user selectable modes: nominally intermittent – where the vacuum acts in a pulsed manner - and continuous - where the vacuum is constantly active - by the laptop controller (Figure 11-4c). The black sample-out line exits the vehicle and delivers the aerosol sample from the enclosure, minus the fraction removed by the TAMIC, to the measurement trolley (Figure 11-4b).
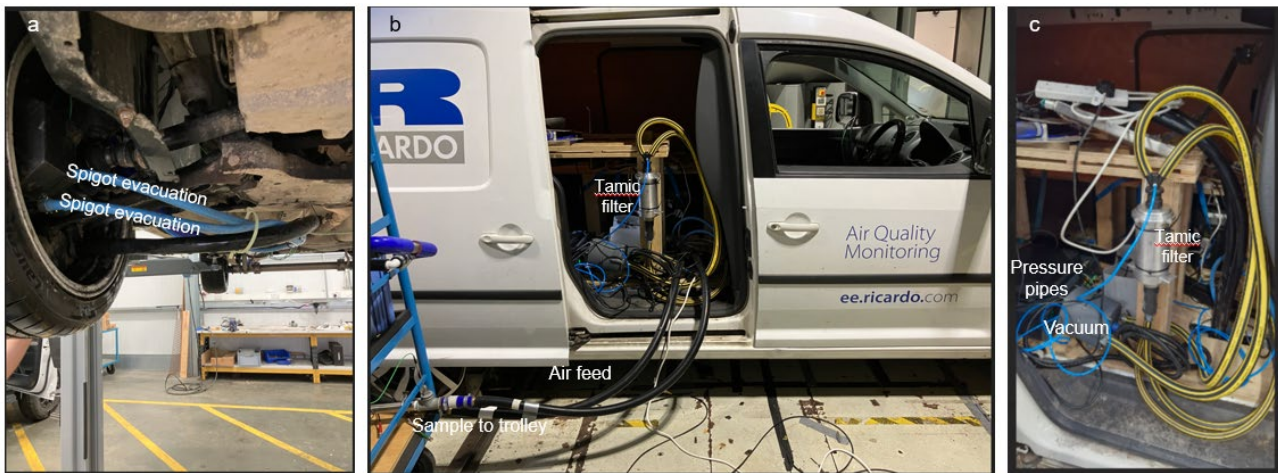
Figure 11-4: a) transport of the PM removed by TAMIC, b) the filter unit, and c) the aerosol sample to the trolley.

The measurement trolley includes all the sampling system pumps and filters to move filtered air into the enclosure and send the sample back for analysis by the various instruments (Figure 11-5a). The two MPECs and the eFilter are also mounted on the trolley, while the DMS500 and APC10 are positioned on the floor nearby (Figure 11-5b).

Figure 11-5: a) sample trolley, b) floor-based measurement instruments, and c) TAMIC laptop.

11.1.3 Experimental Approach

Following installation of the TAMIC device, testing was performed on the chassis dynamometer in the VATF. Testing included both intermittent and continuous modes of operation, with the focus being the primary intermittent mode. The initial plan was to conduct the tests summarised in Table 11-1 and compare them with the data from the original test project results from pad 3 with disc 1 (P3D1). Original P3D1 data comprised 3 x PG42 repeats and 1 x dyno RDE repeat.

Table 11-1: Original planned testing of the TAMIC system.

	Set#1	Set#2	Set#3
PG42#1	TAMIC intermittent (1)	TAMIC continuous (1)	TAMIC intermittent (3)
PG42#2	TAMIC intermittent (2)	TAMIC continuous (2)	TAMIC intermittent (4)
Dyno RDE 1825kg	TAMIC intermittent (1)	TAMIC continuous	TAMIC intermittent (2)

From initial test results it appeared possible that there was an evolutionary trend in the initial pair of PG42 results that may have arisen from the reinstallation of the pads conducted by Tallano. This may have temporarily altered the contact characteristics of the pad and disc surfaces compared to the original P3 measurements. Consequently, some additional tests were performed to evaluate stability of emissions, as shown in Table 11-2.

Table 11-2: Final testing of TAMIC system.

	Set#1	Set#2	Set#3	Set#4
PG42#1	TAMIC intermittent (1)	TAMIC continuous (1)	TAMIC intermittent (3)	TAMIC intermittent (5)
PG42#2	TAMIC intermittent (2)	TAMIC continuous (2)	TAMIC intermittent (4)	TAMIC intermittent (6)
Dyno RDE 1825kg	TAMIC intermittent (1)	TAMIC continuous	TAMIC intermittent (2)	[-]

Measurements were made using the same instrumentation employed during the earlier brake system evaluations, including the testing of P3. Instrumentation and metrics are summarised in Table 11-2.

- The eFilter was employed to provide an indicative real-time $PM_{2.5}$ cumulative mass emissions signal, and a filter-based $PM_{2.5}$ measurement.
- The APC10 provided a non-volatile PN10 measurement, while the hot MPEC provided a similar measurement, but using an evaporation tube rather than a catalyst to eliminate volatiles.
- The cold MPEC provided a total PN10 measurement, including both volatile and non-volatile particles, while the DMS500 provided a particle size distribution in the $PM_{2.5}$ regime.

Table 11-3: Instrumentation used during TAMIC Evaluations.

Metric	TTC evaluation
$PM_{2.5}$ (real-time & gravimetric)	eFilter
"Non-volatile" PN10	APC+ (PN10); hot MPEC+
Total PN10	Cold MPEC+
Particle size distribution < 2.5 μm	DMS500

11.1.4 Results

11.1.4.1 Initial PG42 results - repeatability

Repeatability from the various particle measurement instruments across the first 4 PG42 tests is shown in Figure 11-6. P3D1 represents the original brake emissions evaluation project's test results, and these are shown in dark blue (columns 1-3). This project's PG42 tests 1 and 2, from Set#1, are shown as columns 4 and 5 in purple and mauve and PG42 tests 3 and 4, from Set#2, are shown as red and pink columns 6 and 7. These can be identified as P3*T_int_D1, which identifies Pad 3 modified by Tallano tested in intermittent mode with disc 1. In Figure 11-6 the data from each instrument are normalised to the emissions value of the first P3 repeat (column 1). Note that there was a logging malfunction with the eFilter on PG42 test 1, so no data point is shown.

Results from all instruments and filter PM (eFilter real-time data excepted), appear to show emissions dropping from a peak with PG42 test 1 to test 2, and then stabilising with tests 3 and 4. The difference between the initial two PG42 tests is larger than the typical repeatability shown for P3D1. For this reason results from PG42 test 1 and test 2 (Set 1 in Table 11-1 and Table 11-2) were discarded and comparisons between P3D1 and P3*T_int_D1 made using tests 3 and 4 and two extra repeats: PG42 tests 5 and 6 (sets 3 and 4).
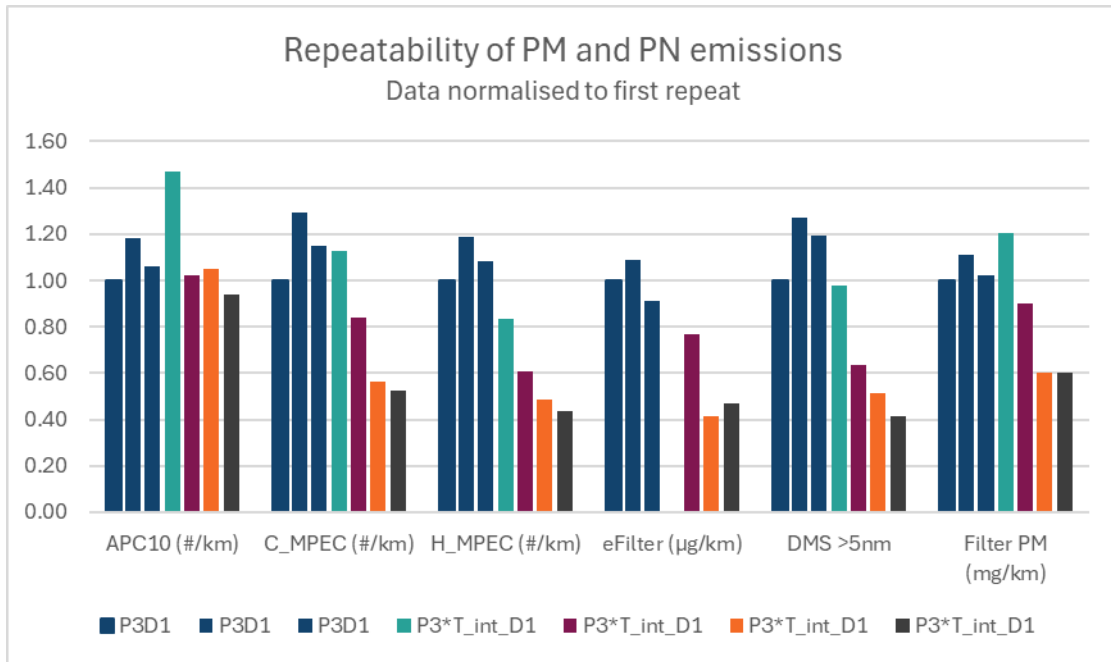
Figure 11-6: Repeatability of PM and PN emissions for 3 PG42 cycles, P3D1 and PG42 tests 1-4 in intermittent mode.

11.1.4.2 Extra PG42 tests – repeatability

Similarly normalised emissions data from P3D1 and PG42 tests 3 to 6 are shown in Figure 11-7. These show much improved consistency across tests 4-6, compared to test 1 and 2, indicating generally stable emissions from the tests with the TAMIC system. These data were then used, along with the P3D1 data, to evaluate the effect of the TAMIC system.
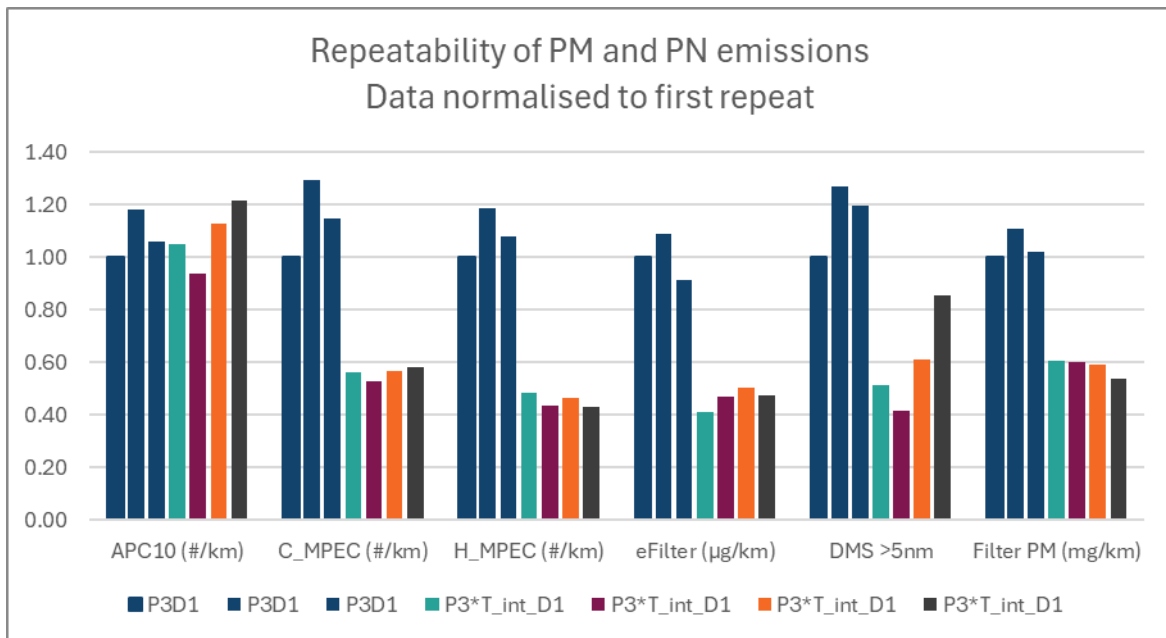

Figure 11-7: Repeatability of PM and PN emissions for 3 PG42 cycles, P3D1 and PG42 tests 3-6 in intermittent mode.

11.1.4.3 Effect of the TAMIC system from PG42 cycles under intermittent operation

Comparative particle number emissions from P3D1 and P3*T_D1 tests using APC10, hot MPEC, cold MPEC and DMS500 instruments respectively are shown in Figure 11-8a-d.

The CPC-based APC10 measurement does not show any obvious effect of the TAMIC system on non-volatile PN emissions, while the two MPEC systems and the DMS500 do indicate reductions in PN. Given that known particle losses in the hot MPEC would indicate ~20% lower emissions, and emissions from the cold MPEC are typically 40-50% higher than those of the hot MPEC, this does suggest a reduction in some volatile or semi-volatile materials with the TAMIC system. This may at least partially explain why three of the PN instruments indicate reductions with the TAMIC system, while the non-volatile APC10 does not. In particular, this might apply to the DMS500 results.

The other factor could be the presence of a relatively few large particles that are multiply charged in the P3D1 and TAMIC system results. These have a disproportionate impact on both PN and PM as measured by an electrometer, and if removal by the TAMIC system of the largest particles in the size regime <100nm, for example above 1 μm, is higher than removal nearer 100nm, then the charge-based measurements will indicate a stronger effect than the CPC-based instrument. This does seem to be case, as the particle size distribution from the measurements made with the TAMIC system are shifted to a smaller particle size (Figure 11-8a). Additionally, the ratio of the size distribution from the average TAMIC system results to the average P3D1 results (Figure 11-8b) decreases steadily above 100nm. Together these indicate fewer particles that will adopt large numbers of charges from the TAMIC system measurements, and these fewer charges likely result in reduced reported PN levels (and higher apparent removal efficiencies).

The DMS size distribution data shown in Figure 11-9a does appear to indicate an increase in particle emissions below ~65nm. These may be volatile particles that are able to remain free of the brake particle agglomerates with the TAMIC system due to a reduction in the surface area available for adsorption. These particles will have minimal effect of mass and the increase in this size range relative to P3D1 results is smaller than the reduction in the >65nm region.
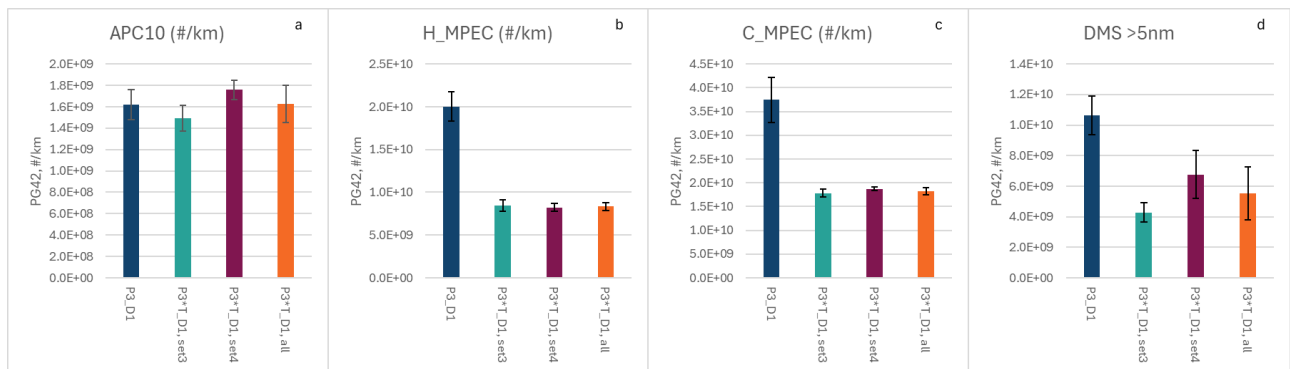

Figure 11-8: Comparative impacts of TAMIC system during the PG42 cycles in intermittent operation on particle number, measured by a) APC, b) hot MPEC, c) cold MPEC and d) DMS500.
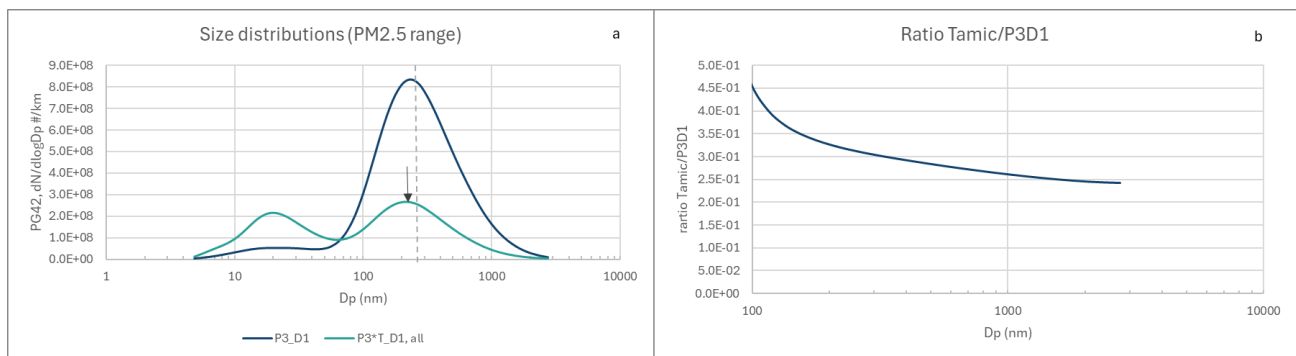

Figure 11-9: a) Size distributions and b) ratio of TAMIC/P3D1 for the PG42 cycles.

Both the charge-based eFilter measurement and gravimetric filter measurement indicate reductions in particulate mass with the TAMIC system (Figure 11-10a,b). The mass reduction mechanism is consistent with the removal of larger particles by the TAMIC system as described above.
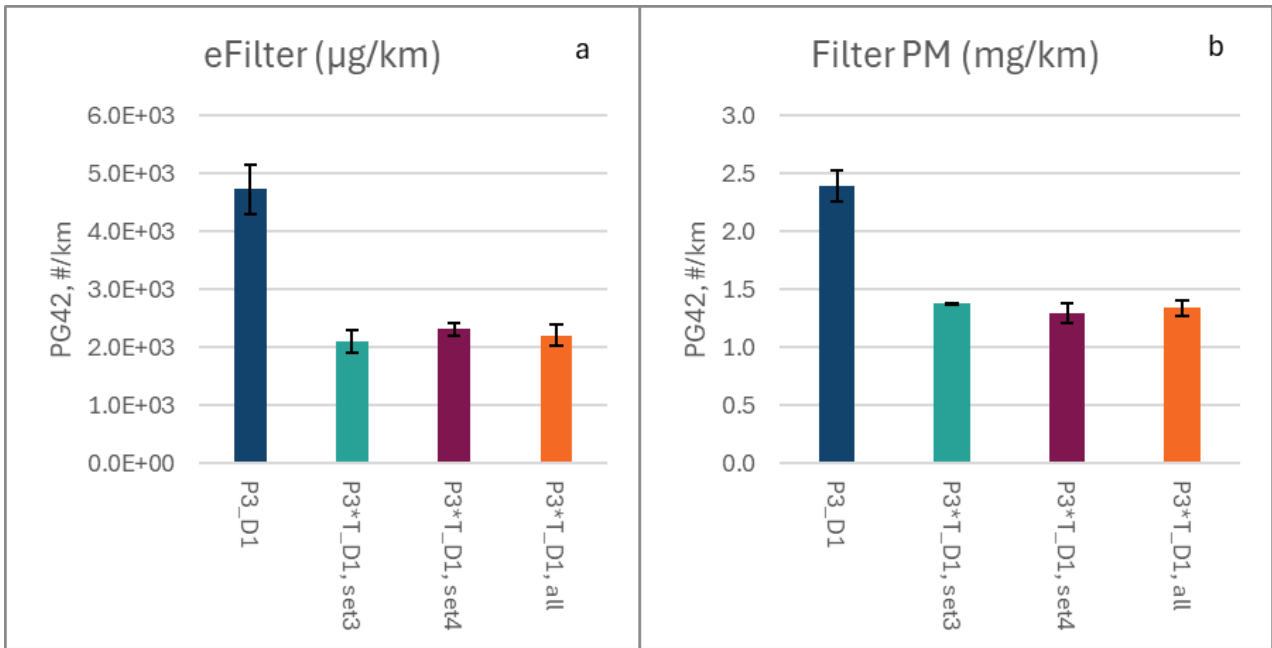
Figure 11-10: Comparative impacts of TAMIC system during the PG42 cycles in intermittent operation on particle mass, measured by a) eFilter real-time data and b) gravimetric PM.

Efficiencies for the tests for the intermittent TAMIC system operation during PG42 cycles are shown in Figure 11-11a, for total particle number and mass emissions and Figure 11-11b for size-related efficiencies.
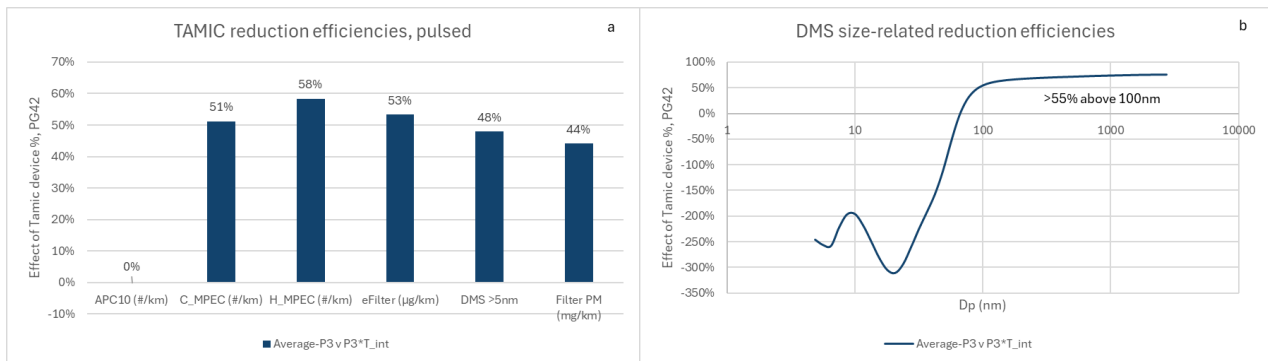

Figure 11-11: Efficiencies of the intermittent TAMIC system during PG42 cycles a) PN and PM emissions, b) size related.

Non-volatile PN emissions were not significantly reduced by the TAMIC system, although charge-based PN measurement systems reported reductions of 48-58%. Gravimetric $PM_{2.5}$ was reduced by ~44%, with the eFilter also showing reductions of that order. In addition, the size-related reduction efficiency of the TAMIC system appears to grow as particle diameter increases above 100nm, which might indicate higher reduction efficiencies for PM_{10} than reported here for $PM_{2.5}$.

11.1.4.4 Effect of the TAMIC system from PG42 cycles under continuous operation

To evaluate the continuous operation of the TAMIC system, the same three PG42 P3D1 test results, as were used for the intermittent operation, were compared with two TAMIC system PG42 tests. These two tests showed repeatability levels broadly similar to those of the P3D1 tests (Figure 11-12), and so were not considered to be substantially impacted by the evolutionary effect seen in the initial intermittent tests that preceded them in the test sequence.
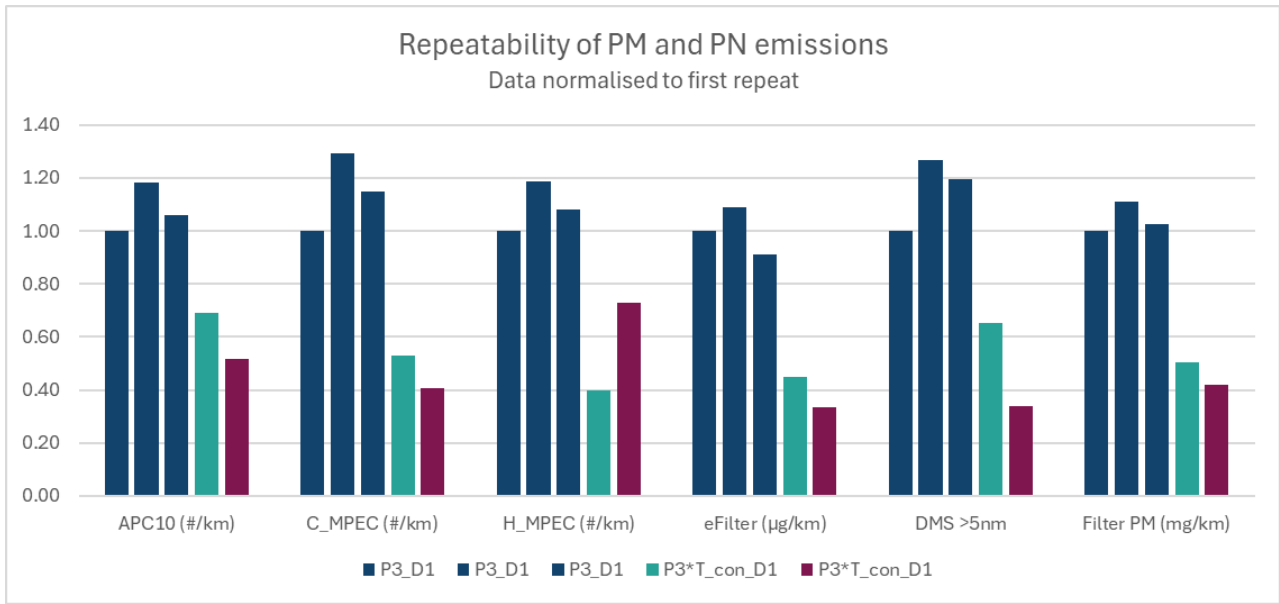
Figure 11-12: Repeatability of PM and PN emissions for 3 PG42 cycles, P3D1 and PG42 tests 1-2 in continuous mode.

Results with the TAMIC system were significantly lower (at one-standard deviation) than from P3D1 for all the PN instruments (Figure 11-13a-d), including the APC10 (Figure 11-13a). This indicates that the continuously operating mode of the TAMIC system may have improved capture ability for small non-volatile particles, when compared to the intermittent mode.
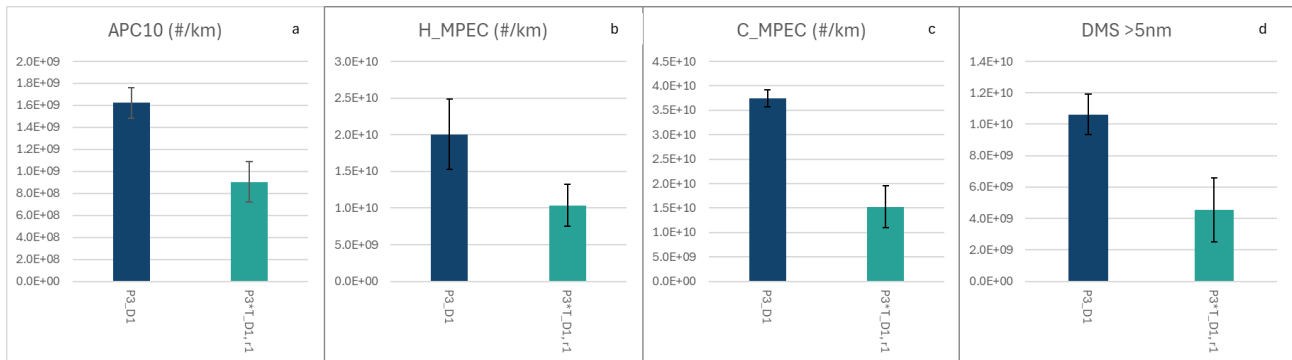

Figure 11-13: Comparative impacts of TAMIC system during the PG42 cycles in continuous operation on particle number, measured by a) APC, b) hot MPEC, c) cold MPEC and d) DMS500.

PM emissions were also significantly lower from the TAMIC system measurements than from the P3D1 data, with both real-time and gravimetric PM results showing a similar effect (Figure 11-14).
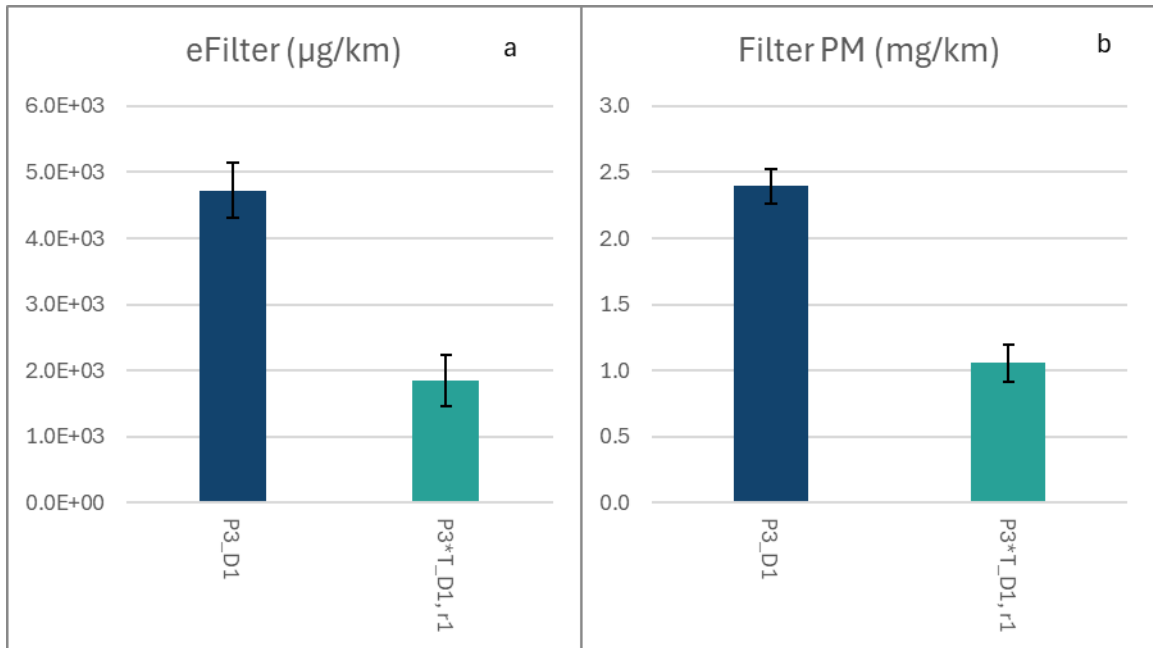
Figure 11-14: Comparative impacts of TAMIC system during the PG42 cycles in continuous operation on particle mass, measured by a) eFilter real-time data and b) gravimetric PM.

PN reduction efficiency was ~44% for the APC10 and 48% to 59% for the charge-based instruments (Figure 11-15a), with filter-based $PM_{2.5}$ reduced by 56%. Size-related reduction efficiencies in the region above 100nm were higher than recorded for the intermittent mode, at 70% or greater. Higher efficiencies were observed with continuous operation (con), when compared to intermittent operation (int), for almost all metrics from PG42 cycles (Figure 11-16).
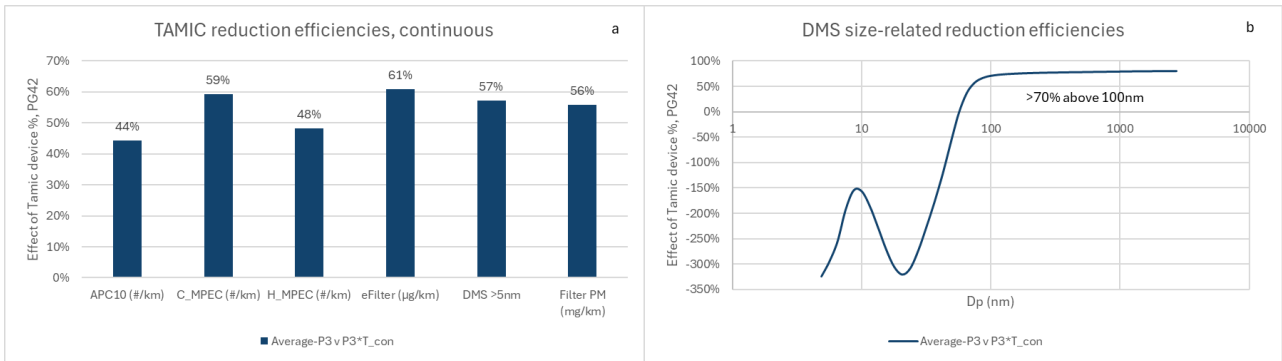
Figure 11-15: Efficiencies of the continuous TAMIC system during PG42 cycles a) PN and PM emissions, b) size related.
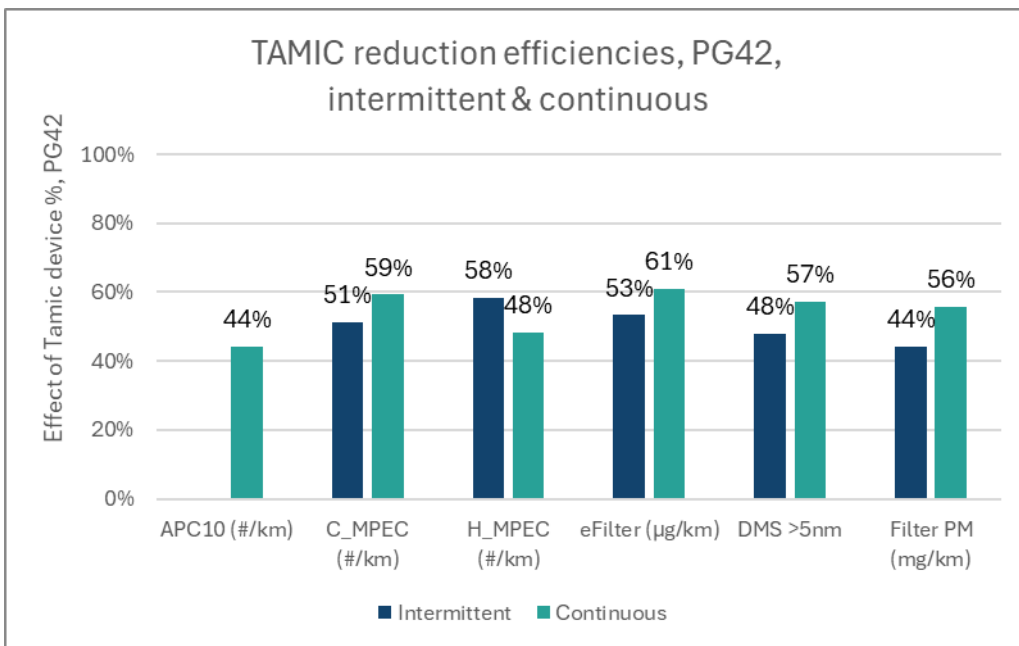
Figure 11-16: Comparative TAMIC system efficiencies during PG42 cycles, in intermittent and continuous modes.

11.1.4.5 Effect of the TAMIC system from dyno RDE cycles under intermittent and continuous operation

The effect of the TAMIC system during chassis dyno RDE tests was similar to that observed in the PG42 testing. Reduction efficiencies for intermittent and continuous operation are shown in Figure 11-17 and Table 11-4. These indicate the following:

- Consistently higher reduction efficiencies for both PN and $PM_{2.5}$ in continuous operation than for intermittent operation

- No reduction of PN10 in intermittent mode, and some reduction in continuous mode, but lower than the $PM_{2.5}$ efficiency

- Highest apparent filtration efficiencies measured by charge-based measurement approaches

Figure 11-17: Comparative TAMIC system efficiencies during chassis dyno RDE cycles, in intermittent and continuous modes.
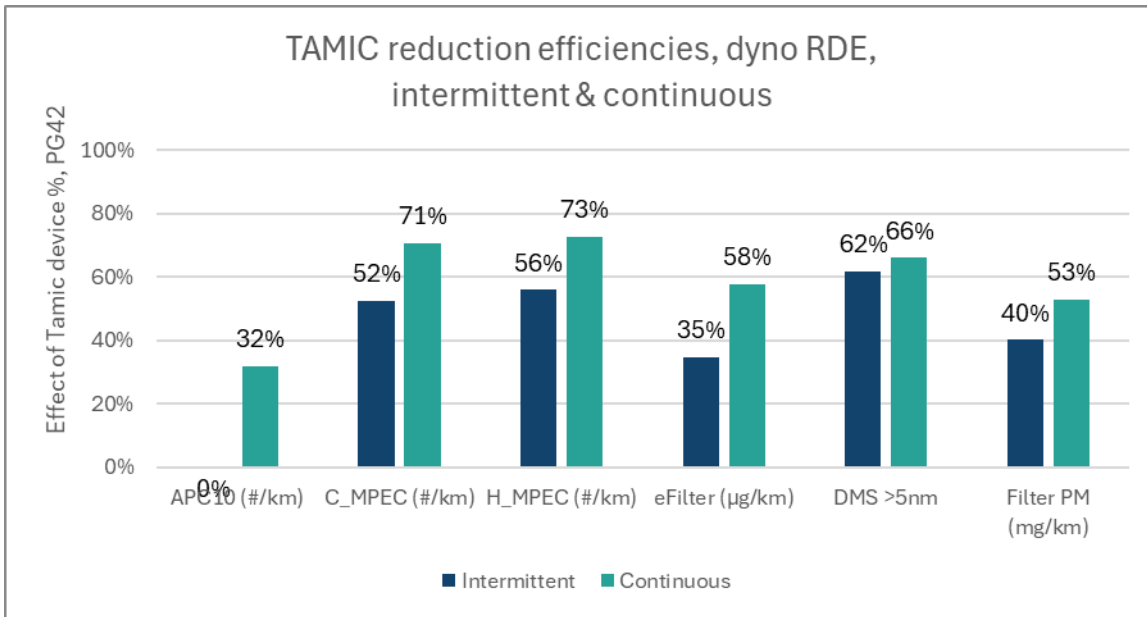
Table 11-4: Comparison of reduction efficiencies of the TAMIC system, measured in the intermittent and continuous modes.

Measurement	Average reduction efficiency in intermittent mode (%)	Average reduction efficiency in continuous mode (%)
APC10 (#/km)	0	32
Cold MPEC (#/km)	52	71
Hot MPEC (#/km)	56	73
eFilter (µg/km)	35	58
DMS > 5nm	62	66
Filter PM (mg/km)	40	53

11.1.4.6 *Consideration of the differences between intermittent and continuous TAMIC operation*

Continuous operation of the TAMIC system will capture emissions events that are missed by intermittent operation. For example, particles may be released outside the duration of a pad to disc contact event through residual heat and oxidation effects, through brake stiction and from vibration. In addition, the spin-up time of the vacuum (~1s) may mean that only ~50% of the duration of a 2s braking event will be efficiently sampled, and this may be slightly compromised by the need to clear the dead volume of the transfer system, although the dead volume will begin to clear as soon as the spin-up commences.

A comparison of 1Hz data between intermittent and continuous operation of the TAMIC (Figure 11-18) indicates a roughly consistent offset between the emissions of the two modes, with emissions from the continuous mode lower. It also indicates that there may be some slight brake drag present. While not noticeable to the driver, this slight touching of the pad and disc may lead to the generation of measurable levels of PN10, with a lesser effect on $PM_{2.5}$. The lack of vibration on the chassis dyno compared to on the road may delay, or inhibit, the brake system naturally correcting this drag.

Data from a highly transient part of the PG42 cycle between 250s and 550s (Figure 11-19) does indicate more pronounced double peaks in intermittent mode from some braking events, for example between 330s and 350s, which appears to be related to the driver's dual application of the brakes during the braking event.
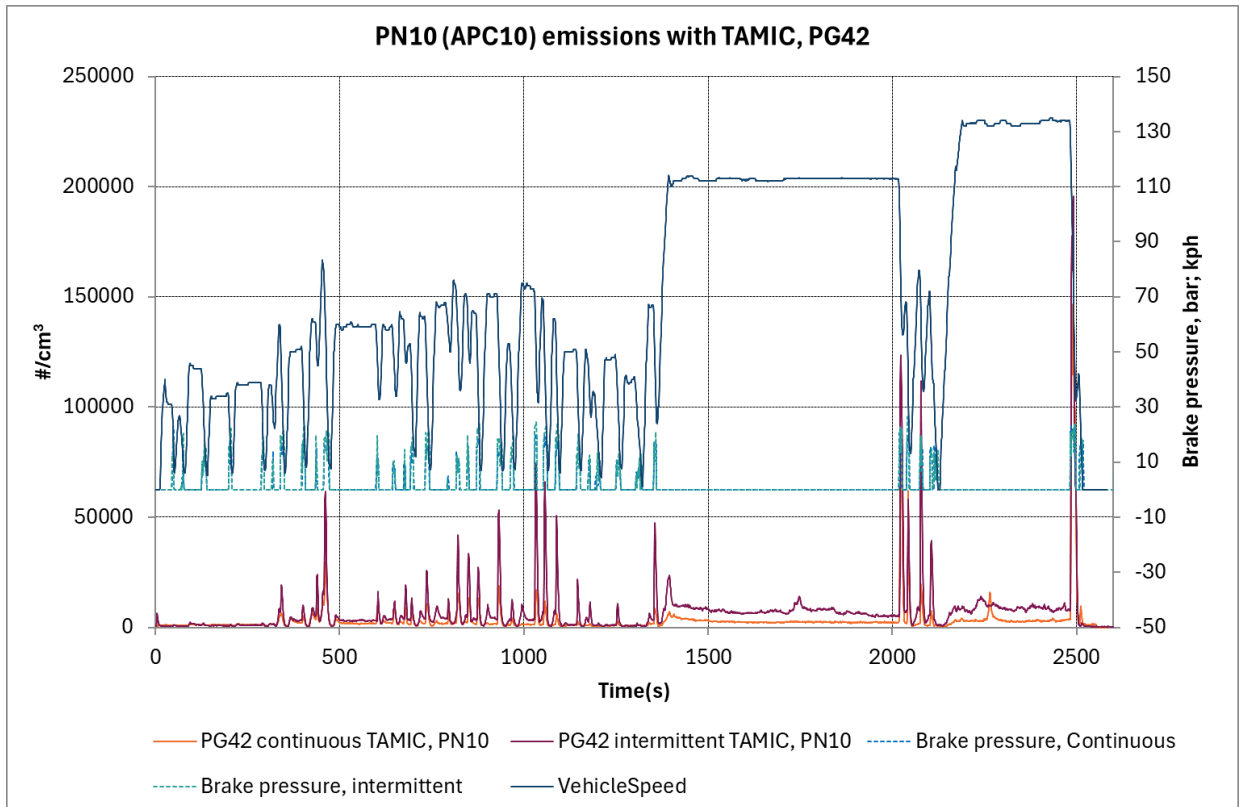
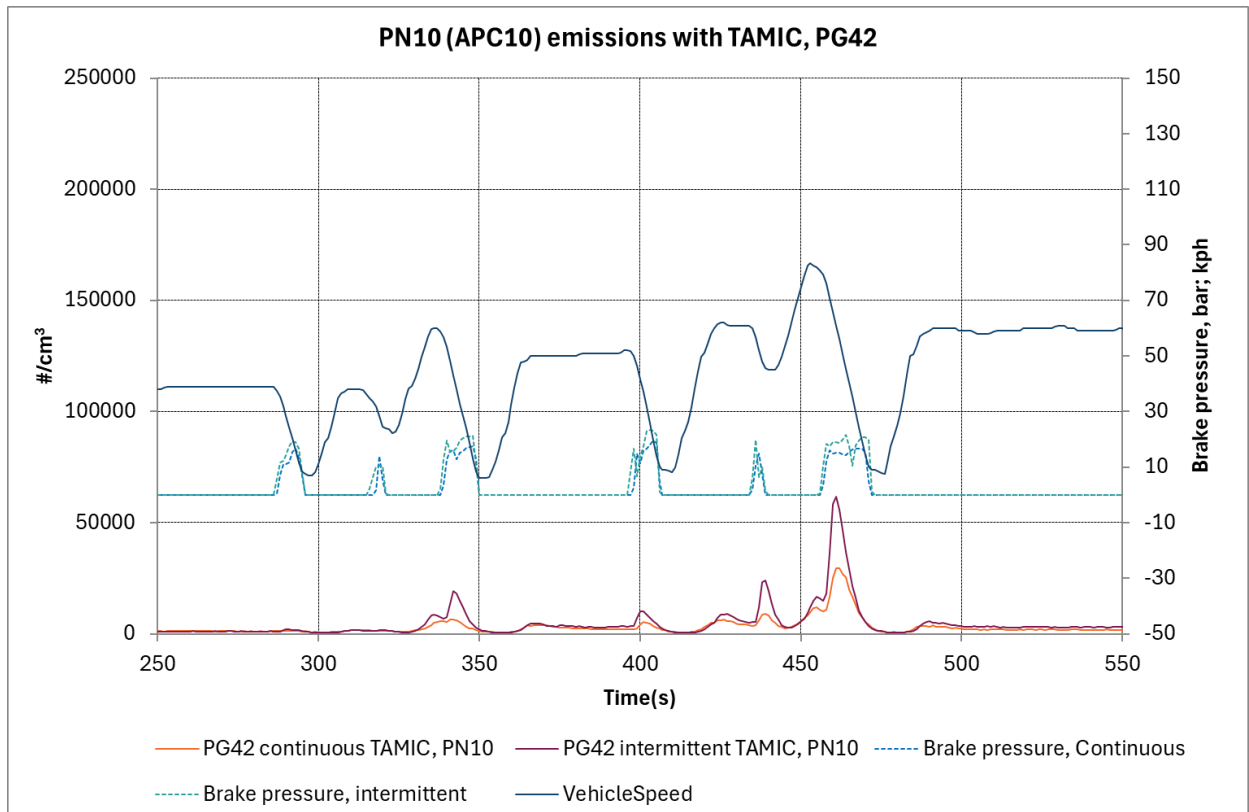Figure 11-18: PG42 cycle showing PN10 emissions from the TAMIC in Intermittent and Continuous modes.

Figure 11-19: PG42 PN10 emissions from the TAMIC in Intermittent and Continuous modes, 250 - 550s.

11.1.5 Outcomes of TAMIC evaluations

The TAMIC system had a consistent positive impact on gravimetric $PM_{2.5}$ emissions, with a greater effect observed in continuous mode than in intermittent mode. In intermittent mode $PM_{2.5}$ reductions were ~44% from PG42 cycles and ~40% from dyno RDE testing, while in continuous mode $PM_{2.5}$ reductions were ~56% and ~53% from PG42 and dyno RDE testing respectively.

Reductions in non-volatile PN10 emissions from the APC10 were not observed from either PG42 or dyno RDE cycles in intermittent mode, but the TAMIC system was able to reduce emissions by ~44% (PG42) and ~32% (dyno RDE) in continuous mode.

PN emissions were apparently reduced by much greater percentages in measurements made by the cold MPEC, hot MPEC and DMS500 systems. These reductions are likely a combination of the elimination of volatile/semi-volatile particles by the TAMIC system, and the positive impact of the TAMIC system in altering the particle size distribution so that the largest particles that carry the greatest number of charges are reduced. This shift in the size distribution to smaller sizes may have reduced the number of particles reported when testing the TAMIC system and leading to higher reported particle removal efficiencies.

Nevertheless, the TAMIC system demonstrates $PM_{2.5}$ reductions of above 40% in both operational modes and is able to reduce both PN10 and $PM_{2.5}$ by in excess of 30% in the more effective continuous mode.

In a recent publication, Tallano has observed background contributions to PN when assessing TAMIC on a brake dynamometer, and state that these should be subtracted to demonstrate highest possible particle removal efficiencies (Adamczak, 2023). No background subtraction was made in this study. Tallano also stated that brake drag between braking events maybe a reason for the efficiency difference between intermittent and continuous modes of the TAMIC. There is some evidence of this – brake particles being released on accelerations – shown in Figure 11-19 and a slightly elevated baseline of particle emissions during the long cruises of the PG42 cycle (Figure 11-18). Higher levels of particle emissions between braking events, in the TAMIC evaluation, would result in lower apparent TAMIC particle removal efficiencies, with a greater effect on PN10 than on $PM_{2.5}$, in both intermittent and continuous modes, and so efficiencies measured in this study should be considered as lower limits.

11.2 TYRE PARTICLES

The Tyre Collective device (TTC) was tested over three days between the 16th and 18th October 2024, on the chassis dynamometer in the VATF.

11.2.1 The Tyre Collective's device

The TTC device employs electrostatic plates, situated parallel to the incoming flow, to attract and capture naturally charged particles. These particles are released, and the charges generated, by the friction between the tyre and the road surface. On a vehicle, the TTC would be positioned in a location optimised to receive particles released from the tyre-road contact patch, to maximise capture. Consequently, a proportion of the tyre emissions will pass into the TTC, but not all the particles released from the tyre would necessarily be harvested.

In the evaluation at Ricardo, the TTC was placed in the sample line downstream of the sampling duct (Section 11.2.2), ensuring that all the particles entering the duct would pass through the TTC.

11.2.2 Installation

For testing, the TTC was installed at a location between the sampling duct and the measurement points in the sampling line, some way upstream of the sample tunnel fan, as indicated in Figure 11-20 (a modified version of Figure 3-9). The bypass air valve was fully closed. The existing sampling line was pre-equipped with v-band connectors to allow a component equipped with the same connector types to be simply added into the sampling line. Samples of the v-bands were supplied by Ricardo to the Tyre Collective, who 3d-printed interfaces for the inlet and outlet sides of the TTC - including suitable flanges to enable its inclusion in the sampling line.
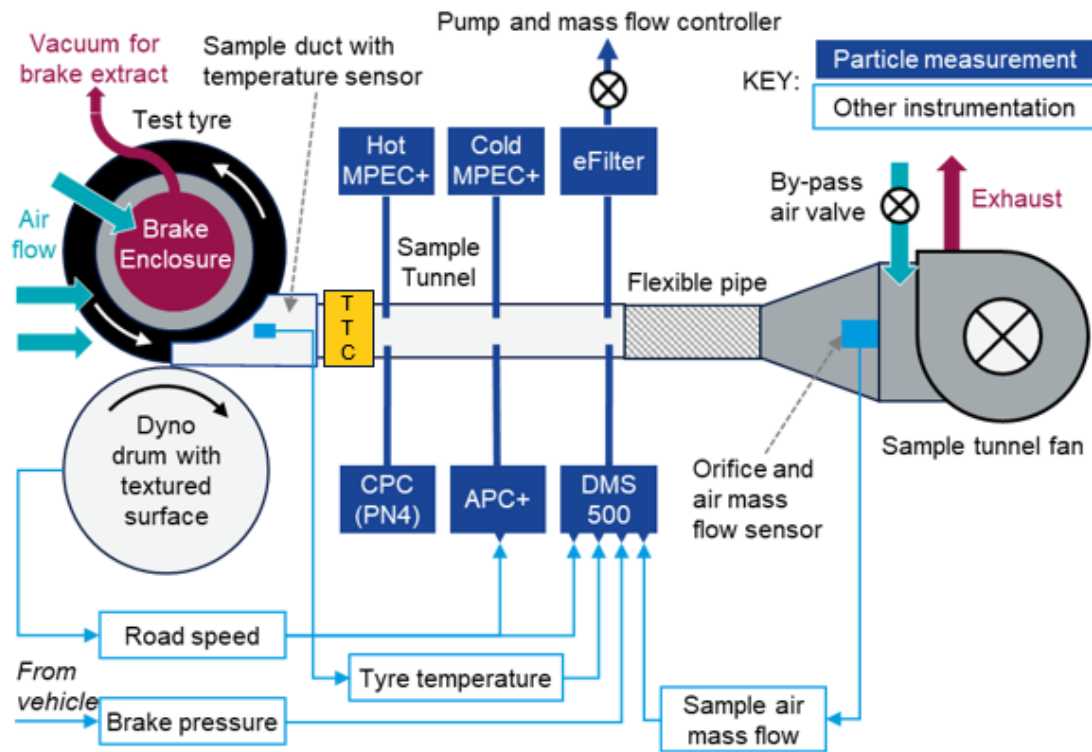
Figure 11-20: Tyre sampling system including TTC installation.

Figure 11-21: TTC installed in the sampling line with the test vehicle on the chassis dynamometer.

11.2.3 Experimental approach

Once placed in the sampling line, the TTC was checked and declared ready for testing. It was tested in active (powered-up; TTC ON) and inactive (powered-down modes; TTC OFF). During the three days of testing, nominally identical tests (excepting the operational status of the TTC) were performed over three repeat PG42 cycles and a single 1850 kg dyno RDE, as shown in Table 11-5. Together these tests represent ~200 km of driving. Between the third PG42 test and the dRDE test, the tyres were allowed to cool for 60 minutes.

Table 11-5: Tests performed to evaluate the TTC.

Test	Day#1	Day#2	Day#3
PG42#1	TTC-ON	TTC-OFF	TTC-ON
PG42#2	TTC-ON	TTC-OFF	TTC-ON
PG42#3	TTC-ON	TTC-OFF	TTC-ON
Dyno RDE (dRDE)	TTC-ON	TTC-OFF	TTC-ON

In addition to the emissions tests, background measurements were performed before and after each day's sequence of tests, with samples acquired for ~45 minutes to match the duration of the PG42 cycles.

The combination of tyre 12 and wheel 12 (W12) was used to evaluate the TTC, since this had shown highly consistent emissions over repeated PG42 tests during the main programme. In addition to comparing the TTC ON and TTC OFF modes, the main programme W12 data from the PG42 and dRDE were compared, since these represented a "non-installed" TTC data set. These earlier W12 results can be identified in later charts as W12_[18].

The instruments shown in Table 11-6 were employed for the measurements from emissions cycles and backgrounds. All instruments and ancillary devices such as pumps were located externally to the vehicle on a specially designed trolley. In addition, photographs of the TTC electrodes were taken following TTC ON (Day#1) and TTC OFF (Day#2) testing to visually assess the collection of particles during the day's testing. Electrodes were cleaned following each day's tests. At the end of Day#3 (TTC ON) Tyre Collective staff cleaned the electrodes with distilled water to remove and collect the particles.

Table 11-6: Instruments employed in the TTC evaluation

Metric	TTC evaluation
PM$_{2.5}$ (real-time & gravimetric)	eFilter
"Non-volatile" PN10	APC+ (PN10); hot MPEC+
Total PN4 and PN10	CPC-PN4; Cold MPEC+
Particle size distribution < 2.5 µm	DMS500

11.2.4 Results

11.2.4.1 Images of particle collection by TTC

A photographic image of the TTC electrodes following a day's testing with the TTC OFF is shown in Figure 11-22a, with a TTC ON result shown in Figure 11-22b. While the TTC OFF image shows clean electrodes with minimal collection of particles, the TTC ON image (Figure 11-22b) clearly shows that a substantial number of black particulates have been captured. This is consistent with large particles that carry natural substantial charges being attracted to the electrodes when the TTC device is active and flowing straight through the device when it is inactive.

To be visible on the TTC surface, these particles must be in the range 50 – 100 µm, or larger, as this is the lower limit of human eyesight. Given the wide scattering of the deposited material, it is unlikely that these particles are agglomerated materials and so would be single particles. These particles are at least an order of magnitude larger than the PM$_{2.5}$ emissions targeted in this study. It is possible that smaller particles are also collected but these would be invisible to the naked eye.
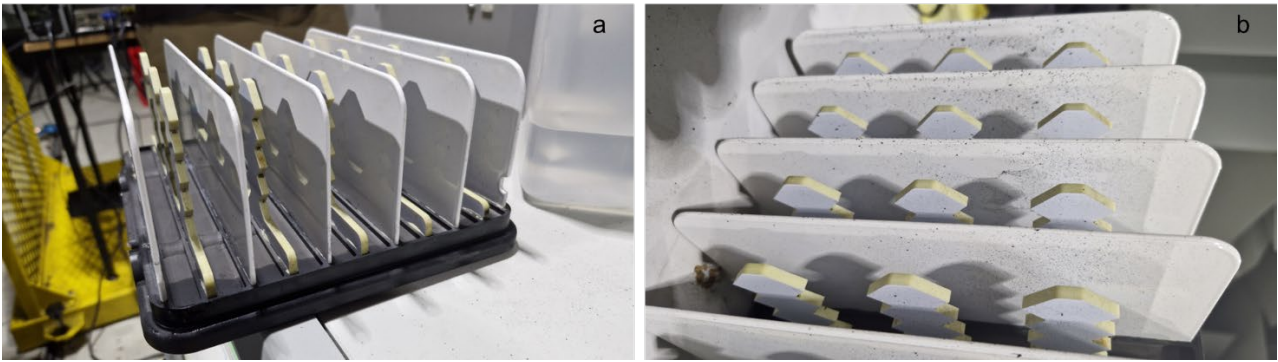
Figure 11-22: Images of electrodes following a) TTC OFF and b) TTC ON testing.

It can be assumed that the difficulty of charging particles is approximately inversely proportional to their surface area, given matched composition and surface characteristics. On this basis, it is 100 times more difficult to charge a 10 µm particle than a 100 µm particle and 10000 times more difficult to charge a 1 µm particle. Hence, when activated, the TTC would be expected to be much more effective at capturing particles in the range ~100 µm than for smaller ones such as in the PM$_{2.5}$ range.

11.2.4.2 Comparison of background and sample emissions

This section compares average particle emissions in particles/s (#/s) for number-based instruments and mass/s (µg/s) for the eFilter gravimetric and real-time data, adds commentary on the levels and consistency backgrounds sampled and presents a judgement on the suitability of subtracting backgrounds from the samples measured.

Figure 11-23 shows six backgrounds taken using the PN4 measurement system. It's apparent that while some backgrounds are relatively consistent across the sampling period, others show erratic particle levels. In addition, the background levels vary considerably, even between the pre-test (start) background and post-test (end) background.
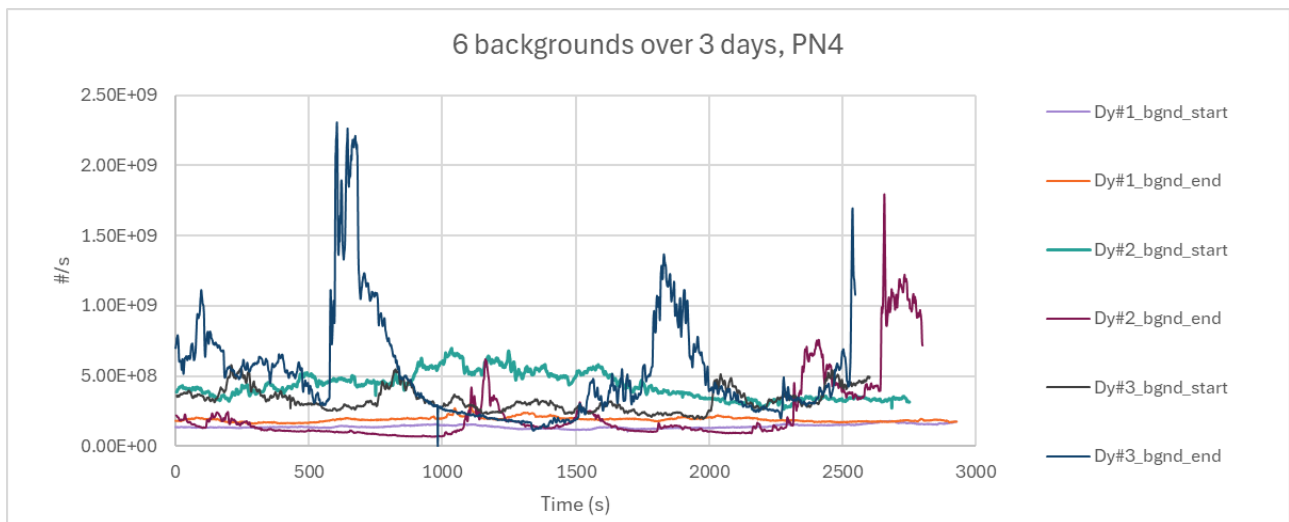

Figure 11-23: Six backgrounds measured by the PN4 instrument, collected over three days.

When background levels are compared with average particle emissions rates from PG42 and RDE tests (Figure 11-24), it's clear that test emissions from PG42 cycles are consistently above the background levels, but that dRDE emissions can be below background levels collected on the same day.
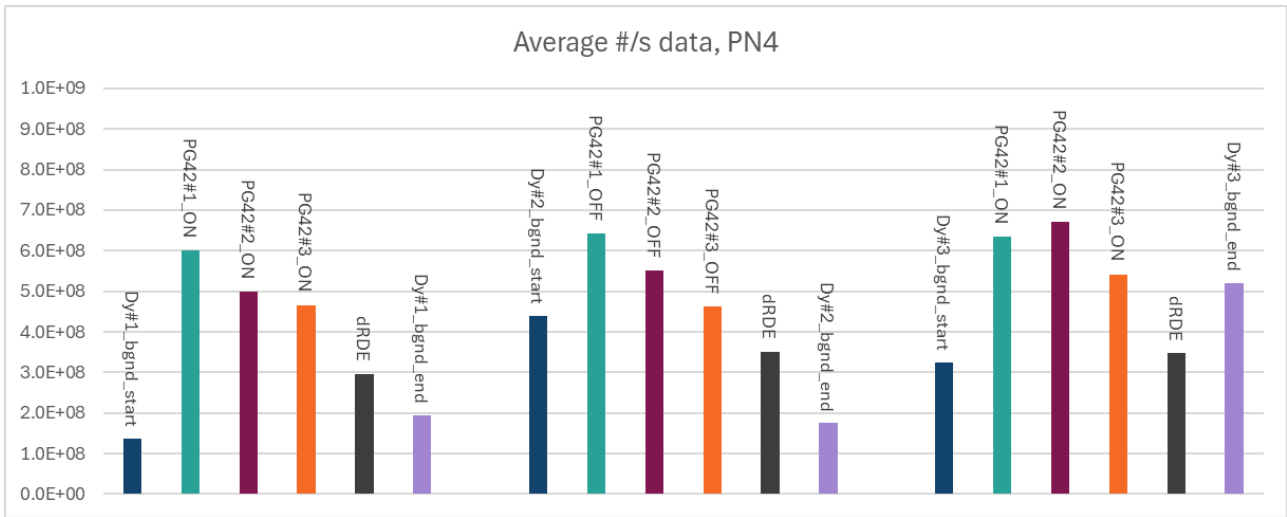
Figure 11-24: Comparisons of average concentrations measured by the PN4 instrument, from PG42 cycles, dRDE cycles and background measurements.

From PG42 tests there is a dominant peak of emissions present at around 2500s. This is a good indicator of whether emissions can be observed above background contributions and instrument noise. When real-time emissions are considered, for example comparing Day 1 and Day 3, backgrounds can be well below the levels of the samples (Day 1, Figure 11-25), but also show periods where background emissions peak and approach those of the highest point in the emissions cycle at 2500s (Day 3, Figure 11-26).
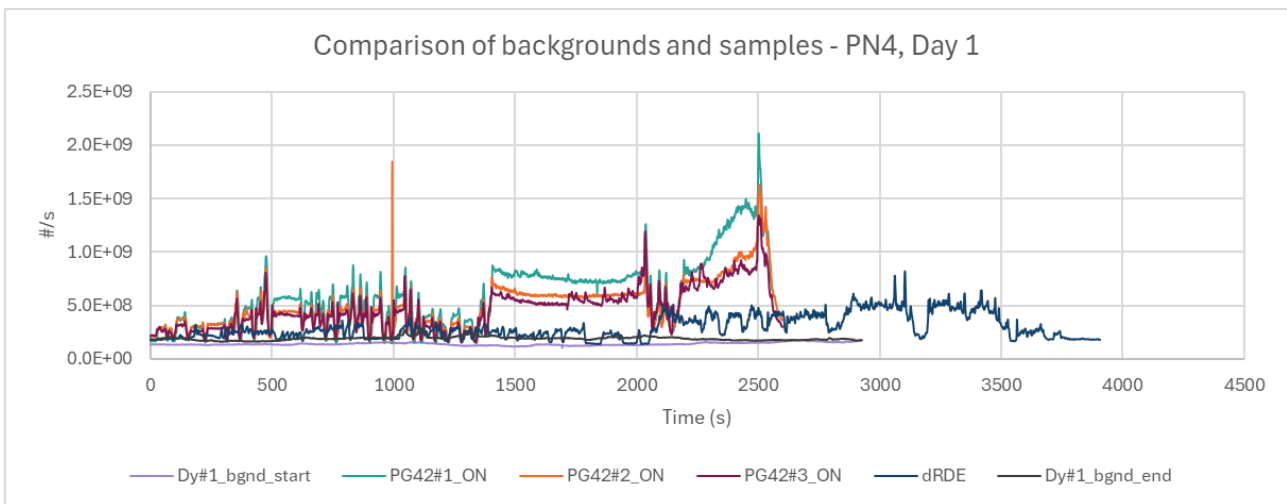
Figure 11-25: Real-time traces of PG42, dRDE and backgrounds from Day 1.
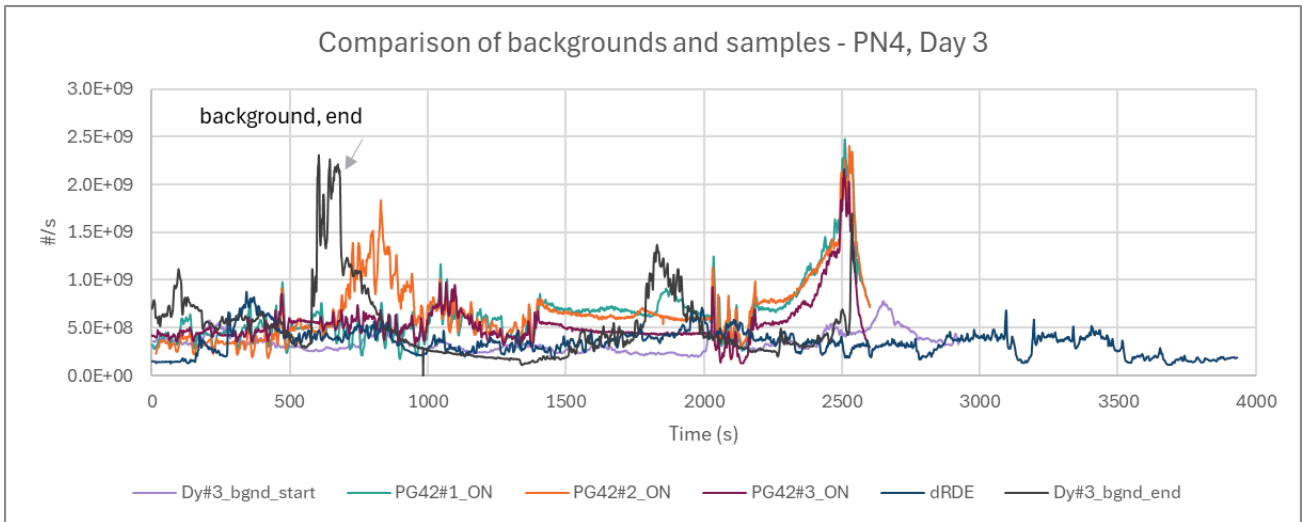
Figure 11-26: Real-time traces of PG42, dRDE and backgrounds from Day 3.

There was also a substantial difference between the initial background on Day 3 and the final background. This again highlights the issue that unless a background is sampled simultaneously with the test, and from a location that provides a representative sample of the air drawn in through the sampling duct to carry the tyre emissions to the measurement devices, it is impossible to know if the background is representative. Currently, it is not known what the source (or sources) of the particles that introduce variability is.

Backgrounds from other instruments showed similarly variable behaviour e.g., APC10 (Figure 11-27), cold MPEC (Figure 11-28) and hot MPEC (Figure 11-29), and these instruments did reveal that the high background at the end of Day 3 comprised both solid and volatile particles.
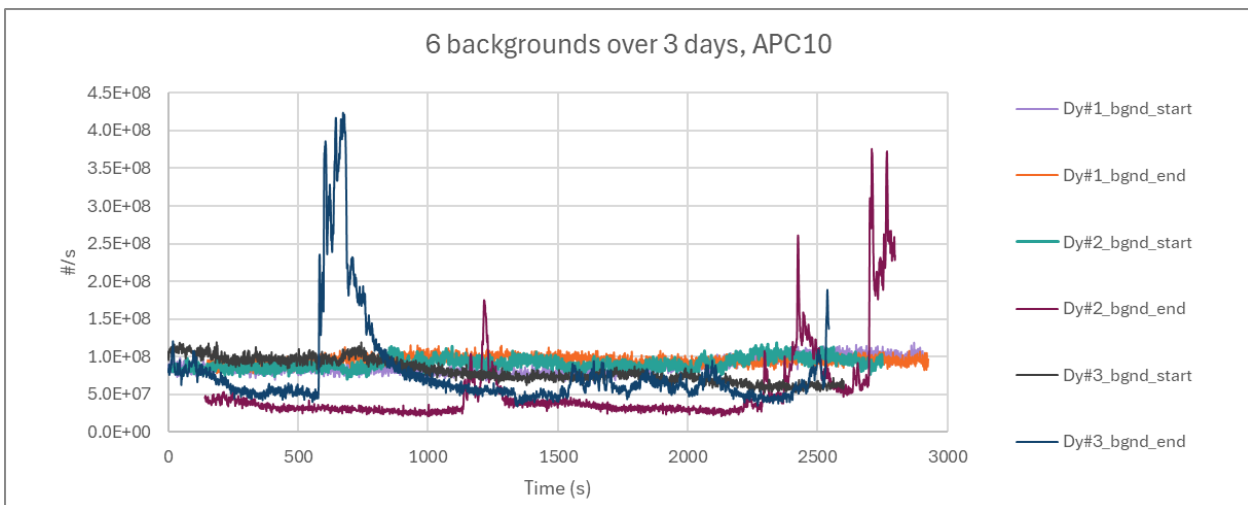
Figure 11-27: Six APC10 backgrounds collected over three days.
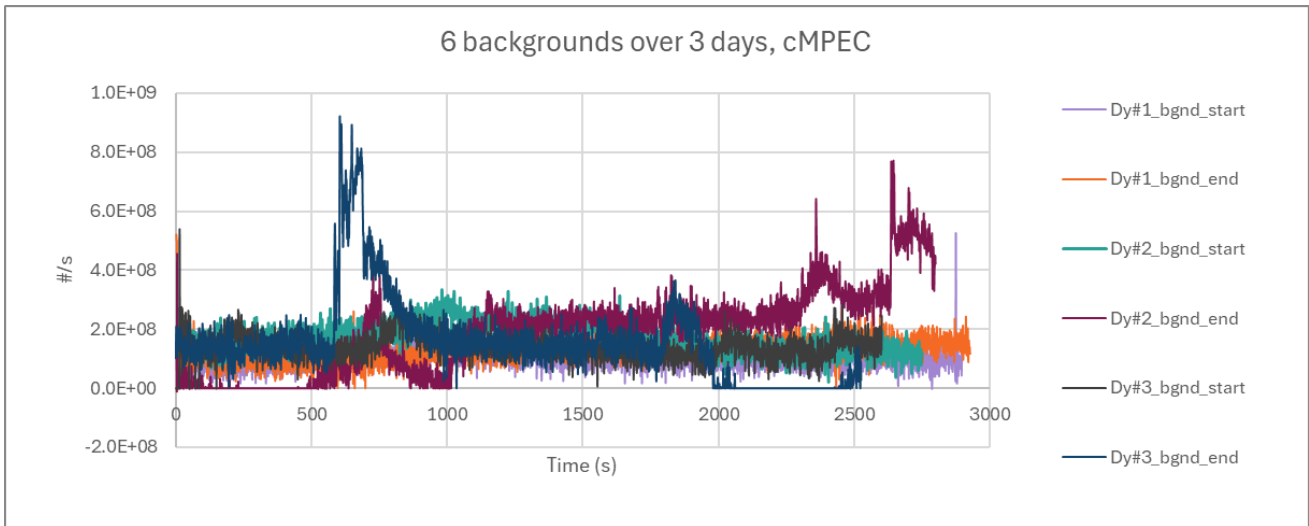
Figure 11-28: Six cold MPEC backgrounds collected over 3 days.
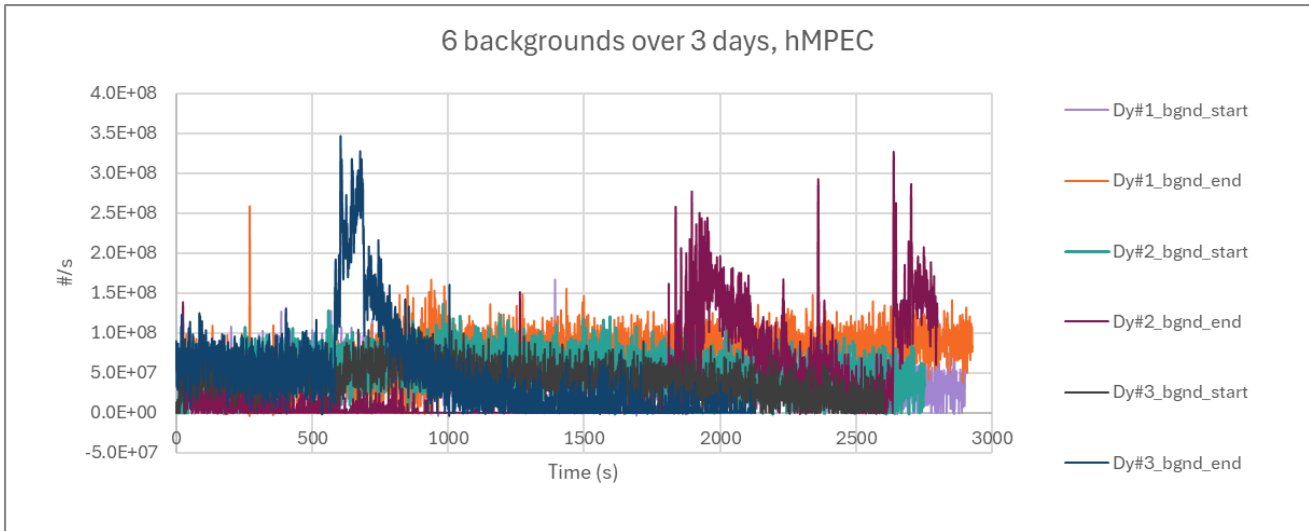
Figure 11-29: Six hot MPEC backgrounds collected over 3 days.

Comparative emission of APC, cold MPEC, hot MPEC and eFilter with backgrounds are shown in Figure 11-30. These figures show that almost all APC10 emissions are at or above background levels and more than half of cMPEC results are above background levels. However, relatively few hot MPEC results are above background levels. It should be noted that there was an issue with the eFilter real-time data during these measurements and the results should be disregarded.

Average #/s data, APC10

Average #/s data, cMPEC

c

Average #/s data, hMPEC

d

Average µg/s data, real-time eFilter

Conversely, the cumulative gravimetric $PM_{2.5}$ emissions from the eFilter, when calculated to a µg/s basis, were predominantly higher than background levels (Figure 11-31). Note that the result from PG42#2 on Day#3 arises from a negative filter weight.
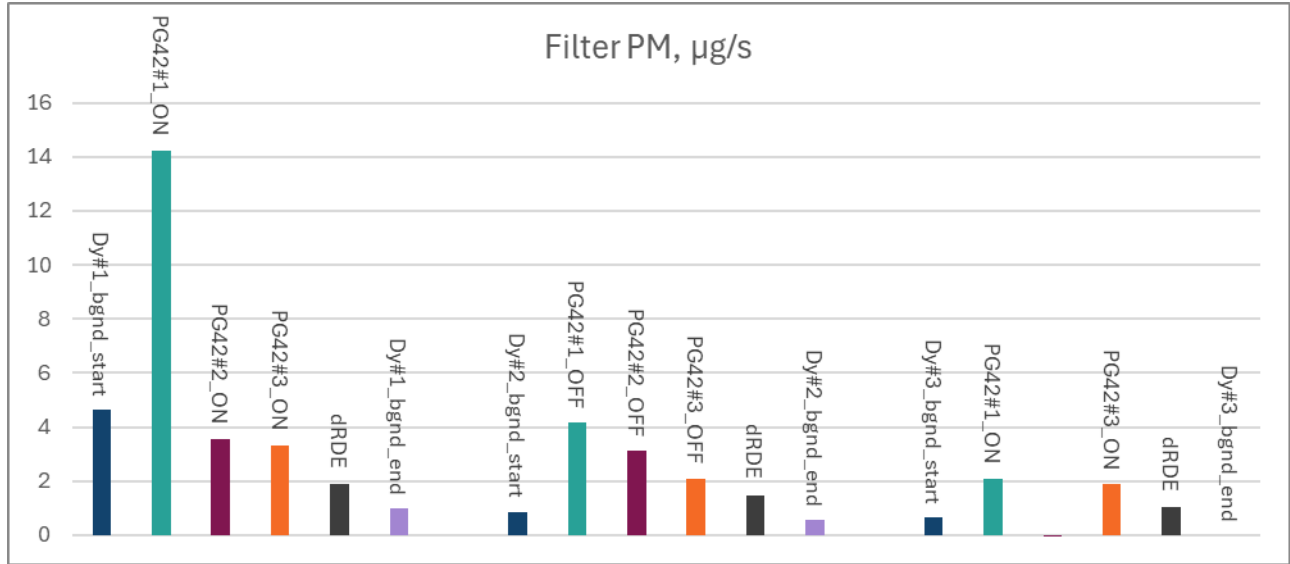
Figure 11-31: Average $PM_{2.5}$ emissions compared from PG42, dRDE and backgrounds.

These results indicated that it was not justified to subtract a background from the samples collected during the TTC ON and TTC OFF measurements, and that analysis of comparative data should focus on PN4, APC10, cMPEC and gravimetric $PM_{2.5}$.

11.2.4.3 Effectiveness of the TTC system at capturing particles in the $PM_{2.5}$ range

Figure 11-32 comprises four sub-figures each showing four columns that represent the averages of the triplicate PG42 test results collected during the W12_[18] non TTC tests, the first batch of TTC ON tests, the TTC OFF tests and the second batch of TTC ON tests. Results are shown for APC10 in sub-figure a, for the cold MPEC in sub-figure b, PN4 emissions in sub-figure c and for filter $PM_{2.5}$ in sub-figure d.

Results for the PN metrics (Figure 11-32a-c) do not indicate obvious differences between the blue TTC OFF/TTC absent results and the green TTC ON results, nor any obvious trend with time.
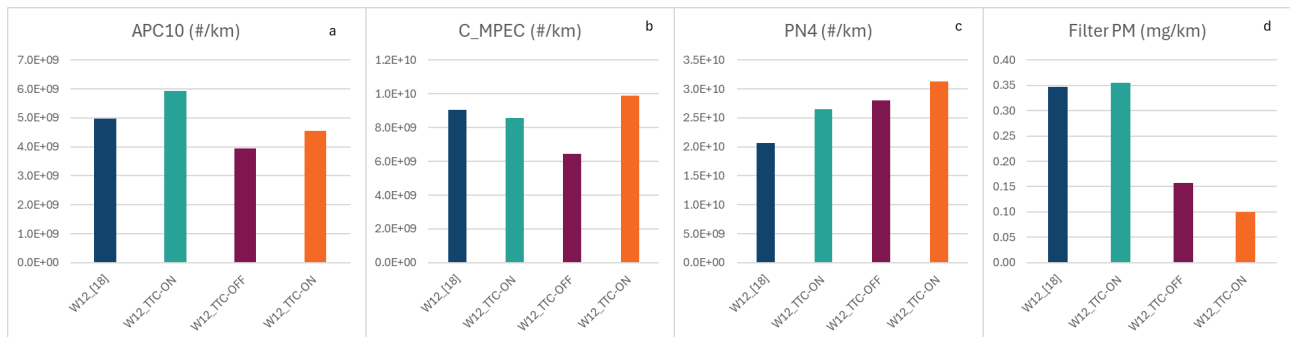
Figure 11-32: Per km emissions for PN and PM from TTC evaluations during PG42 tests measured by a) APC, b) cold MPEC, c) PN4 and d) gravimetric PM.

The PM results do show higher averaged results from the initial W12_[18] tests and the first TTC ON tests, than the later tests, Figure 11-32d. Previously the tendency of a tyre to produce lower PM emissions in a sequence of tests conducted on a single day was observed. This leads to high variability in averaged PM

results. The full sequence of PM results in test order is shown in Figure 11-33, this confirms the trend of highest PM from the initial test and lower subsequent tests. This high variability makes evaluation of the TTC device for PM emissions difficult, but it seems unlikely that any effect is present.
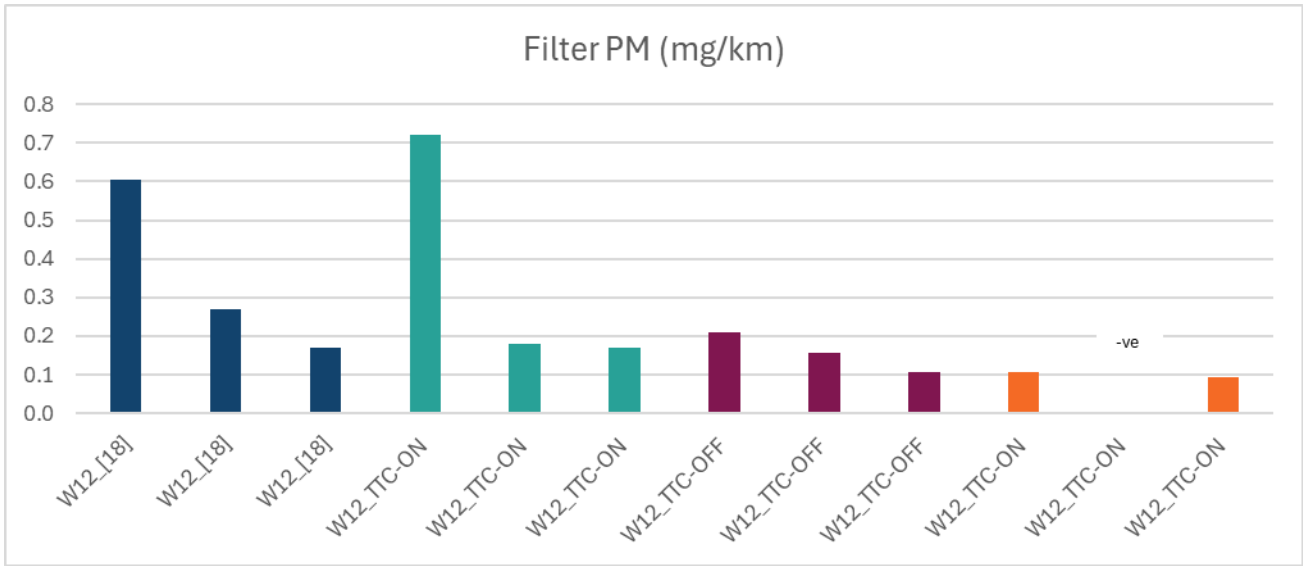
Figure 11-33: PM emissions results in test order.

Comparison between PN emissions, Figure 11-34a, and PM emissions, Figure 11-34b, does not indicate any effect of the TTC device in the $PM_{2.5}$ regime. Even if the PM data are selected to include similar emissions – for example, columns 5, 6, 10, 12 for TTC ON and columns 7, 8 and 9 for TTC OFF, these produce similar results at 1-sigma: TTC ON = 0.137 ± 0.048 and TTC OFF = 0.158 ± 0.052.

Figure 11-34: Comparative per km emissions during PG42 cycles with TTC ON vs. TTC OFF or TTC absent for a) APC10, cold MPEC and PN4, and b) gravimetric PM.

Figure 11-35 shows negative or zero reduction efficiencies for all measurements, indicating no positive reduction efficiencies for PN or PM (Figure 11-35a) or for particle size distributions measured by DMS500 (Figure 11-35b).
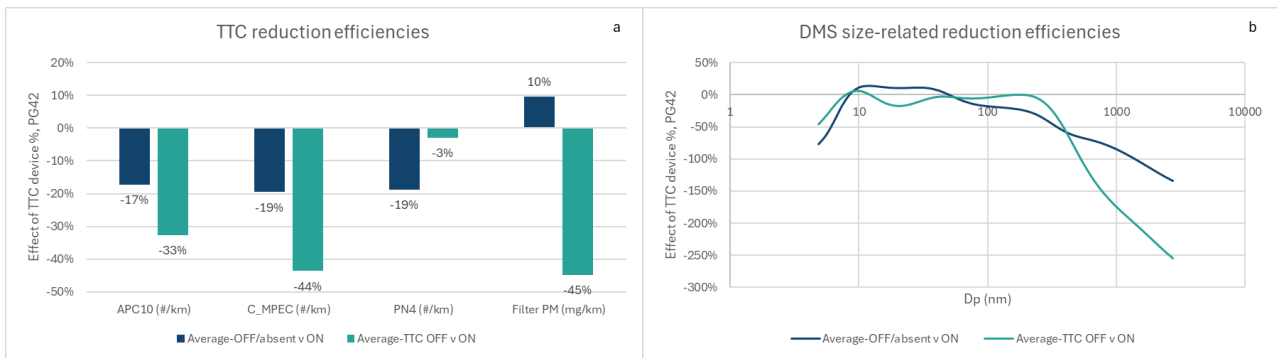
Figure 11-35: Efficiencies of TTC device during PG42 cycles for a) PN and PM emissions, b) size related.

Similar evaluations of the TTC were also performed on the dRDE cycle, except that only single tests were conducted for W12_[18], TTC ON, TTC OFF and repeat TTC ON measurements. Figure 11-36a-c confirm the observation from the PG42 cycle that there is no obvious reduction in PN with the TTC ON.

Figure 11-36d shows that the W12_[18] PM data are probably not comparable with the TTC data, and that similar levels of emissions were observed from both TTC ON and TTC OFF tests. Figure 11-37a confirms that there is no evidence of reduced PN emissions with the TTC ON. Figure 11-37b and c show comparative TTC ON/TTC absent v TTC OFF and TTC ON v TTC OFF PM data. The latter figure, with the W12_[18] data disregarded, confirms no effect on PM.

TTC reduction efficiencies, show no appreciable reductions with TTC on in either PN and PM (Figure 11-38a) or size distribution data (Figure 11-38b).
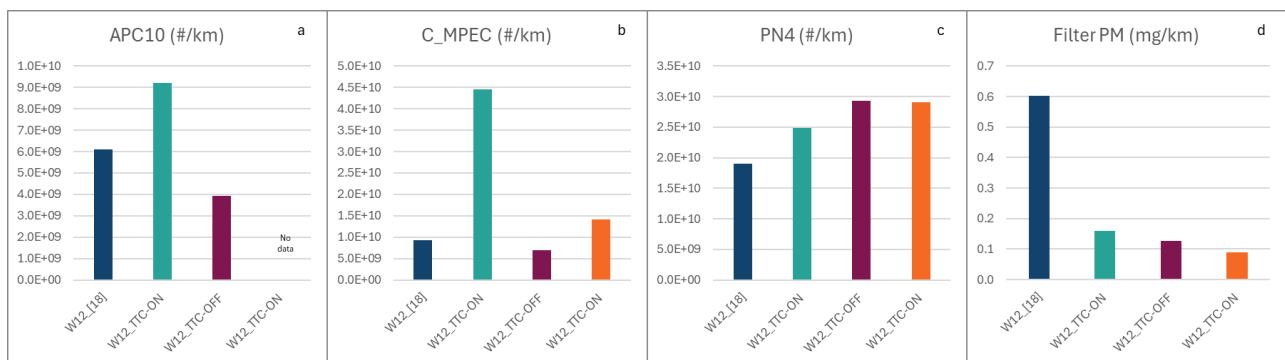
Figure 11-36: Comparative per km emissions during dRDE tests with TTC ON vs. TTC OFF or TTC absent for a) APC10, b) cold MPEC, c) PN4, and d) gravimetric PM.
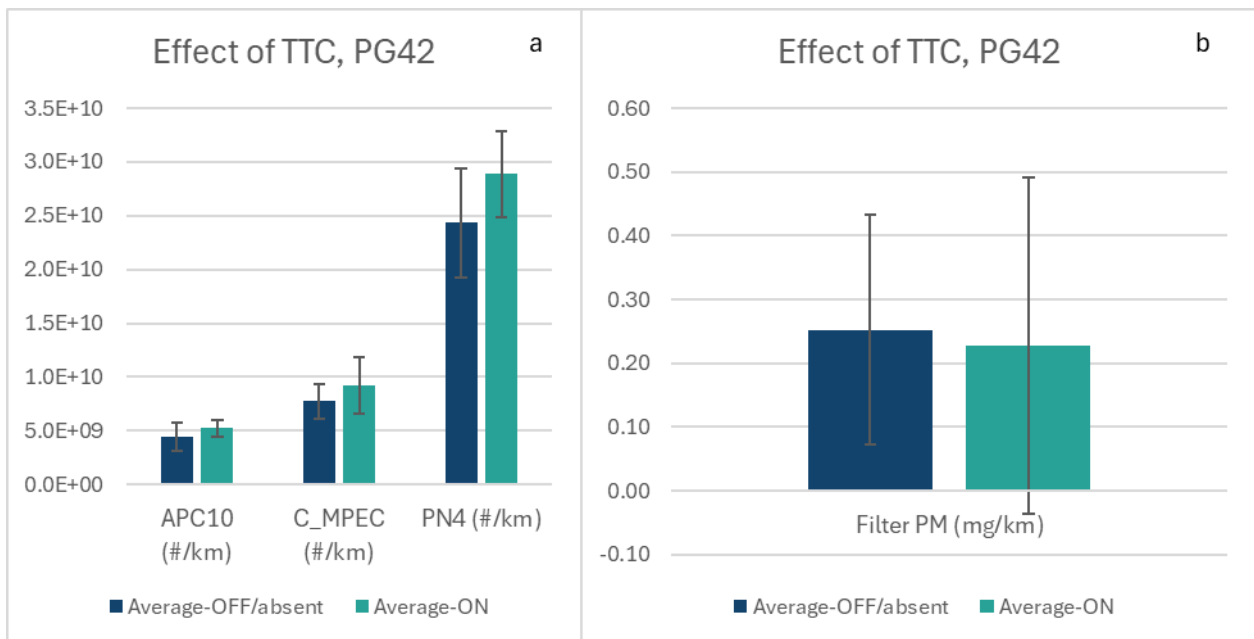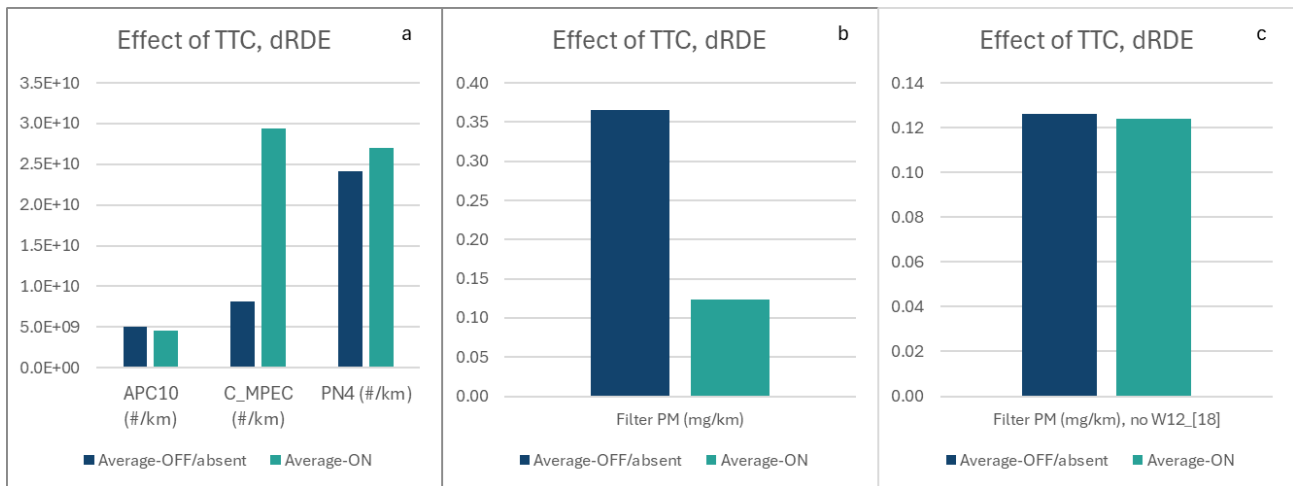
Figure 11-37: Comparative per km emissions during dRDE cycles with TTC ON vs. TTC OFF or TTC absent for a) APC10, cold MPEC and PN4, and b) gravimetric PM, c) gravimetric PM with W12_[18] PM data removed.
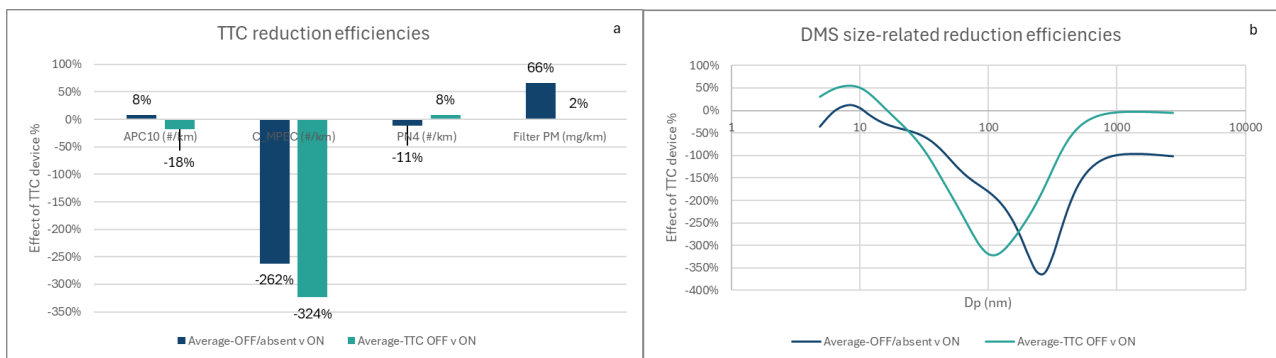
Figure 11-38: Efficiencies of TTC device during dRDE tests for a) PN and PM emissions, b) size related.

11.2.5 Outcomes of TTC experiments

When the TTC was active, it captured large particles (>50-100 µm) on the electrodes, which are visible to the human eye. In contrast, with the TTC off, minimal particle collection was observed.

Background particle levels showed significant variability, both within the same sampling period and between pre-test and post-test measurements. This inconsistency makes it challenging to determine if the background is representative. Emissions levels from PG42 tests with some PN instruments, e.g., PN4 and APC10, were consistently above background levels, while dRDE emissions were sometimes below background levels. Real-time data showed that background levels occasionally fluctuated significantly, sometimes approaching the highest emission levels during the test cycles. This variability indicated that subtracting background levels from test samples was not justified.

No significant differences were observed in particle number (PN) emissions between TTC ON and TTC OFF tests across different instruments.

$PM_{2.5}$ emissions showed high variability, with initial tests generally producing higher emissions than subsequent tests, making it difficult to evaluate the TTC's effectiveness. Comparing the results of similar tests (e.g., the first results in the sequence of PG42 tests) did not indicate any effect of the TTC. Consequently, experimental data did not show any clear trend or significant reduction in $PM_{2.5}$ emissions when the TTC system was active.

Overall, the TTC system did not show reductions in either PN or PM emissions in the $PM_{2.5}$ range but did demonstrate the capacity to collect large particles likely to be categorised as microplastics. The difficulty of

charging particles is approximately inversely proportional to their surface area, thus the TTC is significantly more effective at capturing larger particles (~100 µm) compared to smaller particles, such $PM_{2.5}$.

12. DISCUSSION OF SAMPLING SYSTEM AND INSTRUMENTATION

12.1 COMMENTS ON DIFFERENCES IN TYRE SAMPLING COMPARED TO PHASE 1 AND BENEFITS

Phase 1 aimed to develop a system that could be used to measure NEE particles under real-world operating conditions, the proof-of-concept system enabled either brake or tyre emissions measurements on a vehicle while on the public roads. The size and position of the sample duct was constrained by the dynamic window between the vehicle floor and the road, accounting for road imperfections and traffic calming measures and the geometry of the steering, and by the sample flow rate that was possible with pumps and battery packs on board the vehicle. Brake particles were isolated using the same enclosure system as used for brake measurements in which filtered air was pumped in and brake particles pumped out, although the enclosure could not be completely sealed. Tyre particulate emissions levels were very low concentration and proved difficult to distinguish from background levels on the road.

Phase 2 aimed to explore the variables influencing NEE particulate emissions, and so it was clear that a controlled environment would be needed for repeatable, comparable results. Testing on a vehicle dyno minimises external variables and removes many constraints for the sampling system design, while retaining the whole-vehicle approach. The sample duct could now fill the space between the ground and the underside of the vehicle with a small margin for vehicle movement, and a significantly larger and more powerful fan could be used to increase the sample flow rate. Separating tyre measurements from brake measurements allowed the brake enclosure system to be optimised for its role in isolating brake particles from tyre sampling, air was not pumped into the enclosure but drawn out under vacuum, ensuring the enclosure is always at a negative pressure and particles do not escape through the gap between static and rotating components. Comparing tyre measurements in phase 2 to those of phase 1 suggests those in phase 1 may have seen some contamination by brake particles.

Following initial tests with the revised sample system which had very low readings, further development took place including moving to a test facility with a textured surface roller and in which dyno pit extract fans could be isolated, and the addition of PN4 measurement to identify smaller particles at low concentrations. The sample points were also moved closer to the sample duct, and a tyre temperature sensor added.

The key changes between the sample system used in phase 1 and that in phase 2 are:

- Vehicle dyno only testing – minimising some external factors.
- A larger sample duct.
- Increased sample flow.
- Brake enclosure system optimised for isolating brake particles from tyre sampling.
- Disabled dyno pit extract fan.
- Dyno roller with a textured surface more representative of tarmac.
- Addition of PN4 measurement.
- Instrument sampling close to the tyre sample duct.

Together, these changes allowed phase 2 to compare different types/compositions and sizes of tyre, the effects of ageing, and the effectiveness of a particle emission reduction technology. Challenges remain since the tyre particle emission concentrations are very low, and even in vehicle laboratory, background sources are not eliminated. This was exacerbated by the need for high sampling flows to ensure that larger particles would be efficiently drawn into the sampling duct. Higher sampling flows improved particle transport but also introduced a substantial dilution effect. Background measurements were variable and may not be representative of those reaching the sampling system during testing due to the changes in airflow with the wheel rotating, and even a static tyre could emit volatile particles. Although much larger than that used in phase 1, the sample duct still only covers a small portion of the tyre. The low concentrations and range of

particle sizes and solid and volatile material are challenging for measurement instruments, and there is a trade-off between the benefits of increasing sample flowrate to maximise the collection of particles at the tyre verses the increasing sample dilution that causes.

Approaches that could be adopted to address these challenges include:

- Use a particle-free test chamber, rather like a Sealed Housing for Evaporative Emissions (SHED). However, developing such a facility including a suitable dyno and instrumentation would be complex.

- Fully enclose the wheel in a chamber fed with filtered air. This was considered, but in practice the chamber cannot be fully sealed while the wheel is on a dyno drum, and the chamber cannot be fitted within the vehicle wheelarch. Extending the axle so the wheel can be fitted in an outboard chamber is possible as shown by the Institute of Combustion Technology (DLR) (Bondorf, 2023), although this was considered a significant deviation from the aim of being representative of vehicle use.

- The sample duct itself may be studied using computational fluid dynamics (CFD) to understand the airflows around the wheel and into the duct with different flow velocities, and how the likelihood of particles entering the sample system is changed by sample velocity/flow rate or duct design. The smoke tests (section 3.1.2.1) showed a great deal of turbulence around the wheel, and some particles being entrained close to the surface of the tyre as it rotated.

- Reduce the sample flow to reduce dilution by experimentation, using the presence of larger (>50µm) particles to ensure particles are penetrating the sampling system (i.e. flow is just above the point that particles start to drop out). However, a low sample flow means a low inlet velocity around the tyre and so there is a risk that particles do not enter the sampling system, the path of smaller particles being more susceptible to airflow.

- A mass comparison between total tyre abrasion and particles collected by the sampling system could be carried out, over a long duration mileage accumulation test, depending on tyre and drive cycle perhaps 300-500 miles might be expected to abrade around 20g of tyre material (at 50 µm/km, see 10.3.1). A cyclone installed just downstream of the sample duct could collect the material of significant mass (>50µm) entering the sample system for weighing and comparison with the weight loss of the tyre.

12.2 COMMENTS ON DIFFERENCES IN BRAKE SAMPLING COMPARED TO PHASE 1 AND BENEFITS

Phase 1 revealed several challenges in brake sampling that highlighted the need for improvements to optimize Phase 2, as described in Section 3.1. The most significant limitation identified was the constrained airflow, with a maximum rate of 180–190 lpm, which fell short of the 300+ lpm required for efficient particle transport. This issue was attributed to the suboptimal axial fan design and restrictions at the brake enclosure inlet which proved to be a challenge for the axial fan to overcome in delivering high flows. In Phase 2, we addressed this by implementing blowers designed to operate under more extreme conditions and optimizing the flow path before and after the brake enclosure. The brake enclosure itself was deemed to have an optimal design, considering the constraints of the enclosure and the clearance required for other components critical to the operation of the vehicle braking system and wheel. As a result, we achieved flow rates exceeding 400 lpm.

Flow stability was another issue in Phase 1, with fluctuations caused by system vibrations within the moving vehicle, pressure buildup ahead of the brake enclosure restriction, resulted in outgassing from the dilution boxes and any connections with a suboptimal seal. In Phase 2, we minimized these effects by reducing expansion impacts on the filter boxes and improving connections and hoses, resulting in consistent flow at higher pressures upstream of the brake enclosure and greater data reliability. Additionally, Phase 1's reliance on open rear doors for ventilation and cooling created challenges in testing during adverse weather. In Phase 2, we addressed this by introducing a more compact and enclosed system with reduced heat generation, achieved by selecting better equipment.

Heat buildup from high-powered vacuum pumps, which had been partially mitigated in Phase 1 by leaving the doors open, was further addressed in Phase 2 through the incorporation of more portable and energy-efficient components. This not only resolved heat-related issues but also enabled longer and more practical field testing due to the reduced power demand on the onboard battery generators. These advancements collectively

enhanced transport efficiency, ensured consistent sampling, and improved system reliability, adaptability, and durability for real-world applications.

12.3 FRACTION OF VOLATILE PARTICLES PRESENT (HOT V COLD MPEC) IN MEASUREMENTS COMPARED TO DIFFERENCES EXPECTED THROUGH LOSSES IDENTIFIED IN CALIBRATION

Prior to any testing, the cold and hot MPEC systems were calibrated with solid particles and the results revealed that there were ~20% thermophoretic losses in the hot MPEC, when directly compared with the cold system (Section 5.2.1.2). This implied that when the two systems are compared using measurement data from brake and tyre evaluations, any results that show the cold MPEC results to be substantially higher than 1.2x the hot MPEC results would be an indication of the presence of volatile particles.

When this comparison was made for brake wear particles, including different cycles' data, results showed a very strong correlation, and indicated that cold MPEC levels were ~22% higher than hot MPEC levels (Figure 12-1). This finding, that the $PM_{2.5}$ particles contain ~2% volatiles, is consistent with the thermogravimetric analysis results in Phase 1 that showed PG42 filters to contain >95% of non-volatile, non-oxidisable, materials.
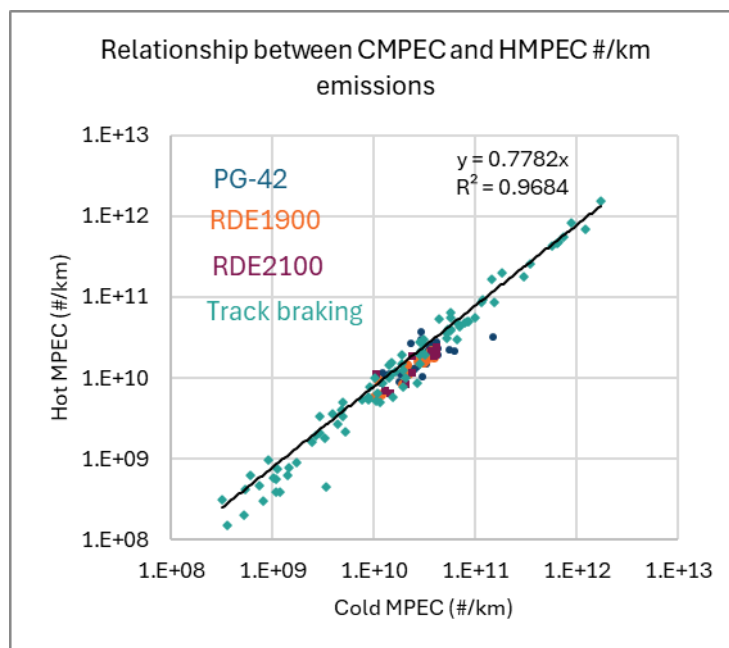
Figure 12-1: Correlation between cold MPEC and hot MPEC results – brake $PM_{2.5}$ emissions.

Comparing cold and hot MPEC results from tyre emissions tests over multiple cycles, and accounting for 20% losses, indicates a much higher volatile fraction, perhaps around 45%, than seen from the brake emissions measurements. In the Phase 1 study, a thermogravimetric analysis of a tyre emissions $PM_{2.5}$ filter showed ~35% volatiles, but this filter may have collected some non-volatile brake wear materials and so the actual volatile fraction would have been slightly higher.

Due to the instrumental sensitivity and low levels of particles measured, plus the uncontrollable influence of background contributions, the correlation between instruments is relatively poor compared to the brake emissions comparison (Figure 12-2).
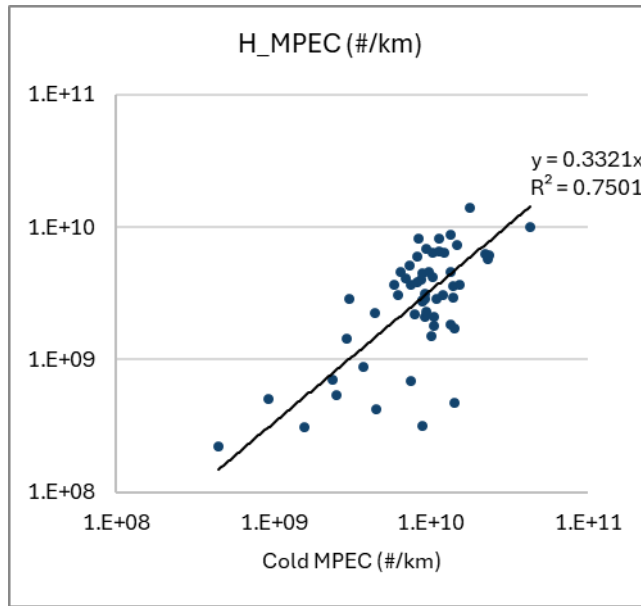
Figure 12-2: Correlation between cold MPEC and hot MPEC results – tyre PM$_{2.5}$ emissions.

12.4 CORRELATIONS BETWEEN INSTRUMENTS USED IN BRAKE AND TYRE PHASES

It is worthwhile comparing the results of instruments or approaches that measure the same or a similar metric in different ways. For example, consider the measurement of non-volatile PN10 particles using the APC10 and hot MPEC. The APC10 is a laboratory-based instrument featuring a condensation particle counter, whereas the hot MPEC is a diffusion charger-based system. The Hot MPEC is smaller, lighter, and has lower power-demand making it more suited to on-vehicle measurements where size and power requirements will be critical factors.

12.4.1 Hot MPEC and APC10

For brake wear emissions a satisfactory correlation is observed between hot MPEC and APC10. However, the hot MPEC reports ~10x higher emissions (Figure 12-3). The reasons for this tenfold difference are discussed below (Section 12.4.1.1) along with a potential correction factor.
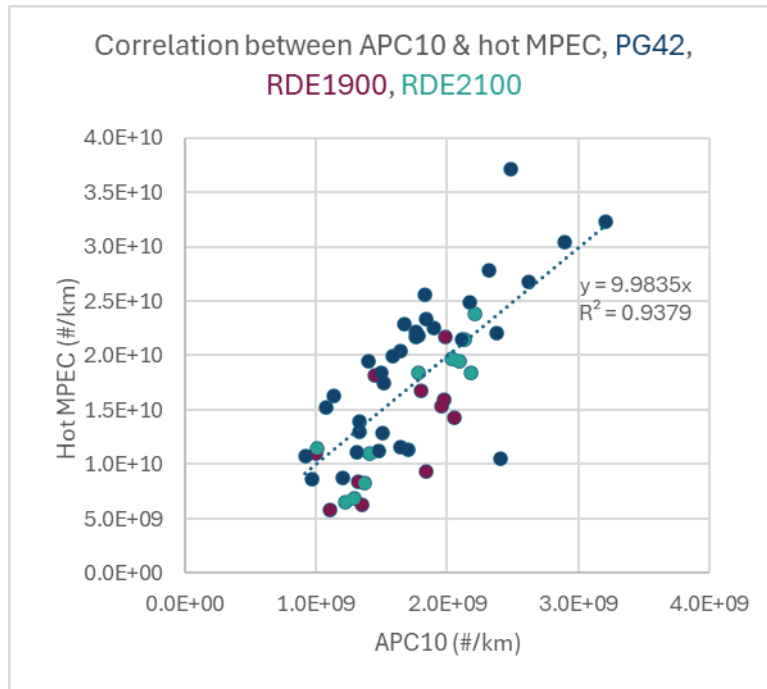
Figure 12-3: Correlation between APC10 and hot MPEC results – brake PM$_{2.5}$ emissions.

Tyre emissions measurements showed more similar levels between APC10 and hot MPEC, but the correlation was poor (Figure 12-4). Despite this, the results do suggest a general trend of higher PN from the MPEC as APC10 emissions rise. The closer agreement between the two instruments, than with brakes, will likely be due to the absence of solid particles in the size distribution above ~500nm. The poor correlation is attributed to high effective dilution of the tyre emissions sample. This occurs due to the significant volumetric airflow rates used to transport wear particles from the duct to the instruments, which compromises the electrometer-based hot MPEC. Additionally, the APC10 introduces further dilution, by a factor of approximately 150x.
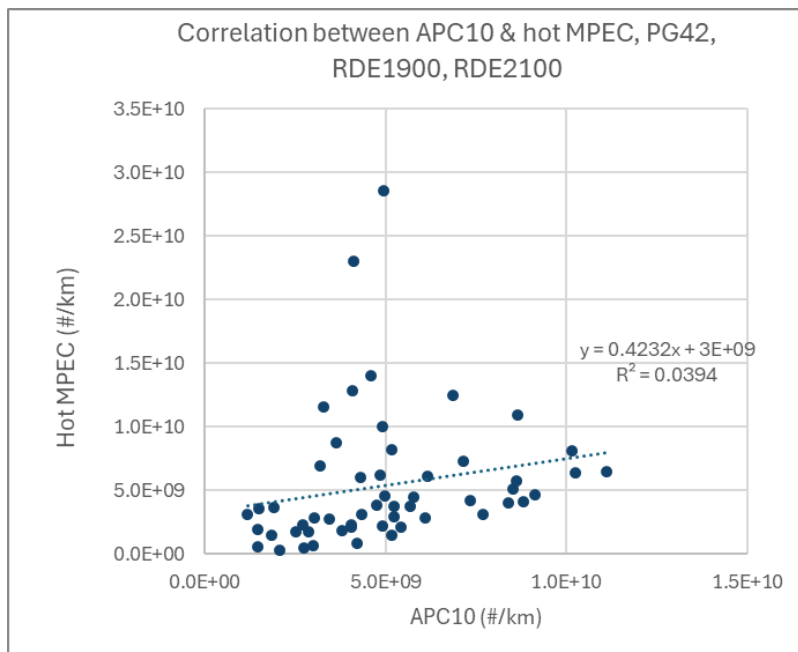

Figure 12-4: Correlation between APC10 and hot MPEC results – tyre PM$_{2.5}$ emissions.

The mismatch between the hot MPEC and APC10 results for brake emissions indicates that, for a diffusion charger-based PN10 measurement system to be viable in a regulatory context, either a correction factor must be applied, or alternative actions, such as that described in Section 12.4.1.2, should be considered.

12.4.1.1 Diffusion charger considerations

The Dekati MPEC+ detector technology relies on particle charge interaction to generate a voltage response for individual particles. However, larger particles, particularly those exceeding 100 nm, can affect diffusion chargers in a number of ways.

As a result, steps are taken during the calibration process to limit the formation and presence of multiply charged particles, identify the likelihood of such particles remaining after mitigation efforts, and apply a correction for multiple charges to the reported data. In real-world testing, where the particle distribution is often polydisperse, ranging from a few nanometres to several microns, larger particles, even in small quantities, can lead to overcounting. This is because diffusion charger-based systems, like the MPEC+, may overestimate particle numbers due to the effects of multiple charges carried by larger particles, particularly those above 200 nm.

Under laboratory conditions, this overcounting issue might go undetected because of proper checks and controlled processes. However, for future calibrations, it may be advisable to include a calibration point at 0.5 µm or 1 µm. A more practical approach, especially in regulatory emissions testing, could involve using an impactor for particles larger than 0.5 µm. This would ensure that particle number detection technologies operate within similar size ranges and detection thresholds as there are some differences in reported concentrations for devices counting particles below 1 µm.

A hypothesis was proposed to explain the influence of particles larger than 1 µm on MPEC+ data compared to the DMS and APC. However, the discrepancy proved more complex than initially anticipated. The working hypothesis suggests that the MPEC+ reports higher values due to the presence of particles near 1 µm in the sample, while the DMS is less effective at measuring particles in this size range. Additionally, no data confirms the measurement efficiency of the APC10 for particles above 200 nm. However, given the APC's optical particle counter methodology, it is unaffected by multiple-charged particles and maintains consistent counting efficiency from 70 nm up to 1 µm. That said, potential particle losses within the APC10 due to impaction and deposition of larger particles must be considered. Therefore, validating the APC's particle penetration efficiency above 100 nm is advisable when measuring particles approaching 1 µm,

A conclusion was reached by comparing the diffusion collector signal of the MPEC+ to the Faraday cup electrometer signal. The ratio between these signals is typically between 0.1 and 0.15 for most of the data. Based on the collection efficiency of the diffusion collector, this ratio could indicate that either there are very few particles larger than 100 nm in the sample, nearly all particles are larger than ~700 nm, or that particles smaller than 100 nm and larger than 700 nm dominate the number concentration. The latter scenario seems most plausible, as the high charging efficiency of large particles would cause the MPEC+ to drastically overestimate the results. Based on this analysis, a rough correction for the MPEC+ data can be proposed, though it would be more of an estimation than an accurate correction.

12.4.1.2 Regulatory PN emission limit approaches

In conclusion, the most effective approach for particle number (PN) measurement in brake and tyre emissions using a diffusion charger is to implement a pre-cut size of approximately 500 nm, as this excludes contributions from larger particles; while a 500 nm cut may not be strictly necessary for tyres, maintaining consistency between brake and tyre measurement systems would support the alignment of calibration approaches. It is essential that the calibration of the PN technology adheres consistently to the ISO 17025 international standard. This approach ensures that all technological methods are measuring the same particle size range and distribution, thereby minimizing the risks of over-counting or under-counting particle numbers (PN). Consequently, any observed differences in emission factors will be attributable to the emission source itself rather than discrepancies in the PN counting devices. By minimising uncertainty in emission factor estimations, this strategy supports more accurate assessments that can inform modelling and regulatory limit determinations. Such best-practice approaches should also be considered for any emissions-based regulatory limits, whether currently enforced or under development.

13. CONCLUSIONS

13.1.1 Brake wear emissions

13.1.1.1 Emissions characteristics

- Real-time brake particle emissions were closely related to instantaneous braking events.
- There was no evidence of volatile outgassing during braking events, suggesting low volatile content in all pads and discs.
- Occasional emission spikes, likely due to brake stiction and release, could potentially lead to overestimations during certification tests.
- Dynamic braking caused the highest $PM_{2.5}$ and PN emissions, while gentle braking produced the lowest, demonstrating braking intensity's impact on emissions.
- Exponential temperature-emission curves fit well for brake emissions, especially for aged pads like P10A, indicating stabilized emissions with use.

13.1.1.2 Impact of Brake Pad and Disc Characteristics

- Aged brake pads produced lower $PM_{2.5}$ and PN emissions than lower mileage pads, suggesting improved emission characteristics with use.
- Low dust (e.g., P8, P9) and ceramic pads demonstrated the lowest $PM_{2.5}$ and PN emissions across all test conditions.
- Organic (e.g., P5) and budget pads produced the highest emissions, indicating material composition significantly influences emissions.
- Volatile materials in pads affected emission variability, with ceramic pads showing emissions of lower volatility components than organic pads.
- There were no significant differences between $PM_{2.5}$ and PN emissions of low-cost and premium discs, and no correlation of emissions levels with brake pad cost.
- Optimized pad-disc pairings may deliver better results than the disc pairs tested in this study.

13.1.1.3 Test Mass and Speed Influences

- Increased test mass (2100 kg vs. 1900 kg) consistently resulted in higher brake PN and $PM_{2.5}$ emissions.
- Moderate braking emissions increased linearly with speed, while dynamic braking emissions followed a quadratic trend, suggesting greater localized heat effects.
- Increased disc temperatures during dynamic braking indicated the possibility of localized heat spikes that may not be fully represented by bulk disc temperature measurements.

13.1.1.4 Wear and Aging Effects

- High-mileage pads (e.g., P10A) exhibited higher wear rates by weight but slower thickness reduction than lower milage pads, suggesting differences in wear mechanisms over time.
- Initial wear rates for pads over the first ~1000 km were ~3 mg/km, with premium and ceramic pads showing lower wear compared to budget options.
- Pad aging and disc curing reduce emissions variability over time, supporting the need for through-life testing in brake system evaluations.

13.1.1.5 Comparisons Across Testing Methods

- Real-time eFilter measurements aligned well with gravimetric $PM_{2.5}$ data, confirming reliability across methodologies.
- Emissions trends were similar across chassis dynamometer and on-road RDE tests, confirming consistent performance of pad-disc combinations in controlled and real-world scenarios.
- Test track results revealed repeatable emissions trends for moderate and dynamic braking, with moderate braking showing more predictable linear increases in emissions.

13.1.1.6 Overall Emissions Performance

- Average PN10 emissions for tested disc and pad combinations were approximately 2×10^9 #/km, with gravimetric $PM_{2.5}$ emissions between 1.5 and 2.5 mg/km.

- The highest PM$_{2.5}$ emissions (e.g., 3.5 mg/km) were observed from organic and budget pads, while the lowest (~1 mg/km) came from ceramic and low dust pads.
- Enclosure temperatures may have elevated reported emissions compared to real-world conditions, but differences are likely relatively small.

13.1.1.7 Recommendations for Emissions Reduction

- Low dust and ceramic pads appeared to outperform other pads in producing lower emissions.
- A break-in period of ~500 km was essential for brake discs and pads to stabilize PN emissions, particularly volatile PN10 emissions.

13.1.1.8 PM$_{2.5}$ and PN10 Whole-Vehicle Emissions Estimation

- Whole vehicle brake emissions (on the basis that braking was 100% by the two front wheels, but would actually be spread 70% to the front wheels and 30% to the rear wheels) were estimated at PM$_{2.5}$ of ~3 to ~5 mg/km with PN10 emissions at ~4 × 10^9 #/km.

13.1.2 Brake wear technology effects

13.1.2.1 Mass and Regenerative Braking Combined

- Only limited differences were observed between PN10 emissions of different vehicle types (ICE, PHEV and EV), with slightly elevated emissions from ICE at 1900 kg during bespoke cycles. Increased regenerative braking and lower test mass appears have minimal effect on non-volatile particles.
- ICE at 1900 kg showed the highest total PN10 emissions, followed by PHEV, with EVs showing the lowest emissions. Cold MPEC emissions were consistently higher than hot MPEC emissions, even accounting for particle losses
- Higher test mass (1900 kg) in ICE vehicles leads to significantly higher emissions compared to PHEV and EV, both tested at 1700 kg. The EVs benefited from higher regenerative braking levels, resulting in lower brake particle emissions
- Highest gravimetric PM$_{2.5}$ emissions were seen from ICE vehicles (2-3 mg/km), followed by PHEV (0.6-1.6 mg/km), and lowest from EVs (0.3-1.2 mg/km). Real-time eFilter data supported these trends
- Particle size distributions showed bimodal character, with peaks below 20 nm and between 200 and 300nm. The >100 nm mode showed the highest emissions from 1900 kg ICE, followed by PHEV, with lowest from EV.
- Reduction in test mass from 1900kg to 1500 kg with ICE did not reduce emissions to the levels seen with the higher mass PHEV and EV that feature regenerative braking
- PN10 and PM$_{2.5}$ emissions were higher from a hot braking system than from a cool one.Emissions increased with braking dynamicity and were always highest when braking from the highest speed, 110 kph

13.1.2.2 Emissions from ICE, PHEV, and EV Using matched 1900 kg Test Mass

- Minimal differences in PN10 emissions were observed between ICE, PHEV, and EV across both PG42 and RDE cycles, with similar levels of around 1x10^9 #/km for PG42, and 2x10^9 #/km for dyno RDE tests
- Cold and hot MPEC PN emissions were highest from ICE vehicles, likely due to volatile and semi-volatile particle emissions. ICE vehicles may also emit more of the larger (0.5µm+) particles that carry higher charge levels
- PM mass emissions were highest from ICE vehicles, around 2 mg/km from both PG42 and dyno RDE cycles, with PHEV and EV emissions being 20-30% of ICE levels and well below 1 mg/km. Higher brake system temperatures in ICE vehicles suggest higher emissions of volatile materials that would contribute to PM

13.1.3 Brake wear reduction device – evaluation of the TAMIC system

13.1.3.1 PM$_{2.5}$ Emissions Reduction

- The TAMIC system consistently reduced gravimetric PM$_{2.5}$ emissions, with greater reductions observed in continuous mode (~56% and ~53%) compared to intermittent mode (~44% and ~40%).
- The system demonstrated PM$_{2.5}$ reductions above 40% in both operational modes.

13.1.3.2 PN10 Emissions Reduction

- In continuous mode, the TAMIC system reduced non-volatile PN10 emissions by ~44% (PG42) and ~32% (dyno RDE), but no reductions were observed in intermittent mode.

13.1.3.3 Efficiency Considerations

- The efficiencies measured in this study should be considered as lower limits due to the potential impact of background contributions and brake stiction on particle removal efficiencies
- Brake pad stiction between braking events may contribute to the observed efficiency difference between intermittent and continuous modes, with evidence of brake particles being released on accelerations
- Higher levels of particle emissions between braking events, particularly during long cruises of the PG42 cycle, could result in lower apparent TAMIC particle removal efficiencies.

13.1.3.4 TAMIC System Effectiveness

- The TAMIC system demonstrated the capacity to reduce both PN10 and PM$_{2.5}$ by over 30% in continuous mode.
- The system's effectiveness is influenced by operational mode, and potentially by background contributions and brake stiction. Careful consideration of these factors is required in evaluating its performance, but it has the potential to reduce both PN10 and PM$_{2.5}$.

13.1.4 Tyre wear emissions

13.1.4.1 Phase-Specific Observations

- When both were tested in the VERC, Audi A4 measurements (Phase 2) showed lower tyre particle emissions than the levels seen from the VW Caddy in Phase 1.
- The promotion of sticky tyre surfaces, when running on relatively smooth steel rollers, may restrict particle release, including those in the PM$_{2.5}$ range.
- Cross-contamination of tyre wear measurements by brake particle emissions may have affected Phase 1 measurements, indicating the erroneous presence of solid particles.

13.1.4.2 Testing Methodologies and Facilities

- A hard-wearing textured roller surface stimulated higher tyre wear emissions from the Audi A4 in the VATF than had been seen in the VERC.
- Brake enclosure evacuation eliminated particle leakage and cross-contamination, of tyre emissions with brake particles, in Phase 2.
- Background level and measurement inconsistencies prevented confident background subtraction.
- No significant changes in PN10 or PM$_{2.5}$ emissions were observed with ageing of the textured roller surface in the VATF across the test programme.

13.1.4.3 Differentiation between PM$_{2.5}$ and PN10 emissions of tyre size, tyre age and tyre types

- In general, due to high measurement variability and low emissions concentrations, it was not possible to categorically identify any general effect of tyre size, tyre age/mileage or tyre type on PN10 or PM2.5 emissions

13.1.4.4 Influences on Total Particle Number Emissions from Tyres

- Several factors were observed to increase the release of total PN from tyres, including higher initial speed of braking, more aggressive braking and higher initial tyre temperature

- PN were observed to be constantly released from the tyre when the vehicle is moving, with faster cruise speeds having higher emissions
- Tyre Total PN emissions are dominated by volatiles

13.1.4.5 Tyre Wear Characteristics and Variability

- Larger 18" tyres potentially showed higher wear rates than 16" tyres.
- Wear rate levels of single front tyres ranged from ~20 to 120 mg/km.
- On one single tyre type evaluated, a ~23,500 km mileage tyre showed a ~300 times faster mass emissions rate than a ~1000 km mileage tyre.
- Average mass wear rate for tyres with ≤ 1000 km mileage was 65.8 ± 45 mg/km.
- No correlation was found between tyre wear and fuel economy ratings.
- No correlations between tyre wear and $PM_{2.5}$ or PN10 emissions were apparent.

13.1.4.6 Tread Wear Dynamics

- There were no obvious differences in tyre tread wear rates between 16" and 18" tyres
- On one single tyre type evaluated, higher mileage increased tread depth loss rates significantly, with wear accelerating at higher mileages. Tread wear loss correlated with tyre mass loss for this tyre type
- Tread wear rates for 18" tyres were 0.2–0.6 μm/km (2 mm to 6 mm per 10,000 km).

13.1.4.7 Real-Time Emissions

- Higher emissions were observed in PN4 measurements, than PN10. Peak emissions were seen during aggressive braking and high-speed operation.
- Non-volatile PN10 emissions constituted a small fraction of total PN4 levels, in one case as low as 1%.

13.1.4.8 Emissions Factors

- Typical non-volatile PN10 emissions were ~5×10^9 #/km ± 44%.
- Total PN10 emissions were ~1.1×10^{10} #/km ± 76%, with PN4 emissions approximately double the PN10 values
- $PM_{2.5}$ emissions were low, but highly variable (~0.19 mg/km ± 103%).

13.1.4.9 Size Distributions and Filter Collection

- Super-micron particle size distributions of tyre wear dust showed modes at ~53 μm, 250 μm, and 600 μm.
- Collected $PM_{2.5}$ filter masses varied widely, from ~20 μg to > 1 mg.
- Most $PM_{2.5}$ filters appeared clean, suggesting minimal solid particle collection.

13.1.4.10 $PM_{2.5}$ and PN10 Whole-Vehicle Emissions Estimation

- There is little evidence to suggest that there are substantial levels of $PM_{2.5}$ emitted by tyres during normal operation.
- Tyre wear mass loss is dominated by particles larger than 2.5 μm, with most particles being an order of magnitude, or more, larger.
- Typical single front wheel non-volatile PN10 tyre emissions were ~5×10^9 #/km, just below 1% of the Euro 7 tailpipe limit value (6×10^{11} #/km).
- Whole vehicle tyre emissions (on the basis that braking was 100% by the two front wheels, but would actually be spread 70% to the front wheels and 30% to the rear wheels) were estimated at $PM_{2.5}$ of ~0.38 mg/km with whole vehicle PN10 emissions at ~1×10^{10} #/km.
- Since average mass wear rate for tyres with ≤ 1000 km mileage was 65.8 ± 45 mg/km, total vehicle emissions would be twice this, at 131.6 mg/km. Measurements of emissions were on a 2-wheel drive chassis dynamometer so total emissions would actually be split 70:30 between front and rear axles, and a typical emission for a front wheel would therefore be estimated at 46.1 ± 31 mg/km

13.1.5 Comparative brake and tyre emissions levels

- On average, tyre PN10 emissions were higher than brake PN10 emissions, at 5×10^9 #/km per front wheel and $\sim 2 \times 10^9$ #/km per front wheel.
- However, $PM_{2.5}$ emissions from brakes averaged around 2 mg/km per front wheel, with tyre $PM_{2.5}$ emissions at ~ 0.2 mg/km.
- Particles of ≤ 2.5 µm from brakes are substantially larger, more dense, or both, when compared to tyre particle emissions.

13.1.6 Tyre wear reduction device

- The TTC system effectively captured large particles (>50-100 µm) when active, which were visible to the human eye, but minimal particle collection occurred when the TTC was switched off.
- It was not possible to discern reductions of either PN or PM emissions in the $PM_{2.5}$ range, but the TTC system demonstrated the capacity to collect large particles, likely categorized as microplastics. The system was significantly more effective at capturing larger particles (~ 100 µm) compared to smaller particles like $PM_{2.5}$.

14. FUTURE RESEARCH

This study provides an in depth investigation into a number of variables that can affect particle emissions from brake and tyre wear. However, not all variables could be covered in the scope of this study, are gaps have also been identified where further research is needed. This includes studies focussing on other variables that were not covered here, further experiments to improve some of the uncertainties in the results, and research into the health impacts of the brake and tyre wear particles that become airborne. Recommendations for further research are summarised below.

Brake technology testing

- High variability was observed when testing the brake emissions from the EV, PHEV and ICE vehicles. It is suggested that further tests are undertaken on the three vehicle types to improve uncertainties and increase confidence in the brake wear differences.

Tyre testing

- The tyre particle number emissions were highest with the PN4 CPC measurements. The system could be run with a catalytic stripper upstream of the CPC to determine what proportion of these emissions may be solids particles.
- Initial tyre temperatures during the tests performed in this study were around 20-24 C. However it is expected under real world conditions, tyre temperatures will be lower during winter months. To investigate the effect of lower tyre temperatures on emissions, the vehicle could be preconditioned to a designated temperature before testing starts.
- Underinflated tyres can result in disproportionate wear on both the inner and outer edge of the tyre, whereas high tyre pressures can result in greater wear in the centre of the tyre. During Phase 1 of this study, PG42 tests were undertaken in the chassis dynamometer to assess any effect of a reduced tyre pressure on emissions. A reduction in the tyre pressure from 2.9 to 2.0 bar resulted in an increase in particle number and particle mass emissions. However, these tests were performed on a smooth roller and only one tyre type. It is recommended that further tests are undertaken using the abrasive surface material used in Phase 2, and with different tyres, to assess the effect of both under- and over-inflated tyres on particle emissions.
- Tyre pressure, wheel alignment also impacts tyre wear and could have an effect on the particle emissions. Similar tests to those for the tyre pressure could also be performed with variations in wheel alignment.

Chemical composition and health impacts of tire and brake wear particles
- For this study filter samples were collected for all tests undertaken on the chassis dynamometer and on road/track. Gravimetric analysis was performed on all filters, and some were also selected for thermogravimetric analysis to calculate the proportion of non-volatile and non-oxidizable material in

the samples. However, these samples could also be analysed in the laboratory to determine their chemical composition and compare to the brake pad/disc or tyre chemistry. Filter samples may also be used for studies on the toxicological effects of brake and tyre wear particles

15. REFERENCES

Adamczak, L., 2023. *At source brake dust active filtering system.* s.l., s.n.

Bondorf, K. G. E. P. S., 2023. Airborne Brake Wear Emissions from a Battery Electric Vehicle. *Atmosphere,* 1 March.14(3).

Giechaskiel, B. et al., 2024. Contribution of Road Vehicle Tyre Wear to Microplastics and Ambient Air Pollution. *Sustainability,* 16(2), p. 522.

Schläfle, S., Unrau, H.-J. & Gauterin, F., 2023. Influence of Load Condition, Tire Type, and Ambient Temperature on the Emission of Tire–Road Particulate Matter. *Atmosphere,* 14(7).